

**MODIFICATION OF HETEROAROTINOIDS
TO ENHANCE THEIR RETINOIC ACID
RECEPTOR-BINDING SPECIFICITY
AND ANTI-CANCER
ACTIVITY**

By

JOZEF KLUCIK

Bachelor of Science

Cameron University

Lawton, Oklahoma

1996

**Submitted to the Faculty of the
Graduate College of the
Oklahoma State University
in partial fulfillment of
the requirements for
the Degree of
DOCTOR OF PHILOSOPHY
July 2000**

MODIFICATION OF HETEROAROTINOID
TO ENHANCE THEIR RETINOIC ACID
RECEPTOR-BINDING SPECIFICITY
AND ANTI-CANCER
ACTIVITY

Thesis approved:

K D Berlin

Thesis Advisor

Eldon C Nelson

Richard A. Bumer

W. Neil A. P.

Alfred Sarluzzi

Dean of Graduate College

ACKNOWLEDGMENTS

I would like to express my sincere gratitude to Dr. K. D. Berlin for being an excellent “coach both on and off the field”. His professional as well as personal advise was, is, and will be respected and appreciated for years to come. Thank you for your positive outlook on things and knowing how to extract the best even from my failures. Most of all, thank you for showing me the light at the end of the tunnel and hopefully making me a better scientist and person as whole.

I wish to thank Dr. Mottola, Dr. El Rassi, and Dr. Nelson for being on my committee and for their encouragement throughout the years of my graduate studies. My special thanks go to Dr. Bunce, Dr. Mort, Dr. Rivera for their advice, knowledge and efforts in writing all those letters of recommendation. I am also grateful to Dr. Benbrook for her doing the biological testing and to Dr. White for his feedback on molecular modeling project.

I thank all my colleagues in Dr. Berlins group: Matora, Sameer, Kevin, Dr. Liu, and Chad for always being there when help was needed and for sharing your experiences with me. Thanks are also due to Mark Wirtz for being honest, critical, and encouraging when I needed it most and for your sense of humor. I would like to also thank the entire Chemistry Department: professors, graduate students and secretaries for their friendliness and help.

Special thanks to my wife, Wanda, for her idea of me going back to school and her endless support of me in achieving my goal. Thanks also to my children, Bianca and Veronica, for understanding “what daddy has to do” and putting up with my absence and brightening up every day. Finally, I’d like to thank my family and my wife’s family (especially Lydia) for their loving support.

My very special thanks go to God and Jesus, for providing the necessary means of existence, health, wisdom and love. I would like to dedicate this dissertation to those who made this country what it is today and those who allowed me to come here, work, live and learn.

TABLE OF CONTENTS

Chapter	Page
I.	HISTORICAL 1
	Introduction 1
	Nuclear Receptors for Natural and Synthetic Retinoids..... 3
	Retinoic Acid Receptor (RAR)..... 3
	Retinoic Acid X Receptor (RXR)..... 8
	Retinoic Acid Z Receptor (RZR)..... 11
	Distribution of Retinoic Acid Receptors in Major Organ Tissues..... 11
	Metabolism of retinoids and Mechanism of Action for Retinoids and Retinoic Acid Receptors..... 12
	Classification of Synthetic Retinoids Based on Their Biological Effects on Retinoic Acid Receptor..... 20
	Detection and Measurement of Retinoic Acid Receptor Activity..... 30
	Toxicity of Retinoids..... 32
	Molecular Modeling..... 33
II.	RESULTS AND DISCUSSION..... 35
	RAR and RXR Isotype Specific Heteroarotinoids..... 35
	Oxygen Heteroarotinoids..... 37
	Nitrogen Heteroarotinoids..... 40
	Sulfur Heteroarotinoids..... 43
	Computer-Aided Activity Prediction..... 45
	Synthesis of Oxygen Heteroarotinoids..... 51
	Synthesis of Nitrogen Heteroarotinoids..... 55
	Synthesis of Sulfur Heteroarotinoids..... 60
	Structure-Activity Relationship Study Via Molecular Modeling 65
	Summary..... 78
	Suggestions for Future Work..... 78
III.	EXPERIMENTAL SECTION 80
	Molecular Modeling..... 80
	Compound Drawing and Energy Minimization..... 80
	Protein Modification..... 81
	Docking..... 82
	Docking Procedure..... 83

Chapter	Page
Superimposition of the Receptor Conformations	86
Conformational Search	87
Activity Prediction	88
Chemistry General Information	91
[(6-Methoxy-1,1,4,4-tetramethylisochroman-5-yl)amino]- [(4-nitrophenyl)amino]methane-1-thione (48)	92
<i>N</i> -{[(6-Methoxy-1,1,4,4-tetramethylisochroman-5-yl)amino]- tioxomethyl}(4-nitrophenyl)carboxamide (49)	92
Ethyl 4-{{[<i>N</i> -(6-Methoxy-1,1,4,4-tetramethylisochroman-5-yl)- carbamoyl]amino}benzoate (50)	93
{{[(1 <i>E</i> ,3 <i>E</i>)-1-Aza-4-(4,4-dimethylchroman-6-yl)-3-fluoropenta-1,3- dienyl]amino}aminomethane-1-thione (51)	94
Ethyl 4-{{[(4,4-Dimethylchroman-6-yl)ethoxy]carbonylamino}- benzoate (52)	95
Ethyl 4-{{[(1,2,2,4-Tetramethyl(1,2-dihydroquinol-6-yl)- carbamoyl]amino]benzoate (53)	96
Ethyl 4-({[(1,2,2,4-Tetramethyl-1,2-dihydroquinol-6-yl)- amino]thioxomethyl}amino) benzoate (54)	97
[(4-Nitrophenyl)amino][(1,2,2,4-tetramethyl(1,2-dihydroquinol-6- yl))amino]methane-1-thione (55)	98
Ethyl (6 <i>Z</i> ,2 <i>E</i> ,4 <i>E</i> ,8 <i>E</i>)-3,7-Dimethyl-9-(1,2,2,4-tetramethyl(1,2- dihydroquinolyl))nona-2,4,6,8-tetraenoate (56)	98
{{[(3 <i>Z</i> ,1 <i>E</i> ,5 <i>E</i>)-1-Aza-4-methyl-6-(1,2,2,4-tetramethyl(1,2-dihydro- quinolyl))hexa-1,3,5-trienyl]amino}aminomethane-1- thione (57)	99
{{[(1 <i>E</i> ,3 <i>E</i>)-1-Aza-3-fluoro-4-(1,2,2,4-tetramethyl-(6-1,2-dihydro- quinolyl))buta-1,3-dienyl]amino}aminomethane-1-thione (58).....	100
{{[(1 <i>E</i> ,3 <i>E</i>)-1-Aza-4-(1,2,2,4-tetramethyl-(6-1,2-dihydroquinolyl))- buta-1,3-dienyl]amino}aminomethane-1-thione (59).....	101
Ethyl (2 <i>E</i> ,4 <i>E</i> ,6 <i>E</i>)-6-Fluoro-3-methyl-7-(2,2,4,4-tetramethyl- (3 <i>H</i> -benzo[3,4- <i>e</i>]thian-6-yl))octa-2,4,6-trienoate (60)	102
Ethyl (2 <i>E</i> ,4 <i>E</i> ,6 <i>E</i>)-6-Fluoro-3,8-dimethyl-7-(2,2,4,4-tetramethyl- (3 <i>H</i> -benzo[3,4- <i>e</i>]thian-6-yl))nona-2,4,6-trienoate (61)	103
Ethyl (2 <i>E</i> ,4 <i>E</i> ,6 <i>E</i>)-6-Fluoro-3,9-dimethyl-7-(2,2,4,4-tetramethyl- (3 <i>H</i> -benzo[3,4- <i>e</i>]thian-6-yl))deca-2,4,6-trienoate (62)	104
Ethyl (6 <i>Z</i> ,2 <i>E</i> ,4 <i>E</i>)-6-Fluoro-3-methyl-7-(2,2,4,4-tetramethyl- (3 <i>H</i> -benzo[3,4- <i>e</i>]thian-6-yl))octa-2,4,6-trienoate (63)	105
Ethyl (6 <i>Z</i> ,2 <i>E</i> ,4 <i>E</i>)-6-Fluoro-3,8-dimethyl-7-(2,2,4,4-tetramethyl- (3 <i>H</i> -benzo[3,4- <i>e</i>]thian-6-yl))nona-2,4,6-trienoate (64)	106
(2,2,4,4-Tetramethyl(3 <i>H</i> -benzo[3,4- <i>e</i>]thian-6-yl))ethyl-4- (methoxycarbonyl)benzoate (65)	107
2-Methyl-1-(2,2,4,4-tetramethyl(3 <i>H</i> -benzo[3,4- <i>e</i>]thian-6-yl))- propyl-4-(methoxycarbonyl)benzoate (66)	107

3-Methyl-1-(2,2,4,4-tetramethyl(3 <i>H</i> -benzo[3,4- <i>e</i>]thian-6-yl))- butyl-4-(methoxycarbonyl)benzoate (67)	108
{{(1 <i>E</i> ,3 <i>E</i>)-1-Aza-3-fluoro-4-(2,2,4,4,7-pentamethyl(3 <i>H</i> -benzo- [3,4- <i>e</i>]thian-6-yl))penta-1,3-dienyl}amino} aminomethane- 1-thione (68)	109
6-Methoxy-1,1,4,4-tetramethyl-5-nitroisochromane (70)	110
(6-Methoxy-1,1,4,4-tetramethylisochroman-5-yl)amine (71)	111
Ethyl (2 <i>E</i>)-3-(4,4-dimethylchroman-6-yl)-2-fluorobut-2-enoate (73)	111
Ethyl (2 <i>E</i>)-3-(4,4-dimethylchroman-6-yl)-2-fluorobut-2-en-1-ol (74)	112
Ethyl (2 <i>E</i>)-3-(4,4-dimethylchroman-6-yl)-2-fluoro-2-butenal (75)	113
1-(4,4-Dimethylchroman-6-yl)ethan-1-ol (76)	115
2,2,4-Trimethyl-1,2-dihydroquinoline (78)	115
1,2,2,4-Tetramethyl-1,2-dihydroquinoline (79)	115
Bis(2,2,2-trichloroethyl) Azodicarboxylate (81)	116
1,2,2,4-Tetramethyl-1,2-dihydroquinol-6-yl amine (82)	117
1,2,2,4-Tetramethyl-1,2-dihydroquinoline-6-carbaldehyde (83)	118
4-Methyl-6-(1,2,2,4-tetramethyl(1,2-dihydroquinolyl))-5,6- dihydropyran-2-one (84)	119
4-Methyl-6-(1,2,2,4-tetramethyl(1,2-dihydroquinolyl))-5,6- dihydropyran-2-ol (85)	120
(2 <i>Z</i> ,4 <i>E</i>)-3-Methyl-5-(1,2,2,4-tetramethyl(1,2-dihydroquinolyl))- penta 2,4-dienal (86)	120
Ethyl (2 <i>E</i>)-2-fluoro-3-(1,2,2,4-tetramethyl(6-1,2-dihydroquinolyl))- prop-2-enoate (87)	121
(2 <i>E</i>)-2-Fluoro-3-(1,2,2,4-tetramethyl(6-1,2-dihydroquinolyl))- prop-2-en-1-ol (88)	122
(2 <i>E</i>)-2-Fluoro-3-(1,2,2,4-tetramethyl(6-1,2-dihydroquinolyl))- prop-2-enal (89)	123
Ethyl (2 <i>E</i>)-3-(1,2,2,4-tetramethyl(6-1,2-dihydroquinolyl))prop- 2-enoate (90)	123
(2 <i>E</i>)-3-(1,2,2,4-Tetramethyl(6-1,2-dihydroquinolyl))prop- 2-en-1-ol (91)	124
(2 <i>E</i>)-3-(1,2,2,4-tetramethyl(6-1,2-dihydroquinolyl))prop- 2-enal (92)	125
1-(2,2,4,4-Tetramethyl-3 <i>H</i> benzo[<i>e</i>]thiane)ethan-1-one (94a)	126
2-Methyl-1-(2,2,4,4-tetramethyl(3 <i>H</i> -benzo[3,4- <i>e</i>]thian-6-yl))- propan-1-one (94b)	127
3-Methyl-1-(2,2,4,4-tetramethyl(3 <i>H</i> -benzo[3,4- <i>e</i>]thian-6-yl))- butan-1-one (94c)	127
Ethyl (2 <i>E</i>)-2-Fluoro-3-(2,2,4,4-tetramethyl(3 <i>H</i> -benzo[3,4- <i>e</i>]- thian-6-yl))but-2-enoate (95a)	129
Ethyl (2 <i>E</i>)-2-Fluoro-4-methyl-3-(2,2,4,4-tetramethyl(3 <i>H</i> -benzo- [3,4- <i>e</i>]thian-6-yl))pent-2-enoate (95b)	130

Chapter	Page
Ethyl (2 <i>E</i>)-2-Fluoro-4-methyl-3-(2,2,4,4-tetramethyl(3 <i>H</i> -benzo[3,4- <i>e</i>]thian-6-yl))pent-2-enoate (95c)	130
(2 <i>E</i>)-2-Fluoro-3-(2,2,4,4-tetramethyl(3 <i>H</i> -benzo[3,4- <i>e</i>]thian-6-yl))but-2-en-1-ol (96a) and (2 <i>Z</i>)-2-Fluoro-3-(2,2,4,4-tetramethyl(3 <i>H</i> -benzo[3,4- <i>e</i>]thian-6-yl))but-2-en-1-ol (98a)	131
(1 <i>E</i>)-1-Fluoro-4-methyl-3-(2,2,4,4-tetramethyl(3 <i>H</i> -benzo[3,4- <i>e</i>]thian-6-yl))pent-2-en-1-ol (96b) and (1 <i>Z</i>)-1-Fluoro-4-methyl-3-(2,2,4,4-tetramethyl(3 <i>H</i> -benzo[3,4- <i>e</i>]thian-6-yl))pent-2-en-1-ol (98b)	132
(1 <i>E</i>)-1-Fluoro-4-methyl-3-(2,2,4,4-tetramethyl(3 <i>H</i> -benzo[3,4- <i>e</i>]thian-6-yl))pent-2-en-1-ol (96c) and (1 <i>E</i>)-1-Fluoro-4-methyl-3-(2,2,4,4-tetramethyl(3 <i>H</i> -benzo[3,4- <i>e</i>]thian-6-yl))pent-2-en-1-ol (98c)	133
(2 <i>E</i>)-2-Fluoro-3-(2,2,4,4-tetramethyl(3 <i>H</i> -benzo[3,4- <i>e</i>]thian-6-yl))but-2-enal (97a)	135
(2 <i>E</i>)-2-Fluoro-4-methyl-3-(2,2,4,4-tetramethyl(3 <i>H</i> -benzo[3,4- <i>e</i>]thian-6-yl))pent-2-enal (97b)	135
(2 <i>E</i>)-2-Fluoro-4-methyl-3-(2,2,4,4-tetramethyl(3 <i>H</i> -benzo[3,4- <i>e</i>]thian-6-yl))pent-2-enal (97c)	136
(2 <i>Z</i>)-2-Fluoro-3-(2,2,4,4-tetramethyl(3 <i>H</i> -benzo[3,4- <i>e</i>]thian-6-yl))-but-2-enal (99a)	137
(2 <i>Z</i>)-2-Fluoro-4-methyl-3-(2,2,4,4-tetramethyl(3 <i>H</i> -benzo[3,4- <i>e</i>]thian-6-yl))pent-2-enal (99b)	137
2-Methyl-1-(2,2,4,4-tetramethyl(3 <i>H</i> -benzo[3,4- <i>e</i>]thian-6-yl))-ethan-1-ol (100a)	138
2-Methyl-1-(2,2,4,4-tetramethyl(3 <i>H</i> -benzo[3,4- <i>e</i>]thian-6-yl))-propan-1-ol (100b)	139
3-Methyl-1-(2,2,4,4-tetramethyl(3 <i>H</i> -benzo[3,4- <i>e</i>]thian-6-yl))-butan-1-ol (100c)	140
6-(1-Chloro-2-isobutyl)-2,2,4,4-tetramethyl-3 <i>H</i> -benzo[<i>e</i>]thione (101b)	141
1-(2,2,4,4,7-Pentamethyl-3 <i>H</i> benzo[<i>e</i>]thiane)ethan-1-one (103)	141
Ethyl (2 <i>E</i>)-2-Fluoro-3-(2,2,4,4,7-pentamethyl(3 <i>H</i> -benzo[3,4- <i>e</i>]thian-6-yl))but-2-enoate (104)	142
(2 <i>E</i>)-2-Fluoro-3-(2,2,4,4,7-pentamethyl(3 <i>H</i> -benzo[3,4- <i>e</i>]thian-6-yl))-but-2-en-1-ol (105)	143
(2 <i>E</i>)-2-Fluoro-3-(2,2,4,4,7-pentamethyl(3 <i>H</i> -benzo[3,4- <i>e</i>]thian-6-yl))-but-2-enal (106).....	144
BIBLIOGRAPHY	356

LIST OF TABLES

Tables	Page
I. The Collection of Endogenous Retinoids, Arotinoids, and Heteroarotinoids That Exhibit Some or Total Specificity for Isoforms of RAR or RXR.	25
II. Predicted EC ₅₀ Values For Compounds 48-68 in Activating Transcription of CV-1 Cell Line	47
III. NMR Analysis of $^4J_{\text{H-F}}^{19}$ Coupling In the <i>E/Z</i> Isomers	65
IV. EC ₅₀ Values and Efficacy Data For the Transactivation of Retinoic Acid Receptors by Compounds 107- 109	68
V. Data from Docking the Flexible Ligands into the Fixed Conformation of RAR γ LBD Crystallographic Structure	69
VI. Interaction Energies Between the Ligands and the LBP of RAR γ in the Flexible Ligand-Flexible Receptor Docking Mode	72
VII. Energies of Interaction from Docking Flexible Ligand Into Fixed LBP of RAR γ	85
VIII. The q ² and r ² values from PLS analysis	89

LIST OF FIGURES

Figures	Page
1. Schematic Representation of Mouse RAR Isoforms	5
2. Schematic representation of P-Box and D-Box	6
3. The crystallographic structure of RAR γ co-crystallized with <i>t</i> -RA (2)	7
4. Crystallographic structure of the ligand binding domain (LBD) of RXR α	10
5. Schematic representation of dietary retinoid metabolism	12
6. Crystallographic structure of RXR/THR heterodimer DNA binding domains bound to DNA	17
7. Schematic representation of RXR/RAR heterodimer interaction with DNA and transcriptional machinery of DNA	18
8. Schematic representation of reporter plasmid for measuring the transcriptional activity of RAR or RXR	31
9. Docking of heteroarotinoids 53 (A), 54 (B), and 55 (C) into the LBP of the crystallographic structure of RAR γ	42
10. Docking of flexible heteroarotinoid 48 (A) and 50 (B) into the rigid LBP of the crystallographic structure of RAR γ	51
11. Compounds 2 (A), 3 (B), 40 (C), 107 (D), 108 (E), and 109 (F) docked into the flexible LBP of RAR γ	73
12. The LBP conformation resulting from <i>t</i> -RA (2) docking superimposed upon conformations of the LBP which resulted from docking of 107 , 108 , 109 , and 3	74
13. Comparison of <i>t</i> -RA [(2), A] with 110 (B) and 9- <i>c</i> -RA [(3), C] with 111 (D)	80

Graph

	Page
1. Relative percentage of EC ₅₀ for compounds 2 and 45-65 When compared to pan-agonist 9- <i>c</i> -RA (3)	48
2. Percent inhibition of cancer growth in ovarian cancer cell lines by compounds 48-52	50
3. Percent of growth inhibition of cancerous vulvar cell lines SW954 and SW962	67

LIST OF PLATES

Plate	Page
I. IR Spectrum of 48	145
II. ^1H NMR Spectrum of 48	146
III. ^{13}C NMR Spectrum of 48	147
IV. IR Spectrum of 49	148
V. ^1H NMR Spectrum of 49	149
VI. ^{13}C NMR Spectrum of 49	150
VII. IR Spectrum of 50	151
VIII. ^1H NMR Spectrum of 50	152
IX. ^{13}C NMR Spectrum of 50	153
X. IR Spectrum of 51	154
XI. ^1H NMR Spectrum of 51	155
XII. ^{13}C NMR Spectrum of 51	156
XIII. ^{19}F NMR Spectrum of 51	157
XIV. IR Spectrum of 52	158
XV. ^1H NMR Spectrum of 52	159
XVI. ^{13}C NMR Spectrum of 52	160
XVII. IR Spectrum of 53	161

Plate	Page
XXVIII. ^1H NMR Spectrum of 53	162
XIX. ^{13}C NMR Spectrum of 53	163
XX. IR Spectrum of 54	164
XXI. ^1H NMR Spectrum of 54	165
XXII. ^{13}C NMR Spectrum of 54	166
XXIII. IR Spectrum of 55	167
XXIV. ^1H NMR Spectrum of 55	168
XXV. ^{13}C NMR Spectrum of 55	169
XXVI. IR Spectrum of 56	170
XXVII. ^1H NMR Spectrum of 56	171
XXVIII. ^{13}C NMR Spectrum of 56	172
XIX. 2D COSY NMR Spectrum of 56	173
XXX. 2D HETCOR NMR Spectrum of 56	174
XXXI. IR Spectrum of 57	175
XXXII. ^1H NMR Spectrum of 57	176
XXXIII. ^{13}C NMR Spectrum of 57	177
XXXIV. IR Spectrum of 58	178
XXXV. ^1H NMR Spectrum of 58	179
XXXVI. ^{13}C NMR Spectrum of 58	180
XXXVII. ^{19}F NMR Spectrum of 58	181
XXXVIII. IR Spectrum of 59	182
XXXIX. ^1H NMR Spectrum of 59	183

Plate	Page
XL. ^{13}C NMR Spectrum of 59	184
XLI. IR Spectrum of 60	185
XLII. ^1H NMR Spectrum of 60	186
XLIII. ^{13}C NMR Spectrum of 60	187
XLIV. ^{19}F NMR Spectrum of 60	188
XLV. IR Spectrum of 61	189
XLVI. ^1H NMR Spectrum of 61	190
XLVII. ^{13}C NMR Spectrum of 61	191
XLVIII. ^{19}F NMR Spectrum of 61	192
XLIX. IR Spectrum of 62	193
L. ^1H NMR Spectrum of 62	194
LI. ^{13}C NMR Spectrum of 62	195
LII. ^{19}F NMR Spectrum of 62	196
LIII. IR Spectrum of 63	197
LIV. ^1H NMR Spectrum of 63	198
LV. ^{13}C NMR Spectrum of 63	199
LVI. ^{19}F NMR Spectrum of 63	200
LVII. IR Spectrum of 64	201
LVIII. ^1H NMR Spectrum of 64	202
LIX. ^{13}C NMR Spectrum of 64	203
LX. ^{19}F NMR Spectrum of 64	204
LXI. IR Spectrum of 65	205

Plate	Page
LXII. ^1H NMR Spectrum of 65	206
LXIII. ^{13}C NMR Spectrum of 65	207
LXIV. IR Spectrum of 66	208
LXV. ^1H NMR Spectrum of 66	209
LXVI. ^{13}C NMR Spectrum of 66	210
LXVII. IR Spectrum of 67	211
LXVIII. ^1H NMR Spectrum of 67	212
LXIX. ^{13}C NMR Spectrum of 67	213
LXX. IR Spectrum of 68	214
LXXI. ^1H NMR Spectrum of 68	215
LXXII. ^{13}C NMR Spectrum of 68	216
LXXIII. ^{19}F NMR Spectrum of 68	217
LXXIV. IR Spectrum of 70	218
LXXV. ^1H NMR Spectrum of 70	219
LXXVI. ^{13}C NMR Spectrum of 70	220
LXXVII. IR Spectrum of 71	221
LXXVIII. ^1H NMR Spectrum of 71	222
LXXIX. ^{13}C NMR Spectrum of 71	223
LXXX. IR Spectrum of 73	224
LXXXI. ^1H NMR Spectrum of 73	225
LXXXII. ^{13}C NMR Spectrum of 73	226
LXXXIII. ^{19}F NMR Spectrum of 73	227

Plate	Page
LXXXIV. IR Spectrum of 74	228
LXXXV. ¹ H NMR Spectrum of 74	229
LXXXVI. ¹³ C NMR Spectrum of 74	230
LXXXVII. ¹⁹ F NMR Spectrum of 74	231
LXXXVIII. IR Spectrum of 76	232
LXXXIX. ¹ H NMR Spectrum of 76	233
XC. ¹³ C NMR Spectrum of 76	234
XCI. IR Spectrum of 73	235
XCII. ¹ H NMR Spectrum of 73	236
XCIII. ¹³ C NMR Spectrum of 73	237
XCIV. IR Spectrum of 79	238
XCV. ¹ H NMR Spectrum of 79	239
XCVI. ¹³ C NMR Spectrum of 79	240
XCVII. IR Spectrum of 81	241
XCVIII. ¹ H NMR Spectrum of 81	242
XCIX. ¹³ C NMR Spectrum of 81	243
C. IR Spectrum of 82	244
CI. ¹ H NMR Spectrum of 82	245
CII. ¹³ C NMR Spectrum of 82	246
CIII. IR Spectrum of 83	247
CIV. ¹ H NMR Spectrum of 83	248
CV. ¹³ C NMR Spectrum of 83	249

Plate	Page
CVI. IR Spectrum of 84	250
CVII. ¹ H NMR Spectrum of 84	251
CVIII. ¹³ C NMR Spectrum of 84	252
CIX. IR Spectrum of 85	253
CX. ¹ H NMR Spectrum of 85	254
CXI. ¹³ C NMR Spectrum of 85	255
CXII. IR Spectrum of 86	256
CXIII. ¹ H NMR Spectrum of 86	257
CXIV. ¹³ C NMR Spectrum of 86	258
CXV. IR Spectrum of 87	259
CXVI. ¹ H NMR Spectrum of 87	260
CXVII. ¹³ C NMR Spectrum of 87	261
CXVIII. IR Spectrum of 88	262
CXIX. ¹ H NMR Spectrum of 88	263
CXX. ¹³ C NMR Spectrum of 88	264
CXXI. ¹⁹ F NMR Spectrum of 88	265
CXXII. IR Spectrum of 89	266
CXXIII. ¹ H NMR Spectrum of 89	267
CXXIV. ¹³ C NMR Spectrum of 89	268
CXXV. ¹⁹ F NMR Spectrum of 89	269
CXXVI. IR Spectrum of 90	270
CXXVII. ¹ H NMR Spectrum of 90	271

Plate	Page
CXXVIII. ¹³ C NMR Spectrum of 90	272
CXXIX. IR Spectrum of 91	273
CXXX. ¹ H NMR Spectrum of 91	274
CXXXI. ¹³ C NMR Spectrum of 91	275
CXXXII. IR Spectrum of 92	276
CXXXIII. ¹ H NMR Spectrum of 92	277
CXXXIV. ¹³ C NMR Spectrum of 92	278
CXXXV. IR Spectrum of 94a	279
CXXXVI. ¹ H NMR Spectrum of 94a	280
CXXXVII. ¹³ C NMR Spectrum of 94a	281
CXXXVIII. IR Spectrum of 94b	282
CXXXIX. ¹ H NMR Spectrum of 94b	283
CXL. ¹³ C NMR Spectrum of 94b	284
CXLI. IR Spectrum of 94c	285
CXLII. ¹ H NMR Spectrum of 94c	286
CXLIII. ¹³ C NMR Spectrum of 94c	288
CXLIV. IR Spectrum of 95a	289
CXLV. ¹ H NMR Spectrum of 95a	290
CXLVII. ¹⁹ F NMR Spectrum of 95a	291
CXLVIII. IR Spectrum of 96a	292
CXLIX. ¹ H NMR Spectrum of 96a	293
CL. ¹³ C NMR Spectrum of 96a	294

Plate	Page
CLI. ¹⁹ F NMR Spectrum of 96a	295
CLII. IR Spectrum of 96b	296
CLIII. ¹ H NMR Spectrum of 96b	297
CLIV. ¹³ C NMR Spectrum of 96b	298
CLV. ¹⁹ F NMR Spectrum of 96b	299
CLVI. IR Spectrum of 96c	300
CLVII. ¹ H NMR Spectrum of 96c	301
CLVIII. ¹³ C NMR Spectrum of 96c	302
CLIX. ¹⁹ F NMR Spectrum of 96c	303
CLX. IR Spectrum of 97a	304
CLXI. ¹ H NMR Spectrum of 97a	305
CLXII. ¹³ C NMR Spectrum of 97a	306
CLXIII. ¹⁹ F NMR Spectrum of 97a	307
CLXIV. IR Spectrum of 97b	308
CLXV. ¹ H NMR Spectrum of 97b	309
CLXVI. ¹³ C NMR Spectrum of 97b	310
CLXVII. ¹⁹ F NMR Spectrum of 97b	311
CLXVIII. IR Spectrum of 97c	312
CLXIX. ¹ H NMR Spectrum of 97c	313
CLXX. ¹³ C NMR Spectrum of 97c	314
CLXXI. ¹⁹ F NMR Spectrum of 97c	315
CLXXII. IR Spectrum of 98a	316

Plate	Page
CLXXIII. ¹ H NMR Spectrum of 98a	317
CLXXIV. ¹³ C NMR Spectrum of 98a	318
CLXXV. ¹⁹ F NMR Spectrum of 98a	319
CLXXVI. IR Spectrum of 98b	320
CLXXVII. ¹ H NMR Spectrum of 98b	321
CLXXVIII. ¹³ C NMR Spectrum of 98b	322
CLXXIX. ¹⁹ F NMR Spectrum of 98b	323
CLXXX. ¹ H NMR Spectrum of 98c	324
CLXXXI. ¹³ C NMR Spectrum of 98c	325
CLXXXII. ¹⁹ F NMR Spectrum of 98c	326
CLXXXIII. ¹ H NMR Spectrum of 99a	327
CLXXXIV. ¹³ C NMR Spectrum of 99a	328
CLXXXV. ¹⁹ F NMR Spectrum of 99a	329
CLXXXVI. IR Spectrum of 100a	330
CLXXXVII. ¹ H NMR Spectrum of 100a	331
CLXXXVIII. ¹³ C NMR Spectrum of 100a	332
CLXXXIX. IR Spectrum of 100b	333
CXC. ¹ H NMR Spectrum of 100b	334
CXCI. ¹³ C NMR Spectrum of 100b	335
CXCII. IR Spectrum of 100c	336
CXCIII. ¹ H NMR Spectrum of 100c	337
CXCIV. ¹³ C NMR Spectrum of 100c	338

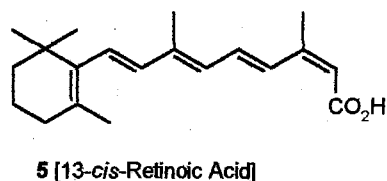
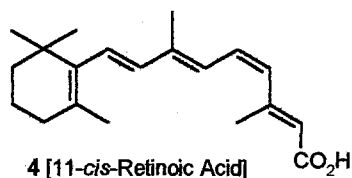
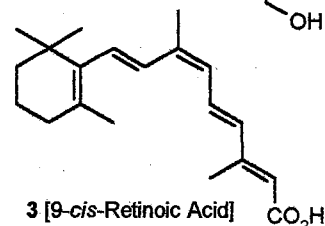
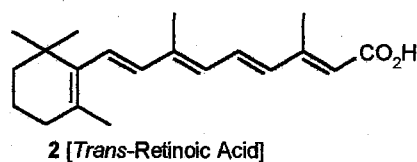
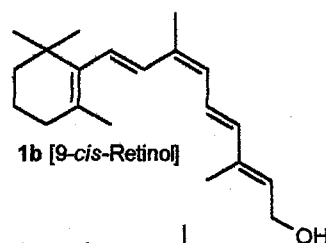
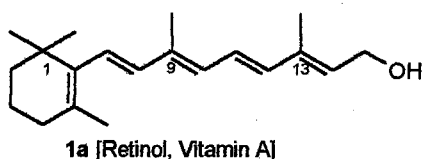
Plate	Page
CXCV. IR Spectrum of 101b	339
CXCVI. ¹ H NMR Spectrum of 101b	340
CXCVII. ¹³ C NMR Spectrum of 101b	341
CXCVIII. IR Spectrum of 103	342
CXCIX. ¹ H NMR Spectrum of 103	343
CC. ¹³ C NMR Spectrum of 103	344
CCI. ¹ H NMR Spectrum of 104	345
CCII. ¹³ C NMR Spectrum of 104	346
CCIII. ¹⁹ F NMR Spectrum of 104	347
CCIV. IR Spectrum of 105	348
CCV. ¹ H NMR Spectrum of 105	349
CCVI. ¹³ C NMR Spectrum of 105	350
CCVII. ¹⁹ F NMR Spectrum of 105	351
CCVIII. IR Spectrum of 106	352
CCIX. ¹ H NMR Spectrum of 106	353
CCX. ¹³ C NMR Spectrum of 106	354
CCXI. ¹⁹ F NMR Spectrum of 106	355

CHAPTER I

HISTORICAL

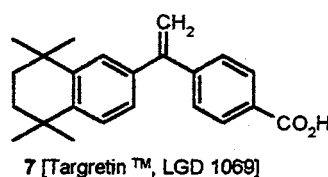
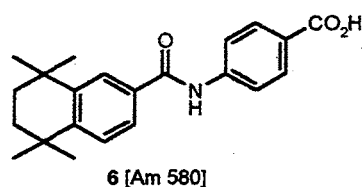
Introduction

The retinoids are a group of compounds that can be defined as molecules (natural or synthetic) that are structurally similar to retinol (**1a**, vitamin A), 9-*cis*-retinol (**1b**), 11-*cis*-retinol, and 13-*cis*-retinol (see discussion on retinoid metabolism) and can elicit specific biological responses via binding to a specific receptor or set of receptors.¹²² A natural retinoid molecule consists of four isoprenoid units [$\text{H}_2\text{C}=\text{C}(\text{CH}_3)\text{CH}=\text{CH}_2$] joined in a head-to-tail manner and can be divided into three parts, namely a trimethylated cyclohexene ring, a conjugated tetraene side chain, and a polar carboxylic acid end group. All-*trans*-retinoic acid (**2**, *t*-RA), 9-*cis*-retinoic acid (**3**, 9-*c*-RA), 11-*cis*-retinoic acid (**4**, 11-*c*-RA), and 13-*cis*-retinoic acid (**5**, 13-*c*-RA) are some of the examples of naturally occurring retinoids.¹²²

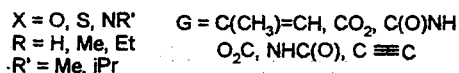
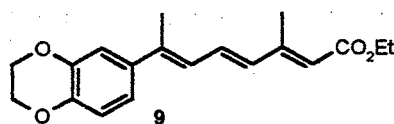
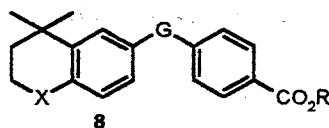


Molecular modifications of natural retinoids has led to a wide variety of synthetic retinoids including arotinoids (molecules that have at least one aryl group in their basic structure), such as Am-580 (**6**)⁵⁵ and Targretin (**7**, LGD 1069),¹² and heteroarotinoids (molecules with at least one aryl moiety and a heteroatom in a fused ring) such as **8**⁹ and **9**.⁸ Many others are known.¹²²

AROTINOIDS



HETEROAROTINOIDS



Experimentally, the role of vitamin A in regulating the epithelial cell differentiation and maintenance was first demonstrated by Wolbach and Howe.¹³⁵ They showed that feeding animals a diet deficient in vitamin A resulted in the appearance of hyperkeratinization, squamous metaplasia, and gross tumors in a variety of epithelial tissues in the experimental animals. This process resembled the induction of tumors by certain chemical carcinogens.⁴⁵ Since carcinogen-induced metaplasia appeared similar to that resulting from vitamin A deficiency, attempts have been made to study the effects of retinoids on the inhibition of induction and progression of cancer in various organ tissues

including pancreas, esophagus, lung, stomach, intestine, liver, urinary bladder, nervous system, mammary gland, and skin.⁶⁰ Clinically, retinoids are useful for the treatment of skin disorders,¹¹⁹ in the inhibition of early stages of tumor progression,¹³⁶ and are also being investigated in several other therapeutic areas including arthritis,¹³² dyslipidimias,¹¹⁵ and with prevention of HIV-induced lymphopenia.¹³⁸ The ability of retinoids to regulate proliferation and differentiation in both normal and malignant cells *in vitro* and *in vivo* presents the opportunity for the use of retinoids in the treatment of a variety disorders.

Nuclear Receptors for Natural and Synthetic Retinoids

The identification of cellular retinol and retinoic acid-binding proteins (CRBP and CRABP, respectively) led to the proposal that such retinoids might represent a specific intracellular receptor system.⁸⁵ However, despite extensive biochemical research, no evidence has been presented to establish a decisive role of CRBP and CRABP as direct mediators of retinoid action on transcription.⁸⁵ In late 1987, two independent groups were studying the steroid hormone receptors and discovered the novel nuclear receptors for retinoids, that is, retinoic acid receptor (RAR) and retinoid X receptor (RXR).^{48,106} This discovery not only offered an opportunity to analyze in detail the structure of the two members of the nuclear receptors but it also provided the necessary tools to study the influence of retinoids on the developmental control of genes and cell differentiation.

Retinoic Acid Receptors (RARs)

The first isoform of the RAR family of nuclear receptors to be discovered was RAR α , a polypeptide composed of 462 amino acid residues.⁴⁸ However, there was evidence that RAR α was not the only nuclear receptor responsible for transduction of the retinoid signal. The discoveries of the several loci present in the human genome related to the

RAR α and the family of RAR α -related genes, together with a close resemblance of gene product to that of RAR α , led to new evidence that another isotype of RAR family receptors existed.⁹² The newly discovered, putative receptor has also been shown to respond to retinoic acid and was named RAR β .⁵ In 1989, while attempting to clone the mouse homologs of RAR α and RAR β , Chambon and colleagues discovered the third isotype of RARs and named it RAR γ .²¹ In addition to finding three different isotypes of the RAR family, each of the isotypes has different functional isoforms that are distinguished from each other in the number of amino acids that make up the amino terminus domain.^{72,81,142} Thus, the RAR α isotype has isoforms RAR α_1 and RAR α_2 ,⁸¹ RAR β has four isoforms RAR β_1 , RAR β_2 , RAR β_3 , and RAR β_4 ,¹⁴² and RAR γ isotype has isoforms RAR γ_1 and RAR γ_2 .⁷² Each isoform of the RAR can be divided into five domains:

- ligand-independent-activation function (AF-1) (domain A/B),
- DNA binding domain (DBD) (domain C),
- hinge (domain D),
- ligand binding domain (LBD) (domain E) which incorporates the ligand dependent-activation function (AF-2),
- and the functionally undefined C-terminus (F domain).³³

The A/B domain, located at the amino terminus of the polypeptide chain, is rich in proline, serine, and threonine which are non-acidic amino acid residues. The A/B domain of RARs belongs to a distinct class of transcriptional regulators.⁹⁷ The sequence and number of amino acid residues of the A/B domain vary from one isoform of RAR to another. It is one of the lowest conserved regions of the receptor (see Figure 1).³³ The central core of the RAR receptor contains the DNA-binding region (domain C), which is responsible for the

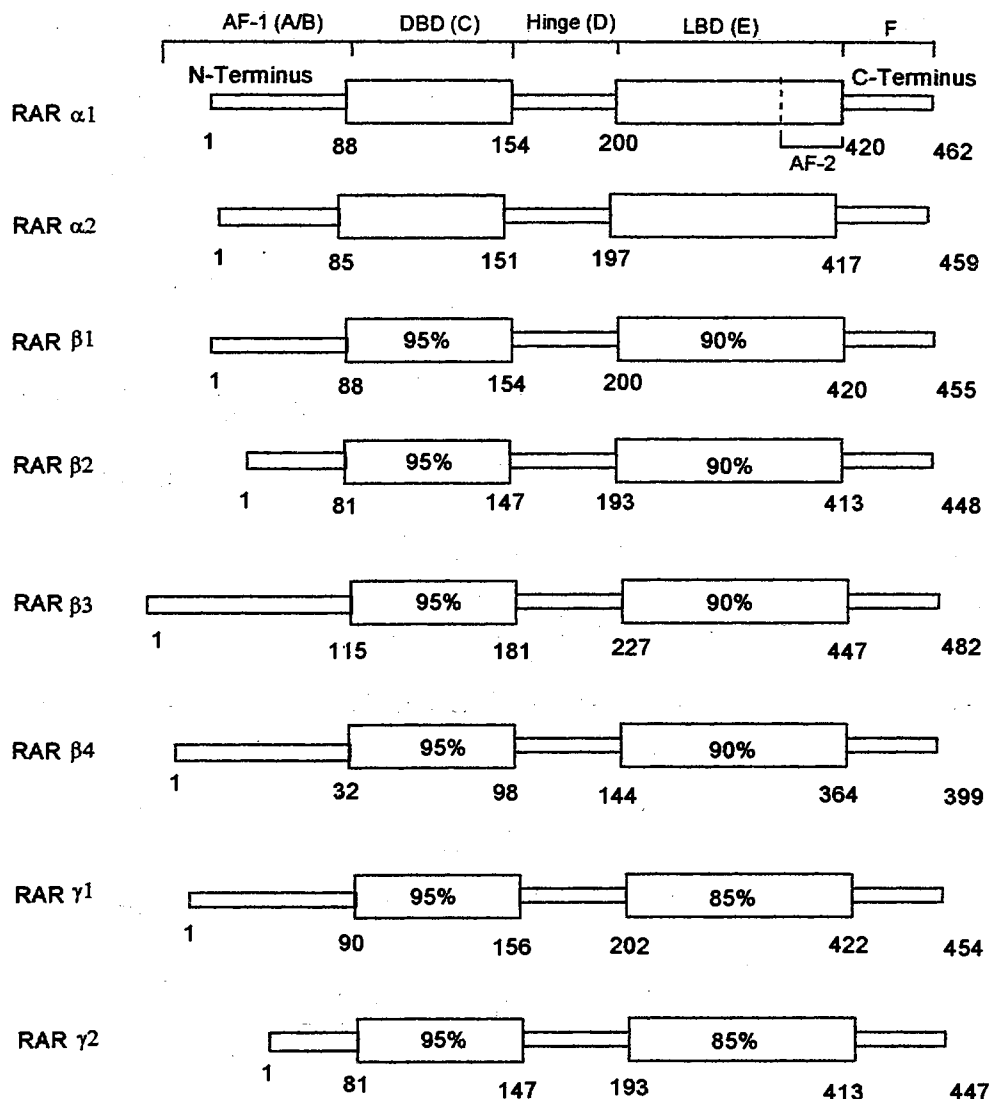


Figure 1. Schematic representation of mouse RAR isoforms. The highly conserved DNA- and ligand-binding domains are represented by large open boxes, and less conserved regions are represented by thin open boxes. The numbers within larger boxes are the percent amino acid identity when compared to RAR α . The numbers below the boxes represent domains as well as total length (last number) of the receptor in the terms of amino acid residues.^{72,81,142}

recognition of a DNA sequence, the so called hormone response element [HRE, in the case of retinoids is the retinoic acid response element (RARE)].⁴³ This domain consists of two

motifs known as the ‘zinc finger’³² and the ‘zinc twist’ (Figure 2).¹³¹ The three amino acid residues, which are different among all isoforms of RAR isotypes, are located at the P-box

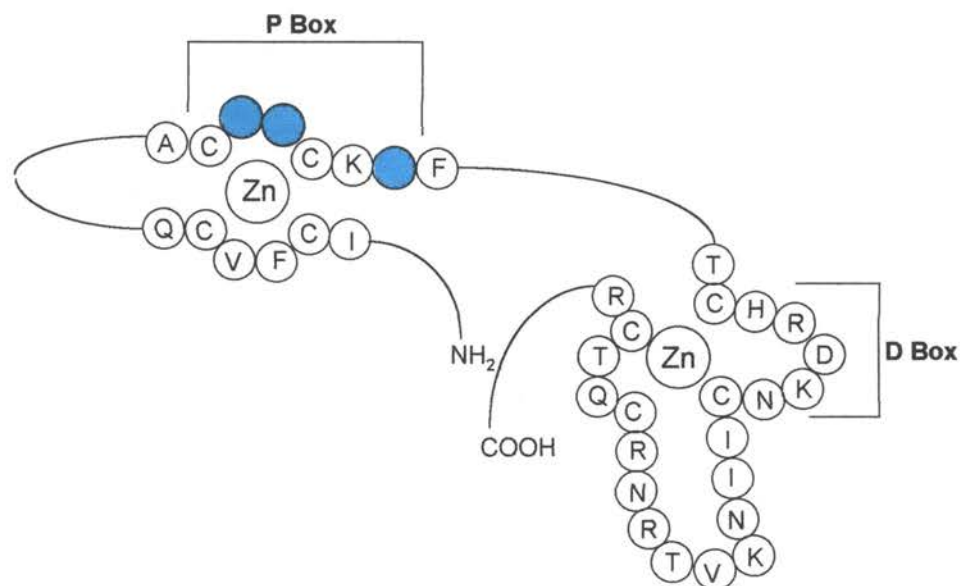


Figure 2. Schematic representation of P-Box and D-Box. The colored circles represent the amino acids responsible for specificity of binding to RARE.¹³¹

(‘zinc finger’) and are responsible for the recognition and specificity of binding of RAR to the RARE⁵⁰ by insertion and making contact within the major groove of the DNA double helix.¹²⁸ The D-box [‘zinc twist’] is required for the recognition of half-site spacing of RARE¹³⁰ and the formation of homo- or heterodimers with another nuclear receptor.⁵⁴ The ligand binding domain (LBD) of RAR is complex and fulfills multiple functions.⁴⁶ The LBD spans approximately 220 amino acid residues at the C-terminus of the receptor.³³ The degree of similarity of the LBD between RAR isoforms is about 85-95%, which suggests a different affinity for binding of the natural ligands *t*-RA (2) and 9-*c*-RA (3) to the RAR.

The crystal structure of the human LBD of RAR γ_2 bound to *t*-RA (holo-LBD) has been determined by Renaud and co-workers (Figure 3).¹⁴ The LBD is composed of 229 amino acid residues which make up 9 α -helical structures (H1 to H12), two Ω (omega) loops, and two β -sheets. The numbering system was adopted from the crystal structure of apo-RXR α ,¹⁵ and the α -helices were numbered according to the resemblance and in comparison to RXR α , but not sequentially. For example, helices H2, H5 and H11 were omitted from the holo-LBD of the RAR γ crystallographic structure because their helices do not exist after the receptor is bound to a ligand.¹⁴ The nine α -helices remaining were organized into a three-layered structure with H4, H6, H8, and H9 positioned between H1 and H3 on one side and H7, H10, and H11 on the other.¹⁴

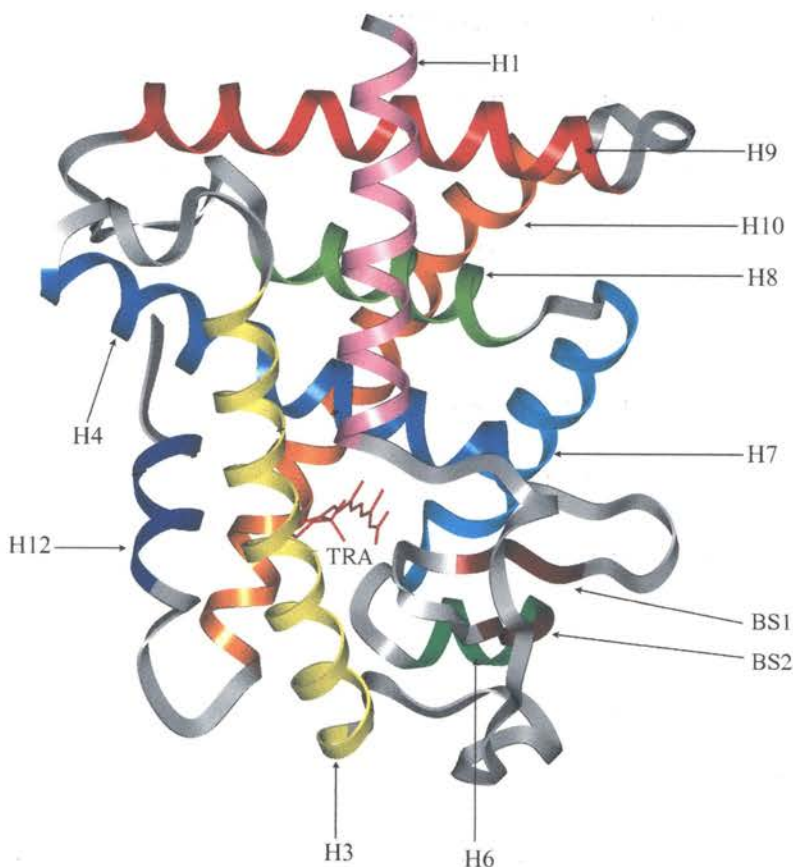


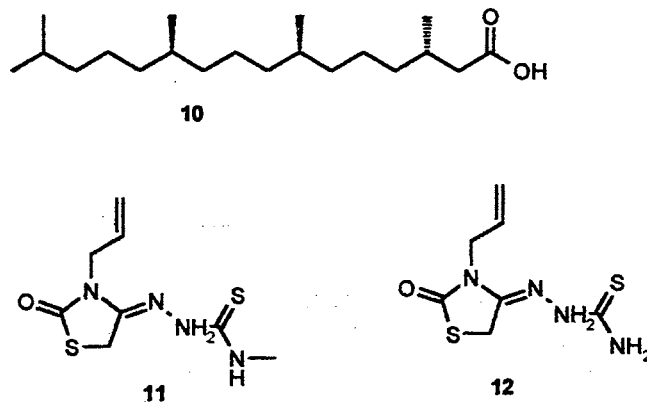
Figure 3. The crystallographic structure of RAR γ co-crystallized with *t*-RA [(2), TRA].¹⁴

Two topologically conserved β -strands (BS1 and BS2) form the β -turn inserted between loop 1-3 (connecting H1 and H3) and H3.¹⁴ Twenty four amino acid residues of the LBD, which include Phe 201, Thr 227, Phe 230, Ser 231, Leu 233, Ala 234, Lys 236, Cys 237, Leu271, Met 272, Arg 274, Ile 275, Arg 278, Phe 288, Ser 289, Gly 303, Phe 304, Ala 394, Arg 396, Ala 397, Leu 400, Met408, Ile 412, and Met 415, make up the ligand-binding pocket (LBP).¹⁴ The ligand-dependent activation-function 2 (AF-2) is located at the carbonyl terminus of the ligand binding domain (α -helix H12).⁷⁹ In addition to the two functionally important regions of the LBD (LBP, AF-2), the structural motif spanned by the amino terminus of α -helix H7, the amino terminus of H10, the loop between α -helices H9 and H10, and the carboxyl terminus of H9 provides a dimerization surface for the formation of homo- or heterodimers with other nuclear receptors including vitamin D₃, thyroid hormone receptor, RXR, and others.³⁵ This dimerization domain has features in common with both the leucine zipper and helix-loop-helix motif which has been proposed as the dimerization structure in other DNA binding proteins.⁴⁰

Retinoic Acid X Receptors (RXR)

The studies of orphan nuclear receptors led to the discovery of a novel retinoic acid-responsive receptor with the same type of domain composition (domains A to F) as RAR and referred to as retinoid X receptor (RXR).⁸⁸ The family of RXR consists of three different isotypes, RXR α , RXR β , and RXR γ , with sequence alignment homologies for DBDs of 92% and 95% and LBDs of 86% and 89% for RXR β and RXR γ , respectively, as compared to RXR α .⁹⁰ Each isotype of the RXR family also has two isoforms, namely RXR $\alpha_{1,2}$, RXR $\beta_{1,2}$, and RXR $\gamma_{1,2}$.⁹⁰ Because of the low degree of homologies between RXR α and RAR α over the entire length of the protein sequence, 27% for LBDs, and 61% for DBDs

(the highest),⁵³ it was discovered that 9-*c*-RA (3) was a natural activating ligand for the RXR family.⁵⁷ However, the 9-*c*-RA (3) can also activate RARs with equal potency,⁹ which suggests that a more specific RXR ligand may exist. There is some evidence that phytanic acid (10) binds to RXR α , promotes the formation of the RXR/RAR response element



complex, and induces RXR α conformational changes similar to that induced by 9-*c*-RA (3).⁸⁰

The crystallographic structure of the LBD of RXR α (apo-LBD, not ligand bound to LBD-RXR α) has been elucidated by Bourguet and co-workers (Figure 4).¹⁵ The LBD topology of RXR α can best be described as an antiparallel, α -helical sandwich with the dimension of 38 x 74 x 25 Å organized into a three-layered structure.¹⁵ The α -helices H4, H5, H8, H9, and the N-terminus of H11 are sandwiched between H1, H2, and H3 on one side and H6, H7, and H10 on the other.¹⁵ Two short β -strands (BS1 and BS2), forming a β -hairpin, are the only β -structures of the domain.¹⁵ The LBD of RXR α also has a dimerization surface (α -helices H10, H5, and H8), the C-terminal activation domain AF-2 (amino acid residues sequence 450-FLMEMLE-458), and two proposed locations of the ligand binding pocket.¹⁵ The letters in the 450-FLMEMLE-458 represent various amino acids.

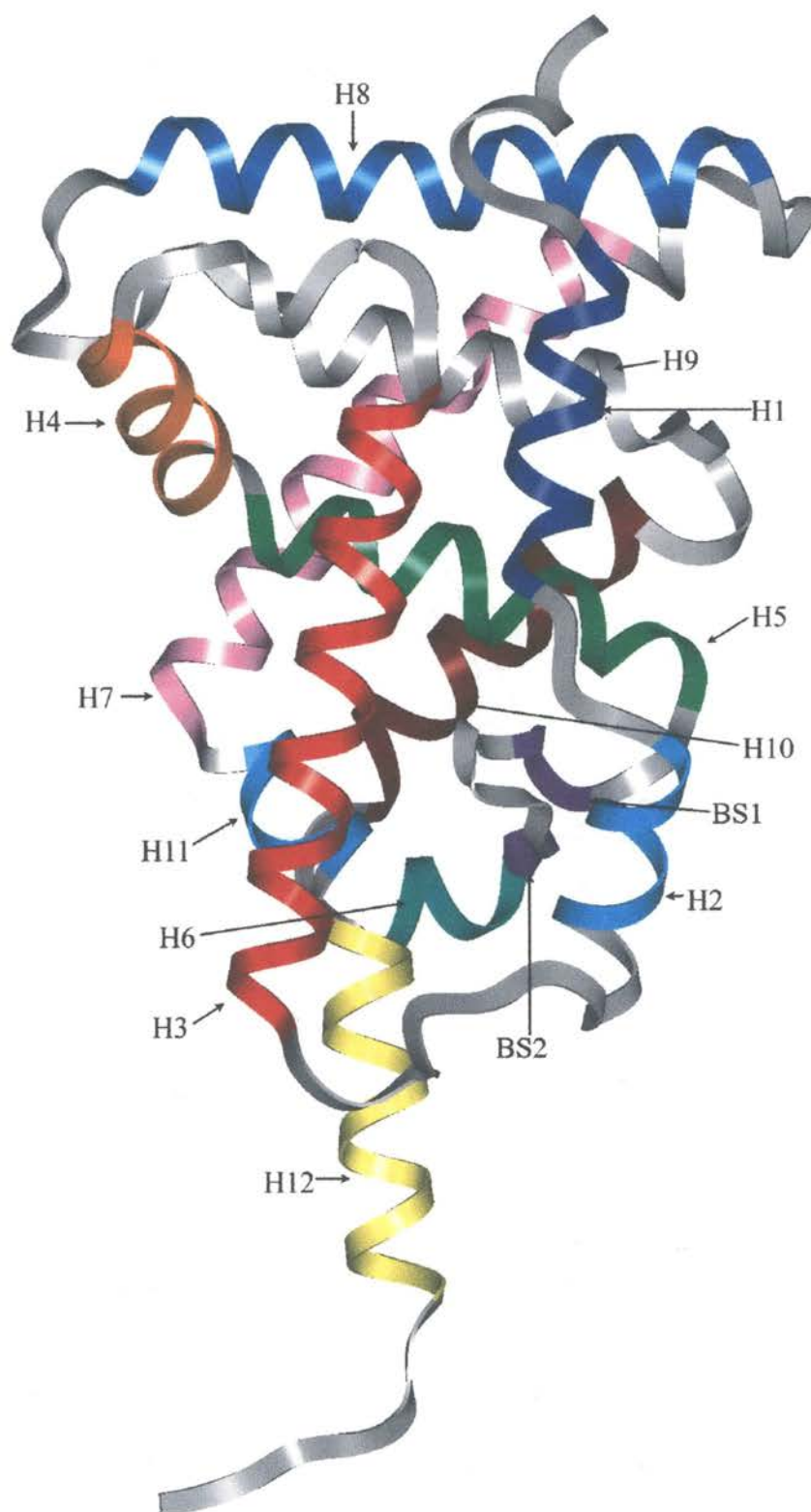
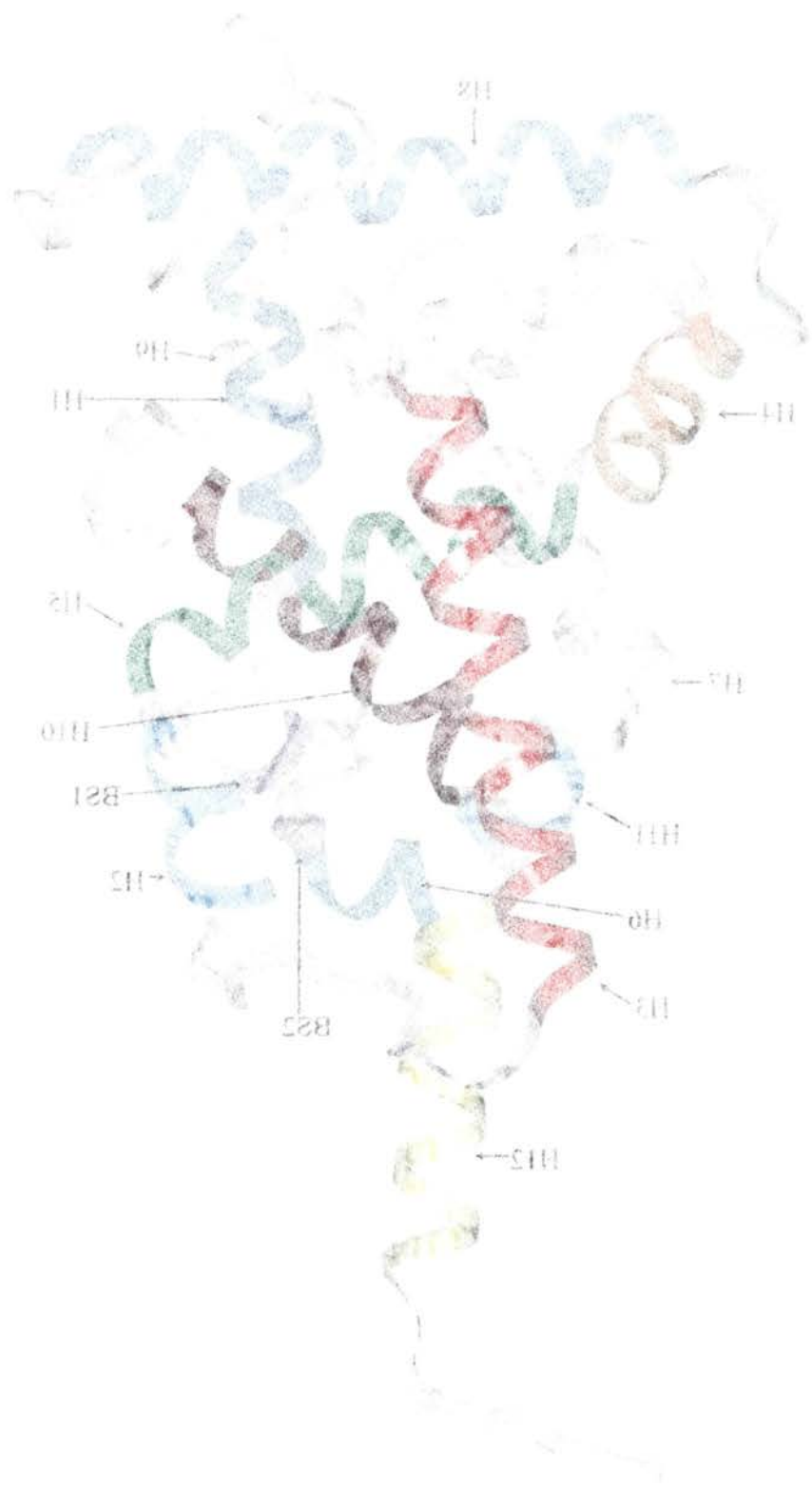


Figure 4. Crystallographic structure of the ligand binding domain (LBD) of RXR α .¹⁵



Retinoic Acid Z Receptor (RZR)

The RZR, whose name was proposed arbitrarily by its discoverer Carlberg and co-workers,³ is a member of the orphan receptors and exhibits a highly restricted brain-specific expression pattern.⁵¹ However, no natural ligand to activate this receptor has been identified, and the role and the function of RZR has yet to be determined.³ Due to a high expression of RZR in the pineal, thalamus, and hypothalamus glands, it has been suggested that RZR is important for physiological and developmental regulation of the central nervous system and for regulation of the circadian rhythm.⁴ Melatonin was suggested as a natural ligand for RZR, but more studies are needed to substantiate this claim.^{3,51} The thiazolidine diones 11 and 12, which are synthetic moieties, have proven to be RZR specific ligands and induce potent RZR antiarthritic activity.⁹⁶

Distribution of the Retinoic Acid Receptors in Major Organ Tissues

A broad spectrum of biological activities are effected by retinoids, which suggests that these receptors play a unique role in mammalian development and homeostasis. The RAR α isotype is highly concentrated in brain tissue, specifically in the hippocampus and cerebellum, suggesting importance in the development and maintenance of the central nervous system.⁹² High levels of RAR β expression genes were found in the kidney, prostate, spinal cord, cerebral cortex, and pituitary gland, with average levels detected in the liver, spleen, uterus, ovary, brain, and testes.⁴ The RAR γ form was found in high levels in skin,⁹⁸ lung, and urogenital tissue,⁶⁶ as well as in average levels in cardiovascular tissue.⁶³ The RXR isoforms are widely distributed and display both unique and combinatorial patterns of regulating transcription.⁸⁹ The RXR α is abundant in visceral tissues such as the liver,

spleen, kidney, lung, and muscle.⁶⁶ The $RXR\beta$ is expressed in various levels in all tissues, and $RXR\gamma$ predominates in liver, kidney, lung, brain, retina, and adrenal tissues.^{61,98,116,118}

Metabolism of Retinoids and the Mechanism of Action for Retinoids and Retinoic Acid Receptors

The retinoids exert a variety of activities on the functions of numerous biological systems (Figure 5).³¹ Metabolism of dietary β -carotene or hydrolysis of dietary retinyl esters produces the parent and major circulating, natural occurring retinol which has no known biological activity but rather serves as a parent substrate for the biosynthesis of functional retinoids.^{17,18} β -Carotene is metabolized in the small intestine to retinal which then binds to a cellular retinol-binding protein (CRBP), which, in turn, protects the retinal from oxidizing

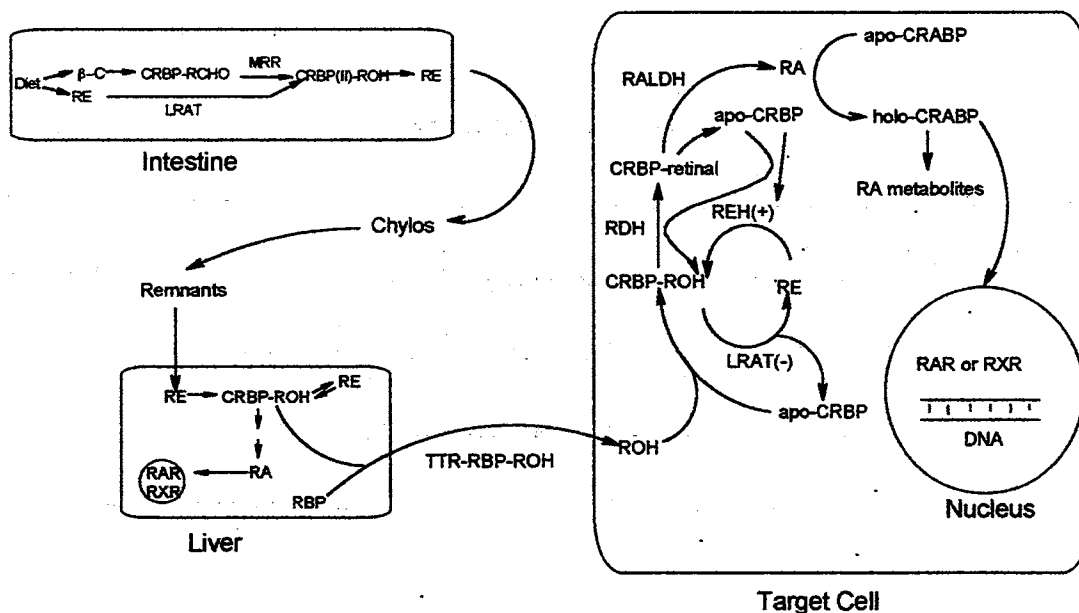


Figure 5. Schematic representation of dietary retinoid metabolism.^{2,11,13,65,82,108,109}

to retinoic acid.⁶⁵ However, retinal is reduced to retinol by microsomal retinal reductase.⁶⁵

Retinol produced from the hydrolysis of retinyl esters also complexes with CRBP and serves

as a reserve for the production of retinyl ester in a reverse reaction catalyzed by the enzyme lecithin:retinol acyltransferase (LRAT).⁸⁶ The retinyl esters are then packaged into chylomicrones with triacylglycerides and other fat-soluble vitamins and then are secreted into the lymph system.¹¹ Triacylglycerides are then removed from the chylomicrones by lipoprotein lipase, and the retinyl esters remain with chylomicrone remnants.⁶⁵ The retinyl esters are delivered to hepatic parenchyma cells of the liver where they are stored for future use or hydrolyzed back to retinol.⁶⁵ Retinol is then bound to a retinol binding protein (RBP), which protects it from oxidation and isomerization, and is secreted into the plasma where the RBP-ROH further complexes with transthyretin (TTR, a plasma transport protein), thus protecting retinol from degradation in the kidney.⁶⁵ Retinol palmitate constitutes 95% of stored retinyl ester in the liver.¹²²

The precise mechanism of the uptake of retinol by a target cell is not known, but, there is some evidence for the existence of RBP receptors in the cell membrane.² Once inside the cell, retinol is bound by an apo-cellular retinoid-binding protein (apo-CRBP, different from mucosal CRBP II in the small intestine), specific for retinol and retinal only, and a holo-CRBP-retinol complex is formed.⁸² The concentration ratio of holo-RBP/apo-RBP controls the conversion of retinol to either retinoic acid or to a cellular retinyl ester via the inhibition of enzymes LRAT by apo-CRBP and the subsequent activation of retinyl ester hydrolase (REH).^{13,56} The holo-CRBP also serves as a substrate for microsomal retinol dehydrogenase (RDH) which oxidizes the retinol to retinaldehyde that remains bound to the CRBP, although with lesser affinity.¹⁰⁸ It is assumed that the CRBP also mediates the transfer of retinal from RDH to the retinal dehydrogenase (RALDH) which converts retinal to retinoic acid.¹⁰⁹ The newly formed retinoic acid is then bound with cellular apo-retinoic

acid-binding protein (apo-CRABP), resulting in holo-CRABP, and this complex plays a major role in retinoic acid metabolism and delivery to the nucleus of the cell.^{16,103} Retinoic acid is metabolized oxidatively through dehydrogenation resulting in the formation of 4-oxo-retinoic acid or 18-hydroxyretinoic acid, which then undergoes further metabolism.³⁶ There is no evidence that 9-*cis*-RA (3), 11-*cis*-RA (4), or 13-*cis*-RA (5) are enzymatically isomerized from all-*trans*-retinoic acid,¹⁰¹ with an exception of a proposal made by Hyaman and co-workers⁵⁷ that *t*-RA (2) may be isomerized to the 9-*c*-RA (3) in certain cells. The 9-*cis*-RA (3) originates from dietary 9-*cis* retinol (1b) or from the conversion of all-*trans*-retinyl esters, as in the case of 11- and 13-*cis*-retinol.¹²³

The isomeric retinoic acids transported to the nucleus dissociate from CRABP and bind to one of the retinoic acid receptors [with *t*-RA (2) as the agonist, binding is restricted only to RAR isoforms, and 9-*c*-RA (3) as a pan-agonist binds to both RAR and RXR].^{20,83} In unbound RARs or RXRs, helix H12 of the LBD points away from the core of the LBD.^{14,15} This creates an opening for the retinoic acids to enter the ligand binding pocket (LBP) of the ligand binding domain (LBD).¹⁴ The carboxylic end of the retinoic acids enters first by means of being drawn into the LBP via an electrostatic field gradient induced by basic amino acid residues in the LBP. These acids are then locked in this position through hydrophobic interactions induced by a bend of the α -helix H11 which creates a continuous loop between H10 and H12.¹⁴ Helix H12 then covers and traps the ligand in the LBP by the formation of a salt bridge [CO₂⁻...H-N⁺H₂] between the glutamic residues of AF-2 (part of H12) and lysine residues in H4.¹⁴ After binding of the ligand (retinoic acid or a synthetic retinoid which have agonistic effects), the receptors, which exist as tetramers²⁰ in the nucleus in the absence of a ligand, dissociate into monomers. This prompts dramatic conformational changes

throughout the LBD region and directs the receptor toward the formation of homo- or heterodimers via the D-box (located in DBD, Figure 2) and the newly formed dimerization surfaces at the LBD.^{14,35,67,95,130} In addition to the dimer formation, the agonist-induced conformational change in the AF-2 domain (carboxyl-terminal of LBD, Figure 1) causes it to bind to and form complexes with transcriptional intermediary factors (TIF) such as estrogen receptor associating protein 160 (ERAP 160),⁵² receptor interacting protein 140 (RIP 140),²⁷ TIF 1,^{26,75} unidentified protein profile/thyroid hormone receptor interacting protein 1 (SUG1/TRIP1),⁷⁸ and the transcription recognition sequence TATA binding protein (TBP).¹¹⁷ As a result of the complex formed between AF-2 and TIFs and the conformational change in the receptor, displacement of transcriptional silencing factors such as nuclear co-repressor (N-Cor)^{59,101} and silencing mediator of retinoic acid and thyroid hormone receptor (SMRT)⁷³ in RARs occurs which, in the absence of an agonist, are bound to the hinge region (domain D) of the RAR (not RXR).²⁴ Retinoic acid receptor homo- or heterodimers are then directed toward the DNA to initiate transcription.^{101,123}

The release of the repressors (N-cor, SMRT) from the hinge region not only depends upon binding of the agonist to the RAR member of a heterodimeric pair but also upon the binding polarity of the heterodimer to the DNA (if the RAR occupies the 3' end of the DNA, a repressor is released; if the RAR member of a dimeric pair binds to the 5' side, the repressor remains bound to the RAR).⁴⁹ Once the tetramers dissociate into monomers because of retinoid binding, the ligand-independent-transactivation function AF-1 (A/B domain) complexes with transcriptional factors that are specific to the promoter of the target gene.⁹⁴ The homo- or heterodimeric pair of receptors binds to the DNA at a specific location of the promoter region named the retinoic acid response element (RARE).⁹¹ RAREs are

nucleotide sequences arranged in direct or inverted polydromic repeats, spaced by one, two, four, or five nucleotides. For instance, a DR2 designation is assigned to direct polydrome repeats (AGGTCA) spaced by 2 nucleotides (AA) such as the DNA sequence AGGTCA(AA) AGGTCA.^{59,73} The RAR/RXR heterodimer binds to DR2 and DR5 in such a manner that the RXR is positioned on the 5' end and the RAR on the 3' end of the DNA.⁷³ The polarity of binding is reversed in the case of association of the RAR/RXR heterodimer with DR1, where the RAR occupies the 5' position and RXR the 3' position.^{59,123} The RXR/thyroid hormone receptor (THR) heterodimer recognizes the DR4,⁹¹ and RXR/vitamin D₃ receptor (VD₃R) heterodimer recognizes DR3.⁴⁰ The crystallographic structure of the RXR/THR heterodimer bound to the DNA has been solved (Figure 6).^{42,112} The connecting loop of RXR α , made up of basic amino acid residues, runs perpendicular to the DNA, and, together with the basic residues of P-box, makes a series of H-bonds with the negatively charged backbone of the DNA.⁴² Furthermore, the attachment of RXR in the major groove of the DNA is strengthened via a salt bridge formed at the dimerization surface which is made up of the THR's aspartate and the RXR α 's arginine residues.⁴² After binding of the homo- or heterodimeric pair to RARE, the DNA makes a loop and is positioned in such a manner that interaction of the TIFs bound to RAR or RXR, with transcriptional machinery (elements needed for initiation and specification of transcription), located up- and downstream from the TATA box, is possible (Figure 7).^{59,73}

One major use of retinoids as potential anticancer agents is in their ability to induce programmed cell death (apoptosis) in malignant cells. The apoptosis of a cell is induced by the binding of an agonist and/or antagonist to the retinoic acid receptor and the receptor

acting through the mechanism as described above (Figure 7 and related description).^{59,73,84,91}

An antagonist is described as a compound that, after incorporation into the nuclear receptor,

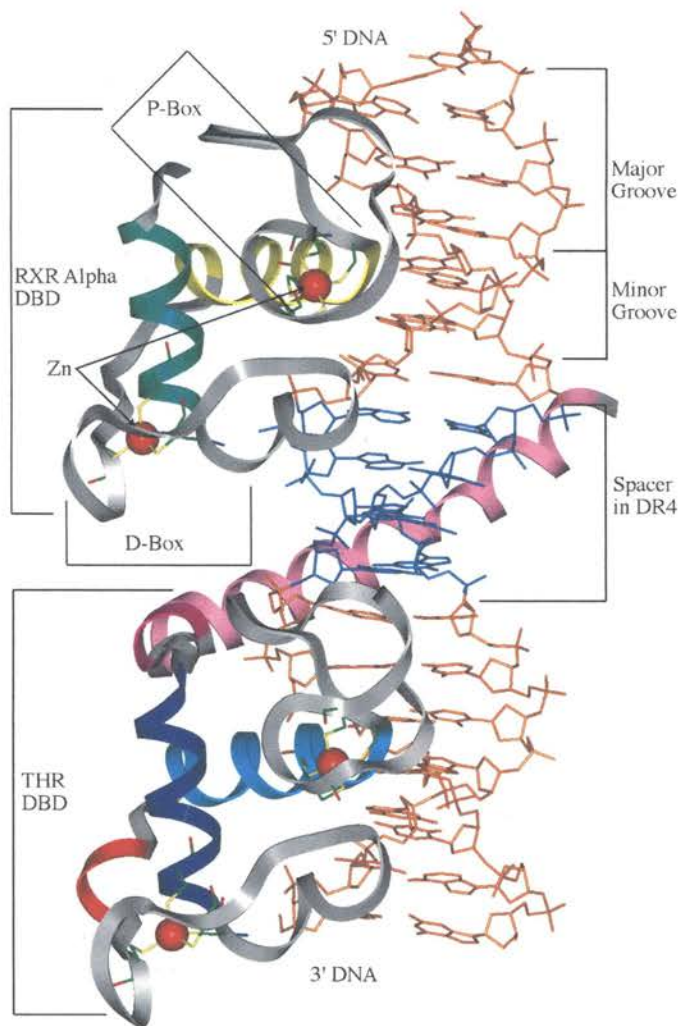
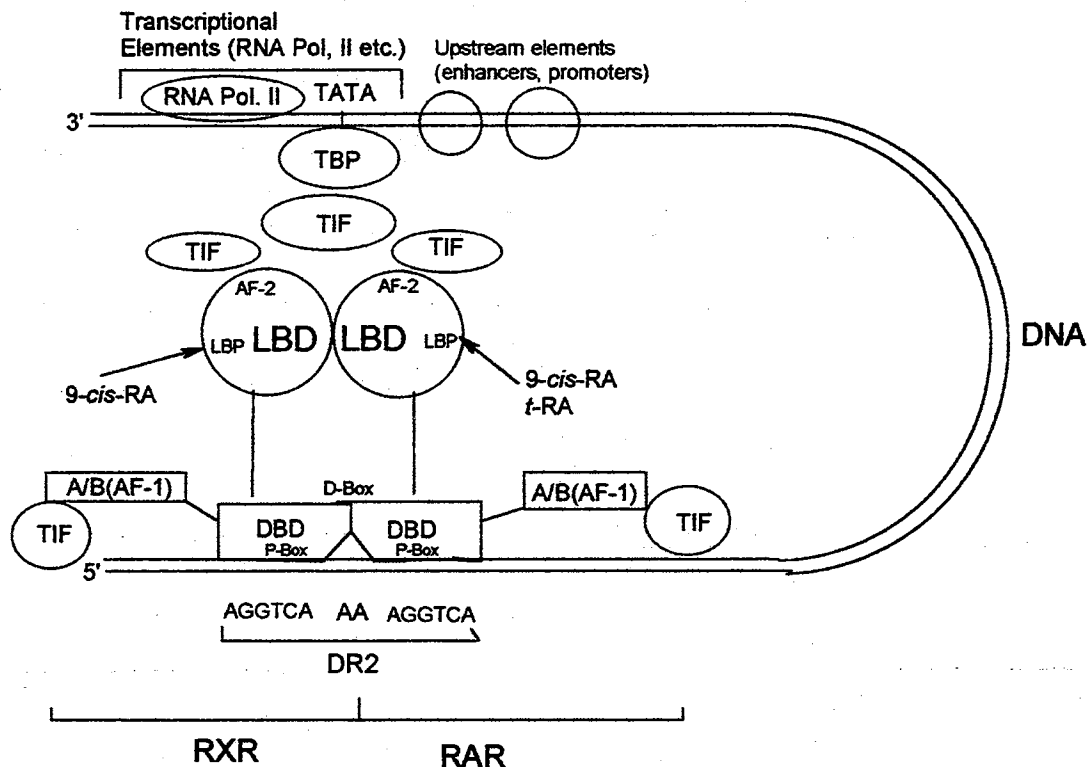


Figure 6. Crystallographic structure of RXR/THR heterodimer DNA binding domains bound to DNA.⁴² Each Zn atoms (red balls) is coordinated to four cysteine residues.

abolishes or greatly reduces a basal transcriptional activity.⁶⁹ The mechanism for binding an antagonist to the LBP of RAR or RXR, and the subsequent receptor activity after the antagonist is bound, is not well understood. It has been proposed that an antagonist enters the LBP in the same way as an agonist.⁴⁷ However, because of structural differences

between the agonist and antagonist, the AF-2 of the LBD is not able to establish the same salt bridge between H12 and H4. This situation results in the receptor undergoing a different

Figure 7. Schematic representation of RXR/RAR heterodimer interaction with DNA and transcriptional machinery of DNA.^{82,88} After activation of the



receptors by a ligand, the newly-formed heterodimer binds to the promoter region of the gene, located upstream from the TATA box, via DNA binding domains (DBD). Due to loop formation by DNA, the transcription intermediary factors (TIF) bound to the ligand binding domain (LBD) of the heterodimer are able to engage in chemical communication with transcriptional machinery proteins, such as TATA binding protein (TBP), etc. The A/B domain, which also recruits the TIFs, is responsible for specificity of DNA binding and cross-talk with enhancers of transcription.^{40,59}

conformational change than the one induced by an agonist.⁴² The induced conformational changes by ligands depend upon the structure of the LBP, which in turn means that what is perceived as an antagonist for one isotype of receptor may act as an agonist in another.^{42,91}

The differences in conformational changes of the receptors' dimeric pair, induced by antagonist binding, may cause the receptors to be incapable of complex formation with RAREs.^{40,91} However, a new antagonist-induced conformation of a receptor can bind the activation protein-1 [(AP-1), c-fos and c-jun genes products], nuclear factor-kappaB [(NF-κB) activator for c-myc, egr-1, LRF-1 cancer genes], and nuclear factor-IL6 (NF-IL6) proteins which are associated with the malignant transformation of cells.³⁷ The binding of RAR/RXR heterodimer to AP-1, and/or NF-κB, and/or NF-IL6, or binding with transcription intermediary factors, such as cyclic-AMP binding protein (CBP), and competitively displacing these oncogenic proteins, protects DNA from such influence and essentially silences the activity of AP-1, NF-κB, and NF-IL6.⁹⁴ Deactivation of the oncogenic proteins (AP-1, NF-κB), or their activity, reverses the action of the transcriptional machinery, and normal cell differentiation, which includes apoptosis induced by the agonist activated nuclear receptor, takes place.⁹⁴

A third avenue by which retinoids can influence the homeostasis of cell is through the action of inverse agonism.⁴⁰ An inverse agonist is defined as a compound which, upon binding to the retinoic acid receptor, causes a shift of receptor activity towards that of an active repressor as opposed to an active enhancer of transcription when the receptor is activated by an agonist.⁴⁰ The conformational change of the receptor that is induced by the inverse agonist does not displace the co-repressor from the hinge (domain D), and, as a result, the retinoic acid receptor is actively involved in the transcriptional repression of target genes.⁴²

In addition to these proposed mechanisms of action for the biological activity of retinoic acid receptors and their heterodimeric partners, RAR and RXR is believed to be

involved in a variety of positive and negative cross-talks mediated by the transcriptional integrator c-AMP binding protein (CBP), RNA polymerase II, and other transcription activating proteins.^{25,143}

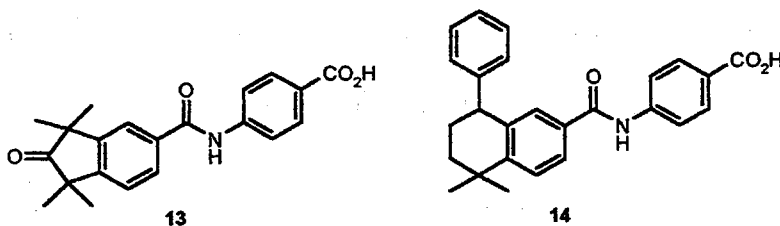
Classification of Synthetic Retinoids Based on Their Biological Effect on Retinoic Acid Receptor

Since the discovery of retinoic acid receptors and because of a high interest in retinoids as potential anticancer agents, many new compounds have been synthesized to gain a better understanding in the nature of biological activity of retinoic acid receptors. Synthetic retinoids can be described according to RAR or RXR biological activity when induced by a retinoid in four ways:

- synthetic retinoids that can act as an agonist or an antagonist,
- retinoids that can exhibit either RAR or RXR selectivity or act as pan-agonists,
- retinoids that can show RAR α , RAR β , or RAR γ isotype selectivity,
- and some retinoids that can preferentially induce target gene transactivation or AP-1 trans-repression.⁴⁷

The existence of different types of receptors, response elements, and intermediary transcriptional proteins implies that retinoid physiology is mediated not by a single pathway, but by multiple pathways. Non-selective retinoids that can activate multiple pathways are likely to be associated with a high incident of adverse effects, and therefore the design of

new retinoids is aimed at specificity of ligand binding to only one isotype of retinoic acid receptor. These compounds and their agonist/antagonist activities are then separated into two classes of synthetic retinoids – Class I and Class II.⁴⁷ Class I retinoids are defined as mono-specific agonistic or antagonistic ligands, like BMS753 (13), that act specifically on a given isotype within the retinoic acid family (RAR or RXR families of receptors). Moreover, this Class I group, even at the highest concentration tested, do not bind or only



weakly bind and activate other isotypes within the given family.⁴⁷ Class II retinoids, such as BMS411 (14), bind with the same or similar affinity to all isotypes of the retinoic acid family (RAR or RXR family) but act as agonists for one isotype within the family and as antagonists for other isotypes.⁹¹

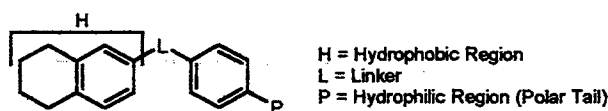
Mutational studies and sequence alignments of the LBDs of RAR α , RAR- β , and RAR- γ show that only three residues inside the binding pocket of the LBD are different for each isotype.¹⁴ The alanine 234 (Ala 234) in RAR γ corresponds to serine 232 (Ser 232) and alanine 225 (Ala 225) in RAR α and - β , respectively.¹⁴ Furthermore, methionine 272 (Met 272) and alanine 397 (Ala 397) in RAR γ correspond to isoleucine 270 (Ile 270) and valine 395 (Val 395), respectively, for RAR α residues and to isoleucine 263 (Ile 263) and valine 388 (Val 388) for RAR β residues.¹⁴ Therefore, these residues were considered as prime candidates responsible for ligand binding selectivity within the RAR family. This hypothesis

was further supported by mutational studies by Ostrovsky and co-workers.¹⁰⁴ However, the same sequence alignment also pointed to additional differences in the LBD of RAR's, but such may be of lesser importance in ligand binding selectivity. Site-directed mutagenesis of RAR α (and RAR β and RAR γ) strongly suggests that polar amino acid residues, such as arginine and/or lysine, are needed for proper hydrogen bonding or salt-bridge formation between the carboxylic end of the ligand and the receptor.⁷⁴

Due to the conformational adaption of 9-*cis*-RA (3) and the spacial arrangement of the RARs' binding pocket, RARs are also able to bind this pan-agonist. However, the activation by 9-*cis*-RA (3) of RAR γ was less than the activation of this receptor by *t*-RA (2), whereas with RAR α and RAR β , the activation by 9-*cis*-RA (3) equaled or in some cases surpassed the activation by *t*-RA (2) of these two receptors.⁶⁸ From the crystallographic structures of RAR γ [co-crystallized with *t*-RA (2) and 9-*cis*-RA(3)], it was pointed out that a possible reason for the activity difference is that RAR γ binds the 9-*cis*-RA (3) less favorably than RAR α and RAR β , a situation due to the interaction of 9-*cis*-RA (3) with amino acid residue Met 272.⁴⁷ This interaction of the Met 272 residue with the ligand in RAR γ corresponds to an interaction of the 9-*cis*-RA (3) with less bulkier residues in RAR α (Ile 270) and RAR β (Ile 263), which in turn results in a smaller distortion of the "active" conformation of the binding pocket.⁴⁷ Mutation of the amino acid residue phenylalanine 230 (Phe 230) by glycine (Phe 230/Gly 230) in RAR γ resulted in the inactivation of the receptor.¹¹² This fact was further substantiated by docking the RAR γ specific ligand into the LBP, where, in a ligand-receptor flexible system, the orientation of the phenyl group of Phe 230 did not change. However, in docking a ligand that does not initiate biological activity of the receptor, the orientation of the phenyl group changed by a rotation of

approximately 60 degrees.⁹ Therefore, P230, although not important for selectivity of ligand binding, has to be taken into consideration because of its function as a “switch” between activity and inactivity of the receptor and its close 3-D proximity to the Ala 234, and Met 272.⁹

The activation of the RXR family receptors by *t*-RA (2) has not been observed.⁵⁷ One possible explanation for this phenomenon is that homologues of the Ala 397 (valines in RAR α and RAR β) are leucine residues in all RXRs.⁵⁷ In RXRs, these leucine residues interact directly with the C(19) methyl group of 9-*cis*-RA (3) and, as a result, these bulkier residues restrict the size of the ligand bound to the receptor.¹³⁷ Moreover, isoleucine 275 (Ile 275) in the LBP of RARs corresponds to phenylalanine 313 (Phe 313) in RXR, and the orientation of Phe 313 sterically interferes with the binding of the more extended *t*-RA (2). This problem is overcome with 9-*cis*-RA (3) because it can assume a low energy “curved” conformation.⁹ However, in contrast to RARs, the amino acid sequence alignment of the LBD of RXRs does not reveal any major differences within the RXR family subtypes.¹³⁷ This fact would suggest potential difficulties in designing specific ligands for RXR α , RXR β , or RXR γ . If the RAR specific subtype activation stems from the interaction of the whole hydrophobic region of the ligand involving certain amino acid residues in the binding pocket and the simultaneous interaction between the linker of the ligand and the amino acid residues, ligand design should concentrate on an alteration of the hydrophobic region (heterocyclic ring fused to aryl ring) of a ligand. The hydrophilic, polar tail of the ligand



should remain intact so as to mimic the property of natural ligands [*t*-RA (2) and 9-*cis*-RA (3)]. If part of the linker and hydrophilic moiety of a ligand prove to be vulnerable to the activity of isomerases *in vivo* such as, for example, where a trans conformation is easily converted to a *cis* and vice versa, more rigid linkers (e.g. L = aryne or aryl) might be required in the ligand in order to avoid isomerization and to allow P313 in RXRs to exclude the RAR specific ligands from binding. Designs of RAR specific Class I antagonists (having a large group in the hydrophobic region of the molecule) and Class II antagonists (having bulky hydrophobic and acidic moieties) are also feasible.¹²⁹ Since agonists and antagonists have different mechanisms of action, co-administration of agonists and antagonists for the treatment of an undesirable condition may have a synergistic effect of value in chemotherapy. The benefit of co-administration of both types of ligands could arise from attack on a cancerous cell via induction of normal cell differentiation (action of agonist), induction of apoptosis (action of agonist and antagonist), and via disrupting the transcriptional machinery of the cancerous cell by competitive deactivation of AP-1 and NF- κ B cancer cell messenger proteins (action of antagonist).

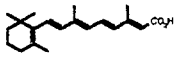
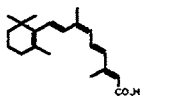
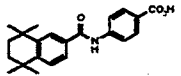
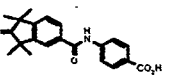
Multiple compounds, which act on a retinoic acid receptor either as an agonist or antagonist with specificity of binding to only one family of receptors or only one isoform, have been synthesized.¹²² The Am 580 (6, page 2)^{10,55} has 70 times higher affinity for binding to RAR α than to RAR β or to RAR γ . Another highly specific agonist for RAR α is BMS 753 (13, Table 1).⁴⁷ This compound possesses a structural resemblance to compound 6. BMS 411 (14, Table 1)⁴⁷ is an interesting compound because it acts as an antagonist for RAR α and RAR γ , but at the same time has an agonistic effect on RAR β , which would suggest large conformational differences between RAR β and the remaining two isotypes or

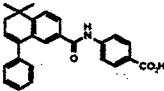
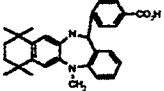
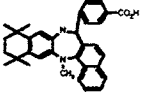
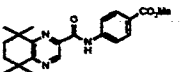
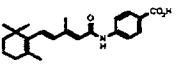
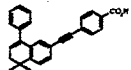
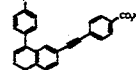
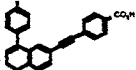
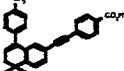
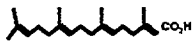
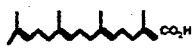
perhaps the conformation of the AF-2 region in RAR β 's LDB can complex to TIFs without a major change induced by ligand binding.

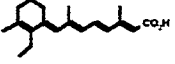
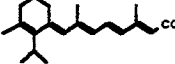
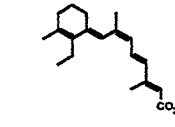
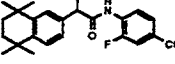
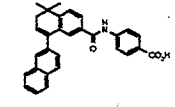
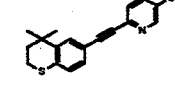
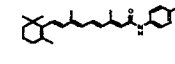
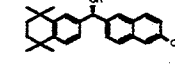
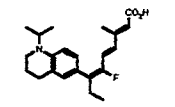
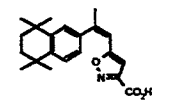
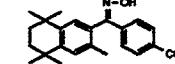
The compounds LE 135 (15)⁸⁴ and LE 540 (16)⁸⁴ have bulky residues which bind to the RAR β with high affinity and are potent AP-1 activity inhibitors (Table I). Amides 17¹²⁹ and 18⁶² have very good activity via inducing differentiation in human promyelotic leukemia cells and in mouse embryonal carcinoma. Arotinoids 19-22,¹⁰ with locked geometries and additional bulky moieties at the hydrophobic region of the ligand, possess excellent inverse and antagonistic effects and structurally resemble 15 which also possesses similar effects on RAR β and RAR γ .

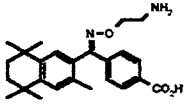
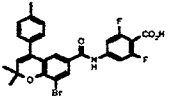
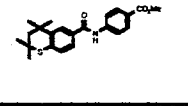
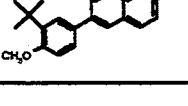
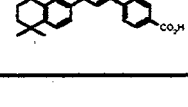
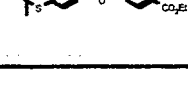
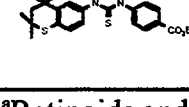
TABLE I

THE COLLECTION OF ENDOGENOUS RETINOIDS, AROTINOIDS, AND HETEROAROTINOIDS THAT EXHIBIT SOME OR TOTAL SPECIFICITY FOR ISOFORMS OF RAR OR RXR.^a

Compound Structure, Name and Number		Isoform Selectivity						Activity Comments	Ref.
		RAR			RXR				
		α	β	γ	α	β	γ		
	<i>t</i> -RA (2)	A	A	A				Natural ligand; binds and transactivates RAR family of receptors only.	122
	9- <i>c</i> -RA (3)	A	A	A	A	A	A	Pan-agonist; activates both families of receptors RXR and RAR (slight lower).	122
	Am 580 (4)	A						EC ₅₀ = 0.36 nM in assay where EC ₅₀ = 2.12 nM for <i>t</i> -RA (2).	55
	BMS 753 (13)	A						As active as <i>t</i> -RA (2) in transcription activity at 10-fold higher concentration.	47

	BMS 411 (14)	T	A	T				The binding affinity to RAR receptors is compatible to <i>t</i> -RA (2), activation of transcription in RAR β is the same as in <i>t</i> -RA (2).	47
	LE 135 (15)		T					Anti-AP-1 activity in breast cancer cell lines when co-administered with <i>t</i> -RA (2).	84
	LE 540 (16)		T					Anti-AP-1 activity in breast cancer cell lines when co-administered with <i>t</i> -RA (2).	84
	9 O (17)	A	A	A				Induction differentiation in HL60 and P19 cell lines 83.5%, and 92.5%, respectively, as compared to <i>t</i> -RA (2). ED ₅₀ = 8.3 nM	129
	10 A (18)	A	A	A				Induction differentiation in HL60 and P19 cell lines by 83.5% and 79%, respectively, as compared to <i>t</i> -RA (2). ED ₅₀ = 32 nM	62
	AGN 192817 (19)		A	T				Binding IC ₅₀ = 32 nM in an antagonism assay using 10 nM <i>t</i> -RA (2).	10
	AGN 193840 (20)		A	T				Binding IC ₅₀ = 32 nM in an antagonism assay using 10 nM <i>t</i> -RA (2).	10
	AGN 193109 (21)			I				Binding IC ₅₀ = 32 nM in an antagonism assay using 10 nM <i>t</i> -RA (2).	10
	AGN 193385 (22)			I				Binding IC ₅₀ = 32 nM in an antagonism assay using 10 nM <i>t</i> -RA (2).	10
	GGA (23)	A	A	A				90% upregulation of transcription of RAR β in CAT assay as compared to <i>t</i> -RA (2). Much less toxic.	1
	4,5-dd-GGA (24)	A	A	A				100% upregulation of transcription of RAR β in CAT assay as compared to <i>t</i> -RA (2). Much less toxic.	1

	UAB 7 (25)			A				At EC ₅₀ = 2.5 nM, UAB8 is 5% better in preventing mouse skin papiloma than <i>t</i> -RA (2) whose EC ₅₀ = 3.0 nM; Lower toxicity than <i>t</i> -RA (2).	99
	UAB 8 (26)			A				At EC ₅₀ = 1.5 nM, UAB8 is 5% better in preventing mouse skin papiloma than <i>t</i> -RA (2) whose EC ₅₀ = 3.0 nM; Lower toxicity than <i>t</i> -RA (2).	99
	(9Z) UAB 7 (27)				A	A	A	At 1 mM concentration, 95% as effective as 9- <i>c</i> -RA (3) which is 7 nM in transcription activation, advantage RXR specific, not an pan-agonist.	99
	BMS 961 (28)		A	A				Compatible to <i>t</i> -RA (2) in initiation of transcription assay which is at 10-fold higher concentration.	47
	BMS 614 (29)	T						At 1 μM concentration completely antagonizes <i>t</i> -RA (2) (10 nM) transcriptional activity.	47
	Tazarotene (30)		A	A				In clinical trial to treat skin disorders; highly receptor specific; very low toxicity and high RARγ selectivity.	23
	4 HPR (31)			A				Used in clinical trials in combination with tamoxifen, same transactivation CAT activity as <i>t</i> -RA (2)	34
	S1 (32)			A				Stereoselective, at 100 nM concentration achieves 90% efficacy in transactivation of transcription as compared to <i>t</i> -RA (2) which is 1 mM	140
	14 B (33)				A	A	A	Efficacy is over 120% in α and β isotype and 233% in γ isotype of RXR as compared to 9- <i>c</i> -RA (3).	58
	I 14 B (34)				T	T	T	Low transactivation activity, but superior inducer of apoptosis 4 times as good as apoptotic activities of 9- <i>c</i> -RA (3).	120
	C 3 (35)				A	A	A	Co-transfection activity EC ₅₀ values are low, total RXR selectivity, EC ₅₀ compatible to 9- <i>c</i> -RA (3).	70

	C15 (36)					A		RXR β selectivity with EC_{50} values is 5 times lower than that for RXR α and RXR γ , although not as good as for 9- <i>c</i> -RA (3).	70
	AGN 194574 (37)	T						Low concentration of AGN 194574 are needed to repress the <i>t</i> -RA (3) transcriptional activity, competitively displaces <i>t</i> -RA from RAR α .	127
	SL-I-50 (38)	A	A	A	A			Partial pan-agonist, interestingly the efficacy for RXR β and RXR γ are low. Excellent repressor of AP-1 activity, and RARE transactivator with low toxicity.	8
	CD 417 (39)		A					$EC_{50} = 3.56 \text{ mM}$ in assay where $EC_{50} = 3.62 \text{ nM}$ for <i>t</i> -RA (2)	140
	CD 666 (40)			A				$EC_{50} = 1.40 \text{ mM}$ in assay where $EC_{50} = 2.46 \text{ nM}$ for <i>t</i> -RA (2)	140
	SL-I-70 (41)			A				Believed to be RAR γ -specific because of its excellent activity in inhibition of growth in vulvar cancer cell lines	u
	SL-I-72 (42)			A				Believed to be RAR γ -specific because of its excellent activity in inhibition of growth in vulvar cancer cell lines	u

^aRetinoids and their specificity of binding.

A = agonist, T = antagonist, I = inverse agonist, u = unpublished data. IC_{50} = concentration of the retinoid that is required to displace 50% bound *t*-RA (2) from a receptor; EC_{50} = concentration that is required to induce 50% of maximal retinoic acid receptor activity. Empty blocks indicate no or minimal binding or activation of a receptor by a retinoid. For more details please see recommended references.

Somewhat unusual acyclic and highly flexible retinoids that are very active in the CAT assay (see page 30) are compounds 23 and 24.¹ These compounds are not bound by CRABP and have very low toxicity toward the environment.¹²⁹ Somewhat flexible retinoids, such as 25-27,⁹⁹ mimic the structural features of *t*-RA (2) and 9-*c*-RA (3). However, the

specificity of binding by these compounds is only enhanced marginally whereas **25** and **26** are RAR γ specific, and **27** recognizes only the RXR family receptors.

A three-atom linker compound (three atoms between the aryl groups), namely BMS 961 (**28**),⁴⁷ proved to be a specific agonist for RAR γ and also bound with lesser affinity to RAR β (Table 1). The highly specific RAR α antagonistic effects of **29**⁴⁷ were accomplished by the presence of a large naphthalene residue in the hydrophobic region of this ligand. Tazarotene (**30**) is a rigid, RAR γ and RAR β specific agonist that is currently in clinical trials for the treatment of skin diseases.²³ Compound **31**,³⁴ whose mechanism of action is not well understood, but appears to bind selectively the RAR γ and transactivate it through an agonistic effect, has a 10 atom linker between the hydrophobic moiety and aryl group. This structural feature is in agreement with that found in other RAR γ specific ligands whose linker groups between aryl moieties are also longer than that for the ligands that are specific for RAR α or RAR β .

The stereospecific arotinoid **32**,¹⁴⁰ which has the S configuration at the linker, specifically activates RAR γ and to a lesser extent RAR β , but not RAR α , whereas its R isomer is less active. This would suggest that the molecular geometry of the ligand will enhance the receptor's specificity.

A fluorine atom has also been incorporated in the synthesis of flexible compounds, such as **33**, with structures resembling the 9-*c*-RA (**3**), but unlike 9-*c*-RA (**3**), which also binds to the RAR family of receptor, **33** (Table I) is only RXR specific.⁵⁸ Heteroarotinoid **34** containing a 5-membered heterocyclic ring did not induce the activation of transcription. However, compound **34** is one of the most potent inducers of apoptosis, perhaps through an

antagonistic effect on the RXR receptors.¹²⁰ Compounds **35** and **36**, with C=N systems, are RXR specific, the latter being one of the few compounds that is isotype-specific within the RXR family.⁷⁰

Heteroarotinoid **37**, a complex structure with an amide linker, exhibits high binding affinity for RAR α and influences the receptor through the induction of antagonistic activities.¹²⁷ Interestingly, heteroarotinoid **38** is a partial agonist, where it induces activity in all of the RAR isoform, but is somewhat selective for the α -isoform in the RXR family.⁸ These compounds are reported to have the same transactivation effect on the RAR family of receptors as does *t*-RA (**2**).^{34,140} The structural differences of the very recent RAR β specific **39** and RAR γ specific **40** are believed to be major contributors to their specificity.¹⁴⁰ Compounds **41** and **42** exhibited excellent inhibition of cancer growth in vulvar cancer cell lines (unpublished data from Dr. Benbrook). Due to a high expression of RAR γ in urogenital tissue⁶⁶ and an unusually high inhibition of cancer growth, these compounds are believed to express specificity for the RAR γ .

Detection and Measurement of Retinoic Acid Receptor Activity

There are several methods for the detection of RAR or RXR ligand-induced activities. One of the most frequently used methods is the use of reporter assay to measure quantitatively the transcriptional activity of RAR, and RXR homo- or heterodimers.¹³⁴ The reporter plasmid construct (Figure 8) consists of a reporter gene, such as *lacZ* or luciferase, driven by a minimal promoter containing a TATA motif on RARE.¹³⁴ At the 5' end position of the RARE is a silencer (S) which acts to dampen any transcriptional activity originating upstream from the RARE.¹³⁴ Additionally, there are several antibiotic selective genes (Ab'),

restriction sites (RS), and an origin of replication (ORI) to ensure proper analysis of RARE's transcriptional influence on the reporter gene.¹³⁴

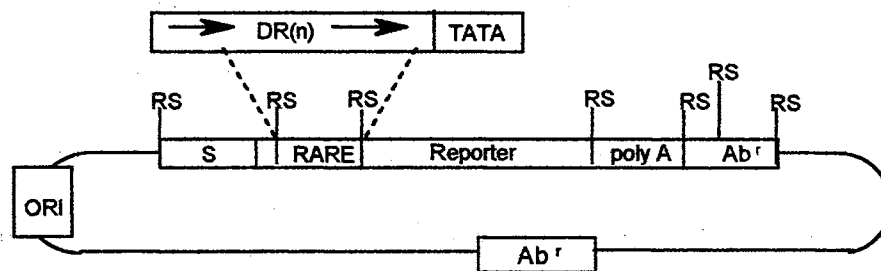
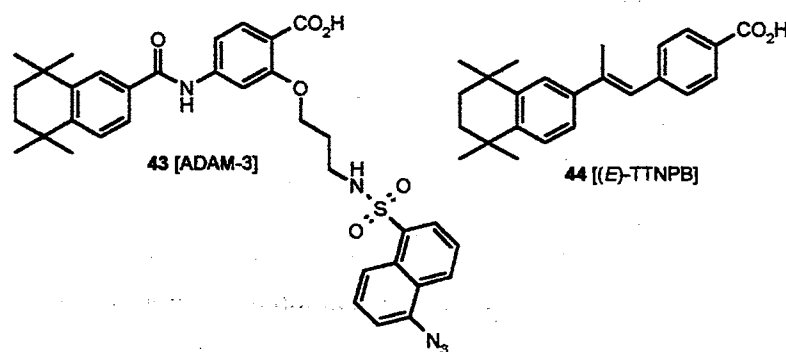


Figure 8. Schematic representation of reporter plasmid for measuring the transcriptional activity of RAR or RXR after activation by a ligand.¹³⁴

A superior and convenient method in investigating the structural features of ligand-receptor complexes is the photoaffinity labeling assay.¹³⁴ The sequence of events for the photoaffinity assay are as follows: (1) design and synthesis of an isoform specific,



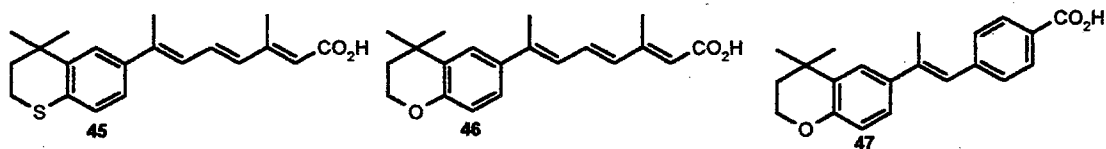
photoreactive ligand, (2) photoaffinity labeling of the receptor, (3) sequential digestion of the labeled receptor by endoproteinases, (4) HPLC separation of digests to determine the amino acid sequence of the labeled site, and (5) mapping of the labeled site for comparison with the known amino acid sequence of the receptor.¹³⁴ The compound ADAM-3 (43),

which is a photo-labeled derivative of the RAR α specific agonist Am 580 (6), was successfully utilized in the mapping of the ligand-receptor complex.¹³⁴

Toxicity of Retinoids

Many retinoids are administered primarily for dermatological conditions, such as psoriasis, acne, and disorders of keratinization.^{6,124} Toxicity has proven to be a significant problem in the long-term administration of retinoids.¹⁰² The most common, unwanted side-effects from the administration of higher than normal doses of retinoids (hypervitaminosis) are skin desquamation, hyperbilirunemia, transaminase elevation, leupenia, diarrhea, headaches, mucocutaneous toxicity, and hypercalcemia.¹¹⁴ The synthetic retinoid TTNPB (44) is a more potent inducer of RAR transcriptional activity than *t*-RA (2) despite the fact that the binding affinity of TTNPB (44) to RARs is 10 times lower. However, arotinoid 44 is 1000 times more toxic than *t*-RA (2).¹⁰⁷ It has been suggested that the higher activity and toxicity of TTNPB is due to an inability to complex with CRABP.¹²⁴ The CRABP regulates the levels of retinoic acid in the cell and its transport to the nucleus where the *t*-RA (2) interacts with RARs.¹⁰⁷ Since the concentration of TTNBP (44), which can't bind to CRABP, is not regulated and its metabolism is slowed down, TTNBP (44) remains in the cell and nucleus for long periods of time and therefore interacts more significantly with RARs. This may well be the major contributing factor for the TTNPB (44) teratogenicity.¹⁰⁷ Intriguingly, when RAR α specific antagonist AGN 193109 (21) was co-administered with TTNBP (44) or administered to mice with preexisting toxicity from 44, 21 was able to accelerate significantly the recovery of the mice from the toxic effects of TTNPB.¹²⁴

Targretin (7, page 2) is a RXR specific agonist and has an organic composition and structure which only slightly differs from TTNPB, but is much less toxic than TTNPB (44).⁷⁰



Another possible avenue for decreasing the toxicological effect of retinoids is the utility of heteroarotinoids which are comparable in receptor activation to that activation induced by natural retinoids.⁶ Nearly full toxicity studies of heteroarotinoids 45, 46, and 47 revealed that the maximum tolerated dose (MTD) was 34 mg/kg/day, 32 mg/kg/day, and 9.4 mg/kg/day, respectively.⁶ These data compared to the MTD of *t*-RA (2), which is 10 mg/kg/day, shows reduced toxicity of 45 and 46. Therefore 45 and 46 are 3-fold less toxic than *t*-RA (2) and 3000-fold less toxic than TTNPB (44) whose MTD is 0.01 mg/kg/day.⁶ Design and synthesis of isoform-specific arotinoids or heteroarotinoids can also significantly decrease the unwanted side effect of retinoic acid receptors.²³

Molecular Modeling of Retinoids

Molecular modeling is a useful tool for the investigation of structure-activity relationships (SAR) in a variety of proteins-ligands complexes. Unfortunately, with exception of unrelated modeling work to our type of research, not much molecular modeling in the field of retinoid research has been done.³⁹ Only in a recently published work by Gronemeyer and colleagues was consideration given to a study of SAR via docking of synthetic arotinoids into RAR isotypes in combination with mutagenic studies of the receptors.⁴⁷ The data from docking of synthetic arotinoids were in agreement with the

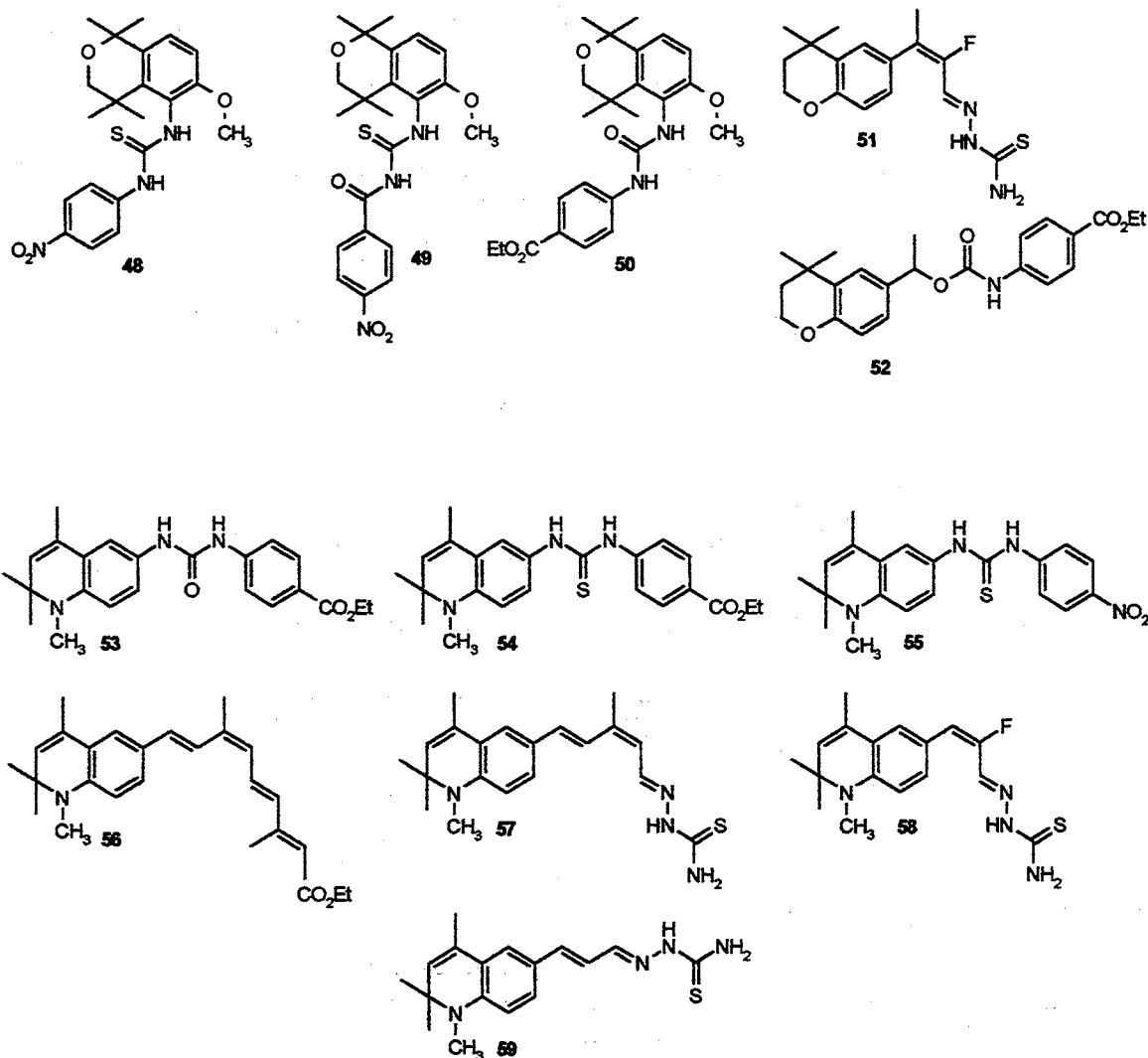
biological data, where the specificity of binding was dependent only on a few residues. The computer-aided analysis was based on the existence of the LBD crystallographic structure of human holo-RAR γ co-crystallized with *t*-RA (**2**). The LBP of RAR γ was prepared for modification by extraction of **2** to obtain apo-RAR γ LBP.¹⁴ The apo-RAR γ was then modified by computer-aided mutagenesis to obtain the LBPs for RAR α and RAR β . The use of QUANTA/CHARMS, a module in a molecular modeling software package from Molecular Simulation Inc. (MSI),³⁰ was utilized, and the amino acid residues of the LBP in RAR γ that are responsible for selectivity were substituted with homologous amino acids of RAR α and RAR β (see Experimental for details).⁴⁷ The computer-aided mutation allowed for creation of the new LBP of RAR α and RAR β with different amino acid composition which essentially translates to different shapes of the hydrophobic surface of the binding pockets of the receptors which resulted in new interaction property (energy of interaction, positioning of in the LBP) with the ligand. Conformational searches and evaluations of the selected arotinoids provided conformations of various energies which was done before the ligands were docked into the LBPs of RAR isotypes. The interaction energy values and visual inspection of docked ligands in the LBPs provided a possible explanation as to how the ligand might interact with the receptors. These data could then serve as valuable tools for the future design of RAR isotype-specific retinoids.

CHAPTER II

RESULTS AND DISCUSSION

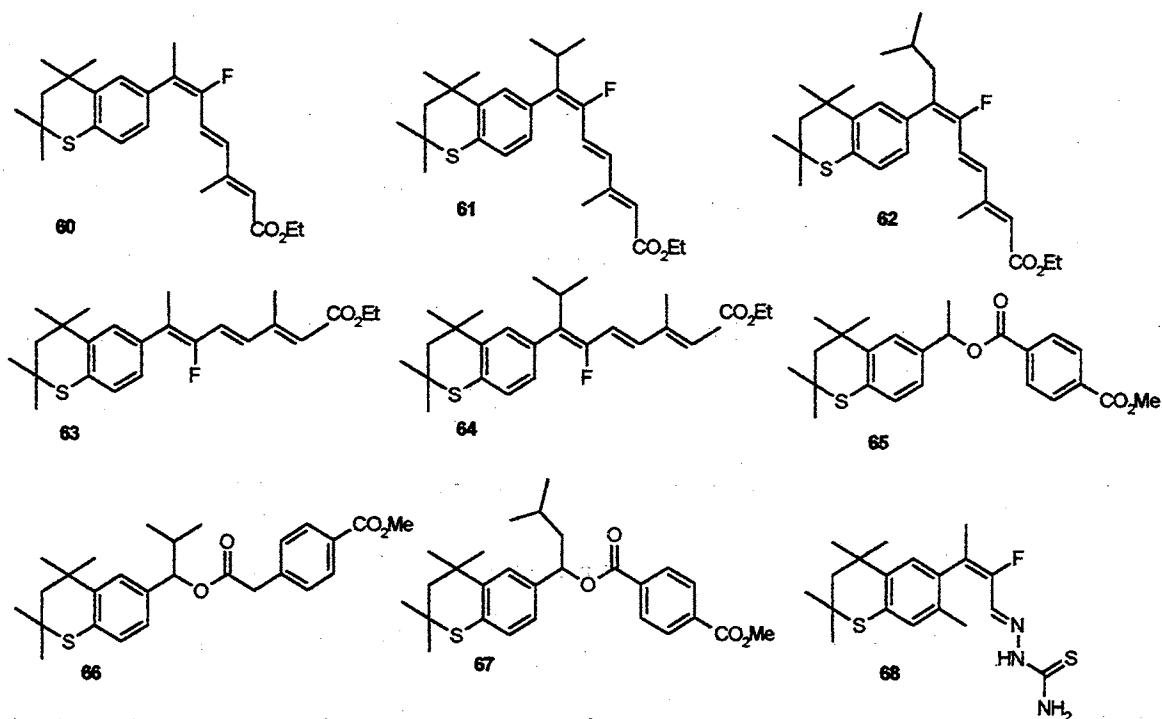
RAR and RXR Isotype Specific Heteroarotinoids

The work addressed in this thesis had two central themes, namely the synthesis of several receptor-specific, or projected receptor-specific, heteroarotinoids and the development of a computer assisted analysis of the heteroarotinoids as a ligand in binding to a specific receptor. The new compounds **48-68** which were prepared are listed below.



An approach to determine the suitability of a heteroarotinoid as a ligand to bind with the retinoic acid receptor was developed using several commercial programs and the computer in the Department of Biochemistry. Such programs addressed the following situations with respect to creating a “fixed” and “flexible” binding pocket in the receptor as well as a “fixed” and “flexible” ligand such as a heteroarotinoid. These programs were as follows along with their particular function in the analysis: The Molecular Simulation Inc. (MSI)³⁰ molecular modeling software package and its program modules were used in drawing and optimizing the conformations of compounds (Builder, MOPAC and Conformational Search Engine) and modification of the LBD of RAR γ crystallographic structure (Biopolymer). The Sybyl 6.5¹²⁶ molecular modeling package, which has modules QSAR with Comfa, Flexidock, and Superimposition, were used in predicting the activity, docking, and analysis of resulting ligand and receptor conformations, respectively.

The goal of the research was to synthesize a number of heteroarotinoids to be RAR isotype (RAR α , RAR β , or RAR γ) or RXR isotype specific. The structure-activity investigation of previously prepared compounds in our laboratory, via the aid of computer modeling programs described later in this chapter and biological data published by us and other research groups, served as guide in designing heteroarotinoids 48-68. The ligand binding domain (LBD) of the crystallographic structure of RAR γ bound to *t*-RA (2) also provided a means for further exploration of the ligand-receptor interaction via docking of the ligands into the ligand binding pocket (LBP) of the receptor. Based on the type of heteroatom contained in the fused ring system, heteroarotinoids 48-68 were divided into three groups:

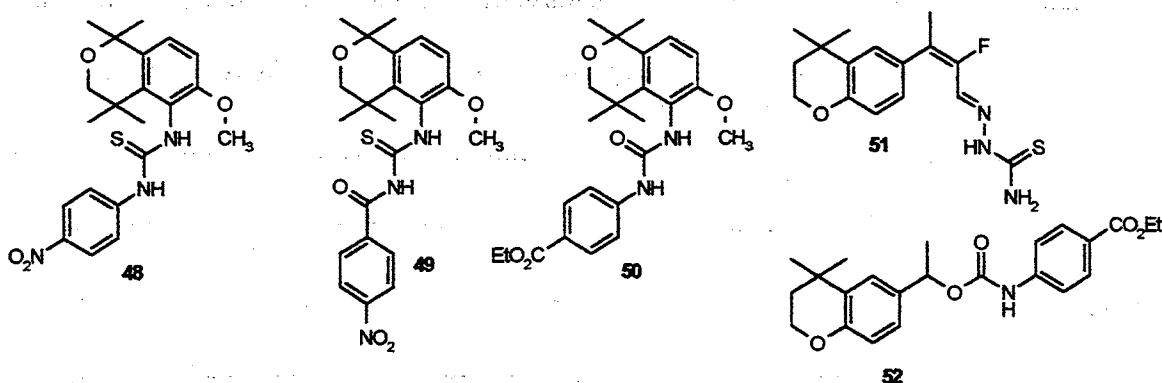


- oxygen heteroarotinoids, compounds 48-52,
- nitrogen heteroarotinoids, 53-59, and
- sulfur heteroarotinoids, 60-68.

Oxygen Heteroarotinoids

Oxygen heteroarotinoids 48-50, where oxygen is part of the isochroman ring and the linker group is placed at the C5 position of the hydrophobic aryl moiety (which is different from previously made retinoids) were synthesized to map the hydrophobic region of the ligand binding pocket. Furthermore the methoxy group at the C6 position was added to the enhance the bulk of the ligands in the hydrophobic region and to alter the bond rotational barrier of the linker group. The unusual nature of the linker group, with respect to the hydrophobic aryl moieties, was expected to reduce binding to the RAR family of receptors, and thus, the compounds might be RXR family specific. The other assumption was that if

the ligand was drawn into the binding pocket of RAR γ , via an electrostatic attraction of its anionic tail to the basic residues, such as arginine 278 (R278) and arginine 274 (R274) in the LBP, to form hydrogen bonds, the hydrophobic bulk of the ligand would prevent the receptor from trapping the ligand through a conformational change of α -helix H12, which could ultimately lead to antagonistic activity of the RAR receptors. The results from the docking of these compounds by rendering them as flexible molecules (the ligand was allowed three degrees of freedom to translate within the LBP, and possessed free rotation around single bonds with restrained dihedral angles being altered) into the LBP of RAR γ being rendered as “fixed,” with the exception of **48**, suggest that these compounds might not be RAR γ active due to the unfavorable energies of interaction (see Experimental).



However, heteroarotinoid **48** interacted favorably with the receptor's binding site without any significant steric hindrance. Compound **49**, which differs from **48** in that the linker is extended by one carbonyl moiety, did *not* dock favorably. Sufficiently strong H-bonds formed by the nitro group of **49** with basic residues of the LBP, the extra atom in the linker, and the limiting space in the LBP resulted in repulsive energies between the region of the amino acids that make up α -helix H12 and the hydrophobic region of the ligand. After

deleting α -helix H12 from the LBD of the crystallographic structure of the RAR γ , **49** interacted favorably with the receptor. This would suggest that **49** may express its influence on the receptor in the form of antagonistic activities.⁴⁷ Compound **50**, which has a urea linker and a carboxylic ester at the polar end, instead of a thiourea linker and a nitro group, respectively (as compared to **48**), did not exhibit the same binding property as heteroarotinoid **48** when docked in the RAR γ LBP (for details, see discussion on pages 46-51).

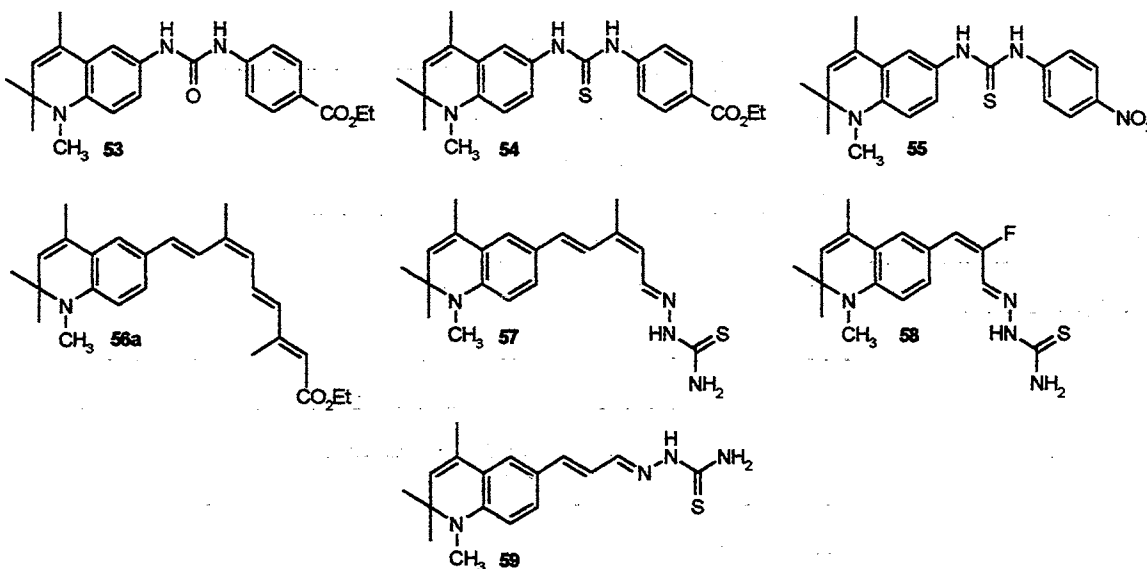
Heteroarotinoid **51**, in which the replacement of hydrogen by a larger fluorine atom at the C10 position could influence the E/Z isomer ratio at the C9-C10 double bond, was designed as a ligand to specifically bind only to the RXR family of receptors. Additionally, a polyene side chain was retained in **51**, and the terminal group was changed to a semicarbazone. This change switches the function of the ligand's polar tail from being an H-bond acceptor to an H-bond donor at a physiological pH via interaction of NH₂ group with the hydroxy group of serine 289 (Ser 289) and the carbonyl oxygen in the receptor's backbone moieties located at the polar end binding region. This agent allowed a study of the importance of electrostatic interactions between the receptor and the ligand. Docking of **51** into the LBP of RAR γ resulted in a positive (unfavorable) energy of interaction which suggested steric hindrance between the ligand and the receptor due to bending of the side chain, and thus **51** could be specific for RXR.

The behavior of **52** with a four-atom linker between the aryl groups resembled that of compound **49** when the former was docked into the LBP of RAR γ . Thus, it could be concluded that a four-atom linker between two aryl moieties may be slightly too long for

receptor activation. However, these compounds may act as antagonists.

Nitrogen Heteroarotinoids

Nitrogen heteroarotinoids **53-59** have a double bond incorporated into the fused ring



of the hydrophobic region. This addition to the heterocyclic ring changes the conformation of the hydrophobic portion of the ligand, as compared to previously synthesized retinoids. The double bond also serves as a probe in terms of the possible interaction or stacking of the π -electrons of the ligand with the phenyl rings of phenylalanine residues in the hydrophobic region of the LBP. It is not known what influence the latter has on the receptor activity. Additionally, the 3-D geometry of the hydrophobic region in **53-59** was altered by deleting one methyl group from the C4 position. Moreover, different bond lengths and conformations of the flexible linkers and the side chain were varied slightly for comparison of effects on activity. Modulation of the polar tails of the ligand was done to explore the

region of the LBP which is responsible for H-bonding.

Compounds **53-55**, which have three-atom linkers between aryl moieties, showed excellent interaction energies when docked as flexible molecules in the rigid LBP of RAR γ (Figure 9, see Experimental for energy of interaction data). Heteroarotinoids **53-55** with a 3-atom linker between the aryl groups are similar to previously designed arotinoids with 3-atom linkers in exhibiting RAR γ specificity.^{47,140} However, the urea and thiourea groups provide a semi-flexible linker region of the ligand for possible enhanced adaptation of the compounds around the amino acid residues responsible for selectivity in the RAR γ . Furthermore, possible H-bonding with the receptor is likely strengthened by the heteroatoms of the urea group present in the linker.

Based on visual inspection, the docked heteroarotinoids **56** and **57**, which were designed to discriminate against the RAR family, resembled the docked 9-*c*-RA (**3**) in the LBP of RAR γ . However, due to the *cis* double bond arrangement at the C11-C12 position in **56** and **57**, which is different from the *cis* double bond position in 9-*c*-RA [**3**], C9-C10], an unfavorable interaction of **56** and **57** with RAR γ occurred. This differs from the interaction of **3** with RAR γ . Considerable steric hindrance was observed with both heteroarotinoids between the hydrophobic region of the ligands and the residues Met 272, Ala 397, and Ile 275 of the LBP of RAR γ . In addition to being RXR specific, **56** and **57**, which have linker moieties extended by two atoms compared to the polyene chain of 9-*cis*-RA (**3**), were originally designed to explore the LBP of RXRs and, hopefully, bind to only one of the RXR isoforms.

Compound **58** was conceived as being RXR specific due to its *E* conformation

around the C9-C10 double bond. However, unlike 9-*c*-RA (**3**), compound **58** did not show a favorable interaction with the LBP of RAR γ upon docking into the receptor (see Experimental). Placement of heteroarotinoid **59** within the cavity of the LBP of RAR γ was

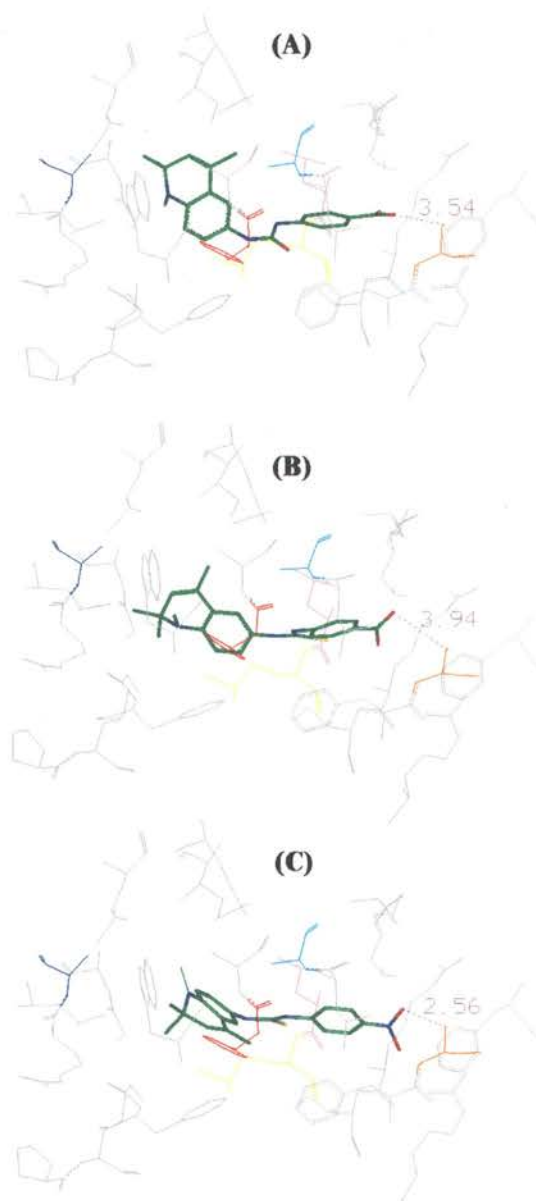
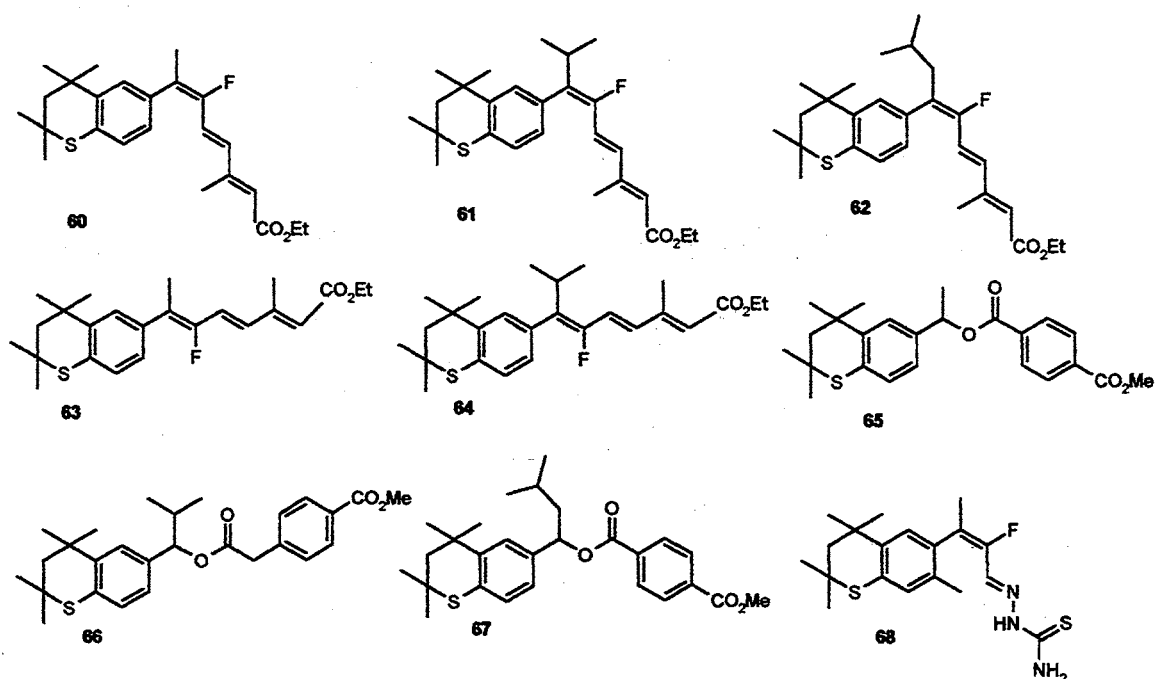


Figure 9. Docking of heteroarotinoids **53** (A), **54** (B), and **55** (C) into the LBP of the crystallographic structure of RAR γ . The distance (\AA) from Ser 289 to the closest polar end oxygen of the ligand is shown for comparison.

accomplished without any major steric or electrostatic repulsion of the ligand by the receptor (see Experimental). Consequently, **59** may act as an pan-agonist, with possible lower toxicity than 9-*c*-RA (**3**).⁴⁴

Sulfur Heteroarotinoids

The synthesis of sulfur heteroarotinoids **60-68** added yet another structural variation to studies on the mechanism of activation of retinoic acid receptors. The differences in stereochemistry of the linker groups due, in part, to the influence of the incorporated fluorine atom, were designed to discern activity differences among the two families of receptors RAR and RXR. The difference in size and electronic density of the fluorine atom at the C9 position, as compared to hydrogen, was also intended to explore the interactions of the ligand with the amino acid residues (such as Ala 234, Met 272, Leu 271, Ala 397, and Phe 230) which were responsible for ligand selectivity and the flexibility in the LBD of RAR γ .¹⁴



Docking of flexible **60** into the rigid LBP of RAR γ did not result in a favorable interaction, and the results worsened as docking progressed to **61** and then to **62**. However, heteroarotinoids **63** and **64**, which are the *Z*-isomer counterparts of compounds **60** and **61**, respectively, showed excellent interactive energies with RAR γ when docked in the LBD of RAR γ (see Experimental). Compounds **60**, **61**, and **62** were designed specifically to activate the RXR family due to their *E* configuration, and **63** and **64**, because of the *Z* configuration about the C9-10 double bond, should activate the RAR. Furthermore, **64** was intended to be RAR β specific since similar compounds with bulky groups around the C9 position had shown RAR β specificity.⁴⁷ Heteroarotinoid **65**, a three-atom linker ligand, showed marginal energies of interaction when docked into the LBP of RAR γ , and thus could be RAR γ specific.⁴⁷ Interestingly, **66** and **67**, in which the bulk of the substituent group at C9 was increased, were rejected by the receptor's LBP due to spacial limitations. The intention to modify **65** at the C9 position with larger substituents (and progress to **66** and **67**) was to explore the limit of selectivity of the RAR receptors, since the ligands interact near the C9 area with the amino acid residues responsible for selectivity.¹⁴ The 3-atom linker system with an ester moiety in **65-67** was devised to achieve RAR γ specificity.⁴⁷

Compound **68** was expected to have pan-agonist activity, since the linker and polar end are somewhat flexible. However, some restrictions on single bond rotations within the ene side chain were discovered when a computer-aided search for other conformations of the ligand was performed. One restriction arose from the addition of the methyl group at the C7 position which forced the fluoro-substituted linker and thiosemicarbazone polar tail into *only one conformation with minimum energy*. Docking of flexible **68** into the rigid LBP

of RAR γ was unfavorable, and the behavior of the compound did not resemble that of 9-*c*-RA (3) with respect to interaction with RAR γ (see Experimental). Therefore, heteroarotinoid 68 was expected to have preferential binding for the RXR family.

Computer-Aided Activity Prediction

In addition to docking flexible ligands into LBP of the rigid crystallographic structure of RAR γ ,¹⁴ attempts were made to predict the activity of RAR and RXR isotypes (RAR α , RAR β , and RAR γ) upon induction by heteroarotinoids 48-68. The Comparative Molecular Field Analysis (CoMFA) is a three-dimensional, Quantitative Structure-Activity Relationship (QSAR) technique which ultimately allows the design and prediction of biological activities of molecules (see user manual for CoMFA use, also see reference 39). The idea underlying CoMFA is that *differences in a target property are often related to the shapes of the non-covalent fields surrounding the test molecules*. In order to input the shape of the molecular field into a QSAR table, the magnitudes of its steric (Lennard-Jones) and electrostatic (Coulomb) energy fields were sampled at regular intervals throughout a defined region. The most important parameter for the CoMFA calculation is the relative alignment of individual molecules when their molecular fields are calculated. The alignment of the ligands was done by mimicking the positioning of *t*-RA (2) in the LBP of RAR γ in the absence of receptor. This resulted in the X, Y, and Z, coordinates of the hydrophobic and hydrophilic moieties of ligands to be in close approximation to X, Y, and Z coordinates of *t*-RA (2), respectively. Therefore, properly aligned molecules have similar orientations in Cartesian space, and the generation of a QSAR by Partial Least Square (PLS) analysis gives a higher cross-validation number q^2 . The number q^2 obtained from cross-validation of a

PLS analysis is a number which represents a percentage of “explained variation” in a ligand-activity relationship. For example, $q^2 = 0.55$, means, that the variation in activity exerted on the receptor by ligands can be explained (with 55% certainty) with respect to the variation in the hydrophobic and electrostatic force field (arrangements in 3-D space) of the aligned ligands. The same q^2 also implies that 45 % of the variation in structure-activity relationship cannot be justified. With a correlation coefficient of $r^2 = 0.95$ applied to the cross-validated PLS analysis, accuracy of about 52 % (55×0.95) would be predicted for activity of new molecules. The $q^2 = 0.4$ (minimum) and $r^2 = 0.95$ (minimum) are acceptable numbers for this type of calculation.¹⁰⁰

The database of retinoids (conformations obtained from docking ligands in the RAR γ and in pseudo-RAR α and in RAR β ; see Experimental for the latter two receptor modifications) with known and unknown biological activity was aligned through structural superimposition using the command “Align Database” in Sybyl 6.5.¹²⁶ The same type of alignment of the database was performed for the compounds to be correlated in the prediction of activity in RXR isotypes. However, since the location of the LBP of RXR has not been elucidated,¹⁵ several different conformations of the same ligand had to be evaluated for this type of calculation (see Experimental for details). The CoMFA for each compound was calculated and stored in a molecular spread sheet. The known biological data, which in this case were EC_{50} values for the induction of transcription in CV-1 cells, were entered as $\log(1/EC_{50})$ and saved in a molecular spread-sheet. The summary of predicted EC_{50} values [the $\log(1/EC_{50})$ was converted back to EC_{50} values] for heteroarotinoids **48-68** are in Table II. The cross-validation q^2 values ranged from 0.43 to 0.58, and the correlation

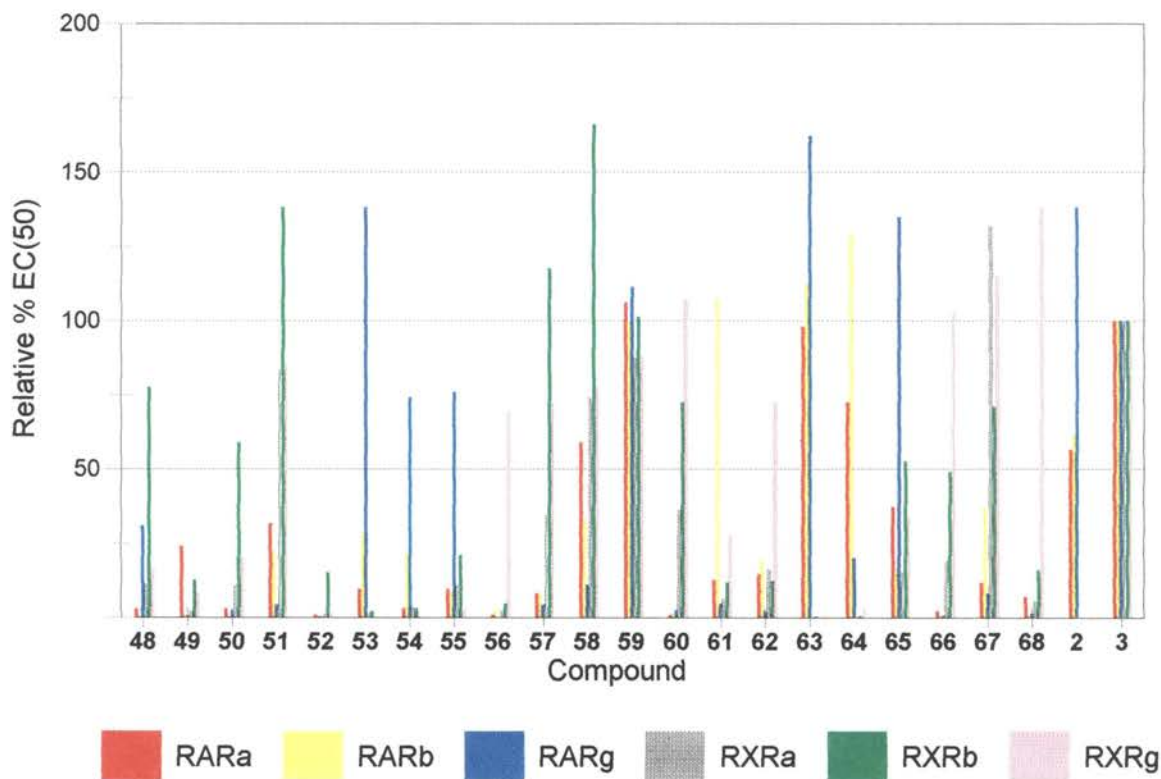
coefficient r^2 values range from 0.95 to 0.98. This indicated that the accuracy percentage for prediction ranged from 41% to 58%.

TABLE II
PREDICTED EC₅₀ VALUES FOR COMPOUNDS 48-68 IN ACTIVATING
TRANSCRIPTION OF THE CV-1 CELL LINE ^a.

Compound	Predicted EC ₅₀ (μM)					
	RARα	RARβ	RARγ	RXRα	RXRβ	RXRγ
<i>t</i> -RA (2)	0.347	0.080	0.030	N/A	N/A	N/A
9- <i>c</i> -RA(3)	0.195	0.050	0.040	0.100	0.200	0.140
48	6.610	14.500	0.140	0.890	0.260	0.870
49	0.813	7.760	8.910	5.010	1.620	1.700
50	6.460	10.700	2.240	0.930	0.350	0.710
51	0.617	0.220	1.050	0.120	0.150	0.170
52	22.390	9.330	13.500	7.410	1.350	12.000
53	2.040	0.180	0.030	6.760	9.550	89.100
54	6.310	0.230	0.060	2.950	6.760	41.700
55	2.040	0.590	0.060	0.930	0.980	5.750
56	22.390	1.860	30.900	4.900	4.370	0.200
57	2.400	0.660	1.050	0.290	0.170	0.190
58	0.330	0.150	0.410	0.130	0.120	0.180
59	20.890	4.270	1.820	0.280	0.280	0.130
60	0.350	0.040	0.030	72.400	70.800	166.000
62	0.520	0.310	0.030	0.650	0.350	0.420
62	0.148	0.040	0.220	67.600	42.700	4.680
63	1.550	0.050	0.980	1.620	1.740	0.510
64	1.350	0.260	2.450	0.620	1.660	0.190
65	8.910	9.550	7.760	0.520	0.420	0.140
66	1.660	0.130	0.550	0.080	0.290	0.120
67	2.820	5.750	3.470	1.820	1.290	0.100
68	3.450	5.980	4.123	2.134	2.412	0.095

^aThe EC₅₀ (μM) values for *t*-RA (2) and 9-*c*-RA (3) are experimental values.²⁸ The EC₅₀

Graph 1 represents the predicted relative activity of heteroarotinoids **48-68** and *t*-RA [**(2)**, actual experimental value] to that of 9-*c*-RA (**(3)**) which was arbitrarily set to 100% for each RAR and RXR receptor isotype. Heteroarotinoids **59**, **63** and **64** appear to have predictable good activity with RAR α as seen from Graph 1. However, compound **59**



Graph 1. Relative percentage of EC₅₀ for compounds **2** and **45-65** when compared to pan-agonist 9-*c*-RA (**(3)**) which is 100%. When isotype bars are missing for a specific compound, this signifies that the predicted activity is close to zero with respect to 9-*c*-RA (**(3)**). a = α , b = β , g = γ .

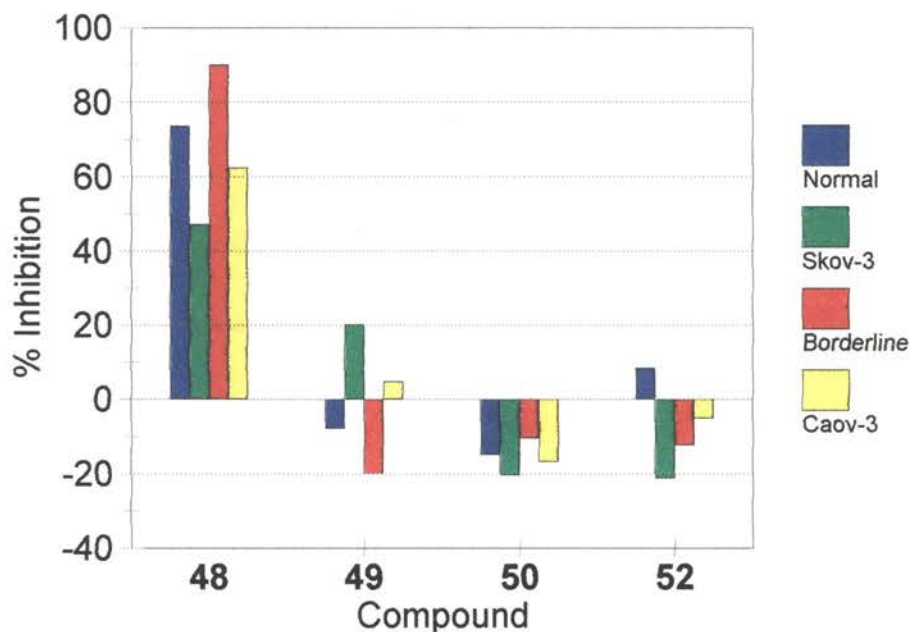
appears to have predictable pan-agonist activity, and **63** and **64** are also predicted to be RAR γ and RAR β active, respectively. Besides moderate predicted activity of compound

appears to have predictable pan-agonist activity, and **63** and **64** are also predicted to be RAR γ and RAR β active, respectively. Besides moderate predicted activity of compound **64** in RAR α , it would appear that **64** may be RAR β specific (yellow bar). Heteroarotinoids **53-55** and **65** have predictable specificity for activation of RAR γ (blue bar). None of the compounds seem to be specific for RXR α (gray bar). Nevertheless, moderate RXR α activity is predicted for heteroarotinoids **51** and **58**, and high activity is predicted with **59** and **67**. The RXR β specific activity (green bar) would appear to be true for **48** and **50**, although with low activity inducement. Heteroarotinoids **51**, **57**, and **58** would have high predicted RXR β activity and specificity.

Somewhat surprising are the predictions for compounds **66** and **68** as RXR γ (magenta bar) specific. Another highly active, but non-specific RXR γ ligand, appears to be compound **67**, and heteroarotinoids **56** and **67** are also envisioned to be highly selective and with high activity for RXR γ .

Of the tested heteroarotinoids **48-50** and **52**, only **48** showed promising activity in the inhibition of cancer growth (Graph 2) in ovarian cancer cells. This finding is in agreement with the data (see Experimental) obtained from docking ligand **48** into the LBP of RAR γ , in which **48** interacted in a favorable fashion with the receptor. However, compounds **49**, **50**, and **52** did not. Compound **50**, which differs from **48** in having oxygen instead of sulfur in the linker moiety and a carboxylic anion instead of a nitro group at the polar end of the molecule, expressed a different mode of docking than did **48** despite conformational similarities (Figure 10). The orientation of the hydrophobic region of ligand **50**, with respect to the amino acid residues of the LBP, was different from the

orientation in **48**. The C6 methoxy group in **48** lays parallel to the Phe 230 (red) whereas in **50** the C6 methoxy is orthogonal to the same residue. The distances between the the Ser 289 residue and carbonyl group of **50** and the nitro group of **48**, with which active retinoids H-bond, are 4.38 Å and 3.07 Å, respectively. Perhaps this is a major reason why compound



Graph 2. Percent inhibition of cancer growth in ovarian cancer cell lines by compounds **48-52**.

50 did not dock favorably into the LBP of RAR γ and why **50** exhibited a poor inhibition effect on the cancer cell lines tested. The nitro group of **48**, because of its polarity, makes stronger H-bonds than the carbonyl group of **50**. After ligand **50** was taken into the LBP, H-bonds were established, and the conformational change that took place resulted in strong hydrophobic interactions between the ligand and the receptor at the *non-polar region of the*

ligand. Because of weaker H-bonds in **50** versus **48** and the strong hydrophobic interaction, the former was pulled deeper into the hydrophobic core of the receptor, which may have caused a weakening in the H-bond. A reorientation of **50** occurred in such a way that it no longer exhibited the same effect on the receptor as did **48**.

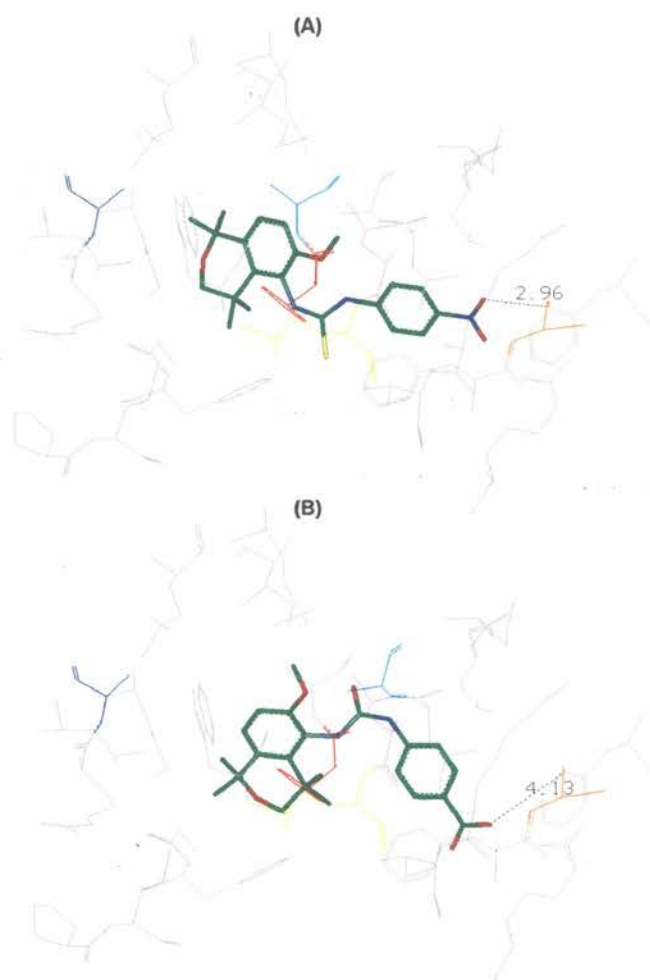
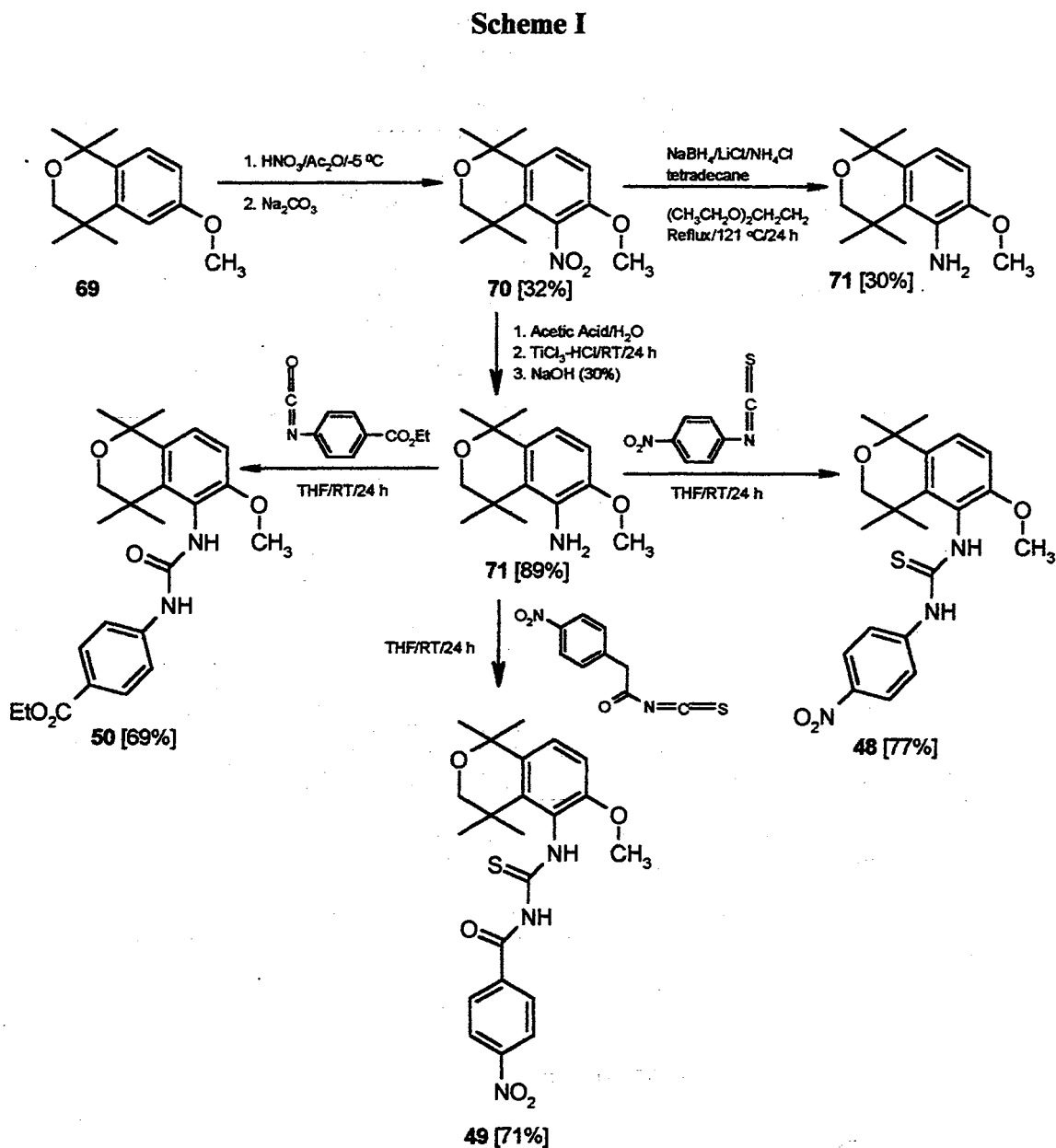


Figure 10. Docking of flexible heteroarotinoid **48** (A) and **50** (B) into the rigid LBP of the crystallographic structure of RAR γ . The nitro group of active **48** in RAR γ was positioned in closer proximity (2.96 Å) to the OH group of Ser 289 (H-bonding site) than was the carbonyl group of RAR γ inactive **50** (4.13 Å). The corresponding distance in the crystallographic structure in the LBP of RAR γ co-crystallized with *t*-RA (**2**), was 2.76 Å.¹⁴

Synthesis of Oxygen Heteroarotinoids

The key starting material for heteroarotinoids **48-50** was 6-methoxy-1,1,4,4-tetra-methylisochromane (**69**), which was synthesized using a published methods (Scheme I).⁸⁷ Nitration of **69** with a mixture of acetic anhydride and concentrated nitric acid at $-5\text{ }^{\circ}\text{C}$ yielded a mixture of products with nitro groups being added at the C5 (30%), and the C7

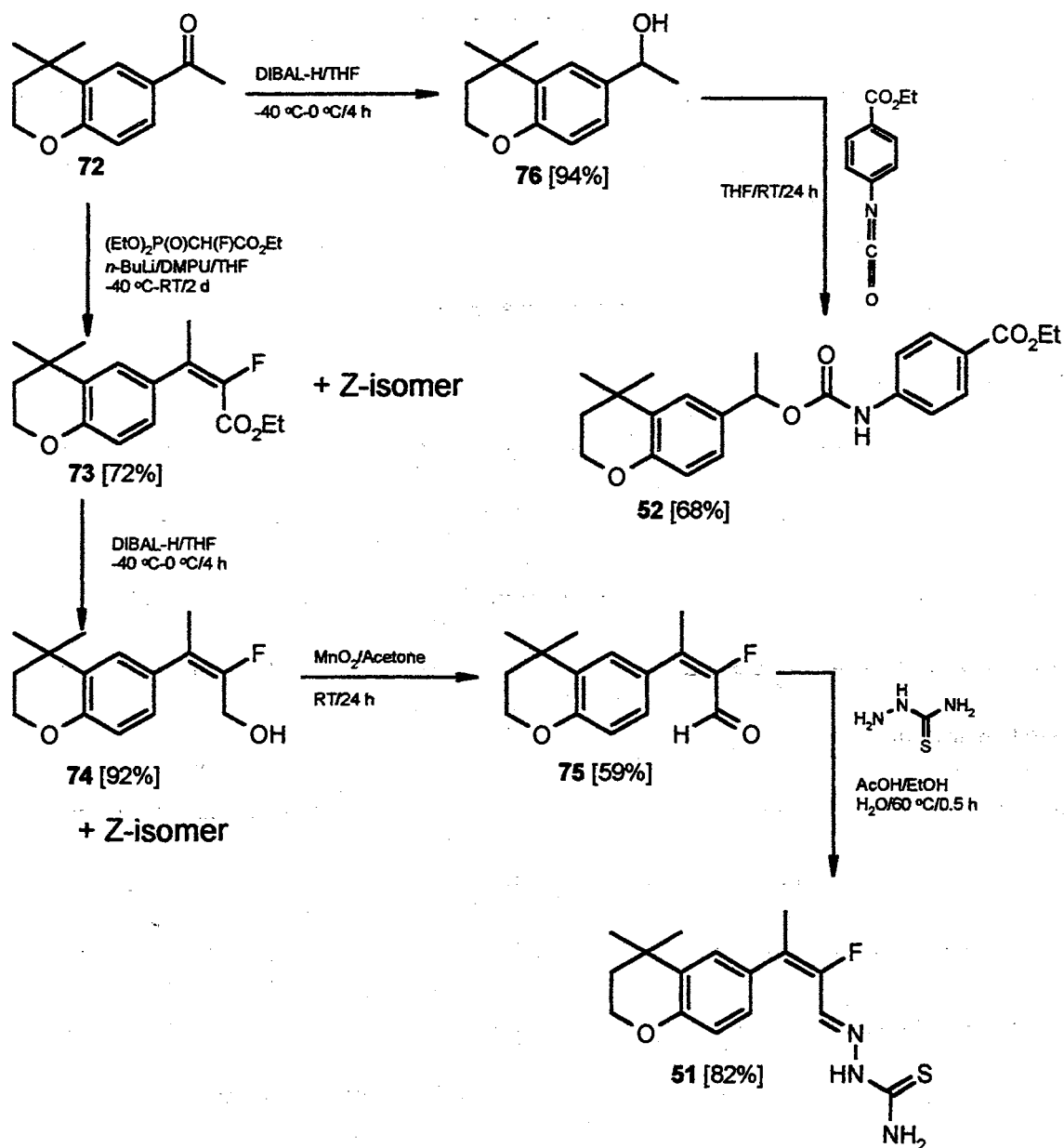


(50%) positions, along with a compound dinitrated at the C5 and C7 (10%) positions of the

benzene ring. The nitrated 5-isomer **70** was separated from the mixture via flash chromatography and then reduced with a $\text{NaBH}_4/\text{LiCl}/\text{NH}_4^+\text{Cl}^-$ complex in ethylene glycol diethyl ether.¹¹³ However, this type of reduction failed to give a reasonable yield (30%) of **71** even at reflux (121 °C) for 24 hours. Reduction of **70** with a titanium (III) chloride-HCl complex¹²⁵ in acetic acid-water as a solvent, followed by workup of the reaction mixture with 30% NaOH, gave 6-methoxy-1,1,4,4,-tetramethylisochroman-5-yl-amine (**71**) in good yield (89%). The reaction of **71** with 4-nitrophenylisothiocyanate, (4-nitrophenyl)oxomethane isothiocyanate, and ethyl 4-isocyanatobenzoate in dry THF at room temperature afforded compounds **48**, **49**, and **50**, respectively, in reasonable yields as shown.

1-(4,4-Dimethylchroman-6-yl)ethan-1-one (**72**), which was synthesized according to a previously published method from our laboratory,⁸⁷ was used as an intermediate for the synthesis of **51** (Scheme II). A Horner-Emmons type reaction of **72** with triethyl 2-fluorophosphono- acetate, in the presence of *n*-BuLi and DMPU in dry THF, gave ester **73** as a mixture of *E* and *Z* isomers.¹²⁰ The separation of the *E* isomer **73** from its *Z* counterpart proved to be more difficult than separating the *E* and *Z* isomers of alcohol **74**. The latter was obtained by the reduction of **73** with DIBAL-H at -40 °C. The *E*-isomer of **74** made up 57% of the mixture. Several attempts to reduce the unsaturated ester **73** directly to aldehyde **75**, as reported by Zakharin and coworkers, failed.¹⁴¹ The product was a mixture of an alcohol and an aldehyde even when 1.0 equivalent of DIBAL-H was added dropwise to **73** at -78 °C, and yields of the desired aldehyde (<10%), after separation from the alcohol, were unacceptable. However, the *E*-aldehyde **75** was obtained from **74** through oxidation with

Scheme II

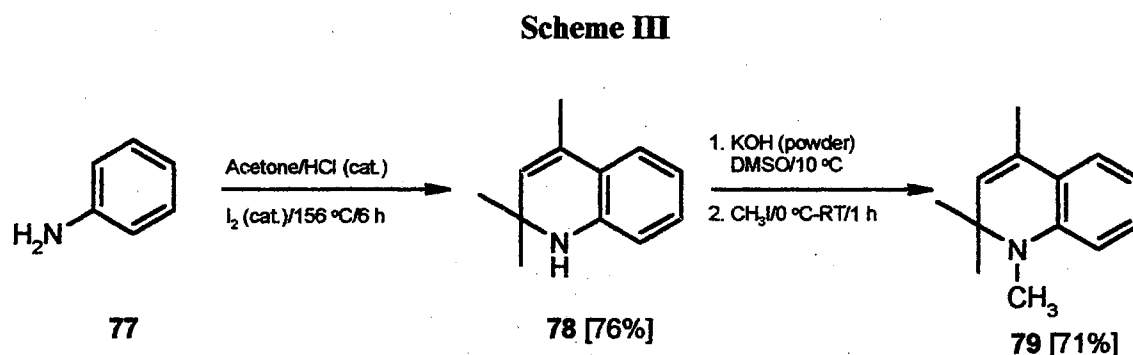


MnO_2 in acetone at room temperature with an overall yield of 54% from **73**. Reacting aldehyde **75** with thiosemicarbazide dissolved in water with few drops of acetic acid afforded heteroarotinoid **51** as a white solid in good yield (82%).⁴⁴ The reduction of ketone **72**, which was followed by a reaction of the resulting alcohol **76** with ethyl isocyanatobenzoate in THF, yielded the 4-atom linker heteroarotinoid **52** as a white solid

(69%).

Synthesis of Nitrogen Heteroarotinoids

A somewhat unusual reaction of aniline (**77**) with acetone, which was added at 156 °C and in the presence of catalytic amounts of HCl and iodine, led to the formation of 2,2,4-trimethyl-1,2-dihydroquinoline (**78**) (Scheme III). Interestingly, compound **78** was obtained

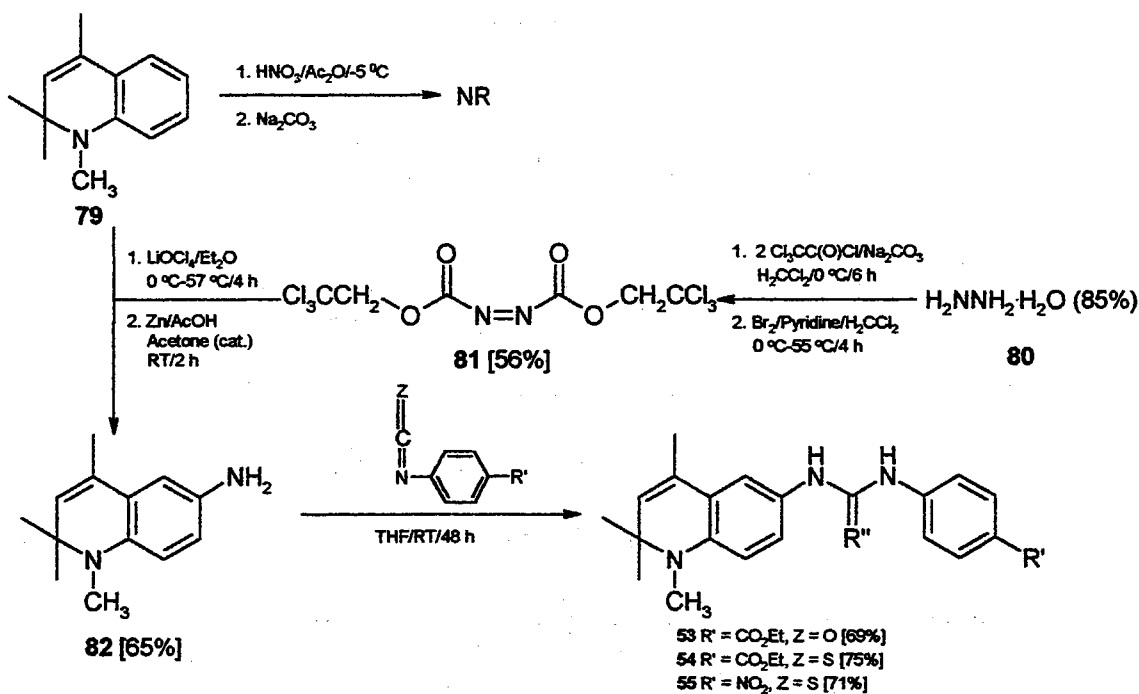


as a by-product as reported by deKoning and co-workers²⁹ in attempts to synthesize 4-(*N*-phenylamino)-4-methyl-2-pentanone [even in absence of HCl, **78** (identified by ¹H NMR) made up 80% of the mixture (52% overall yield) when separated from 4-(*N*-phenylamino)-4-methyl-2-pentanone].²⁹ However, the above method was convenient for our purposes where unsaturation in the heterocyclic ring was desired, and an addition of two equivalents of acetone and the subsequent cyclization of the ring allowed a one pot reaction. The yield (76%) of **78** from **77** was increased by addition of catalytic amount of HCl as compared to reported yields (40%).²⁹ On average, the *N*-methylation of **78** with dimethyl sulfate to give **79** resulted in 20% lower yields as opposed to methylation with methyl iodide in DMSO and KOH. 1,2,2,4-Tetramethyl-1,2-dihydroquinoline (**79**) was the key precursor for the nitrogen heteroarotinoids.

The amination procedure used in the reaction sequence **69**→**70**→**71** (Scheme I) was

not successful for the preparation of amine **82**. Perhaps the harsh acidic conditions for nitration and successive reduction of the nitro moiety to an amine group were responsible for the reaction failure. After reviewing several amination procedures for an arene ring, the most suitable method for **79**→**82**→**53** (**54,55**) appeared to be that reported by Leblanc and co-workers.⁷⁷ The conversion of **80** to **81** [bis(2,2,2-trichloroethyl) azodicarboxylate (**81**)] gave an excellent source of positive nitrogen for electron rich arenes (Scheme IV).⁷⁷ Reagent **81** was synthesized from the reaction of hydrazine hydrate (**80**) with two equivalents of 2,2,2-trichloroethyl chloroformate in the presence of sodium carbonate. Interestingly, after

Scheme IV

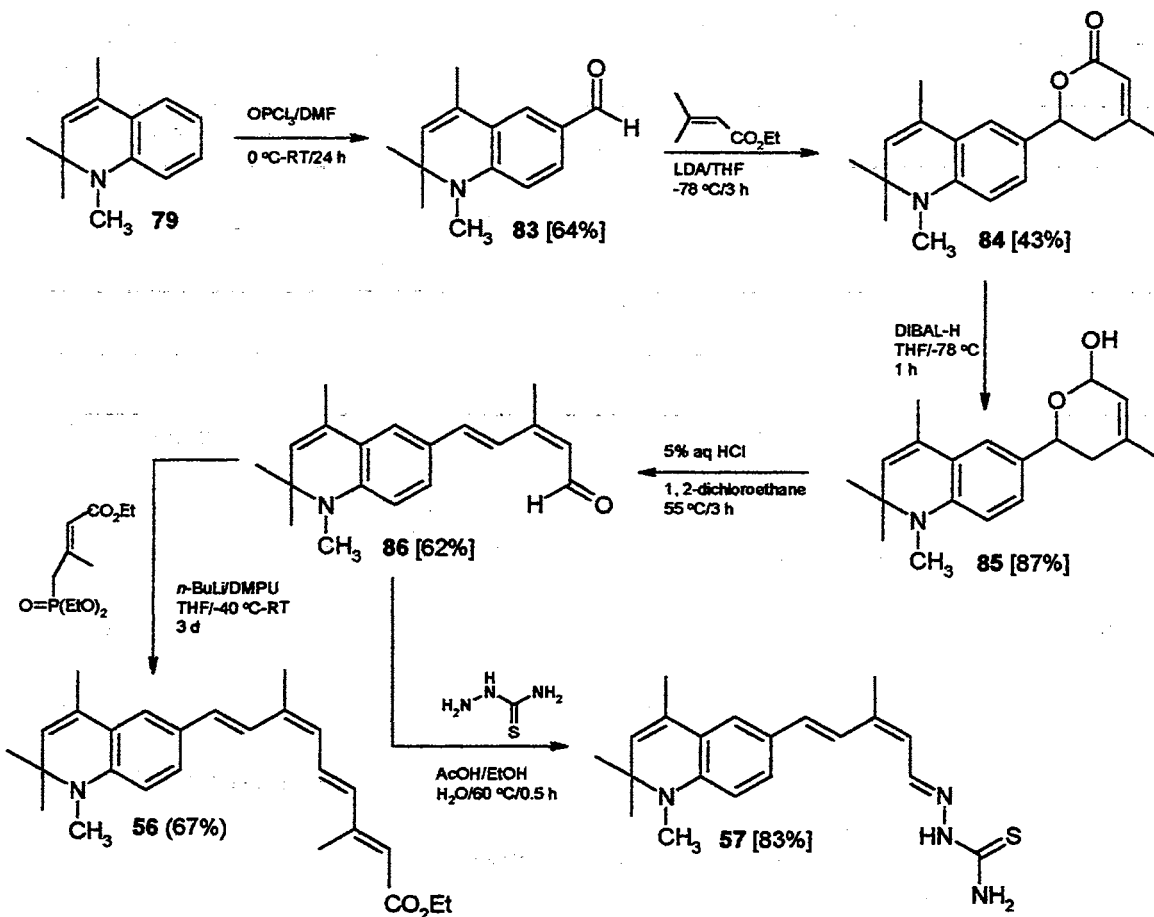


workup, the resulting intermediate from **80** was oxidized with Br_2 in pyridine^{76,121} to yield **81** (56% from **80**). Amine **82** was obtained via a convergent synthesis involving **79** and **81**. 1,2,2,4-Tetramethyl-1,2-dihydroquinoline (**79**) was allowed to react with azo derivative **81** in a solution (3M) of lithium perchlorate dissolved in dry diethyl ether, a process which was

followed by reduction of the product with zinc in acetic acid.⁷⁶ Three-atom linker heteroarotinoids **53-55** were then procured via a reaction of amine **82** with the respective isocyanates or isothiocyanates.

Heteroarotinoids **56** and **57** differ somewhat from 9-*c*-RA (**3**) where the *cis* arrangement of the double bond was moved from the C9 position to C11. Treatment of 1,2,2,4-tetramethyl-1,2 dihydroquinoline (**79**) with a DMF-OPCl₃ complex at 0 °C in a Vilsmeier-Haack reaction resulted in the production of aldehyde **83** (64%) (Scheme V).¹⁹

Scheme V

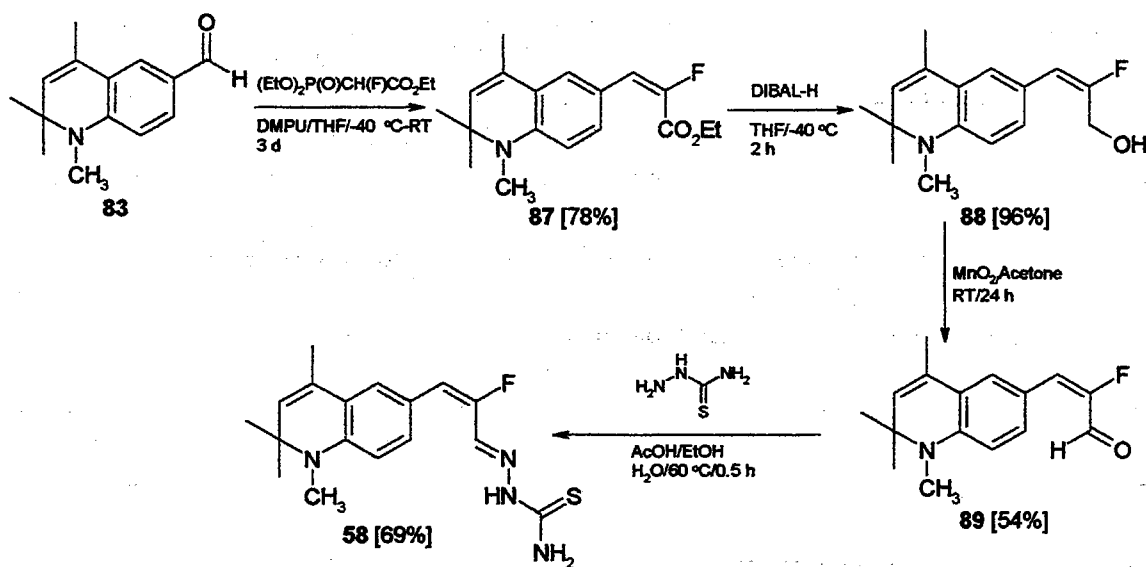


Reaction of aldehyde **83** with the lithium anion derived from ethyl 3,3-dimethylacrylate gave

lactone **84**.⁷ The strategic introduction of the 11-*cis* double bond was efficiently performed by means of a DIBAL-H reduction of **84** to give lactol **85** (87%) which was then transformed upon treatment with HCl in dichloroethane to 11-*cis* aldehyde **86**.⁷ The chain extension of **86** into ester **56** was accomplished by a Horner-Emmons type reaction of triethyl 3-methyl-4-phosphonocrotonate (*trans:cis*, 4:1) with aldehyde **86** in the presence of *n*-BuLi and DMPU. Heteroarotinoid **57** was obtained when 11-*cis*-aldehyde **86** and thiosemicarbazide were allowed to react in an ethanol-water mixture as solvents at 60 °C.

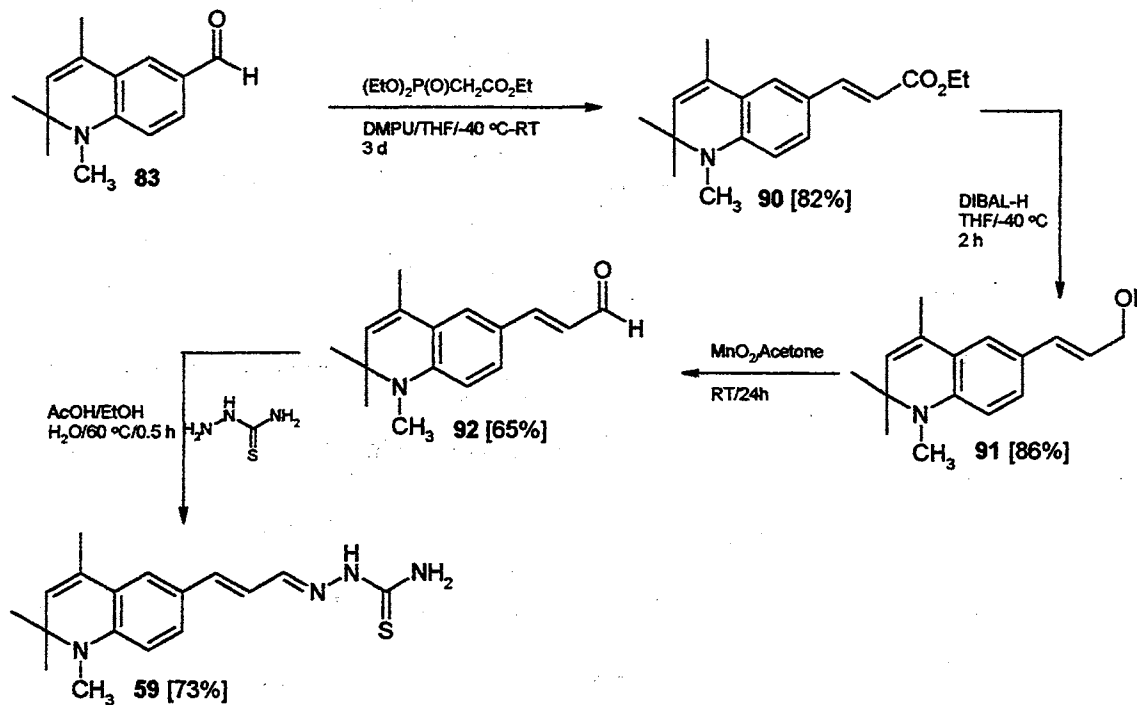
Treatment of aldehyde **83** with the anion of triethyl 2-fluoro-2-phosphonoacetate in THF at -40 °C generated ester **87** as an *E* isomer only (Scheme VI) as opposed to the generation of ester **73** in which both *E* and *Z* isomers were formed (Scheme II) for reasons unknown. The reduction of **87** to **88**, and subsequent oxidation, resulted in aldehyde **89** which was converted to **58** as shown.

Scheme VI



Heteroarotinoid **59** was synthesized by the reaction sequence **83**→**90**→**91**→**92**→**59** (Scheme VII) which is similar to the reaction sequence **83**→**87**→**88**→**89**→**58** described earlier (Scheme VI). Thiosemicarbazide reacted with aldehyde **92** (Scheme VII) and afforded the locked, fluorinated *E*- isomer **59** with different properties at the polar end.

Scheme VII

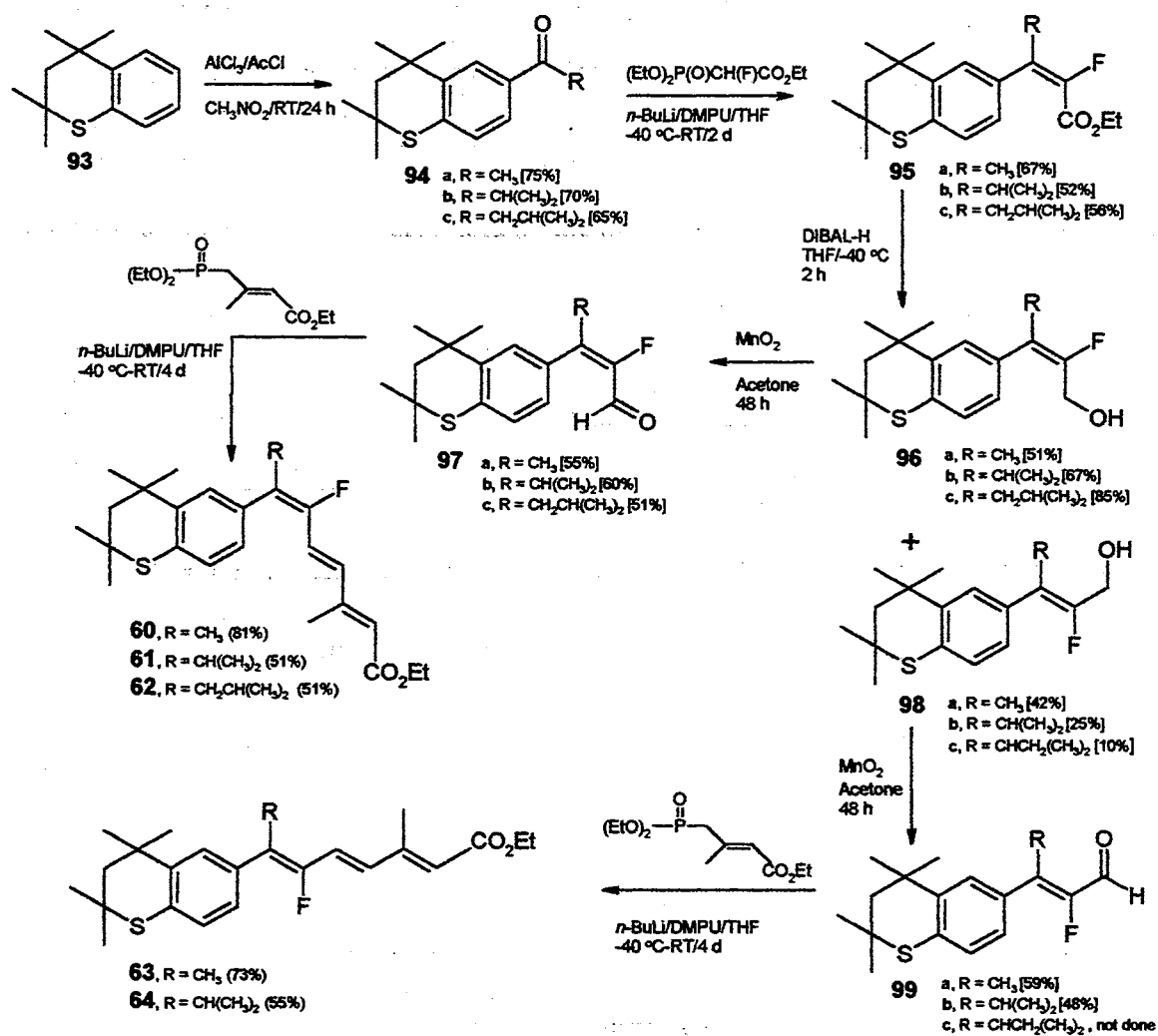


Synthesis of Sulfur Heteroarotinoids

Thiochroman **93** was synthesized (Scheme VIII) according to modified procedures reported from our laboratory.¹²⁵ Acylation of **93** by acetyl chloride, isobutyryl chloride, or isovaleryl chloride in the presence of a Lewis acid, resulted in ketones **94a**, **94b**, and **94c**, respectively. The yields from these reactions were directly proportional to the size of the R group in the acylating reagent. The condensation of the Horner-Emmons reagent, triethyl 2-fluoro-2-phosphonoacetate, with ketones **94a-c** yielded esters **95a-c**. The DIBAL-H reduction of these esters afforded the easily separable *E*- and *Z*-isomers of alcohols **96a-c**

plus **98a** and **98 b**, respectively. Interestingly, the size of the R group may also play a role in determining the *E/Z* isomeric ratio. The larger the R group, the less *Z*-isomer could be recovered. A conformational search, done via computer modeling using the program Discover³⁰ where the torsional force and the V092 algorithm were options for searching and minimizing new conformations, respectively, revealed that the larger the R group, the more the side chain was displaced from conjugation with the arene ring. When the R group was methyl, the angle between the benzene ring and the double bond of the chain for minimal

Scheme VIII

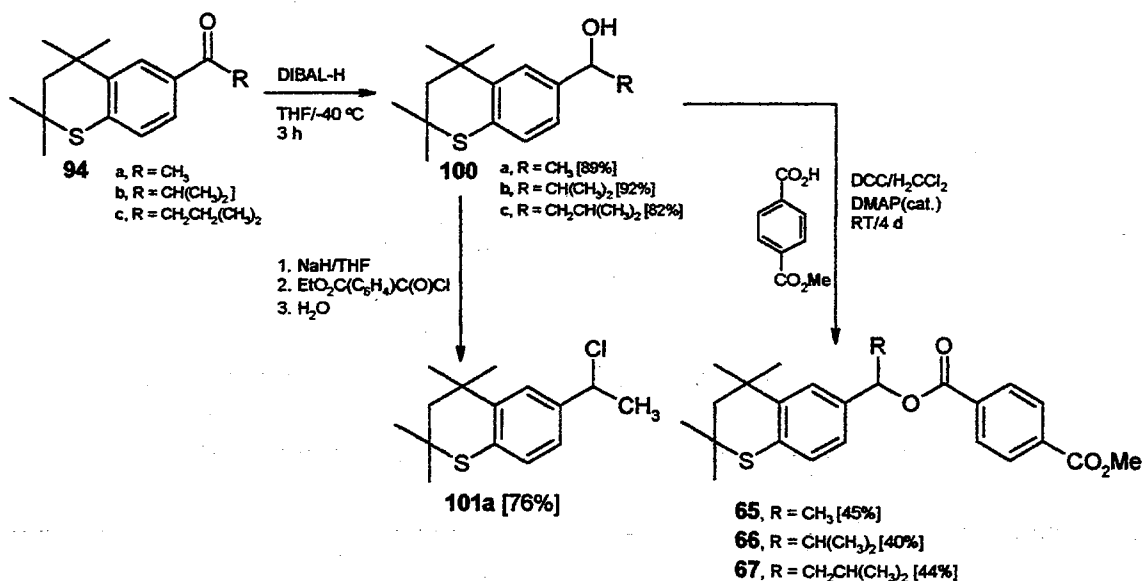


energy conformation was approximately 15 degrees. This angle became $\sim 45^\circ$ and $\sim 60^\circ$ when the R groups were isopropyl and isovaleryl, respectively. Perhaps it may be the combination of the out of plane angle between the arene ring and the side chain double bond and the presence of fluorine that are responsible for the direction of the Horner-Emmons anion attack on the carbonyl carbon. Only a small amount of the alcohol *Z*-isomer **98c** could be recovered after separation from the *E*-isomer **96c**. The alcohols **96a-c** and **98a,b** were oxidized to aldehydes **97a-c** and to **99a,b**, respectively. These aldehydes were then converted to the final heteroarotinoids **60-62**, **63**, and **64**, respectively.

Reduction of ketones **94a-c** by DIBAL-H led to the formation of alcohols **100a-c** in very good yields (Scheme IX). Treatment of alcohol **100a** with sodium hydride in THF, followed by the addition of methyl 4-(chlorocarbonyl)benzoate and workup with water, led to a substitution reaction of the alcohol functional group by chlorine and production of **101a**. The required final product **65** was not obtained (reaction procedure is described in Experimental). Diesters **65-67** were the products of an alternative procedure where alcohols **100a-c** were esterified via the addition of monomethyl terephthalate in the presence of DCC and a catalytic amount of DMAP. However, the yields of these reactions were low possibly due to steric hindrance of the R groups. When R was the isopropyl group, the yields were the lowest, a possible indication that the isopropyl moiety presents a larger bulk than the isovaleryl group in which the tertiary carbon is further removed from the OH group in **100**.

The synthetic procedure to obtain the 7-methylthiochroman **102** was essentially the same as that used to produce thiochroman **93**.¹²⁵ The presence of a methyl group at the C7-position was reasoned to possibly increase the selectivity of the ligand **68** by the RAR γ

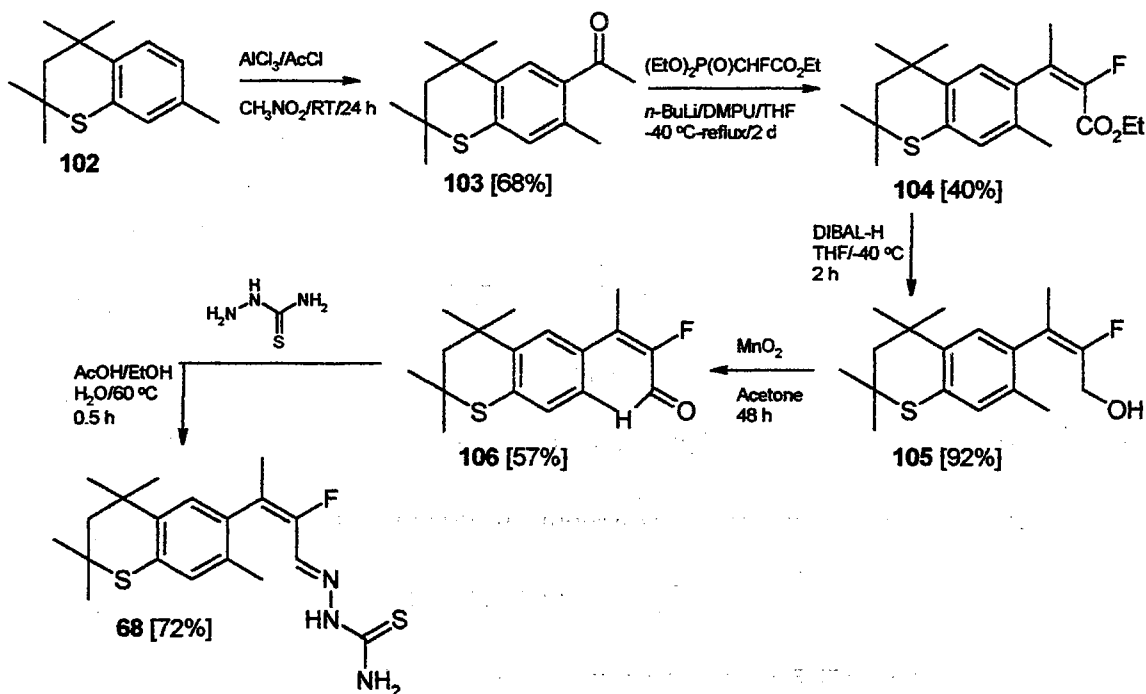
Scheme IX



receptor via altering the rotational barrier of the side chain. The reaction sequence $93 \rightarrow 94 \rightarrow 95 \rightarrow 96 \rightarrow 97$ described previously (Scheme VIII) was the model for the conversion of $102 \rightarrow 103 \rightarrow 104 \rightarrow 105 \rightarrow 106$ (Scheme X). However, the yields for the Horner-Emmons reaction to produce ester **104** were lower (even at reflux) than for its counterpart **95** which does not have a C7 methyl group. Intriguingly, in addition to inducing lower yields, the C7 group may play a vital role in *E/Z* isomer selectivity. The Horner-Emmons reagent used in the condensation with ketone **103** produced an *E/Z* isomer ratio (85:15) that was much higher than in the unmethylated C7 counterpart **95a** (55:45) (Scheme VIII). Molecular modeling also showed that the conformations of intermediates **103-106** had a 20 degree larger angle (35 degrees compared to 15 degrees), with respect to the side chain and the aryl ring than in intermediates **92a-95a**. Therefore, besides reduction of the conjugation between the arene ring and the double bonds of the side chain, the C7 methyl group may also direct the attack of the Horner-Emmons anion on the carbonyl group in **103**.

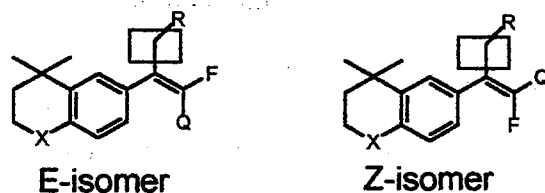
The *E/Z* isomeric ratio for compounds **74**, **96a-c**, **98a-c**, and **105** and proton chemical shifts of the groups attached to the C=C are in the Table III. The ^{19}F chemical shifts were

Scheme X



referenced to the trifluoroacetic acid-OD. It appears that the ^{19}F absorbance in the *E*-isomer is at a lower frequency than in the *Z*-isomer.⁵⁸ This is consistent with the proximity of the fluorine atom to the aryl ring as seen from molecular modeling.

In the *Z* isomers, the fluorine atom is positioned closer to the plane of the benzene ring and more deshielded. Therefore, one might expect ^{19}F chemical shifts to be more downfield in the *Z* isomers than in the *E* isomers. Interestingly, in the *Z* isomers the methyl,



the methylene, and the methine hydrogens (square box in representative compounds below) adjacent to the double bond appear to be more de-shielded than in the respective *E* isomers analogs. The coupling constants between the adjacent hydrogen(s) and fluorine were larger for the *E* isomer, and these values were consistent for all isomeric pairs. This could imply

TABLE III

NMR ANALYSIS OF $^4J_{\text{H-F}}$ COUPLING IN THE *E/Z* ISOMERS. ^a

Compound	<i>E/Z</i> Ratio	δ_{H} (ppm)	$^4J_{\text{H-F}}$ (Hz)	δ_{F} (ppm)
(<i>E</i>)-74	57:43	1.84	3.4	-118.49
(<i>Z</i>)-74		1.97	2.7	-117.21
(<i>E</i>)-96a	55:45	2.02	3.9	-117.76
(<i>Z</i>)-98a		2.03	3.3	-117.58
(<i>E</i>)-96b	61:39	2.86	2.7	-121.86
(<i>Z</i>)-98b		3.15	1.5	-115.28
(<i>E</i>)-96c	90:10	2.26	2.3	-128.49
(<i>Z</i>)-98c		2.64	1.4	-118.86
(<i>E</i>)-105	85:15	1.93	3.3	-120.93
(<i>Z</i>)-105		1.95	2.2	-114.64

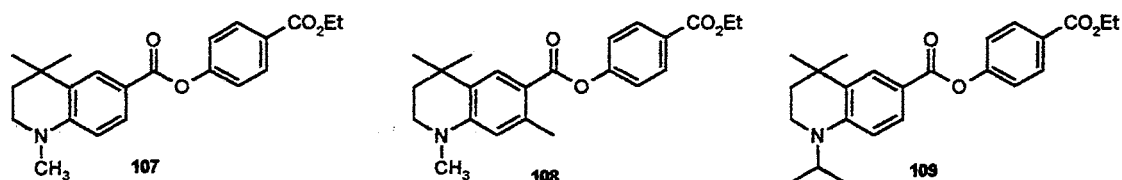
^aThe assignment of stereochemistry was by the Pawson method.¹⁰⁵

that the primary influence of fluorine on the hydrogen atoms mentioned above is due to the size and proximity of the former to the latter, and heteronuclear influence via bond proximity may play role in hydrogen splitting.

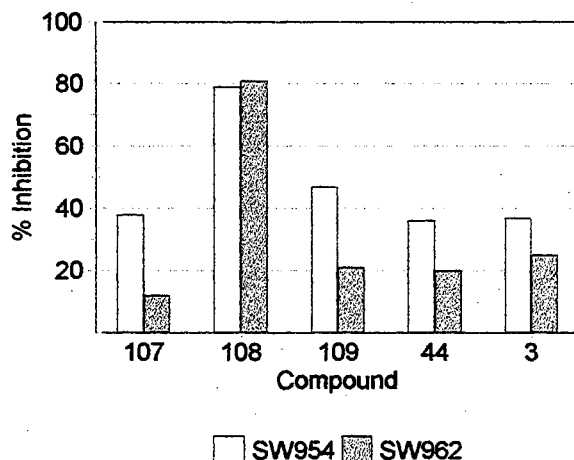
Structure-Activity Relationship (SAR) Study Via Molecular Modeling

The use of computer-aided analyses is becoming a standard method for evaluating structure-activity relationship analysis of new drugs and in the design of new medicinal

agents. To gain better insight into retinoic acid receptor interaction with ligands for the purpose of drug design, the binding of three compounds previously synthesized in our laboratory was assessed in terms of developing a rationale for the interaction with RAR γ . The heteroarotinoids 4-(ethoxycarbonyl)phenyl 1,4,4-trimethyl-1,2,3,4-tetrahydroquino-line-6-carboxylate (**107**), 4-(ethoxycarbonyl)phenyl 1,4,4,7-tetramethyl-1,2,3,4-tetrahydroquino-



line-6-carboxylate (**108**), and 4-(ethoxycarbonyl)phenyl 4,4-dimethyl-1-isopropyl-1,2,3,4-tetrahydroquinoline-6-carboxylate (**109**) were examined for docking in the RAR γ receptor via the use of the SYBYL 6.5¹²⁶ software package along with the docking program “Flexidock.” Due to the structural variations among compounds **107**, **108**, and **109**, differences in the activity of these compounds exist in terms of inhibiting cancer proliferation in two different cancerous vulvar cell lines (Graph 3).⁹ The heteroarotinoid **108** exhibited greater growth inhibition of the various cancer cell lines than did 9-*cis*-RA (**3**) or one of the most potent synthetic retinoids TTNPB (**45**).⁹ Such differences in biological activity may be directly proportional to the ability of an agent to bind and activate the RAR γ . As the data indicated, heteroarotinoid **108** activated the RAR γ better than did 9-*cis*-RA (**3**) (Table IV).⁹ In comparison to compounds **107** and **109**, which transactivate all receptors only moderately and without any specificities, considerable difference can be seen between the activation of RAR γ and the rest of receptors by **108**, where the latter appears to be a RAR γ specific transactivating ligand.⁹



Graph 3. Percent of Growth Inhibition of Cancerous Vulvar Cell Lines SW954 (Empty Bars) and SW962 (Gray Bars)

The activation of RAR γ by **108** posed questions in term of conformations involving the ligand-receptor interaction and differences in receptor activation of **108** from **107** since the former has only an additional methyl group at the C7 position. The latter heteroarotinoid has little or no influence on the activity of the receptor. The heteroarotinoid **109**, which differs from **108** in that an isopropyl moiety is bound to the heteroatom instead of a methyl group and is void of a C7 methyl group, also did not activate the RAR γ to any measurable extent.⁹

Using the Flexidock program, heteroarotinoids **107-109** were docked into the LBP of RAR γ (data taken from the crystallographic structural information)¹⁴ to investigate the ligand-receptor interaction. Compounds *t*-RA (**2**), which is an RAR family agonist, 9-*c*-RA (**3**), (pan-agonist), **6** (RAR α specific), **39** (RAR β specific), **32**, and **40** (RAR γ specific) were docked for comparison purposes (Table I). In addition, the docking of *t*-RA (**2**) was to test the validity of the Flexidock program (see Experimental for molecular modeling). All of the compounds were docked as a carboxylic anion for the closest simulation of the biological

TABLE IV

**EC₅₀ VALUES AND EFFICACY DATA FOR THE TRANSACTIVATION OF
RETINOIC ACID RECEPTORS BY COMPOUNDS 107- 109.^a**

Heteroarotinoid		RAR			RXR		
		α	β	γ	α	β	γ
107	EC ₅₀ (nM) ^a	1128	256	NA	601	33	20
	(% efficacy) ^b	45	64	0	47	53	52
108	EC ₅₀ (nM) ^a	796	92	6	102	70	40
	(% efficacy) ^b	64	63	103	53	55	52
109	EC ₅₀ (nM) ^a	217	41	NA	12	47	27
	(% efficacy) ^b	59	71	0	62	45	47

^a The potency (EC₅₀) is the concentration of the compound that can induce one half of the maximal activity of the receptor. ^b The efficacy is derived from dividing the maximal activity induced by the heteroarotinoid by the maximal activity induced by the 9-*c*-RA (3). NA = not active.⁹

condition where carboxylic esters of retinoids were hydrolyzed and ligands exist as anions at a physiological pH of 7.4.^{17,52} Data from docking of a flexible ligand (a ligand has three degrees of translation, rotational degrees of freedom around each single bond and torsional degrees of freedom around dihedral angles) into the fixed crystallographic structure of the LBD of RAR γ are summarized in Table V. A total of five calculation trials revealed that the interaction energies (interaction energy is equal to the energy of ligand-receptor complex minus the sum of the energy of a receptor before docking plus the energy of the ligand before docking) of heteroarotinoid **108** with RAR γ were better than **107** but not better than for **109** or 9-*c*-RA (3).⁴ These results did not agree with the biological data (Table 4) where the efficacy of **108** was 103% in the vulvar cell line in comparison to **3** and superior in comparison to **109** which did not transactivate the RAR γ . These discrepancies

would suggest that the interaction energies of the flexible ligand-fixed receptor complex may be representative of the binding affinities of the ligand and receptor, but such may not be an indication of the level of receptor activation by the ligand.

TABLE V.

DATA FROM DOCKING THE FLEXIBLE LIGANDS INTO THE FIXED CONFORMATION OF RAR γ LBD CRYSTALLOGRAPHIC STRUCTURE.^a

Ligand	Energy of Interaction (Kcal/mol)				
	R1 (25,000)	R2 (20,000)	R3 (15,000)	R4 (30,000)	R5 (10,000)
<i>t</i> -RA (2)	-64.64	- 58.29	- 34.71	- 75.73	- 33.5
9- <i>c</i> -RA (3)	-15.38	- 9.32	- 7.44	- 17.33	- 5.38
107	8.35	12.58	21.49	5.38	22.98
108	2.47	3.61	5.72	- 1.36	9.34
109	-37.52	- 30.63	- 29.51	- 45.29	-25.61

^aThe notation R1 is the designation for the first trial, R2 for second, etc. The number following the trial designation (25,000) is the generation number, that is the number of calculations which the program generates through adjustments of the translation of ligand in the LPB, rotation around ligand single bonds, and torsion about dihedral angles. Exactly 10,000 new conformations of the ligand are then generated for each generation. The calculation of interaction energies between 10,000 different conformations of the ligand and receptor is followed by scoring the results by picking the 20 conformations of the ligand with the best interaction energies with respect to the receptor. This process is then repeated 25,000 times. The higher the generation number, the more conformations are generated until the program examined that number of conformations where the energies of interaction remain essentially constant, and the results converge toward the 20 best ligand-receptor interacting conformations. Once the receptor is fixed, its conformation does not change.

One of the options for explaining the above observation is that the resulting crystal structure¹⁴ of RAR γ , which was co-crystallized with *t*-RA (2), although it may be in a minimal energy conformation, is not the active conformation of RAR γ . Another possibility is that some of the amino acid conformations within the crystal structure of the LBP of RAR γ are not important in the selectivity and activity of RAR γ . In addition, the more rigid

nature of the system in a flexible ligand-fixed receptor type of docking could prevent 108 from proper orientation for interaction with receptor. Conceivably, the crystal structure of RAR γ may deviate slightly from the active conformation of the receptor. Actually, computer matching of the crystal structure of RAR γ to the resulting conformation of RAR γ after a flexible ligand-flexible receptor docking with *t*-RA (2), and the subsequential removal of the ligand, revealed only small differences in conformational energies. The root-mean-square-deviations (RMSD) of the LBP of RAR γ crystal structural amino acid residues superimposed upon the resulting conformation of the residues of the flexible LBP of RAR γ , after *t*-RA (2) docking, were less than 0.01 Å in most of the cases with only a few differences as in: Phe 201 (RMS = 0.1931 Å), Lys 236 (0.452 Å), Cys 237 (0.420 Å), Arg 278 (0.185 Å), Ser 289 (0.423 Å), Leu 400 (0.128 Å), Ile 412 (0.236 Å), and Met 415 (0.121 Å) observed. These small deviations of RMS values of less than 0.5 Å were considered to be a match via modeling of non-related systems.¹³⁹ The resulting conformation of the LBP of RAR γ after *flexible-flexible* docking, agreed reasonably well with that of the crystallographic structure of the LBP of RAR γ . Nevertheless, the crystallographic structure¹⁴ of RAR γ co-crystallized with *t*-RA (2) may or may not be the active conformation of RAR γ in solution.

The conformations of *all* the amino acids in the LBP of RAR γ , with deviation values noted above, are not considered to play a major role in ligand selectivity and receptor activity.¹⁴ This notion was further supported by mutagenic studies done on the LBD of RAR γ where three amino acid residues (Ala 234, Met 272, Ala 396) were found to be responsible for the selectivity of a ligand and one amino acid (Phe 230) was found to be responsible for the activation of receptor RAR γ .^{14,68,74,104} The interpretation of the results

from Tables 4 and 5 could then imply that compounds **109** and 9-*c*-RA (**3**), which activate RAR γ less than **108**, favorably interact with residues of the LBP which are not important for activation of RAR γ . In contrast, **108** does not interact to the same extent with the same residues of the LBP as do **109** and **3**.

The direct consequence of favorable interactions of compounds **109** and 9-*c*-RA (**3**) with amino acid residues that are *not* important for activation of RAR γ is the unfavorable interaction of **109** and **3** with residues that *are important* for the activation of receptor. This proposition was further supported via docking flexible ligands into the flexible LBP of RAR γ where all bonds in the crystallographic structure of RAR γ were allowed to have the same degree of freedom as a ligand, and backbone rotation was also allowed (Table VI; the lower energy, the more favorable the interactions between the ligand and the amino acid residues; also see Figure 11). The *flexible-flexible* method of docking was to permit the atoms of the ligand and amino acid residues of the LBP to rearrange so as to obtain the minimum interaction energy. The resulting conformations of the LBP of RAR γ (void of the ligand), after docking **107**, **108**, **109**, and **3**, were mathematically analyzed and visually compared with the resulting conformation of the LBP of RAR γ after docking *t*-RA (**2**) which was then removed after docking (Figure 12).

Superimposition of the resulting conformations of the receptor's LBP, after **108** was docked and then removed, on the resulting conformation of the LBP of RAR γ , after *t*-RA (**2**) was docked and removed, revealed only slight differences in RMSD values within the following residues: Phe 201 (0.397Å), Leu 233 (0.805Å), Lys 236 (1.192Å), Cys 237 (0.42Å), Ile 275 (0.185Å), Arg 278 (0.595Å), Ser 289 (0.339Å), Phe 304 (0.134Å), and Met

408 (0.478Å). However, the RMSD values resulting from the superimposition for the amino acid residues important in the selectivity and activity of RAR γ were less than 0.1Å, which signifies a reasonable match. The spatial arrangements of Phe 230, Ala 234, Met 272, and Ala397 residues in the LBP with 108 docked, in comparison to the same residues of the

TABLE VI

INTERACTION ENERGIES BETWEEN THE LIGANDS AND THE LBP OF RAR γ IN THE FLEXIBLE LIGAND-FLEXIBLE RECEPTOR DOCKING MODE.^a

Ligand	Interaction Energy (Kcal/mol)	
	R1 (60,000)	R2 (45,000)
<i>t</i> -RA (2)	- 140.34	- 123.56
9- <i>c</i> -RA (3)	- 120.36	- 99.97
107	- 57.08	- 46.24
108	- 122.49	- 117.69
109	- 88.52	- 85.53

^a In the flexible-flexible docking mode, all ligands docked favorably with different energetic changes for the ligands and receptors, which ultimately produced conformations of receptors that were analyzed.

LBP with docked *t*-RA 2), were essentially the same. The receptor conformation of RAR γ , after 9-*c*-RA (3) was docked, removed, and compared to the conformation of the receptor after *t*-RA (2) was docked, differed in several (residues Phe 230 (0.202Å), Lys 236 (0.698Å), Phe 230 (0.501Å), Ser 231 (0.415Å), Met 272 (1.061Å), Ser 289 (0.378Å), Phe 304 (0.143Å), Leu 307 (0.263Å), Arg 396 (0.151Å), Ile 412 (0.462Å), and Ile 275 (0.435Å). The RMSD values for the amino acid residues for the RAR γ -inactive heteroarotinoid 107 from *t*-RA-induced conformation of the receptor were: Phe 201 (0.274Å), Phe 230 (0.832Å), Ser 231

(0.364Å), Lys 236 (1.655Å), Cys 237 (0.420Å), Met 272 (1.358Å), Ile 275 (0.235Å), Ser 289 (0.524Å), Phe 304 (0.154Å), Arg 396 (0.146Å), Leu 400 (0.338Å), Met 408 (0.174Å), Ile 412 (0.144Å), and Met 415 (0.121Å). The RMSD values for the conformations of residues of the LBP of RAR γ , after the RAR γ -quiescent heteroarotinoid **109** was docked, as

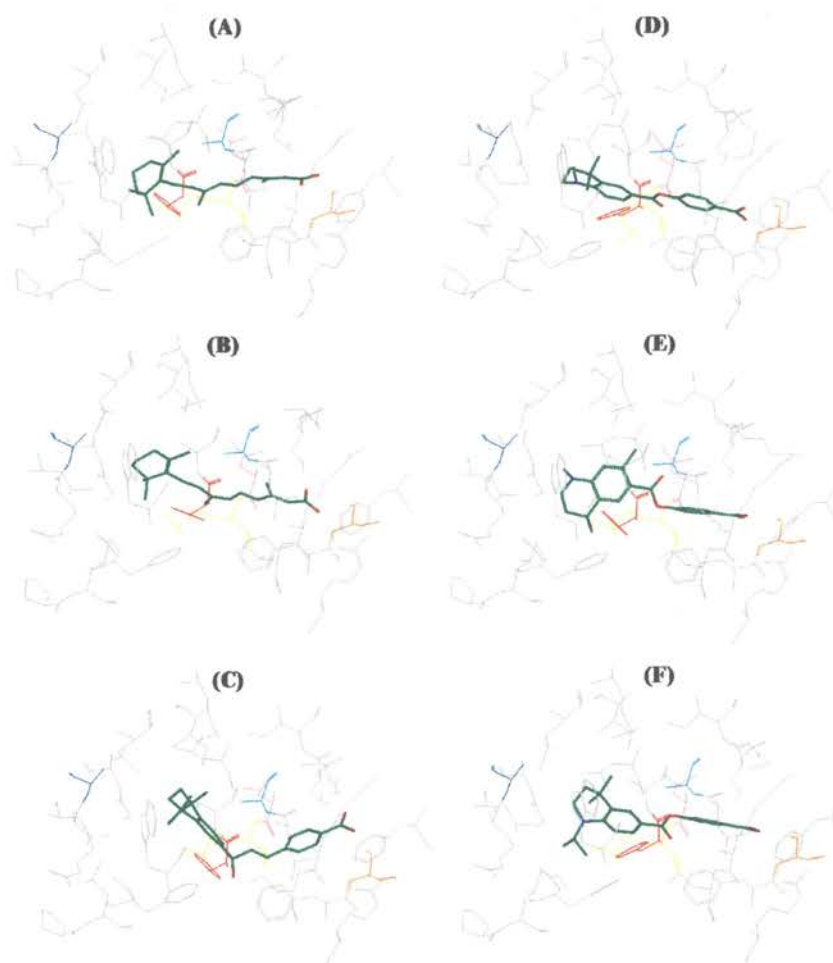


Figure 11. Compounds **2** (A), **3** (B), **40** (C), **107** (D), **108** (E), and **109** (F) docked into the flexible LBP of RAR γ . The amino acids Phe 230 (red), Ala 234 (light blue), Leu 271(magenta), Met 272 (yellow), Ser 289 (orange), and Ala 397 (dark blue) are highlighted.

compared to the amino acids residues of the LBP of RAR γ after **2** was docked, were:

Phe 201 (0.182Å), Trp 227 (0.45Å), Phe 230 (0.893Å), Lys 236 (1.320Å), Cys 237

(0.420Å), Leu 271 (0.244Å), Ile 275 (0.185Å), Ser 289 (0.524Å), Leu 400 (0.128Å), and Met415 (0.121Å).

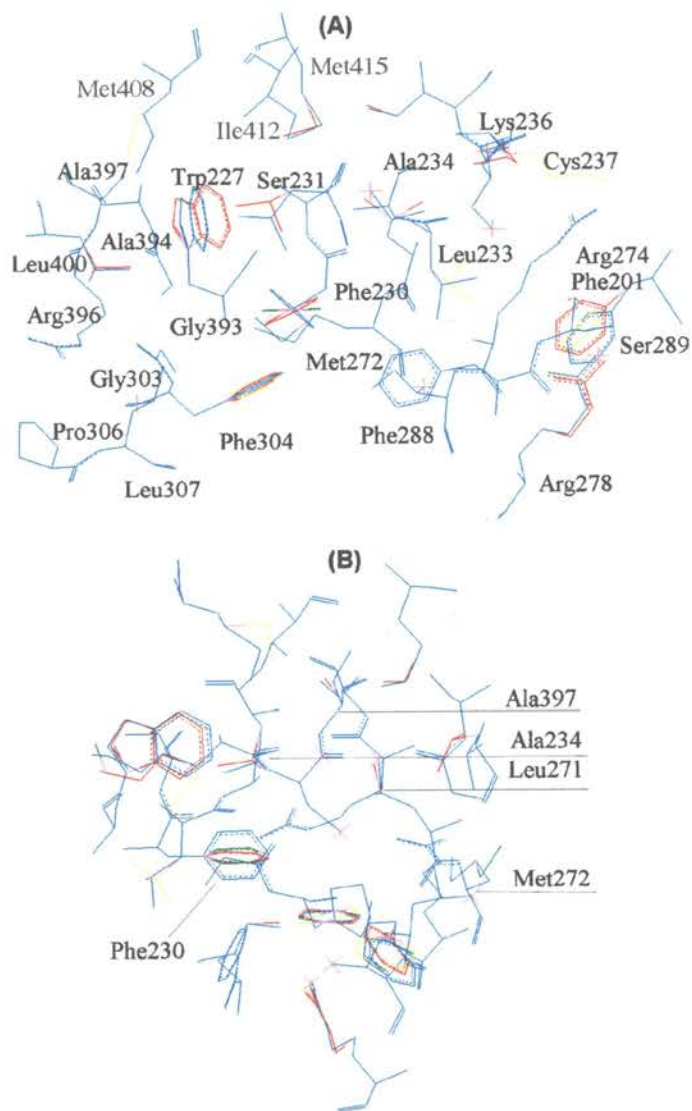


Figure 12. The LBP conformation resulting from *t*-RA (**2**) docking (blue) was superimposed upon conformations of the LBP which resulted from docking of **107** (magenta), **108** (yellow), **109** (red), and **3** (green). (A) side view; (B) view which resulted from (A) after a 90° clockwise rotation about the vertical axis.

After visual inspection and cross-checking the conformational differences where the RMSD value was larger than 0.1Å, it would be appropriate to suggest that in addition to

residues Phe 230, Met 272, Ala 234, and Ala 397, which were responsible for RAR γ activity and selectivity, amino acid residue Leu 271 may also be important in the selectivity of the ligand. If Leu 271 was included as a ligand-selectivity factor residue, this could fill the void in the oval shape conformation within the LBP created by residues Phe 230, Ala 234, and Met 272. However, this conclusion is based only upon visual inspection of the LBP of RAR γ conformation after docking the ligands and needs to be further verified through site-directed mutagenesis of the LBP of RAR γ . Docking the arotinoids **32** and **40** (Table 1), RAR γ specific ligands, via a flexible ligand-flexible receptor method, resulted in similar conformations of the LBP of RAR γ to those conformations of the LBP which were obtained after docking the *t*-RA (**2**) and heteroarotinoid **108**. The docking of arotinoids **6** and **39** (Table I), which are RAR α and RAR β specific, respectively, induced conformational changes in the LBP of RAR γ similar to the conformations of the LBP of RAR γ generated after **107** and **109** were docked (when compared by superimposition and visual inspection).

The orientation of the Phe230 phenyl ring was different with respect to the remaining residues in the LBP of RAR γ after docking the inactive ligands as compared to the orientation found after biologically active ligands were docked into the RAR γ . This fact supports findings from mutagenic studies which implicate Phe 230 as the primary residue responsible for the activity or inactivity of the RAR γ receptor.^{14,37,68,104} The mutation of the Phe 230 residue to Ala 230 or to Gly 230 rendered the receptor inactive.¹⁴ In contrast, mutations in Ala 234, Met 272, and Ala 397 to different residues only partially abolished the activity of the receptor.^{14,37,68,104} In addition to the above mentioned mutagenic studies, a proposal can be made that it is not only the presence of Phe 230 in the LBP that is important

for receptor activity, but it is also the orientation of the Phe 230 towards the remaining residues which may play a role regarding the extent to which the receptor is activated. In other words, Phe 230 can act as a “switch” that regulates the level of RAR γ activity, and that activity can be switched off to deactivate the receptor.

The orientation difference of the Phe 230 phenyl ring between the LBP of RAR γ conformations resulting from docking activating ligands (**2**, **108**) of RAR γ , and conformations that resulted from docking inactive ligands (**107**, **109**) of RAR γ , was a rotation of the ring approximately 60 degrees. This small shift in position of the Phe230 phenyl ring was perhaps of major importance since Phe 230 is part of the loop between α -helices H1 and H3, which in turn is important for the *ligand binding domain's dimerization surface*. Therefore, any changes that occur at the dimerization surface may prevent the formation of homo- or heterodimers and consequently disrupt the proper activity of the receptor. In the case of docking 9-*c*-RA (**3**), the phenyl ring of Phe 230 was rotated nearly 35 degrees apart from that of the active conformation of the receptor when *t*-RA (**2**) was docked. However, this change may not be significant enough to prevent receptor dimer formation. Moreover the interaction between heterodimeric partners at the dimerization surface may be only slightly weakened, and essentially the activity of 9-*cis*-RA-induced RAR γ is not as strong as the activity induced by *t*-RA (**2**). The smaller change in the rotation of the Phe 230 phenyl ring caused by **3** could be due to the conformational change of the Met 272 residue which is pushed away from the core of the LBP cavity by the C19 methyl group of **3**. As a result, the rest of the curved and distorted conformation of 9-*c*-RA (**3**) can be incorporated into the LBP without major disruption of the Phe230 conformation.

The selectivity role of residues Ala 234, Met 272, Ala 397, and Leu 271 would appear to be exhibited through a series of hydrophobic interactions involving parts of the ligand. Since certain amino acid residues occupy the inner core of the LBP of RAR γ , the flexibility of such residues, with the exception of Met272, is somewhat limited. It is this limited flexibility of Ala 234, Leu 271, and Ala 397, that may direct the positioning of the ligand within the binding pocket. *If part of the ligand is positioned in such manner that it can interact with these residues through van der Waals repulsion and attraction forces, as in the case of 108 where the C7 methyl group interacts with Ala 234 and Leu 271, then the rest of the ligand is positioned so as to induce the best interaction with the rest of the LBP.* However, if the structure of the ligand is void of certain groups at specific locations, then the best interactions between the ligand and receptor must come from sources other than from the residues responsible for selectivity, which, in retrospect, may influence the conformation of the remaining residues, such as Phe 230, of the LBP of RAR γ and eventually prevent activation of the RAR γ receptor.

Understanding the ligand-receptor structure-activity relationship is very important in designing isoform specific agents for alleviating of unwanted side-effects. However, more research is needed, and perhaps the discovery of a new method that would enable studies of the dynamic nature of the receptor activities would be a step in the right direction.

Summary

Computer-aided modeling was a good guide in the design of new heteroarotinoids with various linkage groups. The twenty-one new heteroarotinoids should serve as models in the understanding of the role of RAR and RXR families of receptors and, in general, the

mechanisms of action for all nuclear receptors. Furthermore the design of compounds described above was aimed at one receptor isotype-specific activation which eventually could serve as a platform for the invention of potentially effective anticancer agents with high activity and low toxicity. The refinement of heteroarotinoid structures, via adaptation of a fluorine atom property, repositioning of the key groups at the ligands non-polar end, altering the linker flexibility, and changing the polar end functionality could lead to better interaction between the receptor and the ligand.

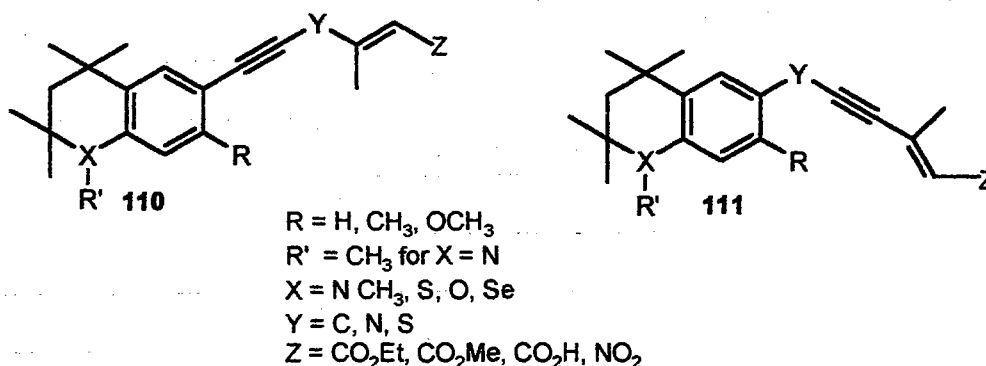
Suggestions for Future Work

Future research in retinoid chemistry should be focused on the generation of isoform specific, non-toxic heteroarotinoids. The specificity of the retinoid could be enhanced either by increasing the rigidity or by fine-tuning and manipulating the structure of ligands so as to create a good match for the three dimensional structure of only one isotype of RAR or of RXR. The former might be accomplished by the attachment of unsaturated rings structures to the linker which could reduce or minimize the ligand flexibility and lock the ligand into one conformation. One problem with this approach, however, is that the toxicity associated with poly-aryl moieties and their metabolites is known to cause variety of disorders.¹³³ The introduction of a triple bond in the linker (as in **30**) of a ligand structure may be another way to increase the rigidity of the heteroarotinoids.²³

Matching the 3-D space of the active conformation in a receptor's LBP can be accomplished through careful studies of the LBP found in the crystallographic structures of a receptor as such become available, mapping the LBP with the aid of computer modeling software, and then deciding which part of the ligand structure needs alteration. A

combination of avenues for ligand design is perhaps another way to address the problem.

Sulfur and nitrogen heteroarotinoids appear to have promising activity with an additional advantage being that the nitrogen compounds can easily be converted to their corresponding water soluble salts (added HX) which is helpful in drug formulation. Heteroarotinoids **110** and **111** are suggested structures for future exploration in retinoid research. Compound **110** has a semi-rigid linker whose orientation and conformation



mimics that of *t*-RA (**2**) (Figure 13) and may specifically bind to the RAR family only. The placement of the Y group in the linker may further reduce the toxic effects of retinoids. When the Y is nitrogen or sulfur, the increased polarity of the compound as a whole may reduce its fat soluble property, and thus the half life of the ligand stored in the fat tissue might be shortened.²² Additionally, such a Y moiety could provide a functional group that could be utilized for further refinement of structures to enhance the receptor selectivity via attachment of different moieties. Rigidity is increased through the introduction of a triple bond (as in **30**) which could also enhance the selectivity by restraining the rotational freedom of the ligand and prohibiting conformational adaptation toward other isotypes. The overall dimensions and conformations of the ligands are still in close proximity to those of

t-RA (**2**) (Figure 13). Heteroarotinoid **111** has the same basic functionality as **110**. However, due to its conformational resemblance to 9-*c*-RA (**3**), the former would likely bind to RXR whereas the latter should bind to RAR only.²²

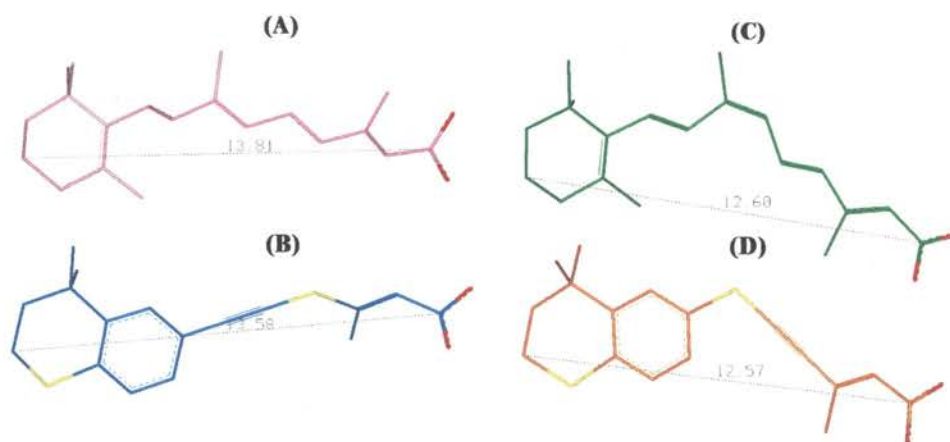


Figure 13. Comparison of *t*-RA [(2), A] with 110 (B) and 9-*c*-RA [(3), C] with 111 (D). The distances (Å) and overall conformation similarities between the two pairs of compounds were noted.

CHAPTER III

EXPERIMENTAL SECTION

Molecular Modeling

Compound Drawing and Energy Minimization

All ligands were drawn using the Builder module and fragment library in Insight II Discover 97 (Molecular Simulation Inc. (MSI) 9685 Scranton Road, San Diego, CA, 92121-2777).³⁰ The atom and bond types were assigned accordingly using the consistent valence force-field (cvff) parameters. The geometries of the ligands were optimized with the program MOPAC, a calculation module in the Insight II modeling package. The MOPAC parameters were set as follows:

- The electronic energy state was set to the “lowest” energy level with unrestricted electron spins where different spins use different orbitals,
- the calculation method was AM1,
- the convergent gradient was set to 0.1 kcal/mol Å,
- the gradient minimizing type was Non Linear Least Square (NLLSQ) method which can detect transition state and local minimums, and
- the minimizer for geometry optimization of the ligands was the Broyden-Fletcher-Goldfarb-Shano (BFGS) method.³⁸

The charges of the ligands were calculated using the Gasteiger-Huckel method with pre-assigned formal charges for the carboxylate anion as -0.5 kcal/mol electrons for each oxygen

atom. After the geometry optimization for the ligands, the ligands were saved in "mol2" format for further use in Sybyl 6.5 (Tripos, Inc. 1699 Hanly Road, St. Louis, Mo, 63144-2913).¹²⁶

Protein Modification

The crystallographic structure of RAR γ was obtained from the Protein Data Bank (PDB, Brookhaven National Laboratory, Upton, NY, 11973). The PDB ID number for RAR γ crystallographic structure was "2LBD", and the molecule was downloaded with the co-crystallized *t*-RA (2) and water molecules (~100). The protein was modified with the Biopolymer module in Sybyl 6.5 by deleting water molecules,¹²⁶ extracting *t*-RA (2), checking atom and bond types, adding hydrogens and valencies, and calculating charges via the Kollman method.⁷¹ The total resulting electronic charge of modified RAR γ was -3.04 kcal/mol electrons. The pseudo-LBP of RAR α and pseudo-LBP of RAR β were obtained from a modified LBP of RAR γ by the mutation of three and two amino acid residues, respectively.⁴⁷ The conversion of RAR γ to pseudo-RAR α was done by mutating Ala 234 to Ser 234, Met 272 to Ile 272, and Ala 397 to Val 397. Similarly, the RAR γ to pseudo-RAR β conversion was done by changing two amino acid residues, Met 272 and Ala 397 to Ile 272, and Val 397, respectively. Since Ala 225 in RAR β corresponds to Ala 234 in RAR γ , the change was not made at this position. This mutation procedure was performed by using the Biopolymer module in Sybyl 6.5, and the mutated receptors were then minimized in Sybyl 6.5 via use of Amber force field with the Powell method of line search and the gradient RMS set to 0.005 kcal/mol Å.⁶⁴ The minimization was allowed to proceed for 1000 iterations to give the final pseudo LBPs of RAR α and RAR β .

Docking

The program Flexidock, which is a component of the Biopolymer module in the Sybyl 6.5 molecular modeling software package, was used for docking the ligands into the modified crystallographic structure of RAR γ , pseudo-RAR α , and pseudo-RAR β . Flexidock is a docking program that attempts to fit a mobile, usually flexible, ligand into a region of a fixed or flexible receptor. This can be viewed as a global optimization problem for which Flexidock's genetic algorithm calculation method is well suited. The genetic algorithm mimics evolutionary behavior and expresses potential solutions which are different conformations of a ligand-receptor complexes known as a population of "chromosomes".¹¹⁰ Each chromosome consists of a number of "genes" which are parameters to be optimized, such as torsional angles, rotations around bonds, or translation of the ligand in the binding pocket of the receptor. A fitness scoring function rates each chromosome, and the competition between chromosomes yields a set of results.⁷¹ Evolution occurs by a random change in the numerical value of the gene, referred to as a "mutation" or by chromosomes exchanging genes, known as a "crossover". Since the best solutions of the fittest generation are kept, the quality of the solution increases with time. Flexidock incorporates the van der Waals, electrostatic, torsional and constraint energy terms of the Tripos force field, while the bond stretching, angle bending, and out of plane bending terms, which are invariant in torsion-space optimization, are ignored. To calculate the interaction energy between the site and the ligand atoms, coordinates of the atoms are converted to an index in the lattice field. A simple linear expression then yields the energy of interaction between the site and a particular atom of the ligand, which, when summarized, yields the overall site-ligand

interaction energy. More precisely, the total energy of steric and electrostatic interactions between the ligand and the receptor is given by :

$$E_{\text{interaction}} = \sum_i \sum_j \left(\frac{A_{ij}}{r_{ij}^{12}} - \frac{B_{ij}}{r_{ij}^6} + \frac{q_i q_j}{r_{ij} \epsilon} \right)$$

where:

- A_{ij} and B_{ij} are the Lennard-Jones steric attractive and repulsive contributions between atoms of the ligand and the receptor (units are: $\text{kcal mol}^{-1} \text{Å}^{12}$ and $\text{kcal mol}^{-1} \text{Å}^6$, respectively, for A_{ij} and B_{ij}),
- r_{ij} is the distance between the receptor atom and the grid point nearest to the atom of the ligand (Å),
- the ϵ is the potential well depth for ligand and receptor (kcal mol^{-1})
- the q_i and q_j are the atomic charges ($\text{kcal/mol-electrons}$) in the ligand and receptor, respectively.

Docking Procedure

The validity of the Flexidock program was checked by removing the *t*-RA (2) from the crystallographic structure of RAR γ and docking it back to the rigid structure of RAR γ and then comparing the results (energies and conformations) from docking with the original crystallographic structure. Before re-docking the *t*-RA (2), the receptor was modified as described previously. In addition, the *t*-RA (2) was also modified by adding hydrogen atoms, charges, and checking for correct atom and bond types. The resulting conformation and the positioning of *t*-RA (2) into the binding pocket after docking was

analyzed and compared with the original LBD of RAR γ co-crystallized with *t*-RA (2), via superimposition. The overall RMSD of the docked conformational complex was not larger than 0.4Å for any atoms of *t*-RA (2), a situation generally considered to validate a good match.

For docking the flexible ligand into the rigid receptor, the default parameters of the Flexidock program were used with the exception that the non-rotational (“non_rot”) bonds were activated to allow for rotation around amide and ester bonds in the ligand. The ligands were pre-positioned in the ligand binding pocket (LBP) defined by the following residues: Phe 201, Thr 227, Phe 230, Ser 231, Leu 233, Ala 234, Lys 236, Cys 237, Leu 271, Met 272, Arg 274, Ile 275, Arg 278, Phe 288, Ser 289, Gly 303, Phe 304, Pro 306, Leu 307, Gly 393, Ala 394, Arg 396, Ala 397, Leu 400, Met 408, Ile 412, and Met 415 with a radius of about 6 Å around the defined binding pocket. The random seed number, which specifies the initial population of ligand conformations, was set to 15,000, and the generation number was different for each series of calculations (see Table III in the Discussion).

The tournament method, where a new parent conformation is chosen by competition between pairs of all conformations and the conformation with a predetermined potential that it would produce more-fit conformations of a new generation when mutated, was chosen as the scoring method (See the Flexidock manual). After the calculation was completed, 20 ligand-receptor complexes with the best interaction energies were saved and compared with the resulting conformations involving the same ligand and receptor from previous series of calculations. The energies of interaction energies for compounds 48-68 with RAR γ are in Table VII. The positive energies of interaction signified bad steric hindrance between the atoms of the ligand and the atoms of RAR γ . *The results in Table VII are a representation*

TABLE VII
ENERGIES OF INTERACTION FROM DOCKING FLEXIBLE LIGAND INTO
FIXED LBP OF RAR γ ^a

Heteroarotinoid	Interaction Energies (kcal/mol)	
	R1 (35,000)	R2 (65,000)
<i>t</i> -RA (2)	-55.45	-78.63
48	-23.92	-39.39
49	59.32	48.91
50	24.48	16.92
51	16.34	6.98
52	79.34	66.83
53	-98.45	-129.73
54	-87.32	-138.37
55	-123.99	-166.88
56	89.32	76.15
57	97.66	93.41
58	3.73	-1.39
59	-145.43	-177.82
60	18.49	14.72
61	56.94	44.38
62	101.87	72.45
63	-93.45	-98.71
64	2.76	-1.83
65	-21.38	-32.59
66	49.21	44.82
67	87.38	56.81
68	1.38	-9.42

^aThe negative Energy of Interaction = Favorable; Positive Energy of Interaction = Not favorable

of only the best values for energy of interaction of two separate series of calculations. Each series of calculations resulted in twenty final conformations (millions of conformations are generated during calculations) of the ligand-receptor complex which were then ranked in descending order for energies of interaction between the ligand and the RAR γ .

Docking of a flexible ligand into the flexible receptor required some changes in the parameter default set of the Flexidock program, namely:

- to press for a more rigorous calculation of the interactive energy between the ligand and the receptor,
- the hydrogen van der Waals radii were change from 1.0 Å to 1.5 Å,
- the hydrogen van der Waals epsilon was changed from 0.03 to 0.042,
- and the van der Waals cutoff distance was adjusted from 16 Å to 8 Å,
- the parameter options “use_backbone” and “use_constrains” were turned on.
- the mutational windows for torsion and rotation were changed from 60 degrees to 30 degrees to assure the generation of additional ligand-receptor conformations and
- the generation number for two series of calculations for each docking procedure for a ligand was set at 45,000 and 60,000.

The data from these calculation were saved in an appropriate database for future comparison and analysis.

Superimposition of the Receptor Conformations

Following the flexible ligand-flexible receptor docking operations, the resulting conformations of the LBP of RAR γ were analyzed by superimposition onto the LBP of the RAR γ conformation that resulted from docking *t*-RA (2). Prior to the superimposition of

receptor conformations on each other, the ligand structures were extracted and saved for future use. The Superimpose module in Sybyl 6.5 was used and “all” of the atoms from the ligand docked LBP of RAR γ conformation were chosen to be superimposed on “all” the atoms of the LBP of RAR γ that resulted from docking *t*-RA (2). A database with the Root Mean Square Deviations (RMSD) between two LBPs of RAR γ conformations was created and saved.

Conformational Search

The compounds used in the QSAR and CoMFA calculations and also 9-*c*-RA (3) used for docking purposes were searched for the minimal energy conformations that were best matched to the crystallographic structure¹⁴ of *t*-RA (2) co-crystallized with RAR γ . The crystallographic structure of 2 was then retrieved and modified via the addition of hydrogen atoms and charges. The program “Discover”, which is a module of Insight II from MSI, was used for the conformational search. The method used for this conformational search was “Torsional Force” which is a subroutine of Discover. The Torsional Force employs an external force field that is applied about a specific dihedral angle during minimization. The force constant for this type of calculation was set to 200. The grid scan algorithm of each dihedral angle was set from 0 degrees to 360 degrees with an 18 degree step size. This implies that for each dihedral angle, 20 new conformations were created which were then minimized. Thus, with this set up for ligands with *n* dihedral angles, 20^{*n*} conformations were generated for each ligand. The quasi-Newton-Rapshon algorithm (VA09A),³⁸ which is time efficient, was chosen for the minimization with the derivative set to 0.001 kcal/mol Å, and the minimization of each new conformation was run for 100 iterations. The resulting conformations of the compounds were then screened by the creation of a Ramachandran

plot¹¹¹ with the two torsional angles as the X and Y axes and the energy value as a gradient with an energy rise of 1 kcal/mol. For compounds with more than two torsional angles, the process of screening conformations was repeated until all of the conformations with different torsional angles were evaluated. Twenty conformations of each ligand, which were energetically low, and resembled the crystallographic 3-D orientation of *t*-RA (2) retrieved from RAR γ , were used for QSAR calculations. The conformation of 9-*c*-RA (3) which most resembled that of *t*-RA (2), which was slightly more “linearly stretched” than the minimal energy conformation of 9-*c*-RA (3) and deviated from the minimal energy conformation 9-*c*-RA (3) by only 0.87 kcal/mol (larger, than minimal conformation energy) in energy value, was chosen for the docking.

Activity Prediction

The programs QSAR, CoMFA, and Molecular Spread Sheet were used for predicting the activity of RAR and RXR isotype receptors in the CV-1 cell by compounds 45-65. For predicting the activity in the receptor isotypes of RXR, 20 conformations of each compound with a known EC₅₀ were used, and from these 20 conformations only one, in which the predicted EC₅₀ value was the closest to the actual value, was used in the prediction of activity of the EC₅₀ for the untested compounds 45-65. In the prediction of EC₅₀ values for the RAR isotypes (α , β , and γ), only the conformations of the ligands that were docked into RAR γ , pseudo RAR α , and pseudo-RAR β , and then extracted from the RARs ligand binding pockets (LBPs), were used. A total of six predictions, one for each isotype of RAR and RXR, were run for each heteroarotinoid 45-65. Before the CoMFA calculation were applied, the database with all the compounds (compounds with known EC₅₀ values and 45-65) and their conformations were aligned via the command “Align Database”,

with additional manual positioning for the thiosemicarbazone compounds. The CoMFA field of ligand sets was calculated using the default set-up (Sybyl 6.5) and then entered into the Molecular Spread Sheet. The known EC_{50} values were entered as $\log(1/EC_{50})$, and a Partial Least Square (PLS) analysis was done twice, first with cross-validation analysis (which gave q^2) and second with “non-validation” analysis (which gave r^2). The q^2 and r^2 values are summarized in Table VIII.

The data from QSAR analysis were analyzed via the command “View CoMFA” in which the graphic representation of the compound in steric and electrostatic fields could be viewed

TABLE VIII

THE Q^2 AND R^2 VALUES FROM PLS ANALYSIS.^a

Receptor Isozyme	q^2	r^2	% certainty
RAR α	0.43	0.97	42
RAR β	0.58	0.95	55
RAR γ	0.51	0.99	50
RXR α	0.49	0.95	47
RXR β	0.56	0.99	55
RXR γ	0.45	0.96	43

^a q^2 is the correlation coefficient of explained variation in activity-structure relationship, r^2 is the correlation coefficient, and the percent certainty is $(q^2 \times r^2) \times 100$. The equation for calculating q^2 is given below where Y_{pred} is a predicted value, Y_{actual} is the actual experimental value, and Y_{mean} is the best of the mean of all values that might be predicted.

$$q^2 = 1 - \frac{\sum_Y (Y_{pred} - Y_{actual})^2}{\sum_Y (Y_{actual} - Y_{mean})^2}$$

of the ligands allowed for more detailed analysis and possible explanations of the

predicted activities as opposed to just superimposition of the ligands on each other and then trying to correlate the difference in activity to RMSD of atoms in the ligands. The predicted values were saved for further use.

Chemistry

General Information

Some ^1H , and ^{13}C NMR spectra were recorded on a ^{UNITY}INOVA 400 NB NMR spectrometer operating at 399.99 Hz and 100.01 Hz, respectively. The broadband Gemini 2000 High-Resolution NMR (300 MHz) spectrometer was also used for obtaining a few ^1H , ^{13}C , and ^{19}F spectra operating at 299.97 Hz, 75.12 Hz, and 282.32 Hz, respectively. All ^1H and ^{13}C signals were referenced to TMS, and ^{19}F spectra were referenced to $\text{F}_3\text{CC}(\text{O})\text{OD}$. The common reference for ^{19}F is $\text{F}_3\text{CCO}_2\text{H}$.¹⁰⁵ The instrument's name and the nuclei examined appear in the parameter table which is at the top-left corner of a ^1H and ^{13}C NMR spectra. IR spectra were recorded on a Perkin Elmer 2000 FT-IR as 'neat' or as KBr pellets. GC-MS spectra were obtained using an HP G1800A GCD system with acetone as the solvent of choice. Melting points were determined with a Thomas-Hoover melting point apparatus and were not corrected. All synthesis were carried out under N_2 , unless indicated otherwise, and with the aid of magnetic stirrer.

All commercial reagents and reagent grade solvents were used without further purification unless described otherwise. The chromatography support used was J. T. Baker 40 μm mesh flash chromatographic packing. Elemental analysis were performed by Atlantic Microlabs, Inc. Norcross, GA, 30091.

[(6-Methoxy-1,1,4,4-tetramethylisochroman-5-yl)amino][(4-nitrophenyl)amino]methane-1-thione (48)

(6-Methoxy-1,1,4,4-tetramethylisochroman-5-yl)amine [(71), 200 mg, 0.85 mmol] dissolved in 5 mL of dry THF was placed in an oven-dried, 25-mL, three-necked, round-bottomed flask equipped with a condenser, N₂ inlet, and addition funnel. The reaction mixture was then cooled to -5 °C (ice and NaCl), and 4-nitrophenylisothiocyanate (160.7 mg, 8.92 mmol, 1.05 eq) dissolved in 6 mL of dry THF was then added dropwise (1 h). After the addition, the reaction mixture was allowed to warm to RT and was then stirred for 24 h. The solvent was evaporated (rotovap), and resulting solid was recrystallized (H₂CCl₂:pentane, 1:1) to afford **48** as a light yellow solid (mp 181-2 °C, 251 mg, 71%). IR (KBr pellet) 3368 [N-H], 3214 [N-H] cm⁻¹; ¹H NMR [D₃C(O)CD₃] δ 1.24 [s, 6 H, C(CH₃)₂], 1.46 [s, 6 H, C(CH₃)₂], 3.56 [s, 2 H, OCH₂], 3.87 [s, 3 H, Ar-OCH₃], 7.01 [d, 1 H, J = 8.7 Hz, Ar-H], 7.25 [d, 1 H, J = 8.7 Hz, Ar-H], 7.60 [bs, 1 H, N-H], 8.01 [d, 2 H, J = 8.5 Hz, Ar-H], 8.15 [d, 2 H, J = 8.5 Hz, Ar-H], 8.48 [bs, 1 H, N-H]; ¹³C NMR [D₃C(O)CD₃] ppm 18.06 [C(CH₃)₂], 26.72 [C(CH₃)₂], 28.91 [C(CH₃)₂], 34.54 [C(CH₃)₂], 56.10 [C(CH₃)₂OCH₂], 75.55 [C(CH₃)₂OCH₂], 108.65 [Ar-OCH₃], 122.11-145.87 [Ar-C], 181.15 [C=S]; Anal. Calcd for C₂₁H₂₅O₄N₃S: C, 60.70; H, 6.06; N, 10.11; S, 7.71. Found: C, 60.63; H, 6.01; N, 10.11; S, 7.69.

N-{[(6-Methoxy-1,1,4,4-tetramethylisochroman-5-yl)amino]tioxomethyl}(4-nitrophenyl)-carboxamide (49)

(6-Methoxy-1,1,4,4-tetramethylisochroman-5-yl)amine [(71), 200 mg, 0.85 mmol] dissolved in 5 mL of dry THF was placed in an oven-dried, 25-mL, three-necked, round-bottomed flask equipped with a condenser, N₂ inlet, and addition funnel. The reaction

mixture was then cooled to $-5\text{ }^{\circ}\text{C}$ (ice and NaCl), and ethyl (4-nitrophenyl)oxomethanisocyanate (186 mg, 8.92 mmol, 1.05 eq) dissolved in 5 mL of dry THF was then added dropwise (1 h). After the addition, the reaction mixture was allowed to warm to RT and was then stirred for 24 h. The solvent was evaporated (rotovap), and the resulting solid was recrystallized (HCCl_3 :pentane, 1:2) to afford **49** as a yellow solid [mp $179\text{ }^{\circ}\text{C}$ (dec), 305 mg, 81%]. IR (KBr pellet) 3229 [N-H], 3171 [N-H], 1686 [C=O] cm^{-1} ; ^1H NMR [$\text{D}_3\text{C}(\text{O})\text{CD}_3$] δ 1.33 [s, 6 H, $\text{C}(\text{CH}_3)_2$], 1.56 [s, 6 H, $\text{C}(\text{CH}_3)_2$], 3.57 [s, 2 H, OCH_2], 3.80 [s, 3 H, Ar-OCH_3], 6.85 [d, 1 H, $J = 8.3\text{ Hz}$, Ar-H], 7.10 [d, 1 H, $J = 8.3\text{ Hz}$, Ar-H], 8.10 [d, 1 H, $J = 7.8\text{ Hz}$, Ar-H], 8.39 [dd, 1 H, $J = 7.8\text{ Hz}$, Ar-H], 10.85 [s, 1 H, N-H], 11.82 [s, 1 H, N-H]; ^{13}C NMR ($\text{D}_3\text{C}(\text{O})\text{CD}_3$) ppm 24.10 [$\text{C}(\text{CH}_3)_2$], 26.67 [$\text{C}(\text{CH}_3)_2$], 34.55 [$\text{C}(\text{CH}_3)_2$], 56.05 [$(\text{CH}_3)_2\text{OCH}_2$], 71.34 [$\text{OC}(\text{CH}_3)$], 111.19 [Ar-OCH_3], 124.24-135.77 [Ar-C], 168.77 [C=O], 182.56 [C=S]; Anal. Calcd for $\text{C}_{22}\text{H}_{25}\text{N}_3\text{O}_5\text{S}$: C, 59.58; H, 5.68; N, 9.47; S, 7.23. Anal. Calcd for $\text{C}_{22}\text{H}_{25}\text{N}_3\text{O}_5\text{S} \cdot 0.6\text{ H}_2\text{O}$: C, 58.16; H, 5.70; N, 9.24; S, 7.05. Found: C, 57.98; H, 5.47; N, 9.15; S, 7.02.

Ethyl 4- $\{[N-(6\text{-Methoxy-1,1,4,4-tetramethylisochroman-5-yl})\text{carbamoyl}]\text{amino}\}$ benzoate-
(50)

(6-Methoxy-1,1,4,4-tetramethylisochroman-5-yl)amine [(71), 200 mg, 0.85 mmol] dissolved in 5 mL of dry THF was placed in an oven-dried, 25-mL, three-necked, round-bottomed flask equipped with a condenser, N_2 inlet, and addition funnel. The reaction mixture was then cooled to $-5\text{ }^{\circ}\text{C}$ (ice NaCl), and ethyl 4-isocyanatobenzoate (170.6 mg, 8.92 mmol, 1.05 eq) dissolved in 5 mL of dry THF was the added dropwise (1 h). After the addition, the reaction mixture was allowed to warm to RT and was then stirred for 24

h. The solvent was evaporated (rotovap), and the resulting solid was recrystallized (H_2CCl_2 :pentane, 2:1) to afford **50** as a white solid (mp 147-9 °C, 265 mg, 73%); IR (KBr) 3343 [N-H], 3201 [N-H], 1713 [C=O], 1673 [C=O], cm^{-1} ; $^1\text{H NMR}$ [$\text{D}_3\text{C}(\text{O})\text{CD}_3$] δ 1.23 [s, 6 H, $\text{C}(\text{CH}_3)_2$], 1.26[t, 3 H, OCH_2CH_3], 1.36 [s, 6 H, $\text{C}(\text{CH}_3)_2$], 3.47 [s, 2 H, OCH_2], 3.85 [s, 3 H, Ar- OCH_3], 4.33 [q, 2 H, OCH_2], 6.90 [d, 1 H, $J = 7.3\text{ Hz}$, Ar- H], 7.15 [d, 1 H, $J = 7.3\text{ Hz}$, Ar- H], 7.58 [d, 2 H, $J = 7.6\text{ Hz}$, Ar- H], 7.84 [d, 2 H, $J = 7.6\text{ Hz}$, Ar- H], 8.23 [s, 1 H, N- H], 8.98 [bs, 1 H, N- H]; $^{13}\text{C NMR}$ [$\text{D}_3\text{C}(\text{O})\text{CD}_3$] ppm 14.52 [OCH_2CH_3] 27.93 [$\text{C}(\text{CH}_3)_2$], 28.66 [$\text{C}(\text{CH}_3)_2$], 54.81 [$\text{C}(\text{CH}_3)_2$], 60.88 [OCH_2CH_3], 71.73 [$(\text{CH}_3)_2\text{OCH}_2$], 75.37 [$\text{OC}(\text{CH}_3)$], 107.24 [Ar- OCH_3], 116.80-145.71 [Ar-C], 153.4 [C=O], 156.47 [C=O]; Anal. Calcd for $\text{C}_{25}\text{H}_{30}\text{N}_2\text{O}_5$: C, 67.58; H, 7.08; N, 6.56. Found: C, 67.50; H, 7.10; N, 6.48.

{[(1*E*,3*E*)-1-Aza-4-(4,4-dimethylchroman-6-yl)-3-fluoropenta-1,3-dienyl]amino}amino-methane-1-thione (**51**)

Thiosemicarbazide (35.0 mg, 0.38 mmol) dissolved into 4 mL of water and AcOH (1 drop) was placed in a 10-mL beaker. Then aldehyde [(75), 95 mg, 0.38 mmol] was dissolved in 5 mL of EtOH (95%). The latter solution was warmed to 60 °C and then was added dropwise to the thiosemicarbazide solution while hot. A precipitate formed immediately. The reaction mixture was set aside for 24 h at 0 °C, and then the solid was filtered off. Recrystallization (EtOAc:diethyl ether, 1:1) of the solid afforded a white solid **51** (mp 231-2 °C, 100.1 mg, 82 %). IR (neat) 3444 [N-H], 3304 [N-H], 3205 [N-H] cm^{-1} ; $^1\text{H NMR}$ ($\text{DMSO}-d_6$) δ 1.30 [s, 6 H, $\text{C}(\text{CH}_3)_2$], 1.78 [t, 2 H, OCH_2CH_2], 2.10 [d, 3 H, =C- CH_3], 4.19 [t, 2 H, OCH_2CH_2], 6.27 [d, 1 H, $J = 8.4\text{ Hz}$, Ar- H], 6.98 [dd, 1 H, $J = 8.4\text{ Hz}$, $J = 2.1\text{ Hz}$, Ar- H], 7.24 [d, 1 H, $J = 2.1\text{ Hz}$, Ar- H], 7.44 [s, 1 H, N- H], 7.65 [d, 1 H, $J =$

20.7 Hz, FC=CH], 8.21 [s, 1H, N-H], 11.31 [s, 1 H, N-H], ¹³C NMR (DMSO-d₆) ppm, 17.22 [=C-CH₃], 30.27 [C-(CH₃)₂], 30.57 [C-(CH₃)₂], 36.83 [OCH₂CH₂], 62.58 [OCH₂CH₂], 116.58 [=CH], 121.81-131.67 [CH=C-Ph], 153.32 [FC=CH] 178.75 [C=S]. Anal. Calcd for C₁₆H₂₀FN₃OS: C, 59.79; H, 6.27; N, 13.07. Found: C, 59.67; H, 6.37; N, 13.10.

Ethyl 4-[(4,4-Dimethylchroman-6-yl)ethoxy]carbonylamino}benzoate (52)

Powdered sodium hydride (23 mg, 0.97 mmol, 95%) was suspended in 5 mL of freshly distilled THF (5 mL) in an oven-dried, 25-mL, three-necked, round-bottomed flask equipped with a condenser, N₂ inlet, and two addition funnels. The reaction mixture was then cooled to 0 °C, and 1-(4,4-dimethylchroman-6-yl)ethanol (200 mg, 0.97 mmol) dissolved in 5 mL of THF was added dropwise (30 min). The reaction mixture was stirred at this temperature (1 h) after which time ethyl 4-isocyanatobenzoate (185 mg, 0.97 mmol) dissolved in 5 mL of dry THF was added dropwise (1 h). The reaction mixture was allowed to warm to RT with continuous stirring for 8 h, followed by cooling to 0 °C and quenching with a solution of saturated, aqueous ammonium chloride (4 mL). The organic layer was separated, and the aqueous layer was extracted with ethyl acetate (3 x 20 mL). The combined organic layers were then washed with H₂O (2 x 5 mL) and brine (1 x 10 mL) and dried (MgSO₄, 24 h). Evaporation (rotovap) of the solvent and recrystallization (ethyl acetate:H₂CCl₂:hexane, 1:1:1) afforded **52** as a white solid (mp 109-11 °C, 262 mg, 68%).

IR (KBr pellet) 3302 [N-H], 1744 [C=O], 1732 [C=O] cm⁻¹; ¹H NMR (DCCl₃) δ 1.41 [s, 6 H, C(CH₃)₂], 1.54 [t, 3 H, OCH₂CH₃], 1.90 [d, 2 H, OCH₂CH₂] 4.02 [d, 2 H, OCH₂CH₂], 4.02 [q, 2 H, OCH₂CH₃], 5.81 [q, 1 H, CHCH₃], 6.85 [dd, 1 H, J = 8.3Hz, J = 2.7 Hz, Ar-H], 7.05 [d, 1 H, J = 2.7 Hz, Ar-H], 7.25 [d, 1 H, J = 8.3 Hz, Ar-H], 7.65 [d, 1 H, J = 7.4 Hz, Ar-

H], 8.05 [d, 1 H, *J* = 7.4 Hz, Ar-*H*]; ¹³C NMR (DCCl₃) ppm 14.02 [OCH₂CH₃], 14.10 [C(CH₃)₂], 60.97 [OCH₂CH₂], 61.17 [OCH₂CH₂], 120.32-141.14 [Ar-C], 165.68 [C=O], 178.93 [C=O]; Anal. Calcd for C₂₃H₂₆NO₅: C, 69.40; H, 6.84; N, 3.52. Found: C, 69.27; H, 6.92; N, 3.45.

Ethyl 4-([(1,2,2,4-Tetramethyl(1,2-dihydroquinol-6-yl)carbamoyl]amino]benzoate (53)

(1,2,2,4-Tetramethyl-1,2-dihydroquinol-6-yl)amine (**82**, 150 mg, 0.74 mmol) dissolved in 4 mL of dry THF was placed in an oven-dried, 25-mL, three-necked, round-bottomed flask equipped with a condenser, N₂ inlet, and addition funnel. The reaction mixture was then cooled to -5 °C (ice and NaCl), and ethyl 4-isocyanatobenzoate (148.5 mg, 7.78 mmol, 1.05 eq) dissolved in 5 mL of dry THF was then added dropwise (30 min). After the addition, the reaction mixture was allowed to warm to RT and was then stirred for 24 h. The solvent was evaporated (rotovap), and the resulting solid was recrystallized (HCCl₃:pentane, 1:1) to afford **53** as a white, flaky solid (mp 211-12 °C, 206 mg, 71%). IR (KBr pellet) 3352 [N-H], 3262 [N-H], 1709 [C=O] cm⁻¹; ¹H NMR (DCCl₃) δ 1.29 [s, 6 H, N-C-(CH₃)], 1.36 [t, 3 H, OCH₂CH₃], 1.63 [bs, 1 H, N-*H*], 1.94 [s, 3 H, =C-CH₃], 2.87 [s, 3 H, N-CH₃], 4.37 [q, 2 H, OCH₂CH₃], 5.33 [s, 1 H, =CH], 6.47 [d, 1 H, *J* = 8.3 Hz, Ar-*H*], 6.67 [bs, 1 H, N-*H*], 6.97 [d, 1 H, *J* = 1.9 Hz, Ar-*H*], 7.13 [q, 1 H, *J* = 1.9 Hz, *J* = 8.3 Hz, Ar-*H*], 7.4 [d, 2 H, *J* = 9.0 Hz, Ar-*H*], 7.92 [d, 2 H, *J* = 9.0 Hz, Ar-*H*]; ¹³C NMR (DCCl₃) ppm 14.33 [OCH₂CH₃], 18.50 [=C-CH₃], 27.21 [2 C, C(CH₃)₂], 30.75 [N-CH₃], 56.39 [=C-C(CH₃)₂], 60.70 [OCH₂CH₃], 111.11 [=C-CH₃], 118.14 [=C-C(CH₃)₂], 120.64-143.96 [Ar-C], 154.23 [C=O], 180.45 [C=S]. TLC Analysis for C₂₃H₂₇N₃O₃ showed one spot in the following solvent systems: hexane:diethyl ether:H₂CCl₂, (1:1:1), R_f 0.46; chloroform:pen-

tane, (2:1), R_f 0.40; hexane:EtOAc, (2:1), R_f 0.18. Anal. Calcd for $C_{23}H_{27}N_3O_3$: C, 70.21; H, 6.92; N, 10.65. Anal. Calcd for $C_{23}H_{27}N_3O_3 \cdot 0.3 H_2O$: C, 68.63; H, 7.01; N, 10.44. Found: C, 68.63; H, 6.75; N, 10.35.

Ethyl 4-([(1,2,2,4-Tetramethyl-1,2-dihydroquinol-6-yl)amino]thioxomethyl)amino)-benzoate (54)

(1,2,2,4-Tetramethyl-1,2-dihydroquinol-6-yl)amine (**82**, 150 mg, 0.74 mmol) dissolved in 4 mL of dry THF, was placed in an oven-dried, 25-mL, three-necked, round-bottomed flask equipped with a condenser, N_2 inlet, and addition funnel. The reaction mixture was then cooled to $-5\text{ }^\circ\text{C}$ (ice and NaCl), and ethyl 4-isothiocyanatobenzoate (161 mg, 7.78 mmol, 1.05 eq) dissolved in 5 mL of dry THF was then added dropwise (30 min). After the addition, the reaction mixture was allowed to warm to RT and was then stirred for 24 h. The solvent was evaporated (rotovap), and the resulting solid was recrystallized (H_2CCl_2 :pentane, 1:2) to afford **54** as a pale yellow solid (mp $161\text{-}2\text{ }^\circ\text{C}$, 275 mg, 91%). IR (KBr pellet) 3344 [N-H], 3289 [N-H], 1712 [C=O] cm^{-1} ; ^1H NMR (DCCl_3) δ 1.34 [s, 6 H, N-C-(CH_3)], 1.37 [t, 3 H, OCH_2CH_3], 1.60 [bs, 1 H, N-H], 1.95 [s, 3 H, =C- CH_3], 2.83 [s, 3 H, N- CH_3], 4.35 [q, 2 H, OCH_2CH_3], 5.36 [s, 1 H, =CH], 6.51 [d, 1 H, $J = 8.7\text{ Hz}$, Ar-H], 6.94 [d, 1 H, $J = 2.4\text{ Hz}$, Ar-H], 7.13 [q, 1 H, $J = 2.4\text{ Hz}$, $J = 8.7\text{ Hz}$, Ar-H], 7.60 [d, 2 H, $J = 8.7\text{ Hz}$, Ar-H], 7.75 [bs, 1 H, N-H], 8.01 [d, 2 H, $J = 8.7\text{ Hz}$, Ar-H]; ^{13}C NMR (DCCl_3) ppm 14.30 [OCH_2CH_3], 18.53 [=C- CH_3], 27.77 [2 C, $\text{C}(\text{CH}_3)_2$], 30.86 [N- CH_3], 56.75 [=C- $\text{C}(\text{CH}_3)_2$], 60.92 [OCH_2CH_3], 111.04 [=C- CH_3], 121.66 [=C- $\text{C}(\text{CH}_3)_2$], 123.06-143.56 [Ar-C], 165.97 [C=O], 179.92 [C=S]. Anal. Calcd for $C_{23}H_{27}N_3O_2S$: C, 67.45; H, 6.65; N, 10.26. Found: C, 67.47; H, 6.66; N, 10.17.

[(4-Nitrophenyl)amino][(1,2,2,4-tetramethyl(1,2-dihydroquinol-6-yl))amino]methane-1-thione (55)

(1,2,2,4-Tetramethyl-1,2-dihydroquinol-6-yl)amine (**82**, 150 mg, 0.74 mmol) dissolved in 5 mL of dry THF was placed in an oven-dried, 25-mL, three-necked, round-bottomed flask equipped with a condenser, N₂ inlet, and addition funnel. The reaction mixture was then cooled to -5 °C (ice and NaCl), and 4-nitrophenylisothiocyanate (141 mg, 7.78 mmol, 1.05 eq) dissolved in 5 mL of dry THF was then added dropwise (30 min). After the addition, the reaction mixture was allowed to warm to RT and was then stirred for 24 h. The solvent was evaporated (rotovap), and the resulting solid was recrystallized (EtOAc:hexane, 1:1) to afford **55** as an orange-yellow solid (mp 172-3.5 °C, 184 mg, 65%). IR (KBr pellet) 3338 [N-H], 3181 [N-H] cm⁻¹; ¹H NMR (DCCl₃) δ 1.39 [s, 6 H, N-C(CH₃)], 1.93 [s, 3 H, =C-CH₃], 2.82 [s, 3 H, N-CH₃], 5.30 [s, 1 H, =CH], 6.52 [d, 1 H, J = 8.7 Hz, Ar-H], 6.92 [d, 1 H, J = 2.4 Hz, Ar-H], 7.02 [q, 1 H, J = 2.4 Hz, J = 8.7 Hz, Ar-H], 7.67 [bs, 1 H, N-H], 7.77 [d, 2 H, J = 9.0 Hz, Ar-H], 7.87 [bs, 1 H, N-H], 8.19 [d, 2 H, J = 9.0 Hz, Ar-H]; ¹³C NMR (DCCl₃) ppm 18.52 [=C-CH₃], 27.89 [C(CH₃)₂], 30.91 [N-CH₃], 56.85 [=C-C(CH₃)₂], 111.08 [=C-CH₃], 121.61 [=C-C(CH₃)₂], 122.81-145.44 [Ar-C], 179.65 [C=S]. TLC Analysis for C₂₀H₂₂N₄O₂S showed one spot in following solvent systems: hexane:diethyl ether:H₂CCl₂, (1:1:1), R_f 0.40; chloroform:pentane, (2:1), R_f 0.19; hexane:EtOAc, (2:1), R_f 0.14. Anal. Calcd. for C₂₀H₂₂N₄O₂S: C, 62.81; H, 5.80; N, 14.05. Anal. Calcd. for C₂₀H₂₂N₄O₂S · 1.37 H₂O: C, 59.50; H, 5.95; N, 13.82. Found: C, 59.26; H, 5.57; N, 13.47.

Ethyl (6Z,2E,4E,8E)-3,7-Dimethyl-9-(1,2,2,4-tetramethyl(1,2-dihydroquinolyl))nona-2,4,6,8-

tetraenoate (56)

In a 25-mL, three-necked, round-bottomed flask equipped with a condenser, N₂ inlet was placed a solution of triethyl 3-methyl-4-phosphonocrotonate (145 mg, 0.62 mmol) dissolved in 1 mL of THF which was cooled to 0 °C and then was treated with DMPU (100 mg, 0.78 mmol) and *n*-BuLi (0.4 mL, 0.62 mmol, 1.6 M solution in toluene). The mixture was stirred for 20 min and then cooled to -78 °C. A solution of aldehyde **86** (87 mg, 0.31 mmol) dissolved in 1 mL of THF was added, and the reaction mixture was stirred at -78 °C for an additional 1 h. This mixture was allowed to warm to 0 °C, and a saturated, aqueous solution of ammonium chloride (1.5 mL) was added. An extraction with EtOAc (3 x 1.5 mL) was followed by washing the extracts with water (1 x 2 mL) and brine (1x 1.5 mL each). The organic layer was then dried (MgSO₄, 12 h). The residue was purified with column chromatography (silica gel, hexane:diethyl ether, 2:1, drop rate = 1 drop/s) and then recrystallized (H₂CCl₂:pentane, 1:2) to yield **56** as a bright red solid (mp 52-54 °C, 37 mg, 42%). IR (neat) 1705 [C=O] cm⁻¹; ¹H NMR (DCCl₃) δ 1.26 [t, 3 H, OCH₂CH₃], 1.29 [s, 6 H, C(CH₃)₂], 2.03 [d, 3 H, =CCH₃, J = 10.8 Hz], 2.36 [d, 3 H, =C-CH₃, J = 7.8 Hz], 2.83 [s, 3 H, N-CH₃], 4.18 [q, 2 H, OCH₂CH₃], 5.25 [s, 1 H, =CH], 5.77 [s, 1 H, =CH] 6.31 [d, 1 H, =CH], 6.45 [d, 1 H, =CH], 6.50 [d, 1 H, Ph-H], 7.45 [m, 3 H, Ph-H]; ¹³C NMR (DCCl₃) ppm 12.98 [OCH₂CH₃], 18.57 [=C-CH₃], 26.78 [C(CH₃)₂], 27.75 [C-CH₃], 31.21 [N-CH₃], 56.43 [CH₃-C=C], 59.53 [CH₃-C=C], 110.58 [=CH], 118.20-155.04 [CH=C-Ph], 167.17 [O-C=O]. Anal. Calcd for C₂₆H₃₃NO₂: C, 79.76; H, 8.97; N, 3.57. Found: C, 79.68; H, 9.06; N, 3.23.

{{(3Z,1E,5E)-1-Aza-4-methyl-6-(1,2,2,4-tetramethyl(1,2-dihydroquinolyl))hexa-1,3,5-trienyl}amino}aminomethane-1-thione (57)

Thiosemicarbazide (71.31 mg, 0.76 mmol) dissolved into 4 mL of water and AcOH (1 drop) was placed in a 10-mL beaker. Then 200 mg (0.71 mmol) of aldehyde **86** was dissolved in 5 mL of EtOH (95%). The latter solution was warmed to 60 °C and then added dropwise to the thiosemicarbazide solution while hot. A precipitate formed immediately. The reaction mixture was set aside for 24 h at 0 °C, and then the solid was filtered off. Recrystallization (EtOAc:diethyl ether, 1:1) of the solid afforded a light orange solid **57** (mp 177-179 °C, 123 mg, 41 %). IR (neat) 3428 [N-H], 3254 [N-H], 3156 [N-H] cm⁻¹; ¹H NMR (DCCl₃) δ 1.32 [s, 6 H, C(CH₃)₂], 2.01 [d, 3 H, =CCH₃], 2.06 [d, 3 H, =C-CH₃], 2.84 [s, 3 H, N-CH₃], 5.32 [d, 1 H, =CH], 6.17 [d, 1 H, =CH], 6.47 [d, 1 H, =CH], 6.72 [s, 1 H, =C-H], 7.14-7.25 [m, 3 H, Ph-H]; 7.88 [s, 1 H, N-H], 7.91 [s, 1H, N-H], 9.28 [s, 1 H, N-H], ¹³C NMR (DCCl₃) ppm, 18.57 [=C-CH₃], 27.64 [C-CH₃], 30.79 [N-CH₃], 56.63 [CH₃-C=C], 110.55 [=CH], 121.81-155.04 [CH=C-Ph], 177.75 [C=S]. Anal. Calcd for C₂₀H₂₆N₄S: C, 67.08; H, 7.39; N, 15.64. Found: C, 66.95; H, 7.37; N, 15.52.

{[(1E,3E)-1-Aza-3-fluoro-4-(1,2,2,4-tetramethyl(6-1,2-dihydroquinolyl))buta-1,3-dienyl] amino}aminomethane-1-thione (**58**)

Thiosemicarbazide (33.6 mg, 0.37 mmol) dissolved into 3 mL of water and AcOH (1 drop) was placed in a 10-mL beaker. Then aldehyde [(**89**), 200 mg, 0.77 mmol) was dissolved in 4 mL of EtOH (95%). The latter solution was warmed to 60 °C and then added dropwise to the thiosemicarbazide solution while hot. A precipitate formed immediately. The reaction mixture was set aside for 24 h at 0 °C, and then the solid was filtered off. Recrystallization (EtOAc:diethyl ether, 1:1) of the solid afforded a light yellow solid **58** (mp 77-79 °C, 86 mg, 69 %). IR (neat) 3429 [N-H], 3258 [N-H], 3148 [N-H] cm⁻¹; ¹H

NMR (DCCl₃) δ 1.36 [s, 6 H, C(CH₃)₂], 2.01 [d, 3 H, =CHCH₃], 2.84 [s, 3 H, N-CH₃], 5.36 [d, 1 H, =CH], 5.83 [d, 1 H, FC=CH], 6.47 [d, 1 H, =CH], 7.14-7.25 [m, 3 H, Ph-H]; 7.78 [s, 1 H, N-H], 9.11 [s, 1H, N-H], 9.41 [s, 1 H, N-H], ¹³C NMR (DCCl₃) ppm, 18.62 [=C-CH₃], 28.12 [C-CH₃], 30.98 [C(CH₃)₂], 40.79 [N-CH₃], 56.63 [C-CH=C], 110.08 [=CH], 121.08-145.04 [CH=C-Ph], 150.22 [HC=CF], 177.75 [C=S]. Anal. Calcd for C₁₇H₂₁FN₄S: C, 61.42; H, 6.37; N, 16.85. The compound decomposed very quickly, and no satisfactory elemental analysis could be obtained.

{[(1*E*,3*E*)-1-Aza-4-(1,2,2,4-tetramethyl(6-1,2-dihydroquinolyl))buta-1,3-dienyl]amino}aminomethane-1-thione (59)

Thiosemicarbazide (56.68 mg, 0.62 mmol) dissolved into 4 mL of water and AcOH (1 drop) was placed in a 10-mL beaker. Then aldehyde **92** (150 mg, 0.62 mmol) was dissolved in 5 mL of EtOH (95%). The latter solution was warmed to 60 °C and then added dropwise to the thiosemicarbazide solution while hot. A precipitate formed immediately. The reaction mixture was set aside for 24 h at 0 °C, and then the solid was filtered off. Recrystallization (EtOAc:diethyl ether, 1:1) of the solid afforded an light yellow solid **59** (mp 51-52.5 °C, 150 mg, 73 %). IR (neat) 3426 [N-H], 3262 [N-H], 3151 [N-H] cm⁻¹; ¹H NMR (DCCl₃) δ 1.26 [s, 6 H, C(CH₃)₂], 2.01 [d, 3 H, =CHCH₃], 2.81 [s, 3 H, N-CH₃], 5.36 [d, 1 H, =CH], 5.80 [q, 1 H, HC=CH], 6.50 [d, 1 H, =CH], 6.78 [d, 1 H, =CH], 6.84-7.25 [m, 3 H, Ph-H], 7.38 [bs, 1 H, N-H], 8.20 [bs, 1H, N-H], 10.71 [bs, 1 H, N-H], ¹³C NMR (DCCl₃) ppm, 16.62 [C-CH₃], 18.12 [=C-CH₃], 28.98 [C(CH₃)₂], 30.63 [C-CH=C], 58.79 [N-CH₃], 110.08 [=CH], 116.56 [=CH], 121.08-143.04 [CH=C-Ph], 178.35 [C=S]. Anal. Calcd for C₁₇H₂₂FN₄S: C, 64.93; H, 7.05; N, 17.81. The compound decomposed very quickly, and

no satisfactory elemental analysis could be obtained.

Ethyl (2*E*,4*E*,6*E*)-6-Fluoro-3-methyl-7-(2,2,4,4-tetramethyl(3*H*-benzo[3,4-*e*]thian-6-yl))octa-2,4,6-trienoate (60)

A 25-mL, three-necked, round-bottomed flask equipped with a N₂ inlet and an addition funnel was charged with triethyl 3-methyl-4-phosphonocrotonate (119 mg, 0.45 mmol), DMPU (58 mg, 0.45 mmol), and THF (2 mL). The mixture was cooled to 0 °C, and 0.42 ml (0.67 mmol) of *n*-BuLi (1.6 M) was added by syringe. After stirring for 1 h at 0 °C, 120 mg (0.41 mmol) of aldehyde 97a dissolved in 2 mL of dry THF was added (addition funnel). The new reaction mixture was allowed to warm to RT and was then stirred for 4 days. Quenching the reaction mixture with saturated, aqueous solution of ammonium chloride (1 mL) and extraction of the mixture with ethyl acetate (3 x 10 mL) was followed by washing the organic extracts with water (2 x 2 mL) and brine (1 x 3 mL). The organic extract was then dried (MgSO₄, 12 h), the solvent was evaporated (rotovap), and the residual oil was purified by flash chromatography (H₂CCl₂:hexane, 1:1, drop rate = 1 drop/s) to give 122 mg (81%) of ester 60 as a thick light yellow oil. IR (neat) 1712 [OC=O] cm⁻¹; ¹H NMR (DCCl₃) δ 1.28 [t, 3 H, OCH₂CH₃], 1.39 [s, 6 H, C(CH₃)₂], 1.44 [s, 6 H, SC(CH₃)₂], 1.98 [s, 2 H, SC(CH₃)₂CH₂], 2.18 [2s, 6 H, =CCH₃], 4.18 [q, 2 H, OCH₂CH₃], 5.87 [s, 1 H, =CH], 6.5 [d, 1 H, =CH], 6.59 [d, 1 H, =CH], 6.90-7.26 [m, 3 H, Ar-H]; ¹³C NMR (DCCl₃) ppm 14.29 [OCH₂CH₃], 31.15 [C(CH₃)₂], 32.85 [C(CH₃)₂], 54.17 [=CCH₃], 59.77 [=CCH₃], 63.74 [=CCH₃], 120.45-123.21 [=C], 126.23-151.32 [Ar-C], 166.92 [OC=O]; ¹⁹F NMR (DCCl₃) (ref C₆H₅CF₃ in C₆D₆) ppm -120.99 [m, 1 F, =CF]. Anal. Calcd for C₂₄H₃₁FO₂S: C, 71.60; H, 7.76. Found: C, 71.53; H, 7.82.

Ethyl (2E,4E,6E)-6-Fluoro-3,8-dimethyl-7-(2,2,4,4-tetramethyl(3H-benzo[3,4-e]thian-6-yl)nona-2,4,6-trienoate (61)

A 25-mL, three-necked, round-bottomed flask equipped with a N₂ inlet and an addition funnel was charged with triethyl 3-methyl-4-phosphonocrotonate (58 mg, 0.22 mmol), DMPU (28 mg, 0.22 mmol), and THF (2 mL). The mixture was cooled to 0 °C, and 0.15 ml (24 mmol) of *n*-BuLi (1.6 M) was added by syringe. After stirring for 1 h at 0 °C, aldehyde **97b** (65 mg, 0.20 mmol) dissolved in 2 mL of dry THF was added (addition funnel). The new reaction mixture was allowed to warm to RT, and then it was stirred for 4 days. Quenching the reaction mixture with a saturated, aqueous solution of ammonium chloride (1 mL) and extraction of the mixture with ethyl acetate (3 x 10 mL) was followed by washing the organic extracts with water (2 x 2 mL) and brine (1 x 3 mL). The organic extract was then dried (MgSO₄, 12 h). Evaporation (rotovap) of the solvent and purification of the major component in the residue by flash chromatography (diethyl ether:hexane, 1:1, drop rate = 1 drop/s) gave **63** (1.44 mg, 51%) as a thick, light yellow oil. IR (neat) 1711 [OC=O] cm⁻¹; ¹H NMR (DCCl₃) δ 1.16 [d, 3 H, CH(CH₃)₂], 1.32 [t, 3 H, OCH₂CH₃], 1.45 [s, 6 H, C(CH₃)₂], 1.44 [s, 6 H, SC(CH₃)₂], 1.57 [d, 3 H, =CCH₃], 1.96 [s, 2 H, SC(CH₃)₂CH₂], 2.16 [d, 3 H, =CCH₃], 2.37 [d, 3 H, =CCH₃], 4.27 [q, 2 H, OCH₂CH₃], 5.80 [s, 1 H, =CH], 6.6 [d, 1 H, =CH], 6.78 [d, 1 H, =CH], 6.82 [q, 1 H, J = 8.6 Hz, J = 2.2 Hz, Ar-H], 7.02 [d, 1 H, J = 8.6 Hz, Ar-H], 7.15 [d, 1 H, J = 2.2 Hz, Ar-H]; ¹³C NMR (DCCl₃) ppm 13.41 [OCH₂CH₃], 14.29 [=CCH₃], 21.13 [=CCH₃], 29.70 [C(CH₃)₂], 30.51 [C(CH₃)₂], 54.20 [=CCH₃], 59.77 [=CCH₃], 120.96-125.21 [=C], 127.74-151.07 [Ar-C], 166.88 [OC=O]; ¹⁹F NMR (DCCl₃) (ref C₆H₅CF₃ in C₆D₆) ppm -110.50 [m, 1 F, =CF]. Anal. Calcd for C₂₆H₃₅FO₂S: C, 72.52; H, 8.19. Found: C, 72.66; H, 8.19.

Ethyl (2E,4E,6E)-6-Fluoro-3,9-dimethyl-7-(2,2,4,4-tetramethyl(3H-benzo[3,4-e]thian-6-yl))deca-2,4,6-trienoate (62)

A 25-mL, three-necked, round-bottomed flask equipped with a N₂ inlet and an addition funnel was charged with triethyl 3-methyl-4-phosphonocrotonate (58 mg, 0.22 mmol), DMPU (28 mg, 0.22 mmol), and THF (2 mL). The mixture was cooled to 0 °C, and 0.15 ml (24 mmol) of *n*-BuLi (1.6 M) was added by syringe. After stirring for 1 h at 0 °C, aldehyde **97c** (67 mg, 0.20 mmol) dissolved in 2 mL of dry THF was added (addition funnel). The new reaction mixture was allowed to warm to RT, and then it was stirred for 5 days. Quenching the reaction mixture with a saturated, aqueous solution of ammonium chloride (1 mL) and extraction of the mixture with ethyl acetate (3 x 10 mL) was followed by washing the organic extracts with water (2 x 2 mL) and brine (1 x 3 mL). The organic extract was then dried (MgSO₄, 12 h). Evaporation (rotovap) of the solvent and purification of the major component in the residue by flash chromatography (diethyl ether:hexane, 1:1, drop rate = 1 drop/s) gave **62** (44.3 mg, 51%) as a thick, light yellow oil. IR (neat) 1710 [OC=O] cm⁻¹; ¹H NMR (DCCl₃) δ 0.96 [d, 3 H, CH(CH₃)₂], 1.12 [d, 3 H, CH(CH₃)₂], 1.38 [t, 3 H, OCH₂CH₃], 1.45 [s, 6 H, C(CH₃)₂], 1.44 [s, 6 H, SC(CH₃)₂], 1.62 [m, 1 H, CH(CH₃)₂], 2.13 [d, 3 H, =CCH₃], 2.22 [s, 2 H, SC(CH₃)₂CH₂], 2.66 [m, 2 H, =CCH₂CH], 2.89 [d, 3 H, =CCH₃], 4.21 [q, 2 H, OCH₂CH₃], 5.80 [s, 1 H, =CH], 6.60 [d, 1 H, =CH], 6.688 [d, 1 H, =CH], 6.82 [q, 1 H, J = 8.5 Hz, J = 2.1 Hz, Ar-H], 7.02 [d, 1 H, J = 8.5 Hz, Ar-H], 7.15 [d, 1 H, J = 2.1 Hz, Ar-H]; ¹³C NMR (DCCl₃) ppm 13.41 [OCH₂CH₃], 14.29 [=CCH₃], 21.13 [=CCH₃], 22.36 [CH(CH₃)₂], 29.70 [C(CH₃)₂], 30.55 [C(CH₃)₂], 53.24 [=CCH₃], 59.77 [=CCH₃], 120.96-125.21 [=C], 127.74-142.07 [Ar-C], 151.37 [FC=CH], 166.88 [OC=O]; ¹⁹F NMR (DCCl₃) ppm -122.13.50 [m, 1 F, =CF]. Anal. Calcd for C₂₇H₃₇FO₂S: C, 72.93; H,

8.39. Found: C, 72.66; H, 8.19.

Ethyl (6Z,2E,4E)-6-Fluoro-3-methyl-7-(2,2,4,4-tetramethyl(3H-benzo[3,4-e]thian-6-yl))octa-2,4,6-trienoate (63)

A 25-mL, three-necked, round-bottomed flask equipped with a N₂ inlet and an addition funnel was charged with triethyl 3-methyl-4-phosphonocrotonate (96 mg, 0.36 mmol), DMPU (42 mg, 0.36 mmol), and THF (2 mL). The mixture was cooled to 0 °C, and 0.32 ml (0.51 mmol) of *n*-BuLi (1.6 M) was added by syringe. After stirring for 1 h at 0 °C, aldehyde **99a** (96 mg, 0.41 mmol) dissolved in 2 mL of THF was added (addition funnel). The new reaction mixture was allowed to warm to RT, and then it was stirred for 4 days. Quenching the reaction mixture with saturated, aqueous solution of ammonium chloride (1 mL) and extraction of the mixture with ethyl acetate (3 x 10 mL) was followed by washing the combined organic extracts with water (2 x 2 mL) and brine (1 x 3 mL). The organic extract was then dried (MgSO₄, 12 h), the solvent was evaporated (rotovap), and the residual oil was purified by flash chromatography (H₂CCl₂:hexane, 1:1, drop rate = 1 drop/s) to give 97 mg (73%) of **63** as a thick, light yellow oil. IR (neat) 1710 [OC=O] cm⁻¹; ¹H NMR (DCCl₃) δ 1.24 [t, 3 H, OCH₂CH₃], 1.40 [s, 6 H, C(CH₃)₂], 1.43 [s, 6 H, SC(CH₃)₂], 1.98 [s, 2 H, SC(CH₃)₂CH₂], 2.16 [d, 3 H, =CCH₃], 2.36 [d, 3 H, =CCH₃], 4.20 [q, 2 H, OCH₂CH₃], 5.92 [s, 1 H, =CH], 6.6 [s, 1 H, =CH], 6.81 [d, 1 H, =CH], 7.11-7.56 [m, 3 H, Ar-H]; ¹³C NMR (DCCl₃) ppm 14.32 [OCH₂CH₃], 31.64 [C(CH₃)₂], 32.55 [C(CH₃)₂], 54.29 [=CCH₃], 59.86 [=CCH₃], 61.38 [=CCH₃], 120.88-123.21 [=C-C], 125.74-151.11 [Ar-C], 166.93 [OC=O]; ¹⁹F NMR (DCCl₃) (ref C₆H₅CF₃ in C₆D₆) ppm -122.32 [d, 1 F, =CF]. Anal. Calcd for C₂₄H₃₁FO₂S: C, 71.60; H, 7.76. Found: C, 71.48; H, 7.62.

Ethyl (6Z,2E,4E)-6-Fluoro-3,8-dimethyl-7-(2,2,4,4-tetramethyl(3H-benzo[3,4-e]thian-6-yl))nona-2,4,6-trienoate (64)

A 25-mL, three-necked, round-bottomed flask equipped with a N₂ inlet and an addition funnel was charged with triethyl 3-methyl-4-phosphonocrotonate (124 mg, 0.47 mmol), DMPU (60 mg, 0.47 mmol), and THF (2 mL). The mixture was cooled to 0 °C, and 0.30 ml (0.48 mmol) of *n*-BuLi (1.6 M) was added by syringe. After stirring for 1 h at 0 °C, aldehyde **99b** (137 mg, 0.43 mmol) in 2 mL of THF was added (addition funnel). The new reaction mixture was allowed to warm to RT, and then it was stirred for 4 days. Quenching the reaction mixture with a saturated, aqueous, solution of ammonium chloride (1 mL) and extraction of the mixture with ethyl acetate (3 x 10 mL) was followed by washing the combined organic extracts with water (2 x 2 mL) and brine (1 x 3 mL). The organic extracts were then dried (MgSO₄, 12 h). Evaporation (rotovap) of the solvent and purification of the major component in the residue by flash chromatography ((Et)₂O:hexane, 1:1, drop rate = 1 drop/s) gave **64** (101 mg, 55%) as a thick, light yellow oil. IR (neat) 1712 [OC=O] cm⁻¹; ¹H NMR (DCCl₃) δ 1.06 [d, 3 H, CH(CH₃)₂], 1.24 [t, 3 H, OCH₂CH₃], 1.37 [s, 6 H, C(CH₃)₂], 1.44 [s, 6 H, SC(CH₃)₂], 1.57 [d, 3 H, =CCH₃], 1.98 [s, 2 H, SC(CH₃)₂CH₂], 2.16 [d, 3 H, =CCH₃], 2.36 [d, 3 H, =CCH₃], 4.25 [q, 2 H, OCH₂CH₃], 5.65 [s, 1 H, =CH], 6.6 [d, 1 H, =CH], 6.81 [d, 1 H, =CH], 6.88 [q, 1 H, J = 8.6 Hz, J = 2.2 Hz, Ar-H], 7.05 [d, 1 H, J = 8.6 Hz, Ar-H] 7.45 [d, 1 H, J = 2.2 Hz, Ar-H]; ¹³C NMR (DCCl₃) ppm 13.41 [OCH₂CH₃], 14.29 [=CCH₃], 21.13 [=CCH₃], 29.70 [C(CH₃)₂], 30.51 [C(CH₃)₂], 54.20 [=CCH₃], 59.77 [=CCH₃], 120.37-125.21 [=C], 127.74-151.34 [Ar-C], 166.90 [OC=O]; ¹⁹F NMR (DCCl₃) (ref C₆H₅CF₃ in C₆D₆) ppm -125.01 [d, 1 F, =CF]. Anal. Calcd for C₂₆H₃₅FO₂S: C, 72.52;

H, 8.19. Found: C, 72.32; H, 8.54.

(2,2,4,4-Tetramethyl(3*H*-benzo[3,4-*e*]thian-6-yl))ethyl 4-(methoxycarbonyl)benzoate (65)

In a 50-mL, one-necked, round-bottomed flask equipped with a condenser and a N₂ inlet was added at RT 2-methyl-1-(2,2,4,4-tetramethyl(3*H*-benzo[3,4-*e*]thian-6-yl))propan-1-ol [(101a), 294.4 mg, 0.88 mmol] and 4-(methoxycarbonyl)benzoic acid (158 mg, 0.88 mmol) dissolved in 20 mL of CH₂Cl₂. To this solution were added *N,N'*-dicyclohexylcarbodiimide (DCC) (462 mg, 2.2 mmol, 2.5 eq) and DMAP (10.0 mg, catalytic amount), and the reaction mixture was stirred for 5 days at RT. Filtration of the reaction mixture, evaporation (rotovap) of solvent from the filtrate, and purification of the residue by flash chromatography (hexane:diethyl ether, 10:1, drop rate = 1 drop/s) of the residue after solvent evaporation afforded 65 (200 mg, 51%) as a pale yellow, thick oil. IR (neat) 1729 [C=O], 1722 [C=O] cm⁻¹; ¹H NMR (DCCl₃) δ 1.39 [s, 6 H, C(CH₃)₂], 1.40 [s, 6 H, C(CH₃)₂], 1.69 [d, 3 H, CHCH₃] 1.94 [s, 2 H, CCH₂C], 3.94 [s, 3 H, OCH₃], 6.19 [q, 1 H, OCHCH₃], 7.18 [q, 1 H, J = 7.8 Hz, J = 2.1 Hz, Ar-*H*], 7.09 [d, 1 H, J = 7.8 Hz, Ar-*H*] 7.46 [d, 1 H, J = 2.1 Hz, Ar-*H*], 8.12 [s, 2 H, Ar-*H*], 8.13 [s, 2 H, Ar-*H*]; ¹³C NMR (DCCl₃) ppm, 14.25 [OCHCH₃], 31.65 [CH₂C(CH₃)₂], 32.50 [SC(CH₃)₂], 34.85 [CH₂C(CH₃)₂], 35.37 [SC(CH₃)₂], 42.05 [CH(CH₃)₂] 52.39 [C, OCH₃], 54.23 [CH₂C(CH₃)₂], 81.94 [HOCH₂], 124.37-142.22 [Ar-C], 165.74 [C=O], 166.29 [C=O]. Anal. Calcd. for C₂₄H₂₈O₄S: C, 69.87; H, 6.84. Found: C, 70.11; H, 6.74.

2-Methyl-1-(2,2,4,4-tetramethyl(3*H*-benzo[3,4-*e*]thian-6-yl))propyl 4-(methoxycarbonyl)benzoate (66)

In a 50-mL, one-necked, round-bottomed flask equipped with a condenser and a N₂ inlet was added at RT 2-methyl-1-(2,2,4,4-tetramethyl(3*H*-benzo[3,4-*e*]thian-6-yl))propan-1-ol [(101b), 300 mg 1.08 mmol] and 4-(methoxycarbonyl)benzoic acid (194 mg, 1.08 mmol) dissolved in 20 mL of CH₂Cl₂. To this solution were added *N,N'*-dicyclohexylcarbodiimide (DCC) (557 mg, 2.7 mmol, 2.5 eq) and DMAP (10.0 mg, catalytic amount), and the reaction mixture was stirred for 4 days at RT. Filtration of the reaction mixture, evaporation (rotovap) of solvent from the filtrate, and purification of the residue by flash chromatography (hexane:diethyl ether, 10:1, drop rate = 1 drop/s) of the residue after solvent evaporation afforded 66 as a pale yellow solid (mp 52-3°C, 190 mg, 40%). IR (neat) 1726 [C=O], 1723 [C=O] cm⁻¹; ¹H NMR (DCCl₃) δ 0.89 [d, 3 H, CH(CH₃)₂], 1.04 [d, 3 H, CH(CH₃)₂] 1.34 [s, 6 H, C(CH₃)₂], 1.40 [s, 6 H, C(CH₃)₂], 1.94 [s, 2 H, CCH₂C], 2.25 [m, 1 H, CH(CH₃)₂], 3.94 [s, 3 H, OCH₃], 5.79 [d, 1 H, OCHCH], 7.08 [q, 1 H, J = 7.8 Hz, J = 2.1 Hz, Ar-*H*], 7.09 [d, 1 H, J = 7.8 Hz, Ar-*H*] 7.36 [d, 1 H, J = 2.1 Hz, Ar-*H*], 8.12 [s, 2 H, Ar-*H*], 8.13 [s, 2 H, Ar-*H*]; ¹³C NMR (DCCl₃) ppm, 18.55 [CH(CH₃)₂], 18.68 [CH(CH₃)₂], 31.50 [CH₂C(CH₃)₂], 32.53 [SC(CH₃)₂], 34.85 [CH₂C(CH₃)₂], 35.37 [SC(CH₃)₂], 41.95 [CH(CH₃)₂] 52.37 [OCH₃], 54.46 [CH₂C(CH₃)₂], 81.94 [HOCH₂], 124.37-142.22 [Ar-C], 164.94 [C=O], 166.22 [C=O]. Anal. Calcd. for C₂₆H₃₂O₄S: C, 70.88; H, 7.32. Found: C, 70.81; H, 7.74.

3-Methyl-1-(2,2,4,4-tetramethyl(3*H*-benzo[3,4-*e*]thian-6-yl))butyl 4-(methoxycarbonyl)benzoate (67)

In a 50-mL, one-necked, round-bottomed flask equipped with a condenser and a N₂ inlet was added at RT 3-methyl-1-(2,2,4,4-tetramethyl(3*H*-benzo[3,4-*e*]thian-6-yl))butan-1-ol [(100c), 300 mg, 1.03 mmol] and 4-(methoxycarbonyl)benzoic acid (185 mg, 1.03 mmol)

dissolved in 20 mL of CH_2Cl_2 . To this solution were added, *N,N'*-dicyclohexylcarbodiimide (DCC) (531 mg, 2.57 mmol, 2.5 eq) and DMAP (9.0 mg, catalytic amount), and the reaction mixture was stirred for 4 days at RT. Filtration of the reaction mixture, evaporation (rotovap) of solvent from the filtrate, and purification of the residue by flash chromatography (hexane:diethyl ether, 8:1, drop rate = 1 drop/s) afforded **67** as a white solid (mp 61-3 °C, 200 mg, 43%). IR (neat) 1732 [C=O], 1723 [C=O] cm^{-1} ; ^1H NMR (DCCl_3) δ 0.89 [dd, 6 H, $\text{CH}(\text{CH}_3)_2$], 1.36 [s, 6 H, $\text{C}(\text{CH}_3)_2$], 1.40 [s, 6 H, $\text{C}(\text{CH}_3)_2$], 1.84 [m, 2 H, $\text{O}=\text{CCH}_2\text{CH}$], 1.94 [s, 2 H, CCH_2C], 2.25 [m, 1 H, $\text{CH}(\text{CH}_3)_2$], 3.93 [s, 3 H, OCH_3], 6.05 [m, 1 H, OCHCH], 7.18 [q, 1 H, $J = 7.9$ Hz, $J = 2.0$ Hz, Ar-*H*], 7.19 [d, 1 H, $J = 7.9$ Hz, Ar-*H*] 7.340 [d, 1 H, $J = 2.0$ Hz, Ar-*H*], 8.1 [s, 2 H, Ar-*H*], 8.10 [s, 2 H, Ar-*H*]; ^{13}C NMR (DCCl_3) ppm 22.39 [$\text{CH}(\text{CH}_3)_2$], 23.82 [$\text{O}-\text{CCH}_2\text{CH}$], 31.62 [$\text{CH}_2\text{C}(\text{CH}_3)_2$], 32.50 [$\text{SC}(\text{CH}_3)_2$], 35.55 [$\text{CH}_2\text{C}(\text{CH}_3)_2$], 42.05 [$\text{SC}(\text{CH}_3)_2$], 52.43 [OCH_3], 54.44 [$\text{CH}_2\text{C}(\text{CH}_3)_2$], 75.78 [$\text{C}-\text{OC}=\text{O}$], 124.07-142.62 [Ar-*C*]. 165.08 [C=O], 166.31 [C=O]. Anal. Calcd. for $\text{C}_{27}\text{H}_{34}\text{O}_4\text{S}$: C, 71.33; H, 7.54. Found: C, 71.36; H, 7.65.

{[(1*E*,3*E*)-1-Aza-3-fluoro-4-(2,2,4,4,7-pentamethyl(3*H*-benzo)[3,4-*e*]thian-6-yl)]penta-1,3-dienyl}amino}aminomethane-1-thione (**68**)

Thiosemicarbazide (60.00 mg, 0.65 mmol) dissolved into 4 mL of water and AcOH (1 drop) was placed in a 10-mL beaker. Then 200 mg (0.65 mmol) of aldehyde **106** was dissolved in 5 mL of EtOH (95%). The latter solution was warmed to 60 °C and then was added dropwise to the thiosemicarbazide solution while hot. A precipitate formed immediately. The reaction mixture was set aside for 24 h at 0 °C, and then the solid was filtered off. The recrystallization of the solid (EtOAc:diethyl ether, 2:1) afforded an white

solid **68** (mp 162-3 °C, 178 mg, 72 %). IR (neat) 3379 [N-H], 3233 [N-H], 3151 [N-H] cm^{-1} ; ^1H NMR (DMSO- d_6) 1.89 [s, 6 H, C(CH₃)₂], 1.90 [s, 6 H, C(CH₃)₂], 2.05 [d, 3 H, CHCH₃] 2.10 [s, 2 H, CCH₂C], 3.34 [s, 3 H, Ar-CH₃], 6.98 [s, 1 H, Ar-H], 7.09 [s, 1 H, Ar-H] 7.35 [d, 1 H, J = 14.1 Hz, FC=CH], 7.51 [s, 1 H, N-H], 7.99 [s, 1 H, N-H], 9.91 [s, 1 H, N-H]; ^{13}C NMR (DMSO- d_6) ppm, 17.57 [=CCH₃], 25.05 [Ar-CH₃] 31.30 [CH₂C(CH₃)₂], 32.52 [SC(CH₃)₂], 34.68 [CH₂C(CH₃)₂], 42.05 [SC(CH₃)₂], 53.63 [CH₂C(CH₃)₂] 128.37-142.22 [Ar-C], 151.61 [FC=CH], 179.83.74 [C=S]. Anal. Calcd for C₁₉H₂₆FN₃S₂: C, 60.12; H, 6.90; N, 11.07. Found: C, 60.35; H, 7.07; N, 11.22.

6-Methoxy-1,1,4,4-tetramethyl-5-nitroisochromane (70)

Into a 500-mL, singled necked, round bottomed flask, fitted with a condenser, magnetic stirrer, and N₂ inlet was added 6-methoxy-1,1,4,4-tetramethylisochromane [(69), 18.0 g, 81.70 mmol] dissolved in Ac₂O (36 mL) at -5 °C (ice/salt bath). A mixture of ice-cold concentrated HNO₃ (18 mL) and Ac₂O (36 mL) was added dropwise to the reaction mixture (-5 °C, 10 min) which was then stirred (1 h). The reaction mixture was poured into a solution of saturated NaHCO₃ (300 mL) and extracted with H₂CCl₂ (3 x 120 mL). The organic layer was washed with water (150 mL) and brine (150 mL) and then dried (Na₂SO₄, 12 h). The solvent was evaporated (rotovap) to give a thick yellow oil. The oil was triturated with pentane to give a light yellow solid. Recrystallization (95 % EtOH) gave **70** (6.91 g, 32%) as a white solid; mp 82-83 °C IR (KBr) 1241 [NO₂] cm^{-1} ; ^1H NMR (DCCl₃) δ 1.28 [s, 6 H, C(CH₃)₂], 1.51 [s, 6 H, OC(CH₃)₂], 3.48 [s, 2 H, CH₂], 3.83 [s, 3 H, OCH₃], 6.88 [d, 1 H, J = 2.5 Hz, Ar-H], 7.12 [d, 1 H, J = 2.5 Hz, Ar-H]; ^{13}C NMR (CDCl₃) ppm 24.09 [(CH₃)₂] 30.05 [(CH₃)₂], 56.35 [O-CH₂], 71.68 [O-C(CH₃)₂], 110.65 [Ar-O-CH₃],

128.18-159.34 [Ar-C]; MS (EI) calcd m/z (M^+) for $C_{14}H_{19}NO_4$: 265; Found: 265.

(6-Methoxy-1,1,4,4-tetramethylisochromane-5-yl)amine (71)

Into a 1-L, single-necked, round bottomed flask, equipped with N_2 inlet, condenser, and a magnetic stirrer was placed 6-methoxy-1,1,4,4-tetramethyl-5-nitroisochromane [(70) 5.7 g, 17.71 mmol] dissolved in acetic acid (206 mL) and water (42 mL). Then the $TiCl_3/HCl$ complex (30% solution, 120 g, 177.1 mmol) was added dropwise, and the resulting purple reaction mixture was stirred (13 h, RT). The new mixture was cooled (0 °C), and NaOH (30%, 500 mL) was added (dropwise, 4 h). The reaction mixture was separated, and the aqueous layer was extracted with EtOAc (8 x 50 mL). The combined organic layers were washed with water (2 x 50 mL) and saturated $NaHCO_3$ (2 x 100 mL), and then the organic extract was dried ($MgSO_4$, 12 h). Recrystallization (95 % EtOH) gave amine 71 (4.6 g, 89%) of as a white solid; mp 110-112 °C. IR (KBr) 3449 [NH_2], 3338 [NH_2], cm^{-1} ; 1H NMR ($DCCl_3$) δ 1.37 [s, 6 H, $C(CH_3)_2$], 1.49 [s, 6 H, $OC(CH_3)_2$], 3.53 [s, 2H, CH_2], 3.83 [s, 3 H, OCH_3], 3.98 [s, 1 H, NH_2], 6.50 [d, 1 H, $J=8.5$ Hz, Ar-H], 7.69 [d, 1 H, $J=8.5$ Hz, Ar-H]; ^{13}C NMR ($DCCl_3$) ppm 27.02 [$(CH_3)_2$], 29.73 [$(CH_3)_2$], 55.41 [$O-CH_2$], 71.16 [$C(CH_3)_2$], 74.83 [$O-C(CH_3)_2$], 111.79 [Ar-O- CH_3], 122.73-146.24 [Ar-C]; MS (EI) calcd m/z (M^+) for $C_{14}H_{19}NO_4$: 235. Found: 235.

Ethyl (2E)-3-(4,4-Dimethylchroman-6-yl)-2-fluorobut-2-enoate (73)

Into a 25-mL, three-necked, round-bottomed flask fitted with a condenser, magnetic stirrer, and N_2 inlet, was added ethyl-2-fluorophosphonoacetate (260 mg, 1.08 mmol) and DMPU (138 mg, 1.08 mmol) dissolved in 3 mL of dry THF. The reaction mixture was cooled to

0 °C, and *n*-BuLi (1.6 M, 0.68 mL, 1.08 mmol) was added dropwise by syringe. After stirring the reaction mixture for 1 h, 1-(4,4-dimethylchroman-6-yl)ethan-1-one [(72), 200 mg, 0.98 mmol] dissolved in 4 mL of dry THF was added. The reaction mixture was then stirred for 6 days at RT and then was quenched with a saturated, aqueous solution of ammonium chloride. Extraction with ethyl acetate (3 x 25 mL) was followed by washing the combined organic layers with H₂O (1 x 20 mL) and brine (1 x 25 mL) and then drying (MgSO₄, 5 h). After flash chromatography (hexane:diethyl ether, 2:1, drop rate = 1 drop/s) of the residue and, after solvent evaporation, 7 (206 mg, 72%) was recovered as a clear oil. IR (neat) 1728 [C=O] cm⁻¹; ¹H NMR (DCCl₃) δ 1.15 [t, 3 H, OCH₂CH₃], 1.30 [s, 6 H, CH₃CCH₃], 1.82 [q, 2 H, CH₂CH₂], 2.09 [d, H, =CCH₃], 4.07 [q, 2 H, OCH₂CH₃], 4.20 [q, 2 H, CH₂CH₂], 6.73 [d, 1 H, J = 8.4 Hz, Ar-H], 6.88 [q, 1 H, J = 8.4 Hz, J = 2.4 Hz, Ar-H], 7.07 [d, 1 H, J = 2.4 Hz, Ar-H]; ¹³C NMR (DCCl₃) ppm 13.75 [OCH₂CH₃], 19.20 [CHCH₃], 30.55 [C(CH₃)₂], 30.97 [C(CH₃)₂], 37.47 [CH₂CH₂], 60.88 [OCH₂CH₃], 63.05 [CH₂CH₂], 116.50 [FC=CH], 126.41-145.77 [Ar-C], 153.38 [FC=CH], 160.34 [O-C=O]; ¹⁹F NMR (DCCl₃) ppm -124.15 [q, 1 F, FC=CCH₃].

(2E)-3-(4,4-dimethylchroman-6-yl)-2-fluorobut-2-en-1-ol (74)

Ester 73 (206 mg, 0.70 mmol) dissolved in 5 mL of dry THF was placed in 25-mL, three-necked, round-bottomed flask fitted with a condenser, magnetic stirrer, and N₂ inlet, and then cooled to -40 °C. A solution (1.5 M, 0.93 mL, 1.40 mmol) of DIBAL-H in toluene was then added by syringe. The reaction mixture was stirred for 2 h, and the reaction was monitored by TLC (hexane:ethyl acetate, 1:1). After all of the starting material appeared to have reacted (TLC), the reaction mixture was quenched with 2 mL of a saturated, aqueous

solution of Rochelle salt (sodium-potassium tartrate). The bi-phasic mixture was extracted with ethyl acetate (3 x 25 mL), followed by washing the organic extracts with H₂O (1 x 15 mL) and brine (1 x 20 mL) and then drying (MgSO₄, 12 h). Separation of the major component in the residue, via flash chromatography (hexane:diethyl ether, 1:3, drop rate = 1 drop/s) and, after solvent evaporation, afforded **74** (160 mg, 92%) as a colorless oil. IR (neat) 3412 [O-H], 1651 [C=C-F] cm⁻¹; ¹H NMR (DCCl₃) δ 1.32 [s, 6 H, CH₃CCH₃], 1.82 [q, 2 H, CH₂CH₂], 2.00 [bs, 1H, O-H], 2.09 [d, H, =CCH₃], 4.19 [m, 2 H, H₂COH], 4.20 [q, 2 H, CH₂CH₂], 6.53 [d, 1 H, J = 8.4 Hz, Ar-H], 6.78 [q, 1 H, J = 8.4 Hz, J = 2.4 Hz, Ar-H], 7.27 [d, 1 H, J = 2.4 Hz, Ar-H]; ¹³C NMR (DCCl₃) ppm 16.20 [=CHCH₃], 30.53 [C(CH₃)₂], 30.97 [C(CH₃)₂], 37.47 [CH₂CH₂], 58.88 [HOCH₂], 63.05 [CH₂CH₂], 116.76 [FC=CH], 118.69-152.77 [Ar-C], 156.38 [FC=CH]; ¹⁹F NMR (DCCl₃) ppm -118.51 [m, 1 F, FC=CCH₃].

(2E)-3-(4,4-Dimethylchroman-6-yl)-2-fluoro-2-butenal (75)

Alcohol **74** (162 mg, 0.65 mmol) dissolved in 5 mL of acetone was placed in a 25-mL, one-necked, round-bottomed flask, and MnO₂ (0.75 g, 17.25 mmol, activated grade, size < 5 μm) was then added to the solution at RT. The suspension was stirred for 24 h and then was filtered through a 1-inch thick celite pad. Evaporation (rotovap) of the solvent and purification via flash chromatography (hexane:diethyl ether:ethyl acetate, 1:1:1, drop rate = 1 drop/s) of the major component in the residue, afforded aldehyde **75** (95mg, 59%) as a light yellow oil. IR (neat) 2834 [O=C-H], 1674 [C=O] cm⁻¹; ¹H NMR (DCCl₃) δ 1.37 [s, 6 H, CH₃CCH₃], 1.83 [q, 2 H, CH₂CH₂], 2.09 [d, H, =CCH₃], 4.21 [q, 2 H, CH₂CH₂], 6.73 [d, 1 H, J = 8.1 Hz, Ar-H], 6.98 [q, 1 H, J = 8.1 Hz, J = 2.2 Hz, Ar-H], 7.24 [d, 1 H, J = 2.1

Hz, Ar-H], 9.01 [s, 1H, HC=O]; ^{13}C NMR (DCCl_3) ppm 17.20 [=CHCH₃], 30.43 [C(CH₃)₂], 30.87 [C(CH₃)₂], 37.34 [CH₂CH₂], 63.05 [CH₂CH₂], 116.76 [FC=CH], 118.69-152.77 [Ar-C], 156.38 [FC=CH], 188.87 [HC=O]; ^{19}F NMR (DCCl_3) ppm -121.51 [m, 1 F, FC=CCH₃].

1-(4,4-Dimethylchroman-6-yl)ethan-1-ol (76)

Ketone **72** (150 mg, 0.73 mmol) dissolved in 3 mL of dry THF was placed in a 25-mL, three-necked, round-bottomed flask fitted with a condenser, magnetic stirrer, and N₂ inlet, and cooled to -40 °C. A solution of DIBAL-H in toluene (1.5 M, 1.63 mL, 2.44 mmol) was then added by syringe. The reaction mixture was then stirred for 2 h, and it was monitored by TLC (hexane:ethyl acetate, 1:3). After all of the starting material appeared to have reacted (TLC), the reaction mixture was quenched with 4 mL of a saturated, aqueous solution of Rochelle salt (sodium-potassium tartrate). The bi-phasic mixture was then extracted with ethyl acetate (3 x 25 mL), followed by washing the extracts with H₂O (2 x 10 mL) and brine (1 x 15 mL) and then drying (MgSO₄, 12 h). Separation of the major component after evaporation (rotovap) of the solvent and flash chromatography (hexane:diethyl ether, 1:3, drop rate = 1 drop/s) afforded alcohol **76** (142 mg, 94%) as a clear oil. IR (neat) 3401 [O-H], cm⁻¹; ^1H NMR (DCCl_3) δ 1.23 [s, 6 H, CH₃CCH₃], 1.42 [d, 3 H, HCCH₃], 1.65 [bs, 1H, O-H], 1.82 [q, 2 H, CH₂CH₂], 4.20 [q, 2 H, CH₂CH₂], 4.81 [q, 1 H, HCOH], 6.79 [d, 1 H, J = 8.2 Hz, Ar-H], 7.08 [q, 1 H, J = 8.2 Hz, J = 2.1 Hz, Ar-H], 7.27 [d, 1 H, J = 2.1 Hz, Ar-H]; ^{13}C NMR (DCCl_3) ppm 24.85 [(HO)HCCH₃], 30.58 [C(CH₃)₂], 30.97 [C(CH₃)₂], 37.459 [CH₂CH₂], 63.08 [CH₂CH₂], 70.29 [HOCH₂], 116.76 [FC=CH], 118.69-152.77 [Ar-C].

2,2,4-Trimethyl-1,2-dihydroquinoline (78)

Into a 500-mL, 4-necked, round-bottomed flask equipped with a thermometer, condenser, N₂ inlet, and addition funnel connected to N₂ and placed on top of another condenser, and distillation apparatus was added freshly distilled aniline (20.0 g, 0.21 mol) together with a catalytic amount of iodine (0.3 g) and concentrated HCl (0.2 mL). The reaction mixture was heated to 155 °C, and then acetone (~ 400 mL) was added slowly and at such a rate so that the temperature of the mixture did not fall below 140 °C. The unreacted acetone and H₂O (a reaction byproduct) distilled off during the addition process. After addition of acetone (250 mL, ~3.5 h), the reaction mixture was stirred for an additional 1 h and was then allowed to cool to RT. Extraction with hexane (3 x 100 mL) was followed by washing the combined organic extracts with H₂O (1 x 100 mL) and brine (1 x 100 mL) and then drying (MgSO₄, 12 h). The hexane was evaporated (rotovap), and the resulting product was purified by distillation (bp 109-111 °C/0.75 mm Hg) to yield **78** as a pale yellow oil (27.9 g, 76%). IR (neat) 3301 [N-H] cm⁻¹; ¹H NMR (DCCl₃) δ 1.41 [s, 6 H, N-C(CH₃)], 2.18 [s, 3 H, =C-CH₃], 3.79 [bs, 1 H, N-H], 5.45 [s, 1 H, =CH], 6.55-7.15 [m, 4 H, Ar-H]; ¹³C NMR (DCCl₃) ppm 18.64 [=C-CH₃], 23.44 [2 C, C(CH₃)₂], 54.34 [=C-C(CH₃)₂], 110.53 [=C-CH₃], 111.91 [=C-C(CH₃)₂], 116.12-145.07 [Ar-C].

1,2,2,4-Tetramethyl-1,2-dihydroquinoline (79)

In a 25-mL, three-necked, round-bottomed flask equipped with a condenser, magnetic stirrer, and N₂ inlet, was added powdered KOH (299 mg, 5.7 mmol) dissolved in 10 mL of DMSO. The mixture was stirred at RT until all KOH dissolved, and then the temperature was adjusted to 10 °C (water bath and ice). 2,2,4-Trimethyl-1,2-dihydroquinoline (1.00 g, 5.77 mmol) dissolved in 5 mL of DMSO was added dropwise,

followed immediately by the addition of CH_3I (1.09 g, 7.7 mmol). The reaction mixture was allowed to stir for 30 min and then was poured into 10 mL of ice-cold water. The mixture was extracted with H_2CCl_2 (3 x 5 mL). The combined organic extracts were washed with water (1 x 10 mL) and brine (1 x 10 mL) and then dried (Na_2SO_4 , 12 h). Evaporation (rotovap) of solvent and flash chromatography (silica gel, hexanes as only solvent, drop rate = 1 drop/s) of the residue afforded **2** as a yellow oil (0.784 g, 71 %). IR (neat) 1048 [C-N] cm^{-1} ; ^1H NMR (DCCl_3) δ 1.37 [s, 6 H, N-C-(CH_3)], 2.23 [s, 3 H, =C- CH_3], 2.96 [s, 3 H, N- CH_3], 5.36 [s, 1 H, =CH], 6.87-7.24 [m, 4 H, Ar-H]; ^{13}C NMR (DCCl_3) ppm 18.64 [=C- CH_3], 25.74 [2 C, C(CH_3) $_2$], 30.60 [N- CH_3], 54.53 [=C-C(CH_3) $_2$], 111.43 [=C- CH_3], 112.51 [=C-C(CH_3) $_2$], 118.12-144.56 [Ar-C].

Bis(2,2,2-trichloroethyl) Azodicarboxylate (81)

In a 50-mL, three-necked flask equipped with magnetic stirrer, thermometer, and 25-mL and 25-mL dropping funnels was placed a solution of 1.0 g (0.023 mol) of 85% hydrazine hydrate in 6 mL of 95% ethanol. The reaction flask was cooled in an ice bath, and 9.6 g (0.046 mol) of 2,2,2-trichloroethyl chloroformate was added dropwise so that the temperature was kept below 20 °C. During the addition of 1 equivalent of the chloroformate, a white precipitate formed. After exactly one-half of the chloroformate had been added, a solution of sodium carbonate (2.5 g, 0.024 mol) in 10.0 mL of water was added dropwise (2 h) along with the remaining chloroformate. The rate of addition of these two reagents was such that the flow of the chloroformate was faster than that of the sodium carbonate so that there was always an excess of chloroformate present. The temperature was kept below 20 °C during the addition. As the second equivalent of chloroformate was

added, the white precipitate dissolved. After the addition of the reactants was complete (4 h), the reaction was allowed to stir for an additional 30 min while the solution warmed to RT. The reaction mixture was then transferred to a separatory funnel. The viscous, organic layer (bottom) was separated from the aqueous layer and was dissolved in 20 mL of ether. The reaction vessel was washed with 10 mL of ether, and this ether portion was used to extract the aqueous layer again. The ether layers were combined, dried (MgSO_4 , 5 h), and then filtered, and the solvent was removed under reduced pressure (rotovap).

Bromine (1.6 g, 20.0 mmol) in 150 mL of dichloromethane was added dropwise (1 h) to a dichloromethane (500 mL) solution of hydrazide (7.0 g, 18.2 mmol) and pyridine (1.50 g, 20.0 mmol), and solution was cooled to 0 °C (ice bath) under argon. The reaction mixture turned from colorless to yellow upon the addition. The reaction was complete after 30-60 min at RT as determined by TLC (silica gel, EtOAc:hexane, 1:1). The reaction mixture was then diluted to 1000 mL with dichloromethane, washed with 5% HCl (2 x 300 mL), saturated sodium bicarbonate (300 mL), water (3 x 300 mL) and saturated NaCl (1 x 300 mL) to give azide **81** as light yellow solid [4.26 g, 56%, mp 115-6 °C (lit.⁷⁶ 116.5-117 °C). IR (KBr pellet) 1786 [C=O], 1723 [C=O] cm^{-1} ; ^1H NMR (DCCl_3) δ 5.08 [s, 4 H, Cl_3CCH_2]; ^{13}C NMR (DCCl_3) ppm 77.45 [Cl_3CCH_2], 93.09 [Cl_3CCH_2], 158.42 [C=O].

[1,2,2,4-Tetramethyl-1,2-dihydroquinol-6-yl]amine (82)

1,2,2,4-Tetramethyl-1,2-dihydroquinoline (1.00 g, 5.3 mmol) dissolved in 5 mL of a 3 M solution of LiOCl_4 in diethyl ether was placed in a 25-mL, three-necked, round-bottomed flask equipped with a condenser, addition funnel, and N_2 inlet. To this solution was added dropwise bis(2,2,2-trichloroethyl) azodicarboxylate (4.5 g, 11.8 mmol, prepared

in our lab (see above) via reaction of 2,2,2-trichloroacetyl chloride and hydrazine (85%), followed by reduction with Br₂ in pyridine) dissolved in 5 mL of diethyl ether at 0 °C. The solution was then carefully warmed to 55 °C and stirred at this temperature for 3 h. The new reaction mixture was cooled to 0 °C, and 5 mL of ice water was added. Extraction with H₂CCl₂ (3 x 10 mL), followed by washing the extracts with brine (1 x 5 mL) and drying (Na₂SO₄) overnight, yielded an aryl azide (2.58 g, 85%). This aryl azide was reduced, without purification, by dissolving it in 5 mL of concentrated acetic acid. To this solution was added approximately 1 equivalent by weight of Zn dust (2.6 g). The reaction mixture was stirred for 15 min, and 9 μL of acetone was added by micro-pipette. After stirring the reaction mixture for 3 h at RT, the new mixture was filtered through a 1-cm thick pad of celite. Then 5 mL of a saturated, aqueous solution of NaHCO₃ was added, and the mixture was extracted (H₂CCl₂, 3 x 10 mL). Flash chromatography of the concentrated extracts with silica gel (hexane:EtOAc, 1:1) was used to purify the resulting amine obtained as a light brown solid **3**, (mp 87-9 °C, 546 mg, 51% from **79**). IR (neat) 3338 [N-H], 3224 [N-H] cm⁻¹; ¹H NMR (DCCl₃) δ 1.30 [s, 6 H, N-C-(CH₃)], 1.97 [s, 3 H, =C-CH₃], 2.78 [s, 3 H, N-CH₃], 5.38 [s, 1 H, =CH], 6.42 [d, 1 H, J = 9.3 Hz, Ar-H], 6.48 [d, 1 H, J = 2.3 Hz, Ar-H], 6.55 [q, 1 H, J = 2.1 Hz, J = 9.3 Hz, Ar-H], 6.56 [s, 1 H, N-H], 6.8 [bs, 1 H, N-H]; ¹³C NMR (DCCl₃) ppm 18.53 [=C-CH₃], 25.70 [C(CH₃)₂], 30.68 [N-CH₃], 55.60 [=C-C(CH₃)₂], 111.91 [=C-CH₃], 112.14 [=C-C(CH₃)₂], 115.72-138.78 [Ar-C].

1.2.2.4-Tetramethyl-1,2-dihydroquinoline-6-carbaldehyde (83)

Phosphorus oxychloride (4.1 g, 0.026 mol) was added dropwise to DMF (12 mL) at 0 °C in a 50-mL, three-necked, round-bottomed flask equipped with a condenser and N₂

inlet. After the reaction of OPCl_3 with DMF had subsided, 1,2,2,4-tetramethyl-1,2-dihydroquinoline [(79), 5 g, 0.026 mol] dissolved in 30 mL of DMF was slowly added at 0 °C. The reaction mixture was allowed to stir for 24 h at RT and was then cooled to 0 °C, after which cold water (5 mL) was carefully added. The reaction mixture was extracted with methylene chloride (3 x 30 mL), and the combined organic layers were washed with water (1 x 10 mL) and brine (1 x 10 mL) and dried (MgSO_4 , overnight). After evaporation (rotovap) of the solvents and refrigeration for 24 h, aldehyde **83** crystallized as a pale yellow solid (no purification required, 3.57 g, 64%), mp 39–41 °C. IR (pellet) 2733 [H-C-O], 1669 [C=O] cm^{-1} ; $^1\text{H NMR}$ (DCCl_3) δ 1.38 [s, 6 H, $\text{C}(\text{CH}_3)_2$], 2.03 [s, 3 H, $=\text{CCH}_3$], 2.91 [s, 3 H, N- CH_3], 5.30 [s, 1 H, $=\text{CH}$], 6.50 [d, 1 H, $J = 8.4$ Hz, Ar- H], 7.52 [d, 1 H, $J = 2.4$ Hz, Ar- H], 7.52 [q, 1 H, $J = 8.4$ Hz, $J = 2.4$ Hz, Ar- H], 9.67 [s, 1 H, O=C- H]; $^{13}\text{C NMR}$ (DCCl_3) ppm 18.57 [$=\text{C}-\text{CH}_3$], 28.75 [$\text{C}-\text{C}(\text{CH}_3)_2$], 31.21 [N- CH_3], 57.60 [$=\text{C}-\text{C}(\text{CH}_3)_2$], 109.14 [$=\text{CH}$], 121.76–150.04 [$\text{CH}=\text{C}-\text{Ph}$], 190.19 [C=O].

4-Methyl-6-(1,2,2,4-tetramethyl(1,2-dihydroquinolyl))-5,6-dihydropyran-2-one (84)

To a solution of ethyl 3,3-dimethylacrylate (205 mg, 1.5 mmol) and 3 mL of dry THF in a 25-mL, three-necked, round-bottomed flask equipped with a condenser and N_2 inlet was added dropwise (syringe) LDA (0.51 mL, 1.53 mmol, 3 M solution in toluene) at -78 °C. After the addition, the reaction mixture was stirred for 1 h, after which **83** (0.3 g, 1.46 mmol) dissolved in 2 mL of THF was added. After stirring the reaction mixture for 1 h at -78 °C, the reaction was quenched with 1.5 mL of a saturated, aqueous solution of ammonium chloride. The resulting mixture was allowed to warm to RT and was then stirred for an additional 1 h. Extraction of the mixture with EtOAc (3 x 3 mL) was followed by washing

the combined organic extracts with water (1 x 1 mL) and brine (1 x 1 mL). After drying (MgSO₄, 5 h), the solvent was removed (rotovap), and a thick, dark-red oil was recovered as **84** (171 mg, 43%). IR (neat) 1725 [C=O] cm⁻¹; ¹H NMR (DCCl₃) δ 1.28 [s, 6 H, C(CH₃)₂], 2.03 [s, 3 H, =CCH₃], 2.05 [s, 3 H, =C-CH₃], 2.91 [s, 3 H, N-CH₃], 5.25 [s, 1 H, =CH], 5.91 [s, 1 H, =CH], 6.50 [d, 1 H, Ph-H], 7.45 [m, 2 H, Ph-H], 9.85 [s, 1 H, O=C-H]; ¹³C NMR (DCCl₃) ppm 18.57 [=C-CH₃], 28.75 [C-CH₃], 31.21 [s, 1 C, N-CH₃], 56.60 [=C-C(CH₃)₂], 109.14 [=CH], 121.76-150.04 [Ph-CH=C], 168.35 [O-C=O].

4-Methyl-6-(1,2,2,4-tetramethyl(1,2-dihydroquinolyl))-5,6-dihydropyran-2-ol (**85**)

To a 25-mL, three-necked, round-bottomed flask equipped with a condenser and N₂ inlet was slowly added a solution of **84** (107 mg, 0.36 mmol) in 2 mL of dry THF to a chilled solution (-78 °C) of DIBAL-H in hexane (0.37 mL, 0.59 mmol, 1.6 M). The mixture was stirred for 20 min and was then quenched with 0.75 mL of a saturated, aqueous solution of Rochelle salt (saturated solution of sodium and potassium tartrate, 1:1). After allowing the reaction mixture to warm to RT, the mixture was extracted with EtOAc (2 x 2 mL), and the extracts were washed with water (1 x 1 mL) and brine (1 x 1 mL). After drying (Na₂SO₄, 12 h), the solvent was evaporated (rotovap) to give a thick, red oil **85** [the only product as seen from TLC (hexane:EtOAc, 2:1) (92 mg, 85%)]. Compound **85** was used in the next step without further purification. IR (neat) 3452 [O-H] cm⁻¹.

(2Z,4E)-3-Methyl-5-(1,2,2,4-tetramethyl(1,2-dihydroquinolyl))penta2,4-dienal (**86**)

In a 25-mL, three-necked, round-bottomed flask equipped with a condenser, N₂ inlet, and thermometer holder was placed lactol **85** (150 mg, 0.5 mmol) dissolved in 2 mL of

ClCH₂CH₂Cl (1,2-dichloroethane), and then 2 mL of 5% HCl was added. The reaction mixture was warmed to 55 °C for 3 h. The reaction was monitored by TLC (hexane:EtOAc, 4:1) until completion. The mixture was then cooled to RT and carefully neutralized with a saturated, aqueous solution of NaHCO₃. The aqueous layer was extracted with H₂CCl₂ (2 x 3 mL), and the combined extracts were washed with water (1 x 2 mL) and brine (1 x 2 mL). After drying (MgSO₄, 12 h) and evaporating the solvent (rotovap), the residue was purified with silica gel chromatography (hexane:EtOAc, 1:1) to yield a bright red oil as **86** (87 mg, 62%). IR (neat) 2785 [H-C=O], 1655 [C=O] cm⁻¹; ¹H NMR (DCCl₃) δ 1.28 [s, 6 H, C(CH₃)₂], 2.03 [s, 3 H, =CCH₃], 2.35 [s, 3 H, J = 0.3 Hz, =C-CH₃], 2.91 [s, 3 H, N-CH₃], 5.25 [s, 1 H, =CH], 5.91 [d, 1 H, =CH], 6.25 [s, 1 H, =CH], 6.50 [d, 1 H, Ar-H], 7.45 [m, 2 H, Ar-H], 10.15 [d, 1 H, O=C-H]; ¹³C NMR (DCCl₃) ppm 13.06 [=C-CH₃], 18.57 [=C-CH₃], 27.90 [C-(CH₃)₂], 30.21 [N-CH₃], 56.86 [=C-C(CH₃)₂], 110.14 [=CH], 122.76-136.04 [CH=C-Ph], 191.04 [H-C=O].

Ethyl (2E)-2-Fluoro-3-(1,2,2,4-tetramethyl(6-1,2-dihydroquinolyl))prop-2-enoate (87)

Into a 25-mL, three-necked, round-bottomed flask fitted with a condenser, magnetic stirrer, and N₂ inlet, was added ethyl 2-fluorophosphonoacetate (224 mg, 0.93 mmol) and DMPU (120 mg, 0.93 mmol) dissolved in 3 mL of dry THF. The reaction mixture was cooled to 0 °C, and *n*-BuLi was added dropwise (0.6 mL, 0.94 mmol, 1.6 M) by syringe. After stirring the reaction mixture for 1 h, 1,2,2,4-tetramethyl-1,2-dihydroquinoline-6-carbaldehyde [(**83**), 200 mg, 0.93 mmol] dissolved in 2 mL of dry THF was added. The reaction mixture was then stirred for 3 days at RT and was then quenched with a saturated, aqueous solution of ammonium chloride (1.0 mL). Extraction with ethyl acetate (3 x 25 mL)

was followed by washing the combined organic layers with H₂O (1 x 20 mL) and brine (1 x 25 mL) and then drying (MgSO₄, 5 h). After flash chromatography (hexane:diethyl ether, 1.5:1, drop rate = 1 drop/s) of the residue, and, after solvent evaporation (rotovap), ester **87** (220 mg 78%) of was recovered as a clear oil. IR (neat) 1724 [C=O] cm⁻¹; ¹H NMR (DCCl₃) δ 0.85 [t, 3 H, OCH₂CH₃], 1.35 [s, 6 H, CH₃CCH₃], 1.98 [s, 3 H, =CCH₃], 2.81 [s, 3 H, N-CH₃], 4.27 [q, 2 H, OCH₂CH₃], 5.33 [s, 1 H, =CH], 6.50 [d, 1 H, J = 8.7 Hz, Ar-H], 6.85 [d, 1 H, J = 36.6 Hz, FC=CH], 7.42 [d, 1 H, J = 2.1 Hz, Ar-H], 7.52 [q, 1 H, J = 8.7 Hz, J = 2.1 Hz, Ar-H]; ¹³C NMR (DCCl₃) ppm 14.29 [OCH₂CH₃], 18.53 [=C-CH₃], 25.70 [C(CH₃)₂], 28.68 [N-CH₃], 56.60 [=C-C(CH₃)₂], 61.32 [OCH₂CH₃], 110.91 [=C-CH₃], 118.14 [=C-C(CH₃)₂], 127.72-131.78 [Ar-C], 146.34 [FC=CH], 162.45 [C=O].

(2E)-2-Fluoro-3-[(1,2,2,4-tetramethyl-6-(1,2-dihydroquinolyl)]prop-2-en-1-ol (**88**)

Ester **87** (220 mg, 0.72 mmol) dissolved in 5 mL of dry THF was placed in 25-mL, one-necked, round-bottomed flask, and was then cooled to -40 °C. A solution (1.8 mL, 1.2 mmol, 1.5 M) of DIBAL-H in toluene was then added by syringe. The reaction mixture was stirred for 2 h, and it was monitored by TLC (hexane:ethyl acetate, 1:2). After all of the starting material appeared to have reacted (TLC), the reaction mixture was quenched with 1 mL of a saturated, aqueous solution of Rochelle salt (sodium-potassium tartrate, 1:1). The bi-phasic mixture was extracted with ethyl acetate (3 x 25 mL), followed by washing the organic extracts with H₂O (1 x 15 mL) and brine (1 x 20 mL) and then drying (MgSO₄, 12 h). Separation of the major component in the residue, after solvent evaporation (rotovap), by flash chromatography (hexane:diethyl ether:EtOAc, 1:1:1, drop rate = 1 drop/s) afforded **88** (182 mg, 96%) as a colorless oil. IR (neat) 3371 [O-H] cm⁻¹; ¹H NMR (DCCl₃) δ 1.36

[s, 6 H, CH_3CCH_3], 1.98 [bs, 1 H, O-*H*], 1.98 [d, 3 H, $=\text{CCH}_3$], 2.86 [s, 3 H, N- CH_3], 4.41 [q, 2 H, $\text{H}_2\text{C-OH}$], 6.35 [d, 1 H, $J = 20.4$ Hz, $\text{FC}=\text{CH}$], 6.46 [d, 1 H, $J = 8.4$ Hz, Ar-*H*], 6.93 [d, 1 H, $J = 2.1$ Hz, Ar-*H*], 6.95 [q, 1 H, $J = 8.4$ Hz, $J = 2.1$ Hz, Ar-*H*]; ^{13}C NMR (DCCl_3) ppm 18.53 [$=\text{C-CH}_3$], 27.70 [$\text{C}(\text{CH}_3)_2$], 29.68 [$\text{C}(\text{CH}_3)_2$], 30.68 [N- CH_3], 56.36 [$=\text{C-C}(\text{CH}_3)_2$], 58.83 [HOCH_2], 110.48 [$=\text{C-CH}_3$], 111.34 [$\text{FC}=\text{CH}$], 111.54 [$=\text{C-C}(\text{CH}_3)_2$], 123.72-130.78 [Ar-*C*]; ^{19}F NMR (DCCl_3) ppm -113.65 [q, 1 F, HOCH_2CF].

(2*E*)-2-Fluoro-3-[(1,2,2,4-tetramethyl-6-(1,2-dihydroquinolyl))]prop-2-enal (89)

Alcohol **88** (180 mg, 0.70 mmol) dissolved in 5 mL of acetone was placed in a 25-mL, one-necked, round-bottomed flask and MnO_2 (0.75 g, 8.75 mmol, activated grade, size < 5 μm) was then added to the solution at RT. The suspension was stirred for 24 h and then filtered through a 1-inch thick celite pad. Evaporation (rotovap) of the solvent and purification of the major component in the residue, after solvent evaporation, via flash chromatography (hexane:diethyl ether:ethyl acetate, 2:1:0.1, drop rate = 1 drop/s) afforded aldehyde **89** (98 mg, 54%), as a light yellow oil. IR (neat) 2864 [O=C-*H*], 1682 [C=O] cm^{-1} ; ^1H NMR (DCCl_3) δ 1.34 [s, 6 H, CH_3CCH_3], 1.98 [s, 3 H, $=\text{CCH}_3$], 2.81 [s, 3 H, N- CH_3], 5.33 [s, 1 H, $=\text{CH}$], 6.47 [d, 1 H, $J = 8.4$ Hz, Ar-*H*], 7.06 [d, 1 H, $J = 2.4$ Hz, Ar-*H*], 7.14 [q, 1 H, $J = 8.4$ Hz, $J = 2.1$ Hz, Ar-*H*]; 7.26 [d, 1 H, $J = 18.3$ Hz, $\text{FC}=\text{CH}$], 9.75 [d, 1 H, $J = 19.8$ Hz, $\text{FCC}(\text{O})\text{H}$], ^{13}C NMR (DCCl_3) ppm 18.51 [$=\text{C-CH}_3$], 28.19 [$\text{C}(\text{CH}_3)_2$], 30.86 [N- CH_3], 38.68 [$\text{C}(\text{CH}_3)_2$], 57.36 [$=\text{C-C}(\text{CH}_3)_2$], 110.48 [$=\text{C-CH}_3$], 116.54 [$=\text{C-C}(\text{CH}_3)_2$], 123.72-130.78 [Ar-*C*], 151.34 [$\text{FC}=\text{CH}$], 182.35 [C=O]; ^{19}F NMR (DCCl_3) ppm -131.44 [t, 1 F, O=CHCF].

Ethyl (2*E*)-3-(1,2,2,4-tetramethyl(6-(1,2-dihydroquinolyl)))prop-2-enoate (90)

Into a 25-mL, three-necked, round-bottomed flask fitted with a condenser, magnetic stirrer, and N₂ inlet, was added ethyl 2-phosphonoacetate (217 mg, 0.93 mmol) and DMPU (119 mg, 0.93 mmol) dissolved in 3 mL of dry THF. The reaction mixture was cooled to 0 °C, and *n*-BuLi was added dropwise (64 mL, 1.03 mmol, 1.6 M) by syringe. After stirring the reaction mixture for 1 h, 1,2,2,4-tetramethyl-1,2-dihydroquinoline-6-carbaldehyde [(83), 200 mg, 0.93 mmol] dissolved in 3 mL of dry THF was added dropwise (20 min). The reaction mixture was stirred for 3 days at RT and then was quenched with a saturated, aqueous solution of ammonium chloride (1 mL). Extraction with ethyl acetate (3 x 20 mL) was followed by washing the combined organic layers with H₂O (1 x 20 mL) and brine (1 x 20 mL) and then drying (MgSO₄, 12 h). After flash chromatography (hexane:diethyl ether, 1:2, drop rate = 1 drop/s) of the residue (after solvent evaporation), **90** (217 mg, 82%) was recovered as a clear oil. IR (neat) 1703 [C=O] cm⁻¹; ¹H NMR (DCCl₃) δ 1.33 [t, 3 H, OCH₂CH₃], 1.34 [s, 6 H, CH₃CCH₃], 1.99 [d, 3 H, =CCH₃], 2.84 [s, 3 H, N-CH₃], 4.23 [q, 2 H, OCH₂CH₃], 5.30 [d, 1 H, =CH], 6.18 [d, 1 H, J = 15.9 Hz, HC=CH], 6.48 [d, 1 H, J = 8.4 Hz, Ar-H], 7.21 [d, 1 H, J = 2.1 Hz, Ar-H], 7.30 [q, 1 H, J = 8.7 Hz, J = 2.1 Hz, Ar-H], 7.60 [d, 1 H, J = 15.9 Hz, HC=CH]; ¹³C NMR (DCCl₃) ppm 14.40 [OCH₂CH₃], 18.54 [=C-CH₃], 30.68 [N-CH₃], 56.60 [=C-C(CH₃)₂], 60.32 [OCH₂CH₃], 63.96 [C(CH₃)₂], 110.53 [=C-CH₃], 112.14 [=C-C(CH₃)₂], 121.72-147.78 [Ar-C], 167.92 [C=O].

(2E)-3-[(1,2,2,4-Tetramethyl-6-(1,2-dihydroquinolyl)]prop-2-en-1-ol (91)

Ester **90** (200 mg, 0.7 mmol) dissolved in 3 mL of dry THF was placed in 25-mL, three-necked, round-bottomed flask fitted with a condenser, magnetic stirrer, and N₂ inlet, and then cooled to -40 °C. A solution (1.20 mL, 1.75 mmol, 2.5 eq, 1.5 M) of DIBAL-H in

toluene was then added by syringe. The reaction mixture was stirred for 3 h, and it was monitored by TLC (hexane:ethyl acetate, 1:2). After the starting material appeared to have reacted (TLC), the reaction mixture was quenched with 1 mL of a saturated, aqueous solution of Rochelle salt (sodium-potassium tartrate, 1:1). The bi-phasic mixture was extracted with ethyl acetate (3 x 15 mL), followed by washing the organic extracts with H₂O (1 x 15 mL) and brine (1 x 20 mL) and then drying (MgSO₄, 12 h). Separation of the major component in the residue, after solvent evaporation, by flash chromatography (hexane:diethyl ether, 1:2, drop rate = 1 drop/s) afforded **91** (146 mg, 86%) as colorless oil. IR (neat) 3342 [O-H] cm⁻¹; ¹H NMR (DCCl₃) δ 1.29 [s, 6 H, CH₃CCH₃], 1.58 [bs, 1 H, O-H], 1.99 [d, 3 H, =CCH₃], 2.80 [s, 3 H, N-CH₃], 4.26 [d, 2 H, H₂C-OH], 5.31 [d, 1H, =CH], 6.35 [d, 1 H, J = 20.4 Hz, FC=CH], 6.46 [d, 1 H, J = 8.4 Hz, Ar-H], 6.93 [d, 1 H, J = 2.1 Hz, Ar-H], 6.95 [q, 1 H, J = 8.4 Hz, J = 2.1 Hz, Ar-H]; ¹³C NMR (DCCl₃) ppm 18.56 [=C-CH₃], 27.21 [C(CH₃)₂], 30.65 [N-CH₃], 56.29 [=C-C(CH₃)₂], 64.21 [HOCH₂], 110.49 [=C-CH₃], 121.54 [=C-C(CH₃)₂], 123.72-145.78 [Ar-C].

(2E)-3-[(1,2,2,4-Tetramethyl-6-(1,2-dihydroquinolyl))]prop-2-enal (92)

Alcohol **91** (140 mg, 0.57 mmol) dissolved in 3 mL of acetone was placed in a 25-mL, one-necked, round-bottomed flask and MnO₂ (0.55 g, 6.44 mmol, activated grade, size < 5 μm) was then added to the solution at RT. The suspension was stirred for 24 h and was then filtered through a 1-inch thick celite pad. Evaporation (rotovap) of the solvent and purification of the major component in the residue, after solvent evaporation, via flash chromatography (hexane:diethyl ether:ethyl acetate, 2:1:1, drop rate = 1 drop/s) afforded aldehyde **92** (90 mg, 65%), as a light yellow oil. IR (neat) 2837 [O=C-H], 1697 [C=O] cm⁻¹

¹H NMR (DCCl₃) δ 1.36 [s, 6 H, CH₃CCH₃], 1.98 [d, 3 H, =CCH₃], 2.87 [s, 3 H, N-CH₃], 5.32 [s, 1 H, =CH], 6.47 [d, 1 H, J = 8.4 Hz, Ar-H], 6.55 [dd, 1 H, J = 7.8 Hz, J = 15.9 Hz, =CHC(O)H], 7.21 [d, 1 H, J = 2.4 Hz, Ar-H], 7.30 [q, 1 H, J = 8.4 Hz, J = 2.1 Hz, Ar-H]; 7.26 [d, 1 H, J = 15.9 Hz, HC=CH], 9.57 [d, 1 H, J = 7.8 Hz, HCC(O)H], ¹³C NMR (DCCl₃) ppm 18.50 [=C-CH₃], 28.36 [C(CH₃)₂], 31.86 [N-CH₃], 57.36 [=C-C(CH₃)₂], 110.48 [=C-CH₃], 121.54 [=C-C(CH₃)₂], 122.72-154.78 [Ar-C], 151.34 [FC=CH], 193.70 [C=O].

1-(2,2,4,4-Tetramethyl-3H-benzo[e]thiane)ethan-1-one (94a)

Into a 25-mL, three-necked, round-bottomed flask equipped with a condenser, a N₂ inlet, and an addition funnel was added AlCl₃ (5.17 g, 38.77 mmol) dissolved in 25 mL of freshly distilled CH₃NO₂. A solution of the 2,2,4,4-tetramethyl-3H-benzo[e]thiane [(93), 5.00 g, 24.24 mmol] and acetyl chloride (2.80 g, 40.11 mmol) in freshly distilled CH₃NO₂ (20 mL) was then added dropwise at RT over period of 1 h. The reaction mixture was stirred for 48 h and then poured into a 100-mL beaker containing ~30 g of crushed ice. The layers were separated, and the aqueous layer was then extracted with diethyl ether (2 x 50 mL). Combined organic layers were washed with water (2 x 30 mL) and brine (1 x 30 mL) and then dried (Na₂SO₄, 12 h). Evaporation (rotovap) of solvent and distillation (bp 132-34 °C/0.75 mm Hg) of the residual oil afforded ketone 94a (4.29 g, 75%) as a light yellow oil. IR (neat) 1681 [C=O] cm⁻¹; ¹H NMR (DCCl₃) δ 1.39 [s, 6 H, C(CH₃)₂], 1.40 [s, 6 H, C(CH₃)₂], 1.98 [s, 2 H, CH₂C(CH₃)₂], 2.55 [s, 3 H, C(O)CH₃], 7.18 [d, 1 H, J = 8.7 Hz, Ar-H], 7.62 [q, 1 H, J = 8.7 Hz, J = 1.9 Hz, Ar-H], 8.15 [d, 1 H, J = 1.9 Hz, Ar-H]; ¹³C NMR (DCCl₃) ppm 18.21 [C(O)CH₃], 31.58 [CH₂C(CH₃)₂], 32.53 [SC(CH₃)₂], 35.42 [CH₂C(CH₃)₂], 42.41 [SC(CH₃)₂], 53.78 [CH₂C(CH₃)₂], 125.70-142.51 [Ar-C], 196.78 [C=O].

2-Methyl-1-(2,2,4,4-tetramethyl(3*H*-benzo[3,4-*e*]thian-6-yl))propan-1-one (94b)

Into a 25-mL, three-necked, round-bottomed flask equipped with a condenser, a N₂ inlet, and an addition funnel was added AlCl₃ (5.17 g, 38.77 mmol) dissolved in freshly distilled CH₃NO₂ (25 mL). A solution of the 2,2,4,4-tetramethyl-3*H*-benzo[*e*]thiane [(93), 4.00 g, 19.38 mmol] and isobutyryl chloride (2.61 g, 21.32 mmol) in 20 mL of freshly distilled CH₃NO₂ was then added dropwise (1 h) at RT. The reaction mixture was stirred for 48 h and was then poured into a 100-mL beaker containing ~30 g of crushed ice. The layers were separated, and the aqueous layer was then extracted with diethyl ether (2 x 50 mL). Combined organic layers were washed with water (2 x 25 mL) and brine (1 x 30 mL) and then dried (Na₂SO₄, 12 h). Evaporation (rotovap) of solvent and distillation (bp 153-54 °C/ 0.75 mm Hg) of the residual oil afforded ketone 94b (3.59 g, 70%) as a light yellow oil. IR (neat) 1679 [C=O] cm⁻¹; ¹H NMR (DCCl₃) δ 1.21 [d, 3 H, CH(CH₃)₂], 1.42 [s, 6 H, C(CH₃)₂], 1.43 [s, 6 H, C(CH₃)₂], 3.53 [m, 1 H, CH(CH₃)₂], 7.18 [d, 1 H, J = 8.7 Hz, Ar-*H*], 7.62 [q, 1 H, J = 8.7 Hz, J = 1.9 Hz, Ar-*H*], 8.15 [d, 1 H, J = 1.9 Hz, Ar-*H*]; ¹³C NMR (DCCl₃) ppm 19.21 [CH(CH₃)₂], 31.58 [CH₂C(CH₃)₂], 32.53 [SC(CH₃)₂], 35.42 [CH₂C(CH₃)₂], 42.41 [SC(CH₃)₂], 53.78 [C, CH₂C(CH₃)₂], 125.70-142.51 [Ar-C], 203.59 [C=O].

3-Methyl-1-(2,2,4,4-tetramethyl(3*H*-benzo[3,4-*e*]thian-6-yl))butan-1-one (94c)

Into a 100-mL, three-necked, round-bottomed flask equipped with a condenser, a N₂ inlet and an addition funnel was placed AlCl₃ (6.5 g, 48.46 mmol) dissolved in 25 mL of freshly distilled CH₃NO₂. The solution of 2,2,4,4-tetramethyl-3*H*-benzo[*e*]thiane [(93), 5.00 g, 24.23 mmol] and isovaleryl chloride (3.21 g, 26.65 mmol) in 20 mL of freshly distilled

CH₃NO₂ was then added at RT over period of 1 h. The reaction mixture was stirred for 48 h and was then poured into a 100-mL beaker containing ~30 g of crushed ice. The layers were separated, and the aqueous layer was then extracted with diethyl ether (2 x 50 mL). The combined organic layers were washed with water (2 x 25 mL) and brine (1 x 30 mL) and dried (Na₂SO₄, 12 h). Evaporation (rotovap) of the solvent and distillation (bp 182-85 °C/1.5 mm Hg) of the residual oil afforded ketone **94c** (mp 55-6 °C, 4.60 g, 65%) as a light yellow solid. IR (neat) 1680 [C=O] cm⁻¹; ¹H NMR (DCCl₃) δ 1.01 [d, 6 H, CH(CH₃)₂], 1.40 [s, 6 H, C(CH₃)₂], 1.41 [s, 6 H, C(CH₃)₂], 1.96 [s, 2 H, CCH₂C], 2.25 [m, 1 H, CH(CH₃)₂], 2.80 [d, 2 H, O=CCH₂CH], 7.18 [d, 1 H, J = 8.9 Hz, Ar-H], 7.62 [q, 1 H, J = 8.9 Hz, J = 2.0 Hz, Ar-H], 8.15 [d, 1 H, J = 2.0 Hz, Ar-H]; ¹³C NMR (DCCl₃) ppm 22.76 [CH(CH₃)₂], 25.22 [O=CCH₂CH], 31.60 [CH₂C(CH₃)₂], 32.52 [SC(CH₃)₂], 35.47 [CH₂C(CH₃)₂], 42.44 [SC(CH₃)₂], 53.81 [CH₂C(CH₃)₂], 125.63-142.47 [Ar-C], 198.22 [C=O].

Ethyl (2E)-2-Fluoro-3-(2,2,4,4-tetramethyl(3H-benzo[3,4-e]thian-6-yl))but-2-enoate (95a)

Into a 25-mL, three-necked, round-bottomed equipped with a condenser, a N₂ inlet and an addition funnel flask was added ethyl 2-fluorophosphono-acetate (536 mg, 2.21 mmol) and DMPU (283.2 mg, 2.21 mmol) dissolved in 3 mL of dry THF. The reaction mixture was cooled to 0 °C, and *n*-BuLi was added dropwise (1.38 mL, 2.21 mmol, 1.6 M) by syringe. After stirring the reaction mixture for 1 h, 1-(2,2,4,4-tetramethyl-3H-benzo[3,4-e]thian-1-one [(**94a**), 502 mg, 2.00 mmol] dissolved in 4 mL of dry THF was added dropwise (1h). The reaction mixture was stirred for 6 days at RT and was then quenched with a saturated, aqueous solution of ammonium chloride (2 mL). Extraction with ethyl acetate (3 x 25 mL) was followed by washing the combined organic layers with H₂O (1 x 20 mL) and

brine (1 x 25 mL) and then drying (MgSO₄, 12 h). After solvent evaporation (rotovap), and flash chromatography (hexane:di-ethyl ether, 1:1, drop rate = 1 drop/s) of the residue, **95a** (394 mg, 67%) was recovered as a clear oil which was a mixture of *E* and *Z* isomers clear oils (*E:Z*, 4:1). IR (neat) 1712 [C=O] cm⁻¹; ¹H NMR (DCCl₃) δ 1.00 [t, 3 H, OCH₂CH₃], 1.40 [s, 6 H, CH₃CCH₃], 1.42 [s, 6 H, CH₃CCH₃], 1.98 [s, 2 H, CH₂], 2.15 [d, 3 H, =CCH₃], 4.07 [q, 2 H, OCH₂CH₃], 6.83 [q, 1 H, Ar-*H*], 7.10 [d, 1 H, Ar-*H*], 7.15 [d, 1 H, Ar-*H*]; ¹³C NMR (DCCl₃) ppm 14.25 [OCH₂CH₃], 18.15 [=CCH₃], 26.39 [C(CH₃)₂], 30.43 [C(CH₃)₂], 55.59 [CH₂CS], 60.19 [OCH₂CH₃], 110.65 [=CH], 115.03-131.14 [Ar-C], 140.99 [FC=CH], 165.34 [RO-C=O]; ¹⁹F NMR (DCCl₃) ppm -123.6 [q, 1 F, FC=CCH₃].

Ethyl (2*E*)-2-Fluoro-4-methyl-3-(2,2,4,4-tetramethyl(3*H*-benzo[3,4-*e*]thian-6-yl))pent-2-enoate (**95b**)

Into a 25-mL, three-necked, round-bottomed flask equipped with a condenser, a N₂ inlet, and an addition funnel was added ethyl 2-fluorophosphonoacetate (482 mg, 1.99 mmol), DMPU (255 mg, 1.99 mmol), and 3 mL of dry THF. The reaction mixture was cooled to 0 °C, and *n*-BuLi (1.25 mL, 21.99 mmol, 1.6 M) was added by syringe. After stirring the reaction mixture for 1 h, 2-methyl-1-(2,2,4,4-tetramethyl(3*H*-benzo[3,4-*e*]thian-6-yl))propan-1-one [(**94b**), 495 mg, 1.98 mmol] dissolved in 4 mL of dry THF was added dropwise (30 min). The reaction mixture was then stirred for 4 days at RT and then 2 days at reflux, after which time it was cooled to RT and quenched with a saturated, aqueous solution of ammonium chloride (1 mL). Extraction with ethyl acetate (3 x 25 mL) was followed by washing the combined organic extracts with H₂O (1 x 20 mL) and brine (1 x 25 mL) and drying (MgSO₄, 12 h). After solvent evaporation (rotovap), and flash chromatography (hexane:diethyl ether, 1:1, drop rate = 1 drop/s) of the residue, ester **95b**

(342 mg, 52%) was recovered as a light yellow oil. IR (neat) 1702 [C=O] cm^{-1} ; ^1H NMR (DCCl_3) δ 0.35 [t, 3 H, OCH_2CH_3], 1.23 [d, 3 H, $\text{CH}(\text{CH}_3)_2$], 1.44 [s, 6 H, $\text{C}(\text{CH}_3)_2$], 1.43 [s, 6 H, $\text{C}(\text{CH}_3)_2$], 2.01 [s, 2 H, CCH_2C], 3.48 [m, 1 H, $\text{CH}(\text{CH}_3)_2$], 4.14 [q, 2 H, OCH_2CH_3], 7.18 [d, 1 H, $J = 8.9$ Hz, Ar-*H*], 7.54 [q, 1 H, $J = 8.9$ Hz, $J = 2.1$ Hz, Ar-*H*], 8.02 [d, 1 H, $J = 2.1$ Hz, Ar-*H*]; ^{13}C NMR (DCCl_3) ppm 14.25 [C, OCH_2CH_3], 19.34 [2 C, $\text{CH}(\text{CH}_3)_2$], 31.75 [2 C, $\text{CH}_2\text{C}(\text{CH}_3)_2$], 32.43 [2 C, $\text{SC}(\text{CH}_3)_2$], 35.56 [C, $\text{CH}_2\text{C}(\text{CH}_3)_2$], 42.41 [$\text{SC}(\text{CH}_3)_2$], 53.78 [C, $\text{CH}_2\text{C}(\text{CH}_3)_2$], 60.12 [C, OCH_2CH_3], 110.65 [C, $\text{CH}_3\text{C}=\text{CF}$], 110.65 [C, $\text{CH}_3\text{C}=\text{CF}$], 122.70-140.51 [6 C, Ar-C], 165.45 [C=O]; ^{19}F NMR ppm -123.8 [q, 1 F, $\text{FC}=\text{CCH}_3$].

Ethyl (2*E*)-2-Fluoro-4-methyl-3-(2,2,4,4-tetramethyl(3*H*-benzo[3,4-*e*]thian-6-yl))pent-2-enoate (95c)

Into a 25-mL, three-necked, round-bottomed flask equipped with a condenser, a N_2 inlet, and an addition funnel was added ethyl 2-fluorophosphonoacetate (530 mg, 2.20 mmol), DMPU (280 mg, 2.20 mmol), and 5 mL of dry THF. The reaction mixture was cooled to 0 $^\circ\text{C}$, and *n*-BuLi (1.33 mL, 2.20 mmol, 1.6 *M*) was added by syringe. After stirring the reaction mixture for 1 h, 2-methyl-1-(2,2,4,4-tetramethyl(3*H*-benzo[3,4-*e*]thian-6-yl))butan-1-one [(94c), 580 mg, 2.00 mmol] dissolved in 5 mL of dry THF was added dropwise (30 min). The reaction mixture was then stirred for 6 days at RT and then 2 days at reflux, after which it was cooled to RT and quenched with a saturated, aqueous solution of ammonium chloride (1 mL). Extraction with ethyl acetate (3 x 35 mL) was followed by washing the combined organic extracts with H_2O (1 x 30 mL) and brine (1 x 35 mL) and drying (MgSO_4 , 12 h). After solvent evaporation (rotovap) and flash chromatography

(hexane:diethyl ether, 1:1, drop rate = 1 drop/s) of the residue, ester **95c** (423 mg, 56%) was recovered as a light yellow oil. IR (neat) 1702 [C=O] cm^{-1} ; ^1H NMR (DCCl_3) δ 0.85 [t, 3 H, OCH_2CH_3], 1.25 [d, 3 H, $\text{CH}(\text{CH}_3)_2$], 1.44 [s, 6 H, $\text{C}(\text{CH}_3)_2$], 1.43 [s, 6 H, $\text{C}(\text{CH}_3)_2$], 2.01 [s, 2 H, CCH_2C], 2.14 [m, 2 H, CH_2CH], 3.48 [m, 1 H, $\text{CH}(\text{CH}_3)_2$], 4.24 [q, 2 H, OCH_2CH_3], 7.18 [d, 1 H, $J = 8.7$ Hz, Ar- H], 7.54 [q, 1 H, $J = 8.7$ Hz, $J = 2.4$ Hz, Ar- H], 8.02 [d, 1 H, $J = 2.4$ Hz, Ar- H]; ^{13}C NMR (DCCl_3) ppm 14.25 [C, OCH_2CH_3], 19.34 [2 C, $\text{CH}(\text{CH}_3)_2$], 31.75 [2 C, $\text{CH}_2\text{C}(\text{CH}_3)_2$], 32.43 [2 C, $\text{SC}(\text{CH}_3)_2$], 35.56 [C, $\text{CH}_2\text{C}(\text{CH}_3)_2$], 42.41 [$\text{SC}(\text{CH}_3)_2$], 53.78 [C, $\text{CH}_2\text{C}(\text{CH}_3)_2$], 60.12 [C, OCH_2CH_3], 110.65 [C, $\text{CH}_3\text{C}=\text{CF}$], 110.65 [C, $\text{CH}_3\text{C}=\text{CF}$], 122.70-140.51 [6 C, Ar-C], 165.45 [C=O]; ^{19}F NMR (DCCl_3) ppm -125.8 [q, 1 F, $\text{FC}=\text{CCH}_3$].

(2E)-2-Fluoro-3-(2,2,4,4-tetramethyl(3H-benzof[3,4-e]thian-6-yl))but-2-en-1-ol (96a) and

(2Z)-2-Fluoro-3-(2,2,4,4-tetramethyl(3H-benzof[3,4-e]thian-6-yl))but-2-en-1-ol (98a)

Ester **95a** (631 mg, 1.87 mmol) dissolved in 5 mL of dry THF was placed in 25-mL, three-necked, round-bottomed flask and then cooled to -40 °C. A solution of DIBAL-H in toluene (3.75 mL, 5.61 mmol, 1.5 M) was then added by syringe. The reaction mixture was stirred for 2 h, and it was monitored by TLC (hexane:ethyl acetate, 1:1). After all of the starting material appeared to have reacted (TLC), the reaction mixture was quenched with 2 mL of a saturated, aqueous solution of Rochelle salt (sodium-potassium tartrate, 1:1). The bi-phasic mixture was extracted with ethyl acetate (3 x 25 mL), followed by washing the organic extracts with H_2O (1 x 15 mL) and brine (1 x 20 mL) and then drying (MgSO_4 , 12 h). Separation of the major component in the residue, after solvent evaporation followed by flash chromatography (hexane:diethyl ether, 1:1, drop rate = 1 drop/s), afforded **96a** [(E

isomer) 390 mg, 70%] and **98a** [(*Z* isomer), 127 mg, 23%] as colorless oils. The *E*:*Z* ratio was 3:1; R_f 's were 0.645 and 0.362, respectively, for TLC with hexane:diethyl ether, (1:1).

The spectrum of **96a**: IR (neat) 3402 [O-H], 1659 [C=C-F] cm^{-1} ; $^1\text{H NMR}$ (DCCl_3) δ 1.75 [bs, 1 H, O-*H*], 4.18 [d, 2 H, $H_2\text{COH}$], 6.9-7.3 [m, 3 H, Ar-*H*], $^{13}\text{C NMR}$ (DCCl_3) ppm 31.56 [2 C, CH_3CCH_3], 118.81 [=C CH_3], 119.05 [=CF], 125.70-156.44 [Ar-C]; $^{19}\text{F NMR}$ (DCCl_3) ppm -117.65 [d, 1 F, HOCH_2CF].

The spectrum of **98a**: IR (neat) 3404 [O-H], 1683 [C=C-F] cm^{-1} ; $^1\text{H NMR}$ (DCCl_3) δ 1.65 [bs, 1 H, O-*H*], 4.41 [d, 2 H, $H_2\text{COH}$], 7.1-7.45 [m, 3 H, Ar-*H*], $^{13}\text{C NMR}$ (DCCl_3) ppm 32.56 [2 C, CH_3CCH_3], 120.81 [=C CH_3], 121.05 [=CF], 125.70-154.60 [Ar-C]; $^{19}\text{F NMR}$ (DCCl_3) ppm -117.57 [t, 1 F, HOCH_2CF].

(1*E*)-1-Fluoro-4-methyl-3-(2,2,4,4-tetramethyl(3*H*-benzo[3,4-*e*]thian-6-yl))pent-2-en-1-ol
(**96b**) (1*Z*)-1-Fluoro-4-methyl-3-(2,2,4,4-tetramethyl(3*H*-benzo[3,4-*e*]thian-6-yl))pent-2-en-1-
ol (**98b**)

Ester **95b** (402 mg, 1.1 mmol) dissolved in 4 mL of dry THF was placed in a 25-mL, three-necked, round-bottomed flask equipped with a condenser, a N_2 inlet and an addition funnel and then cooled to $-40\text{ }^\circ\text{C}$. A solution of DIBAL-H (2.20 mL, 3.3 mmol, 1.5 *M* in toluene) was then added by syringe. The reaction mixture was stirred for 1 h and monitored by TLC (hexane:ethyl acetate, 1:1). After all of the starting material appeared to have reacted (TLC), the reaction mixture was quenched with 2 mL of a saturated, aqueous solution of Rochelle salt (sodium-potassium tartrate, 1:1). The bi-phasic mixture was extracted with ethyl acetate (3 x 20 mL), followed by washing the organic extracts with H_2O (1 x 10 mL) and brine (1 x 15 mL). Purification of the major component in the residue (after

solvent evaporation) by flash chromatography (hexane:diethyl ether, 2:1, drop rate = 1 drop/s) afforded 112 mg (31%) of **96b** (E isomer) and 191 mg (53%) of **98b** (Z isomer) (E:Z, 0.6:1, R_f 's were 0.745 and 0.562, respectively) as oils.

The spectrum of **96b**: IR (neat) 3359 [O-H], 1686 [C=C-F] cm^{-1} ; ^1H NMR (DCCl_3) δ 1.01 [d, 3 H, $\text{CH}(\text{CH}_3)_2$], 1.36 [s, 6 H, $\text{C}(\text{CH}_3)_2$], 1.40 [s, 6 H, $\text{C}(\text{CH}_3)_2$], 1.58 [bs, 1 H, O-H], 1.96 [s, 2 H, CCH_2C], 3.18 [m, 1 H, $\text{CH}(\text{CH}_3)_2$], 3.97 [d, 2 H, HOCH_2], 6.98 [q, 1 H, $J = 8.5$ Hz, $J = 2.3$ Hz, Ar-H], 7.15 [d, 1 H, $J = 8.5$ Hz, Ar-H] 7.25 [d, 1 H, $J = 2.3$ Hz, Ar-H]; ^{13}C NMR (DCCl_3) ppm, 20.98 [2 C, $\text{CH}(\text{CH}_3)_2$], 31.51 [2 C, $\text{CH}_2\text{C}(\text{CH}_3)_2$], 32.80 [2 C, $\text{SC}(\text{CH}_3)_2$], 33.56 [C, $\text{CH}_2\text{C}(\text{CH}_3)_2$], 35.31 [$\text{SC}(\text{CH}_3)_2$], 54.25 [C, $\text{CH}_2\text{C}(\text{CH}_3)_2$], 59.54 [C, HOCH_2], 112.34 [C, $\text{CH}_3\text{C}=\text{CF}$], 113.65 [C, $\text{CH}_3\text{C}=\text{CF}$], 127.70-142.16 [6 C, Ar-C]; ^{19}F NMR (DCCl_3) ppm -121.85 [t, 1 F, =CF].

The spectrum of **98b**: IR (neat) 3347 [O-H], 1688 [C=C-F] cm^{-1} ; ^1H NMR (DCCl_3) δ 0.98 [dd, 3 H, $\text{CH}(\text{CH}_3)_2$], 1.38 [s, 6 H, $\text{C}(\text{CH}_3)_2$], 1.44 [s, 6 H, $\text{C}(\text{CH}_3)_2$], 1.60 [bs, 1 H, O-H], 1.96 [s, 2 H, CCH_2C], 2.86 [m, 1 H, $\text{CH}(\text{CH}_3)_2$], 4.40 [d, 2 H, HOCH_2], 6.80 [q, 1 H, $J = 8.0$ Hz, $J = 2.1$ Hz, Ar-H], 7.10 [d, 1 H, $J = 8.0$ Hz, Ar-H], 7.25 [d, 1 H, $J = 2.1$ Hz, Ar-H]; ^{13}C NMR (DCCl_3) ppm, 21.89 [2 C, $\text{CH}(\text{CH}_3)_2$], 30.60 [2 C, $\text{CH}_2\text{C}(\text{CH}_3)_2$], 31.68 [2 C, $\text{SC}(\text{CH}_3)_2$], 32.76 [C, $\text{CH}_2\text{C}(\text{CH}_3)_2$], 41.96 [$\text{SC}(\text{CH}_3)_2$], 54.35 [C, $\text{CH}_2\text{C}(\text{CH}_3)_2$], 61.91 [C, HOCH_2], 110.34 [C, $\text{CH}_3\text{C}=\text{CF}$], 111.34 [C, $\text{CH}_3\text{C}=\text{CF}$], 127.23-142.16 [6 C, Ar-C], ^{19}F NMR (DCCl_3) ppm -115.28 [m, 1 F, =CF].

(1E)-1-Fluoro-4-methyl-3-(2,2,4,4-tetramethyl(3H-benzo[3,4-e]thian-6-yl))pent-2-en-1-ol (96c) and (1E)-1-Fluoro-4-methyl-3-(2,2,4,4-tetramethyl(3H-benzo[3,4-e]thian-6-yl))pent-2-en-1-ol (98c)

Ester **95c** (300 mg, 0.79 mmol) dissolved in 4 mL of dry THF was placed in a 25-mL, three-necked, round-bottomed flask equipped with a condenser, a N₂ inlet and an addition funnel and then cooled to -40 °C. A solution of DIBAL-H in toluene (1.35 mL, 1.98 mmol, 1.5 M) was then added by syringe. The reaction mixture was stirred for 1 h and monitored by TLC (hexane:ethyl acetate, 1:1). After all of the starting material appeared to have reacted (TLC), the reaction mixture was quenched with 2 mL of a saturated, aqueous solution of Rochelle salt (sodium-potassium tartrate, 1:1). The bi-phasic mixture was extracted with ethyl acetate (3 x 15 mL), followed by washing the organic extracts with H₂O (1 x 10 mL) and brine (1 x 15 mL). After solvent evaporation (rotovap) and separation of the major component in the residue by flash chromatography (hexane:diethyl ether, 1:1, drop rate = 1 drop/s), **96c** (225 mg, 85%) and **98c** (21 mg, 8%) were obtained as oils.

The spectrum of **96c**: IR (neat) 3369 [O-H], 1683 [C=C-F] cm⁻¹; ¹H NMR (DCCl₃) δ 0.89 [d, 6 H, CH(CH₃)₂], 1.36 [s, 6 H, C(CH₃)₂], 1.40 [s, 6 H, C(CH₃)₂], 1.54 [m, 1 H, CH(CH₃)₂] 1.88 [bs, 1 H, O-H], 1.96 [s, 2 H, CCH₂C], 2.22 [d, 2 H, CHCH₂], 4.42 [d, 2 H, HOCH₂], 6.98 [q, 1 H, J = 8.5 Hz, J = 2.3 Hz, Ar-H], 7.15 [d, 1 H, J = 8.5 Hz, Ar-H] 7.30 [d, 1 H, J = 2.3 Hz, Ar-H]; ¹³C NMR (DCCl₃) ppm, 22.98 [CH(CH₃)₂], 24.90 [CH(CH₃)₂], 31.51 [CH₂C(CH₃)₂], 32.67 [SC(CH₃)₂], 39.56 [CH₂C(CH₃)₂], 41.31 [SC(CH₃)₂], 54.29 [CH₂C(CH₃)₂], 58.54 [HOCH₂], 120.16 [CH₃C=CF], 126.70-142.16 [Ar-C], 155.21[CH₃C=CF]; ¹⁹F NMR (DCCl₃) ppm -117.36 [t, 1 F, =CF].

The spectrum of **98c**: IR (neat) 3369 [O-H], 1683 [C=C-F] cm⁻¹; ¹H NMR (DCCl₃) δ 0.82 [d, 6 H, CH(CH₃)₂], 1.36 [s, 6 H, C(CH₃)₂], 1.40 [s, 6 H, C(CH₃)₂], 1.69 [m, 1 H, CH(CH₃)₂] 1.82 [bs, 1 H, O-H], 1.94 [s, 2 H, CCH₂C], 2.32 [m, 2 H, CHCH₂], 4.17 [d, 2 H, HOCH₂], 6.95 [q, 1 H, J = 8.4 Hz, J = 2.1 Hz, Ar-H], 7.15 [d, 1 H, J = 8.4 Hz, Ar-H] 7.30

[d, 1 H, $J = 2.1$ Hz, Ar-*H*]; ^{13}C NMR (DCCl_3) ppm, 22.24 [$\text{CH}(\text{CH}_3)_2$], 24.79 [$\text{CH}(\text{CH}_3)_2$], 31.58 [$\text{CH}_2\text{C}(\text{CH}_3)_2$], 32.87 [$\text{SC}(\text{CH}_3)_2$], 38.56 [$\text{CH}_2\text{C}(\text{CH}_3)_2$], 42.31 [$\text{SC}(\text{CH}_3)_2$], 54.43 [$\text{CH}_2\text{C}(\text{CH}_3)_2$], 72.73 [HOCH_2], 122.16 [$\text{CH}_3\text{C}=\text{CF}$], 126.16-142.38 [Ar-C], 156.21 [$\text{CH}_3\text{C}=\text{CF}$]; ^{19}F NMR (DCCl_3) ppm -118.76 [t, 1 F, =CF].

(2E)-2-Fluoro-3-(2,2,4,4-tetramethyl(3*H*-benzo[3,4-*e*]thian-6-yl))but-2-enal (97a)

Alcohol **96a** (390 mg, 1.32 mmol) dissolved in 5 mL of acetone was placed in a 25-mL, one-necked, round-bottomed flask, and MnO_2 (1.5 g, 17.25 mmol, activated grade, size < 5 μm) was then added to the solution at RT. The suspension was stirred for 24 h and then filtered through a 1-inch thick celite pad. Evaporation (rotovap) of the solvent and purification of the major component in the residue (after solvent evaporation) via flash chromatography (hexane:diethyl ether:ethyl acetate, 1:1:0.1, drop rate = 1 drop/s) afforded aldehyde **97a** (212 mg, 55%), as a light yellow oil. IR (neat) 2874 [O=C-H], 1667 [C=O] cm^{-1} ; ^1H NMR (DCCl_3) δ 1.36 [s, 6 H, $\text{C}(\text{CH}_3)_2$], 1.40 [s, 6 H, $\text{C}(\text{CH}_3)_2$], 1.94 [s, 2 H, CCH_2C], 2.30 [d, 3 H, = CCH_3], 7.02 [q, 1 H, Ar-*H*], 7.12 [d, 1 H, Ar-*H*], 7.29 [d, 1 H, Ar-*H*], 9.31 [d, 1 H, HC=O]; ^{13}C NMR (DCCl_3) ppm, 17.98 [$\text{CH}(\text{CH}_3)_2$], 31.58 [$\text{CH}_2\text{C}(\text{CH}_3)_2$], 32.53 [$\text{SC}(\text{CH}_3)_2$], 35.49 [$\text{CH}_2\text{C}(\text{CH}_3)_2$], 42.31 [$\text{SC}(\text{CH}_3)_2$], 53.95 [$\text{CH}_2\text{C}(\text{CH}_3)_2$], 126.16 [$\text{CH}_3\text{C}=\text{CF}$], 126.16-142.86 [Ar-C], 155.70 [$\text{CH}_3\text{C}=\text{CF}$], 182.69 [C=O]; ^{19}F NMR (DCCl_3) ppm -131.32 [m, 1 F, =CF].

(2E)-2-Fluoro-4-methyl-3-(2,2,4,4-tetramethyl(3*H*-benzo[3,4-*e*]thian-6-yl))pent-2-enal (97b)

Alcohol **96b** (112 mg, 0.35 mmol) dissolved in 3 mL of acetone was placed in a 25-mL, one-necked, round-bottomed flask, and MnO_2 (0.5 g, 6.75 mmol, activated grade, size:

<5 μm) was then added to the solution at RT. The suspension was stirred for 24 h and then filtered through a 1-inch thick celite pad. Evaporation (rotovap) of the solvent and purification of the major component in the residue via flash chromatography (hexane:diethyl ether 1:1, drop rate = 1 drop/s) afforded aldehyde **97b** (67 mg, 60%) as a yellow oil. IR (neat) 2814 [O=C-H], 1687 [C=O] cm^{-1} ; ^1H NMR (DCCl_3) δ 1.11 [d, 3 H, $\text{CH}(\text{CH}_3)_2$], 1.38 [s, 6 H, $\text{C}(\text{CH}_3)_2$], 1.42 [s, 6 H, $\text{C}(\text{CH}_3)_2$], 1.96 [s, 2 H, CCH_2C], 3.21 [m, 1 H, $\text{CH}(\text{CH}_3)_2$], 6.88 [q, 1 H, $J = 8.5$ Hz, $J = 2.3$ Hz, Ar- H], 7.05 [d, 1 H, $J = 8.5$ Hz, Ar- H], 7.45 [d, 1 H, $J = 2.3$ Hz, Ar- H], 9.78 [d, 1 H, O=CH]; ^{13}C NMR (DCCl_3) ppm, 20.78 [2 C, $\text{CH}(\text{CH}_3)_2$], 31.65 [2 C, $\text{CH}_2\text{C}(\text{CH}_3)_2$], 32.16 [2 C, $\text{SC}(\text{CH}_3)_2$], 32.56 [C, $\text{CH}_2\text{C}(\text{CH}_3)_2$], 35.45 [$\text{SC}(\text{CH}_3)_2$], 54.23 [C, $\text{CH}_2\text{C}(\text{CH}_3)_2$], 110.34 [C, $\text{CH}_3\text{C}=\text{CF}$], 111.45 [C, $\text{CH}_3\text{C}=\text{CF}$], 125.70-143.16 [6 C, Ar-C], 184.23 [C=O]; ^{19}F NMR (DCCl_3) (ref $\text{C}_6\text{H}_5\text{CF}_3$ in C_6D_6) ppm -128.3 [t, 1 F, =CF].

(2E)-2-Fluoro-4-methyl-3-(2,2,4,4-tetramethyl(3H-benzo[3,4-e]thian-6-yl))pent-2-enal (97c)

Alcohol **96c** (120 mg, 0.35 mmol) dissolved in 3 mL of acetone was placed in a 25-mL, one-necked, round-bottomed flask, and MnO_2 (0.55 g, 6.95 mmol, activated grade, size: <5 μm) was then added to the solution at RT. The suspension was stirred for 24 h and then filtered through a 1-inch thick celite pad. Evaporation (rotovap) of the solvent and purification of the major component in the residue via flash chromatography (hexane:diethyl ether 2:1, drop rate = 1 drop/s) afforded aldehyde **97c** (60 mg, 51%) as a light yellow oil. IR (neat) 2869 [O=C-H], 1687 [C=O] cm^{-1} ; ^1H NMR (DCCl_3) δ 0.90 [d, 3 H, $\text{CH}(\text{CH}_3)_2$], 1.34 [s, 6 H, $\text{C}(\text{CH}_3)_2$], 1.40 [s, 6 H, $\text{C}(\text{CH}_3)_2$], 1.72 [m, 1 H, $\text{CH}(\text{CH}_3)_2$], 1.96 [s, 2 H, CCH_2C], 2.59 [m, 2 H, CHCH_2], 6.88 [q, 1 H, $J = 8.7$ Hz, $J = 2.1$ Hz, Ar- H], 7.15 [d, 1 H, $J = 8.5$ Hz, Ar- H], 7.25 [d, 1 H, $J = 2.3$ Hz, Ar- H], 9.25 [d, 1 H, O=CH]; ^{13}C NMR (DCCl_3)

ppm, 22.38 [CH(CH₃)₂], 26.98 [CCH₂C], 31.58 [2 C, CH₂C(CH₃)₂], 32.61 [SC(CH₃)₂], 32.56 [CH₂C(CH₃)₂], 35.45 [SC(CH₃)₂], 35.42 [CH₂HC(CH₃)₂], 53.93 [C, CH₂C(CH₃)₂], 125.70-142.16 [Ar-C], 183.23 [C=O]; ¹⁹F NMR (DCCl₃) (ref C₆H₅CF₃ in C₆D₆) ppm -132.08 [m, 1 F, =CF].

(2Z)-2-Fluoro-3-(2,2,4,4-tetramethyl(3H-benzo[3,4-e]thian-6-yl))but-2-enal (99a)

Alcohol 98a (121 mg, 0.43 mmol) dissolved in 3 mL of acetone was placed in a 25-mL one-necked, round-bottomed flask, and MnO₂ (0.8 g, 9.8 mmol, activated grade, size < 5 μm) was then added to the solution at RT. The suspension was stirred for 24 h and then filtered through a 1-inch thick celite pad. Evaporation (rotovap) of the solvent and purification of the major component in the residue (after solvent evaporation) via flash chromatography (hexane:diethyl ether:ethyl acetate, 1:1:0.1, drop rate = 1 drop/s) afforded aldehyde 99a (74 mg, 59%) as a light yellow oil. IR (neat) 2874 [O=C-H], 1667 [C=O] cm⁻¹; ¹H NMR (DCCl₃) δ 1.42 [s, 6 H, C(CH₃)₂], 1.44 [s, 6 H, C(CH₃)₂], 1.96 [s, 2 H, CCH₂C], 2.30 [d, 3 H, =CCH₃], 7.12-7.60 [m, 3 H, Ar-H], 9.98 [d, 1 H, HC=O]; ¹³C NMR (DCCl₃) ppm, 17.98 [CH(CH₃)₂], 31.58 [CH₂C(CH₃)₂], 32.53 [SC(CH₃)₂], 35.49 [CH₂C(CH₃)₂], 42.31 [SC(CH₃)₂], 53.95 [CH₂C(CH₃)₂], 126.16 [CH₃C=CF], 126.16-142.86 [Ar-C], 155.70 [CH₃C=CF]; 181.69 [C=O]; ¹⁹F NMR (DCCl₃) ppm -131.86 [m, 1 F, =CF].

(2Z)-2-Fluoro-4-methyl-3-(2,2,4,4-tetramethyl(3H-benzo[3,4-e]thian-6-yl))pent-2-enal (99b)

Alcohol 98b (190 mg, 0.59 mmol) dissolved in 3 mL of acetone was placed in a 25-mL, one-necked, round-bottomed flask, and MnO₂ (1.00 g, 11.5 mmol, activated grade, size < 5 μm) was then added to the solution at RT. The suspension was stirred for 24 h and

then filtered through a 1-inch thick celite pad. Evaporation (rotovap) of the solvent and purification of the major component in the residue via flash chromatography (hexane:diethyl ether, 1:1, drop rate = 1 drop/s) afforded aldehyde **99b** (90 mg, 48%) as a light yellow oil. IR (neat) 2832 [O=C-H] 1686 [C=O] cm^{-1} ; $^1\text{H NMR}$ (DCCl_3) δ 1.10 [d, 3 H, $\text{CH}(\text{CH}_3)_2$], 1.48 [s, 6 H, $\text{C}(\text{CH}_3)_2$], 1.52 [s, 6 H, $\text{C}(\text{CH}_3)_2$], 2.11 [s, 2 H, CCH_2C], 3.01 [m, 1 H, $\text{CH}(\text{CH}_3)_2$], 6.98 [q, 1 H, $J = 8.4 \text{ Hz}$, $J = 2.0 \text{ Hz}$, Ar-H], 7.25 [d, 1 H, $J = 8.4 \text{ Hz}$, Ar-H] 7.68 [d, 1 H, $J = 2.0 \text{ Hz}$, Ar-H], 9.94 [d, 1 H, O=CH]; $^{13}\text{C NMR}$ (DCCl_3) ppm, 21.78 [$\text{CH}(\text{CH}_3)_2$], 33.65 [$\text{CH}_2\text{C}(\text{CH}_3)_2$], 34.16 [$\text{SC}(\text{CH}_3)_2$], 34.56 [$\text{CH}_2\text{C}(\text{CH}_3)_2$], 35.45 [$\text{SC}(\text{CH}_3)_2$], 54.23 [$\text{CH}_2\text{C}(\text{CH}_3)_2$], 112.34 [$\text{CH}_3\text{C}=\text{CF}$], 113.42 [$\text{CH}_3\text{C}=\text{CF}$], 126.70-144.89 [Ar-C], 188.92 [C=O]; $^{19}\text{F NMR}$ (DCCl_3) (ref $\text{C}_6\text{H}_5\text{CF}_3$ in C_6D_6) ppm -129.53 [m, 1 F, =CF].

2-Methyl-1-(2,2,4,4-tetramethyl(3*H*-benzo[3,4-*e*]thian6-yl))ethan-1-ol (100a)

Ketone **94a** (300 mg, 1.20 mmol) dissolved in 5 mL of dry THF was placed in a 25-mL, three-necked, round-bottomed flask equipped with a condenser, a N_2 inlet and an addition funnel and then cooled to $-40 \text{ }^\circ\text{C}$. A solution of DIBAL-H in toluene (2.42 mL, 3.63 mmol 1.5 *M*) was then added by syringe. The reaction mixture was then stirred for 2 h, and it was monitored by TLC (hexane:ethyl acetate, 1:4). After the starting material appeared to have reacted (TLC), the reaction mixture was quenched with 4 mL of a saturated, aqueous solution of Rochelle salt (sodium-potassium tartrate, 1:1). The bi-phasic mixture was then extracted with ethyl acetate (3 x 30 mL), followed by washing the extracts with H_2O (1 x 30 mL) and brine (1 x 30 mL) then drying (MgSO_4 , 12 h). After evaporation (rotovap) and separation of the major component of the solvent by flash chromatography (hexane:diethyl ether, 1:2, drop rate = 1 drop/s), alcohol **100a** (269 mg, 89%) was obtained

as a clear oil. IR (neat) 3352 [O-H], cm^{-1} ; $^1\text{H NMR}$ (DCCl_3) δ 1.39 [s, 6 H, $\text{C}(\text{CH}_3)_2$], 1.41 [s, 6 H, $\text{C}(\text{CH}_3)_2$], 1.46 [d, 3 H, HOCH_2CH_3], 1.82 [bs, 1 H, O-H], 1.95 [s, 2 H, CCH_2C], 1.98 [m, 1 H, $\text{CH}(\text{CH}_3)_2$], 4.84 [dd, 2 H, HOCH_2CH_3], 7.07 [q, 1 H, $J = 7.8$ Hz, $J = 2.1$ Hz, Ar-H], 7.09 [d, 1 H, $J = 7.8$ Hz, Ar-H] 7.38 [d, 1 H, $J = 2.1$ Hz, Ar-H]; $^{13}\text{C NMR}$ (DCCl_3) ppm, 24.98 [HOCH_2CH_3], 31.61 [$\text{CH}_2\text{C}(\text{CH}_3)_2$], 32.53 [$\text{SC}(\text{CH}_3)_2$], 35.60 [$\text{CH}_2\text{C}(\text{CH}_3)_2$], 41.99 [$\text{SC}(\text{CH}_3)_2$], 54.42 [$\text{CH}(\text{CH}_3)_2$], 70.38 [$\text{HO CH}_2\text{C}(\text{CH}_3)_2$], 123.27-142.19 [Ar-C].

2-Methyl-1-[(2,2,4,4-tetramethyl(3*H*-benzo[3,4-*e*]thian-6-yl))]propan-1-ol (100b)

Ketone **94b** (500 mg, 1.81 mmol) dissolved in 6 mL of dry THF was placed in a 25-mL, three-necked, round-bottomed flask equipped with a condenser, a N_2 inlet and an addition funnel and then cooled to -40 °C. A solution of DIBAL-H in toluene (3.63 mL, 5.43 mmol, 1.5 M) was then added by syringe. The reaction mixture was then stirred for 2 h, and it was monitored by TLC (hexane:ethyl acetate, 1:3). After the starting material appeared to have reacted (TLC), the reaction mixture was quenched with 5 mL of a saturated, aqueous solution of Rochelle salt (sodium-potassium tartrate, 1:1). The bi-phasic mixture was then extracted with ethyl acetate (3 x 35 mL), followed by washing the extracts with H_2O (1 x 30 mL) and brine (1 x 25 mL) then drying (MgSO_4 , 12 h). After evaporation (rotovap) and separation of the major component of the solvent by flash chromatography (hexane:diethyl ether, 1:4, drop rate = 1 drop/s), alcohol **100b** (462 mg, 92%) was obtained as a clear oil. IR (neat) 3425 [O-H], cm^{-1} ; $^1\text{H NMR}$ (DCCl_3) δ 0.78 [d, 3 H, $\text{CH}(\text{CH}_3)_2$], 1.01 [d, 3 H, $\text{CH}(\text{CH}_3)_2$] 1.26 [s, 6 H, $\text{C}(\text{CH}_3)_2$], 1.32 [s, 6 H, $\text{C}(\text{CH}_3)_2$], 1.85 [bs, 1 H, O-H], 1.96 [s, 2 H, CCH_2C], 1.98 [m, 1 H, $\text{CH}(\text{CH}_3)_2$], 4.27 [d, 1 H, HOCHCH], 6.98 [q, 1 H, $J = 7.8$ Hz, $J = 2.1$ Hz, Ar-H], 7.09 [d, 1 H, $J = 7.8$ Hz, Ar-H] 7.32 [d, 1 H, $J = 2.1$ Hz, Ar-H]; $^{13}\text{C NMR}$

(DCCl₃) ppm, 18.36 [CH(CH₃)₂], 18.92 [CH(CH₃)₂], 31.51 [CH₂C(CH₃)₂], 32.70 [SC(CH₃)₂], 35.19 [CH₂C(CH₃)₂], 35.36 [SC(CH₃)₂], 41.95 [CH(CH₃)₂], 54.46 [CH₂C(CH₃)₂], 80.35 [HOCH₂], 124.27-140.19 [Ar-C].

3-Methyl-1-[(2,2,4,4-tetramethyl(3*H*-benzo[3,4-*e*]thian-6-yl))]butan-1-ol (100c)

Ketone **94c** (500 mg, 1.72 mmol) dissolved in 6 mL of dry THF was placed in a 25-mL, three-necked, round-bottomed flask equipped with a condenser, a N₂ inlet and an addition funnel and then cooled to -40 °C. A solution of DIBAL-H in toluene (3.44 mL, 5.15 mmol, 1.5 M) was then added by syringe. The reaction mixture was then stirred for 2 h, and it was monitored by TLC (hexane:ethyl acetate, 1:2). After the starting material appeared to have reacted (TLC), the reaction mixture was quenched with 5 mL of a saturated, aqueous solution of Rochelle salt (sodium-potassium tartrate, 1:1). The bi-phasic mixture was then extracted with ethyl acetate (3 x 35 mL), followed by washing the extracts with H₂O (1 x 30 mL) and brine (1 x 35 mL) then drying (MgSO₄, 12 h). After evaporation (rotovap) and separation of the components in the residue, of solvent, by flash chromatography (EtOAc, 1:4, drop rate = 1 drop/s), alcohol **100c** (412 mg, 82%) was obtained as a clear oil. IR (neat) 3385 [O-H] cm⁻¹; ¹H NMR (DCCl₃) δ 0.95 [d, 6 H, CH(CH₃)₂], 1.39 [s, 6 H, C(CH₃)₂], 1.41 [s, 6 H, C(CH₃)₂], 1.47 [m, 1 H, CH(CH₃)₂], 1.65 [bs, 1 H, O-H], 1.78 [m, 2 H, CH₂CH], 1.96 [s, 2 H, CCH₂C], 4.87 [m, 1 H, HOCHCH₂], 7.12 [q, 1 H, J = 7.8 Hz, J = 2.1 Hz, Ar-H], 7.19 [d, 1 H, J = 7.8 Hz, Ar-H] 7.40 [d, 1 H, J = 2.1 Hz, Ar-H]; ¹³C NMR (DCCl₃) ppm, 22.21 [CH(CH₃)₂], 123.16 [CH(CH₃)₂], 24.82 [CH₂CH], 31.59 [CH₂C(CH₃)₂], 32.60 [SC(CH₃)₂], 35.59 [CH₂C(CH₃)₂], 42.00 [SC(CH₃)₂], 48.95 [CH(CH₃)₂], 54.45 [CH₂C(CH₃)₂], 72.35 [HOCH₂], 123.27-142.19 [Ar-C].

6-(1-Chloro-2-isobutyl)-2,2,4,4-tetramethyl-3H-benzo[e]thione (101b)

Into a 25-mL, three-necked, round-bottomed flask equipped with a condenser, a N₂ inlet, and an addition funnel NaH (17.00 mg, 0.72 mmol) was added to 5 mL of dry THF at 0 °C. The reaction mixture was stirred for 2 h, and then ethyl 4-(chlorocarbonyl)benzoate [(101b), 153 mg, 0.72 mmol] dissolved in 4 mL of dry THF was added dropwise. A cloudy precipitate formed during the addition, and the reaction mixture was then stirred for 4 hours after which time 2 drops of de-ionized water were added at RT. The cloudy reaction mixture cleared and was diluted with diethyl ether (20 mL). The organic mixture was then washed with NaHCO₃ (3 x 10 mL), H₂O (1 x 10 mL), and brine (1 x 10 mL) and the dried (MgSO₄, 12 h). Evaporation of solvent (rotovap) and and flash chromatography (hexane:EtOAc, 1:1, drop rate = 1 drop/s) afforded 101b (163 mg, 76%) as a clear oil. IR (neat) 1474 [C-Cl], cm⁻¹; ¹H NMR (DCCl₃) δ 0.82 [d, 3 H, CH(CH₃)₂], 1.05 [d, 3 H, CH(CH₃)₂] 1.40 [s, 6 H, C(CH₃)₂], 1.42 [s, 6 H, C(CH₃)₂], 1.96 [s, 2 H, CCH₂C], 2.20 [m, 1 H, CH(CH₃)₂], 4.60 [d, 2 H, ClCH₂CH], 7.05 [q, 1 H, J = 8.1 Hz, J = 2.1 Hz, Ar-H], 7.07 [d, 1 H, J = 8.1 Hz, Ar-H] 7.32 [d, 1 H, J = 2.1 Hz, Ar-H]; ¹³C NMR (DCCl₃) ppm, 19.61 [CH(CH₃)₂], 20.07 [CH(CH₃)₂] 31.56 [CH₂C(CH₃)₂], 32.62 [SC(CH₃)₂], 35.46 [CH₂C(CH₃)₂], 36.63 [CH(CH₃)₂], 42.34 [SC(CH₃)₂], 54.28 [CH₂C(CH₃)₂], 71.04 [ClCH₂], 124.97-142.30 [Ar-C].

1-(2,2,4,4,7-Pentamethyl-3H/benzo[e]thiane)ethan-1-one (103)

Into a 50-mL, three-necked, round-bottomed flask equipped with a condenser, a N₂ inlet, and an addition funnel was added AlCl₃ (2.53 g, 19.33 mmol) and dissolved in 25 mL of freshly distilled CH₃NO₂. A solution of the 2,2,4,4,7-pentamethyl-3H-benzo[e]thiane [(102), 2.00 g, 9.08 mmol] and acetyl chloride (850 mg, 10.56 mmol) dissolved in 20 mL

of freshly distilled CH_3NO_2 was then added dropwise (1 h) at RT. The reaction mixture was stirred for 48 h and then poured into a 100-mL beaker containing ~30 g of crushed ice. The layers were separated, and the aqueous layer was then extracted with diethyl ether (3 x 50 mL). Combined organic layers were washed with water (2 x 25 mL) and brine (1 x 30 mL) and then dried (Na_2SO_4 , 12 h). Evaporation (rotovap) of solvent and distillation (bp 163-64 °C/0.75 mm Hg) of the residual oil afforded ketone **103** (mp 78-9 °C, 1.47 g, 68%) as a light yellow solid. IR (neat) 1600 [C=O] cm^{-1} ; ^1H NMR (DCCl_3) δ 1.42 [s, 6 H, $\text{C}(\text{CH}_3)_2$], 1.43 [s, 6 H, $\text{C}(\text{CH}_3)_2$], 1.98 [s, 2 H, CCH_2C], 2.45 [s, 3 H, $\text{C}(\text{O})\text{CH}_3$], 2.57 [s, 3 H, Ar-CH_3], 6.97 [s, 1 H, Ar-H], 7.75 [s, 1 H, Ar-H], ^{13}C NMR (DCCl_3) ppm 21.22 [$\text{C}(\text{O})\text{CH}_3$], 29.12 [$\text{CH}_2\text{C}(\text{CH}_3)_2$], 31.54 [$\text{CH}_2\text{C}(\text{CH}_3)_2$], 32.70 [$\text{SC}(\text{CH}_3)_2$], 35.42 [$\text{CH}_2\text{C}(\text{CH}_3)_2$], 42.31 [$\text{SC}(\text{CH}_3)_2$], 53.87 [$\text{CH}_2\text{C}(\text{CH}_3)_2$], 128.70-139.40 [Ar-C], 200.59 [C=O].

Ethyl (2E)-2-Fluoro-3-(2,2,4,4,7-pentamethyl(3H-benzo[3,4-e]thian-6-yl))but-2-enoate (104)

Into a 25-mL, three-necked, round-bottomed equipped with a condenser, a N_2 inlet and an addition funnel flask was added ethyl 2-fluorophosphono-acetate (505 mg, 2.10 mmol) and DMPU (267 mg, 2.10 mmol) dissolved in 3 mL of dry THF. The reaction mixture was cooled to 0 °C, and *n*-BuLi (1.31 mL, 2.10 mmol, 1.6 M) was added dropwise by syringe. After stirring the reaction mixture for 1 h, 1-(2,2,4,4,7-pentamethyl-3H-benzo[3,4-e]thian-1-one (500 mg, 1.90 mmol) dissolved in 4 mL of dry THF was added dropwise (1 h). The reaction mixture was stirred for 6 days at RT and was then quenched with a saturated, aqueous solution of ammonium chloride (3 mL). Extraction with ethyl acetate (3 x 25 mL) was followed by washing the combined organic layers with H_2O (1 x 20 mL) and brine (1 x 25 mL) and then drying (MgSO_4 , 5 h). After solvent evaporation

(rotovap), followed by flash chromatography (hexane:diethyl ether, 1:1, drop rate = 1 drop/s) of the residue and after solvent evaporation, **104** (266 mg, 40%) was recovered as a clear oil. IR (neat) 1712 [C=O] cm^{-1} ; $^1\text{H NMR}$ (DCCl_3) δ 0.85 [t, 3 H, OCH_2CH_3], 1.42 [s, 6 H, $\text{C}(\text{CH}_3)_2$], 1.43 [s, 6 H, $\text{C}(\text{CH}_3)_2$], 1.98 [s, 2 H, CCH_2C], 2.45 [s, 3 H, CCH_3], 2.57 [s, 3 H, Ar-CH_3], 3.97 [q, 2 H, OCH_2CH_3], 6.97 [s, 1 H, Ar-H], 7.75 [s, 1 H, Ar-H], $^{13}\text{C NMR}$ (DCCl_3) ppm 13.61 [OCH_2CH_3], 21.22 [$\text{C}(\text{O})\text{CH}_3$], 29.12 [$\text{CH}_2\text{C}(\text{CH}_3)_2$], 31.54 [$\text{CH}_2\text{C}(\text{CH}_3)_2$], 32.70 [$\text{SC}(\text{CH}_3)_2$], 36.45 [$\text{CH}_2\text{C}(\text{CH}_3)_2$], 43.31 [$\text{SC}(\text{CH}_3)_2$], 52.87 [$\text{CH}_2\text{C}(\text{CH}_3)_2$], 60.88 [OCH_2CH_3], 128.70-139.40 [Ar-C], 145.88 [$\text{FC}=\text{CH}$], 160.98 [$\text{C}=\text{O}$]. $^{19}\text{F NMR}$ (DCCl_3) ppm -124.77 [d, 1 F, $\text{FC}=\text{CCH}_3$].

(2E)-2-Fluoro-3-(2,2,4,4,7-pentamethyl(3H-benzo[3,4-e]thian-6-yl))but-2-en-1-ol (105)

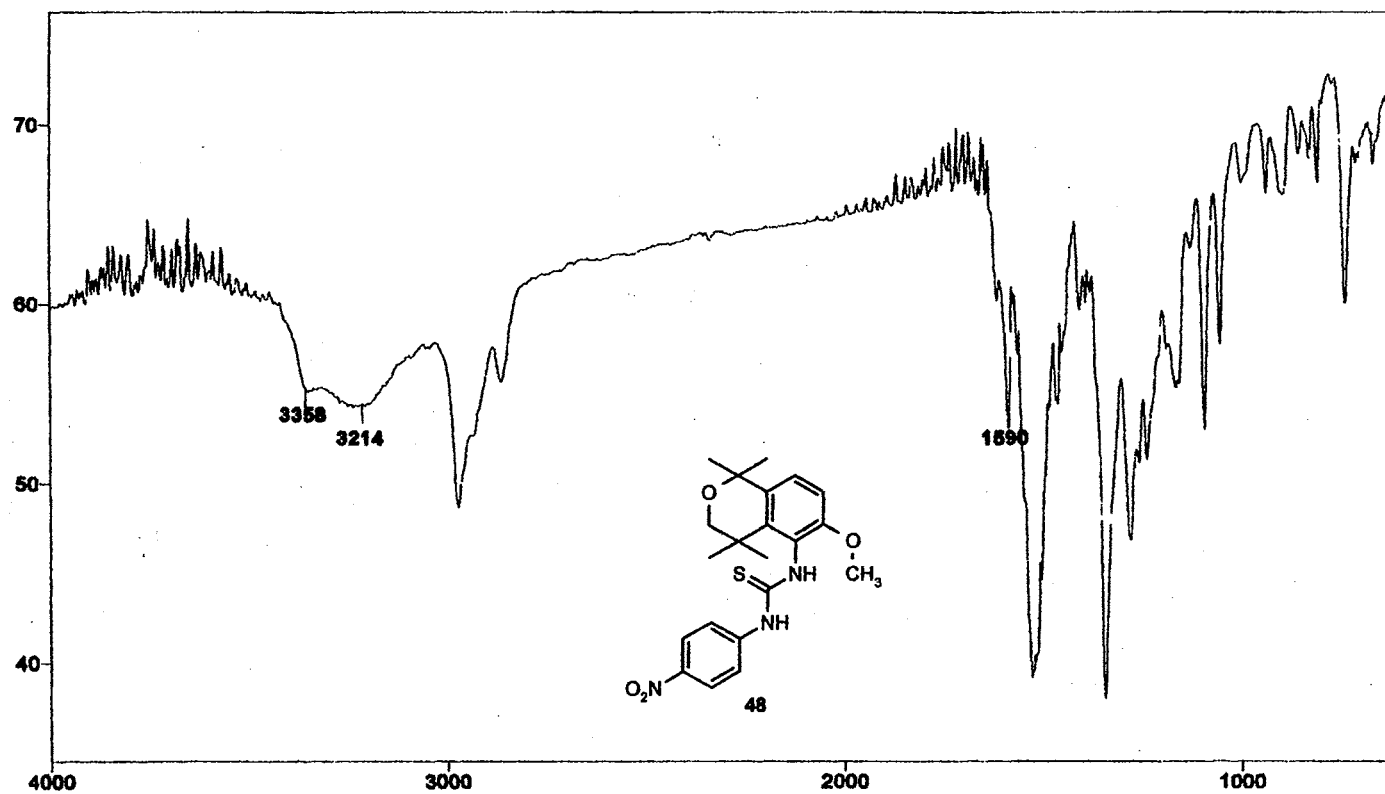
Ester **104** (266 mg, 0.76 mmol) dissolved in 5 mL of dry THF was placed in 25-mL, three-necked, round-bottomed flask equipped with a condenser, a N_2 inlet and an addition funnel and then cooled to $-40\text{ }^\circ\text{C}$. A solution of DIBAL-H in toluene (1.27 mL, 1.90 mmol, 1.5 M) was then added by syringe. The reaction mixture was stirred for 2 h, and it was monitored by TLC (hexane:ethyl acetate, 1:2). After all of the starting material appeared to have reacted (TLC), the reaction mixture was quenched with 2 mL of a saturated, aqueous solution of Rochelle salt (sodium-potassium tartrate, 1:1). The bi-phasic mixture was extracted with ethyl acetate (3 x 25 mL), followed by washing the organic extracts with H_2O (1 x 15 mL) and brine (1 x 20 mL) and then drying (MgSO_4 , 12 h). Separation of the major component in the residue, after solvent evaporation, by flash chromatography (hexane:diethyl ether, 1:1, drop rate = 1 drop/s) afforded alcohol **105** (216 mg, 92%) as a colorless oil. IR (neat) 3353 [O-H], 1659 [C=C-F] cm^{-1} ; $^1\text{H NMR}$ (DCCl_3) δ 1.35 [s, 6 H,

$C(CH_3)_2$], 1.42 [s, 6 H, $C(CH_3)_2$], 1.87 [bs, 1 H, O-H], 1.97 [d, 3 H, CCH_3], 1.98 [s, 2 H, CCH_2C], 2.14 [s, 3 H, Ar- CH_3], 3.97 [d, 2 H, $HOCH_2$], 6.94 [s, 1 H, Ar-H], 7.07 [s, 1 H, Ar-H], ^{13}C NMR ($DCCl_3$) ppm 16.61 [$=CCH_3$], 18.68 [CCH_3], 31.54 [$CH_2C(CH_3)_2$], 32.61 [$SC(CH_3)_2$], 35.04 [$CH_2C(CH_3)_2$] 42.05 [$CH_2C(CH_3)_2$], 54.27 [$SC(CH_3)_2$], 58.88 [$HOCH_2$], 117.66 [$FC=CH$], 127.70-140.05 [Ar-C], 156.28 [$FC=CH$]. ^{19}F NMR ($DCCl_3$) ppm -120.93 [td, 1 F, $FC=CCH_3$].

(2E)-2-Fluoro-3-(2,2,4,4,7-pentamethyl(3H-benzo[3,4-e]thian-6-yl))but-2-enal (106)

Alcohol **105** (200 mg, 0.65 mmol) dissolved in 3 mL of acetone was placed in a 25-mL, one-necked, round-bottomed flask, and MnO_2 (1.0 g, 11.52 mmol, activated grade, size <5 μm) was then added to the solution at RT. The suspension was stirred for 24 h and then filtered through a 1-inch thick celite pad. Evaporation (rotovap) of the solvent and purification of the major component in the residue, after solvent evaporation, via flash chromatography (hexane:diethyl ether:ethyl acetate, 1:1:1, drop rate = 1 drop/s), afforded aldehyde **106** (113 mg, 57%) as a light yellow oil. IR (neat) 2834 [O=C-H], 1692 [C=O] cm^{-1} ; 1H NMR ($DCCl_3$) δ 1.35 [d, 6 H, $C(CH_3)_2$], 1.43 [d, 6 H, $C(CH_3)_2$], 1.96 [s, 2 H, CCH_2C], 2.19 [d, 3 H, CCH_3], 2.21 [s, 3 H, Ar- CH_3], 7.00 [s, 1 H, Ar-H], 7.17 [s, 1 H, Ar-H], 9.15 [d, 1 H, $HC(O)$], ^{13}C NMR ($DCCl_3$) ppm 18.22 [$=CCH_3$], 18.82 [CCH_3], 31.52 [$CH_2C(CH_3)_2$], 32.47 [$SC(CH_3)_2$], 35.03 [$CH_2C(CH_3)_2$] 42.15 [$CH_2C(CH_3)_2$], 54.01 [$SC(CH_3)_2$], 127.66-140.05 [$FC=CH$, Ar-C], 154.73 [$FC=CH$]. 182.44 [$HC(O)$]; ^{19}F NMR ($DCCl_3$) ppm -132.98 [m, 1 F, $FC=CCH_3$].

Plate I



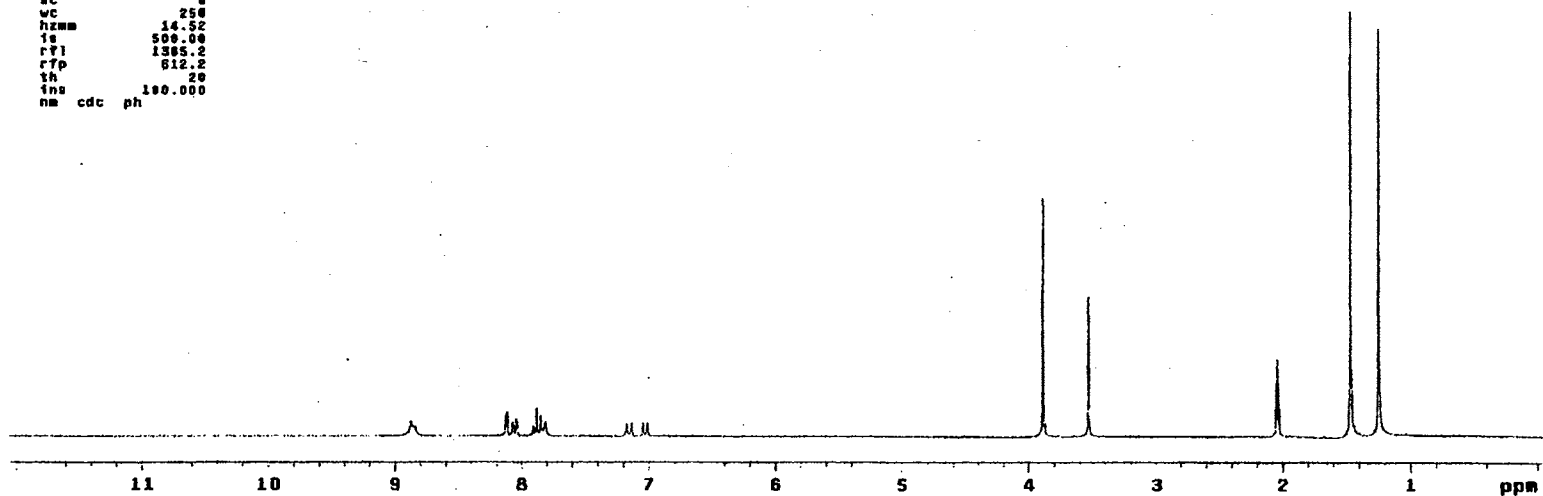
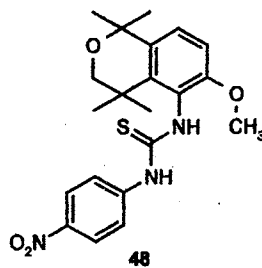
IR Spectrum of 48

Plate II

STANDARD 1H OBSERVE

```

expt stdih
SAMPLE
date Apr 3 2000 dfrq DEC. & VT 300.089
solvent Acetone dn H1
file exp dpwr 30
ACQUISITION exp dof 0
sfrq 300.089 ds nnn c
tn H1 dmw 200
at 3.747 dmf 200
np 33728 PROCESSING
sw 4500.5 wtfile
rb 2000 proc ft
bs 16 tn not used
tpwr 45
pv 6.8 verr
di 8 wexp
tof 0 wbs
nt 16 wnt
ct 16
alock n
gain not used
FLAGS
f1 n
fn y
dp y
DISPLAY
sp -13.0
wp 3831.0
vs 78
sc 8
wc 250
hzmm 14.52
is 500.00
rfl 1305.2
rfp 612.2
th 20
ins 100.000
nm cdc ph
    
```



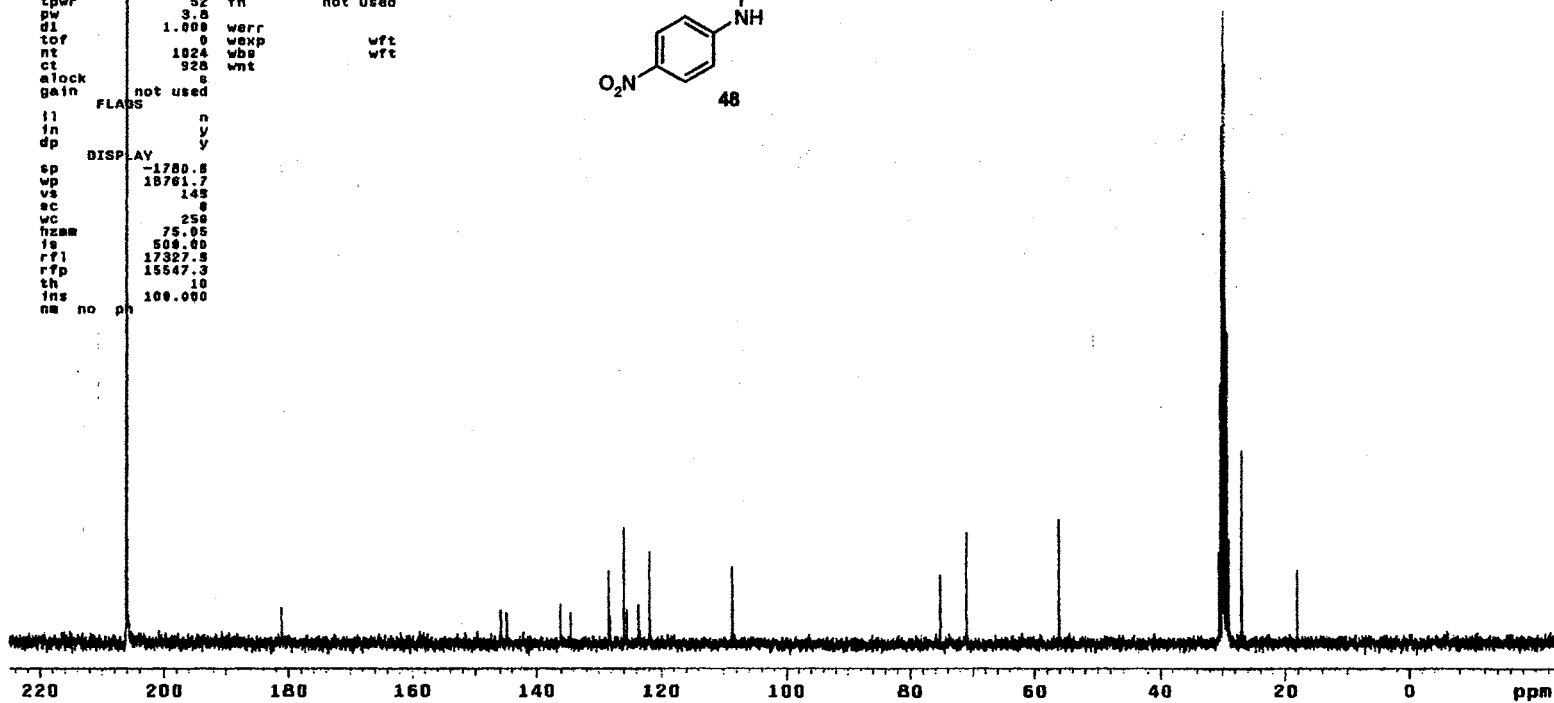
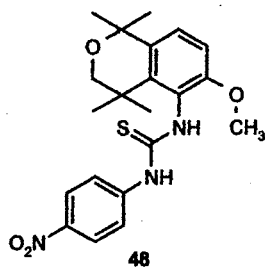
¹H NMR Spectrum of 48

Plate III

13C OBSERVE

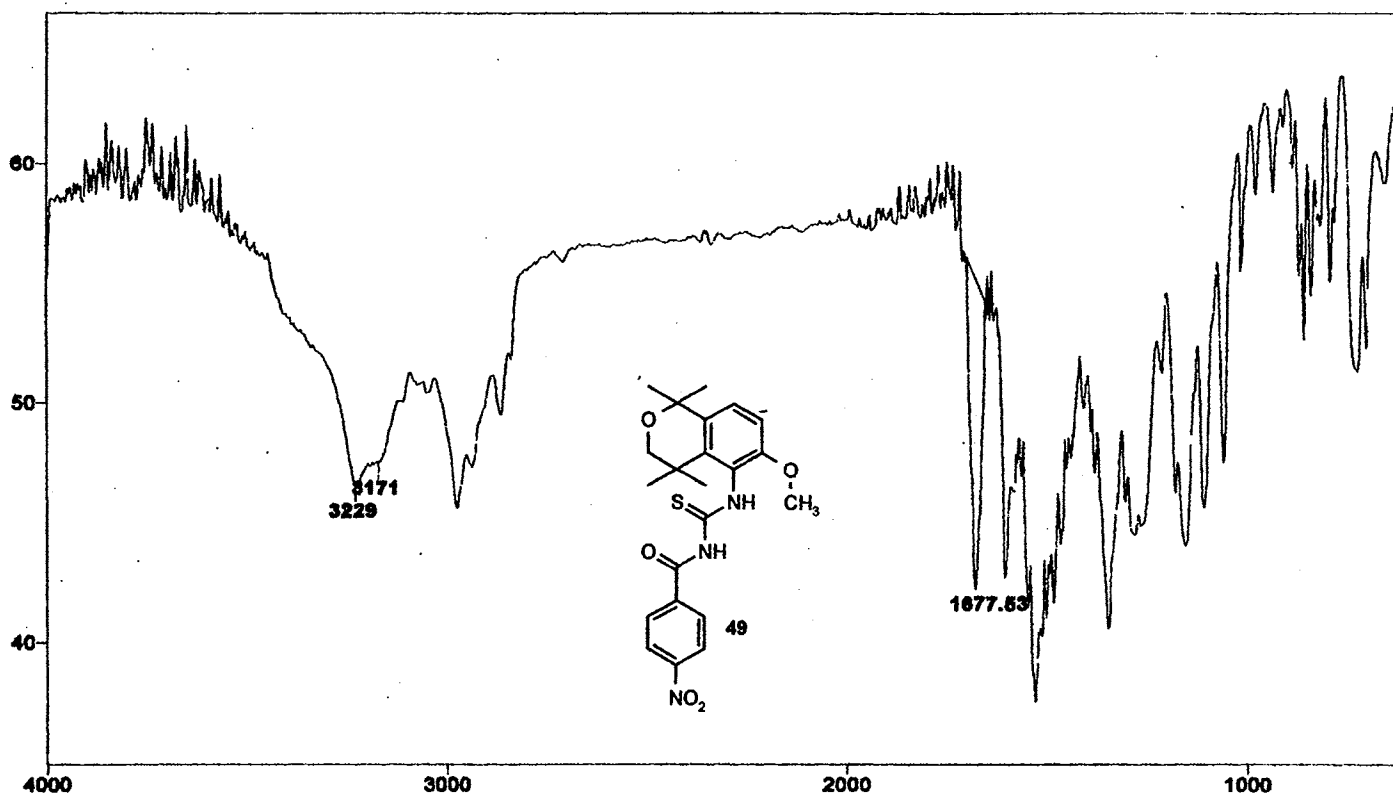
```

expl std13c
SAMPLE
date Apr 3 2000 dfrq 300.089
solvent Acetone dn H1
file exp dpwr 34
ACQUISITION dof 0
efrq 75.465 dm vvv
tn C13 dms w
ac 0.800 dmf 11764
np 30016 PROCESSING
sw 18761.7 lb 1.00
fb 10408 wf11e
bs 16 proc ft
tpwr 52 fn not used
pw 3.3
dl 1.000 werr
tof 0 wexp wft
nt 1024 wba wft
ct 928 wnt
alock s
gain not used
FLAS n
in y
dp y
DISPLAY
sp -1780.8
wp 18761.7
vs 145
ec s
wc 250
hzam 75.05
fs 500.00
rfl 17327.5
rff 15547.3
th 10
ins 100.000
nm no ph
    
```



¹³C NMR Spectrum of 48

Plate IV



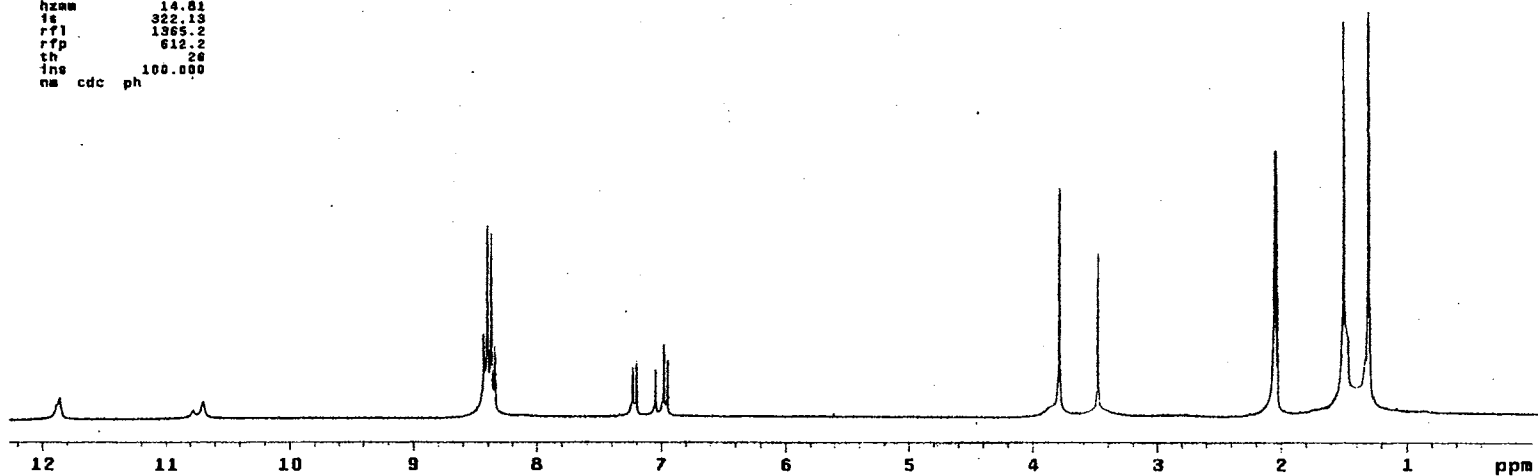
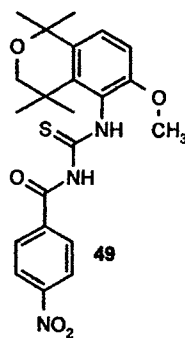
IR Spectrum of 49

Plate V

STANDARD 1H OBSERVE

```

expi stdih
SAMPLE
date Apr 3 2000 dfrq DEC. A VT 300.089
solvent Acetone dn H1
f1le exp dpr 30
ACQUISITION exp dof 0
sfrq 300.089 dm nnn
tn H1 dam c
at 3.747 dmf 200
np 33728 PROCESSING
sw 4500.5 wtfile ft
fb 2600 proc
bs 16 fn not used
tpwr 48
pw 6.3 werr
d1 0 wexp
tof 0 wbs
nt 16 wnt
ct 16
alock n
gain not used
FLADS
f1 n
in y
dp y
DISPLAY
sp -19.6
wp 3702.1
vs 83
sc 0
wc 250
hzaw 14.81
fs 322.13
rfl 1365.2
rfp 612.2
th 20
ins 100.000
na cdc ph
  
```



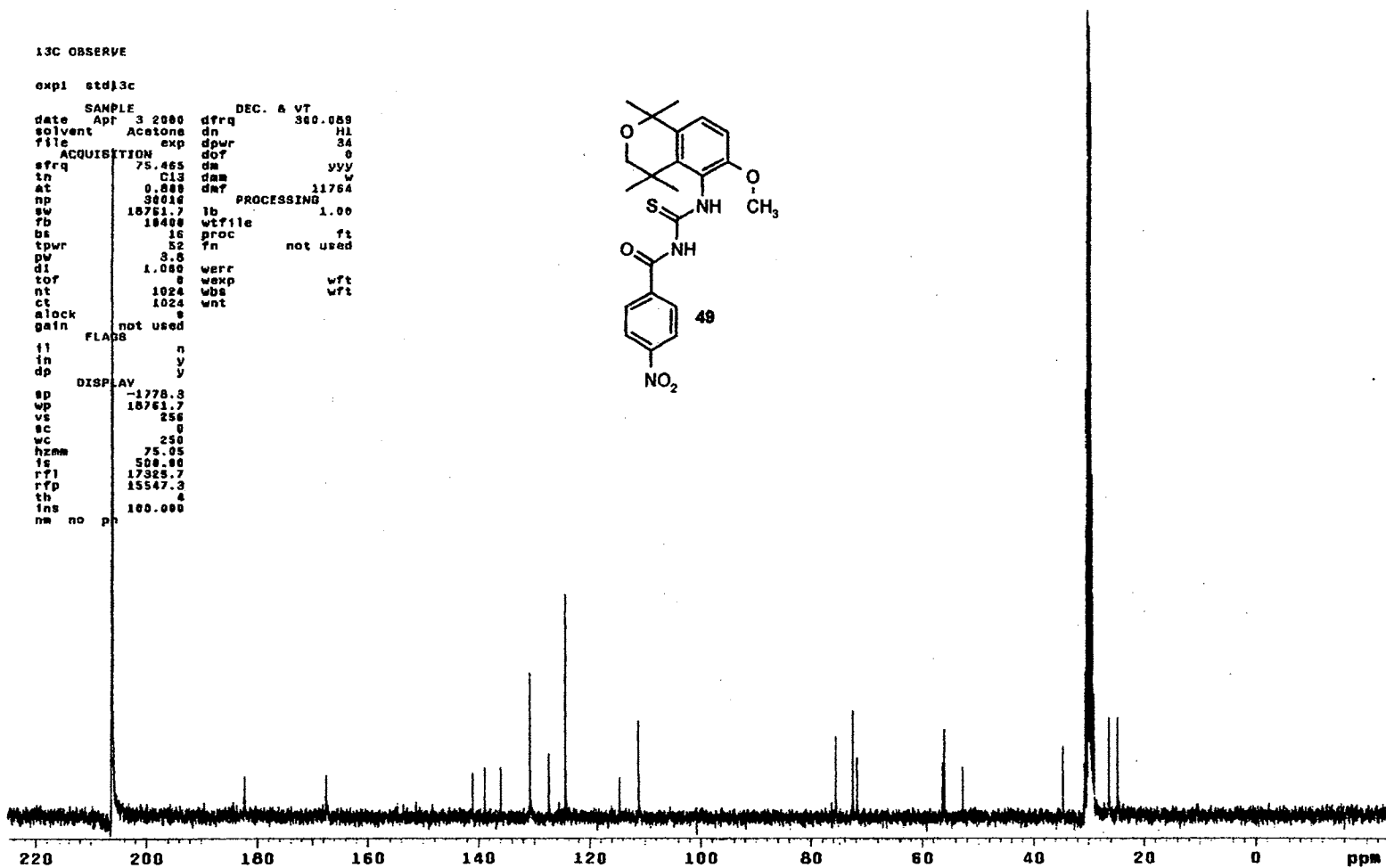
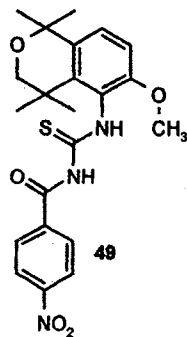
¹H NMR Spectrum of 49

Plate VI

13C OBSERVE

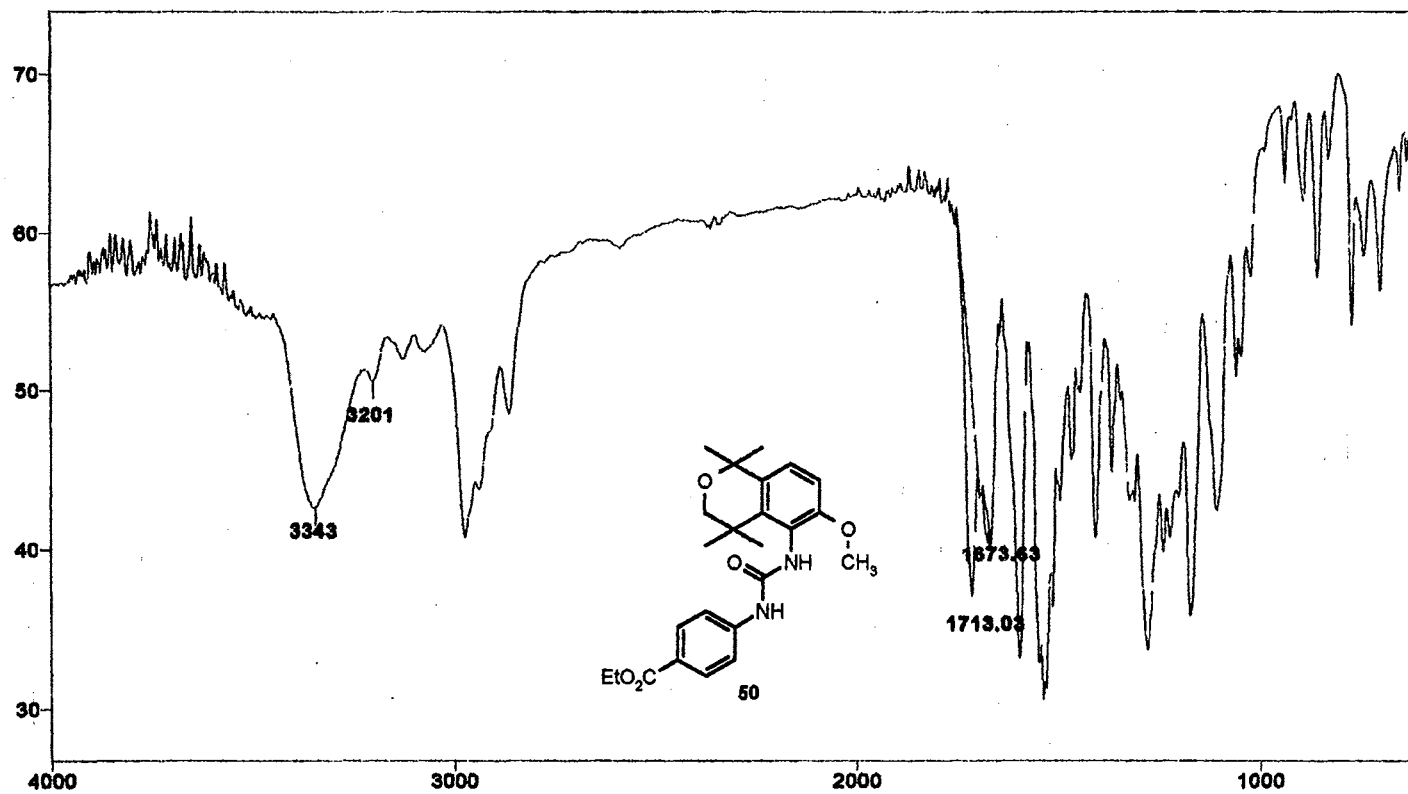
exptl std)3c

SAMPLE		DEC. & VT	
date	Apr 3 2000	dfrq	360.089
solvent	Acetone	dn	H1
file		dpwr	34
ACQUISITION			
exp		dot	0
sfrq	75.465	da	vvv
in	C13	dam	w
at	0.800	daf	11764
np	38016	PROCESSING	
sw	18761.7	lb	1.00
fb	18400	wtfile	
bs	16	proc	ft
tpwr	52	fn	not used
pw	3.8		
d1	1.000	werr	
tor	0	wexp	wft
nt	1024	wds	wft
ct	1024	wnt	
alock	0		
gain	not used		
FLAGS			
f1	n		
in	y		
dp	y		
DISPLAY			
sp	-1778.3		
wp	18761.7		
vs	250		
sc	0		
wc	250		
hznm	75.05		
fs	500.00		
rfl	17325.7		
rfp	15547.3		
th	4		
ins	100.000		
nm	no	ph	



¹³C NMR Spectrum of 49

Plate VII



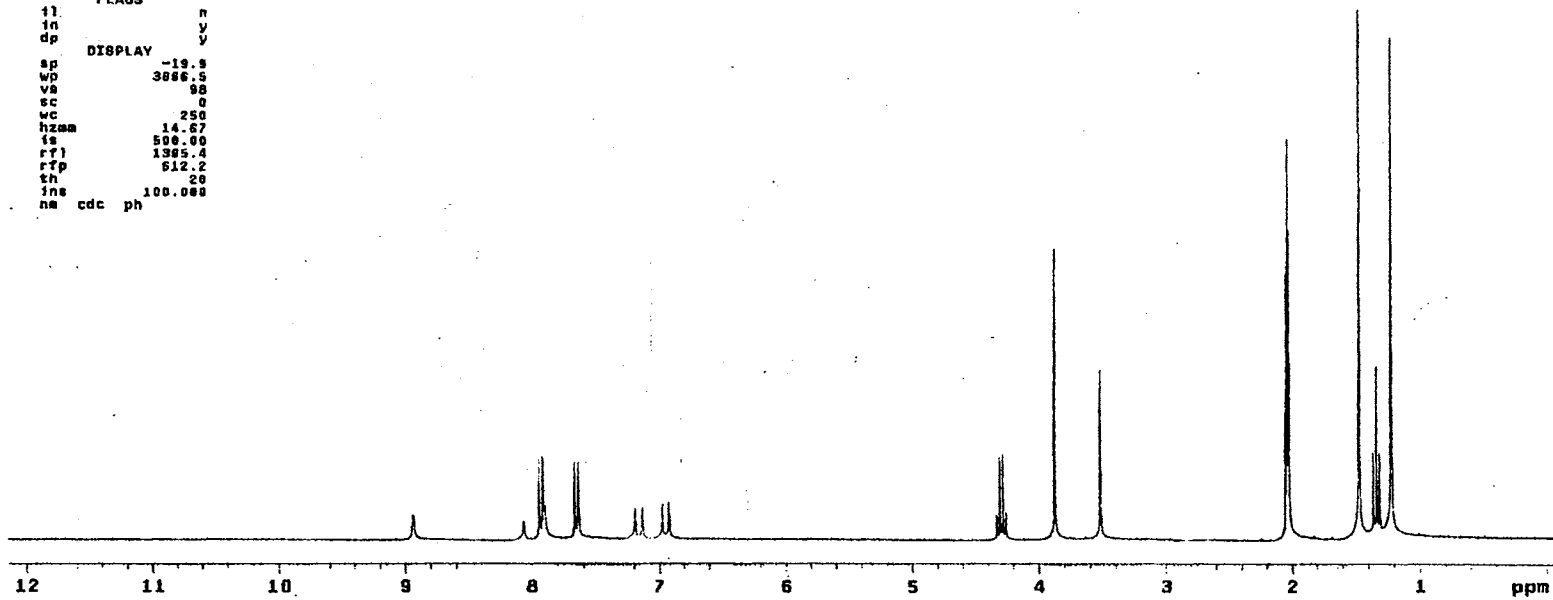
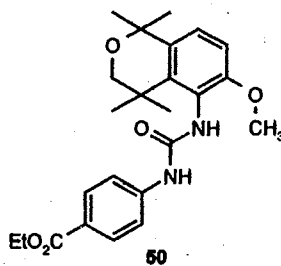
IR Spectrum of 50

Plate VIII

STANDARD IH OBSERVE

```

expl stdih
SAMPLE DEC. & VT
date Apr 3 2000 dfrq 300.089
solvent Acetone dn H1
file exp dpr 30
ACQUISITION dof 0
sfrq 300.089 dm nnn
tn H1 dmm c
at 3.747 dmf 200
np 33728 PROCESSING
sw 4500.5 wtf10 ft
Tb 1600 proc
be 16 fn not used
tpwr 48
pw 6.9 werr
d1 0 wexp
tof 0 wba
nt 16 wnt
ct 16
clock n
gain not used
FLAGS
fl n
in y
dp y
DISPLAY
sp -19.9
wp 3886.5
vs 98
sc 0
wc 250
hzom 14.67
is 500.00
rf1 1305.4
rfp 612.2
th 20
ins 100.000
na cdc ph
    
```



¹H NMR Spectrum of 50

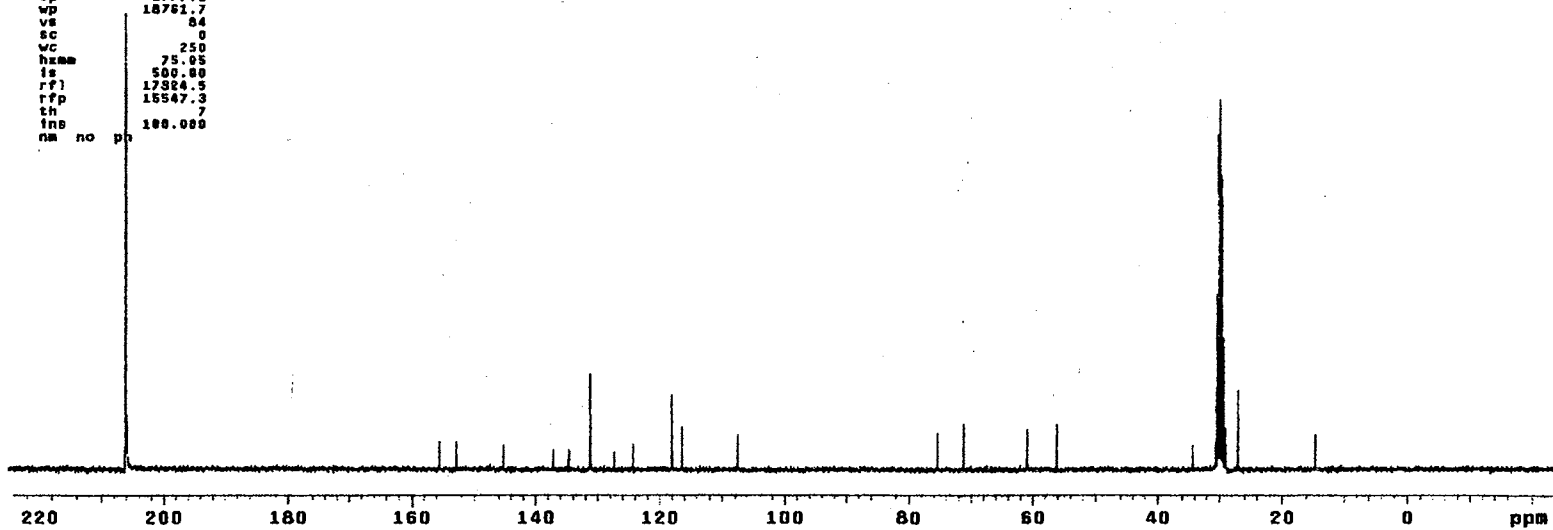
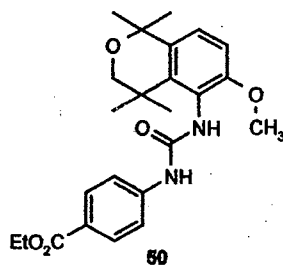
Plate IX

¹³C OBSERVE

exptl std13c

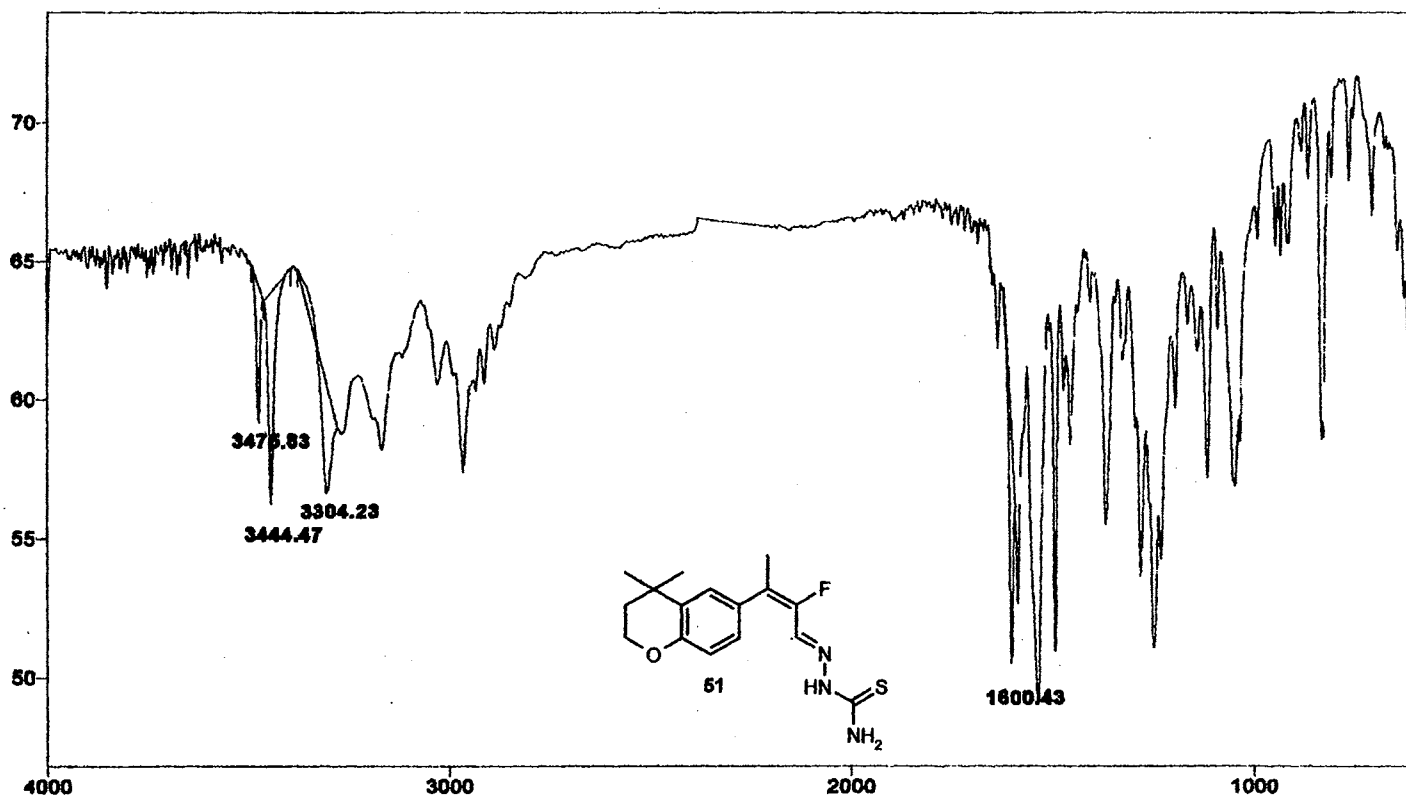
```

SAMPLE          DEC. & VT
date Apr 3 2000 dfrq 300.089
solvent Acetone dn HI
file exp dpwr 34
ACQUISITION    dot 0
sfrq 75.465 da yvy
tn C13 dm w
at 6.800 dat 11764
np 30816 PROCESSING
sw 18781.7 lb 1.00
fb 10400 wtfile
bs 15 proc ft
spwr 52 fn not used
pw 3.8
d1 1.000 werr
tof 0 wexp wft
nt 1824 wbs wft
ct 1824 wnt
alock 6
gain not used
FLAOS n
il y
in y
dp y
DISPLAY
sp -1777.2
wp 18781.7
vs 84
sc 0
wc 250
hzmm 75.05
fs 509.00
rf1 17324.5
rfp 15547.3
th 7
ins 188.000
nm no ph
    
```



¹³C NMR Spectrum of 50

Plate X



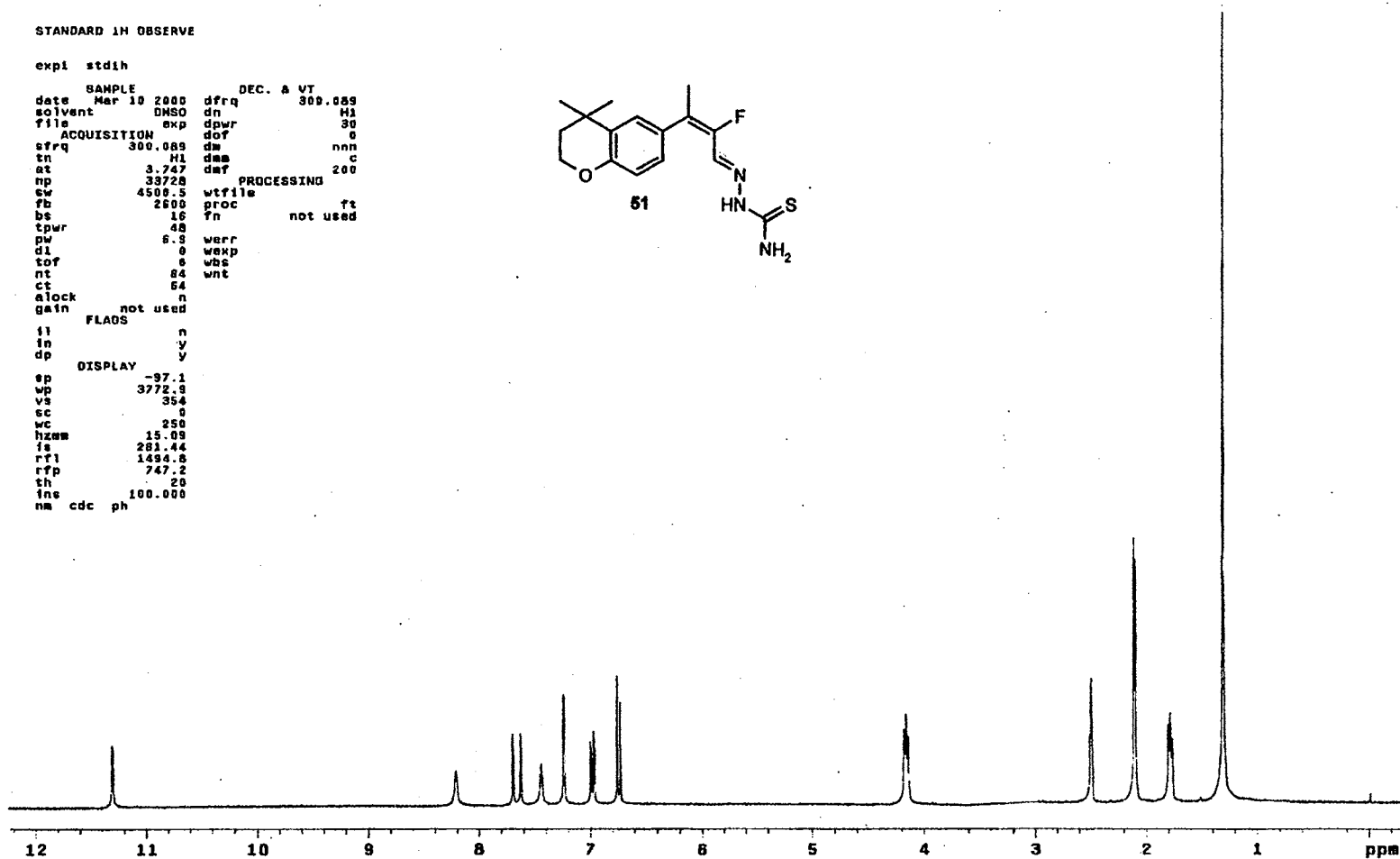
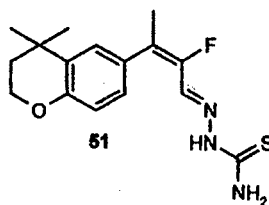
IR Spectrum of 51

Plate XI

STANDARD 1H OBSERVE

```

expt stdih
SAMPLE          DEC. A VT
date Mar 10 2000 dfrq 300.089
solvent DMSO      dn  H1
file ACQUISITION exp  dpwr 30
sfrq 300.089      dm  nnn
tn  H1            dms  c
at  3.747         dmf  PROCESSING 200
np  33728
gw  4500.5        wtfile
fb  2500          proc  ft
bs  16            fn  not used
tpwr 48
pw  6.8          warr
d1  0            wexp
tof  0           wbc
nt  64          wnt
ct  54
alock not used  n
gain  FLAOS     n
ii  n
in  y
dp  y
DISPLAY
sp  -97.1
wp  3772.9
vs  354
sc  0
wc  250
hzms 15.09
is  281.44
rf1  1494.8
rfp  747.2
th  25
ins  100.000
nm  cdc ph
    
```



¹H NMR Spectrum of 51

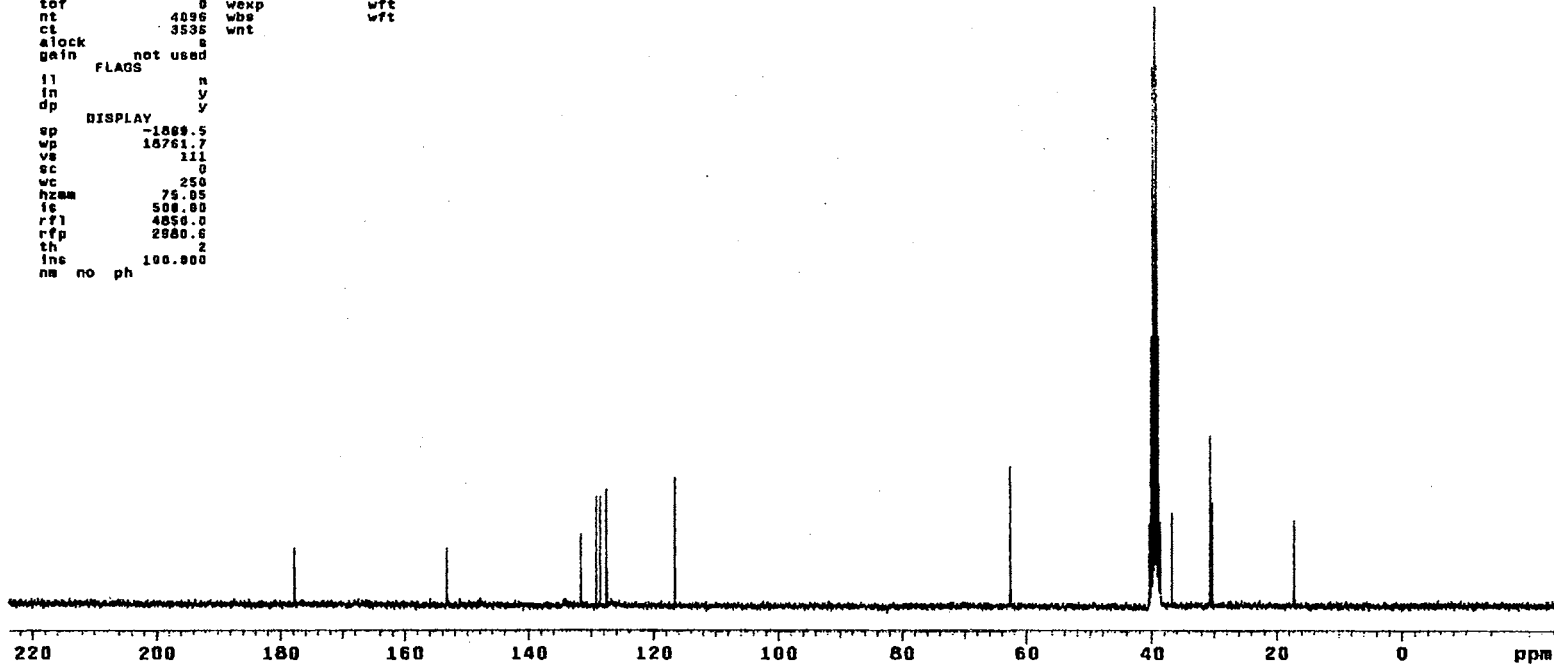
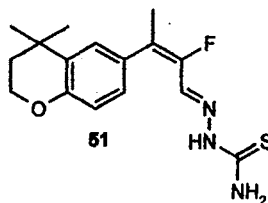
Plate XII

13C OBSERVE

expl stdiac

```

SAMPLE          DEC. & VT
date Mar 10 2000 dfrq          300.083
solvent DMSO   dn             H1
file      exp   dpwr          34
ACQUISITION    dof           0
sfrq       75.464 dm          vvvv
tn         C13  dms          w
at         0.800 daf          11764
np         38018 PROCESSING
sw         18761.7 lb          1.00
fb         10400 wtfile
bs         15   proc          ft
tpwr       52   fn          not used
pw         3.8
d1         1.000 werr
tof         0   wexp          wft
nt         4896 wbs          wft
ct         3536 wnt
alock      s
gain       not used
FLAGS
il         n
in         y
dp         y
DISPLAY
sp         -1000.5
wp         18761.7
vs         111
sc         0
wc         250
hzam       75.05
ic         500.00
rfl        4850.0
rfp        2900.0
th         2
ins        100.000
na no ph
    
```



¹³C NMR Spectrum of 51

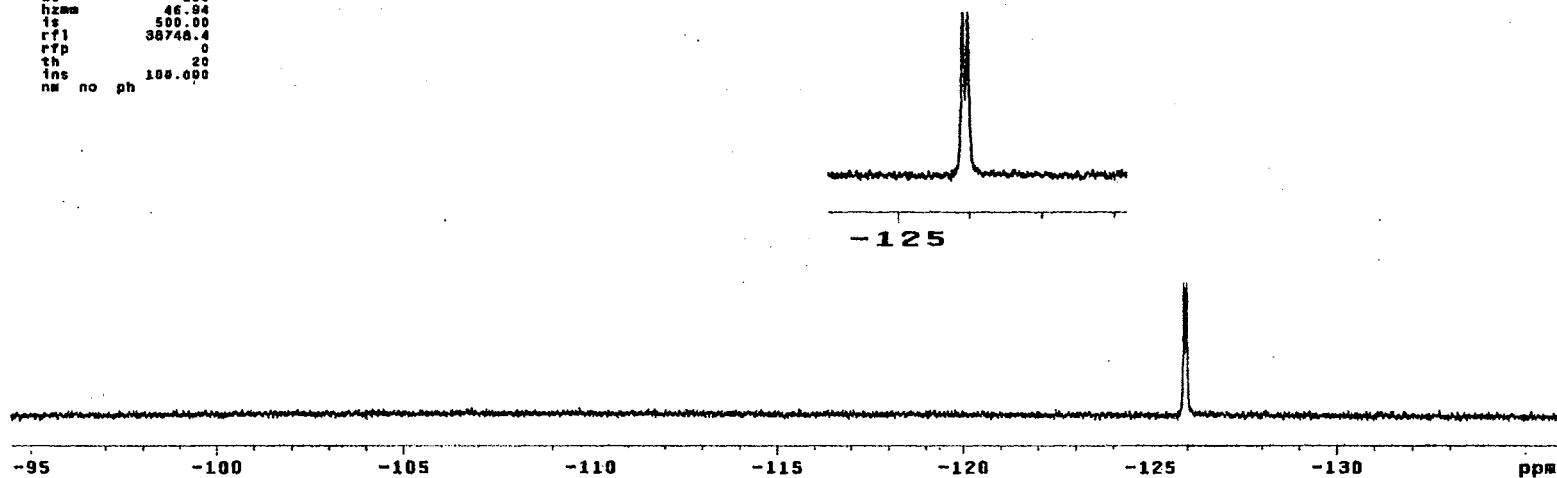
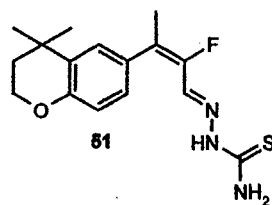
Plate XIII

13C OBSERVE

expl std13c

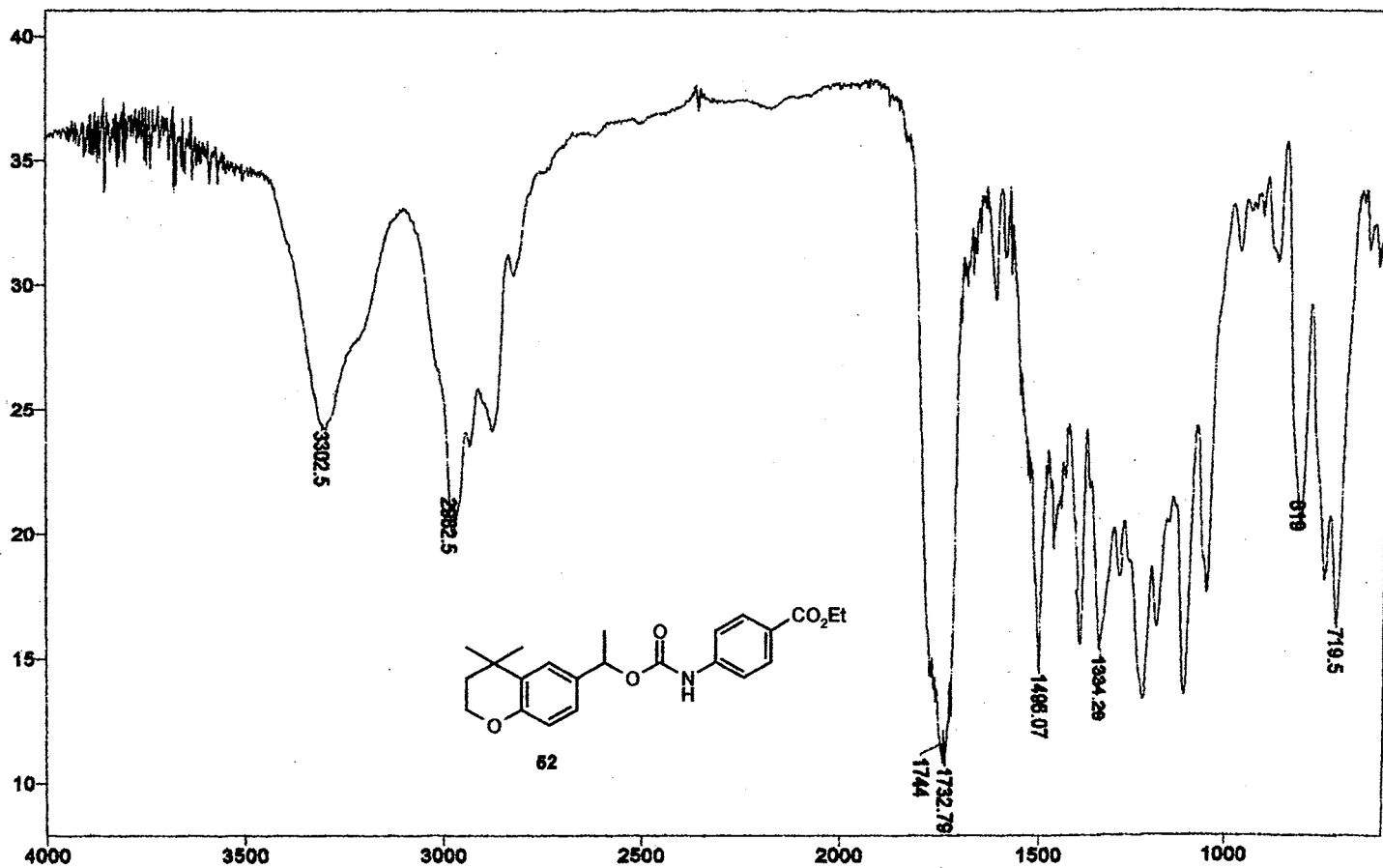
```

SAMPLE          DEC. & VT
date   Mar 10 2000   dfrq      300.089
solvent DMSO        dn         H1
file          exp   dpwr       34
          ACQUISITION   dof         0
sfrq      282.335   dm         nnn
tn         F19      dsm         w
at         0.000   ddf      11784
np         30016   PROCESSING
sw      18761.7   lb         1.00
fb         10400   wtfile
bs         16     proc         ft
tpwr       52     Tn         not used
pu         3.8
dl         1.000   warr
tof         0     wexp         wft
nt         1024   wbs         wft
ct         96     wnt
alock      n
gain      not used
          FLAOS
ii         n
in         y
dp         y
          DISPLAY
sp      -38403.7
wp      11734.8
vs       25
sc        0
wc       250
hzmax    46.94
fs       500.00
rf1      30748.4
rtp       0
th        20
ins      100.000
nm no ph
    
```



¹⁹F NMR Spectrum of 51

Plate XIV



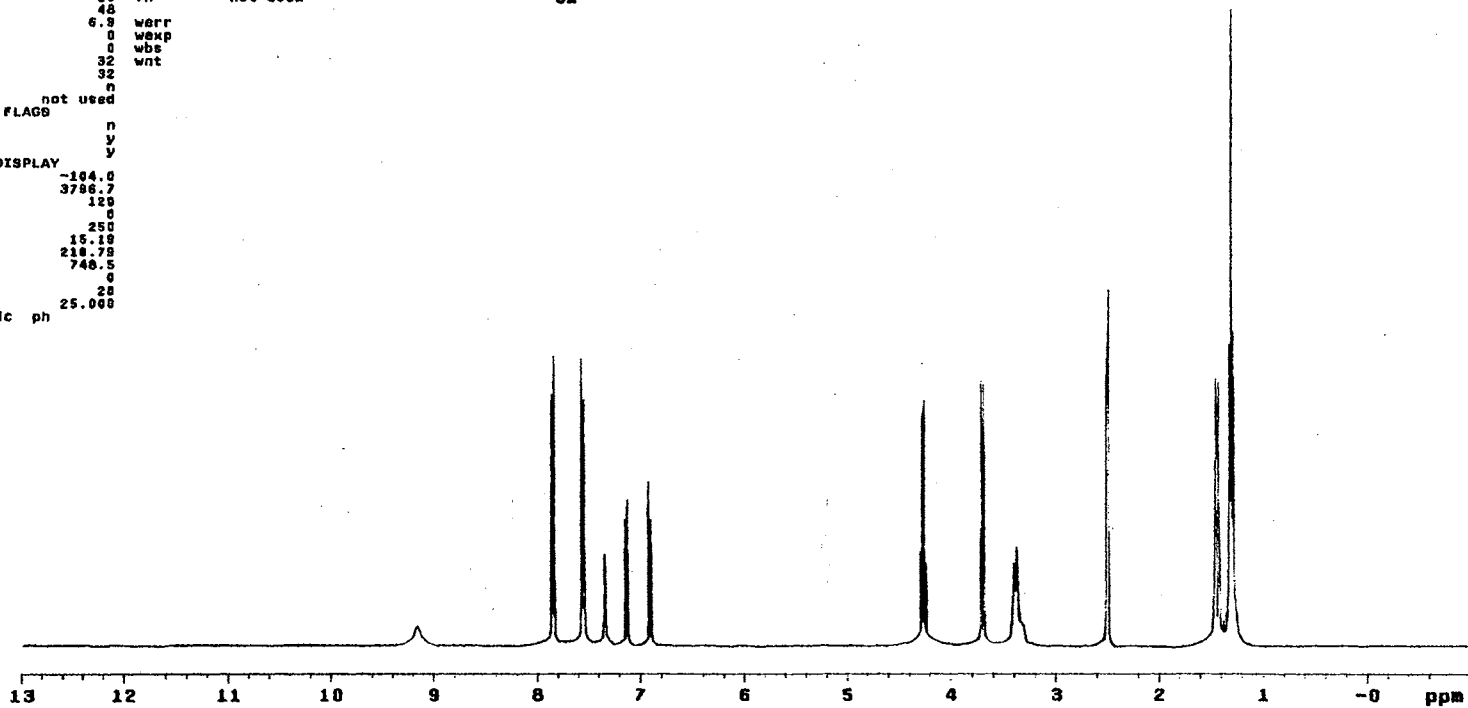
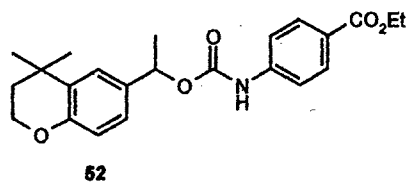
IR Spectrum of 52

Plate XV

STANDARD 1H OBSERVE

```

expl stdh
SAMPLE DEC. & VT
date Nov 11 1989 dfrq 300.067
solvent CDCl3 dn H1
f1la exp dpwr 38
ACQUISITION dof 8
sfrq 300.067 dm nnn
tn H1 dnm c
at 3.747 dmf PROCESSING 200
np 33728
sw 4500.5 wtf1la
fb 2600 proc ft
bs 16 Tn not used
zpw 48
pw 6.9 warr
d1 0 wexp
tof 0 wbs
nt 32 wnt
ct 32
atock n
gain not used
FLAGS
f1 n
in y
dp DISPLAY y
sp -104.0
wp 3786.7
vs 120
sc 0
wc 250
hzmm 15.10
fg 210.78
rf1 740.5
rfp 0
th 20
ins
nm cdc ph 25.000
    
```



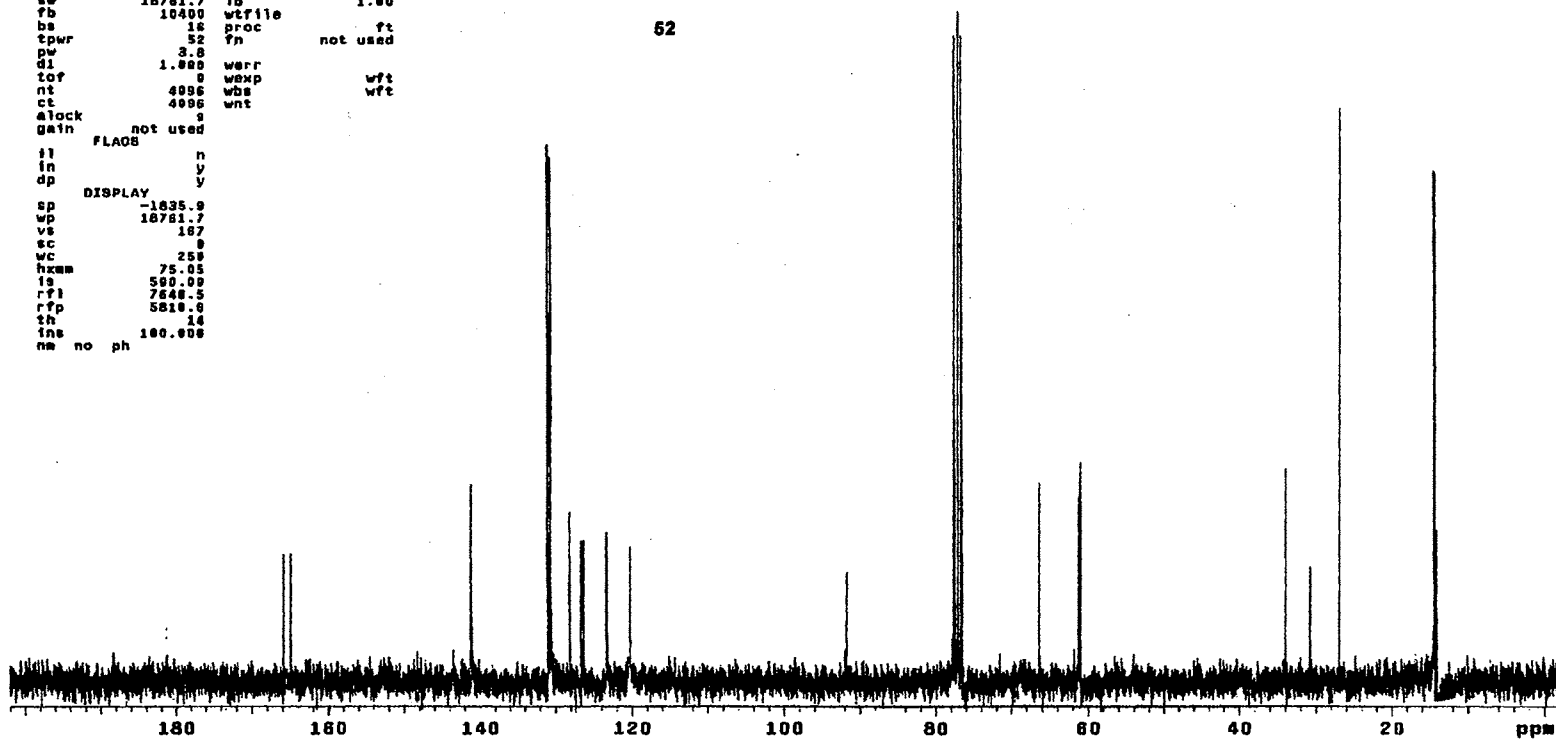
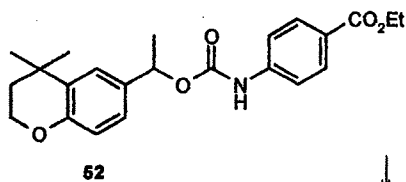
¹H NMR Spectrum of 52

Plate XVI

13C OBSERVE

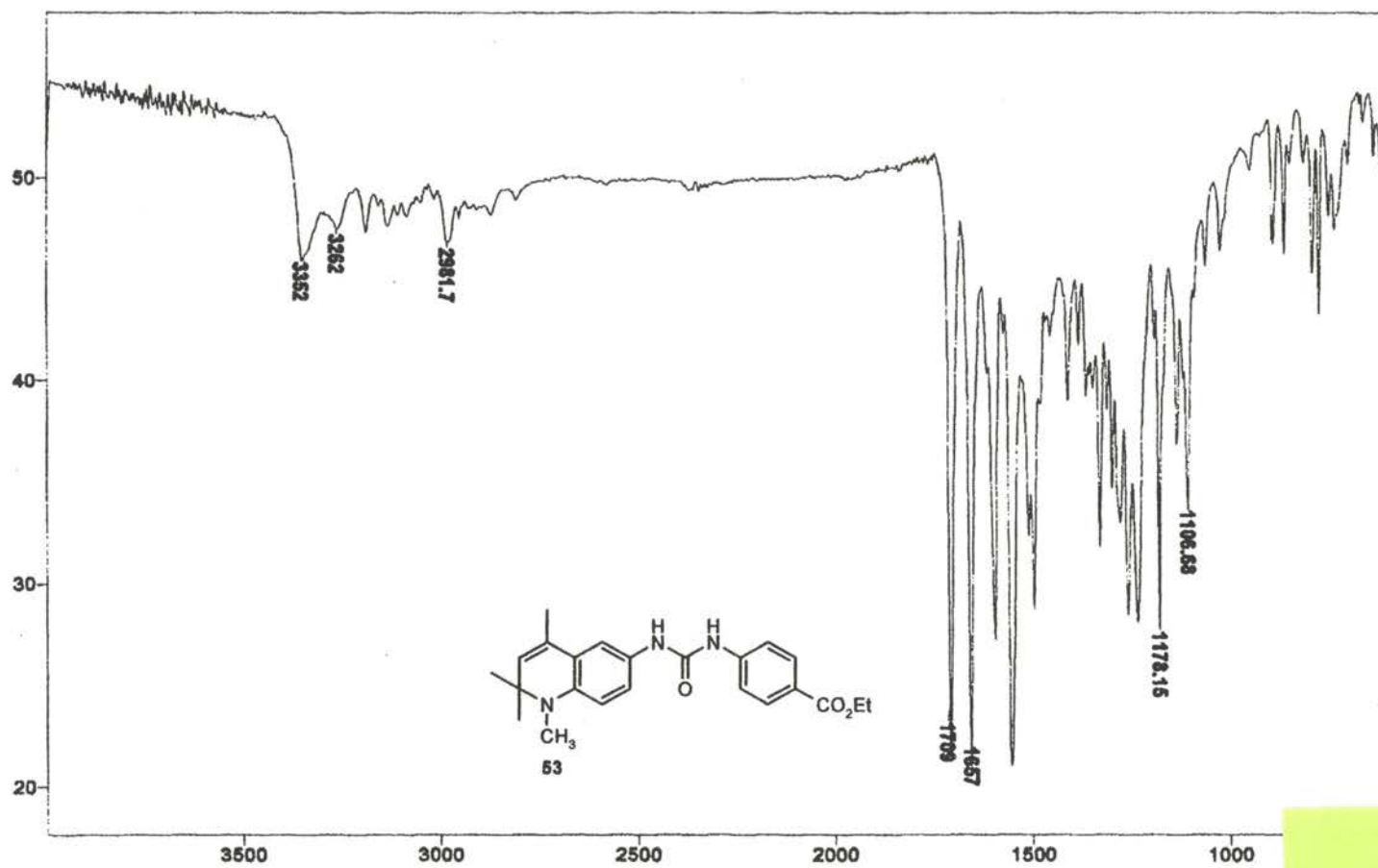
```

exp1 std13c
SAMPLE DEC. & VT
date Apr 19 2000 dfrq 300.087
solvent CDCl3 dn H1
file exp dpr 34
ACQUISITION dot 0
sfrq 75.464 dm vvv
tn 0.137 dm w
at 0.880 dm 11764
np 30016 daf PROCESSING
sw 18781.7 lb 1.00
fb 10400 wtfile
bs 18 proc ft
tpwr 32 yn not used
pw 3.8
d1 1.000 warr
tof 0 wexp wft
nt 4096 wbs wft
ct 4096 wnt
alock s
gain not used
FLAOS
ii n
in y
dp DISPLAY y
sp -1835.9
wp 18781.7
vs 107
sc 0
wc 259
hxam 75.05
is 589.09
rf1 7648.5
rfp 5810.0
th 14
ins 100.008
nm no ph
    
```



¹³C NMR Spectrum of 52

Plate XVII



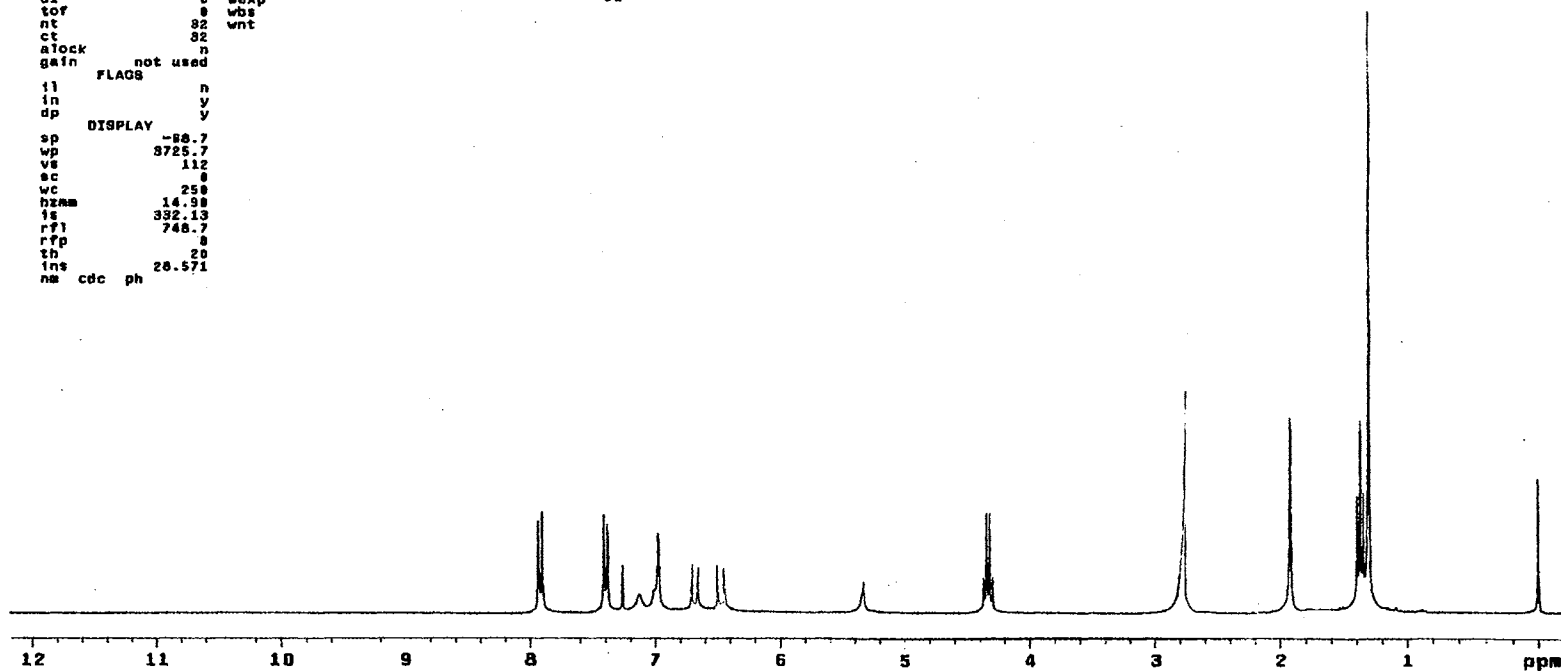
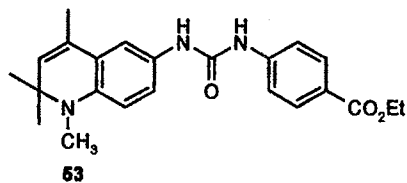
IR Spectrum of 53

Plate XVIII

STANDARD 1H OBSERVE

```

exp1 std1h
SAMPLE
date Nov 11 1999 dfrq DEC. & VT 300.087
solvent CDCl3 dn H1
f1ls exp dpr 30
ACQUISITION dof 0
sfrq 300.087 da nnn
th H1 dm c
at 3.747 dwt 200
np 39728 wtfile PROCESSING
sw 4508.5 wtfile
fb 2600 proc ft
bs 18 yn not used
tdwr 48
pw 6.8 warr
dl 0 wexp
tof 0 wbs
nt 32 wnt
ct 32
atock n
gain not used
FLAG8
il n
in y
dp y
DISPLAY
sp -88.7
wp 3725.7
vs 112
sc 0
wc 250
hzmm 14.98
fs 332.13
rf1 748.7
rfp 0
th 20
ins 20.571
na cdc ph
    
```



¹H NMR Spectrum of 53

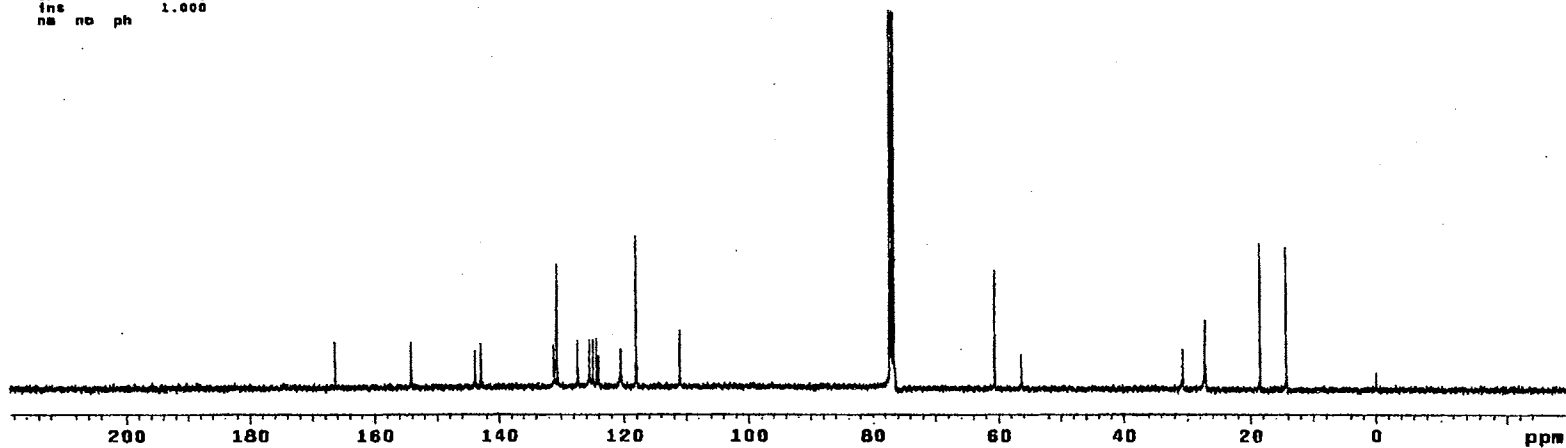
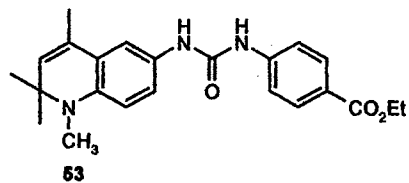
Plate XIX

13C OBSERVE

expl std13c

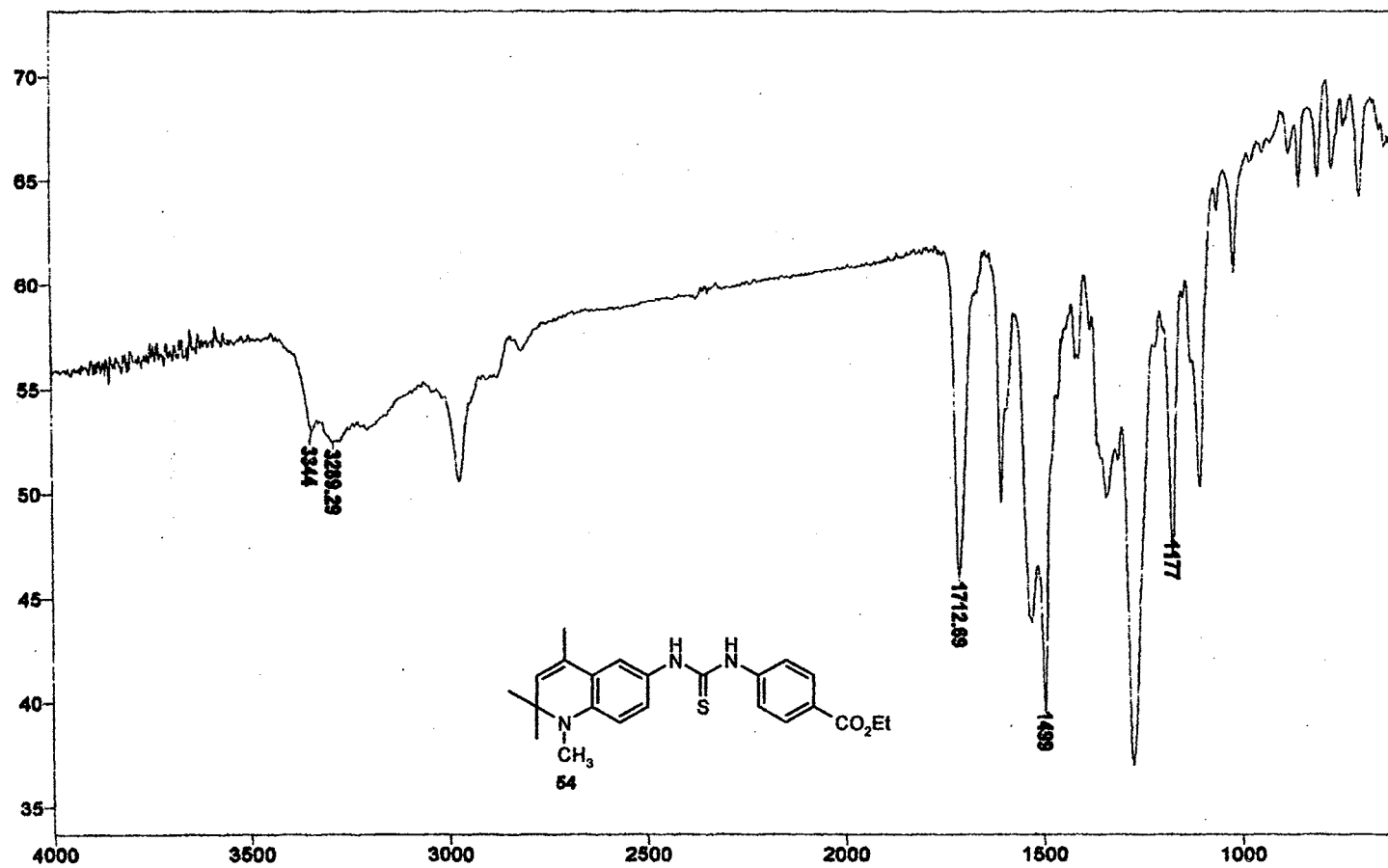
```

SAMPLE          DEC. & VT
date Nov 11 1999 dfrq 395.925
solvent CDCl3   dn      M1
file          exp  dpwr    40
              dot      0
ACQUISITION
dfrq 100.570  dm      nvy
tn    013    dsm      w
at    1.120  dat     12000
np    5996A  dsag
sw    25000.0 dres    1.0
fb    14000  homo
bs    15     PROCESSING
tpwr  53     lb      1.00
pw    7.0   wtfile
d1    1.000 proc    ft
d2    0.500 fn     not used
tor   0     math    f
ns    10000
ct    10000 werr
alock  n    wexp
gain  not used wba    wft
              wnt    wft
              n
              n
              y
              nn
DISPLAY
sp    -9000.4
wp    25000.0
vs    71
sc    0
wc    250
hzwa  100.00
is    500.00
rfl   10750.1
rfp   7743.0
th    5
ins   1.000
na no ph
    
```



¹³C NMR Spectrum of 53

Plate XX



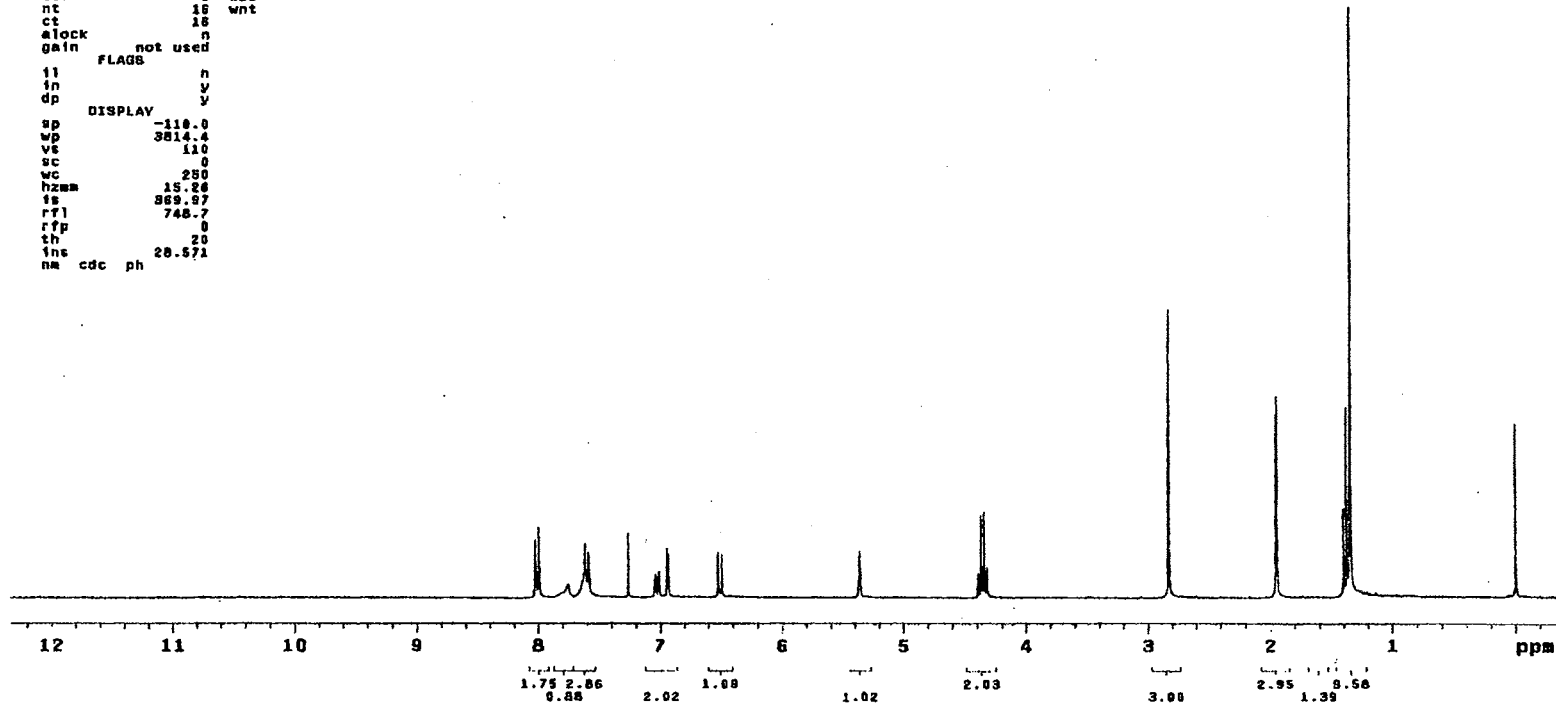
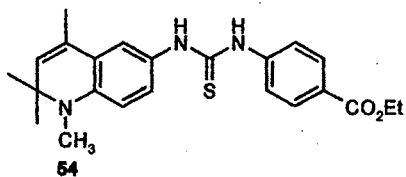
IR Spectrum of 54

Plate XXI

STANDARD 1H OBSERVE

```

expl stdih
SAMPLE
date Nov 11 1989 dfrq DEC. & VT 300.087
solvent CDCl3 dn H1
file exp dpwr 80
ACQUISITION dof 0
sfrq 300.087 dm nnn c
tn H1 dmz 200
at 3.747 dmz
np 33728 PROCESSING
sw 4588.5 wtfile ft
fb 2600 proc not used
bx 15 Yn
tpwr 48
pw 6.0 warr
di 0 wexp
cof 8 wbs
nt 15 wnt
ct 18
alock n
gain not used
FLAGS
ii n
in y
dp y
DISPLAY
sp -110.0
wp 3814.4
vs 110
sc 0
wc 200
hzsm 15.24
is 369.87
rfl 748.7
rfp 0
th 20
tms 20.571
nm cdc ph
    
```



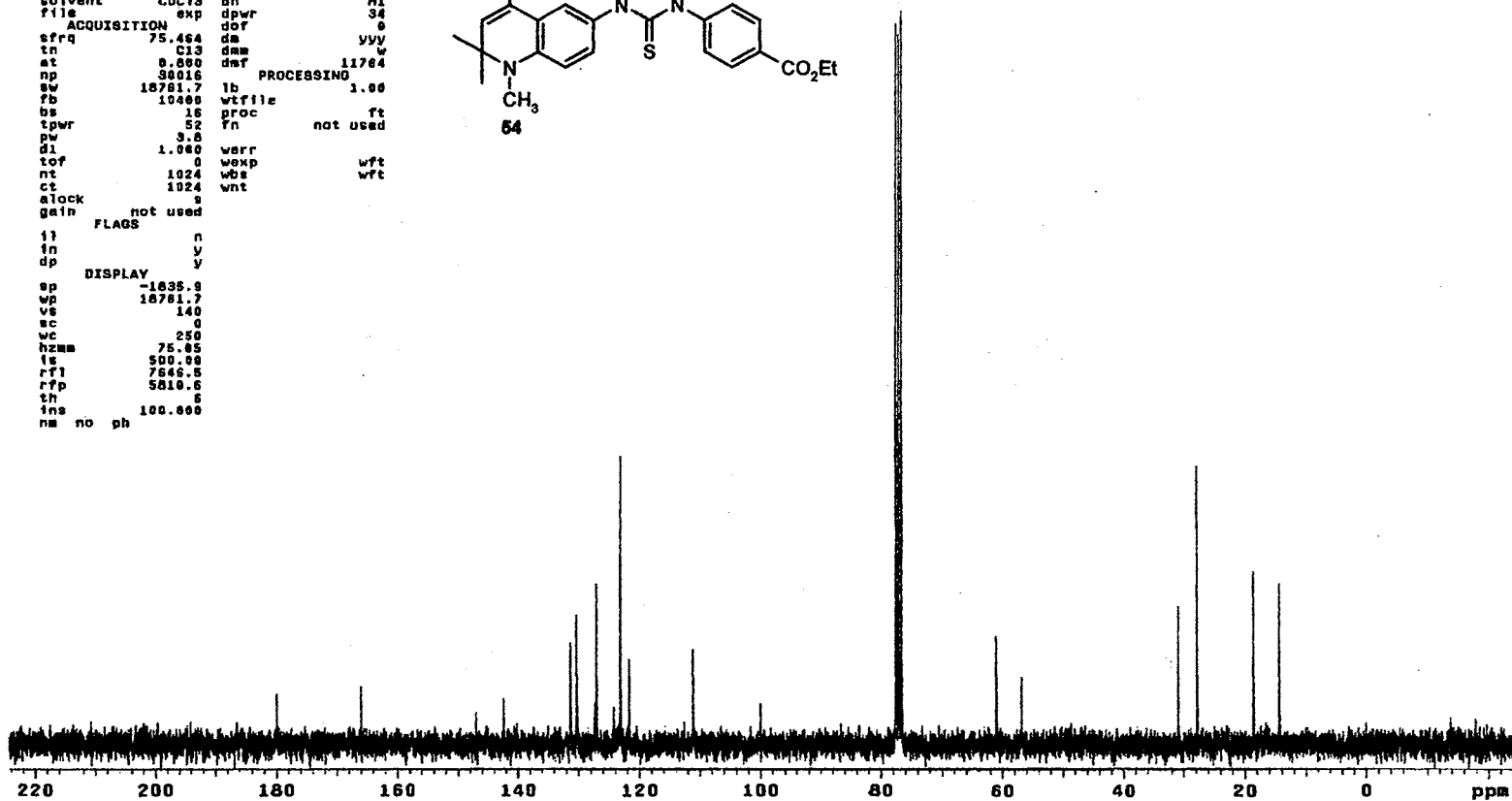
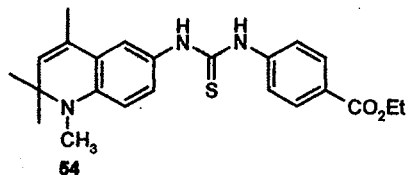
¹H NMR Spectrum of 54

Plate XXII

13C OBSERVE

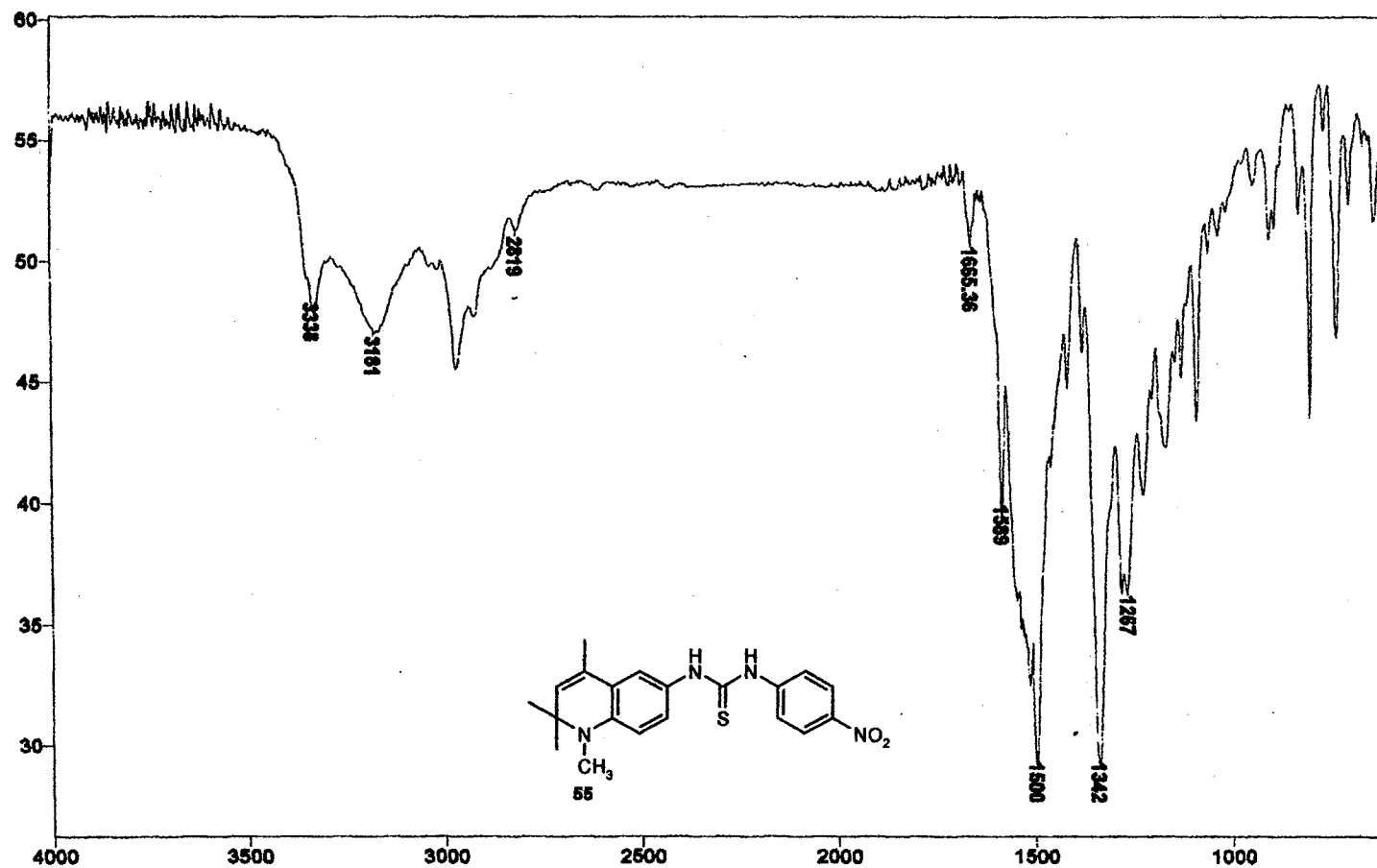
exp1 std13c

date	Nov 11 1999	dfrq	DEC. & VT	300.087
solvent	CDCl3	dn		H1
file	exp	dpwr		34
ACQUISITION				
efrq	75.484	da		0
tn	C13	dmm		VVY
at	0.800	dmf		11764
np	30016	PROCESSING		
sw	18781.7	lb		1.00
fb	10400	wtfile		
bs	16	proc		ft
tpwr	52	fn		not used
pw	3.8			
d1	1.000	werr		
tof	0	wexp		wft
nt	1024	wos		wft
ct	1024	wnt		
elock	s			
gain	not used			
FLAGS				
ij		n		
in		y		
dp		y		
DISPLAY				
ep	-1035.0			
wp	18781.7			
vs	140			
sc	0			
wc	250			
hzmm	75.85			
fs	500.00			
rfl	7546.5			
rtp	5810.6			
th	6			
ins	100.000			
nm	no	ph		



¹³C NMR Spectrum of 54

Plate XXIII



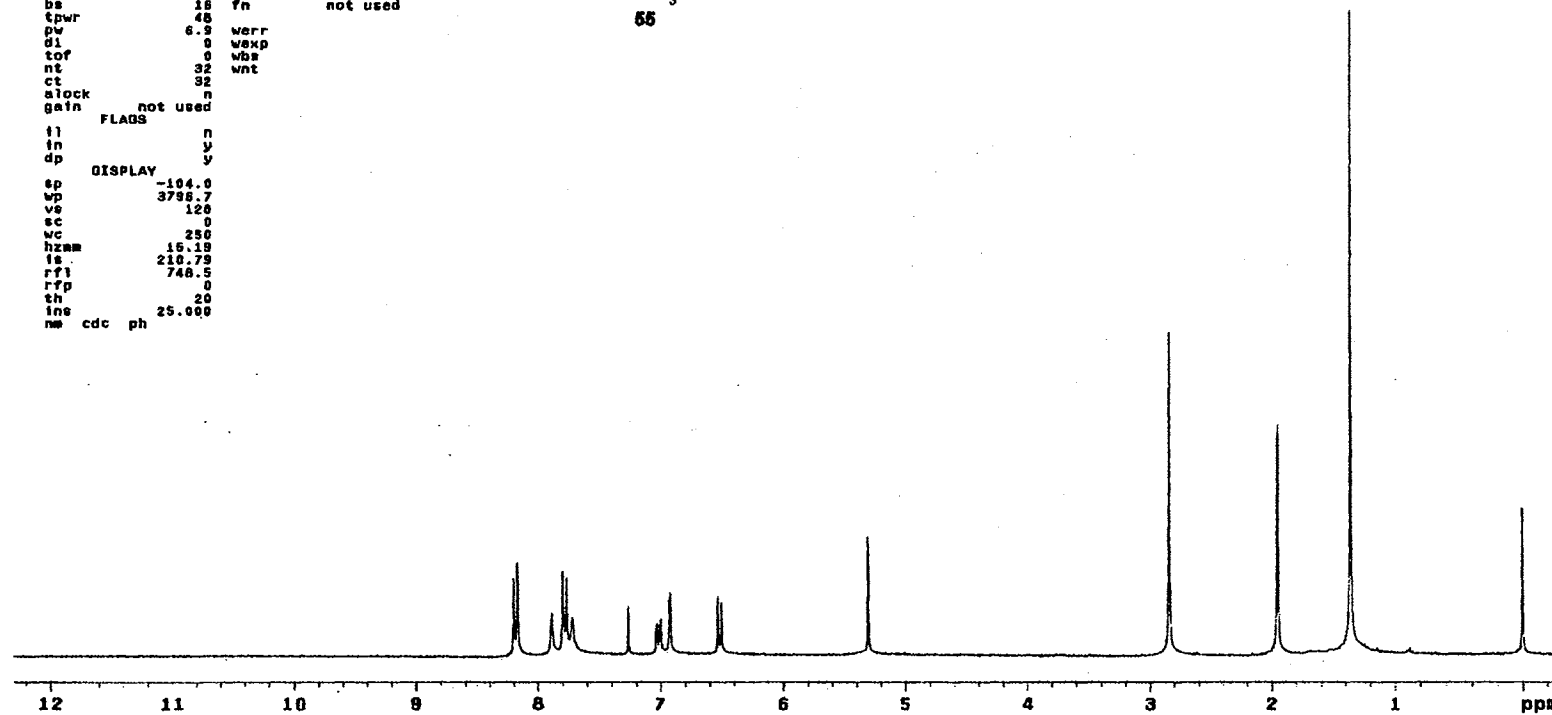
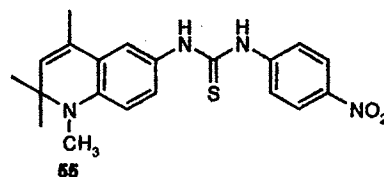
IR Spectrum of 55

Plate XXIV

STANDARD 1H OBSERVE

```

expl stdih
SAMPLE
date Nov 11 1999 dfrq DEC. & VT 300.007
solvent CDCl3 dn H1
file exp dpwr 30
ACQUISITION dof 0
efrq 300.007 dm nnn
tn H1 dm c
ss 3.747 dmf 200
np 33728
sw 4500.5 wtfile PROCESSING
fb 2800 proc ft
ds 18 fn not used
spwr 45
pv 6.9 verr
dl 0 wexp
tof 0 wbs
nt 32 wnt
ct 32
alock n
gain not used
FLAGS
il n
in y
dp y
DISPLAY
sp -104.0
wp 3785.7
vs 120
sc 0
wc 250
hzmm 15.19
ls 210.79
rf1 740.5
rfp 0
th 20
lne 25.000
ne cdc ph
  
```



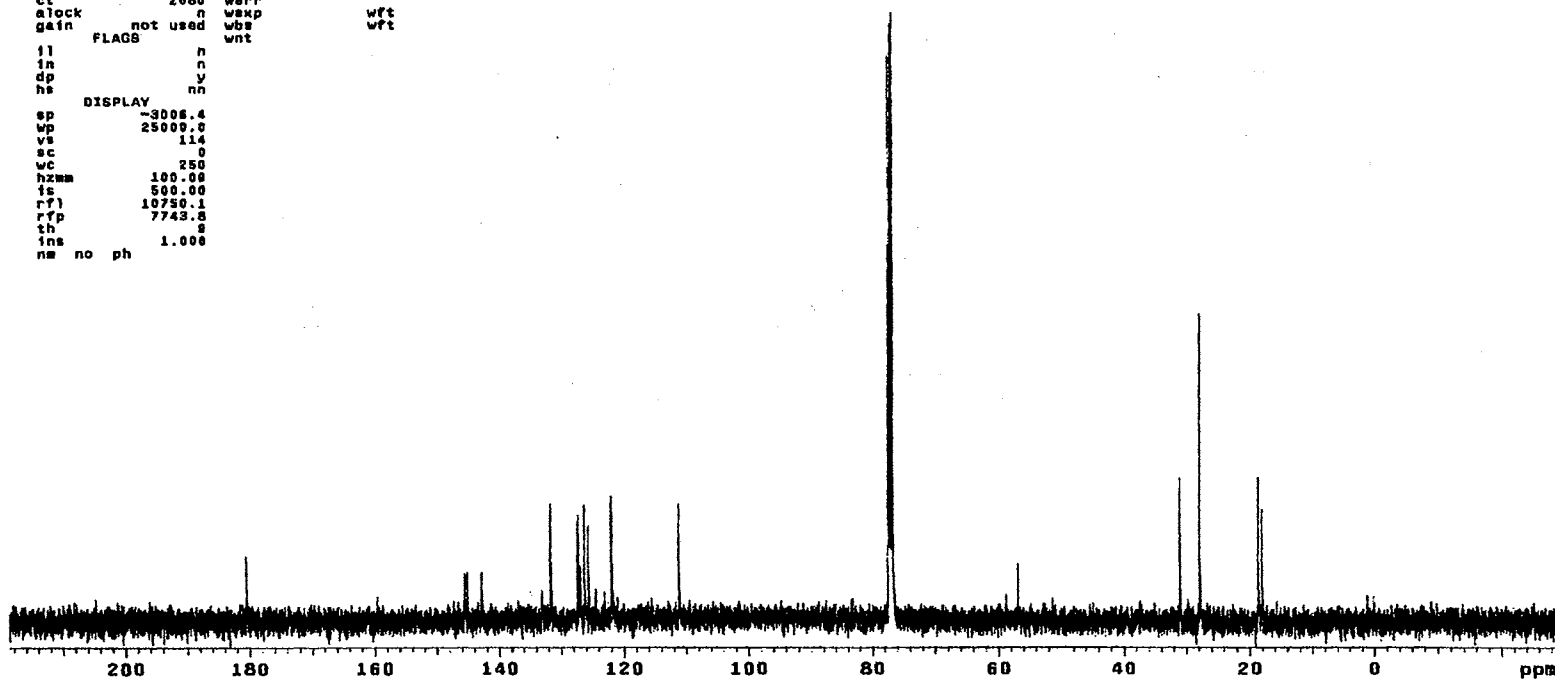
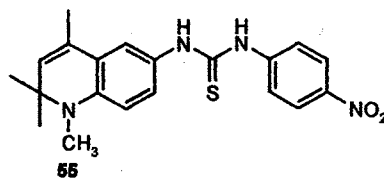
¹H NMR Spectrum of 55

Plate XXV

13C OBSERVE

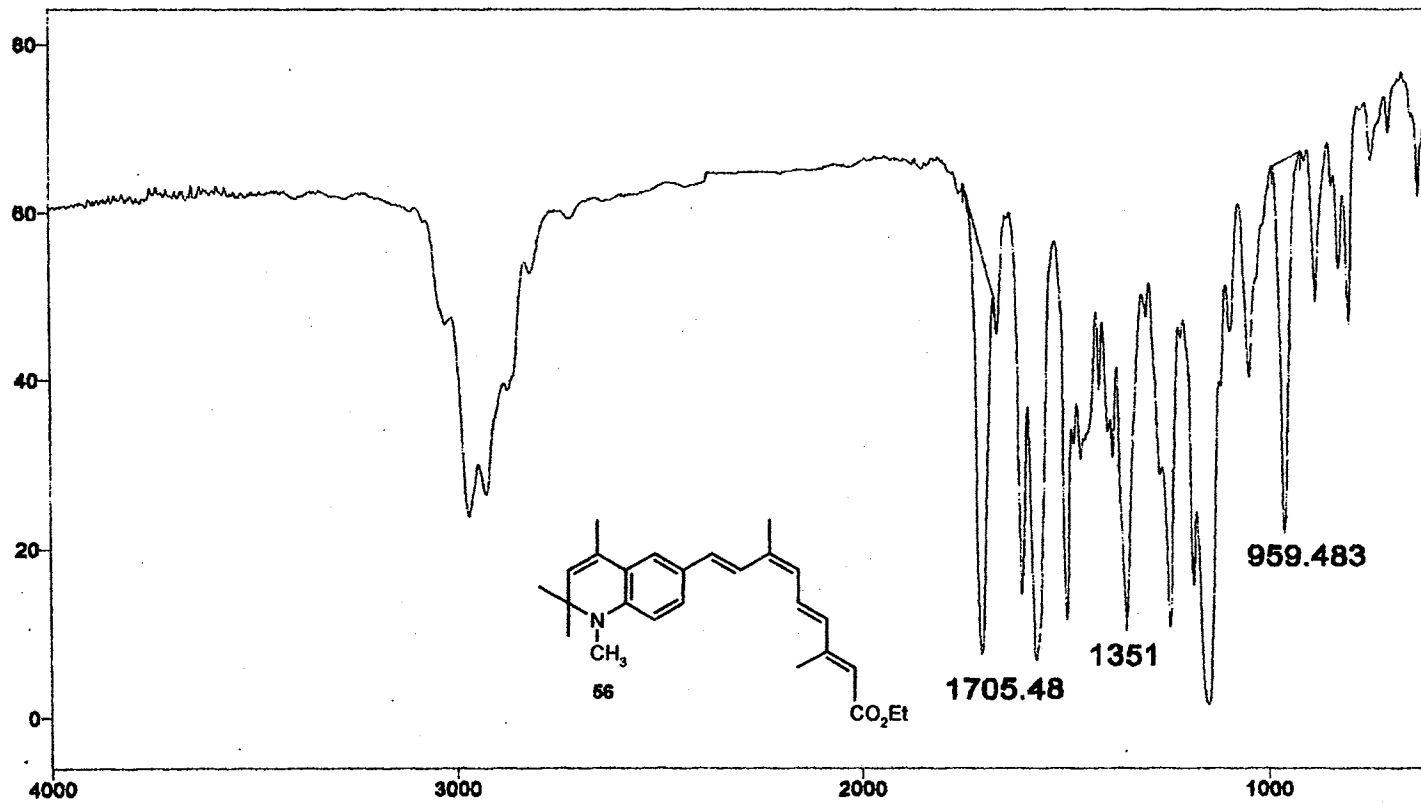
```

expt  std13c
SAMPLE
date  Nov 11 1998  dfrq  398.925
solvent  CDCl3      dn      H1
file      exp      dpwr     40
ACQUISITION  exp  dot      0
sfrq     100.578  da      nyy
tn        C13     dam      w
at        1.188  dar     12000
np        59988  dseq     1.0
sw        25000.0 dres     n
fb        14000  homo     n
bs        18     PROCESSING
tpwr      53     lb      1.00
pw        7.8   wf1file
d1        1.000  proc     ft
d2        0.500  fn      not used
tof        0     math     f
nt        18800
ct        2080  werr     n
atlock    not used  wexp     wft
gain      not used  wbs      wft
        FLAGS
il         n
in         n
dp         y
hs         nn
DISPLAY
sp         -3008.4
wp         25000.0
vs         114
sc         0
wc         250
hzmm      100.00
fs         500.00
rf1       10750.1
rfp       7743.8
th         8
fns       1.000
na no ph
    
```



¹³C NMR Spectrum of 55

Plate XXVI



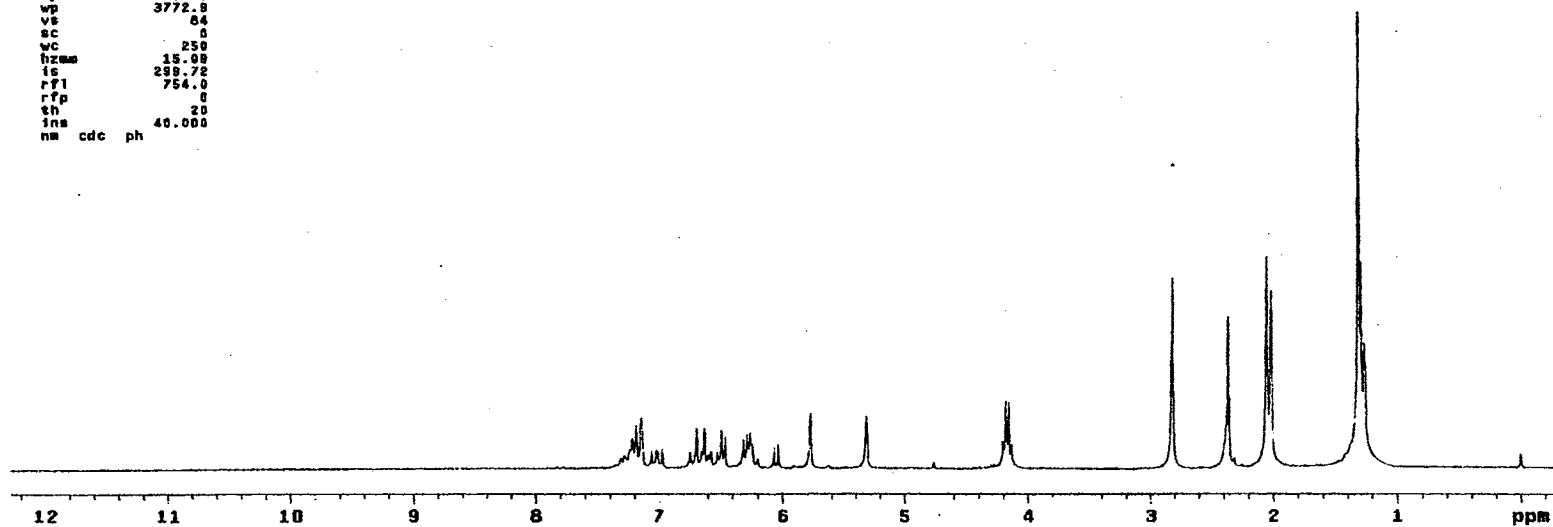
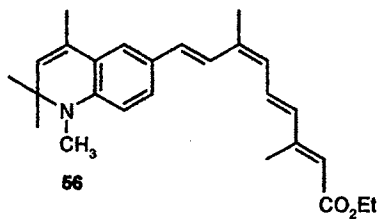
IR Spectrum of 56

Plate XXVII

STANDARD 1H OBSERVE

```

expl stdih
SAMPLE
date Nov 22 1999 dfrq DEC. & VT 300.087
solvent CDC13 dn H1
file ACQUISITION exp dpwr 30
sfrq 300.087 dw nnn
tn H1 dms c
at 3.747 dmf 200
np 33728 PROCESSING
sw 4500.5 wtf file ft
fb 2809 proc not used
bs 16 tn
tpwr 48
pw 4.0 werr
di 0 wexp
tof 0 wds
nt 16 wnt
ct 16
alock not used n
gain FLAOS n
ii n
in y
dp DISPLAY y
sp -85.8
wp 3772.8
ve 84
sc 0
wc 250
hzms 15.09
ic 299.72
rf1 754.0
rfp 0
th 20
na cdc ph 40.000
    
```



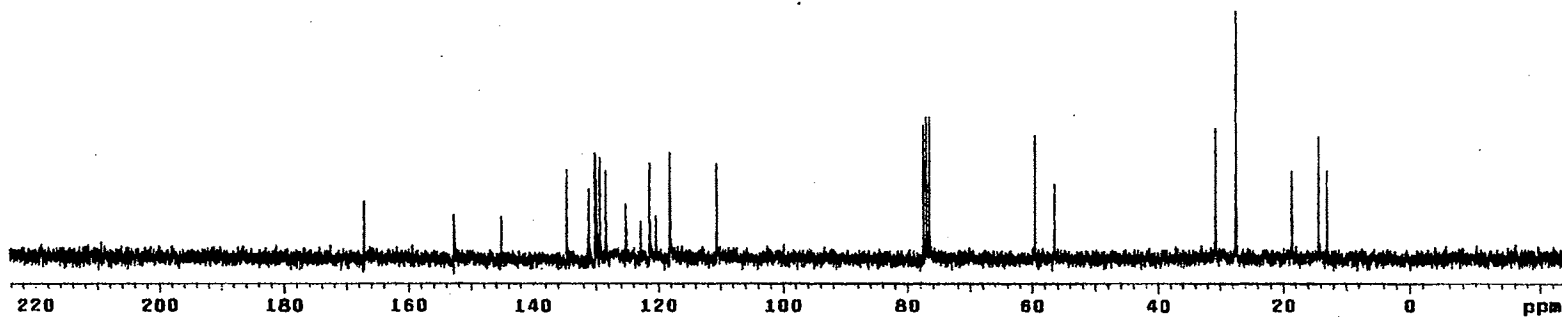
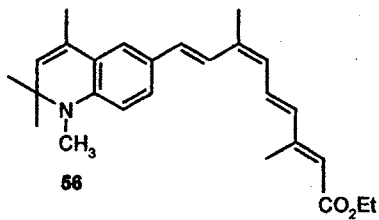
¹H NMR Spectrum of 56

Plate XXVIII

13C OBSERVE

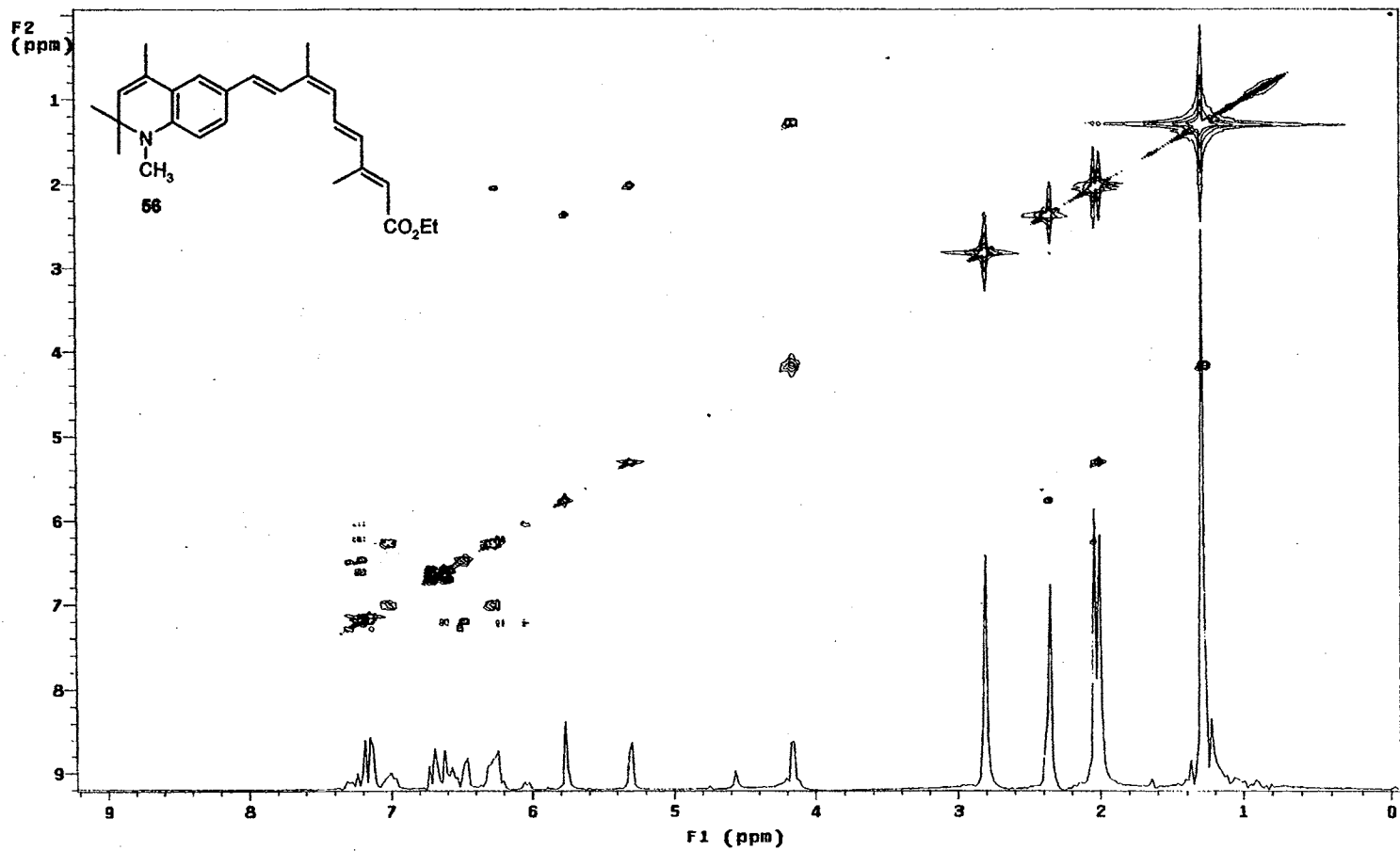
exp1 etd18c

date	Nov 22 1999	dfrq	DEC. & VT	300.067
solvent	CDCl3	dn		M1
file	exp	dpwr		34
ACQUISITION				
sfrq	75.464	ds		0
tn	C13	dsm		VVY
at	0.090	daf		11764
np	30016	PROCESSING		
sw	18761.7	lb		1.00
zb	10490	wtfile		
bs	16	proc		ft
tpwr	52	fn		not used
pv	3.0			
d1	1.000	werr		wft
top	0	wokp		wft
nt	1024	wbs		wft
ct	128	wnt		
alock				s
gain	not used			
FLAGS				
ll		n		
in		y		
dp		y		
DISPLAY				
sp	-1040.4			
wp	18761.7			
vs	48			
sc	0			
wc	250			
hzm	75.05			
is	500.00			
rfl	7651.0			
rtp	5810.6			
tn	20			
inc	100.090			
nm	no	ph		



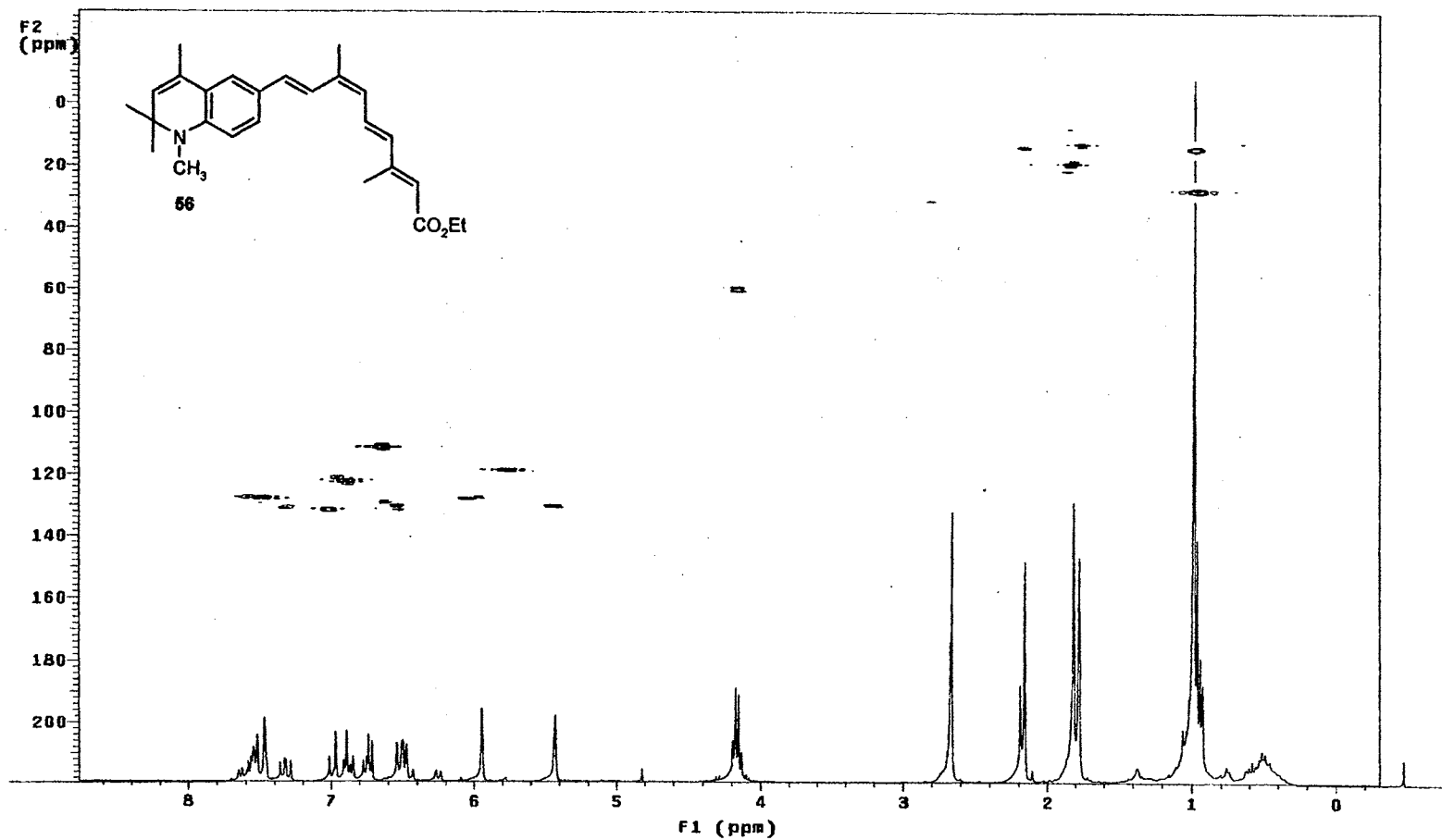
¹³C NMR Spectrum of 56

Plate XXIX



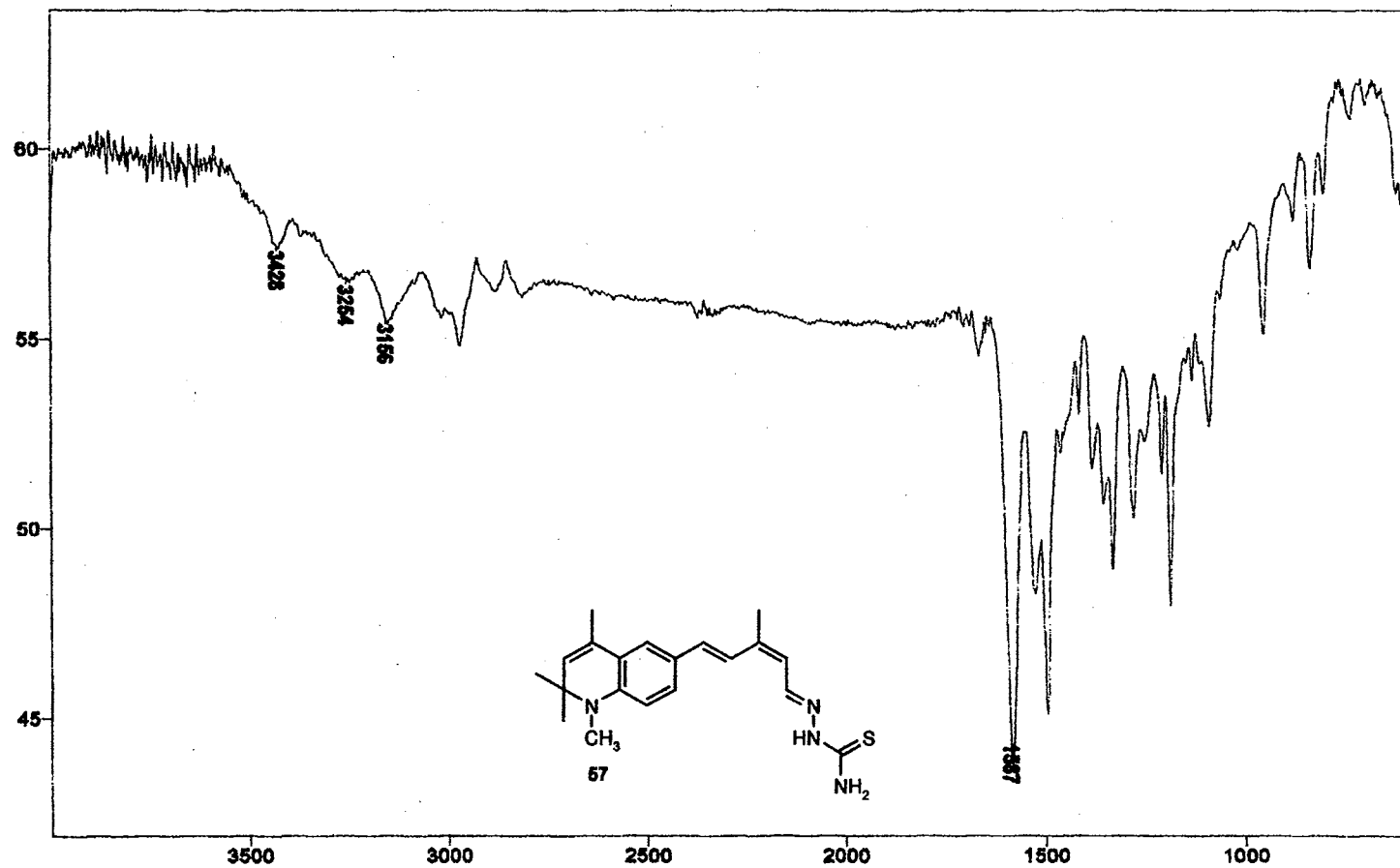
2D COSY NMR Spectrum of 56

Plate XXX



2D HETCOR NMR Spectrum of 56

Plate XXXI



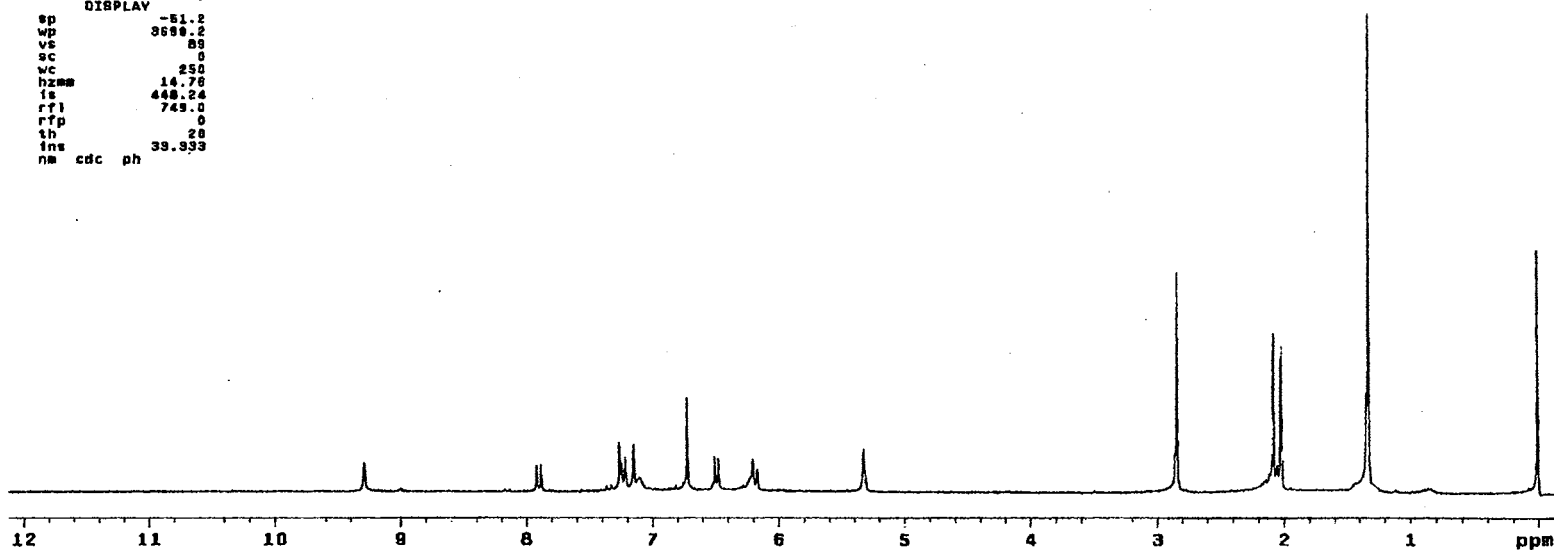
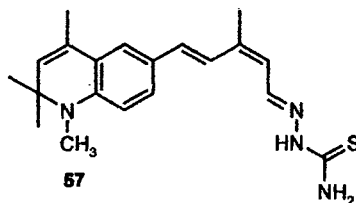
IR Spectrum of 57

Plate XXXII

STANDARD IN OBSERVE

```

expl stdlh
SAMPLE
date Nov 12 1989 dfrq DEC. & VT 300.067
solvent COCl2 dn H1
file exp dpwr 30
ACQUISITION dof 0
sfrq 300.067 dw nnn
tn H1 dam c
at 3.747 dm7 200
np 33728 PROCESSING
sw 4500.5 wtfle rt
fb 2800 proc not used
bs 15 7n
tpwr 48
pw 6.9 werr
di 0 wexp
tof 0 wbs
nt 64 wnt
ct 64
alock n
gain not used
FLAOS
il n
in y
dp y
DISPLAY
sp -51.2
wp 3688.2
vs 88
sc 0
wc 250
hzms 14.76
fs 448.24
rfi 749.0
rfp 0
th 28
ins 39.393
na cdc ph
    
```



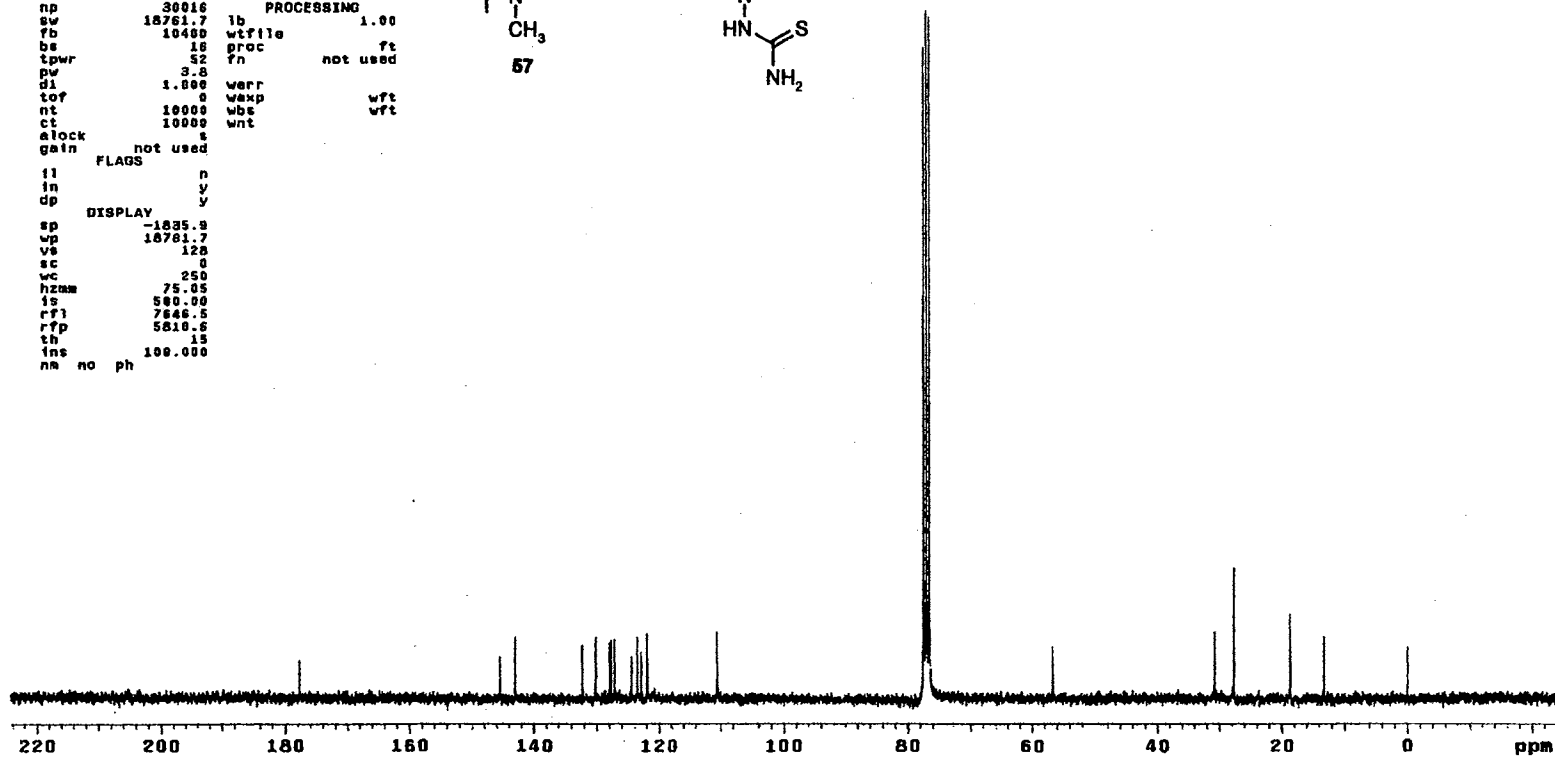
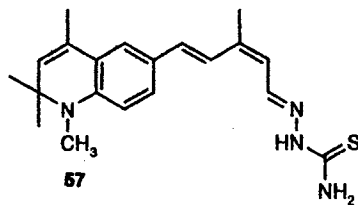
¹H NMR Spectrum of 57

Plate XXXIII

13C OBSERVE

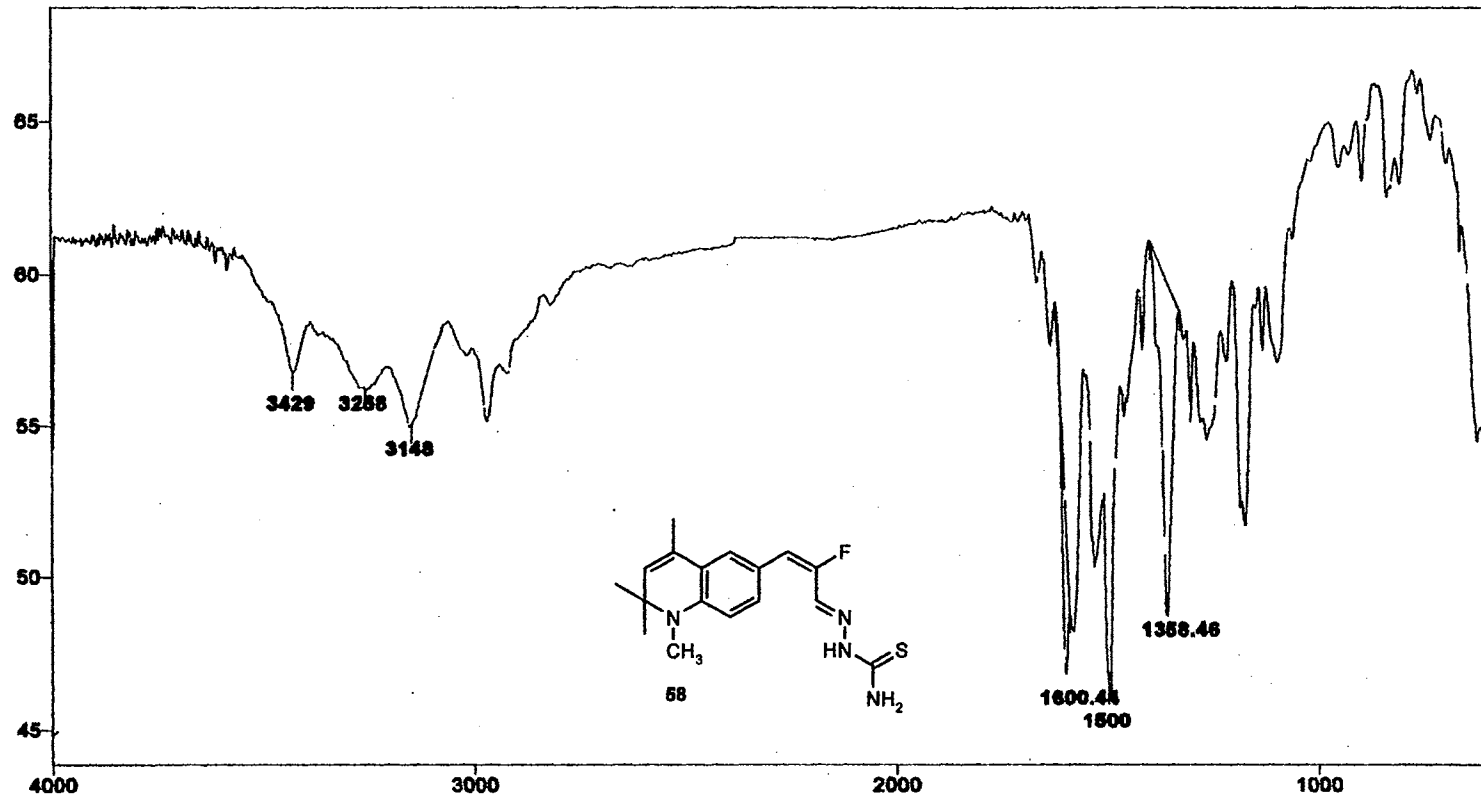
exp1 std13c

data	Nov 11 1999	dfrq	300.007	NI
solvent	CDCl3	dn		34
file	exp	dpwr		0
ACQUISITION				
sfrq	75.404	da		yyv
tn	C13	daw		w
at	0.800	daf	11764	
np	30016	PROCESSING		
sw	18761.7	lb	1.00	
fb	10400	wtfile		
bs	16	proc	ft	
tpwr	52	fn	not used	
pw	3.8			
d1	1.800	verr		
tof	0	wasp	wft	
nt	10000	wbs	wft	
ct	10000	wnt		
alock		s		
gain	not used			
FLAGS				
fl		n		
in		y		
dp		y		
DISPLAY				
sp	-1035.0			
wp	18761.7			
vs	120			
sc	0			
wc	250			
hzmm	75.05			
is	500.00			
rfl	7666.5			
rfp	5810.5			
th	15			
ins	100.000			
nm	no	ph		



¹³C NMR Spectrum of 57

Plate XXXIV



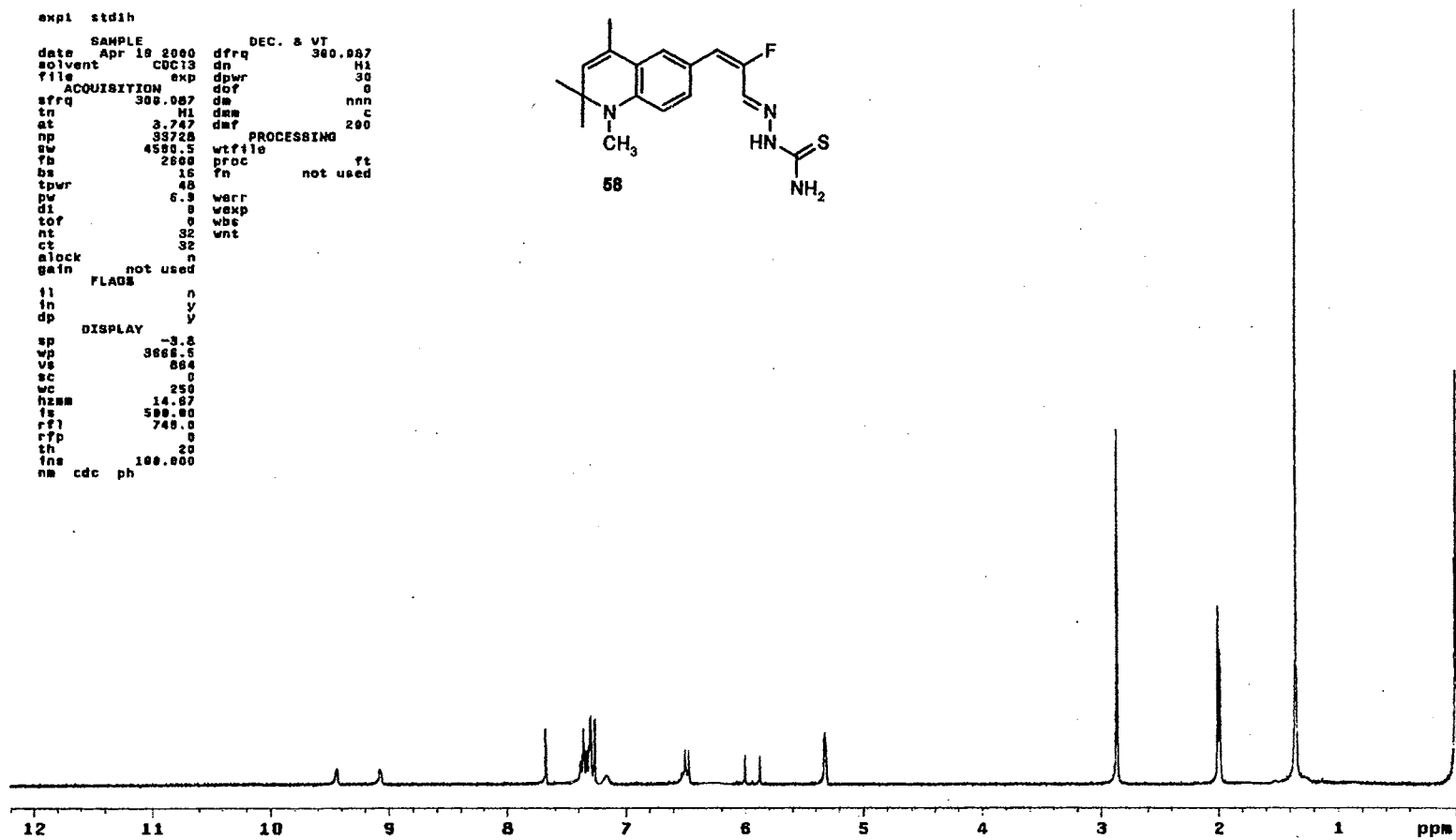
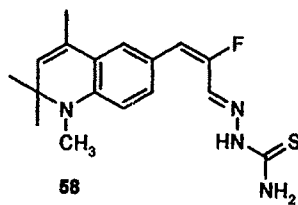
IR Spectrum of 58

Plate XXXV

STANDARD 1H OBSERVE

```

expl stdih
SAMPLE
date Apr 19 2000 dfrq DEC. & VT 300.007
solvent CDCl3 dn H1
file exp dpwr H1
ACQUISITION dof 0
sfrq 300.007 da nnn
tn H1 dms c
at 3.747 dmf 200
np 33720
sw 4500.5 wtf file
fb 2600 proc ft
bs 16 fn not used
tpwr 48
pw 6.9 warr
di 0 wexp
cof 0 wbc
nt 32 wnt
ct 32
alock n
gain not used
FLADE
fl n
fn y
dp y
DISPLAY
sp -3.2
wp 3666.5
vs 804
sc 0
wc 250
hzmm 14.87
ls 500.00
rf1 740.0
rff 0
th 20
ins 100.000
nm cdc ph
    
```



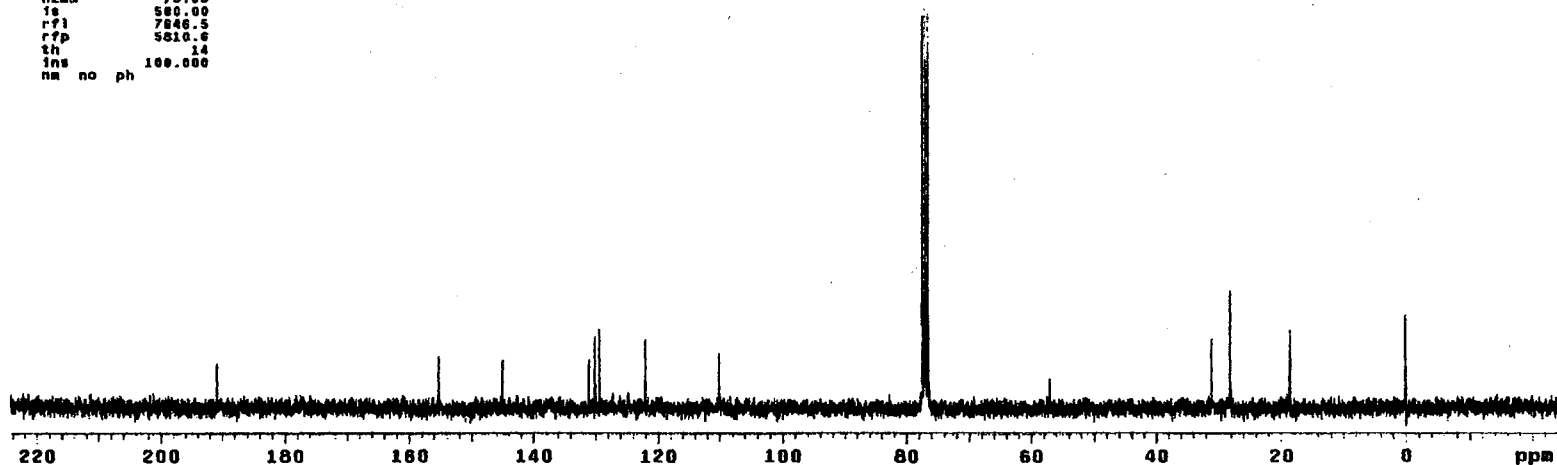
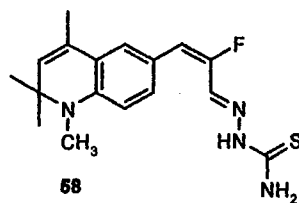
¹H NMR Spectrum of 58

Plate XXXVI

13C OBSERVE

exptl std13c

SAMPLE		DEC. & VT	
date	Apr 19 2000	dfrq	300.007
solvent	CDCl3	dn	H1
file	exp	dpwr	34
ACQUISITION		dsf	0
afrq	75.464	ds	yyv
tn	C13	dsw	w
at	0.800	daf	11764
np	30016	PROCESSING	
sw	10761.7	lb	1.00
fb	10400	wtfile	
bs	16	proc	ft
tpwr	52	fn	not used
pw	3.8		
d1	1.000	verr	
tof	0	wexp	wft
nt	4096	wbs	wft
ct	4096	wnt	
alock	not used	s	
gain	not used		
FLAGS			
fl	n		
fn	y		
dp	y		
DISPLAY			
sp	-1035.0		
wp	10761.7		
vs	167		
sc	0		
wc	250		
hzmm	75.05		
fs	500.00		
rfl	7846.5		
rfp	5810.0		
th	14		
ins	100.000		
nm	no	ph	



¹³C NMR Spectrum of 58

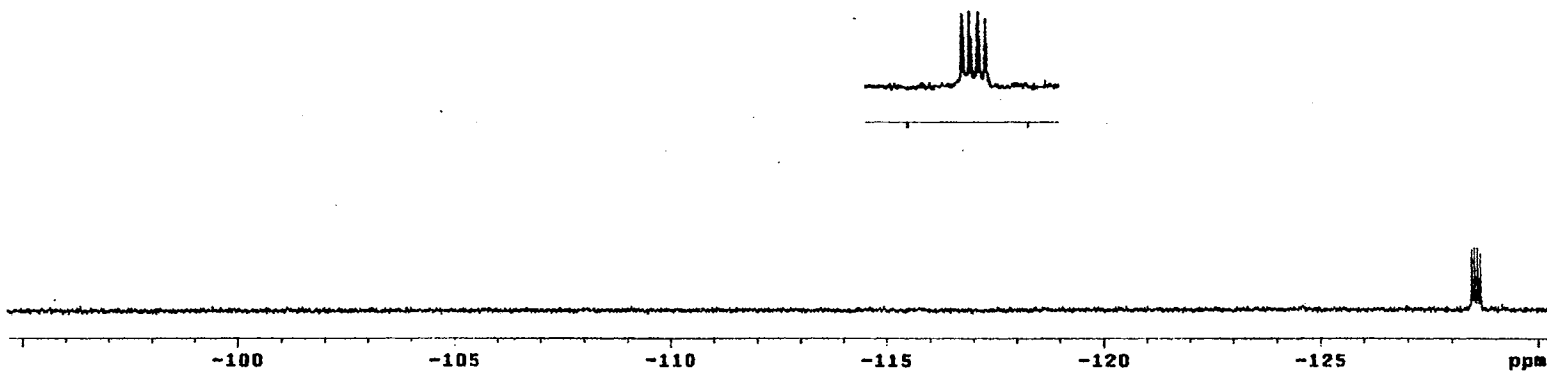
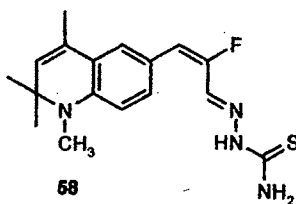
Plate XXXVII

13C OBSERVE

exptl std13c

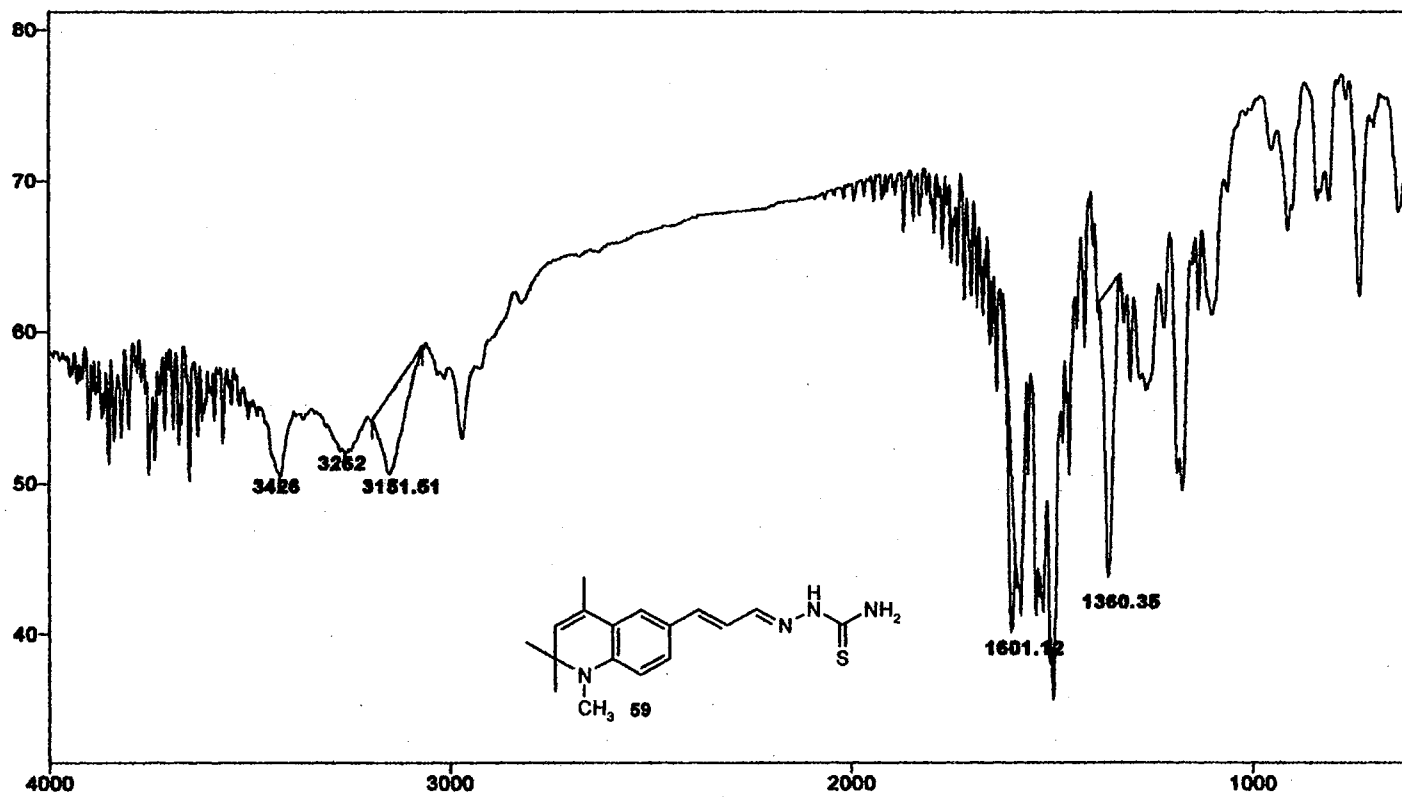
```

SAMPLE          DEC. 8 VT
date    Feb 22 2000  dfrq    300.007
solvent  CDC13      dn      N1
file     exp       dpwr    34
          ACQUISITION  dof      0
sfrq    282.333    dm      nnn
tn      719       dms      w
at      0.500     def      11764
np      30016     PROCESSING
sw      18751.7   lb      1.00
fb      10400    wtfile
bs      16      proc      ft
tprw    52      Tn      not used
pw      3.8
dl      1.000    werr
tof      0      wexp      wft
nt      1024    wbs      wft
cs      112     wnt
slock   n
gain    not used
          FLAGS
ii      n
in      y
dp      y
          DISPLAY
sp      -36001.4
wp      10003.4
vs      12
sc      0
wc      250
hznm    40.33
is      500.00
rf1     38748.2
rtp     6
tb      10
inc     100.000
nm no ph
    
```



¹⁸F NMR Spectrum of 58

Plate XXXVIII



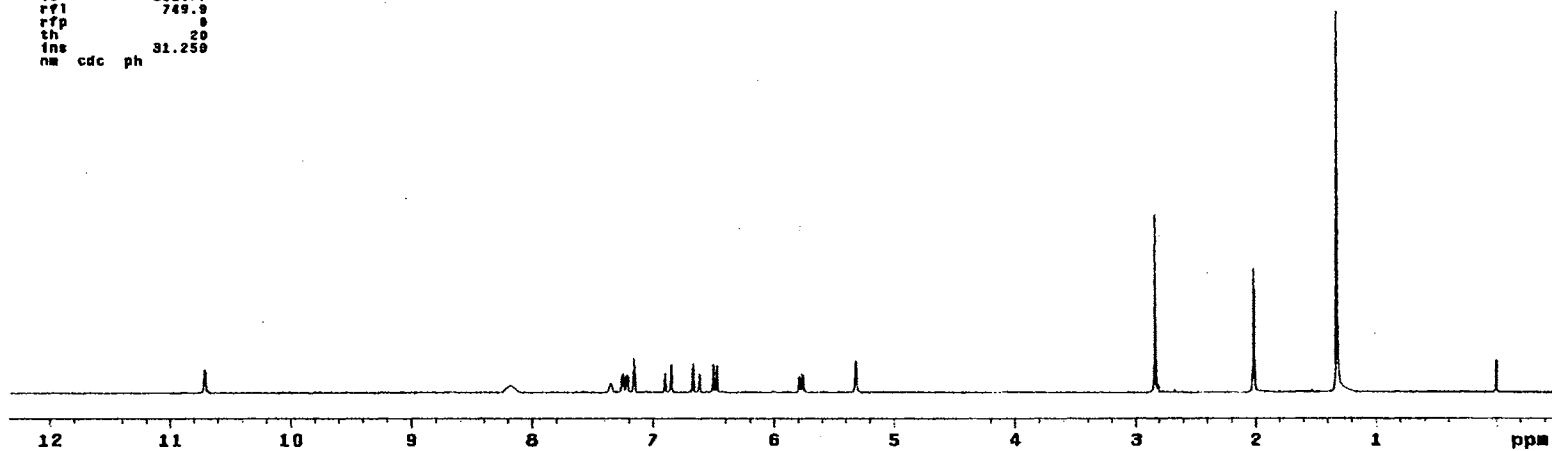
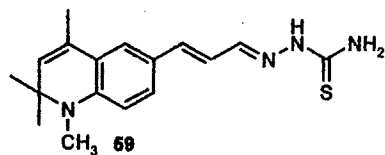
IR Spectrum of 59

Plate XXXIX

STANDARD 1H OBSERVE

```

expl stdh
SAMPLE
date Jul 8 1998 dfrq DEC. & VT 300.007
solvent CDC13 dn H1
file exp dpwr 39
ACQUISITION dof 9
sfrq 300.007 dm nnn
tn H1 dnm c
at 3.747 dm7 PROCESSING 200
np 33728
sw 4500.5 wtfle
fb 2600 proc ft
hs 16 fn not used
tpwr 48
pw 3.0 werr
dl 0 wexp wrt
tor 0 wbs
nt 16 wnt
ct 16
alock n
gain not used
FLABS
f1 n
in y
dp DISPLAY y
ep -146.8
wp 3849.5
vs 81
ec 0
sc 250
hzmm 15.40
is 382.77
rf1 749.9
rff 9
sh 20
ins 31.250
nm cdc ph
    
```



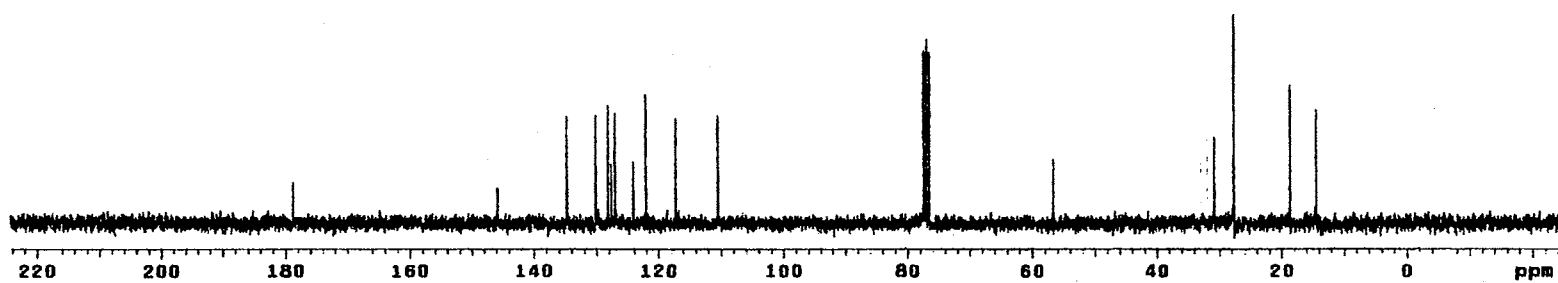
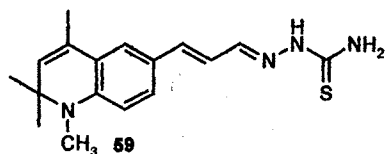
¹H NMR Spectrum of 59

Plate XL

13C OBSERVE

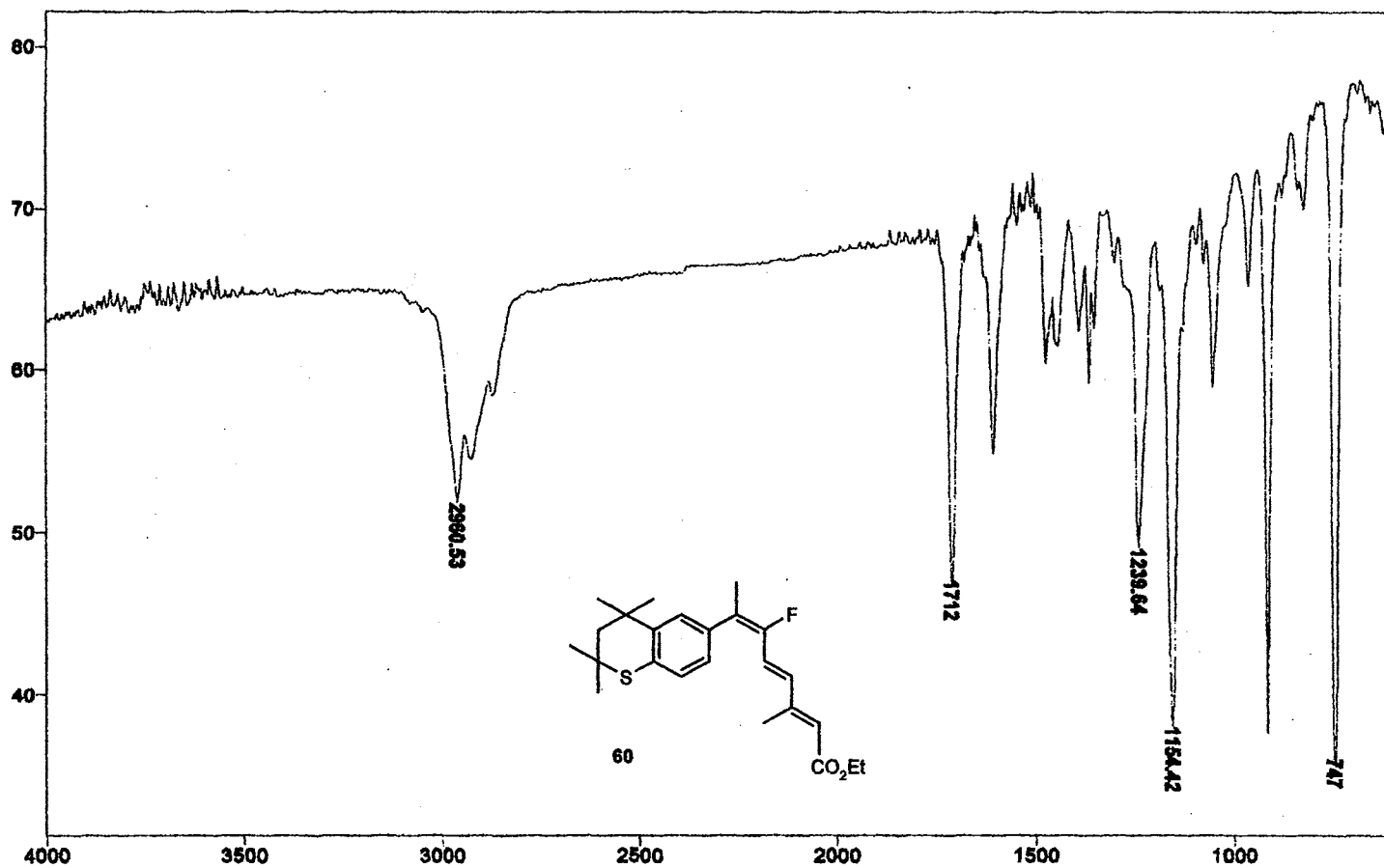
expl std13c

SAMPLE		DEC. & VT	
date	Jul 8 1989	dfrq	300.087
solvent	CDCl3	dn	H1
file	exp	dpwr	34
ACQUISITION		dof	0
efrq	75.464	dm	VVV
tn	C13	dsm	W
at	0.000	daf	11784
np	30018	PROCESSING	
sw	18761.7	lb	1.00
fb	10600	wtfile	
bs	18	proc	ft
tpwr	52	fn	not used
pw	3.6		
di	1.000	werr	
sof	8	wexp	wft
nt	1024	wbs	wft
ct	256	wnt	
alock	9		
gain	not used		
FLABS			
fl	n		
in	y		
dp	y		
DISPLAY			
sp	-1837.0		
wp	18761.7		
vs	52		
sc	8		
wc	256		
hzmm	75.05		
is	500.00		
rfl	7647.6		
rfp	5810.6		
th	4		
ins	100.000		
nm	no	ph	



¹³C NMR Spectrum of 59

Plate XLI



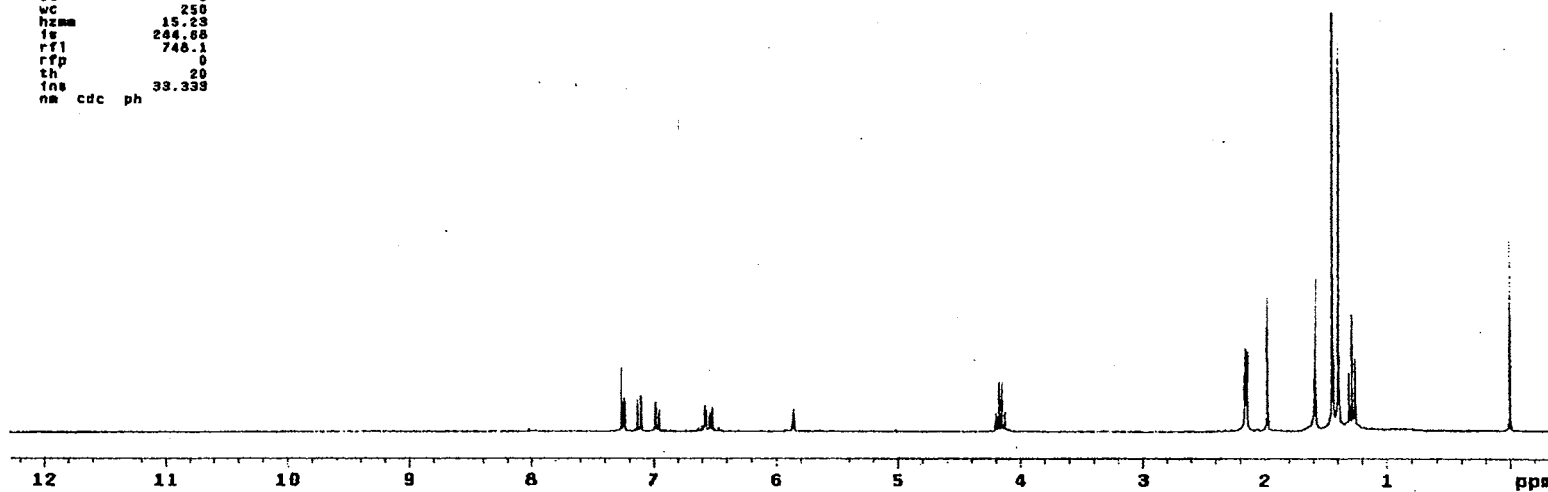
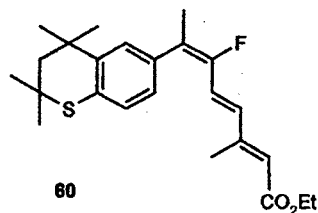
IR Spectrum of 60

Plate XLII

STANDARD 1H OBSERVE

```

expt stdih
SAMPLE
date Oct 30 1995 dfrq DEC. & VT 300.057
solvent CDCl3 dn HI
file exp dpwr 30
ACQUISITION dof 0
sfrq 300.057 ds nnn
tn HI ds c
at 3.747 daf 200
np 39726 PROCESSING
sw 4500.5 wtf file
fb 2680 proc ft
bs 15 fn not used
tpwr 48
pw 6.9 werr
dl 0 wexp
tor 0 wbs
nt 32 wnt
ct 32
clock n
gain not used
FLAOS
il n
in y
dp y
DISPLAY
sp -121.3
wp 3008.5
vs 75
sc 0
wc 250
hzmm 15.23
fs 204.38
rfi 748.1
rfp 0
th 20
ins 33.339
na cdc ph
  
```



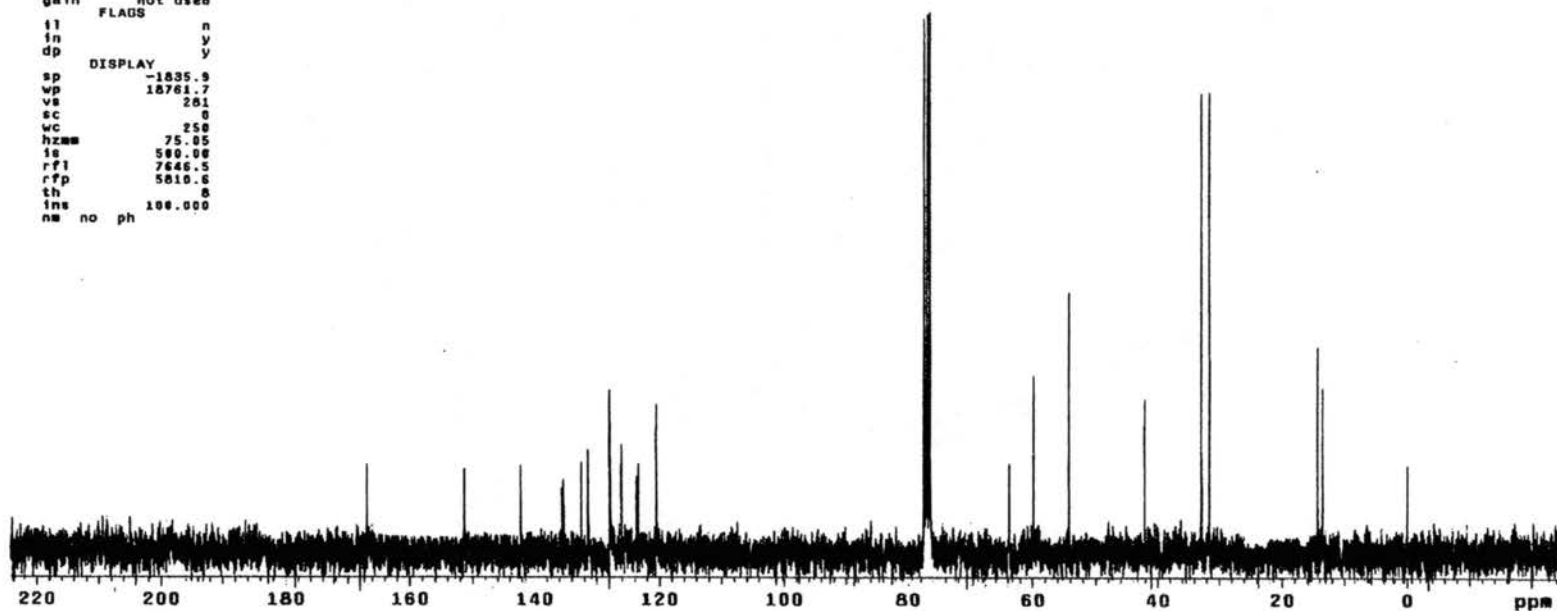
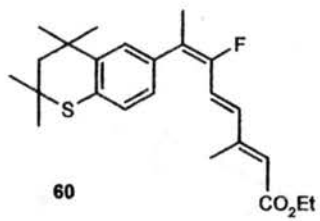
¹H NMR Spectrum of 60

Plate XLIII

¹³C OBSERVE

exp1 std13c

data	Oct 30 1989	dfrq	300.057	DEC. & VT
solvent	CDCl3	dn	H1	
file	exp	dpwr	34	
ACQUISITION				
sfrq	75.464	dof	0	
tn	C13	dm	yyy	w
at	0.800	dwt	11764	
np	30016	PROCESSING		
sw	18761.7	lb	1.00	
fb	10400	wfile		
bs	18	proc	ft	
tpwr	52	fn	not used	
pw	3.8			
di	1.000	werr		
tof	0	wexp	wft	
nt	4096	wba	wft	
ct	2096	wnt		
alock				
gain	not used			
	FLADS			
il		n		
in		y		
dp		y		
DISPLAY				
sp	-1835.9			
wp	18761.7			
vs	201			
sc	0			
wc	250			
hzmm	75.05			
is	500.00			
rfl	7646.5			
rfp	5010.6			
th	0			
ins	100.000			
nm	no	ph		



¹³C NMR Spectrum of 60

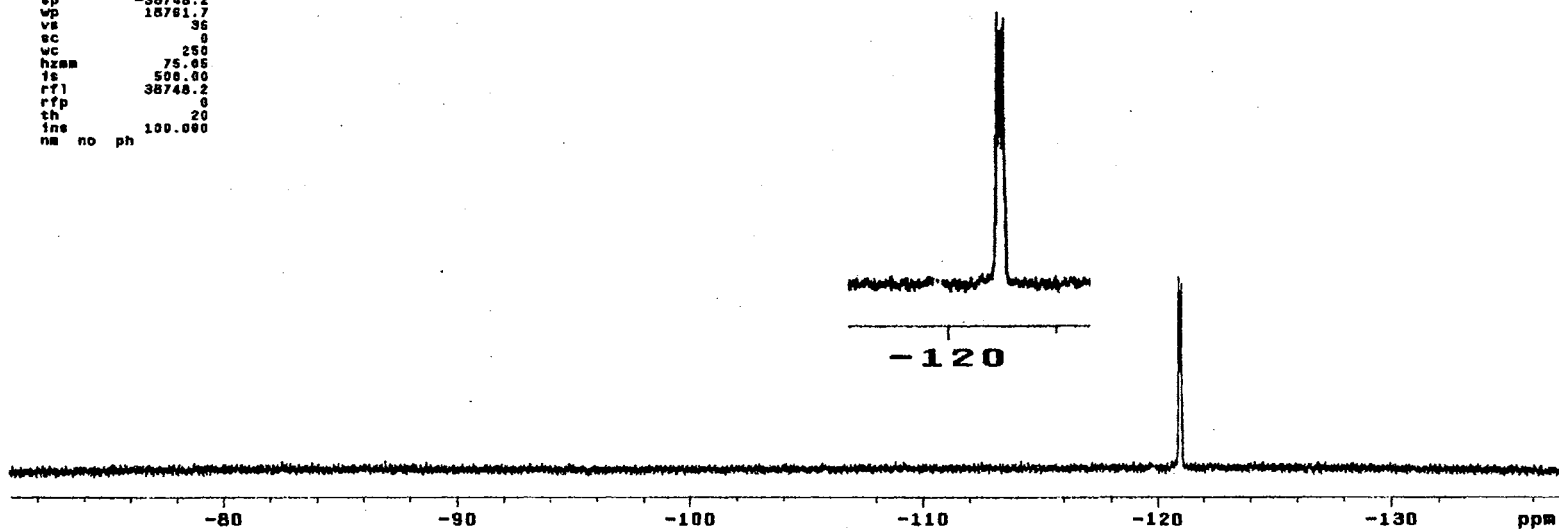
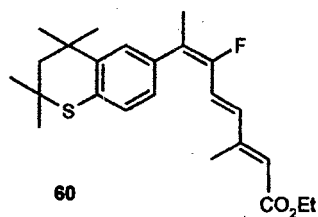
Plate XLIV

13C OBSERVE

exptl std13c

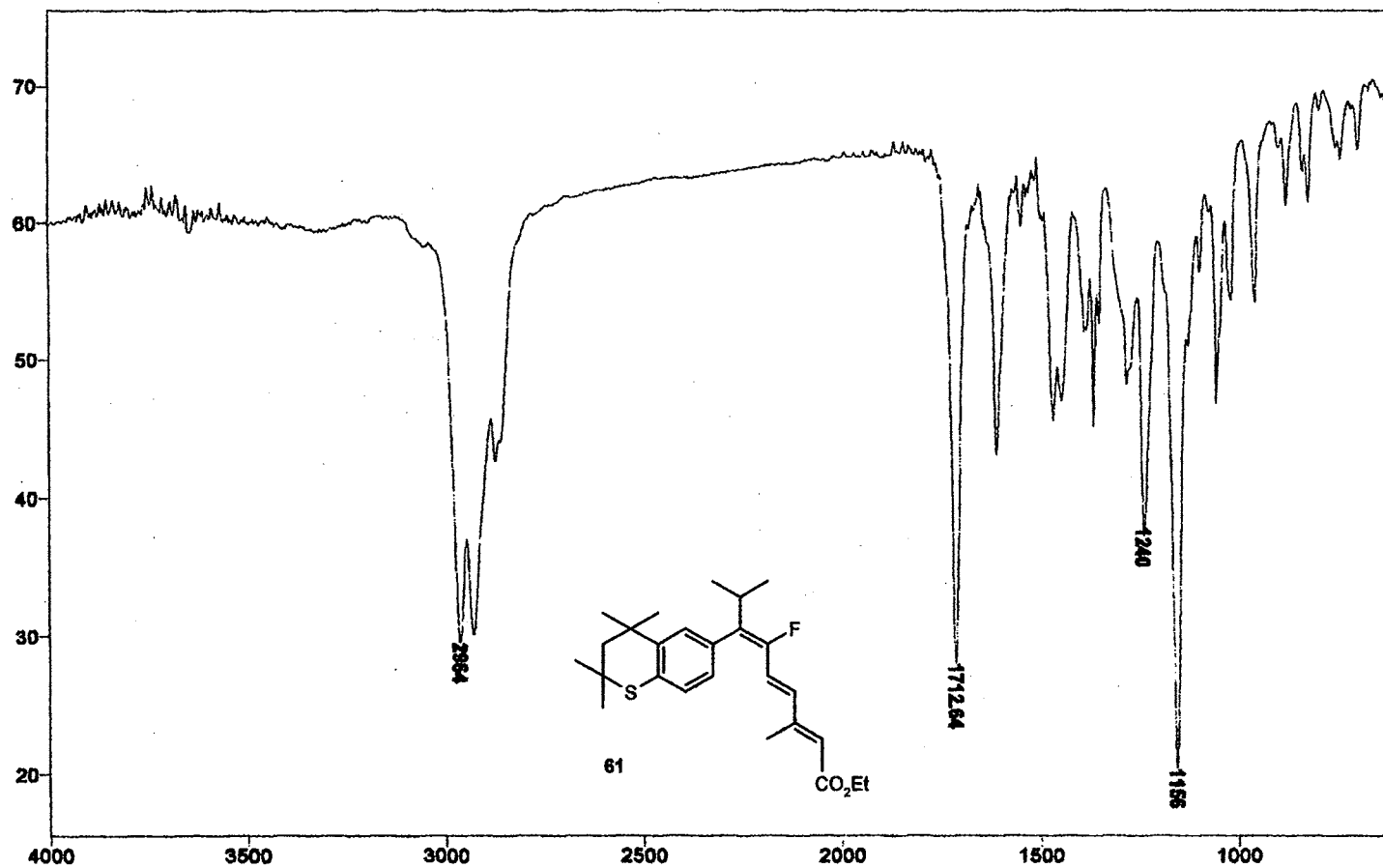
```

SAMPLE
data Oct 30 1999 dfrq DEC. & VT 300.087
solvent CDCl3 dn H1
file exp dpwr 34
ACQUISITION
sfrq 282.333 dm dof 0
tn F13 das w
at 9.800 dat 11764
np 30018 PROCESSING
sw 18751.7 lb 1.00
fb 10400 wtfile
bs 15 proc ft
tpwr 52 yn not used
pw 3.8
d1 1.000 werr
tof 0 wexp wft
nt 1024 wds wft
ct 112 wnt
alock n
gain not used
FLAGS
il n
in y
dp y
DISPLAY
sp -38748.2
wp 18751.7
vs 36
sc 0
wc 250
hzmm 75.05
ts 500.00
rf1 38748.2
rfp 0
th 20
ins no ph
  
```



¹⁹F NMR Spectrum of 60

Plate XLV



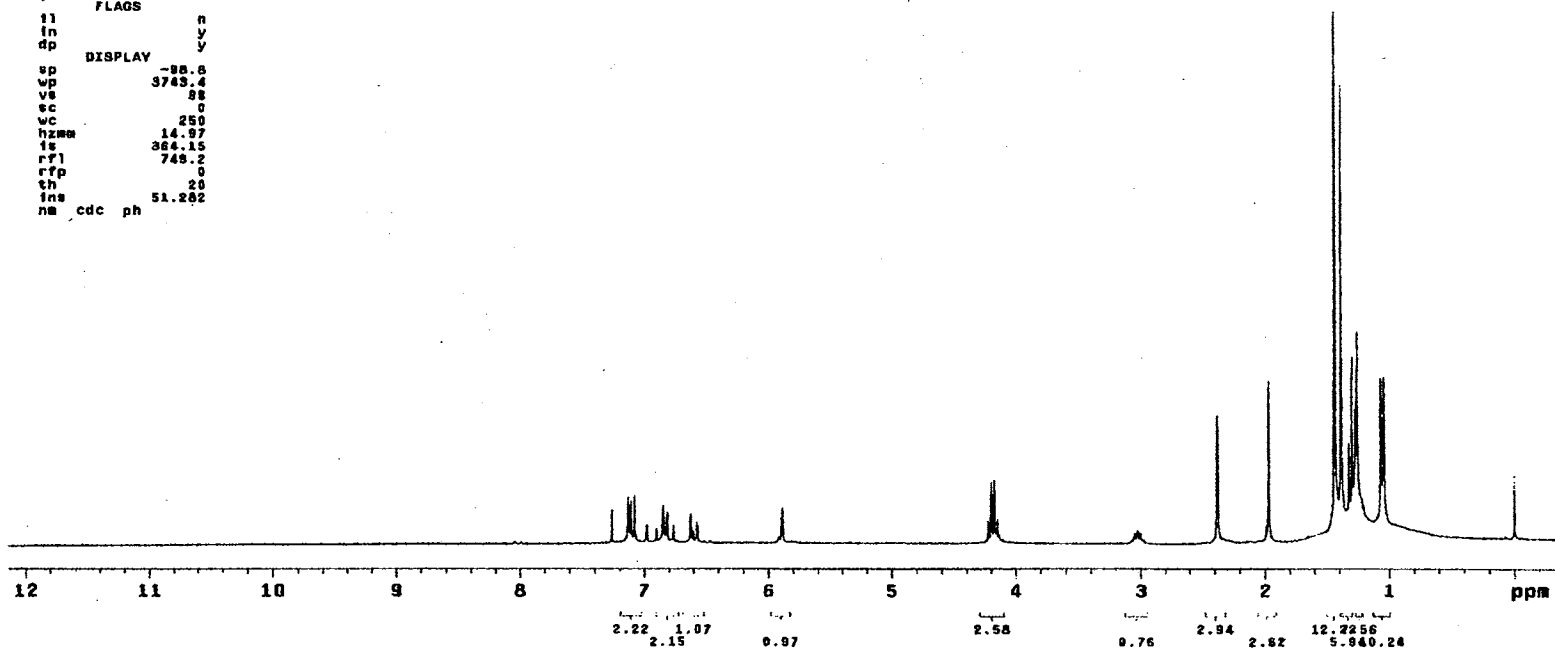
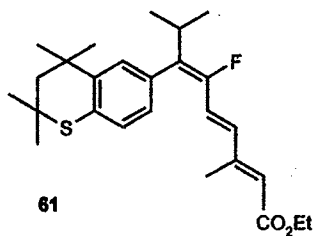
IR Spectrum of 61

Plate XLVI

STANDARD 1H OBSERVE

```

expt std1h
SAMPLE
date Nov 10 1988 dfrq DEC. & VT 300.087
solvent CDCl3 dn H1
file exp dpwr 30
ACQUISITION dof 0
sfrq 300.087 da nnn
tn H1 dm c
at 3.787 dwt 200
np 32728 PROCESSING
sw 4500.5 wtf11s
fb 2800 proc ft
bs 16 fn not used
tpwr 48
pw 6.9 werr
d1 0 wexp
tof 0 wbs
nt 16 wnt
ct 16
alock n
gain not used
FLAGS
t1 n
t2 y
dp y
DISPLAY
sp -88.8
up 3743.4
vs 88
sc 0
wc 250
hzmm 14.97
is 364.15
rf1 745.2
rfp 0
th 20
ins 51.282
nm cdc ph
  
```



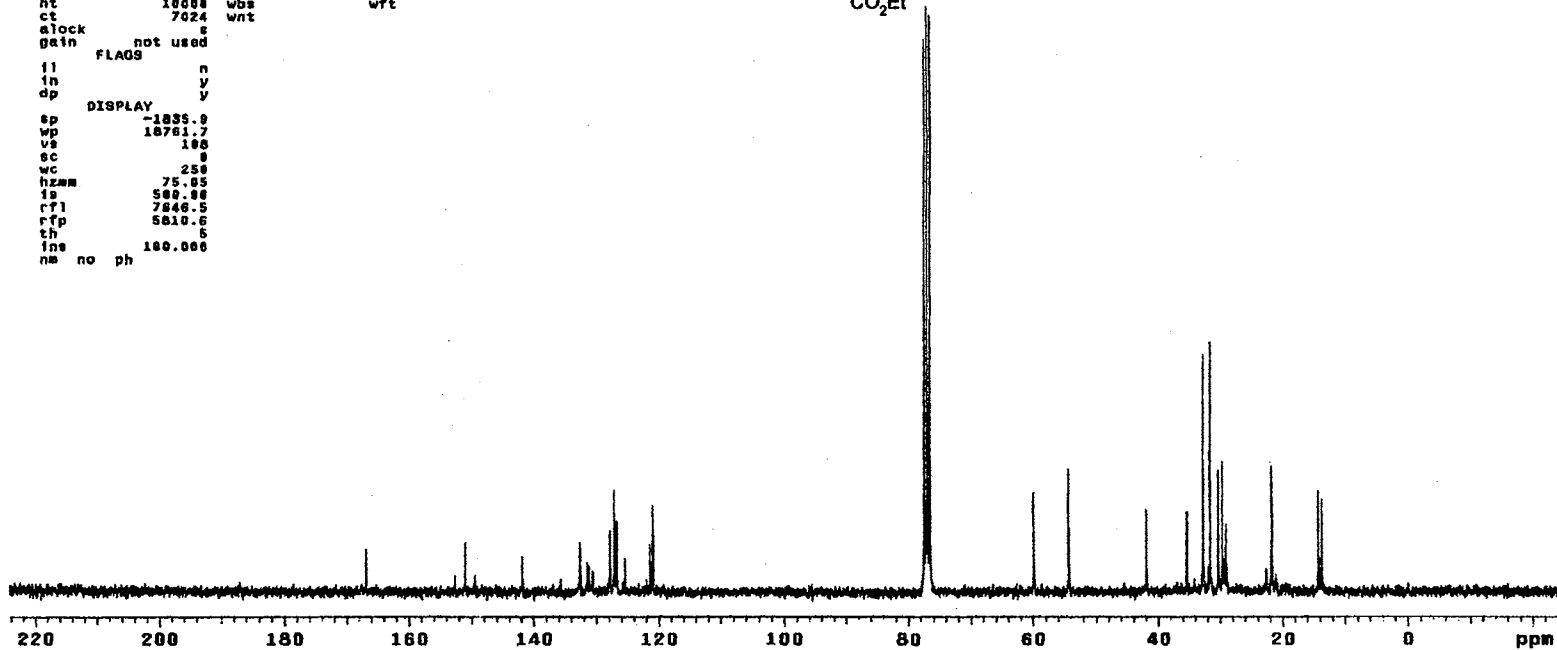
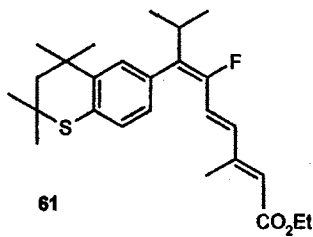
¹H NMR Spectrum of 61

Plate XLVII

13C OBSERVE

expl std13c

data	SAMPLE	DEC. & VT	
Nov 10 1993		300.087	
solvent	CDC13	dn	H1
files	exp	dpwr	34
ACQUISITION	exp	dyf	0
sfrq	75.464	dm	VVV
tn	C13	dsm	w
at	8.800	daf	11764
np	38016	PROCESSING	
sw	18761.7	lb	1.00
fb	10400	wf11e	
bs	16	proc	ft
tpwr	52	fn	not used
pw	3.0		
di	1.000	werr	
cor	0	wkpd	wft
nt	10000	wbs	wft
ct	7024	wnt	
clock	s		
gain	not used		
FLAGS			
fl	n		
fn	y		
dp	y		
DISPLAY			
sp	-1835.9		
wp	18761.7		
vs	100		
sc	0		
wc	250		
hznm	75.05		
fa	500.00		
rfl	7846.5		
rfp	5810.6		
th	5		
lne	100.000		
no	no	ph	



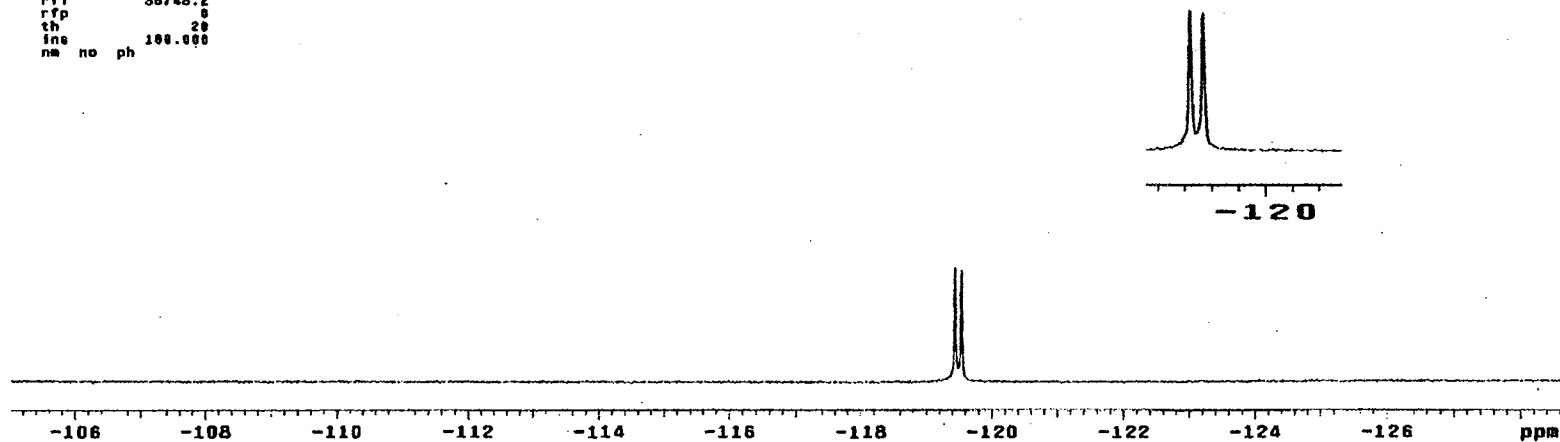
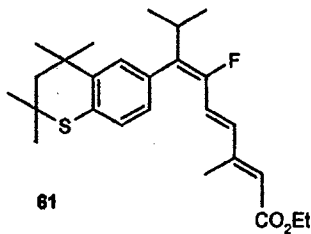
¹³C NMR Spectrum of 61

Plate XLVIII

13C OBSERVE

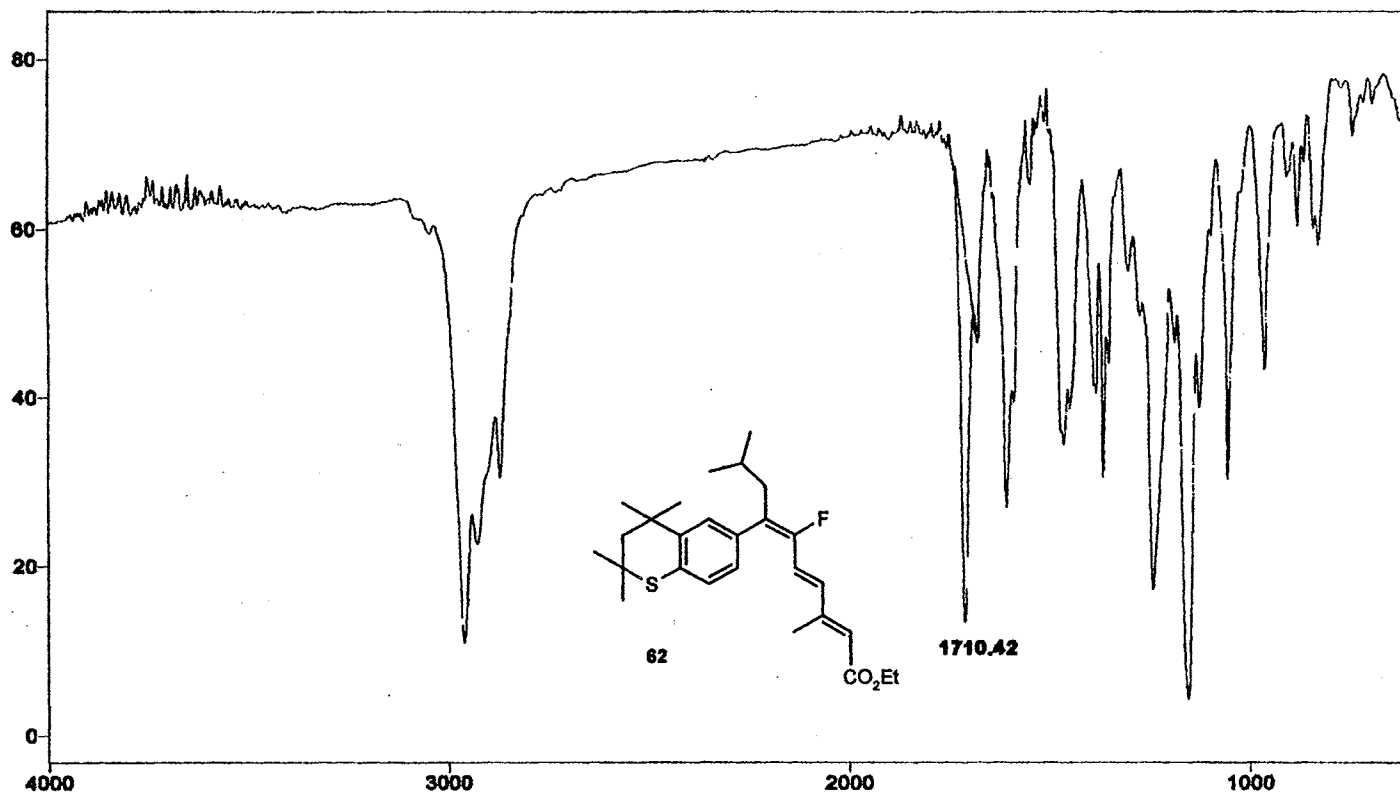
```

exp1 std13c
SAMPLE
date Nov 18 1999 dfrq 300.087
solvent CDC13 dn HI
f1ls exp dpr 32
ACQUISITION exp ddr 0
sfrq 282.333 da nnn
tn F13 dam w
at 0.800 dm7 11764
np 38016 PROCESSING 1.00
sw 18761.7 lb
fb 10400 wtfile ft
bs 16 proc not used
tpwr 32 fn
pw 3.8
d1 1.000 warr wft
tor 0 wexp wft
nt 1024 wba wft
ct 112 wnt
alock n
gain not used
FLAUS
f1 n
in y
dp y
DISPLAY
sp -38333.0
wp 6681.1
vs 22
sc 0
wc 250
hzwm 26.72
is 500.00
rfl 38748.2
rff 0
th 20
ins 100.000
nm no ph
    
```



¹⁹F NMR Spectrum of 61

Plate XLIX



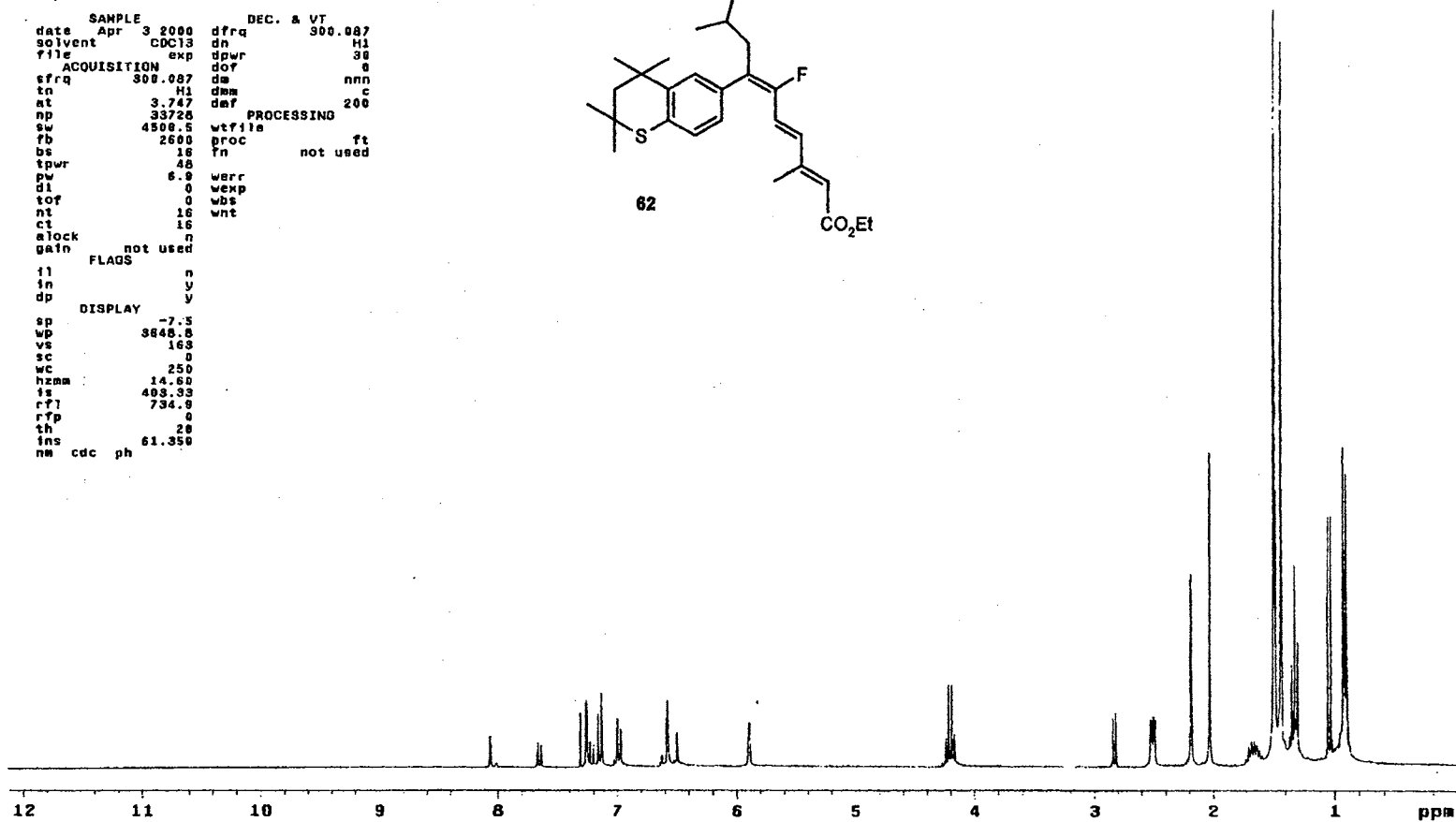
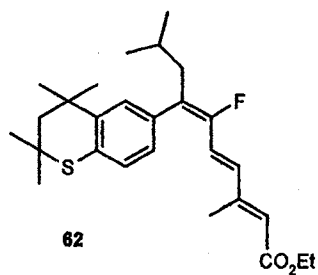
IR Spectrum of 62

Plate L

STANDARD 1H OBSERVE

```

expl stdih
date Apr 3 2000 dfrq DEC. & VT 300.087
solvent CDCl3 dn H1
file exp gpwr 30
ACQUISITION dof 0
tfrq 300.087 dm nmc
tn H1 dmz c
at 3.747 def 200
np 33726 PROCESSING
sw 4500.5 wtfila ft
fb 2500 proc
bs 16 fn not used
tpwr 48
pw 6.9 werr
d1 0 wexp
tof 0 wbs
nt 16 wnt
ct 16
alock n
gain not used
FLAGS
f1 n
f2 y
dp y
DISPLAY
sp -7.5
wp 3648.8
vs 163
sc 0
wc 250
hzmm 14.60
fs 493.33
rfl 734.0
rtp 0
th 20
ins 61.350
nm cdc ph
  
```



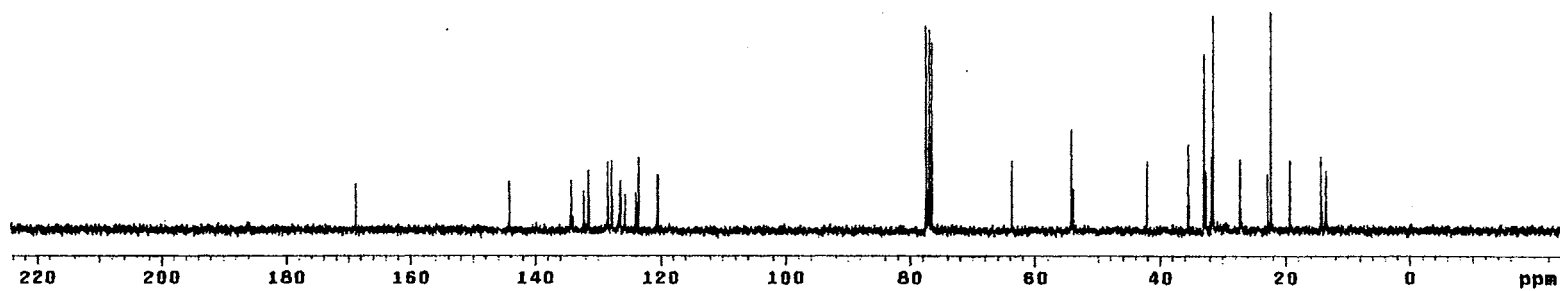
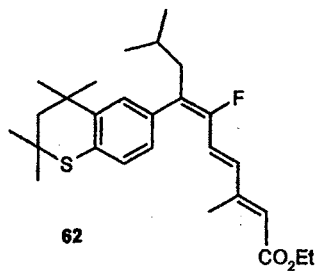
¹H NMR Spectrum of 62

Plate LI

13C OBSERVE

expl std13c

date	SAMPLE	DEC. & VT	dfrq	300.087
Apr 3 2000			dn	H1
solvent	CDC13		dpwr	34
file	exp		dof	0
ACQUISITION				
sfrq	75.484	dm	yvy	w
tn	C13	dmf	11764	
at	0.800	PROCESSING		
np	30016	lb	1.00	
gw	18781.7	wtfile		
fb	10400	proc	ft	
hs	16	fn	not used	
tpwr	52	werr		
pw	3.8	wexp	wft	
d1	1.000	wbs	wft	
tor	0	wnt		
nt	1024			
ct	736			
a)ack	s			
gain	not used			
FLAGS				
il	n			
in	y			
dp	y			
DISPLAY				
sp	-1835.9			
wp	18781.7			
vt	40			
sc	0			
wc	250			
hzw	75.95			
is	500.00			
rfl	7846.5			
rfp	5810.6			
th	4			
ins	100.000			
nm	no ph			



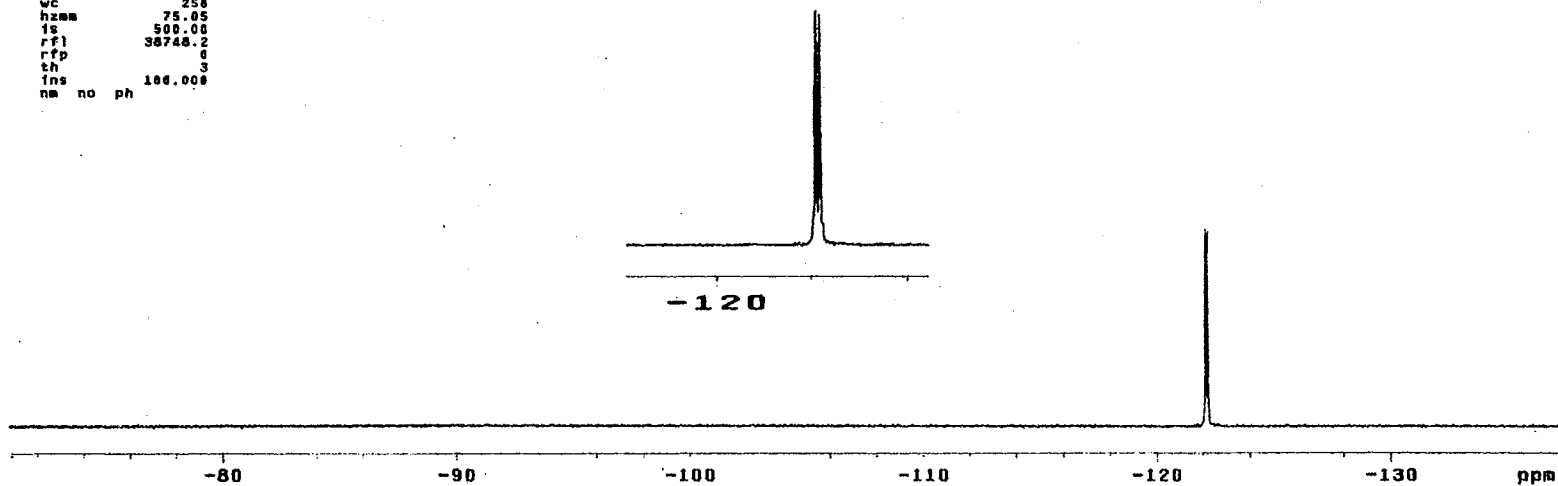
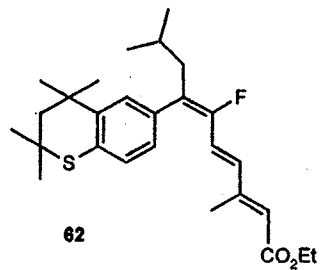
¹³C NMR Spectrum of 62

Plate LII

13C OBSERVE

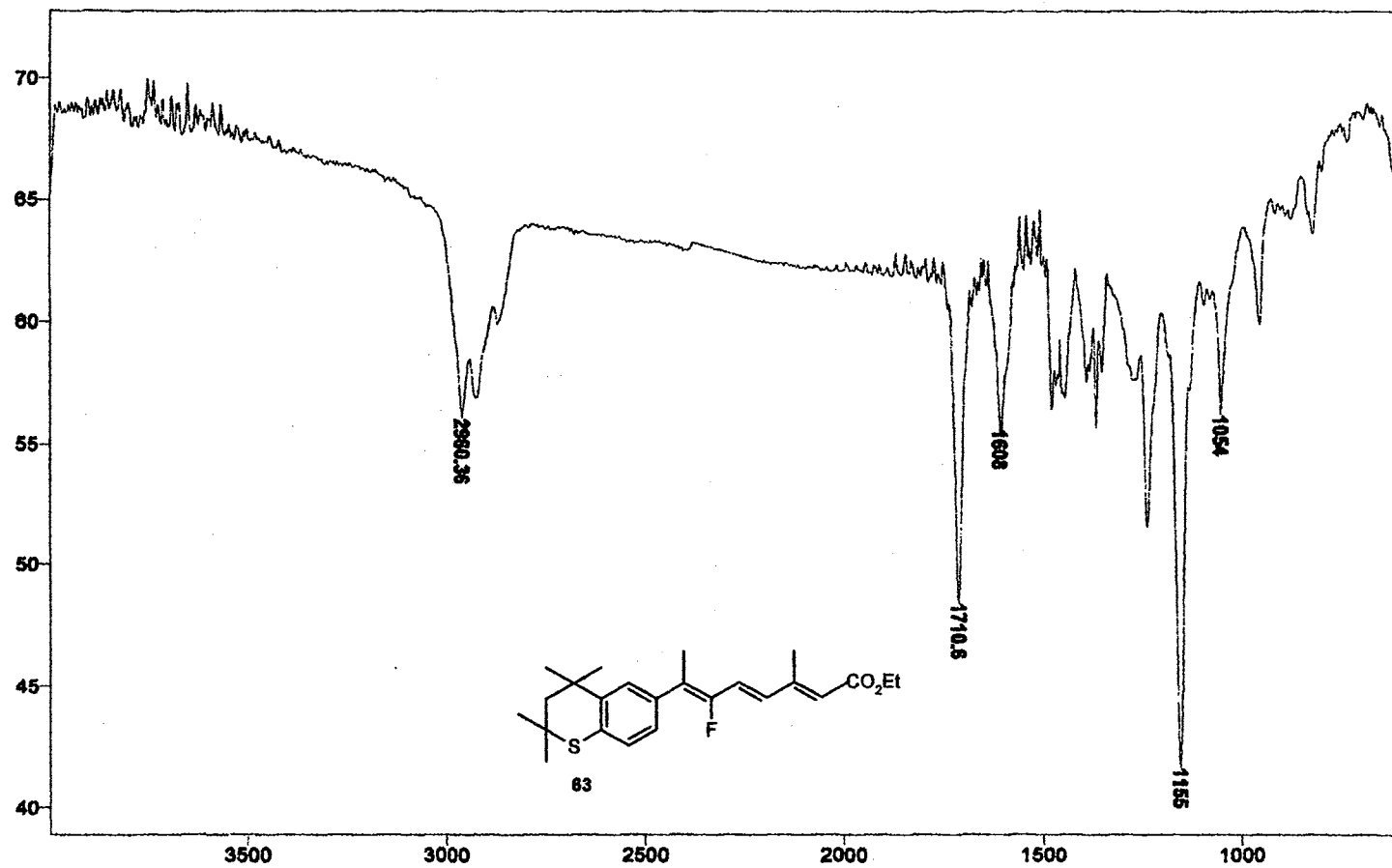
```

exp1 std13c
SAMPLE DEC. & VT
date Apr 3 2009 dfrq 300.087
solvent CDC13 dn H1
file exp dpr 34
ACQUISITION dof 0
sfrq 282.333 dm n
tn F19 dam W
st 0.000 dmf 11764
np 38018 PROCESSING
sw 16781.7 lb 1.00
fb 10400 wtfile
bs 16 proc ft
tpwr 52 fn not used
pw 3.8
d1 1.000 werr
tof 0 wexp wft
nt 1024 wba wft
ct 48 wnt
slock n
gain not used
FLAGS
il n
in y
dp y
DISPLAY
sp -38748.2
wp 16781.7
vs 37
sc 0
wc 256
hzmm 75.05
ls 500.00
rfl 38748.2
rfp 0
th 3
ins 100.000
nm no ph
    
```



¹⁹F NMR Spectrum of 62

Plate LIII



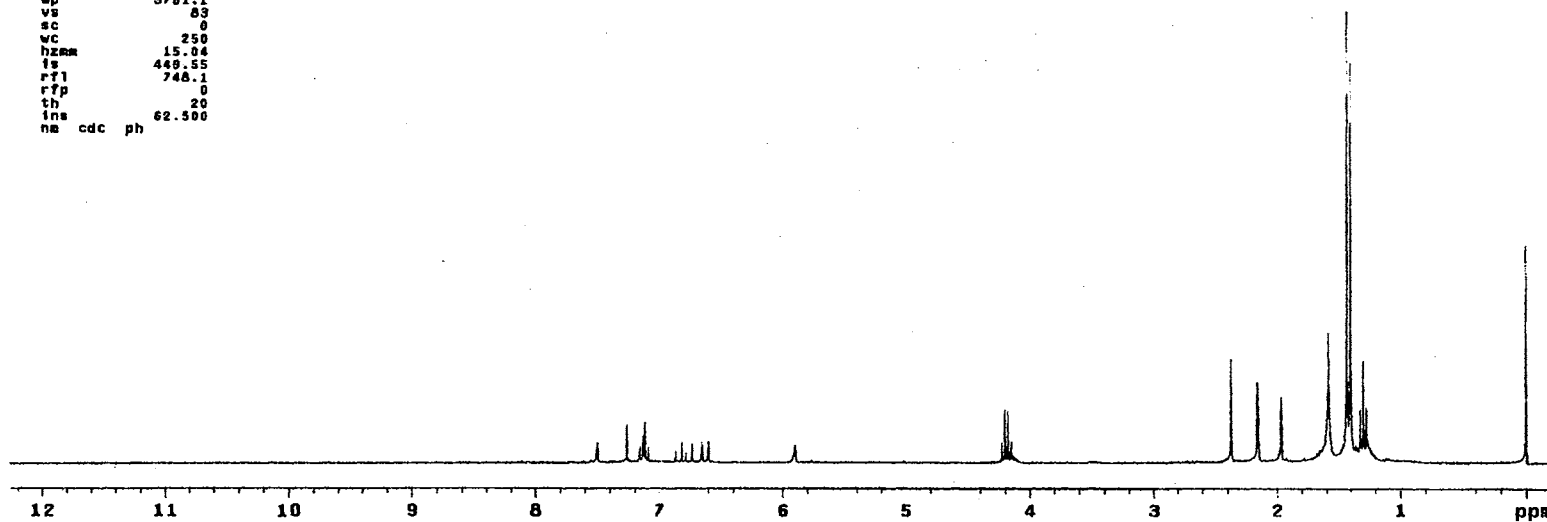
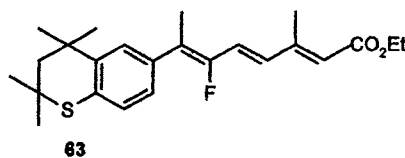
IR Spectrum of 63

Plate LIV

STANDARD 1H OBSERVE

```

expi stdih
SAMPLE
date Oct 30 1999 dfrq DEC. & VT 300.067
solvent CDCl3 dn H1
file exp dpwr 30
ACQUISITION dof 0
sfrq 300.067 da nnn
tn H1 dam c
at 3.747 dmf 200
np 33726 PROCESSING
sw 4588.6 wtfila
fb 2600 proc ft
bs 16 fn not used
tpwr 48
pw 6.3 werr
dl 0 wexp
top 0 wbs
nt 32 wnt
ct 82
alock n
gain not used
FLAOS
tl n
in y
dp y
DISPLAY
sp -79.9
wp 3761.1
vs 63
sc 0
wc 250
hzmm 15.84
fs 449.55
rf1 746.1
rfp 0
th 20
ins 62.500
nm cdc ph
    
```



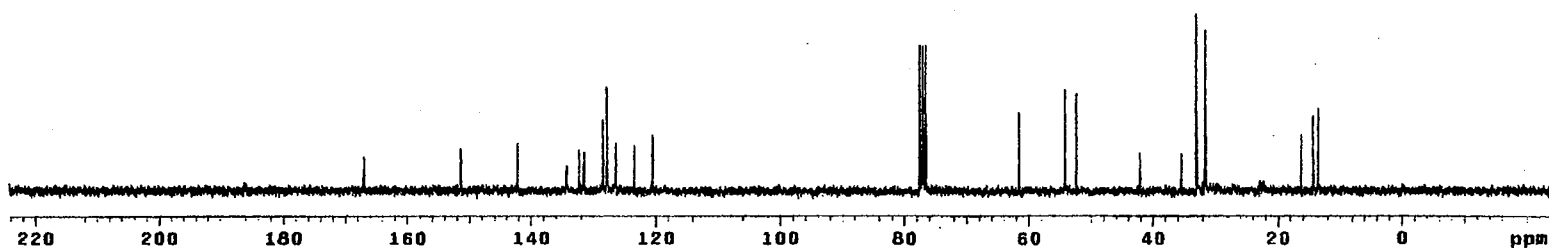
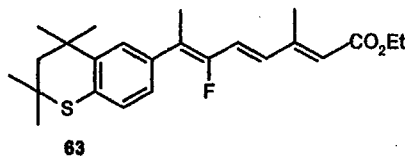
¹H NMR Spectrum of 63

Plate LV

13C OBSERVE

```

expt  std13c
SAMPLE
date  Apr  3 2000  dfrq  DEC. & VT  300.087
solvent  CDCl3  dn  H1
file  exp  dpwr  34
ACQUISITION  dof  0
sfrq  75.464  ds  yyw
tn  C13  dnm
at  0.000  daf  11764
np  30010  PROCESSING
gw  18761.7  lb  1.00
Tb  10490  wtfile
bs  16  proc  ft
tpwr  52  fn  not used
pw  3.8
d1  1.000  werr
tof  0  wexp  wft
nt  1024  wbs  wft
ct  736  wnt
alock  s
gain  not used
FLAGS
il  n
in  y
dp  y
DISPLAY
sp  -1835.0
wp  18761.7
vs  40
sc  0
wc  250
hzmm  75.95
fs  500.00
rf1  7646.5
rfp  5010.6
th  4
ins  160.000
na  no  ph
  
```



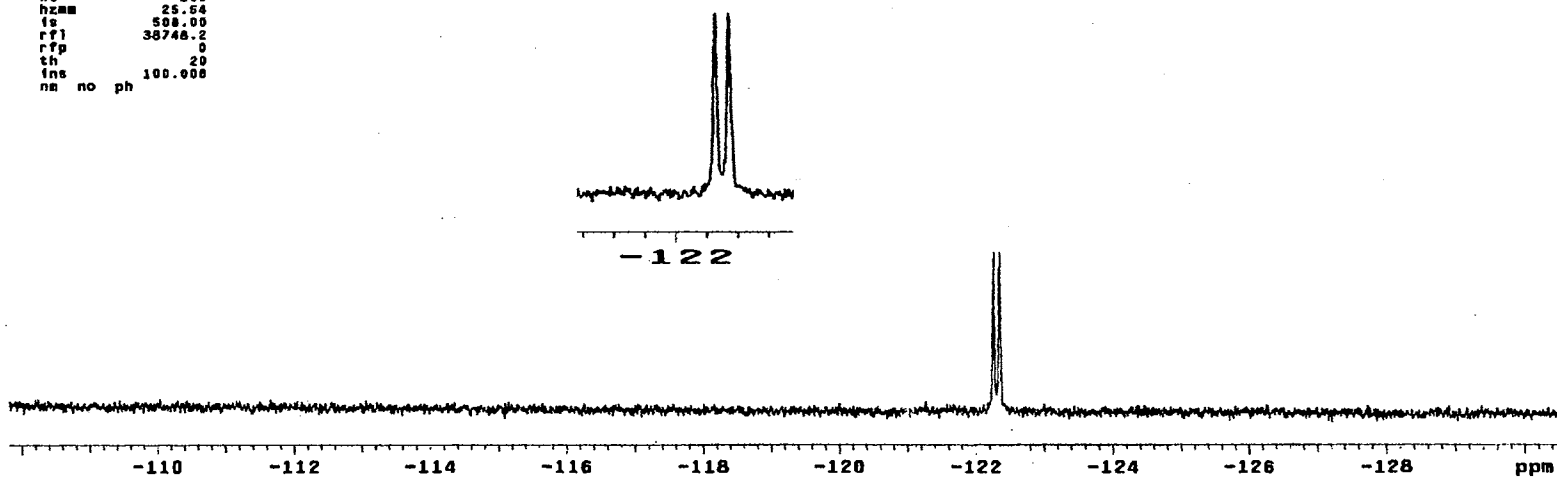
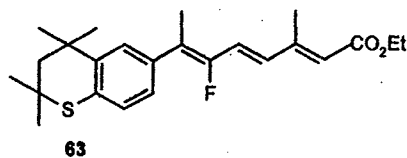
¹³C NMR Spectrum of 63

Plate LVI

13C OBSERVE

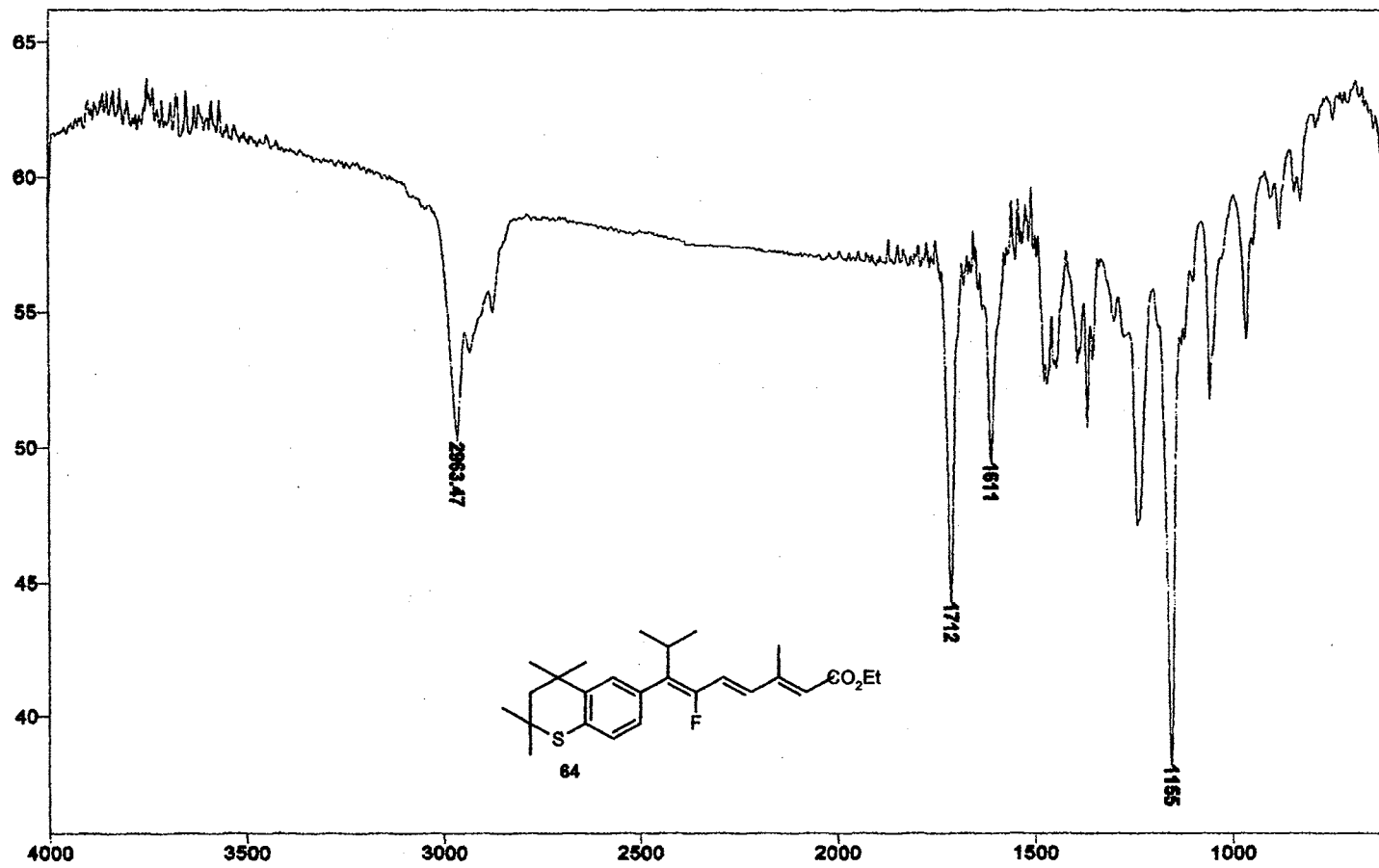
expi std13c

data	Oct 30 1999	dfrq	DEC. & VT	300.067
solvent	CDC13	dn		M1
file	exp	dpwr		34
ACQUISITION				
sfrq	202.393	ds		nn
tn	F18	dsm		w
at	0.800	daf		11764
np	38016	PROCESSING		
sw	10781.7	lb		1.00
fb	10000	wtfile		
bs	16	proc		ft
tpwr	52	fn		not used
pw	3.8			
di	1.000	werr		
tot	0	wexp		wft
nt	1024	wbs		wft
ct	144	wnt		
alock				n
gain	not used			
	FLADS			n
tl				n
in				y
dp				y
DISPLAY				
sp	-36858.6			
wp	8489.7			
vs	31			
sc	0			
wc	250			
hzam	25.54			
fs	500.00			
rfl	38746.2			
rfp	0			
th	20			
ins	100.000			
nr	no	ph		



¹⁹F NMR Spectrum of 63

Plate LVII



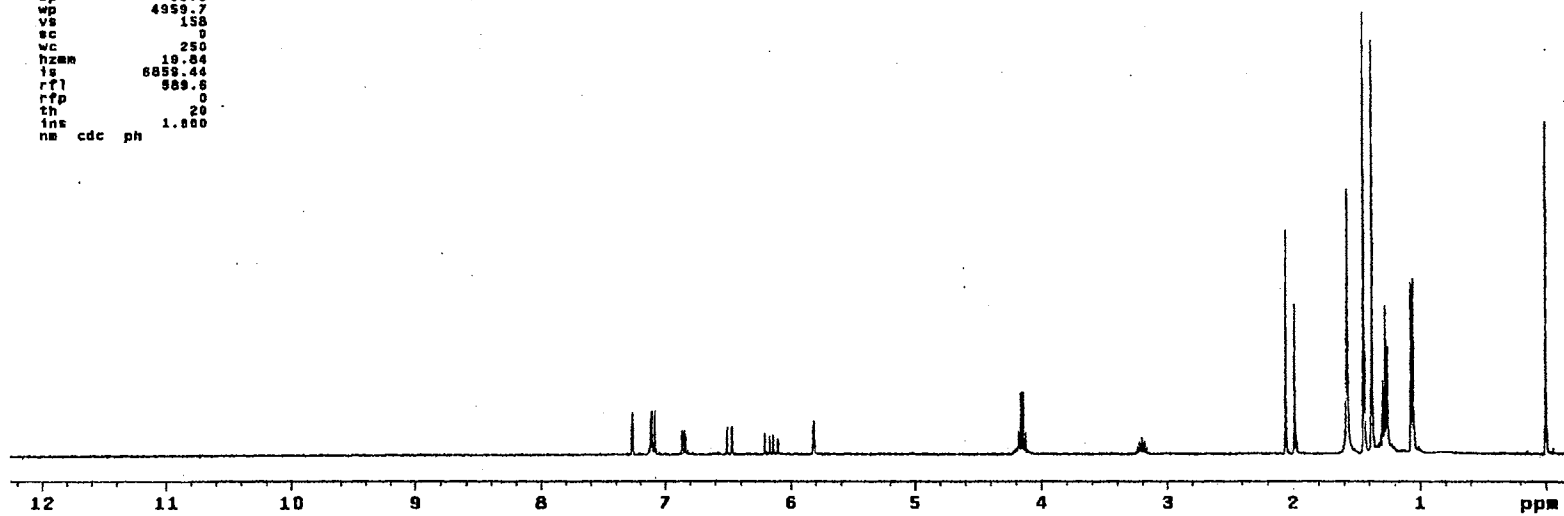
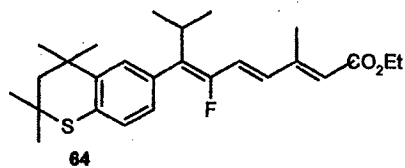
IR Spectrum of 64

Plate LVIII

STANDARD 1H OBSERVE

```

expi stdih
SAMPLE DEC. & VT
date Nov 10 1999 dfrq 300.825
solvent CDCl3 dn H1
file exp dpwr 30
ACQUISITION exp dof 0
sfrq 300.825 da nnn
tn H1 dm c
at 3.744 dmf 200
np 44828 dseq
sw 6000.6 dres 1.0
fb 3080 homo n
bs 16 PROCESSING
tpwr 52 wtf1le
pw 6.0 proc ft
d1 0 fn not used f
tof 0 math
nt 32
ct 32 werr
alock n wexp
gain 35 wss
        wnt
        n
        n
        y
        nn
DISPLAY
sp -59.3
wp 4959.7
vs 150
sc 0
wc 250
hzam 19.84
is 6859.44
rfl 999.6
rfd 0
th 20
ins 1.000
nm cdc ph
    
```



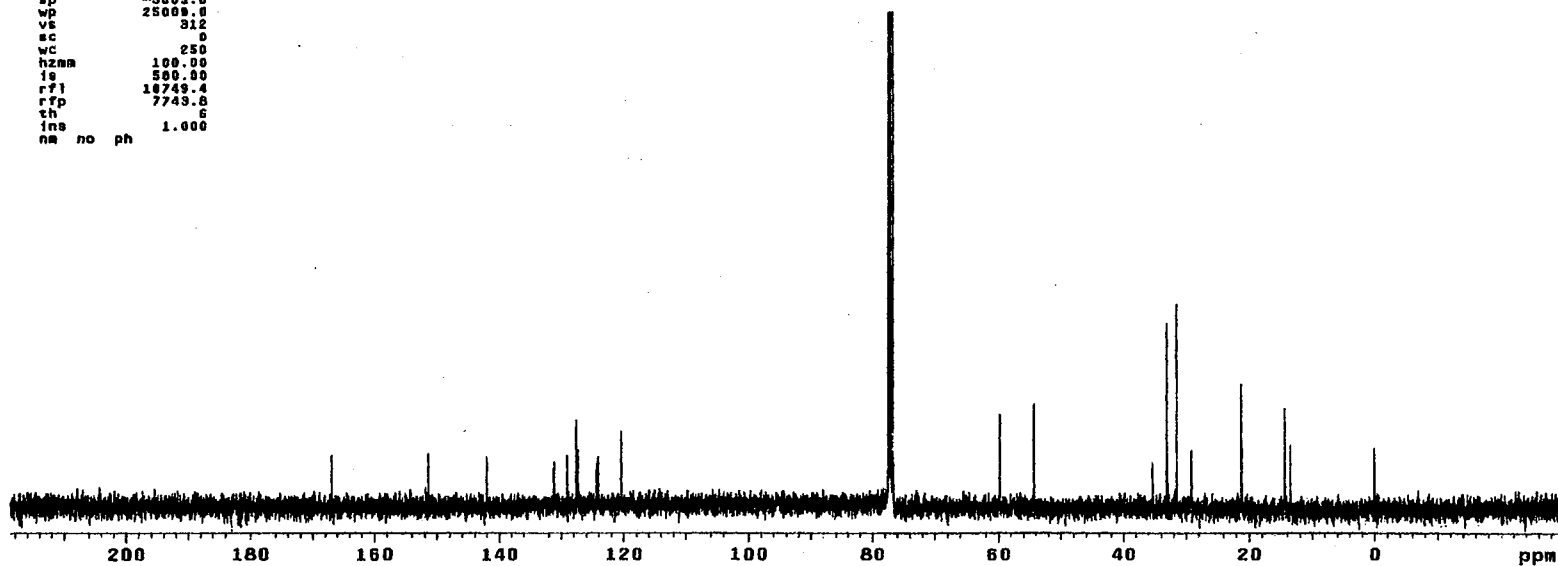
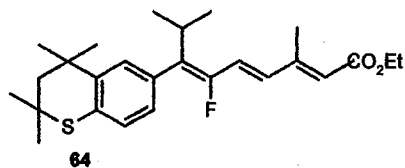
¹H NMR Spectrum of 64

Plate LIX

13C OBSERVE

expt std13c

SAMPLE		DEC. & VT	
date	Nov 10 1988	dfrq	380.025
solvent	CDCl3	dn	H1
file	exp	dpwr	40
ACQUISITION		dot	0
efrq	100.570	dm	nyy
tn	C13	dsm	w
at	1.189	dm7	12000
np	5888	dseq	
sw	25000.0	dres	1.0
fb	14000	homo	n
bs	64	PROCESSING	
tpwr	53	lb	1.00
pw	7.0	wf file	
d1	1.000	proc	ft
d2	0.500	fn	not used
tof	0	math	f
nt	10000		
ct	6144	werr	wft
elock	n	wexp	wft
gain	not used	wbs	wft
	FLAGS	wnt	
il	n		
in	n		
dp	y		
hs	nn		
DISPLAY			
sp	-3003.6		
wp	25000.0		
ve	312		
sc	0		
wc	250		
hzma	100.00		
is	500.00		
rfl	18749.4		
rfp	7743.8		
th	6		
ins	no ph		
na	1.000		



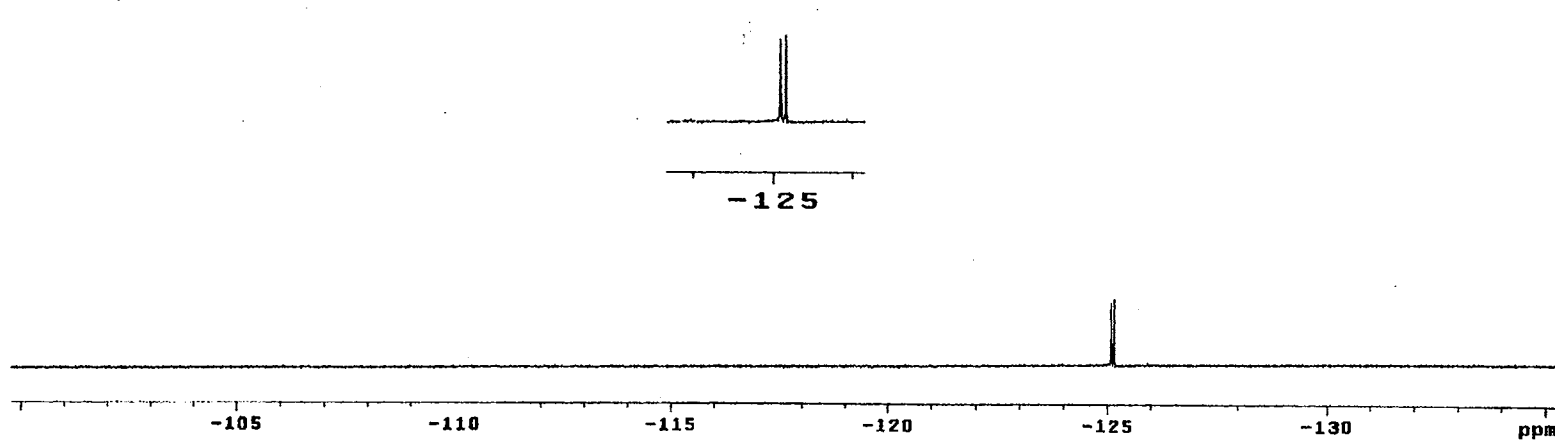
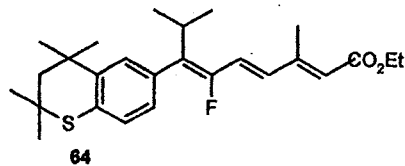
¹³C NMR Spectrum of 64

Plate LX

F19 OBSERVE
STANDARD PARAMETERS

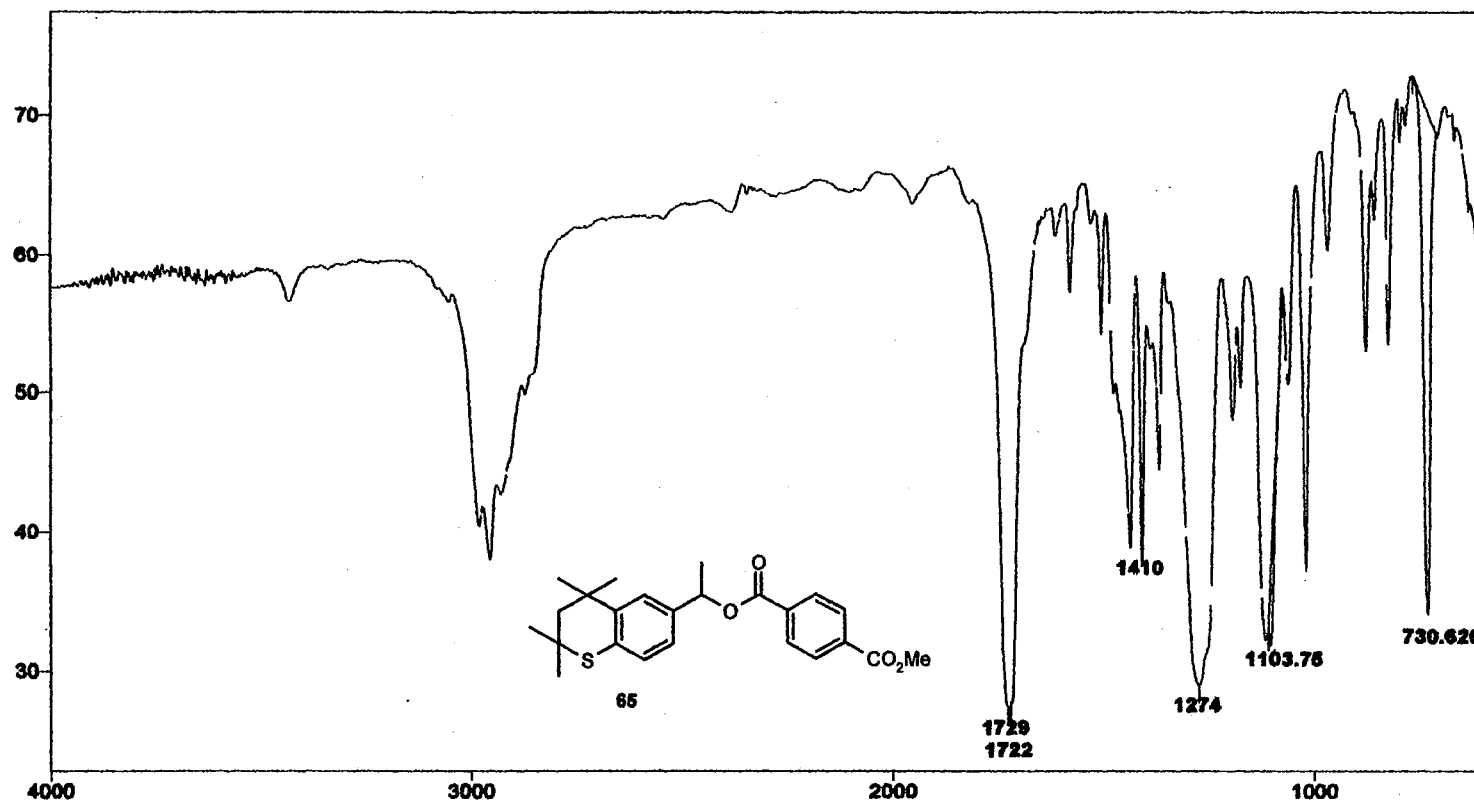
```

exp1 s2pu1
SAMPLE
date Nov 10 1999 dfrq DEC. & VT 399.925
solvent CDC13 dn HI
file exp dpwr 30
ACQUISITION dbf 0
sfrq 376.253 da nnn
tn F19 dm c
at 0.690 dsf 200
np 59968 deeq 1.0
sw 50000.0 dres 1.0
fb 28000 homo n
bs 16
tpwr 55 PROCESSING 0.30
pw 5.0 wtf file
di 4.000 proc ft
tof 0 fn not used r
nt 128 math r
ct 128
aLock n werr
gain not used wexp wft
FLAOS wse wft
il n
in n
dp y
hs nn
DISPLAY
sp -50050.4
wp 19402.2
vs 14
sc 0
wc 250
hzmm 53.81
fs 500.00
rf1 85141.5
rfp 0
sh 20
ins 1.000
nm no ph
  
```



¹⁹F NMR Spectrum of 64

Plate LXI



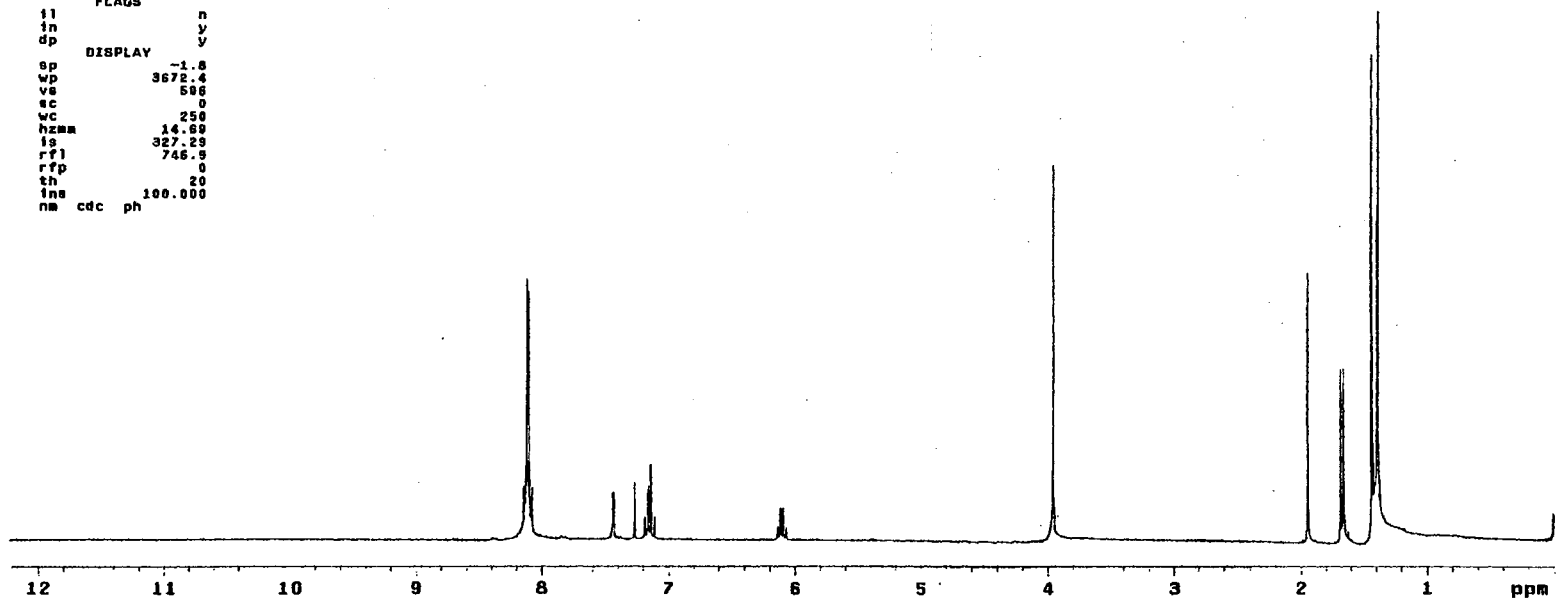
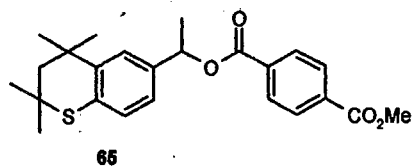
IR Spectrum of 65

Plate LXII

STANDARD 1H OBSERVE

```

expl  stdih
SAMPLE
date  Apr 13 2000  dfrq  DEC. & VT  300.087
solvent  CDC13      dn      HI
file     exp      dpwr     30
ACQUISITION  exp    dof      9
qfrq    300.087  da      nnn
tn      HI      dm      c
at      3.747   dmf     200
np      33728   PROCESSING
aw      4590.5  wtfile
fb      2680   proc   ft
bs      16     fn      not used
tpwr    48
pw      6.9   warr
d1      0     wexp
tof     0     wbs
nt      16   wnt
ct      16
alock   not used
gain    not used
FLAGS
fl      n
fn      y
dp      y
DISPLAY
sp      -1.8
wp      3672.4
vs      500
sc      0
wc      250
hzmm    14.80
ls      327.29
rf1     746.9
rfp     0
th      20
ins     100.000
nm      cdc  ph
    
```



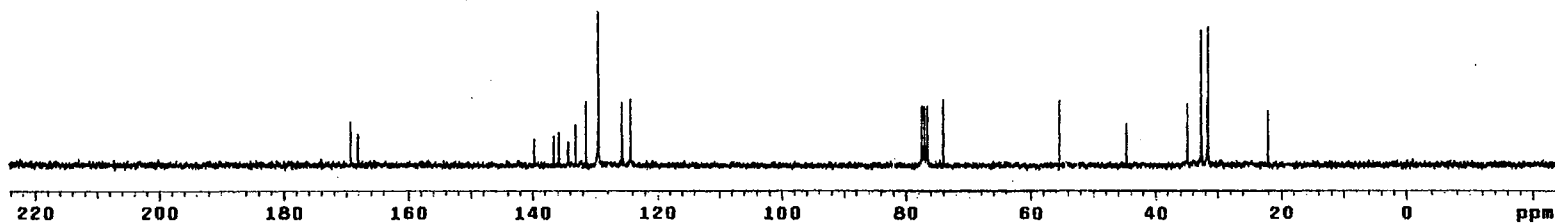
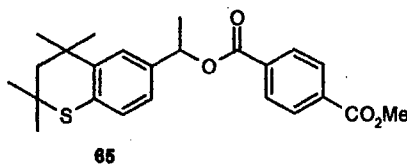
¹H NMR Spectrum of 65

Plate LXIII

¹³C OBSERVE

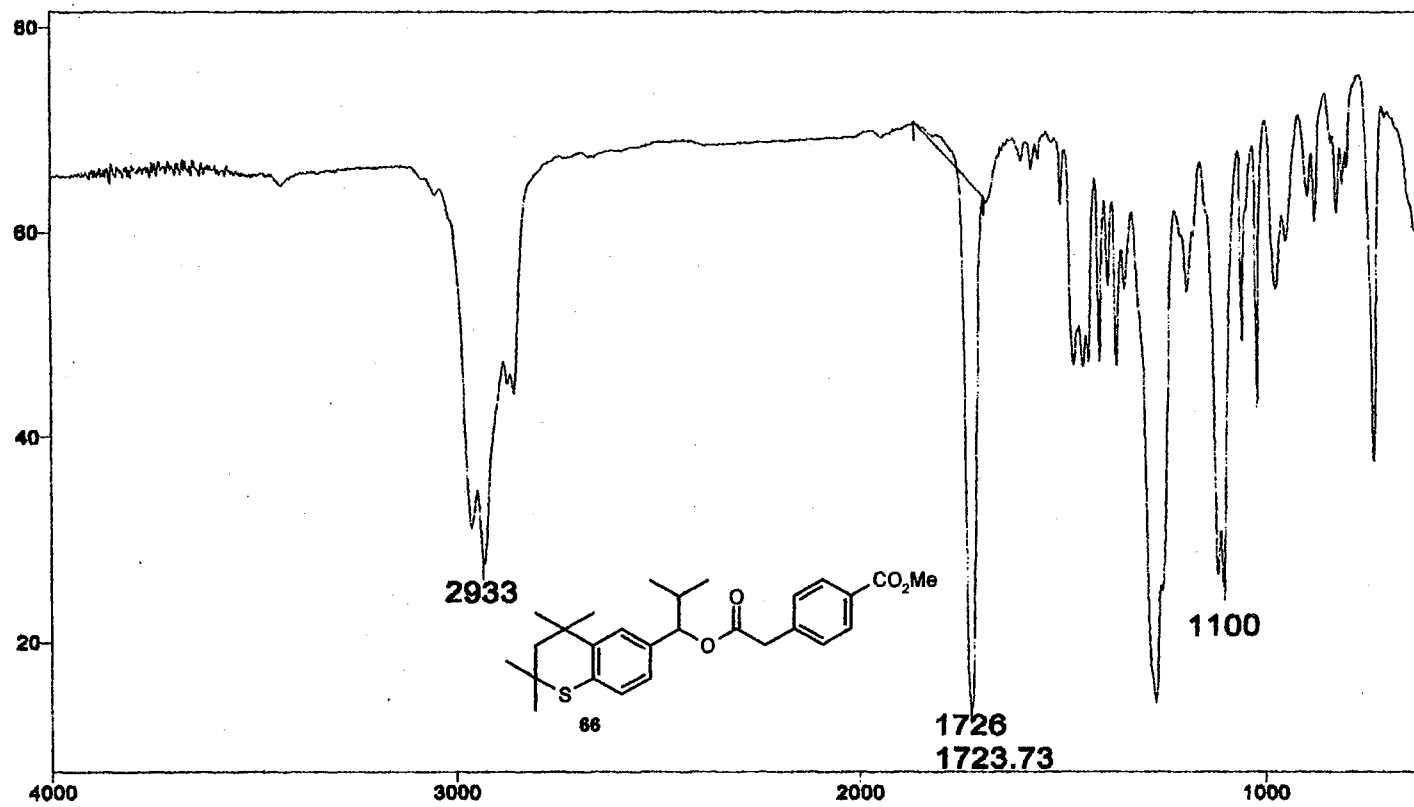
exptl std13c

	SAMPLE	DEC. & VT	
date	Nov 20 1999	dfrq	300.067
solvent	CDCl3	dn	H1
file		dpwr	36
	ACQUISITION	exp	0
sfrq	75.464	dm	yyv
tn	C13	dwm	w
at	8.800	dmf	11764
np	30016	PROCESsing	
sw	18761.7	lb	1.00
fb	10400	wtfile	
bs	16	proc	ft
tpwr	52	fn	not used
pw	3.8		
d1	1.000	werr	
tof	0	wexp	wTt
nt	4096	wbs	wTt
ct	366	wnt	
clock	s		
gain	not used		
	FLAGS		
il	n		
in	y		
dp	y		
	DISPLAY		
sp	-1839.3		
wp	18761.7		
vs	26		
sc	0		
wc	250		
hnm	75.05		
is	500.00		
rfl	7648.8		
rfd	5610.8		
th	5		
ins	100.000		
nm	no ph		



¹³C NMR Spectrum of 65

Plate LXIV



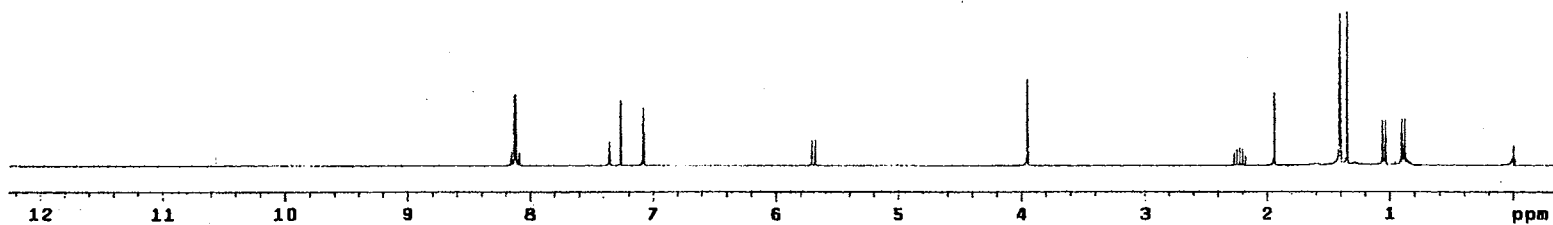
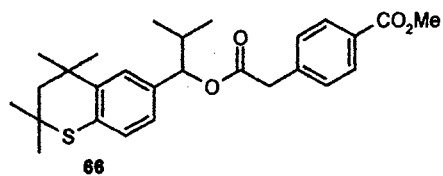
IR Spectrum of 66

Plate LXV

STANDARD 1H OBSERVE

```

exp1 std1h
SAMPLE
date Nov 30 1999 dfrq DEC. A VT 300.087
solvent CDC13 dn H1
file exp dpwr 30
ACQUISITION exp d0f 0
efrq 300.087 da nnn
tn H1 dm c
at 3.747 dat 200
np 33728 PROCESSING
sw 4800.5 wtfls
fb 2800 proc ft
bs 16 tn not used
tpwr 48
pw 6.9 weff
d1 0 wexp
tof 0 wbs
nt 16 wnt
ct 16
alock not used n
gain not used
FLAGS
tl n
tn y
dp y
DISPLAY
sp -184.2
wp 3784.9
vs 47
sc 0
wc 250
hznm 15.14
fs 338.21
rf1 746.8
rfp 0
th 20
ins 40.000
nm cdc ph
    
```



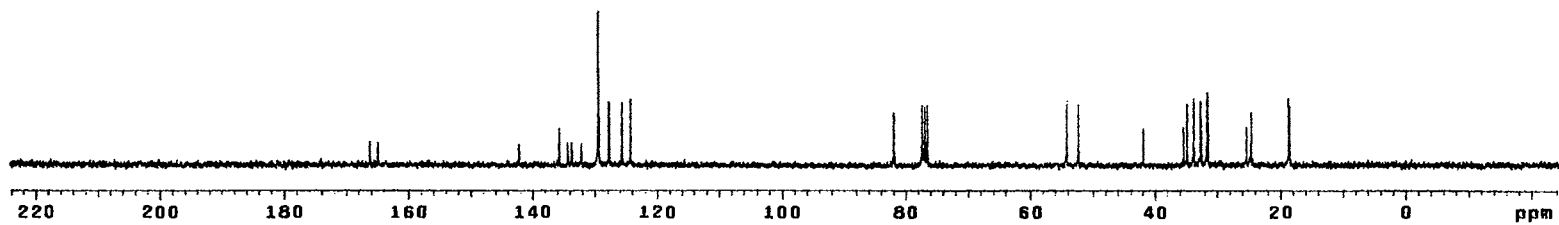
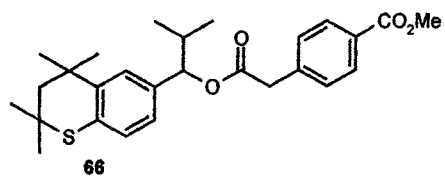
¹H NMR Spectrum of 66

Plate LXVI

13C OBSERVE

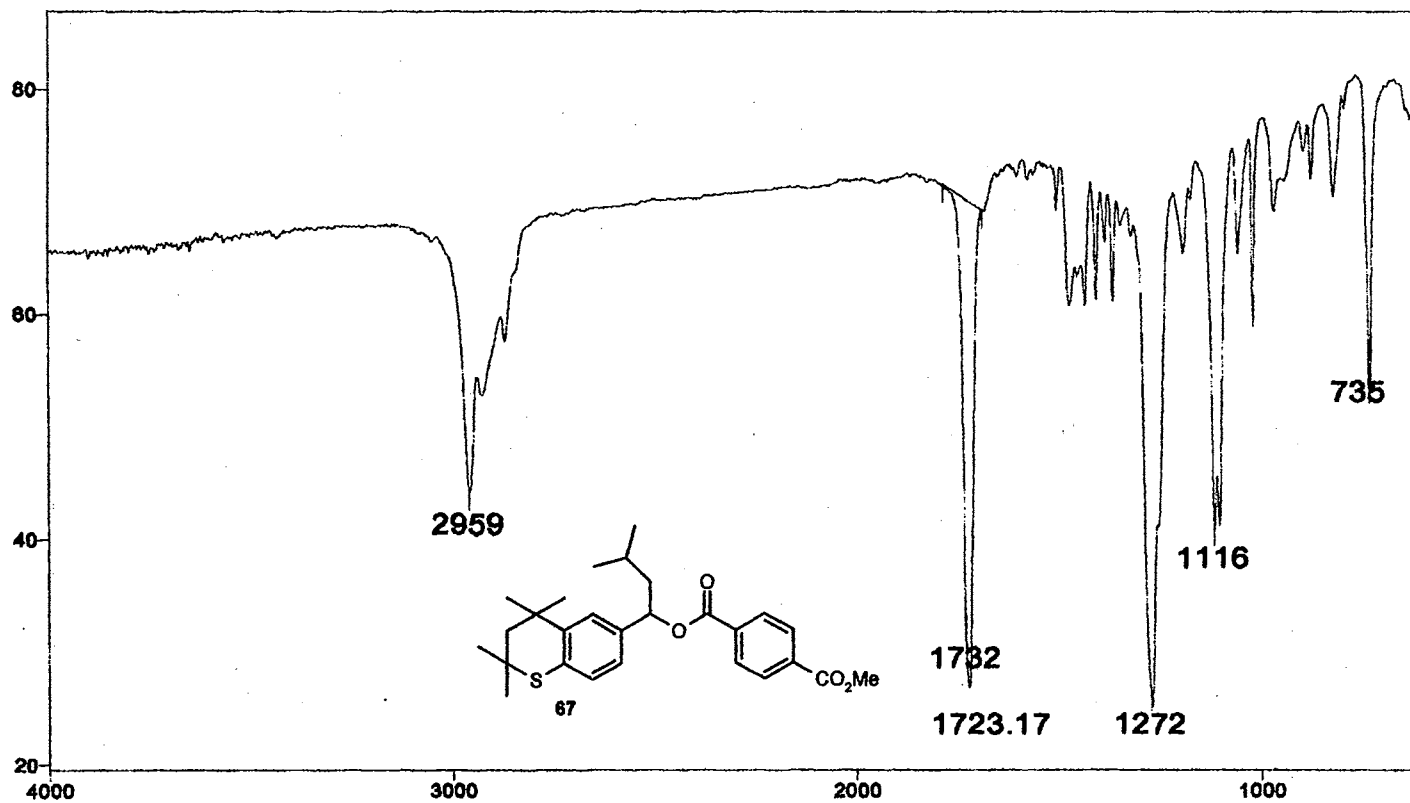
```

exp1 std13c
SAMPLE
date Nov 20 1993 dfrq DEC. a VT 300.027
solvent CDC13 dn H1
file exp dpwr 34
ACQUISITION exp dot 0
sfrq 75.464 da vvy
tn C13 dam w
at 0.800 daf 11764
np 38816 PROCESSING
sw 18761.7 lb wftfile 1.00
fb 16400 wtf1le
bs 16 proc ft
tpwr 52 fn not used
pw 3.0
d1 1.000 werr
top 0 wexp wft
nt 4088 wbs wft
ct 368 wnt
alock s
gain not used
FLAGS
il n
in y
dp y
DISPLAY
sp -1839.3
wp 18761.7
vs 28
sc 0
wc 250
hzmm 75.05
is 500.00
rf1 7649.9
rfp 5810.8
th 5
ins 100.000
nm no ph
    
```



¹³C NMR Spectrum of 66

Plate LXVII



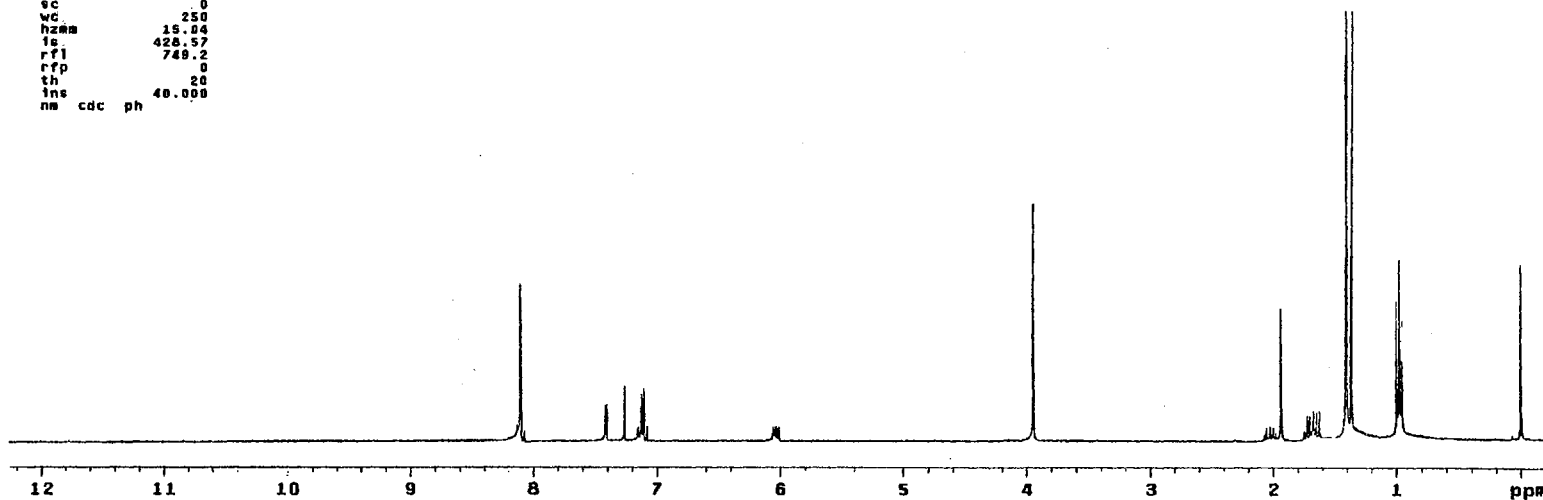
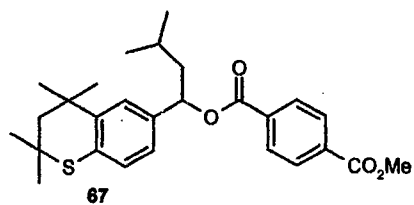
IR Spectrum of 67

Plate LXVIII

STANDARD 1H OBSERVE

```

expl stdlh
SAMPLE
date Nov 20 1999 dfrq DEC. & VT 300.087
solvent CDC13 dn H1
file exp dpwr 30
ACQUISITION dof 0
sfrq 300.087 dm nnn
tn H1 dms c
st 3.747 dmf 290
np 33728 PROCESSING
sw 4500.5 wtfile
fb 2600 proc ft
bs 16 fn not used
tpwr 48
pw 6.9 werr
SI 0 wexp
tof 0 wbp
nz 16 wnt
ct 16
alock n
gain not used
FLAGS
fl n
in y
dp y
DISPLAY
sp -81.0
wp 3781.1
vs 80
sc 0
wc 250
hzmm 15.04
fs 428.57
rfl 748.2
rfp 0
th 20
ins 48.000
nm cdc ph
    
```



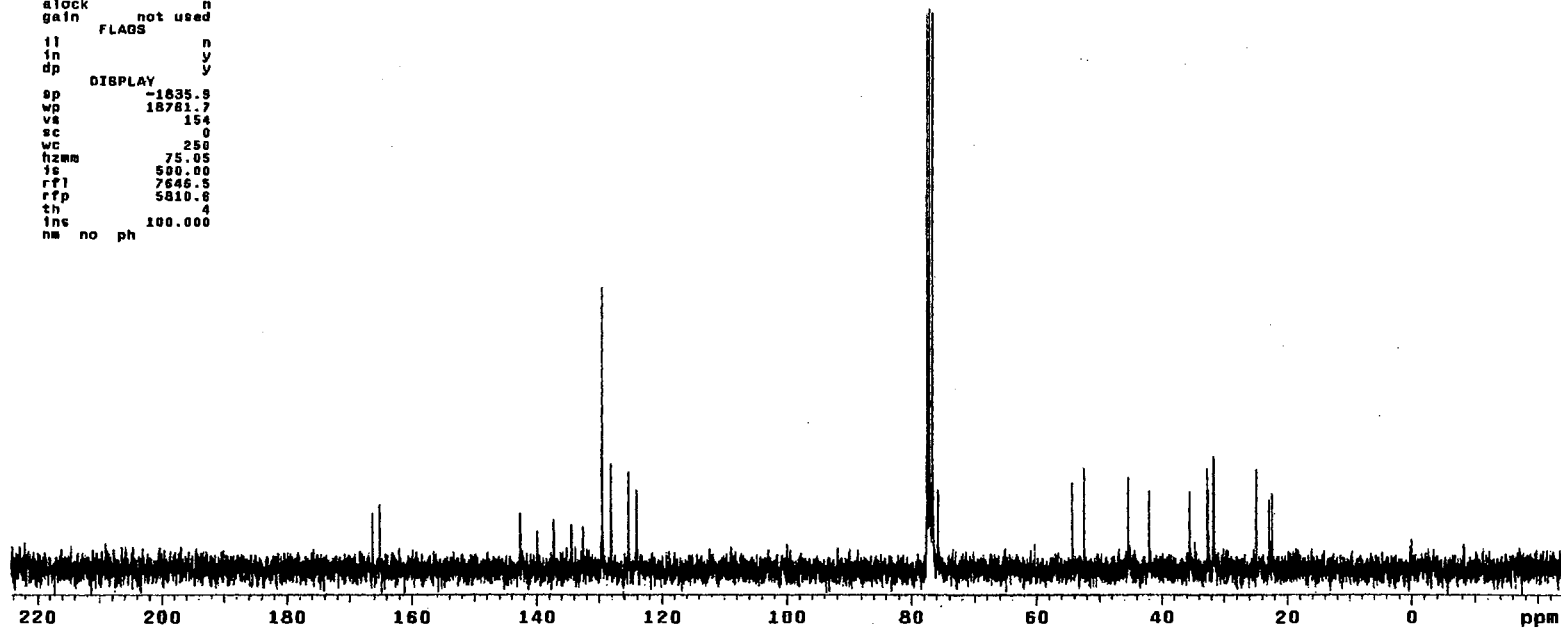
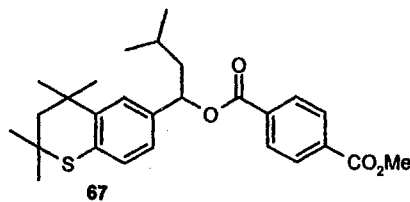
¹H NMR Spectrum of 67

Plate LXIX

13C OBSERVE

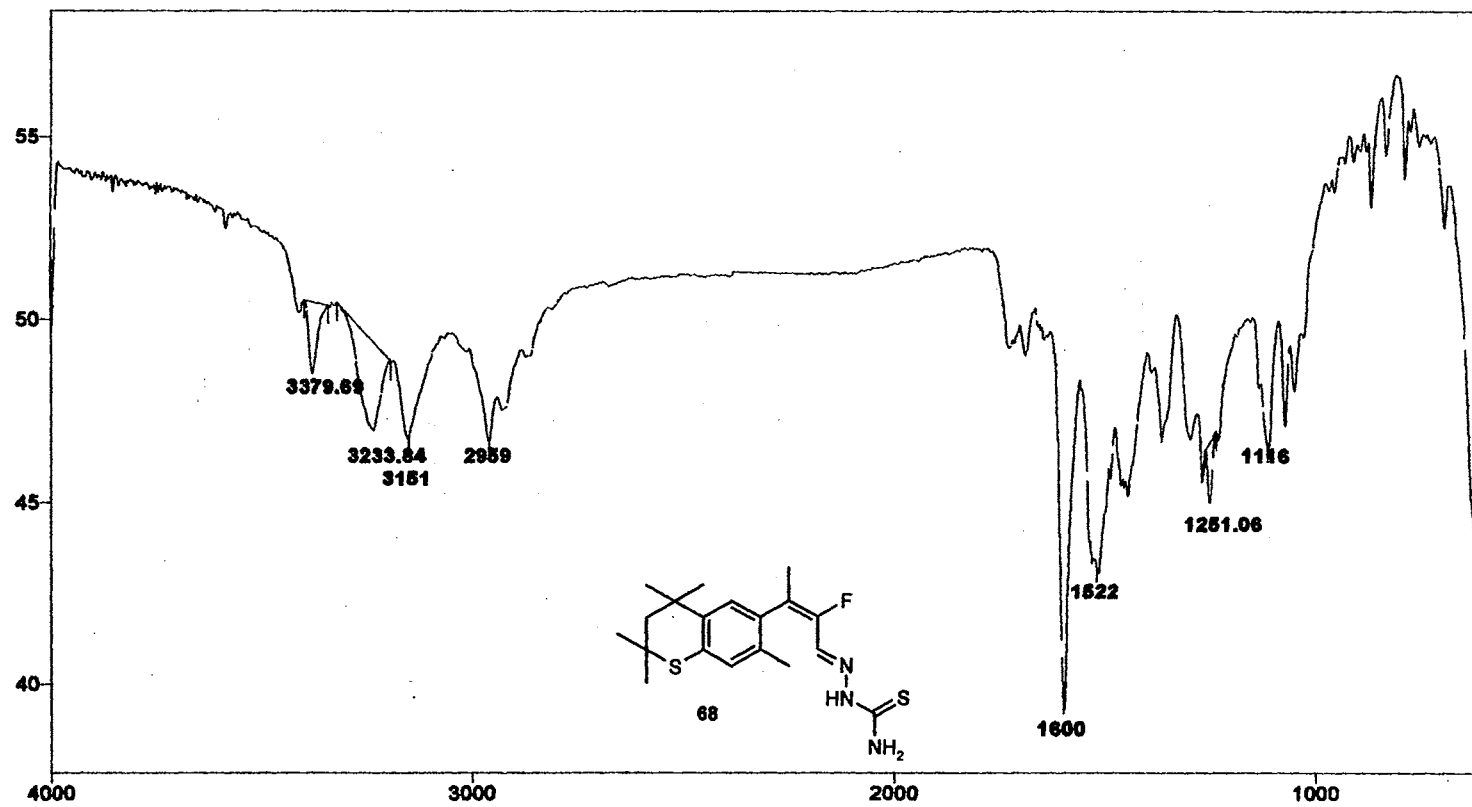
```

expt  std13c
SAMPLE
date  Nov 28 1999  dfrq  300.087
solvent  CDCl3  dn  41
file  exp  dpwr  34
ACQUISITION  dof  0
sfrq  75.464  dm  yvy
tn  C13  dms  w
at  0.800  dmf  11764
np  30018  PROCESSING
sw  18761.7  lb  1.00
fb  10400  wtfile
bs  16  proc  ft
tpwr  52  fn  not used
pw  3.8
d1  1.000  werr
tof  0  wexp  wft
nt  4096  wba  wft
ct  1472  wnt
clock  0
gain  not used
FLAOS
il  n
in  y
dp  y
DISPLAY
sp  -1835.9
wp  18761.7
vs  154
sc  0
wc  250
hzmm  75.05
is  500.00
rfl  7646.5
rff  5810.8
th  4
ins  100.000
nm  no  ph
    
```



¹³C NMR Spectrum of 67

Plate LXX



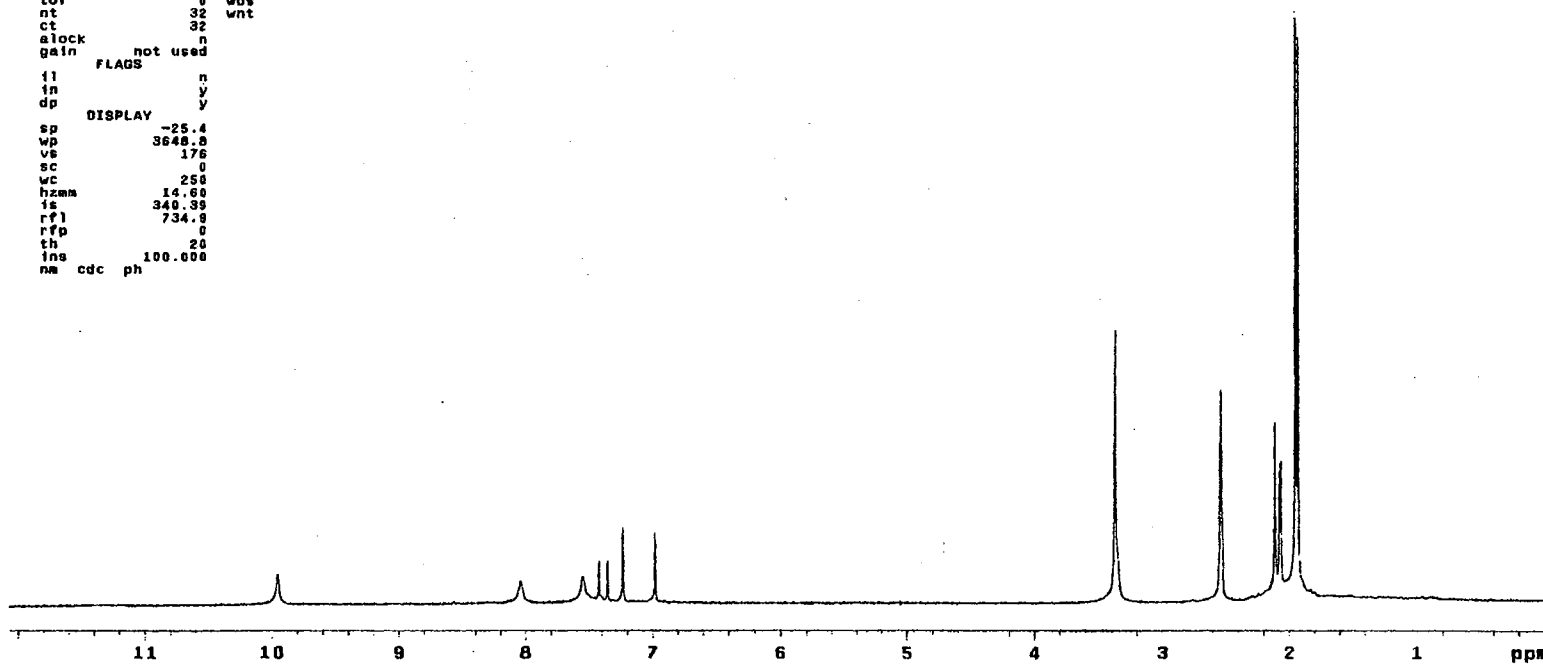
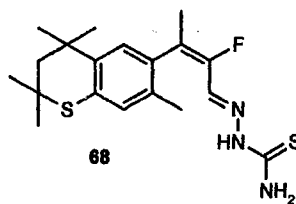
IR Spectrum of 68

Plate LXXI

STANDARD 1H OBSERVE

```

exp1 std1h
SAMPLE
date Apr 4 2000 dfrq DEC. & VT 300.080
solvent DMSO dn H1
file exp dpwr 30
ACQUISITION dof 0
sfrq 300.080 da nnn
tn H1 dam c
at 3.747 day 200
np 33728 PROCESSING
sw 4500.5 wtfile ft
fb 2600 proc
bs 16 fn not used
tpwr 48
pw 6.8 werr
d1 0 wexp
tof 0 wbs
nt 32 wnt
ct 32
alock n
gain not used
FLAGS
fl n
in y
dp y
DISPLAY
sp -25.4
wp 3648.0
vs 176
sc 0
wc 250
hzmm 14.60
is 340.38
rf1 734.8
rfp 0
th 20
ins 100.000
nm cdc ph
    
```



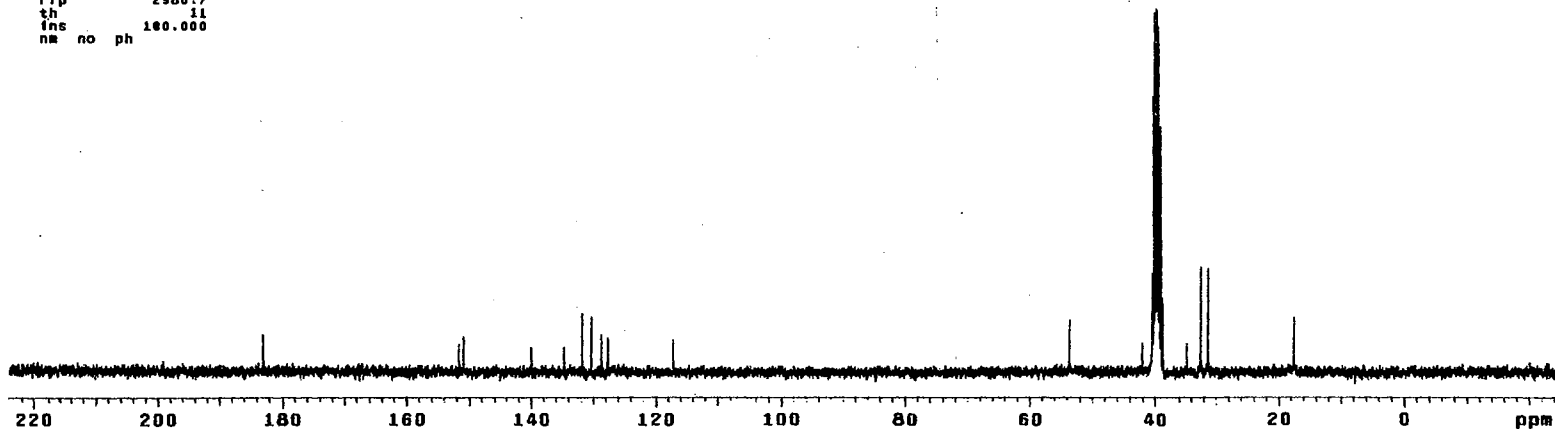
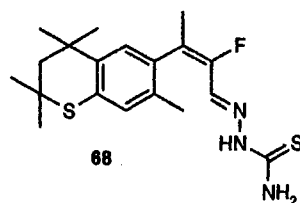
¹H NMR Spectrum of 68

Plate LXXII

¹³C OBSERVE

```

expl  std13c
SAMPLE
date  Apr  4 2000  dfrq  300.089
solvent  DMSO  dn  H1
file  exp  dpwr  30
ACQUISITION  dof  0
sfrq  75.464  dm  vvy
tn  C13  dam  w
at  0.800  dat  11764
np  30016  PROCESSING
sw  18761.7  lb  1.00
fb  10400  wtfile
bs  18  proc  ft
tpwr  52  fn  not used
pw  3.8
d1  1.000  werr
tof  0  wexp  wtt
nt  1024  wbs  wtt
ct  1024  wnt
alock  s
gain  not used
FLAGS
ii  n
in  y
dp  y
DISPLAY
sp  -1868.1
wp  18761.7
vs  107
sc  0
wc  250
hzam  75.05
ts  500.00
rf1  4848.8
rfp  2980.7
th  11
fns  180.000
nm  no  ph
    
```



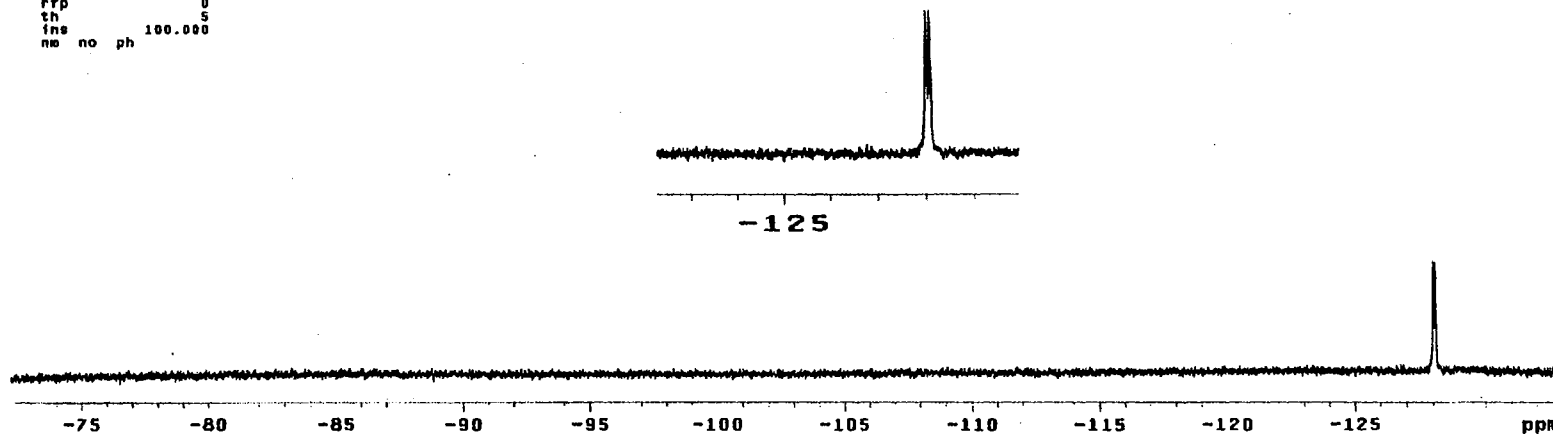
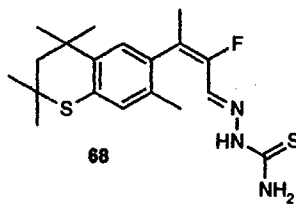
¹³C NMR Spectrum of 68

Plate LXXIII

13C OBSERVE

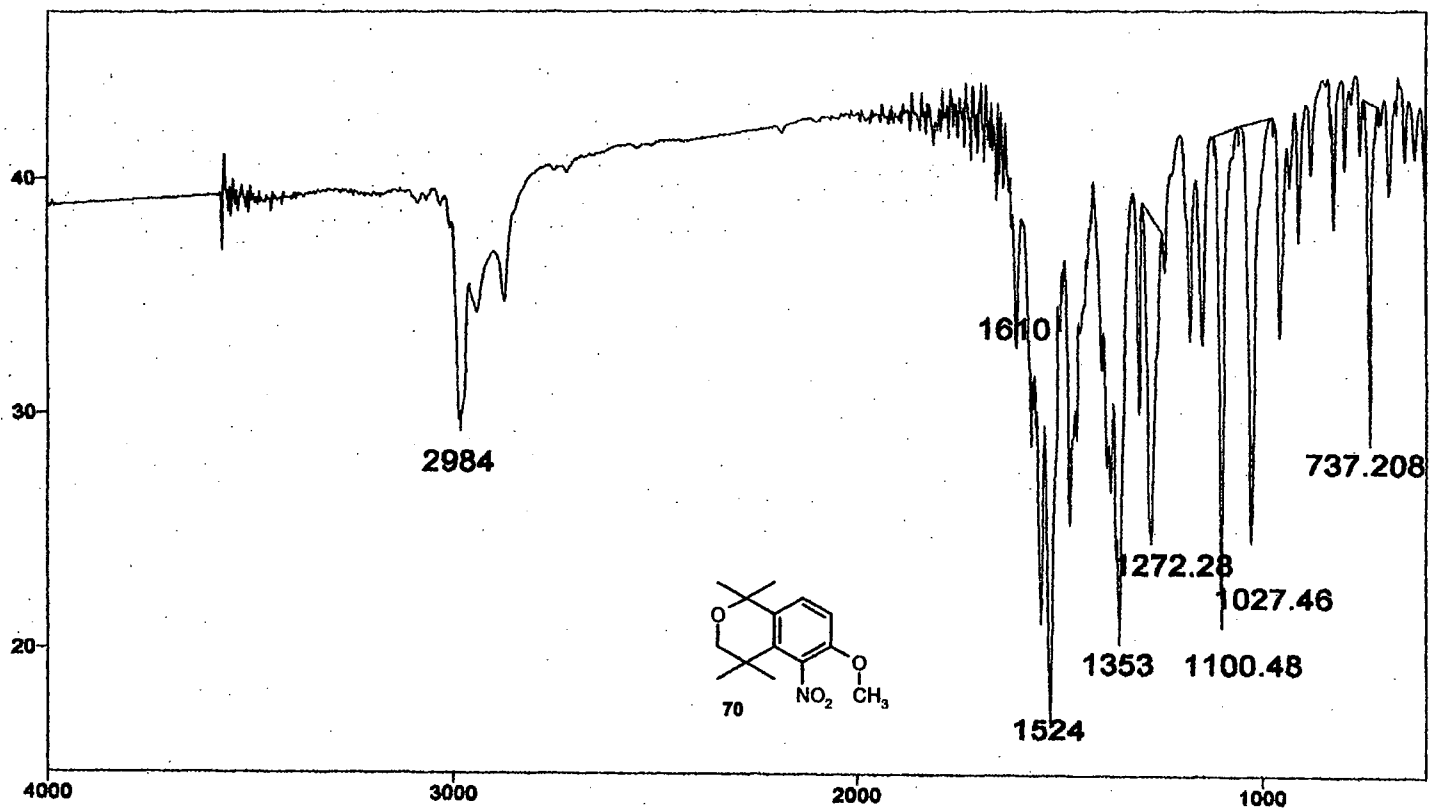
expl std13c

SAMPLE		DEC. & VT	
date	Apr 4 2000	dfrq	300.889
solvent	DMSO	dn	H1
file	exp	dpwr	34
ACQUISITION		dof	0
sfrq	282.335	da	n
tn	F19	dms	w
at	0.809	daf	11764
np	30016	PROCESSING	
sw	18781.7	lb	1.00
fb	10400	wtfile	
bs	16	proc	ft
tpwr	52	fn	not used
pw	3.8		
di	1.000	werr	
tof	0	wexp	wft
nt	1024	wbs	wft
ct	88	wnt	
alock	n		
gain	not used		
FLAGS			
fl	n		
in	y		
dp	y		
DISPLAY			
sp	-37590.6		
wp	17207.7		
vs	21		
sc	0		
wc	250		
hzmw	68.83		
is	500.88		
rfl	98748.4		
rpf	0		
th	5		
ins	100.000		
no	no	ph	



¹⁹F NMR Spectrum of 68

Plate LXXIV



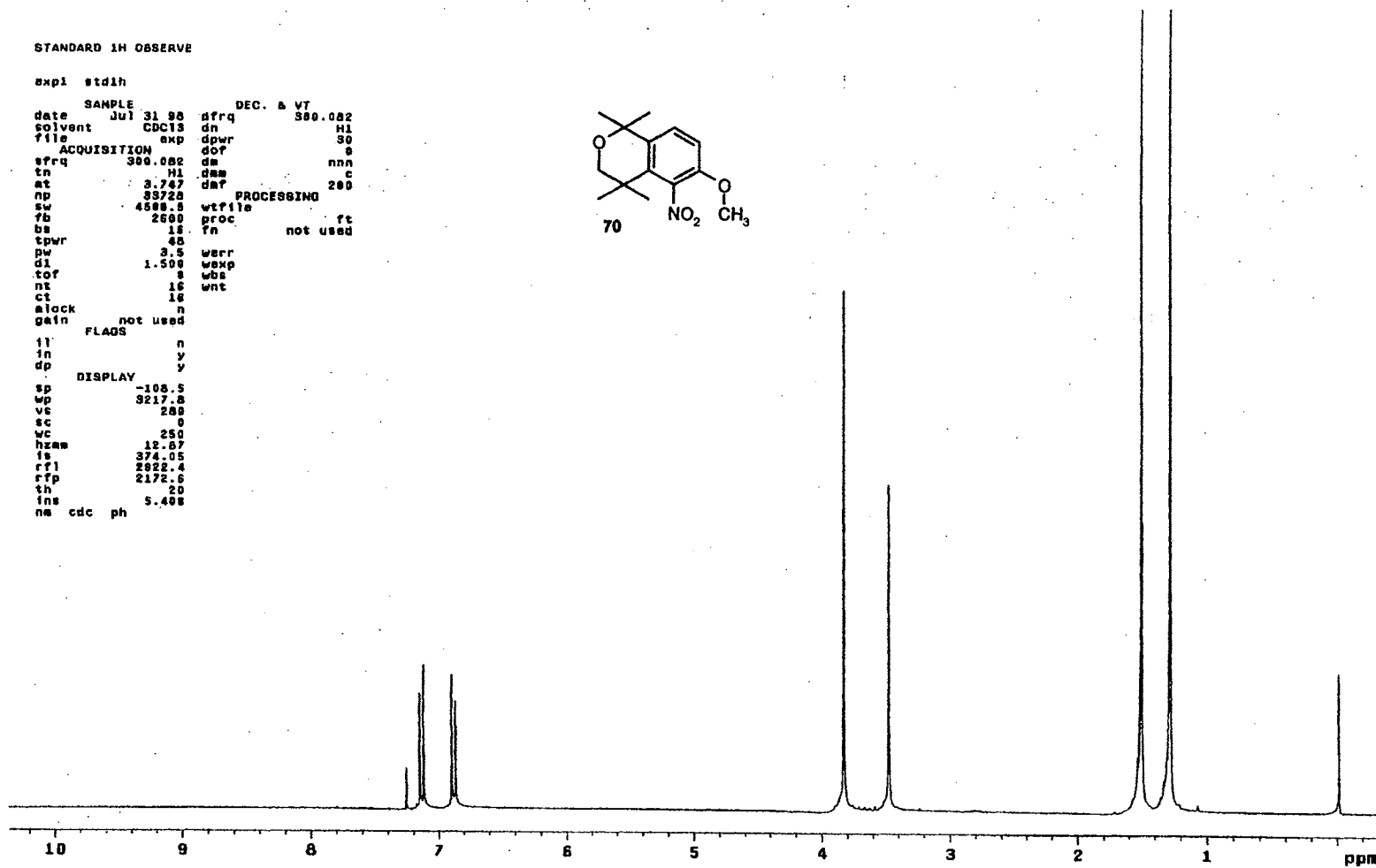
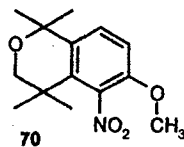
IR Spectrum of 70

Plate LXXV

STANDARD 1H OBSERVE

```

expi stdlh
SAMPLE
date Jul 31 98 dfrq DEC. & VT 500.082
solvent CDC13 dn H1
file exp dpwr 30
ACQUISITION exp dof 8
sfrq 300.082 da nnn c
tn H1 dm c
at 3.747 dat 200
np 83728 PROCESSING
sw 4588.8 wtfile
fb 2600 proc ft
ba 18 tn not used
tpwr 48
pw 3.5 werr
dl 1.500 wexp
tof 8 wbs
nt 18 wnt
ct 18
clock n
gain not used
FLAGS
il n
in y
dp y
DISPLAY
sp -108.5
wp 3217.8
vc 288
sc 0
wc 250
hzaw 12.87
fs 374.05
rf1 2922.4
rfp 2172.6
th 20
ins 5.408
na cdc ph
    
```



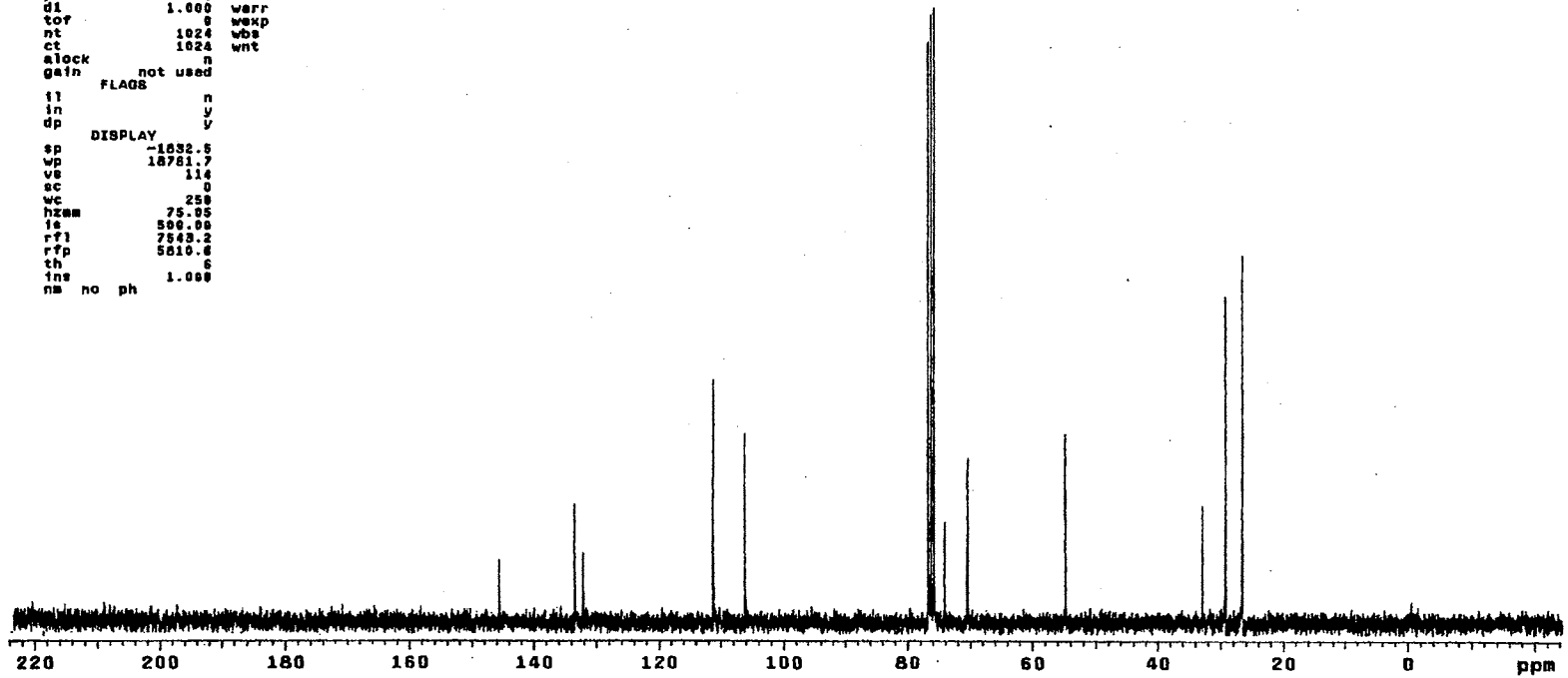
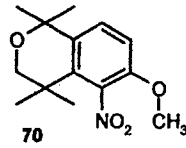
¹H NMR Spectrum of 70

Plate LXXVI

13C OBSERVE

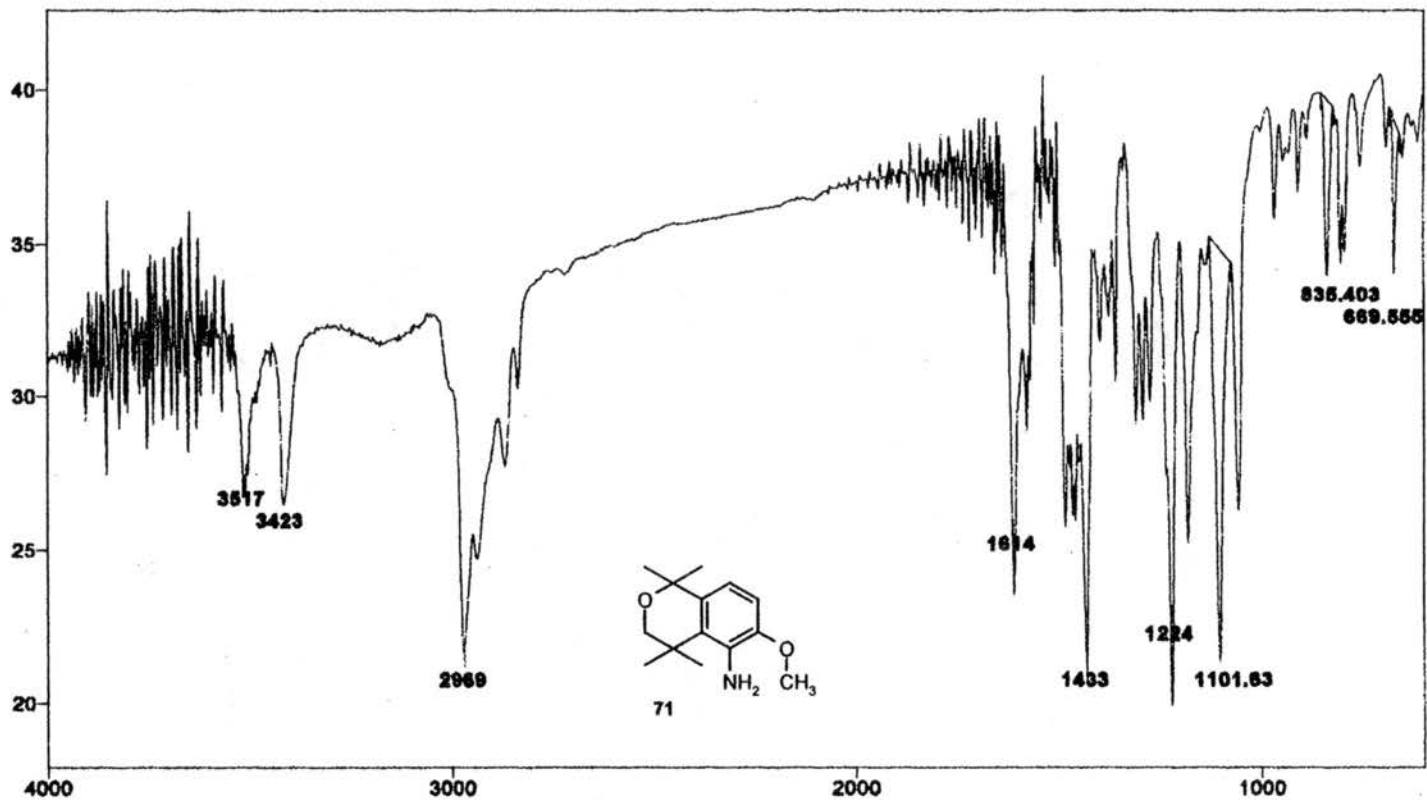
```

exp1 std13c
      SAMPLE          DEC. A VT
date Jul 30 98      dfrq 300.002
solvent CDC13      dn      H1
file ACQUISITION  exp      dpwr 34
      ACQUISITION  exp      dot  0
sfrq 75.463      dm      nyv
tn      C13      dnm      w
at      0.800      dmf      11704
np      30015      PROCESSING
sw      18781.7      lb      1.00
fb      10400      wfile
bs      18      proc      ft
tpwr 52      fn      not used
pw      3.0
di      1.000      werr
tof      8      wexp
nt      1024      wbs
ct      1024      wnt
slock      not used
gain      not used
      FLAGS
fl      n
in      y
dp      y
      DISPLAY
sp      -1632.5
wp      18781.7
ve      114
sc      0
wc      250
hzam 75.05
le      500.00
rfl 7543.2
rff 5610.8
th      5
ins 1.000
nm no ph
    
```



¹³C NMR Spectrum of 70

Plate LXXVII

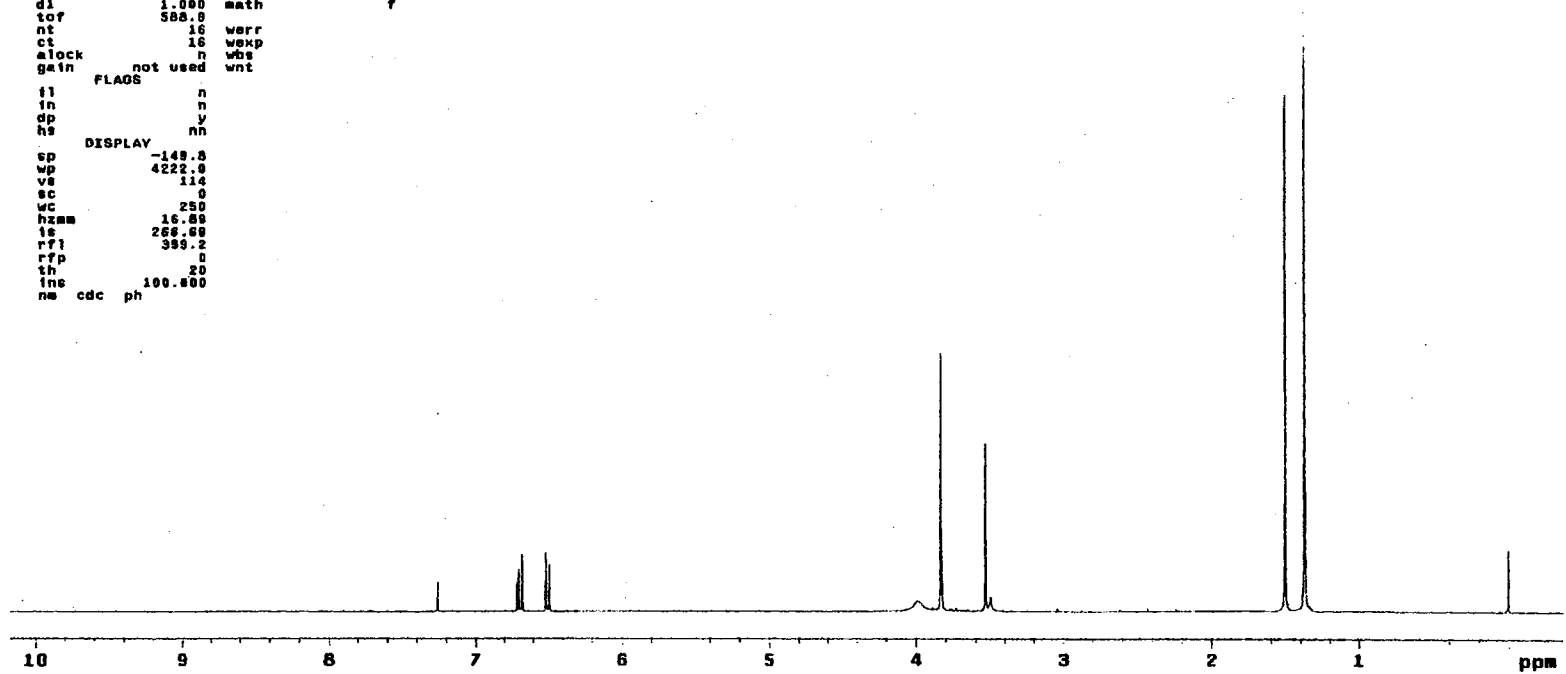
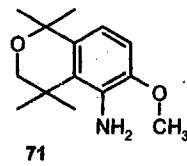


IR Spectrum of 71

Plate LXXVIII

```

Std. 1H Inova400
expl stdih
SAMPLE DEC. & VT
date Aug 5 98 dfrq 399.923
solvent CDC13 dn H1
file exp dpwr 30
ACQUISITION dot 0
sfrq 399.924 dm nnn
tn H1 dm c
at 2.731 dmf 200
np 32768 dseq
sw 6000.2 dres 1.0
fb 3000 homo n
bs 16 PROCESSING
ss 2 wfile
tpwr 52 proc ft
pw 6.6 fn not used
d1 1.000 math f
tor 588.0
nt 16 werr
ct 16 wexp
alock n wbs
gain not used wnt
FLAOS
f1 n
f2 n
dp y
hs nn
DISPLAY
sp -149.0
wp 4222.0
vs 114
sc 0
wc 250
hzam 16.00
ts 268.00
rf1 399.2
rfp 0
th 20
lne 100.000
na cdc ph
    
```



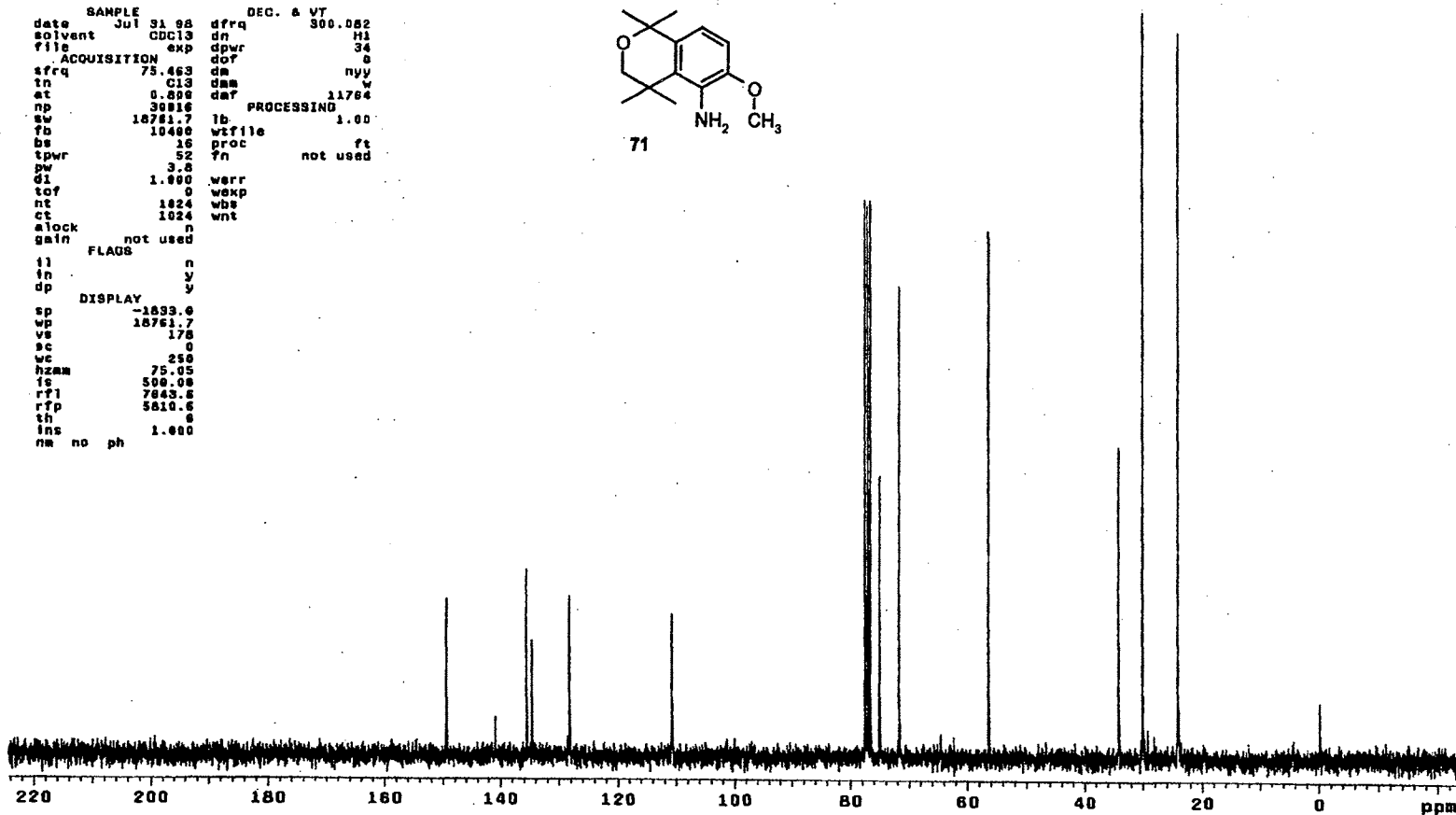
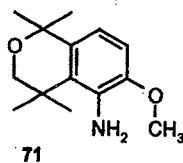
¹H NMR Spectrum of 71

Plate LXXIX

13C OBSERVE

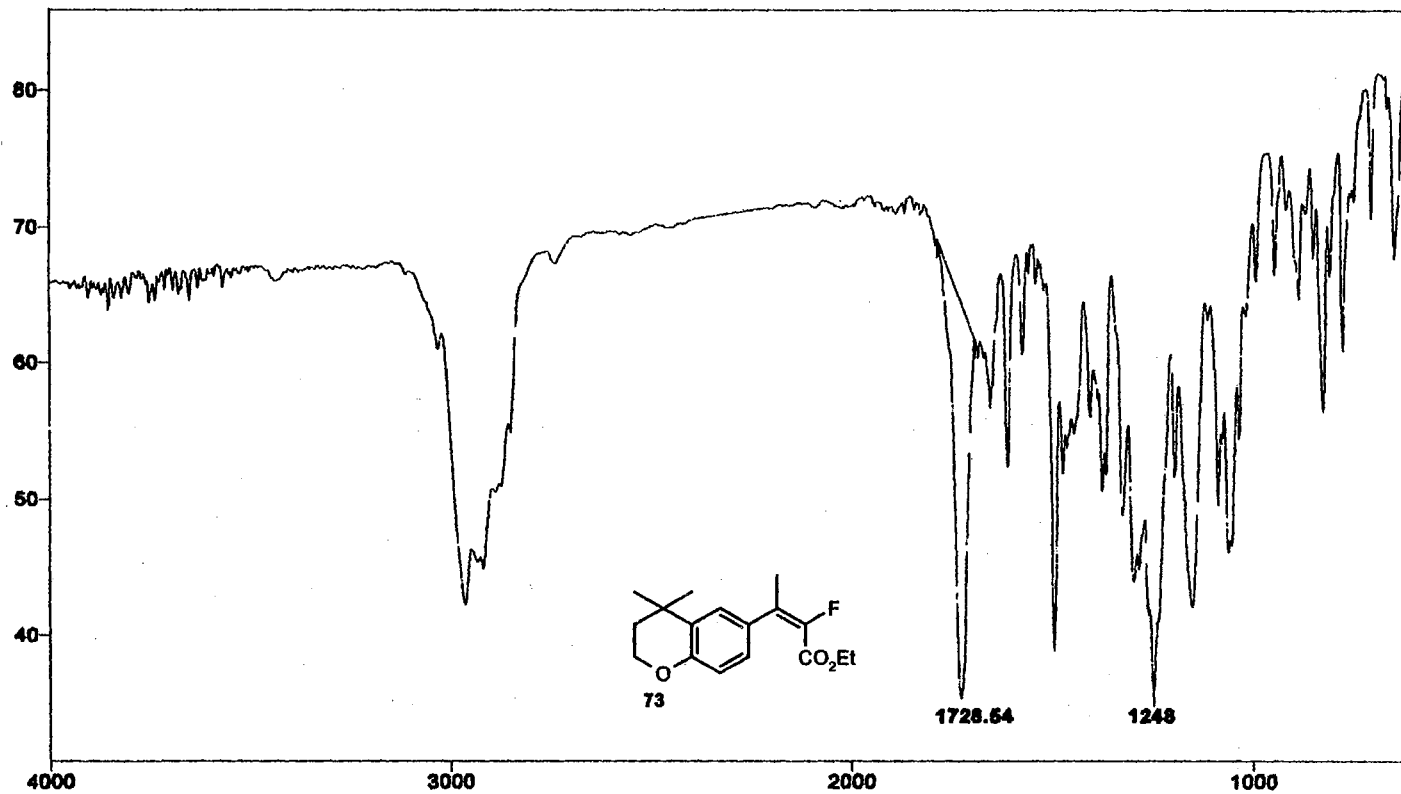
```

expl  std13c
SAMPLE
date  Jul 31 98  dfrq  300.082
solvent  CDCl3  dn  H1
file  exp  dpwr  34
ACQUISITION  exp  dof  0
sfrq  75.463  dm  nyy
tn  C13  dam  w
at  0.898  daf  11784
np  30816  PROCESSING
sw  18761.7  lb  1.00
fb  10400  wf1file
bs  16  proc
tpwr  52  fn  not used
pw  3.8
d1  1.000  warr
tof  0  wexp
nt  1024  wbs
ct  1024  wnt
alock  n
gain  not used
FLAGS
f1  n
fn  y
dp  y
DISPLAY
sp  -1033.0
wp  18761.7
vs  170
sc  0
wc  250
hzam  75.05
is  500.00
rf1  7845.8
rfp  8810.6
th  0
ins  1.000
na  no  ph
    
```



¹³C NMR Spectrum of 71

Plate LXXX



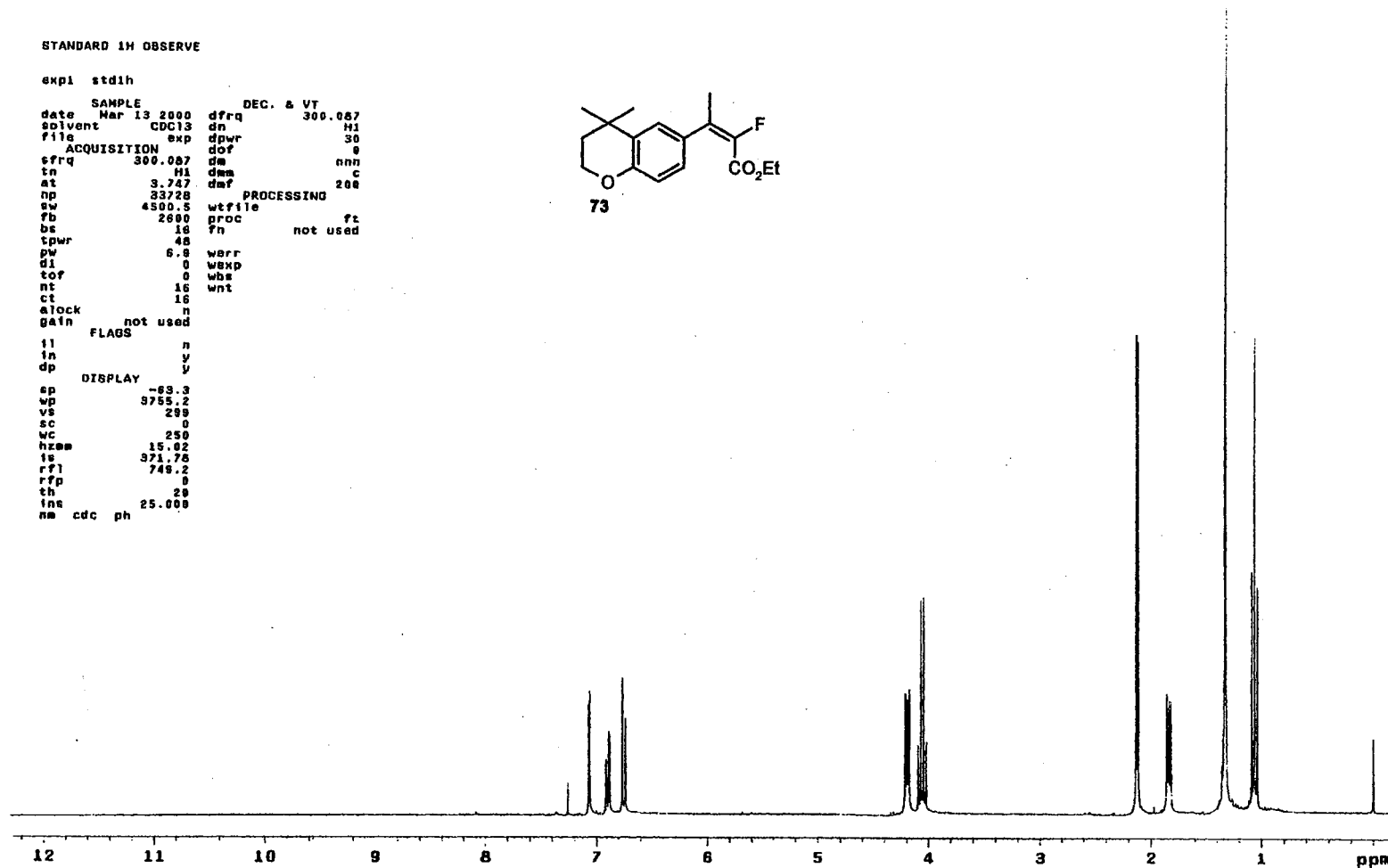
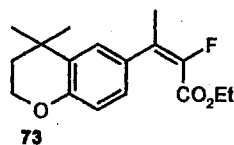
IR Spectrum of 73

Plate LXXXI

STANDARD 1H OBSERVE

```

expt stdih
SAMPLE
date Mar 13 2000 dfrq DEC. & VT 300.067
solvent CDC13 dn H1
file exp dpwr 30
ACQUISITION exp dof 9
sfrq 300.067 dm nnn c
tn H1 dm c
at 3.747 dmf 208
np 83728 PROCESSING
sw 4500.5 wtf file
fb 2680 proc ft
bs 16 fn not used
tpwr 48
pw 6.8 werr
d1 0 wexp
tof 0 wbs
nt 16 wnt
ct 16
alock n
gain not used
FLAGS
fl n
in y
dp y
DISPLAY
ep -63.3
wp 9755.2
vs 289
sc 0
wc 250
hzam 15.82
fs 971.76
rf1 749.2
rfp 0
th 29
ins 25.000
nm cdc ph
    
```



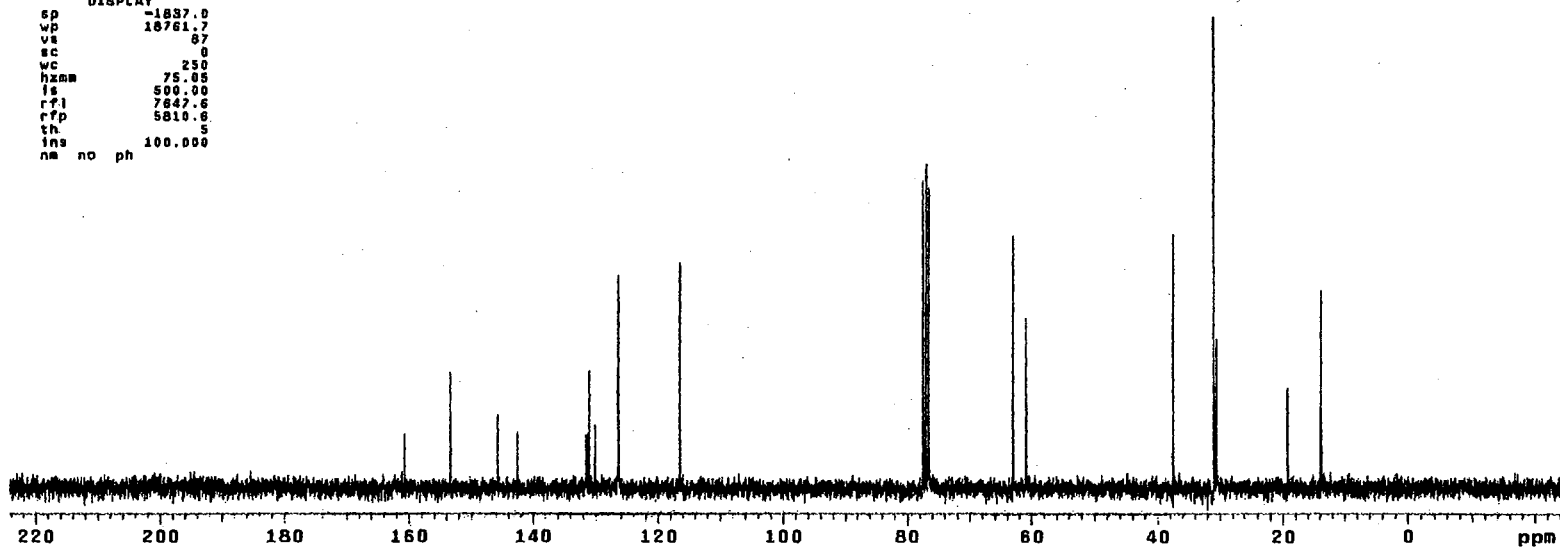
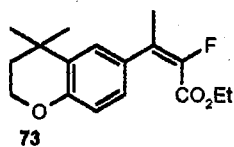
¹H NMR Spectrum of 73

Plate LXXXI

¹³C OBSERVE

exp1 std13c

date	Jan 24 2000	dfrq	DEC. & VT	300.087
solvent	CDCl3	dn		H1
file	exp	dpwr		34
ACQUISITION				
sfrq	75.464	da		0
tn	C13	dm		VVY
at	0.800	dmg		W
np	30016	dpr	PROCESSING	11764
sw	18761.7	lb		1.00
fb	10400	wtfile		
bs	16	proc		ft
tpwr	52	fn		not used
pw	3.6			
d1	1.000	werr		wft
tof	0	wexp		wft
nt	1024	wbs		wft
ct	256	wnt		
clock				
gain	not used			
FLAGS				
fl		n		
fn		y		
dp		y		
DISPLAY				
sp	-1837.0			
wp	18761.7			
vs	87			
sc	0			
wc	250			
hznm	75.05			
fs	500.00			
rfl	7847.6			
rfp	5810.6			
th	S			
ins	100.000			
nm	no	ph		



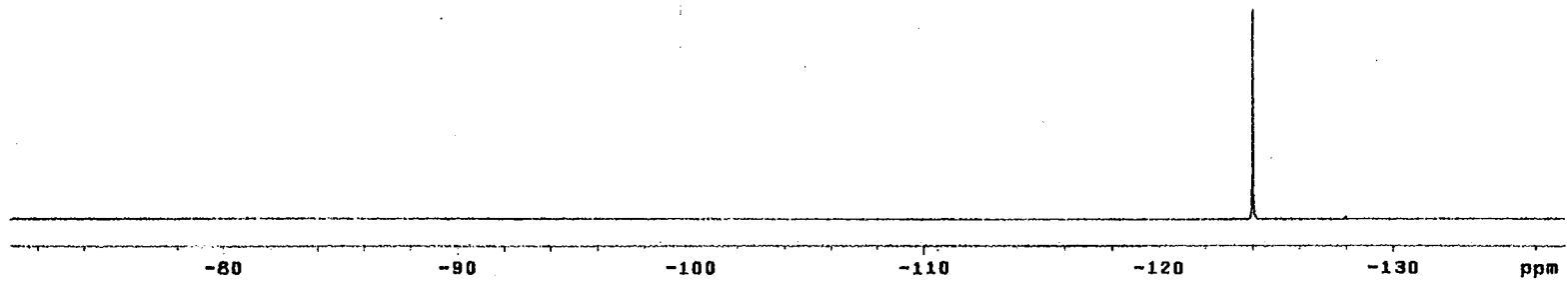
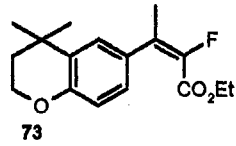
¹³C NMR Spectrum of 73

Plate LXXXIII

13C OBSERVE

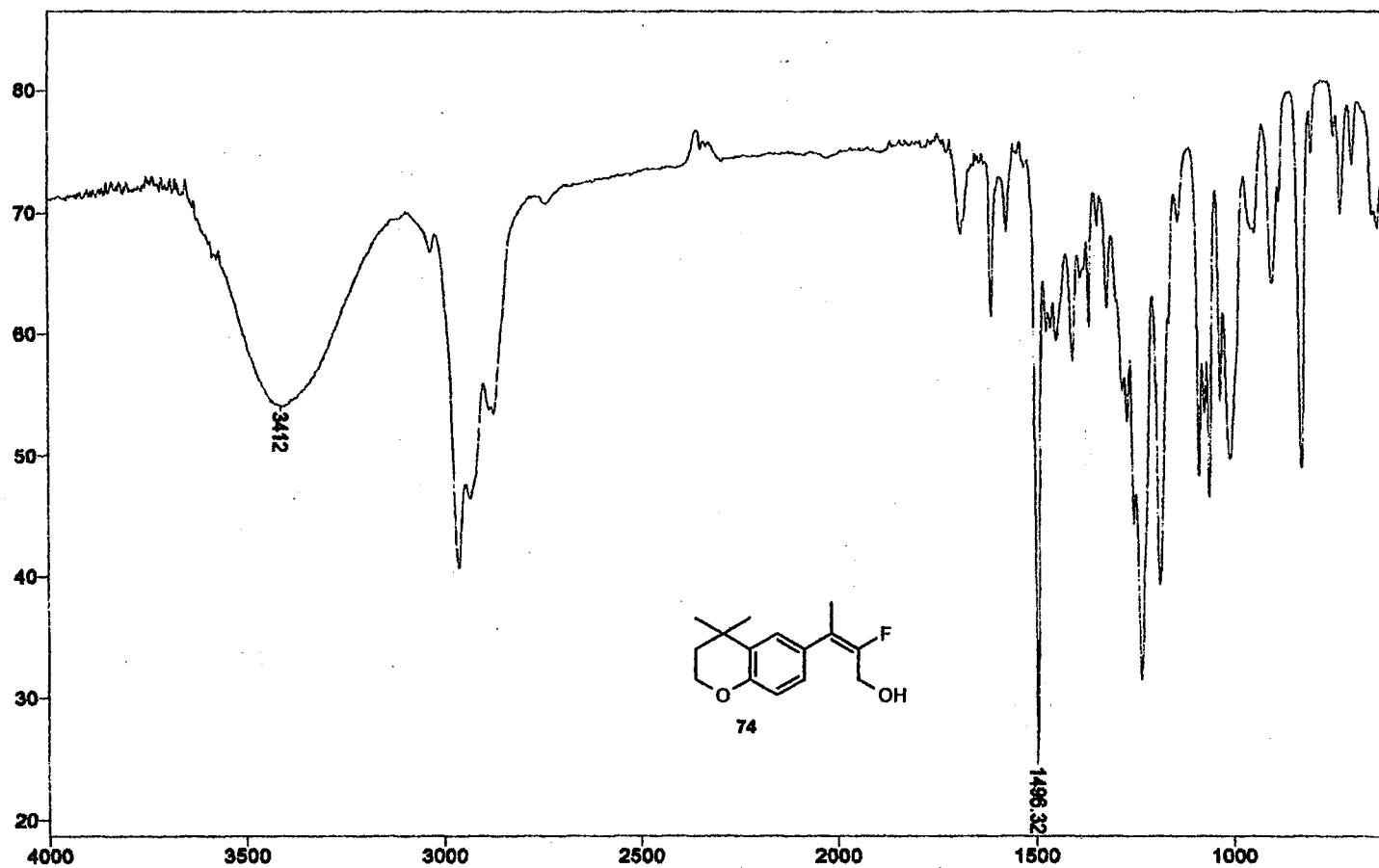
```

exp1 std13c
SAMPLE
date Jan 24 2000 dfrq DEC. & VT 309.087
solvent CDC13 dn H1
file exp dpwr 34
ACQUISITION dof 0
sfrq 282.333 dm nnn
tn F15 dms w
at 0.500 dm7 11764
np 30918 PROCESSING
sw 18761.7 lb 1.00
fb 10400 wtfile
bs 15 pproc ft
tpwr 52 7n not used
pw 3.5
di 1.000 werr
tof 0 wexp wft
nt 1024 wbs wft
ct 32 wnt
slock n
gain not used
FLAGS
ij n
ih y
dp y
DISPLAY
sp -38748.2
wp 18761.7
vs 39
sc 0
wc 250
hzmm 75.05
is 500.00
rf1 38748.2
rfp 0
th 20
ins 100.000
nm no ph
    
```



¹⁹F NMR Spectrum of 73

Plate LXXXIV



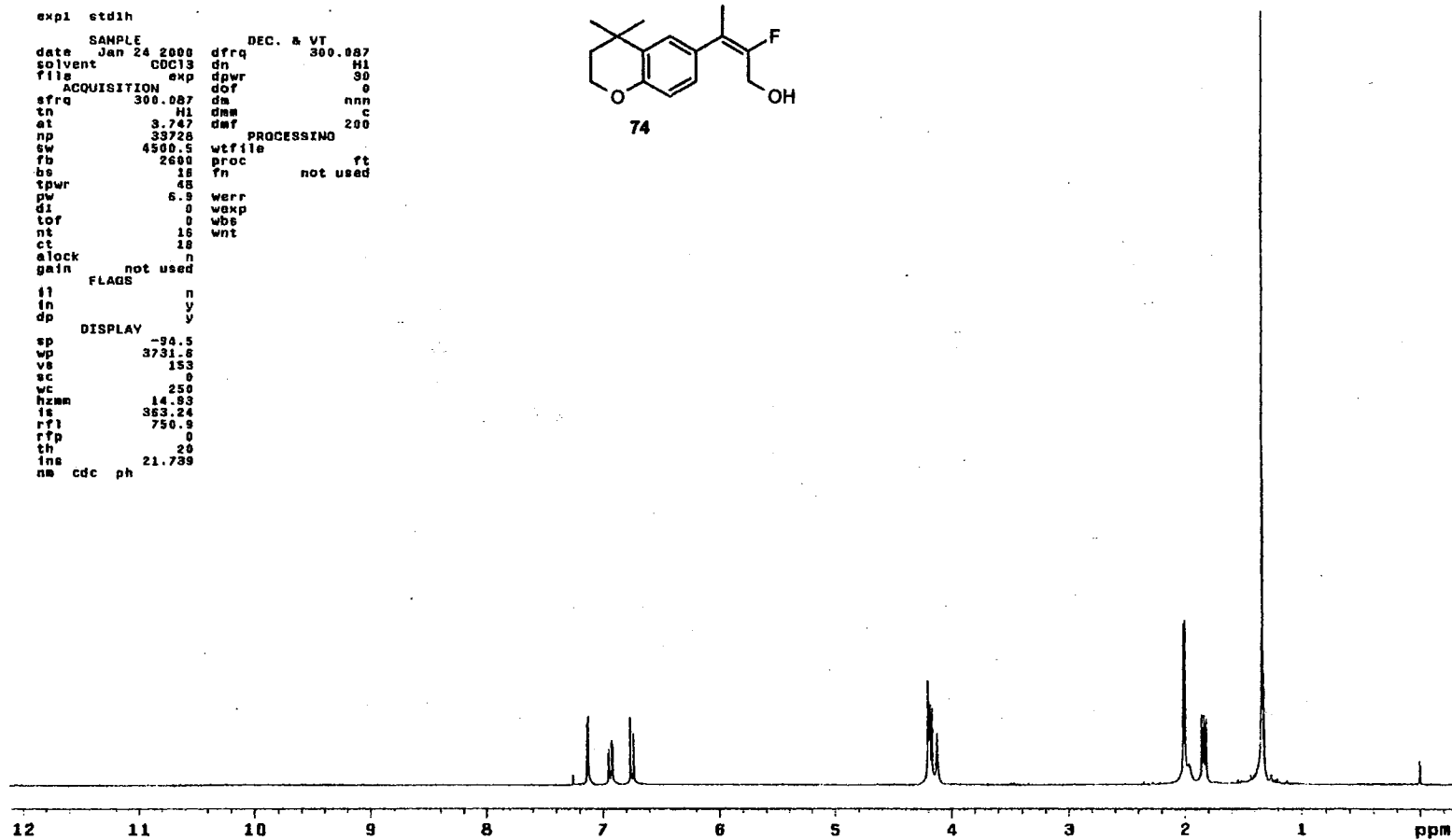
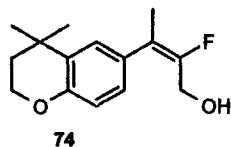
IR Spectrum of 74

Plate LXXXV

STANDARD 1H OBSERVE

```

exp1  etd1h
SAMPLE
date  Jan 24 2000  dfrq  300.007  DEC. & VT
solvent  CDCl3  dn  H1
file  exp  dpwr  30
ACQUISITION  dof  0
sfrq  300.007  da  nnn
tn  H1  dmw  c
at  3.747  dmf  200
np  33720  PROCESSING
sw  4500.5  wtfile
fb  2600  proc  ft
bs  18  fn  not used
tpwr  48
pw  6.9  werr
di  0  wexp
tof  0  wbs
nt  16  wnt
ct  18
alock  n
gain  not used
FLAGS
i1  n
in  y
dp  y
DISPLAY
sp  -30.5
wp  3731.8
vs  153
sc  0
wc  250
hzmm  14.93
is  363.24
rf1  750.9
rfp  0
th  20
ins  21.739
nm  cdc  ph
    
```



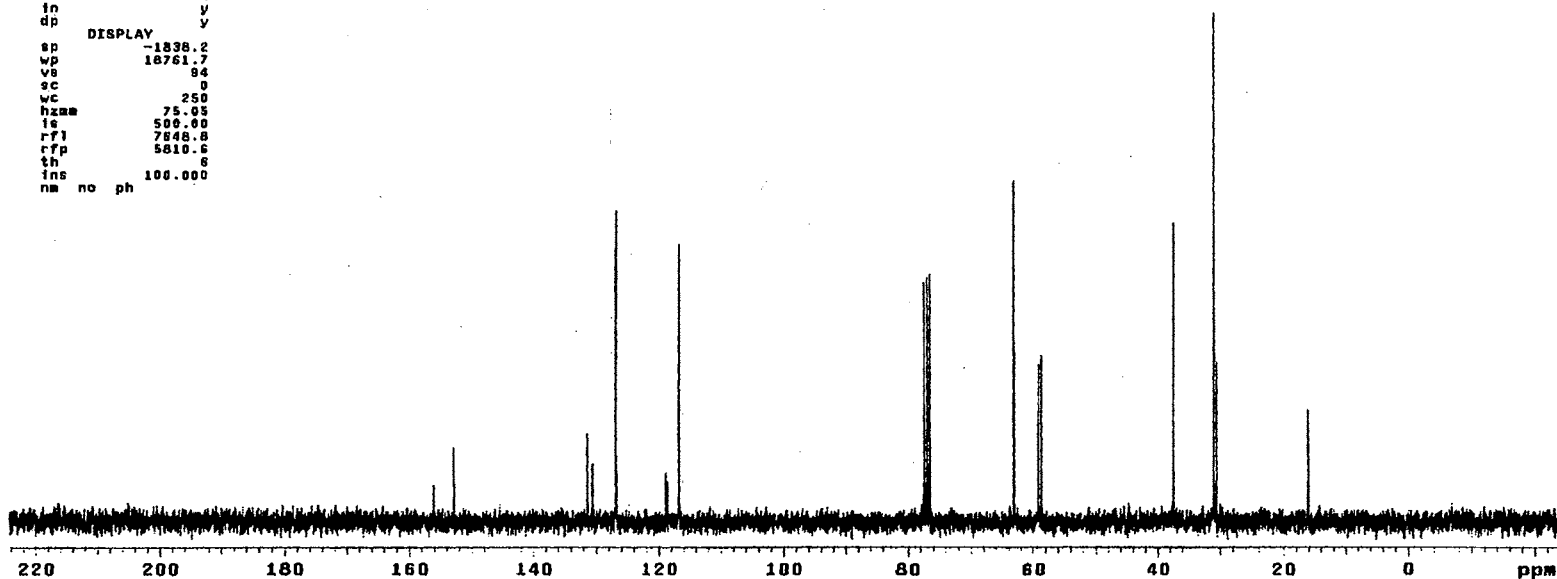
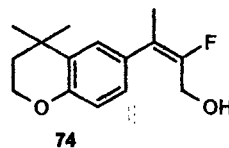
¹H NMR Spectrum of 74

Plate LXXXVI

¹³C OBSERVE

exptl std13c

date	Jan 24 2000	dfrq	DEC. & VT	300.007
solvent	CDC13	dn		H1
file	exp	dpwr		36
		dof		0
ACQUISITION				
sfrq	75.464	da		yvy
tn	C13	dsm		w
at	0.800	daf		11764
np	30016	PROCESSING		
sw	18761.7	lb		1.00
fb	10400	wtfile		
bs	16	proc		ft
tpwr	52	fn		not used
pw	3.0			
d1	1.000	werr		wft
tor	0	wexp		wft
nt	1824	wbs		wft
ct	128	wnt		
alock		s		
gain	not used			
FLAGS				
tl		n		
in		y		
dp		y		
DISPLAY				
sp	-1838.2			
wp	18761.7			
vs	94			
sc	0			
wc	250			
hzm	75.03			
is	500.00			
rfl	7848.8			
rff	5810.6			
th	8			
ins	100.000			
na	no	ph		



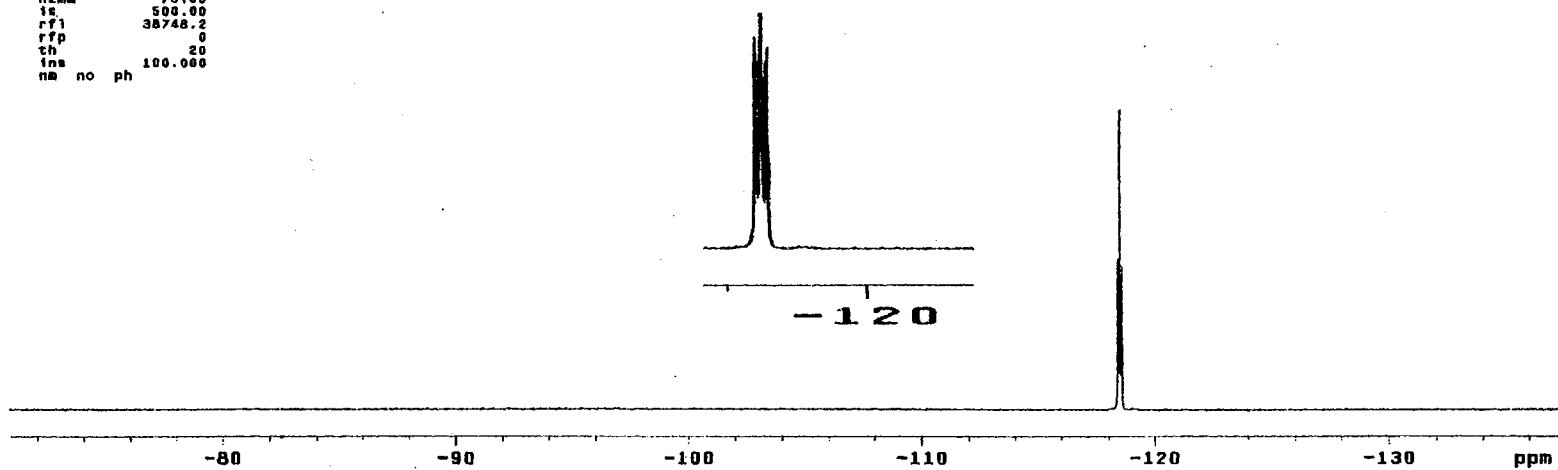
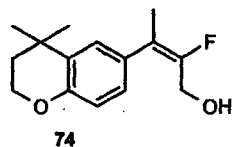
¹³C NMR Spectrum of 74

Plate LXXXVII

13C OBSERVE

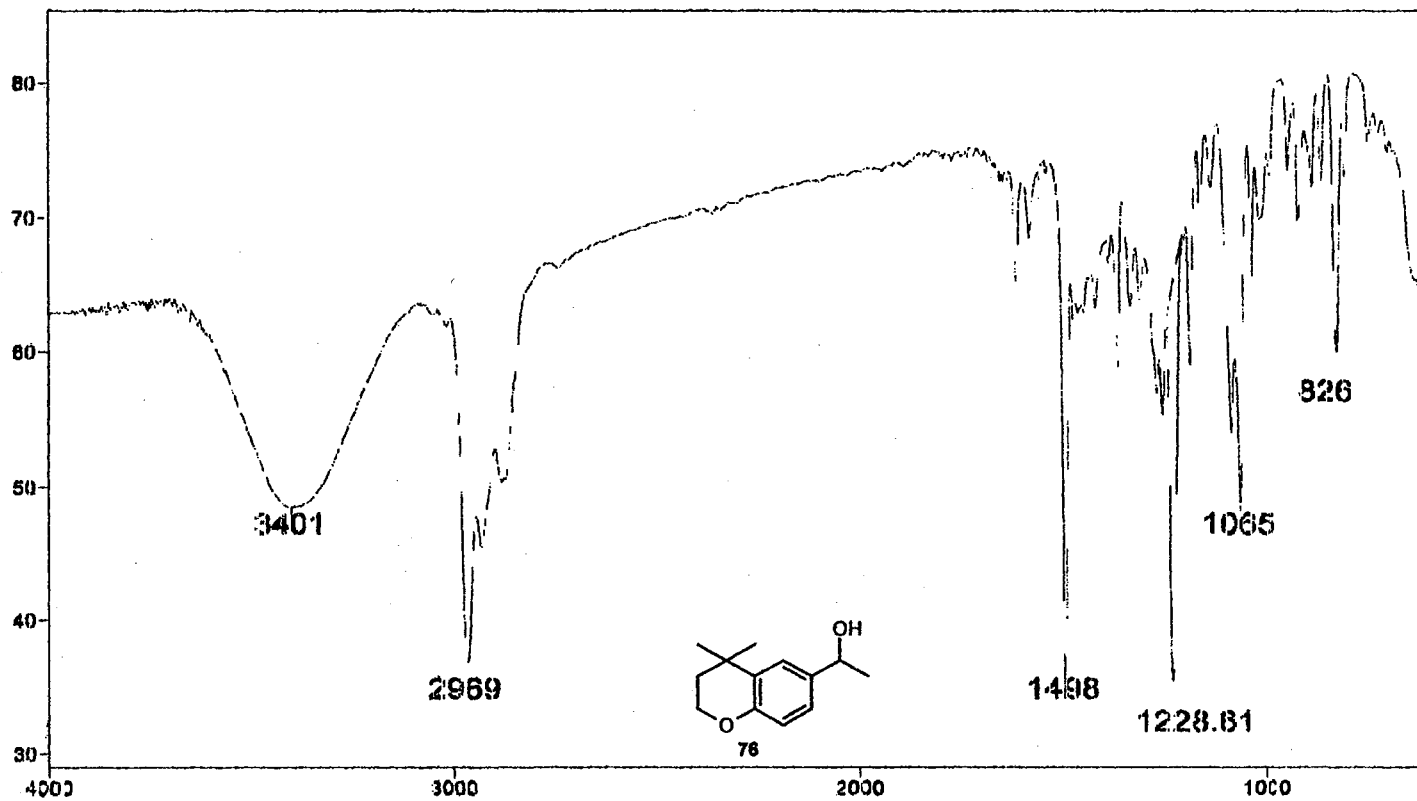
```

expt  std13c
SAMPLE
date  Jan 24 2000  dfrq  DEC. & VT  300.087
solvent  CDCl3  dn  M1
file  exp  dpwr  34
ACQUISITION  dbf  0
sfrq  282.333  ds  nnn
tn  F19  dsm  w
at  0.800  dmf  11764
np  30016  PROCESSING
sw  18781.7  lb  1.00
yb  10480  wtfile
bs  16  proc  ft
tpwr  52  fn  not used
pw  3.8
d1  1.000  werr
tof  9  wexp  wft
nt  1024  wbs  wft
ct  48  wnt
alock  n
gain  not used
FLAGS
f1  n
in  y
dp  y
DISPLAY
sp  -38748.2
wp  18781.7
vs  55
sc  0
wc  250
hzmm  75.05
is  500.00
rf1  38748.2
rfp  0
th  20
ina  100.000
na  no  ph
    
```



¹⁹F NMR Spectrum of 74

Plate LXXXVIII



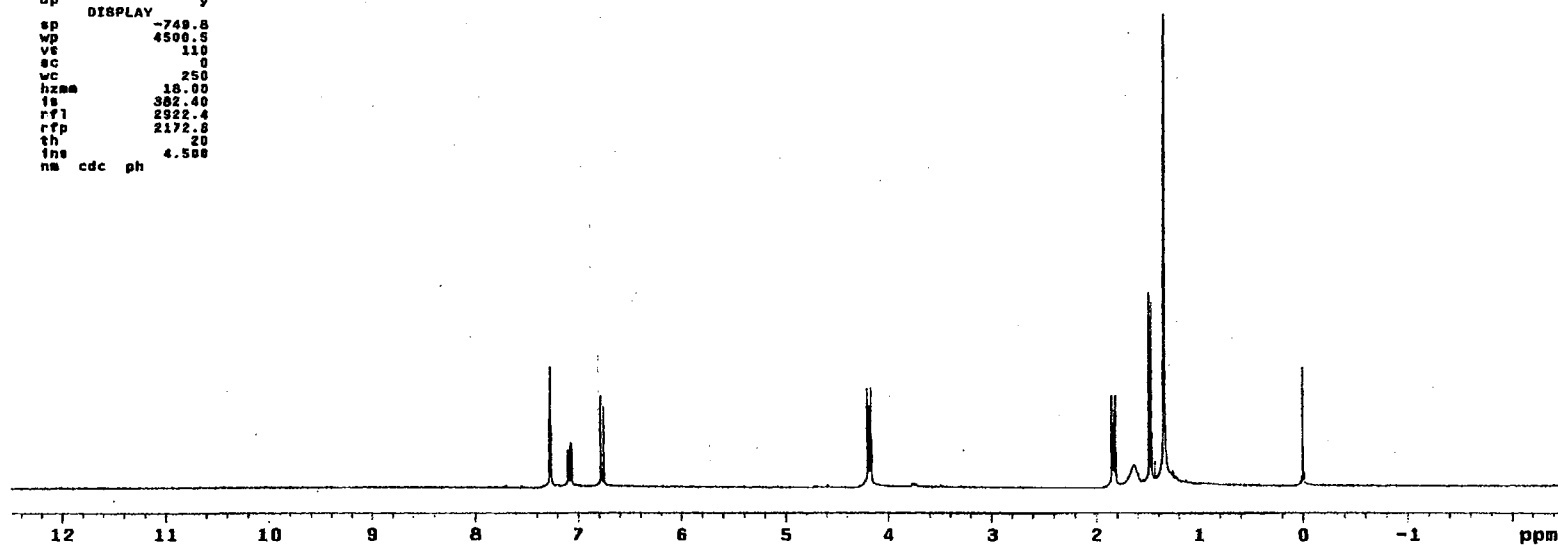
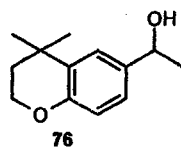
IR Spectrum of 76

Plate LXXXIX

STANDARD 1H OBSERVE

```

expl stdih
SAMPLE
date Aug 18 98 dfrq DEC. & VT 300.082
solvent CDC13 dn HI
file /export/home/~ dpwr 30
Klucik/alcohol5 dof 0
ACQUISITION da nnn
sfrq 300.082 dem c
tn HI dmf 200
at 3.001 PROCESSING
np 27008 wtfile
sw 4500.5 proc ft
fb 2600 fn not used
bs 18
tpwr 48 werr
pw 4.5 wexp
dI 1.500 wbp
tof 0 wnt
nt 18
ct 18
elock n
gain not used
FLAOS
il n
in y
dp y
DISPLAY
sp -749.8
wp 4500.5
vs 110
sc 0
wc 250
hz00 18.00
fs 382.40
rf1 2922.4
rfp 2172.8
th 20
fns 4.500
na cdc ph
    
```



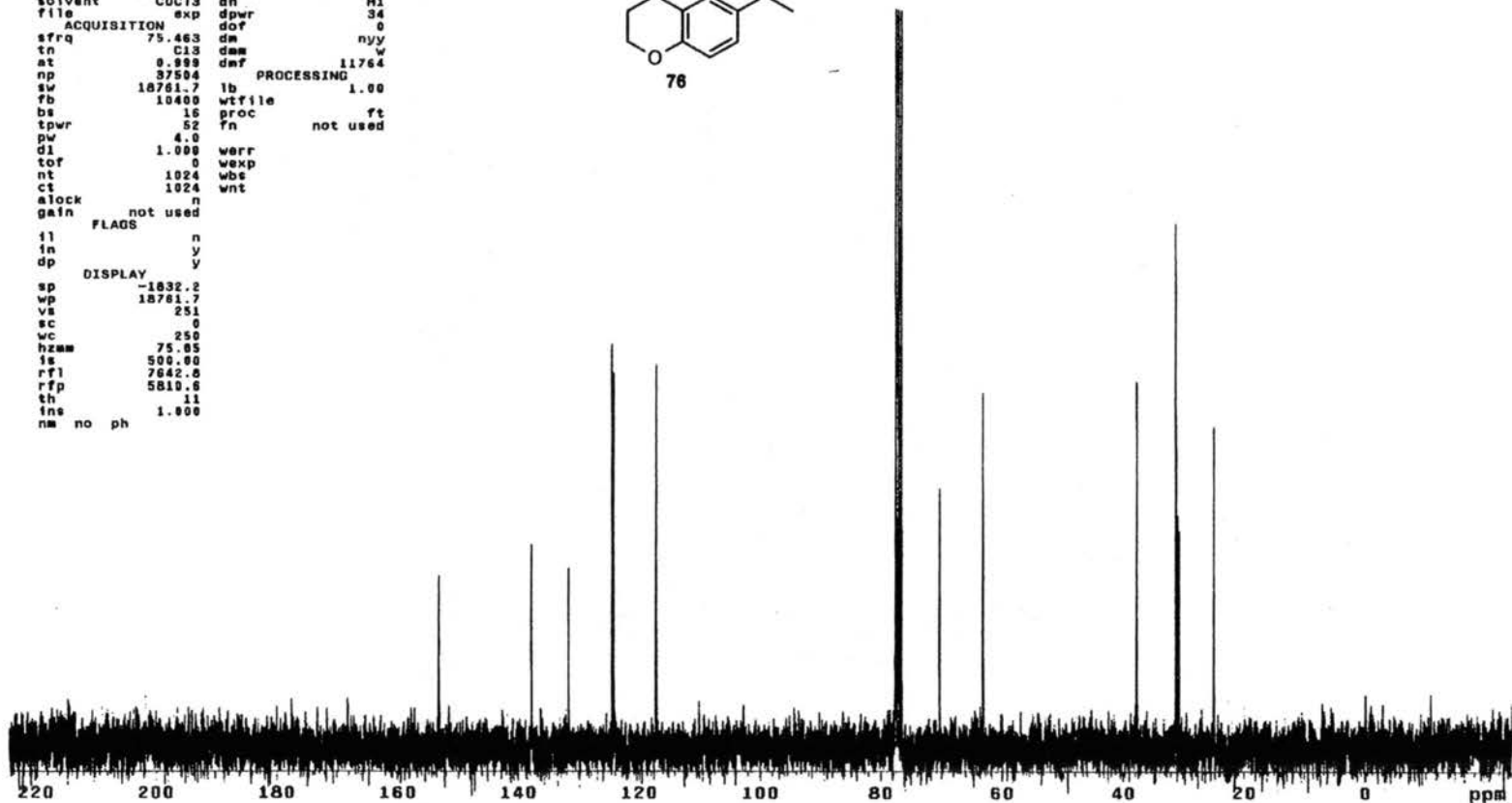
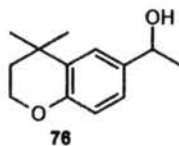
¹H NMR Spectrum of 76

Plate XC

¹³C OBSERVE

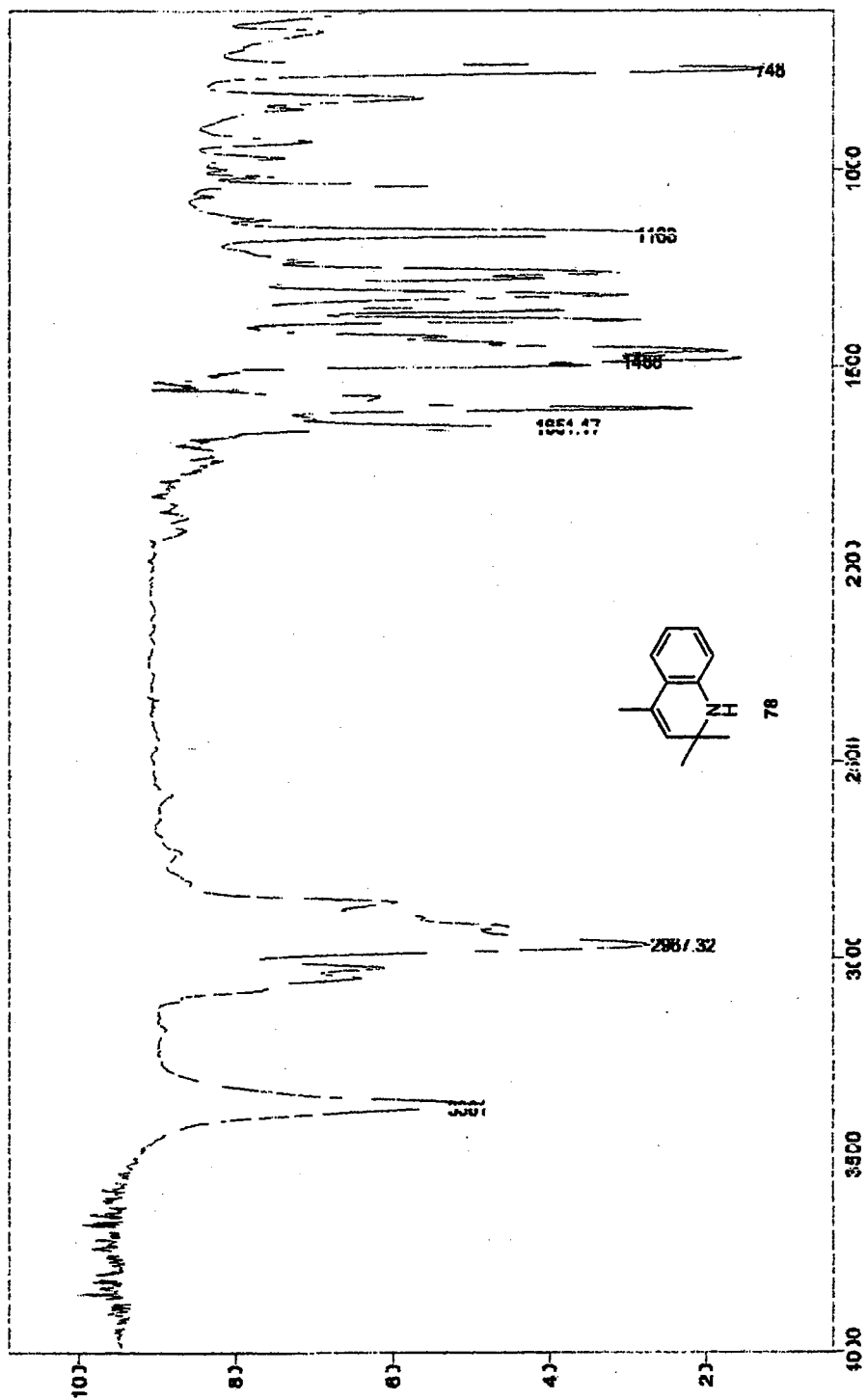
exp1 std13c

data	Aug 18 98	dfrq	300.082
solvent	CDC13	dn	M1
file	exp	dpwr	34
ACQUISITION			
sfrq	75.463	dm	nyy
tn	C13	dsw	w
at	0.999	dwt	11764
np	37504	PROCESSING	
sw	18761.7	lb	1.00
fb	10400	wtfile	
bs	16	proc	ft
tpwr	52	fn	not used
pw	4.0		
d1	1.000	werr	
tor	0	wexp	
nt	1024	wbs	
ct	1024	wnt	
alock	n		
gain	not used		
FLAGS			
i1	n		
in	y		
dp	y		
DISPLAY			
sp	-1832.2		
wp	18761.7		
vs	251		
sc	0		
wc	250		
hzam	75.85		
is	500.00		
rfl	7642.0		
rfp	5810.8		
th	11		
ins	1.000		
nm	no ph		



¹³C NMR Spectrum of 76

Plate XCI



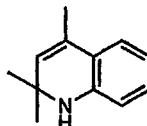
IR Spectrum of 78

Plate XCII

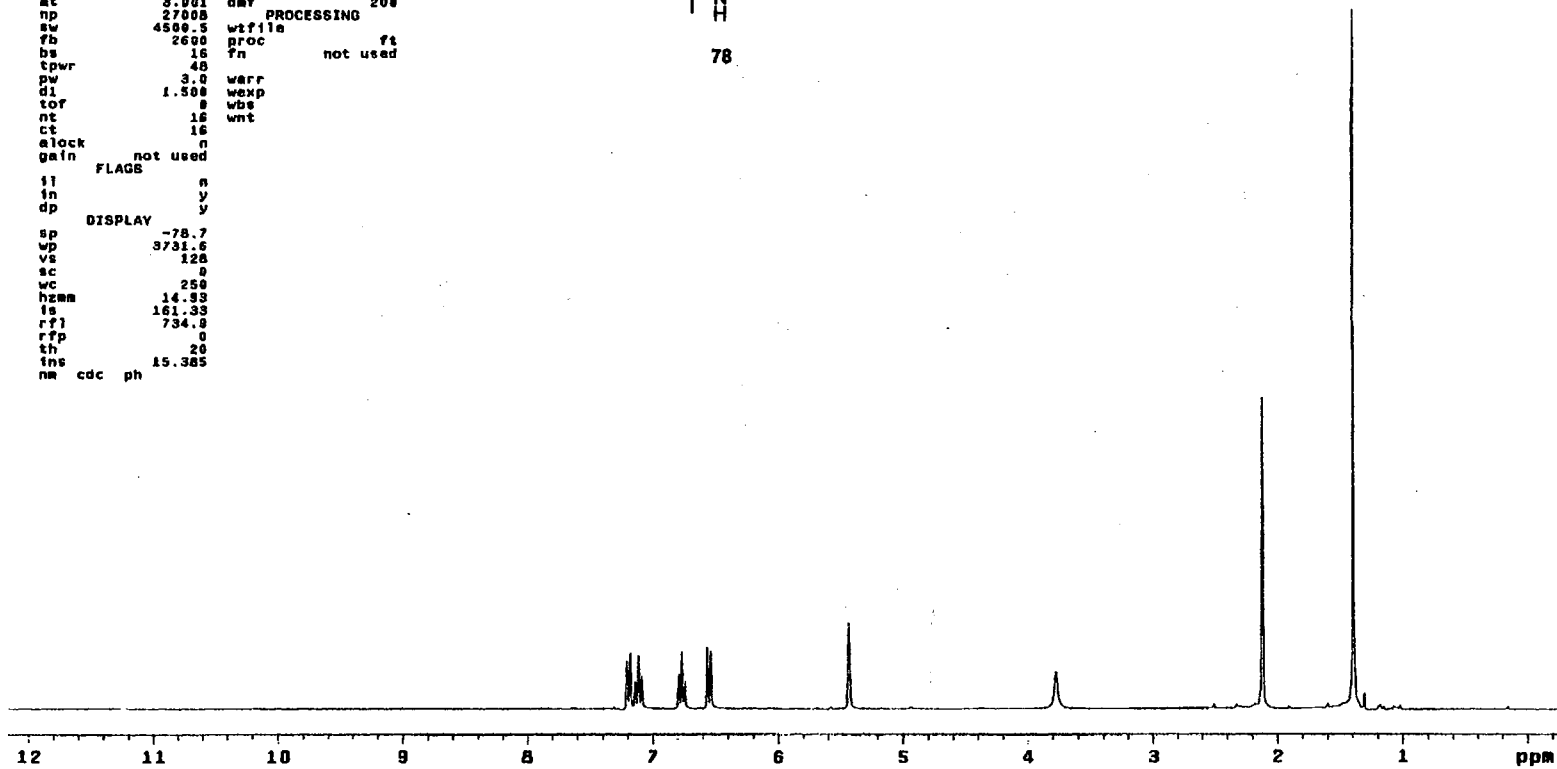
STANDARD 1H OBSERVE

```

expi std1h
SAMPLE
date Feb 22 1988 dfrq DEC. A VT 300.087
solvent CDCl3 dn H1
file exp dpr 30
ACQUISITION dof 8
sfrq 300.087 da nnp
tn H1 dm c
at 3.001 da7 208
np 27008 PROCESSING
sw 4500.5 wifile
fb 2600 proc ft
bs 16 fn not used
tpwr 48
pw 3.0 warr
d1 1.500 wexp
tor 8 wbs
nt 16 wnt
ct 16
clock n
gain not used
FLAGS
il n
in y
dp y
DISPLAY
sp -78.7
wp 3731.6
vs 128
sc 0
wc 250
hzmm 14.33
fs 161.33
rfj 734.8
rtp 0
th 20
ins 15.385
nm cdc ph
    
```



78



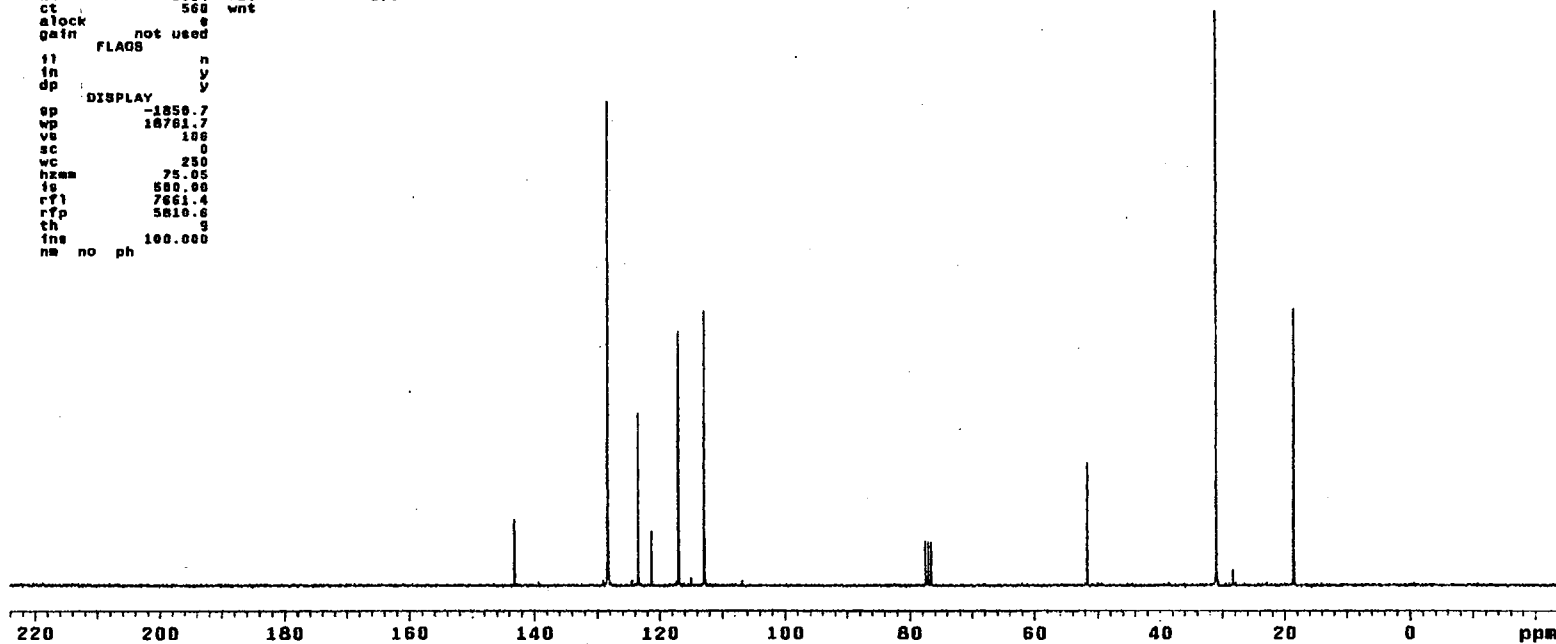
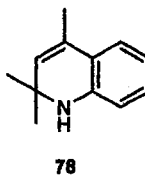
¹H NMR Spectrum of 78

Plate XCIII

13C OBSERVE

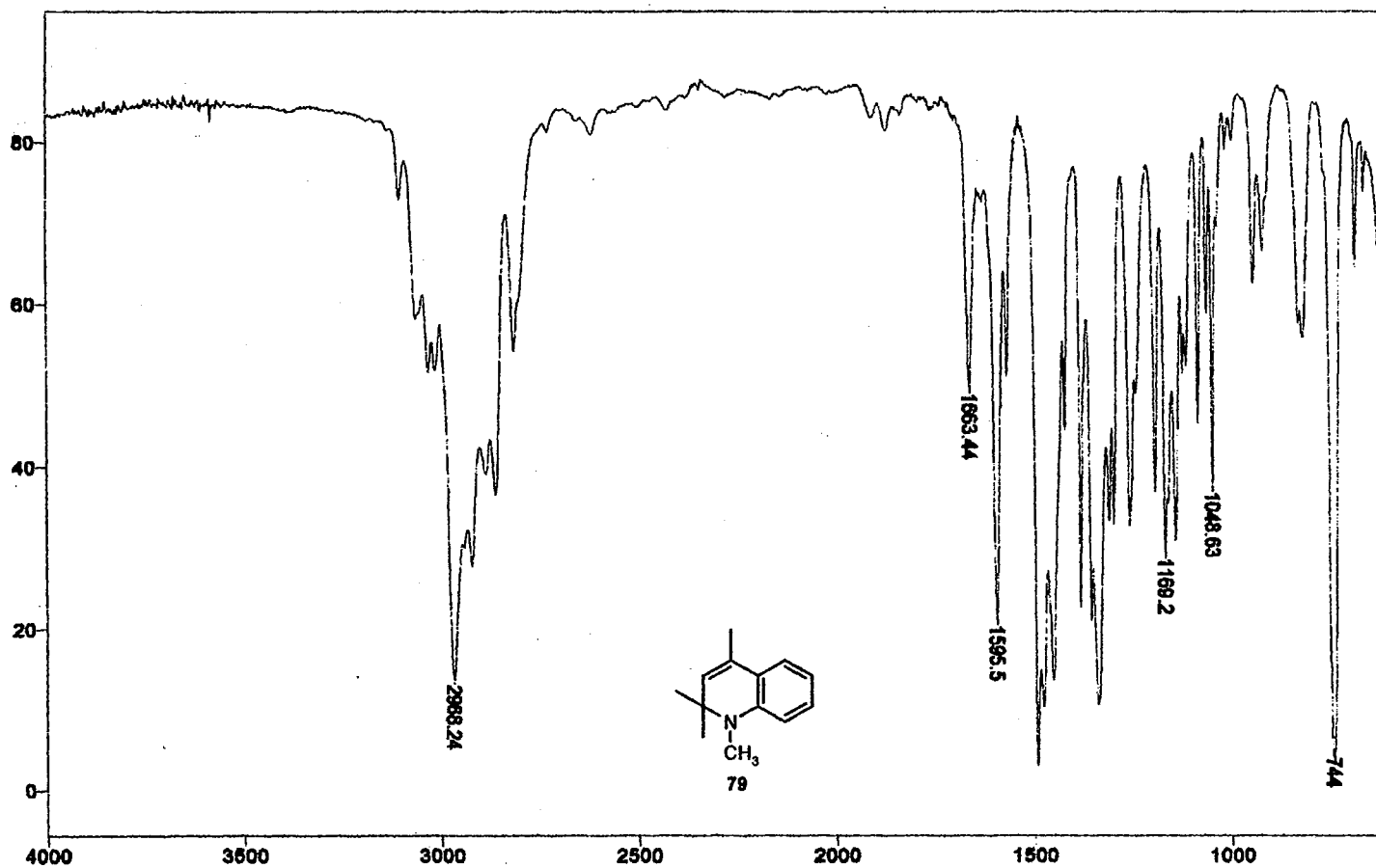
```

expl  std13c
SAMPLE
date  Feb 22 1999  dfrq  300.087
solvent  CDC13  dn  H1
file  exp  dpwr  34
ACQUISITION  exp  dof  0
sfrq  75.464  dm  nvy
tn  C13  dms  w
at  0.800  dmf  11764
np  30016  PROCESSING
sw  18761.7  lb  1.00
fb  10400  wtfile
bs  16  proc  ft
tpwr  52  fn  not used
pw  3.8
si  1.000  warr
tof  0  wexp  wft
nt  1024  wbs  wft
ct  568  wnt
alock  not used  e
gain  not used  s
FLAGS  n
ii  n
in  y
dp  y
DISPLAY
sp  -1850.7
wp  18761.7
vs  108
sc  0
wc  250
hzam  75.05
is  580.00
rfl  7661.4
rfp  5810.6
th  3
ins  100.000
nm  no  ph
    
```



¹³C NMR Spectrum of 78

Plate XCIV

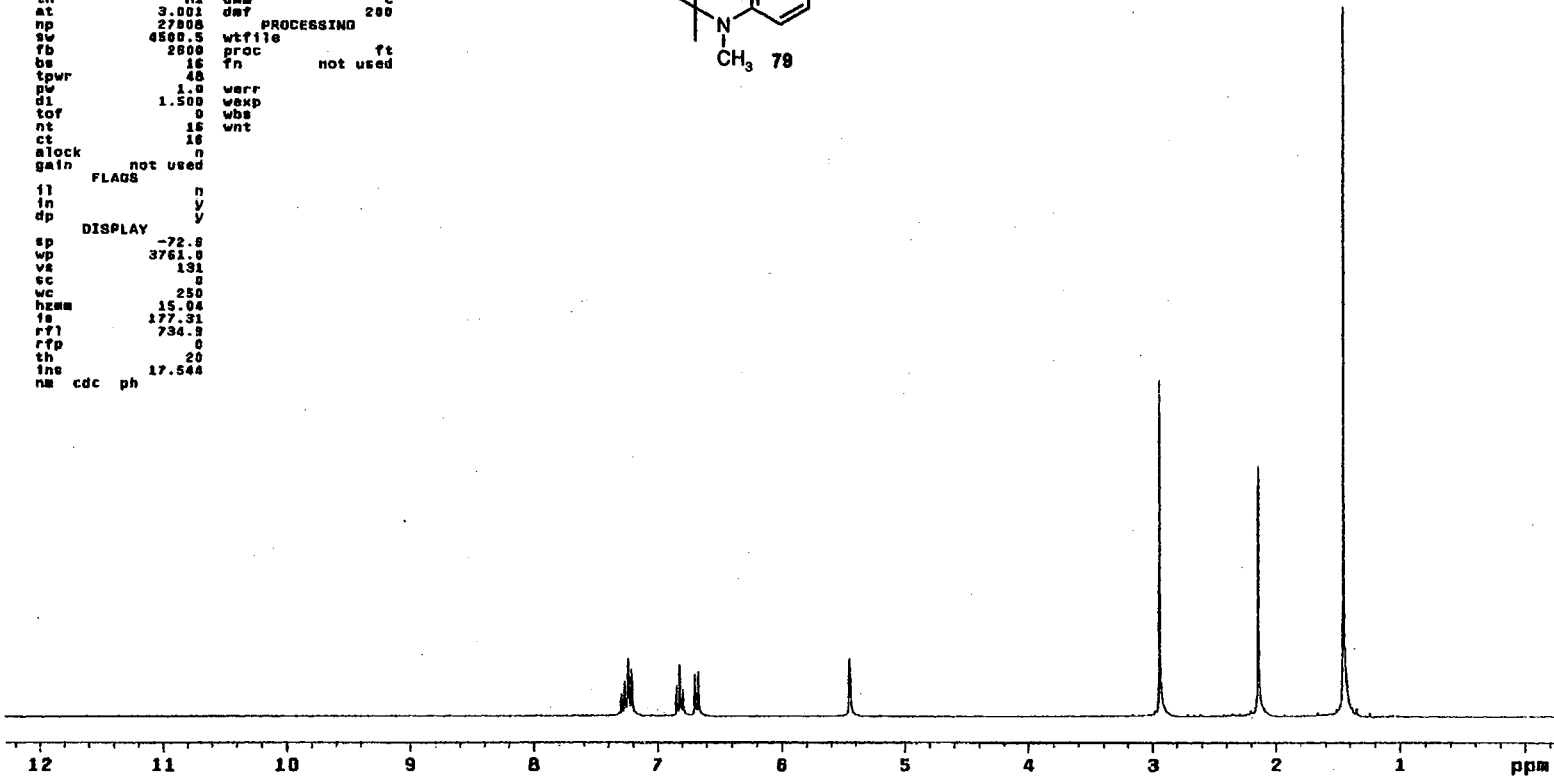
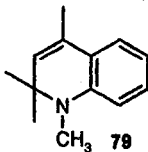


IR Spectrum of 79

Plate XCV

STANDARD 1H OBSERVE

```
expt stdih
SAMPLE
data Mar 2 1999 dfrq DEC. & VT 300.087
solvent Mar CDC13 dn H1
file exp dpwr 30
ACQUISITION
sfrq 300.087 dw nnn
tn H1 dsm c
at 3.001 dwt 200
np 27008 PROCESSING
sw 4500.5 wtfile
fb 200 proc ft
bs 16 fn not used
tpwr 45
pw 1.0 warr
d1 1.500 wexp
tof 0 wbs
nt 15 wnt
ct 16
alock n
gain not used
FLAGS
il n
in y
dp y
DISPLAY
sp -72.8
wp 3761.0
vs 131
cc 0
wc 250
hzmm 15.04
fs 177.31
rfl 734.8
rfp 0
th 20
lne 17.544
nm cdc ph
```



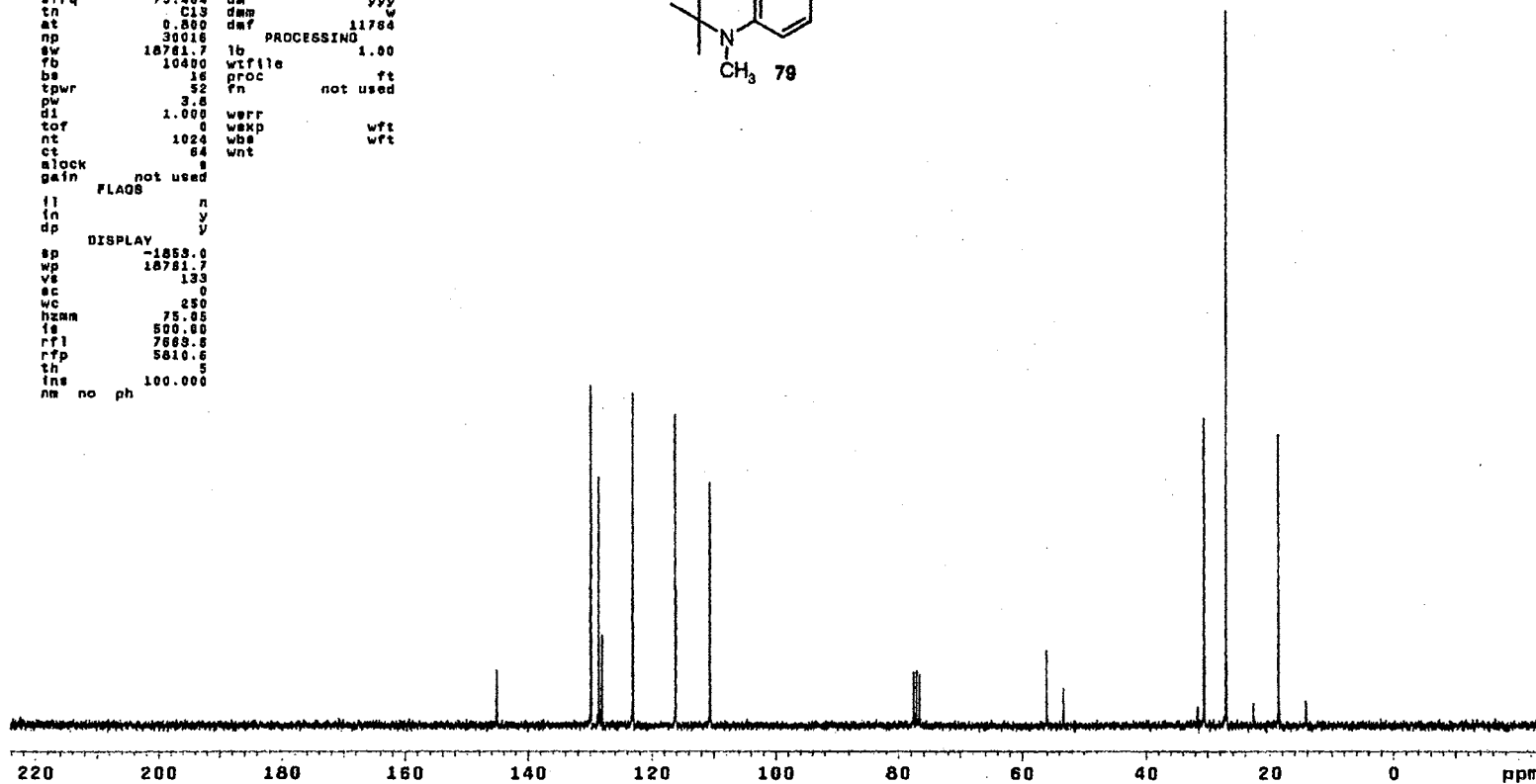
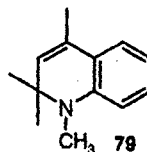
¹H NMR Spectrum of 79

Plate XCVI

13C OBSERVE

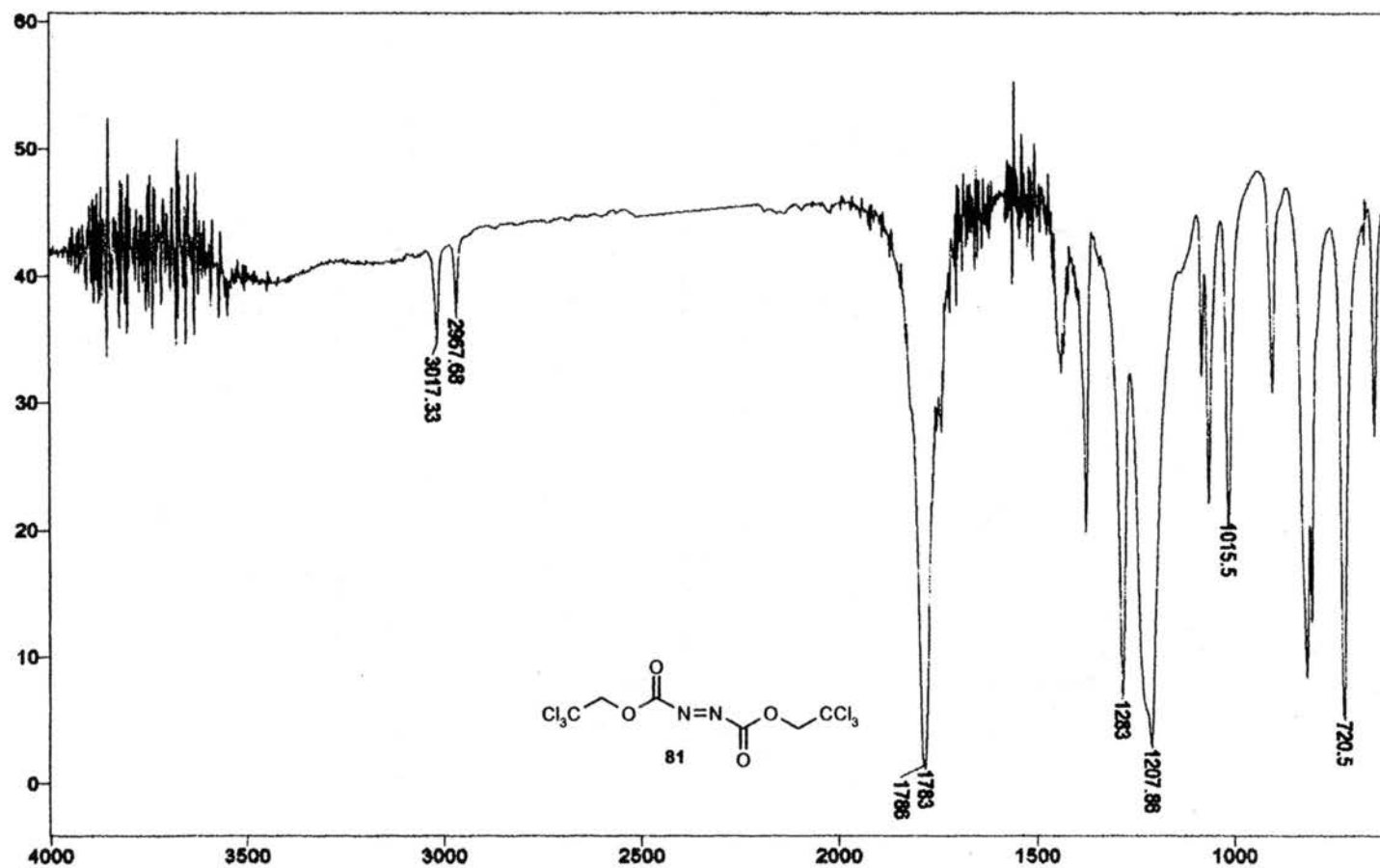
exptl std13c

date	Feb 4 2000	dfrq	DEC. & VT	300.087
solvent	CDCl3	dn		H1
file	exp	dpwr		34
ACQUISITION				
sfrq	75.464	ds		0
tn	C13	dsm		w
at	0.800	daf		11784
np	30016	PROCESSING		
sw	18781.7	lb		1.00
fb	10400	wffile		
be	16	proc		ft
tpwr	52	fn		not used
pw	3.8			
di	1.000	werr		
cor	0	wexp		wft
nt	1024	wss		wft
ct	64	wnt		
clock				
gain	not used			
FLAOS				
fl		n		
fn		y		
dp		y		
DISPLAY				
sp	-1853.0			
wp	18781.7			
vs	133			
sc	0			
wc	250			
hsmn	75.05			
is	500.00			
rfl	7889.8			
rfd	5810.6			
th	5			
ins	100.000			
nm	no	ph		



¹³C NMR Spectrum of 79

Plate XCVII



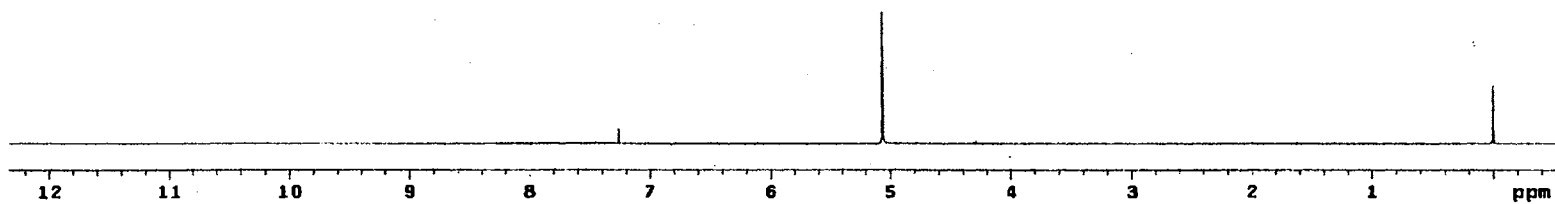
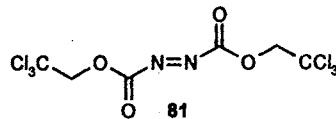
IR Spectrum of 81

Plate XCVIII

STANDARD 1H OBSERVE

```

exp1 stdih
SAMPLE
date Mar 31 1999 dfrq 300.087
solvent CDCl3 dn H1
file exp dpr 30
ACQUISITION 0 dof 0
efrq 300.087 da nnn
tn H1 dm c
at 3.881 daf 200
np 27000 PROCESSING
sw 4500.5 wtfile
fb 2800 proc ft
bs 18 fn not used
tpwr 48
pw 3.0 werr
d1 1.500 wexp
tof 0 wbs
nt 8 wnt
ct 8
alock n
gain not used
FLAGS
f1 n
f2 y
f3 y
DISPLAY
sp -157.7
wp 9861.5
vs 24
sc 0
wc 250
hzmr 15.45
fs 982.28
rft 748.8
rfd 0
th 20
ins 4.800
nm cdc ph
    
```



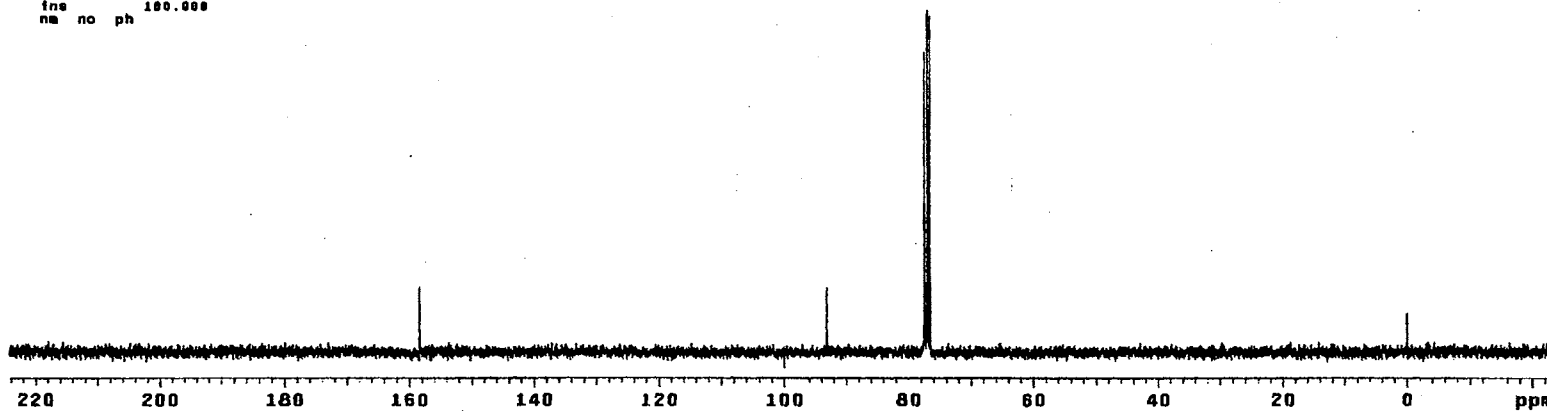
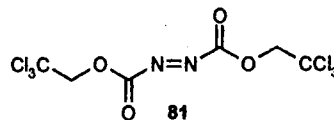
¹H NMR Spectrum of 81

Plate XCIX

13C OBSERVE

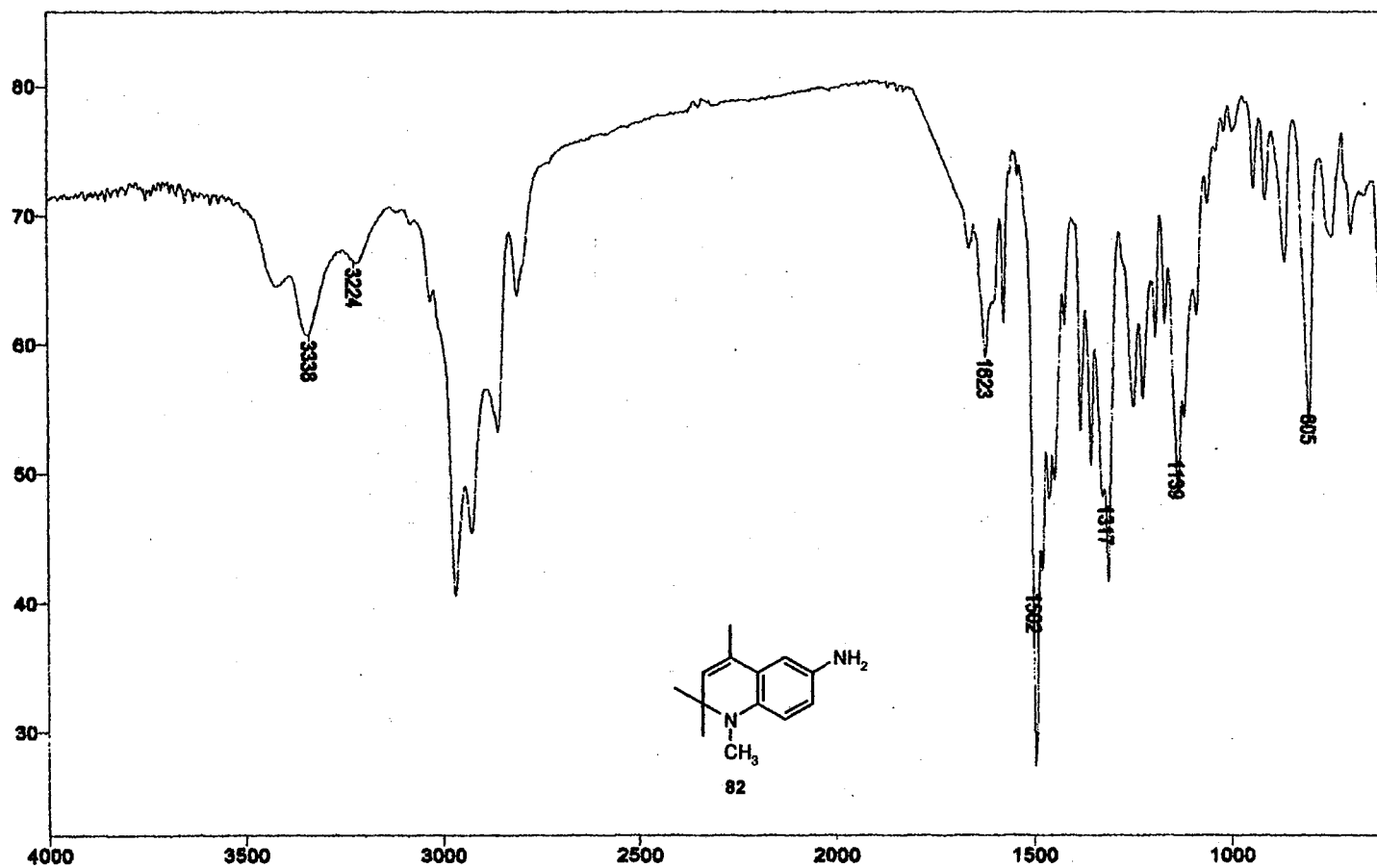
exp1 std13c

date	SAMPLE	DEC. & VT
Mar 31 1988		300.007
solvent	CDC13	dn H1
file	exp	dpwr 34
ACQUISITION		
sfrq	75.464	doF 0
tn	C13	dm vvy
at	9.899	dat 11764
np	30816	PROCESSING
sw	18751.7	lb 1.00
Tb	10400	wfile
bs	18	proc ft
tpwr	52	fn not used
pw	3.6	
di	1.000	werr
cor	0	wexp wft
nt	1024	wss wft
ct	844	wnt
alock	0	
gain	not used	
FLAOS		
fl	n	
in	y	
dp	y	
DISPLAY		
sp	-1005.0	
wp	18751.7	
vs	63	
sc	0	
wc	250	
hzm	75.05	
is	509.00	
rfl	7646.5	
rff	5610.6	
th	0	
ina	100.000	
na	no ph	



¹³C NMR Spectrum of 81

Plate C



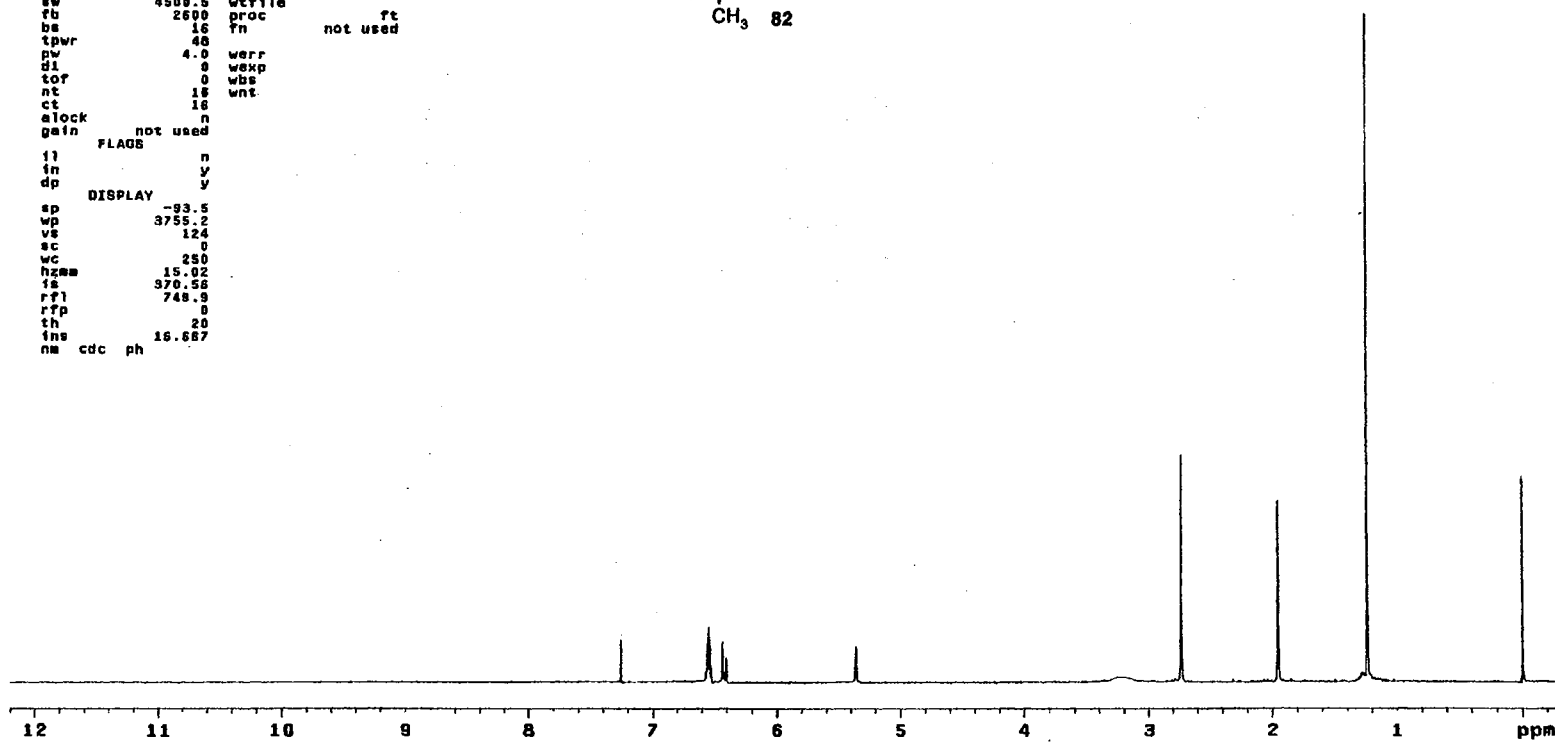
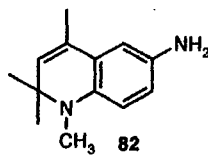
IR Spectrum of 82

Plate CI

STANDARD 1H OBSERVE

```

expl stdih
SAMPLE
date Apr 12 1999 dfrq DEC. & VT 300.087
solvent CDC13 dn M1
file exp dpwr 30
ACQUISITION dof 0
sfrq 300.087 da nnn
in M1 dam c
at 3.747 dmf 200
np 33728 PROCESSING
sw 4500.5 wtfile
fb 2600 proc ft
bs 16 Tn not used
tpwr 48
pw 4.0 werr
d1 0 wexp
tof 0 wbs
nt 18 wnt
ct 18
alock n
gain not used
FLAG
il n
in y
dp y
DISPLAY
sp -93.5
wp 3755.2
vs 124
sc 0
wc 250
hzma 15.02
fs 370.58
rfl 748.9
rfp 0
th 20
ins 16.887
nm cdc ph
    
```



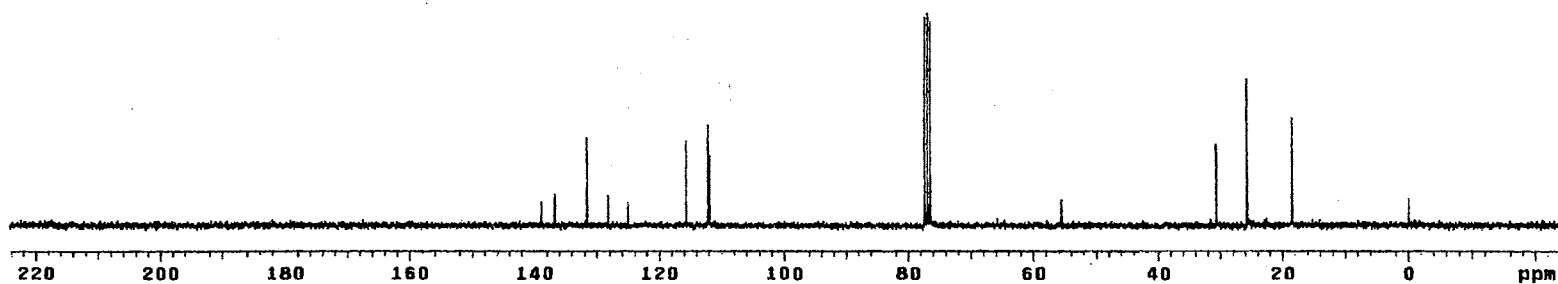
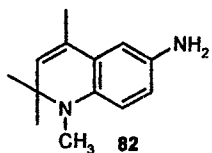
¹H NMR Spectrum of 82

Plate CII

13C OBSERVE

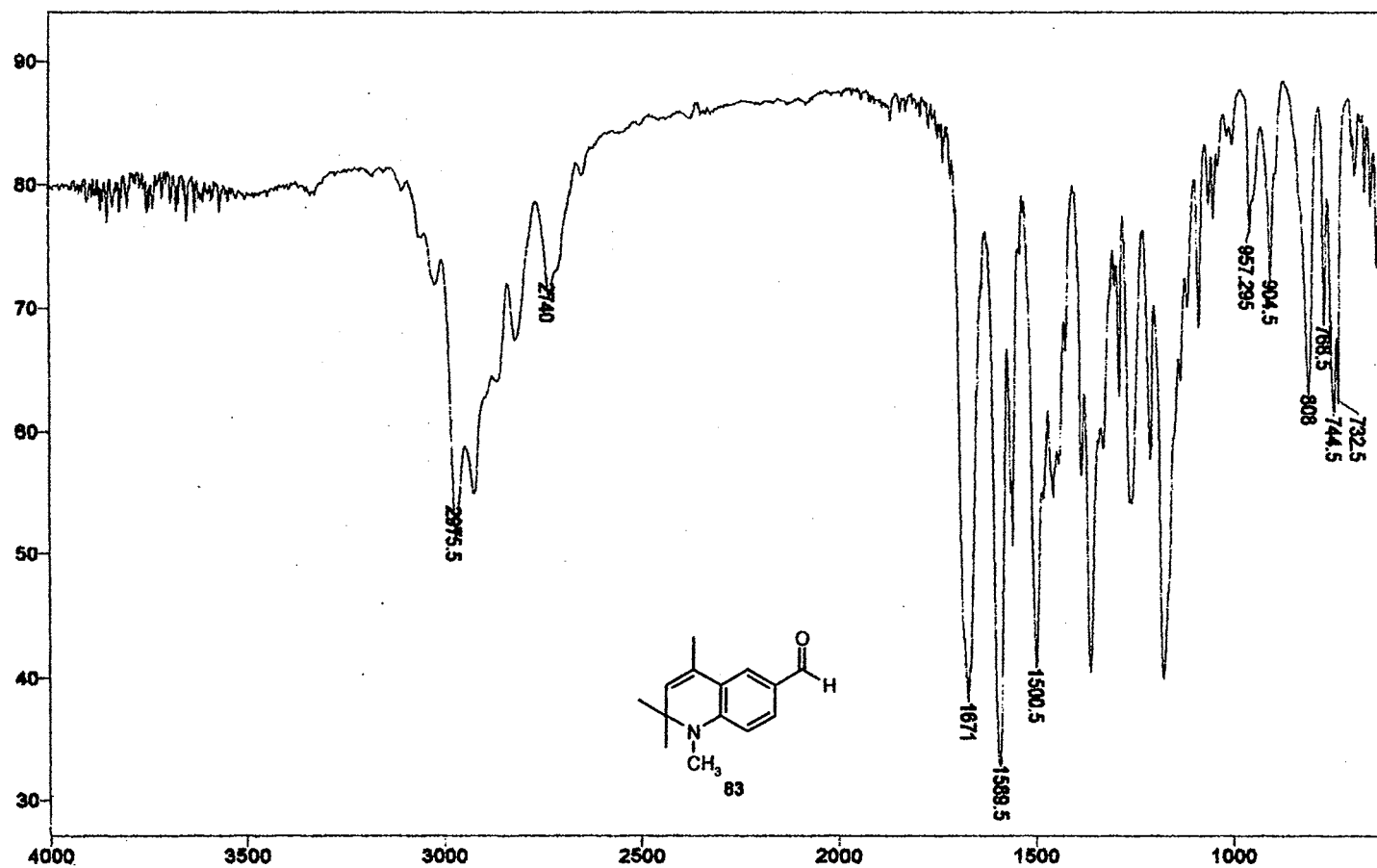
expl std13c

date	Apr 12 1999	dfrq	300.087
solvent	CDC13	dn	H1
file	exp	dpwr	34
ACQUISITION			
sfreq	75.464	dm	vyv
tn	C13	dms	w
at	0.800	dnt	11784
np	38016	PROCESSING	
sw	18761.7	lb	1.00
fb	10400	wf file	
bs	18	proc	ft
tpwr	52	fn	not used
pw	3.8		
d1	1.000	werr	
tof	0	wexp	wft
nt	1024	wbs	wft
ct	1024	wnt	
alock		s	
gain	not used		
FLAGS			
fl		n	
fn		y	
dp		y	
DISPLAY			
sp	-1835.8		
wp	18761.7		
vs	39		
sc	0		
wc	250		
hzam	75.05		
ls	500.00		
rfl	7646.5		
rff	5810.8		
th	4		
ins	100.000		
nm	no	ph	



¹³C NMR Spectrum of 82

Plate CIII



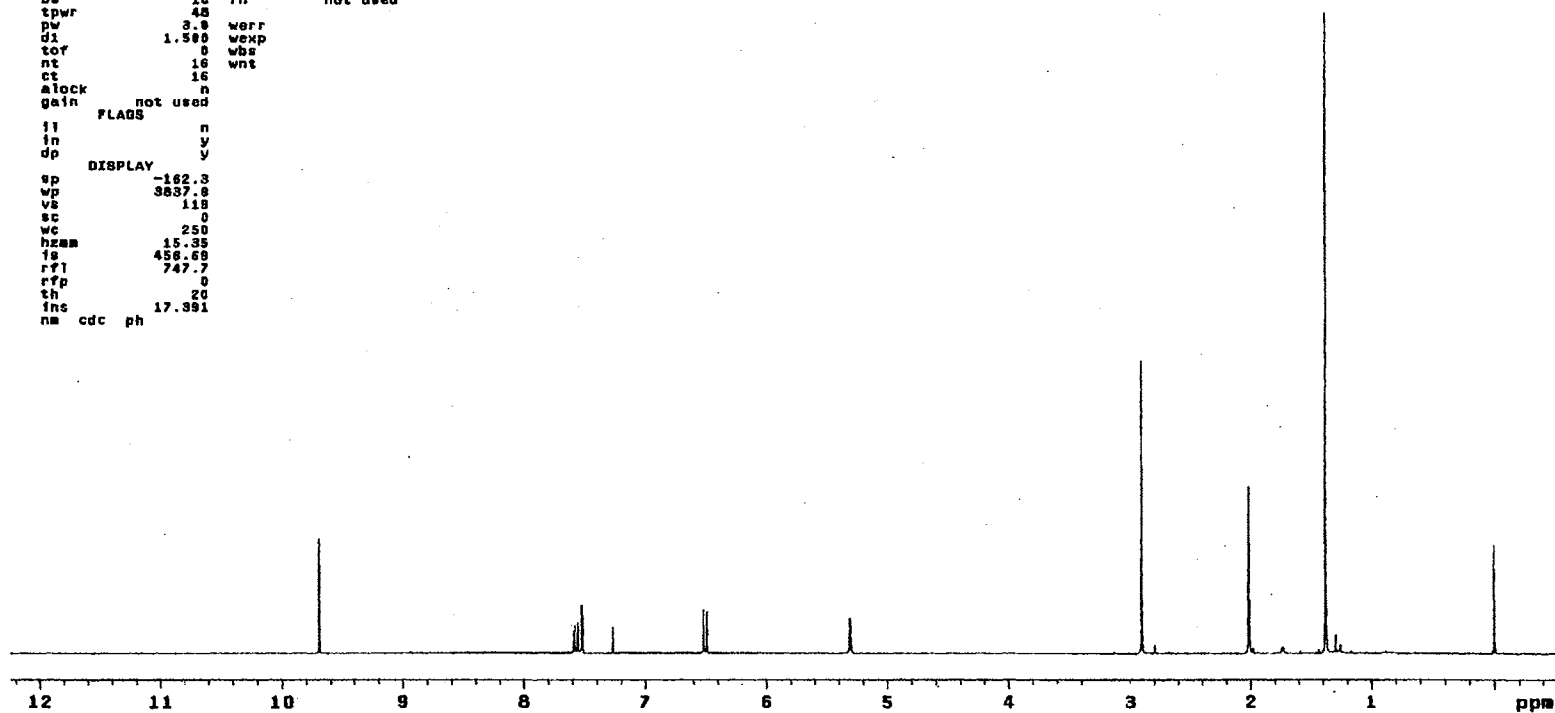
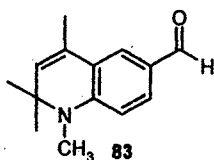
IR Spectrum of 83

Plate CIV

STANDARD 1H OBSERVE

```

exp1 std1h
SAMPLE
date Mar 31 1988 dfrq DEC. & VT 300.087
solvent CDCl3 dn H1
file exp dpwr 38
ACQUISITION dot 0
sfrq 300.087 dm nnn
tn H1 dm c
at 3.081 dm? 200
np 27088 PROCESSING
sw 4500.5 wtfile ft
fb 2600 proc not used
bs 18 fn
tpwr 48
pw 3.0 werr
d1 1.500 wexp
tof 0 wbr
nt 16 wnt
st 16
alock n
gain not used
FLAGS
ll n
in y
dp y
DISPLAY
sp -182.3
wp 3837.8
vs 133
sc 0
wc 250
hzmm 15.35
is 458.69
rf1 747.7
rfp 0
th 20
fns 17.391
nm cdc ph
    
```



¹H NMR Spectrum of 83

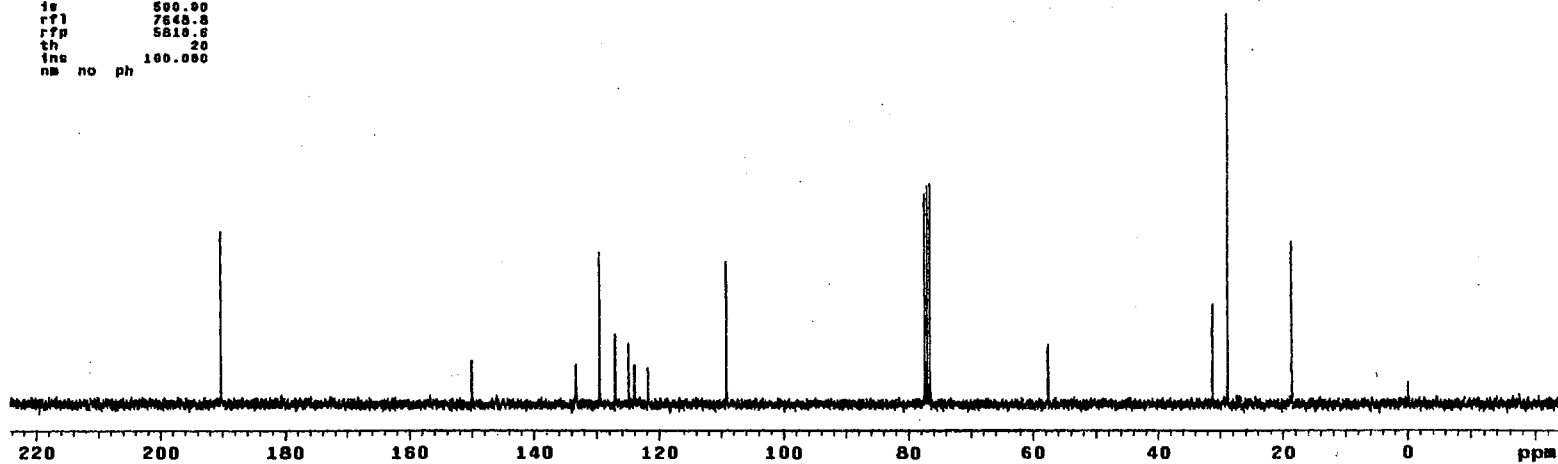
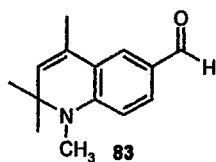
Plate CV

13C OBSERVE

exptl std13c

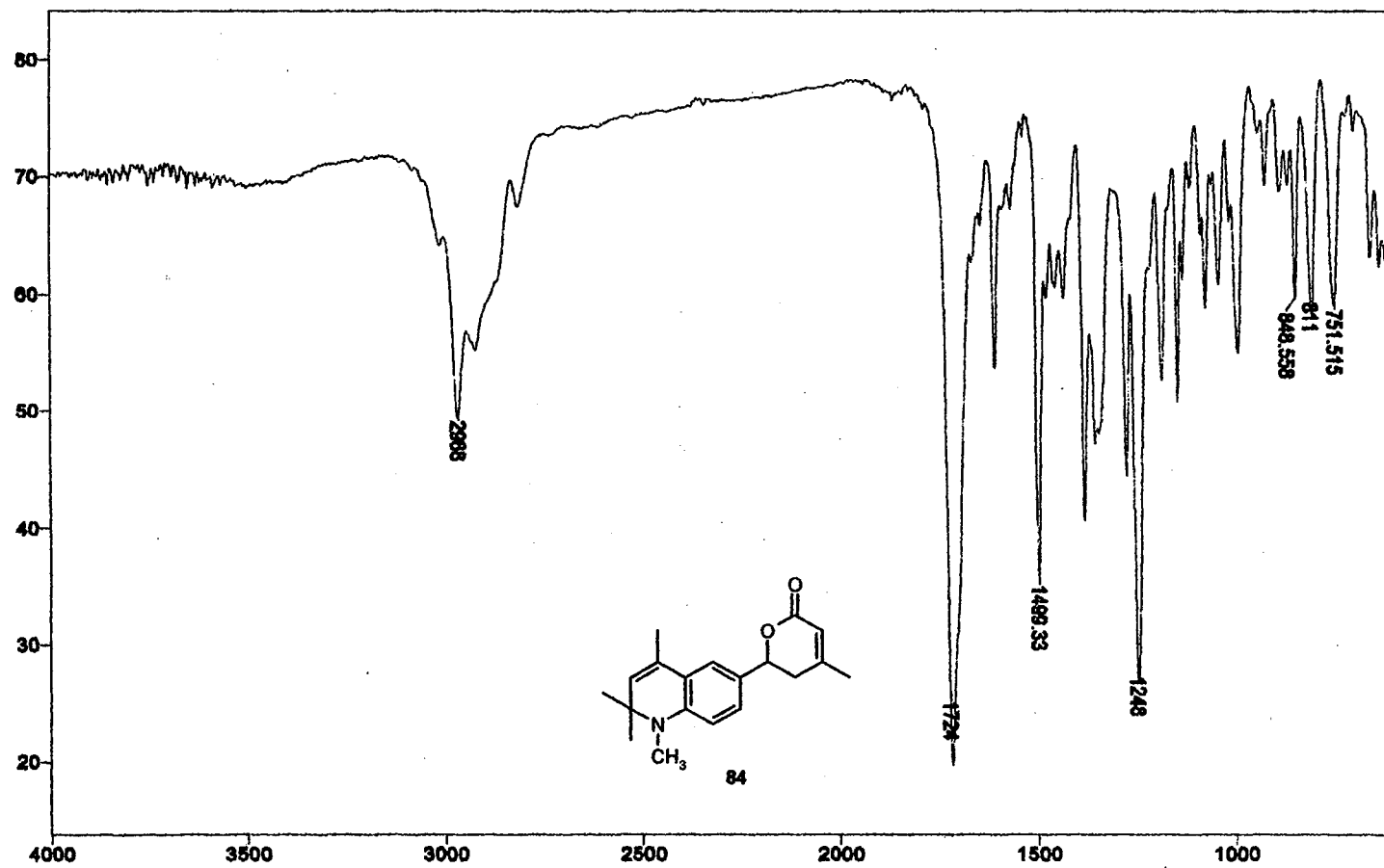
```

SAMPLE
date Mar 31 1988 dfrq DEC. & VT 300.087
solvent CDCl3 dn H1
file exp dpr 34
ACQUISITION
sfrq 75.464 dm vvy
tn C13 dm w
at 0.800 dar 11764
np 30818 PROCESSING
sw 18761.7 lb 1.00
fb 18480 wtfile
hs 15 proc ft
tpwr 52 fn not used
pw 9.8
di 1.000 werr
tof 0 wexp wft
nt 1824 wss wft
ct 288 wnt
alock s
gain not used
FLAGS
il n
in y
dp y
DISPLAY
sp -1838.2
wp 18761.7
vs 72
sc 0
wc 250
hzem 75.05
is 500.00
rf1 7848.3
rfp 5818.6
th 20
ins 180.080
ns no ph
    
```



¹³C NMR Spectrum of 83

Plate CVI



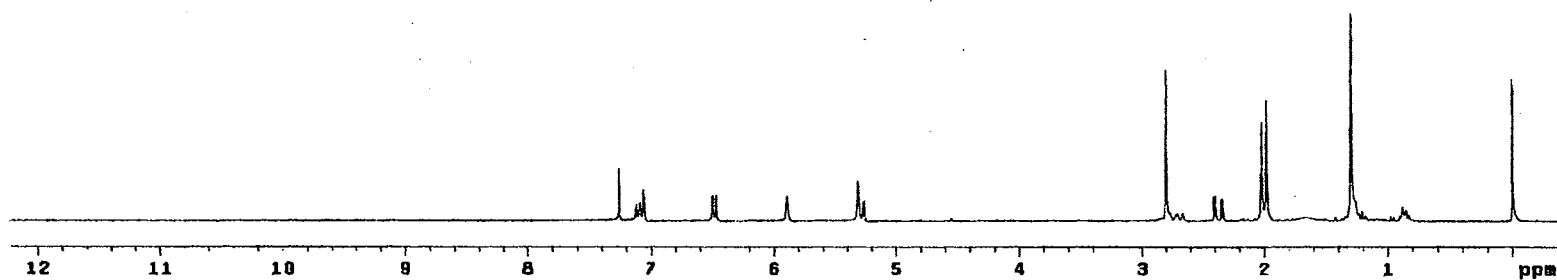
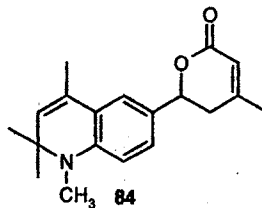
IR Spectrum of 84

Plate CVII

STANDARD 1H OBSERVE

```

expl std1h
SAMPLE
date Apr 13 1988 dfrq DEC. & VT 300.087
solvent CDCl3 dn M1
file ACQUISITION exp dpwr M1
sfrq 300.087 dm 30
tn M1 dnm nnn
st 3.747 dmf 200
np 83728 PROCESSING
sw 4500.5 wtf file ft
fb 2000 proc
bs 16 fn not used
tpwr 48
pw 4.0 werr
di 0 wexp
tof 0 wbs
nt 16 wnt
ct 16
alock not used
gain FLAGG n
il n
in y
dp DISPLAY y
sp -123.8
wp 3780.8
ve 38
sc 0
wc 250
hzmw 7.84
fs 500.00
rfi 750.7
rfp 0
th 34
fns 25.000
nm cdc ph
    
```



¹H NMR Spectrum of 84

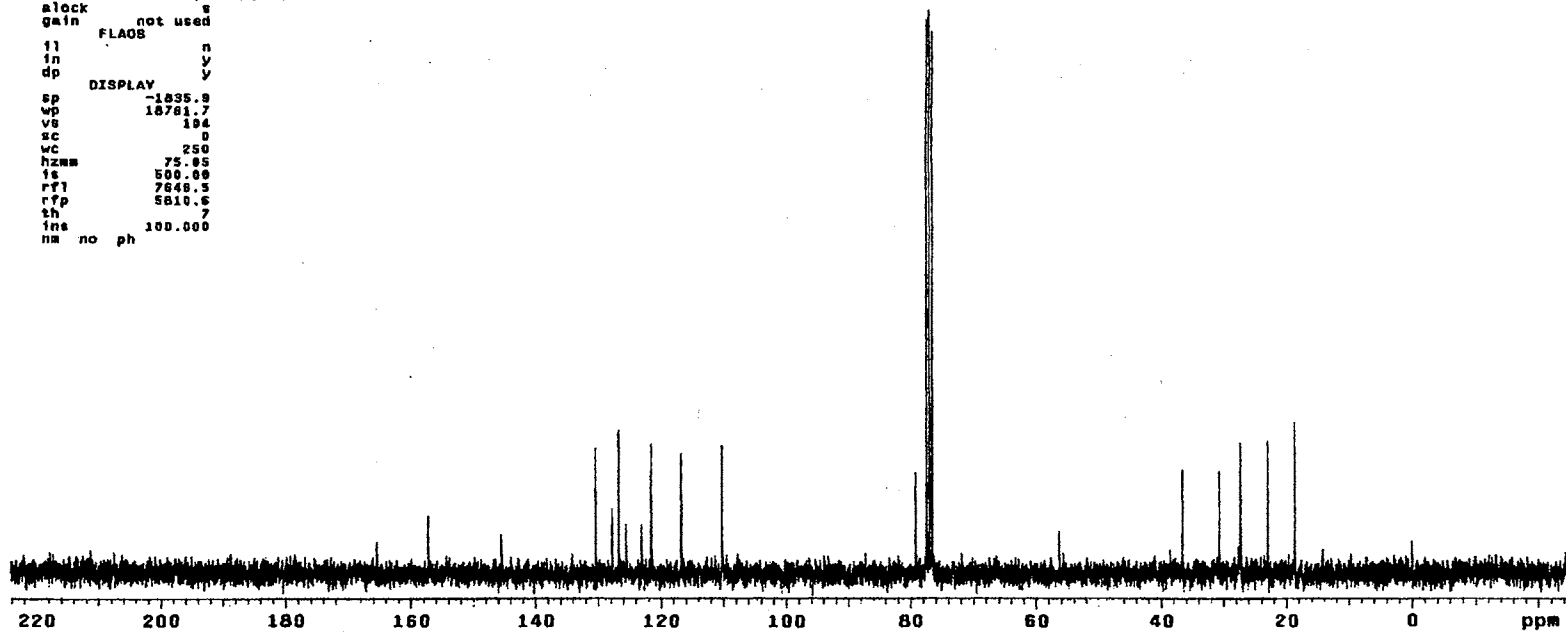
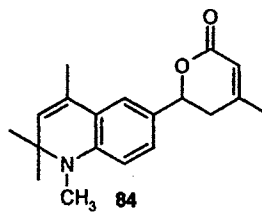
Plate CVIII

13C OBSERVE

expt st13c

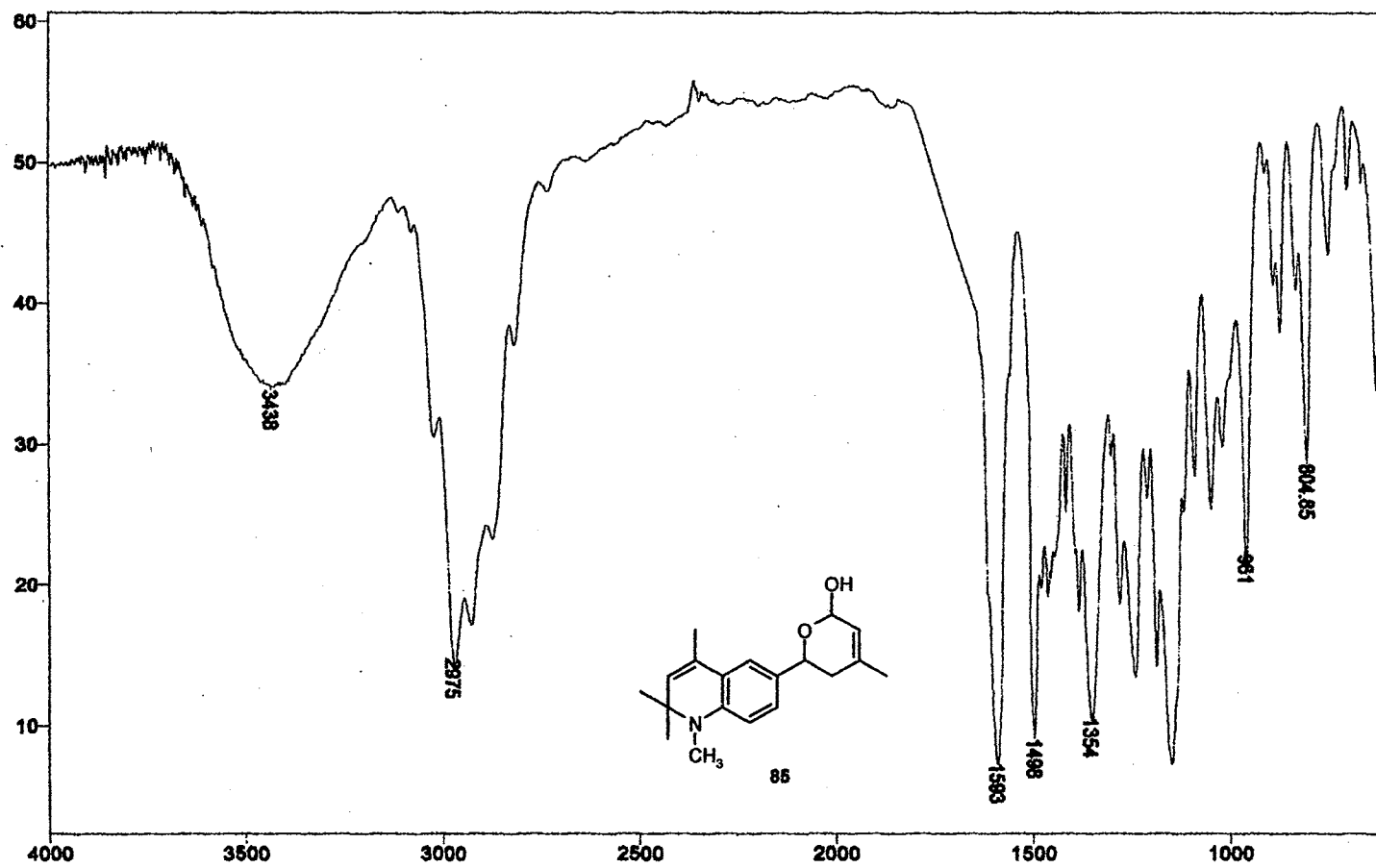
```

SAMPLE          DEC. & VT
date  Apr 13 1988  dfrq  300.007
solvent  CDCl3    dn      H1
file      exp     dpwr    34
ACQUISITION    dof      0
sfrq      75.464  dm      vvy
in        013     dnm      w
at        0.000  dmf     11764
np        30818  PROCESSING
sw        18751.7  lb      1.00
fb        10400  wf file
hs        15     proc     ft
tpwr      52     fn      not used
pw        3.8
d1        1.000  werr
tof       0     wexp
nt        1024  wbs
ct        498  wnt
alock     0
gain      not used
FLAOS     not used
il        n
in        y
dp        y
DISPLAY
sp        -1835.9
wp        18751.7
vs        104
sc        0
wc        250
hznm      75.85
fs        500.00
rf1       7646.5
rfp       5810.6
th        7
fns       100.000
na no ph
    
```



¹³C NMR Spectrum of 84

Plate CIX



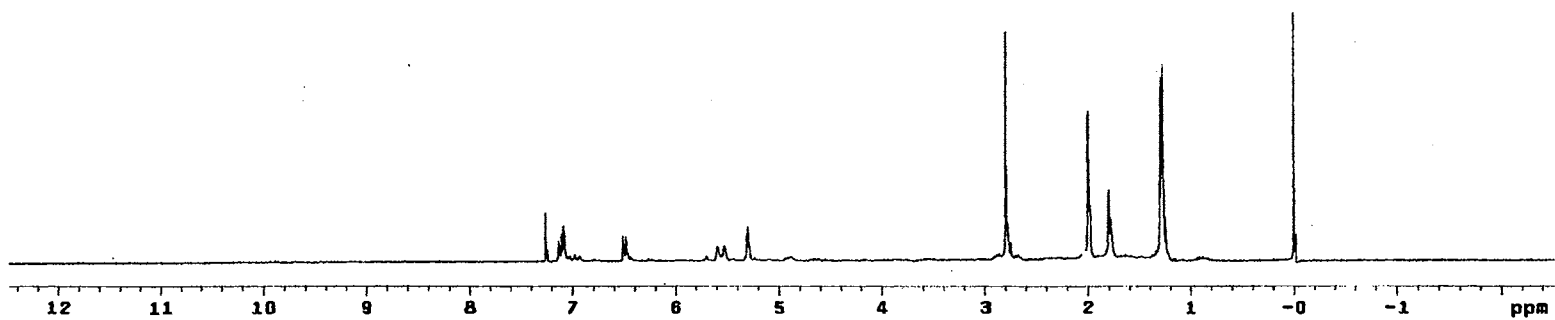
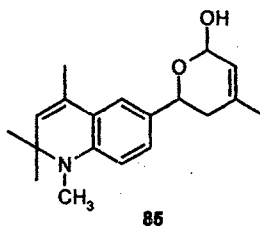
IR Spectrum of 85

Plate CX

STANDARD 1H OBSERVE

```

expi std1h
SAMPLE
date Jun 16 1989 dfrq DEC. & VT 300.087
solvent CDC13 dn H1
file exp dpwr 30
ACQUISITION dof 0
sfrq 300.087 da nnn
tn H1 dm c
at 3.747 dmf 200
np 33728 PROCESSING
sw 4500.5 wtf1le
fs 2608 proc ft
bs 16 fn not used
tpwr 46
pw 6.0 warr
d1 0 wexp
tor 0 wba
nt 32 wnt
ct 32
alock n
gain not used
FLAGS
il n
in y
dp y
DISPLAY
sp -755.0
wp 4500.5
vs 46
sc 0
wc 258
hzmm 16.00
is 588.00
rfl 755.0
rfp 0
th 20
ins 100.000
nm cdc ph
  
```



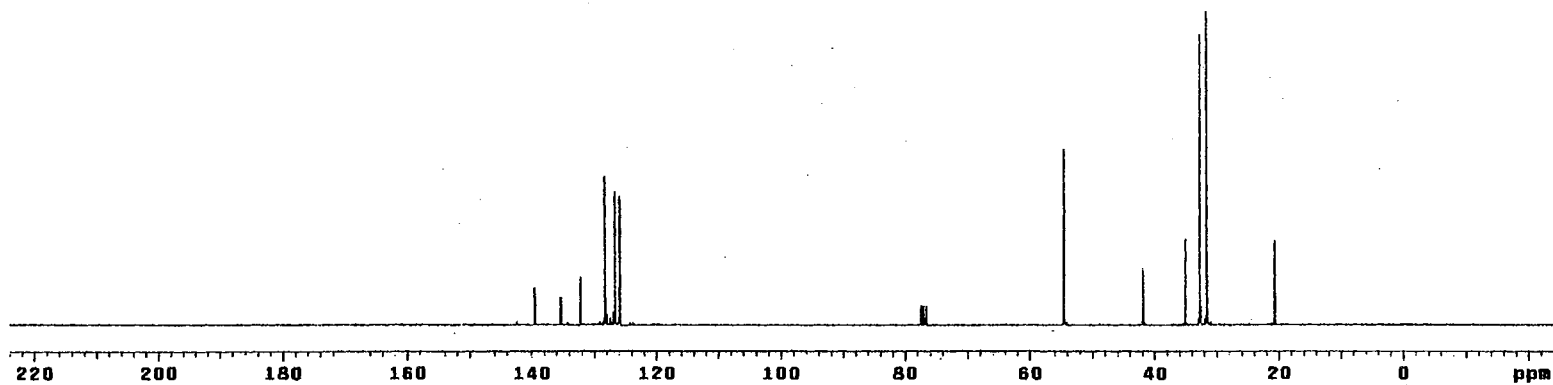
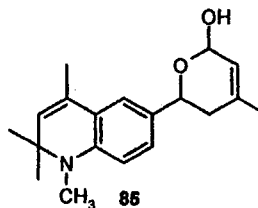
¹H NMR Spectrum of 85

Plate CXI

¹³C OBSERVE

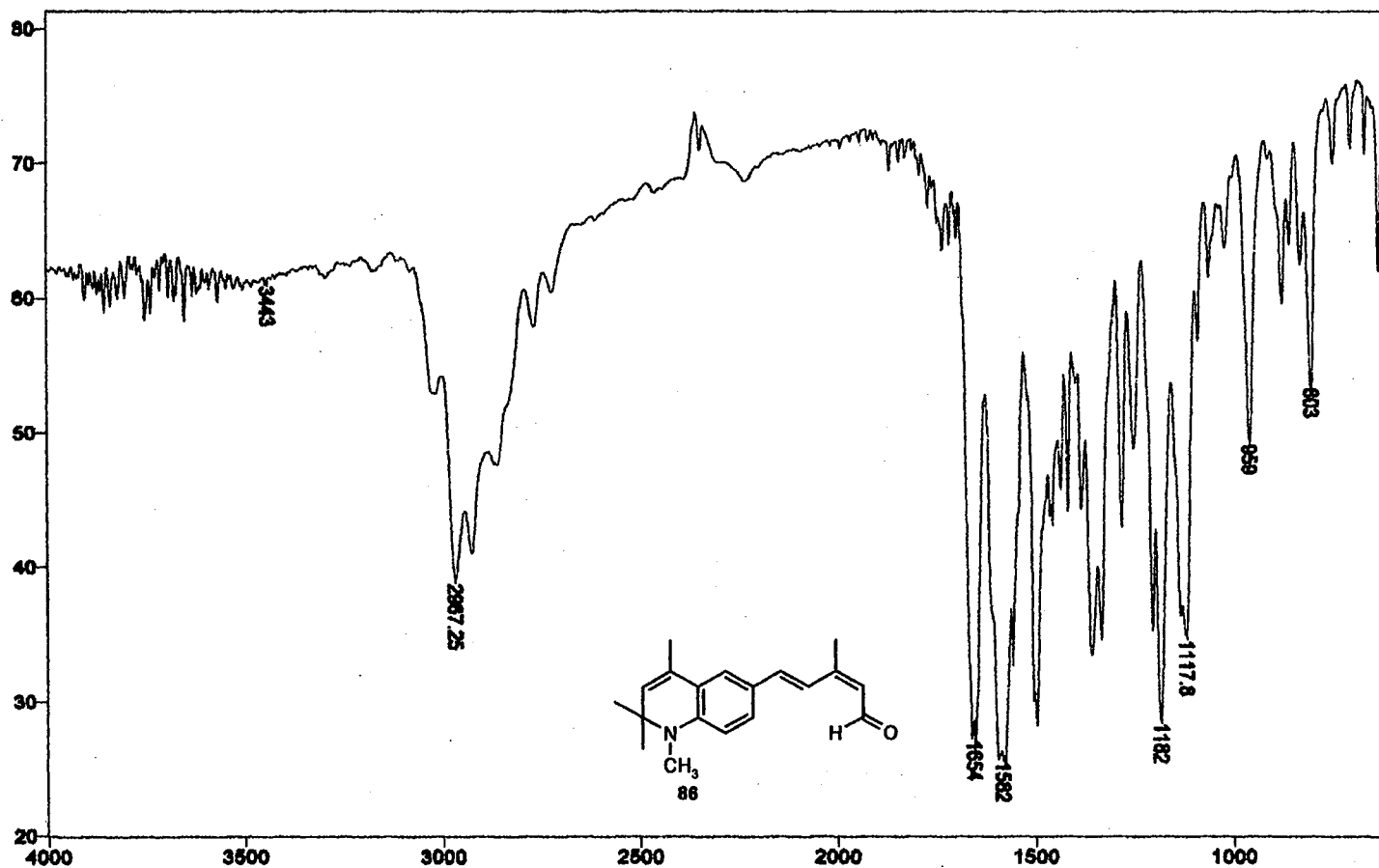
```

expt std13c
SAMPLE
date Jul 8 1999 dfrq DEC. & VT 300.087
solvent CDCl3 dn H1
file ACQUISITION exp dpwr 3A
sfrq 75.464 dm 0
tn C13 dm vvy
at 0.800 dmf 11764
np 30018 PROCESSING
sw 18781.7 lb wtfile 1.00
fb 10400 wnt
bs 16 proc ft
tpwr 52 fn not used
pw 3.8
d1 1.000 werr
tot 0 wexp wft
nt 1024 wbs wft
ct 878 wnt
alock s
gain not used
FLAGS
il n
in y
dp DISPLAY y
sp -1054.2
wp 18781.7
vs 50
sc 0
wc 250
hznm 75.05
ls 500.00
rfl 7664.8
rfp 5810.8
th 3
ins 100.000
nm no ph
    
```



¹³C NMR Spectrum of 85

Plate CXII



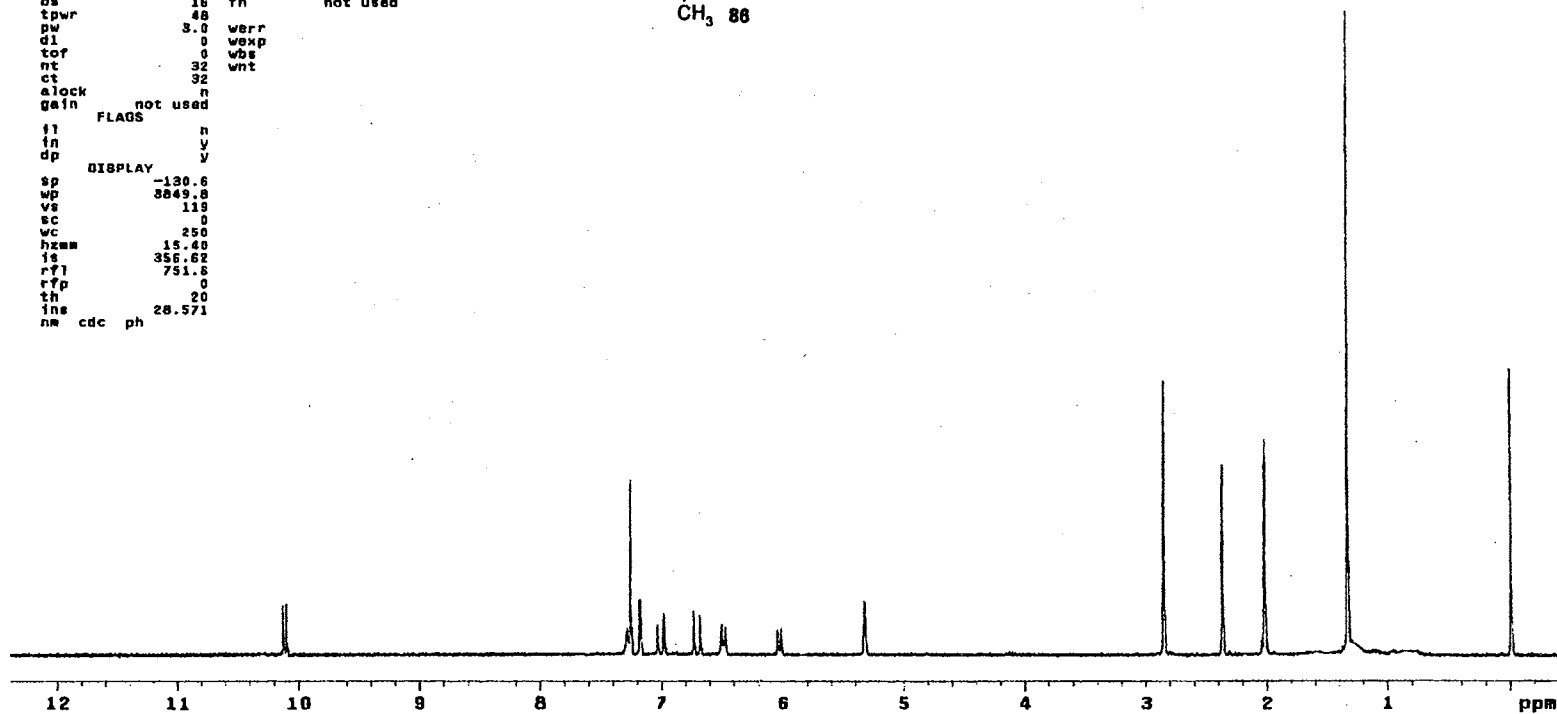
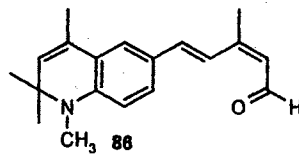
IR Spectrum of 86

Plate CXIII

STANDARD 1H OBSERVE

```

exp1 std1h
SAMPLE
date May 10 1989 dfrq 300.087
solvent CDC13 dn H1
f1s exp dpwr 38
ACQUISITION exp dot 0
sfrq 300.087 dw nnn
tn H1 dm c
at 3.747 dar 200
np 33728 PROCESSING
sw 4500.5 wtfile
fb 2600 proc yt
bs 16 fn not used
tpwr 48
pw 3.0 werr
d1 0 wexp
tof 0 wbs
nt 32 wnt
ct 32
alock n
gain not used
FLAGS
f1 n
f2 y
dp y
DISPLAY
sp -130.6
wp 8849.8
vs 119
sc 0
wc 250
hzmm 15.40
is 356.62
rfl 751.6
rfp 0
th 20
ins 28.571
nm cdc ph
    
```



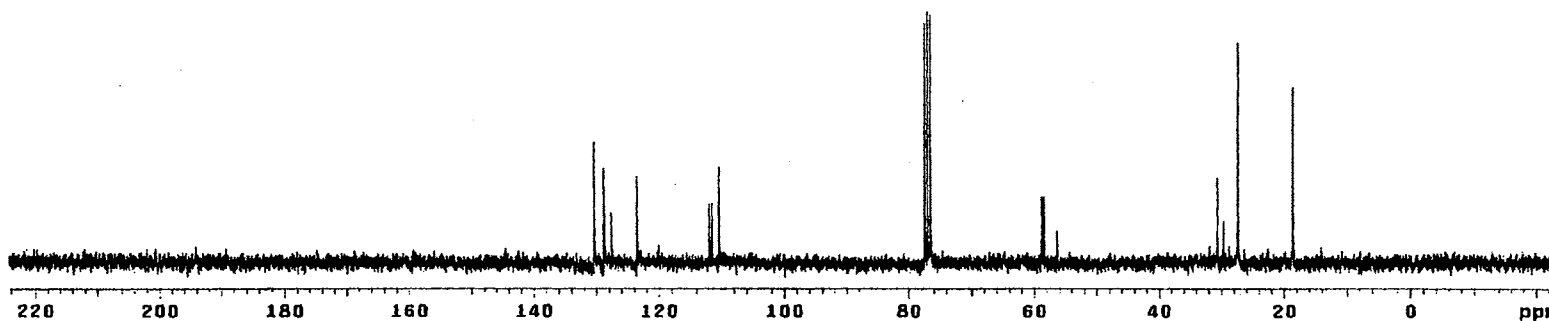
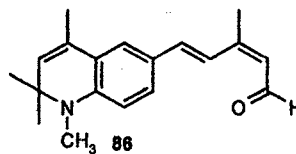
¹H NMR Spectrum of 86

Plate CXIV

¹³C OBSERVE

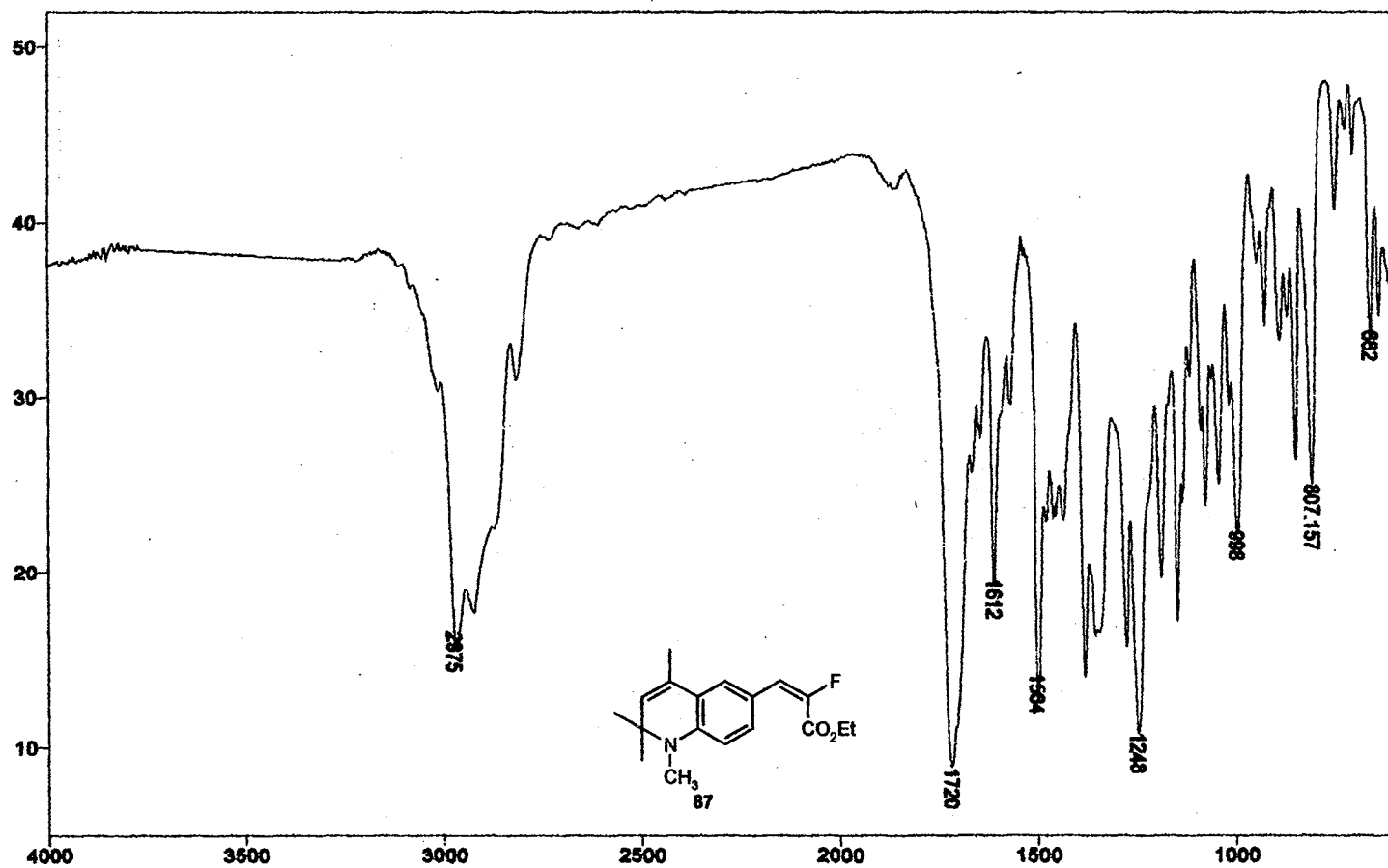
exptl std13c

date	Jan 24 2000	dfrq	DEC. & VT	300.087
solvent	CDCl3	dn		H1
file	exp	dpwr		36
ACQUISITION		dot		0
sfrq	75.464	dm		yyv
tn	C13	dnn		w
at	0.800	dnt	PROCESSING	11764
np	30016	lb		1.00
sw	18781.7	wtfile		
fb	10400	proc		ft
bs	16	fn		not used
tpwr	52			
pw	3.8			
d1	1.000	werr		wft
top	0	wexp		wft
nt	1024	wbs		wft
ct	368	wnt		
alock				
gain	not used			
FLAGS				
ll	n			
ln	y			
dp	y			
DISPLAY				
sp	-1837.0			
wp	18781.7			
vs	46			
sc	0			
wc	250			
hznm	75.05			
is	500.00			
rfl	7647.6			
rfd	5810.6			
th	5			
ins	100.000			
nm	no	ph		



¹³C NMR Spectrum of 86

Plate CXV



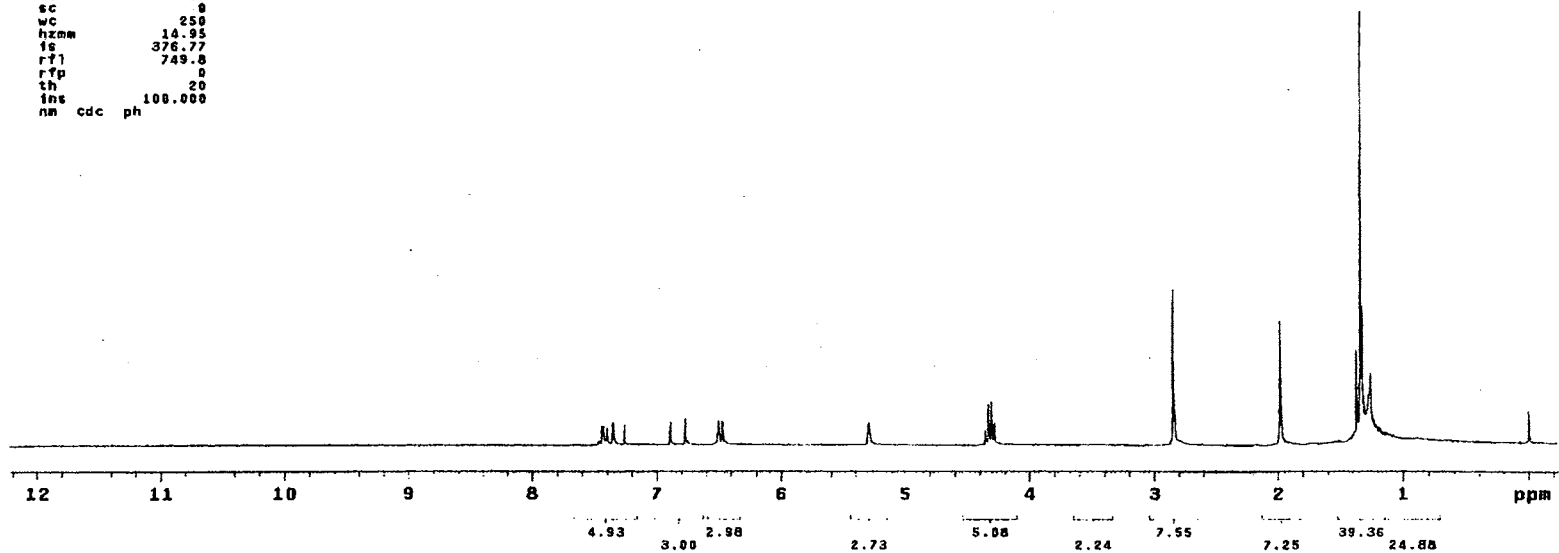
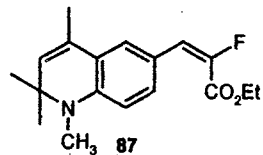
IR Spectrum of 87

Plate CXVI

STANDARD 1H OBSERVE

```

expl stdih
SAMPLE
date Jan 24 2000 dfrq DEC. & VT 300.087
solvent CDCl3 dn H1
file exp dpwr 30
ACQUISITION dof 0
sfrq 300.087 da nnn
in H1 dm c
at 3.747 daf 200
np 33720 PROCESSING
sw 4500.5 wtf file
fb 2800 proc ft
ba 16 fn not used
tpwr 48
pw 6.9 werr
di 9 wexp
tof 8 wbs
nt 16 wnt
ct 10
clock n
gain not used
FLAGS
f1 n
in y
dp y
DISPLAY
sp -89.8
wp 3737.5
vs 53
sc 9
wc 250
hzmm 14.95
fs 376.77
rf1 749.8
rfp 9
th 20
ins 100.000
nm cdc ph
    
```



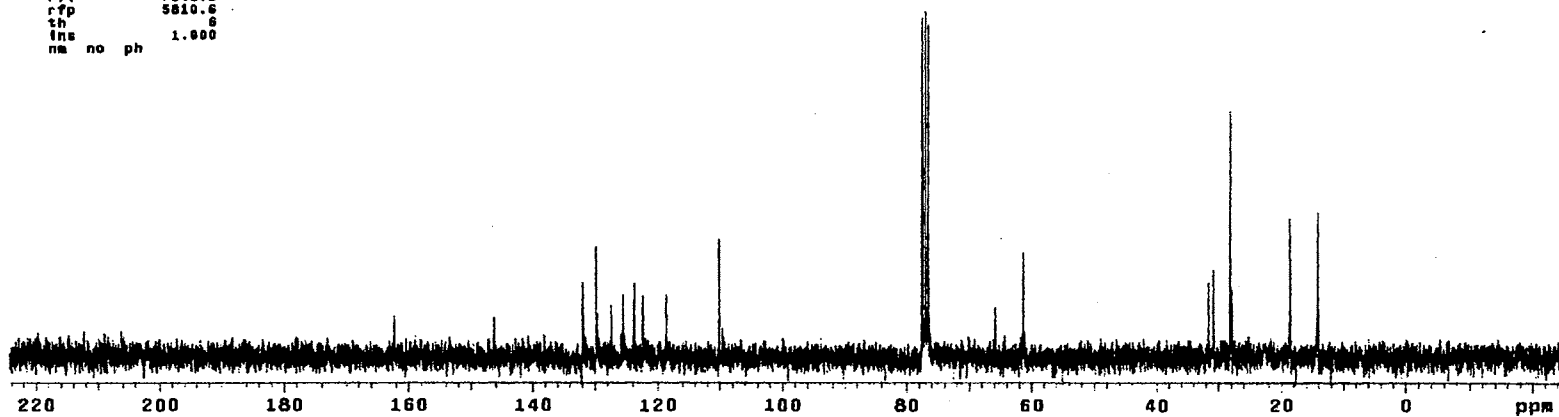
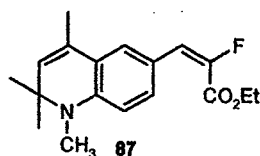
¹H NMR Spectrum of 87

Plate CXVII

13C OBSERVE

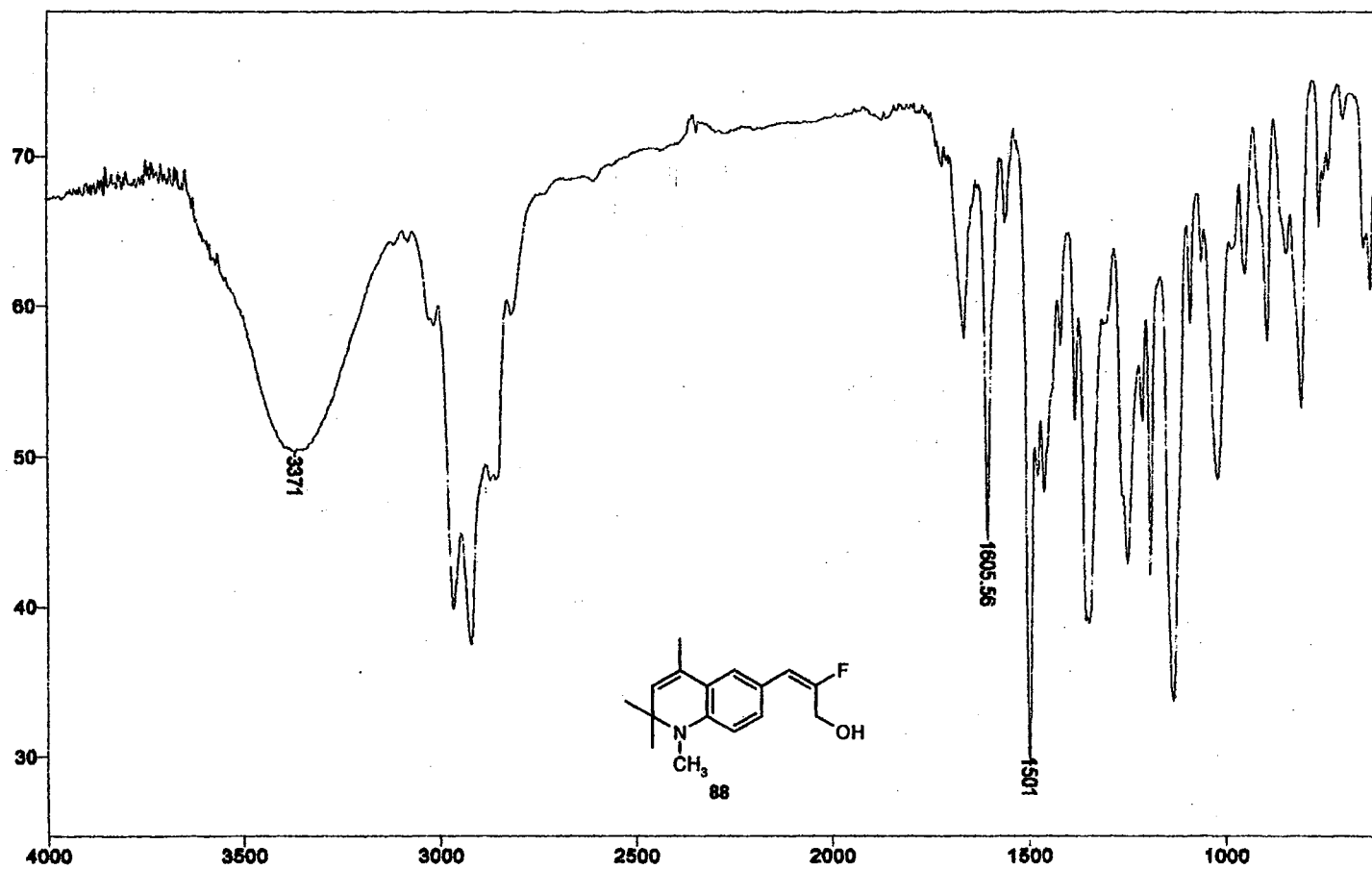
```

expt std13c
SAMPLE
date Jul 31 88 dfrq DEC. & VT 300.082
solvent CDCl3 dn H1
file exp dpwr 34
ACQUISITION dof 0
sfrq 75.463 da nyf
tn C13 daa w
at 6.800 da7 11764
np 30816 PROCESSING
sw 18761.7 lb 1.00
fb 10400 wtfile
bs 15 proc ft
tpwr 52 tn not used
pw 3.0
d1 1.000 warr
tof 0 wexp
nt 1024 wbs
ot 1024 wnt
alock n
gain not used
FLAGS
fl n
in y
dp y
DISPLAY
sp -1833.0
vp 18761.7
vs 178
sc 0
wc 250
hzam 75.85
fs 508.88
rfl 7543.8
rfp 5810.6
th 6
ins 1.000
na no ph
    
```



¹³C NMR Spectrum of 87

Plate CXVIII



IR Spectrum of 88

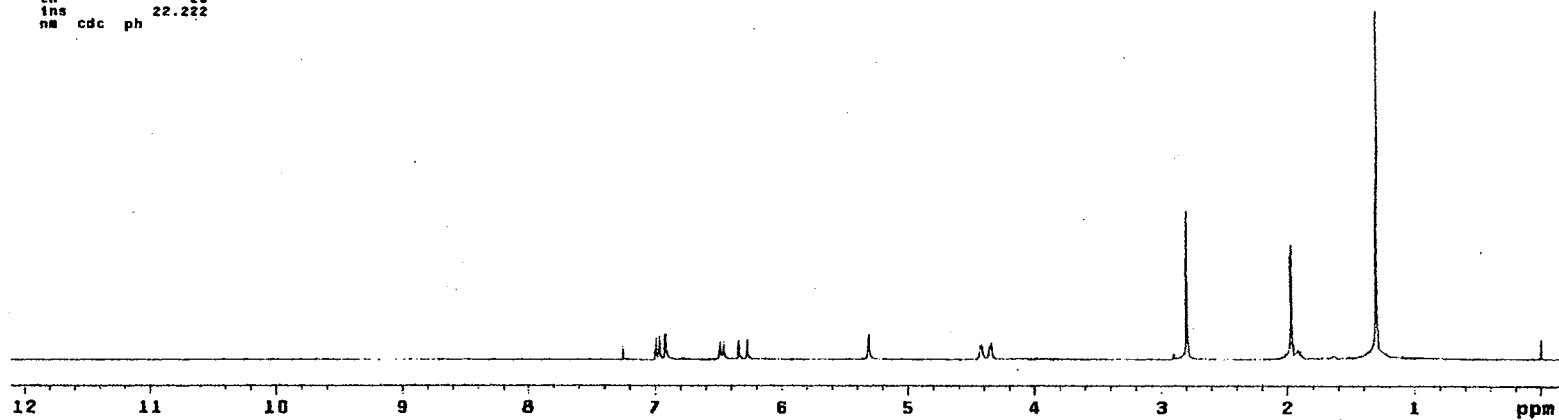
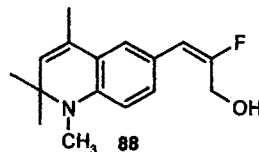
Plate CXIX

STANDARD 1H OBSERVE

expl stdih

```

SAMPLE          DEC. & VT
date   Jan 24 2000   dfrq   300.087
solvent  CDCl3      dn      H1
file     exp        dpwr    30
ACQUISITION      dof      0
sfrq     300.087   dm      nnn
tn       H1       dam      c
at       3.747    daf     200
np       33728    PROCESSING
sw       4500.5   wtfile
fb       2600    proc      ft
bs       16      fn      not used
tpwr     46
pw       6.9    werr
dl       0      wexp
tof      0      wbs
nt       16     wnt
ct       16
a1ock   n
gain    not used
FLAOS   n
fl      y
in      y
dp      y
DISPLAY
sp      -47.8
wp      3684.3
vs      64
sc      0
wc      250
hzmm    14.74
fs      253.53
rf1     751.4
rfp     0
th      20
ins     22.222
nm      cdc ph
    
```



¹H NMR Spectrum of 88

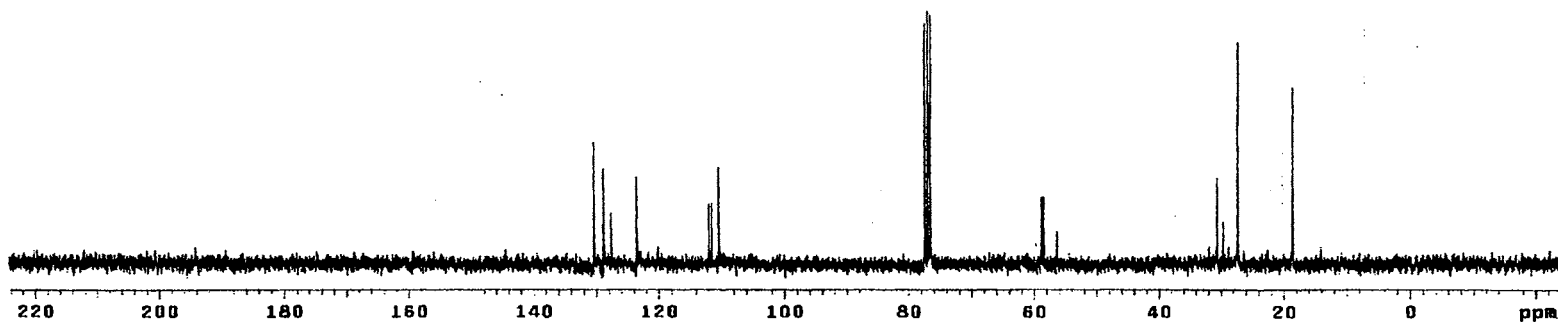
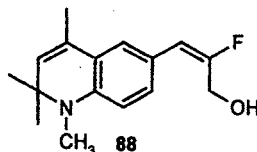
Plate CXX

13C OBSERVE

exptl std13c

```

SAMPLE
date Jan 24 2000 dfrq DEC. & VT 300.067
solvent CDCl3 dn H1
file exp dpwr 34
ACQUISITION
sfrq 75.464 dm yyy 0
tn C13 dnm w
at 0.800 dnt 11764
np 30016 PROCESSING
sw 18781.7 lb 1.00
fb 10400 wtfile
bs 16 proc ft
tpwr 52 fn not used
pw 3.8
dl 1.000 werr
tof 0 wexp wft
nt 1024 wss wft
ct 368 wnt
alock s
gath not used
FLAGS
il n
in y
dp y
DISPLAY
sp -1837.0
wp 18781.7
vs 46
sc 0
wc 250
hzmm 75.05
is 500.00
rfi 7847.6
rfp 5810.6
th 5
ina 100.000
na no ph
    
```



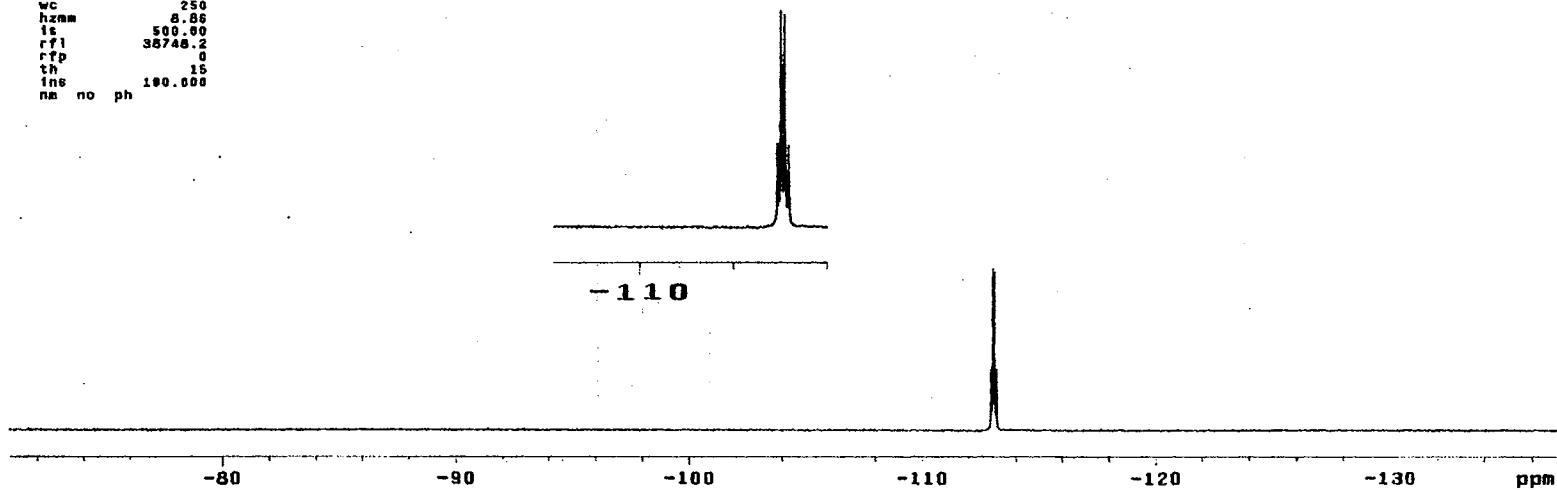
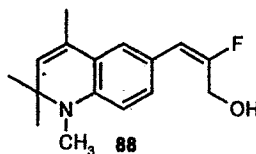
¹³C NMR Spectrum of 88

Plate CXXI

13C OBSERVE

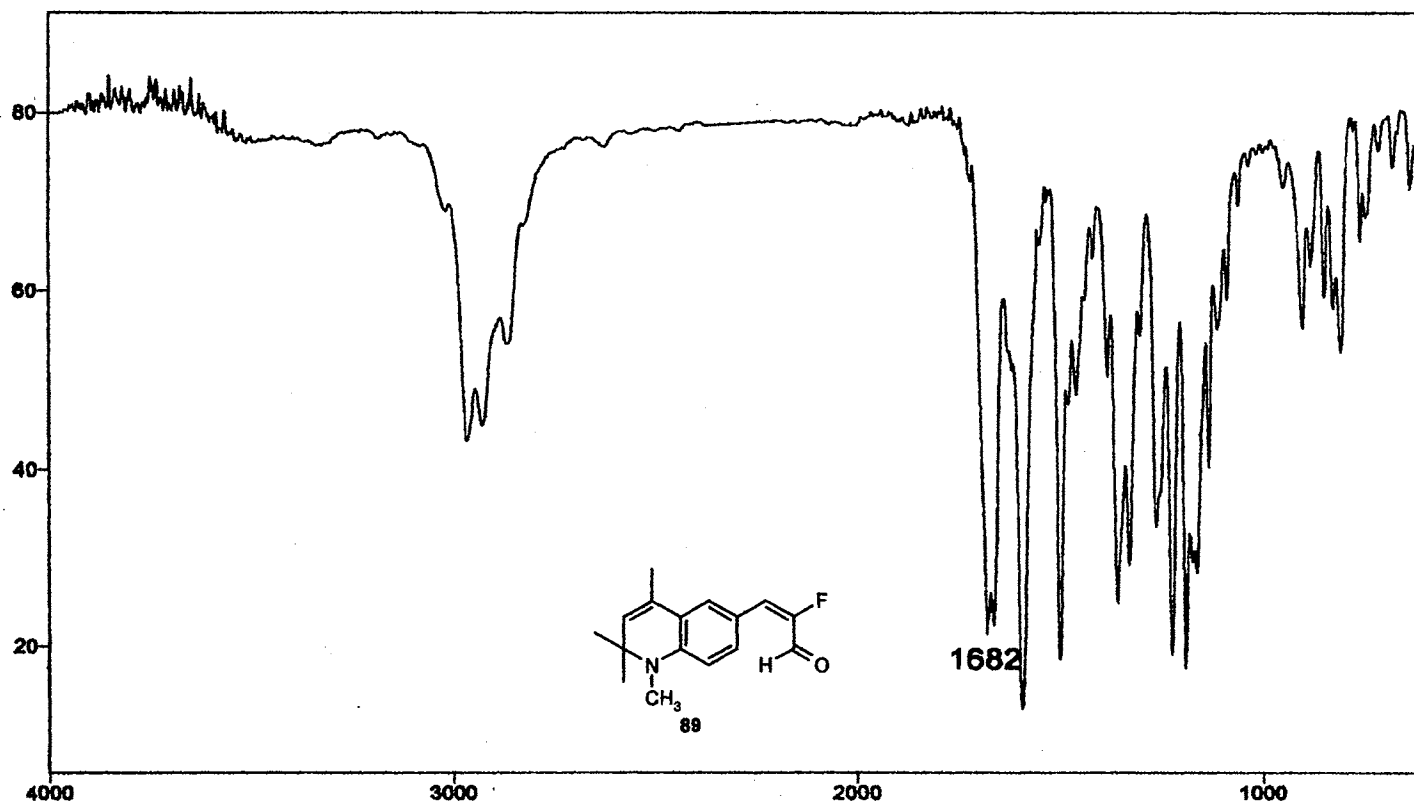
exp1 std13c

SAMPLE		DEC. & VT	
date	Jan 24 2000	dfrq	300.067
solvent	CDCl3	dn	H1
files	exp	dpr	34
ACQUISITION		dot	0
sfrq	282.333	dm	nnn
tn	F18	dwm	w
at	0.500	dwt	11764
np	38916	PROCESSING	
sw	18761.7	lb	1.00
fb	10400	wtfile	
bs	16	proc	ft
tpwr	52	fn	not used
pw	3.8		
d1	1.000	werr	wft
tof	0	wexp	wft
nt	1024	wbs	wft
ct	32	wnt	
clock	n		
gain	not used		
FLAGS			
ll	n		
ln	y		
dp	y		
DISPLAY			
sp	-38748.2		
wp	10761.7		
vs	30		
sc	0		
wc	250		
hznm	8.86		
ls	500.00		
rfl	38748.2		
rfp	0		
th	15		
ins	100.000		
nm	no	ph	



¹⁹F NMR Spectrum of 88

Plate CXXII



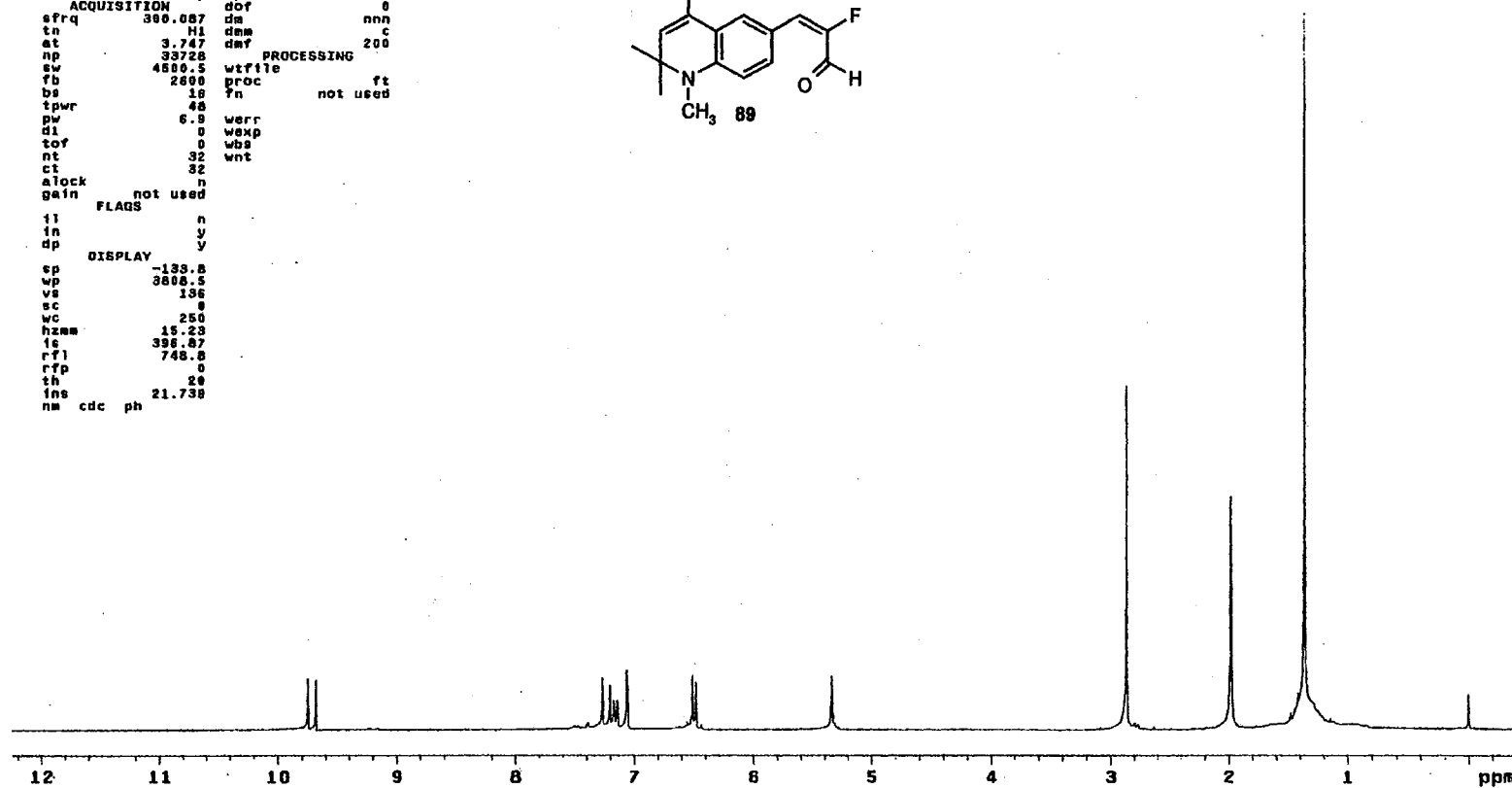
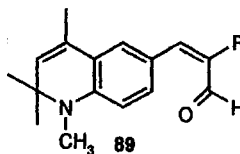
IR Spectrum of 89

Plate CXXIII

STANDARD IN OBSERVE

```

expl  stdih
SAMPLE
date  Feb  8 2000  dfrq  DEC. & VT  300.087
solvent  CDCl3  dn  H1
file  exp  dpwr  30
ACQUISITION  exp  dof  0
sfrq  300.087  da  nnn  c
tn  H1  dmw  200
at  3.747  dmf
np  33728  PROCESSING
sw  4800.5  wtfite
fb  2800  proc  ft
bs  18  ?n  not used
tpwr  48
pw  6.9  werr
dl  0  wexp
tof  0  wds
nt  32  wnt
ct  32
alock  n
gain  not used
FLAGS
fl  n
in  y
dp  y
DISPLAY
sp  -133.8
wp  3808.5
vs  136
sc  0
wc  250
hsum  15.23
ls  396.87
rfl  748.6
rfp  0
th  20
ins  21.738
nm  cdc  ph
    
```



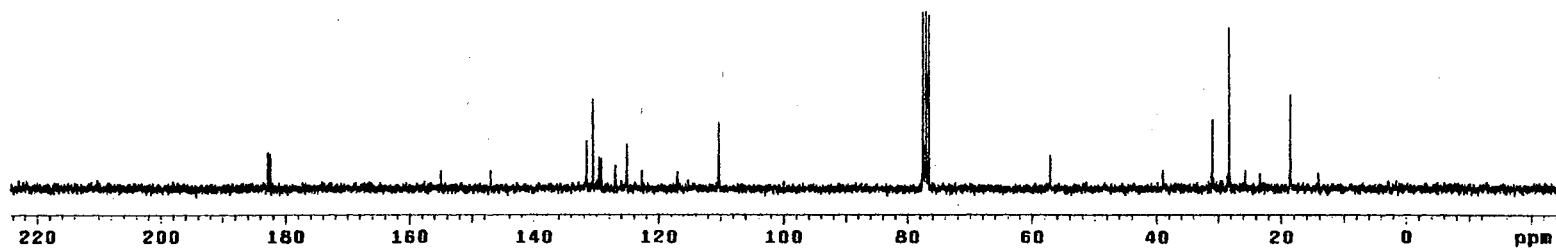
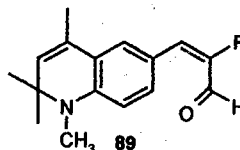
¹H NMR Spectrum of 89

Plate CXXIV

13C OBSERVE

```

expl  stdisc
SAMPLE
date  Feb 8 2000  dfrq  DEC. & VT  300.087
solvent  CDC13  dn  H1
file  exp  dpwr  34
ACQUISITION  exp  dof  0
sfrq  75.454  ds  yyv
tn  C13  dam  w
at  0.800  dmf  11764
np  30016  PROCESSING
sw  18761.7  lb  1.00
rb  10400  wtfile
bs  16  proc  ft
tpwr  52  yn  not used
pw  3.8
d1  1.000  werr
tot  0  wexp  wft
nt  1024  wbs  wft
ct  704  wnt
alock  3
gain  not used
FLABS
fl  n
fn  y
dp  y
DISPLAY
sp  -1837.0
wp  18761.7
vs  32
sc  0
wc  250
hnam  75.05
is  500.00
rf1  7647.6
rfp  5810.6
th  3
ina  100.000
na  no  ph
    
```



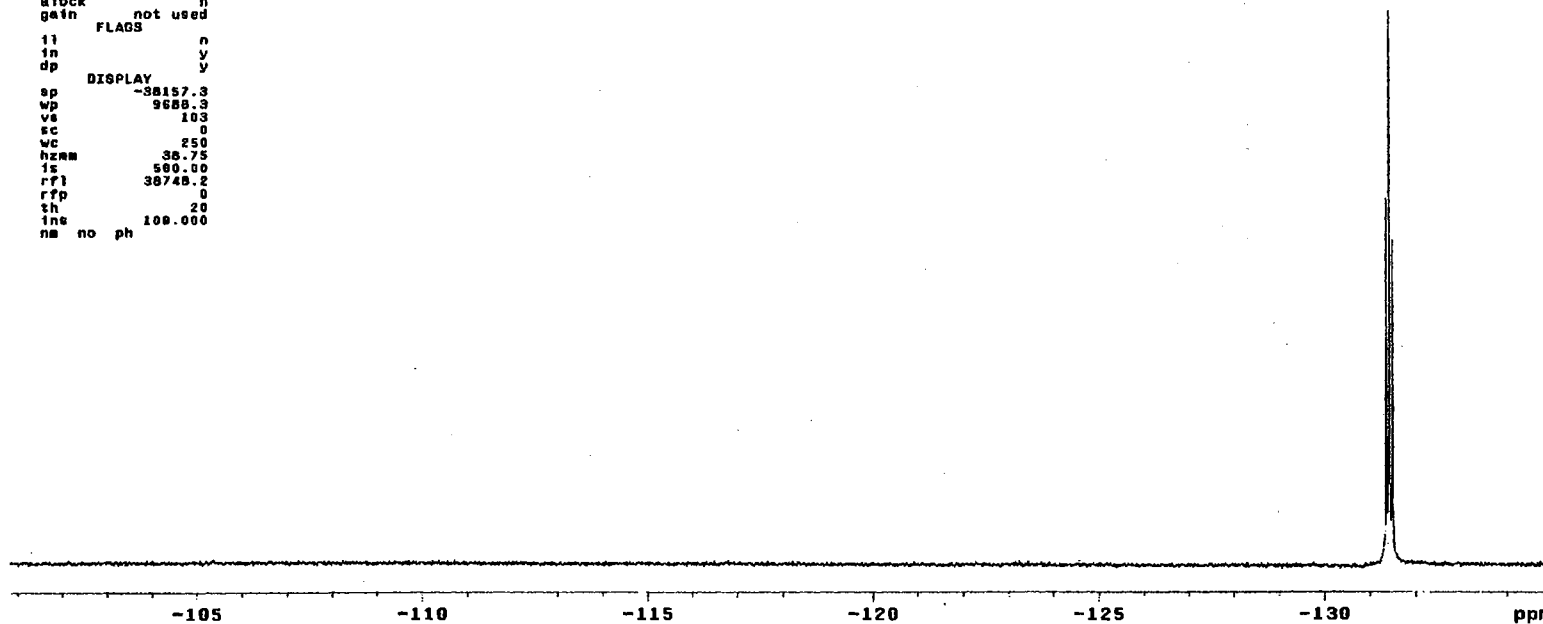
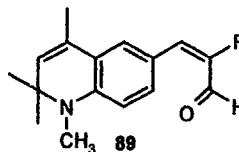
¹³C NMR Spectrum of 89

Plate CXXV

13C OBSERVE

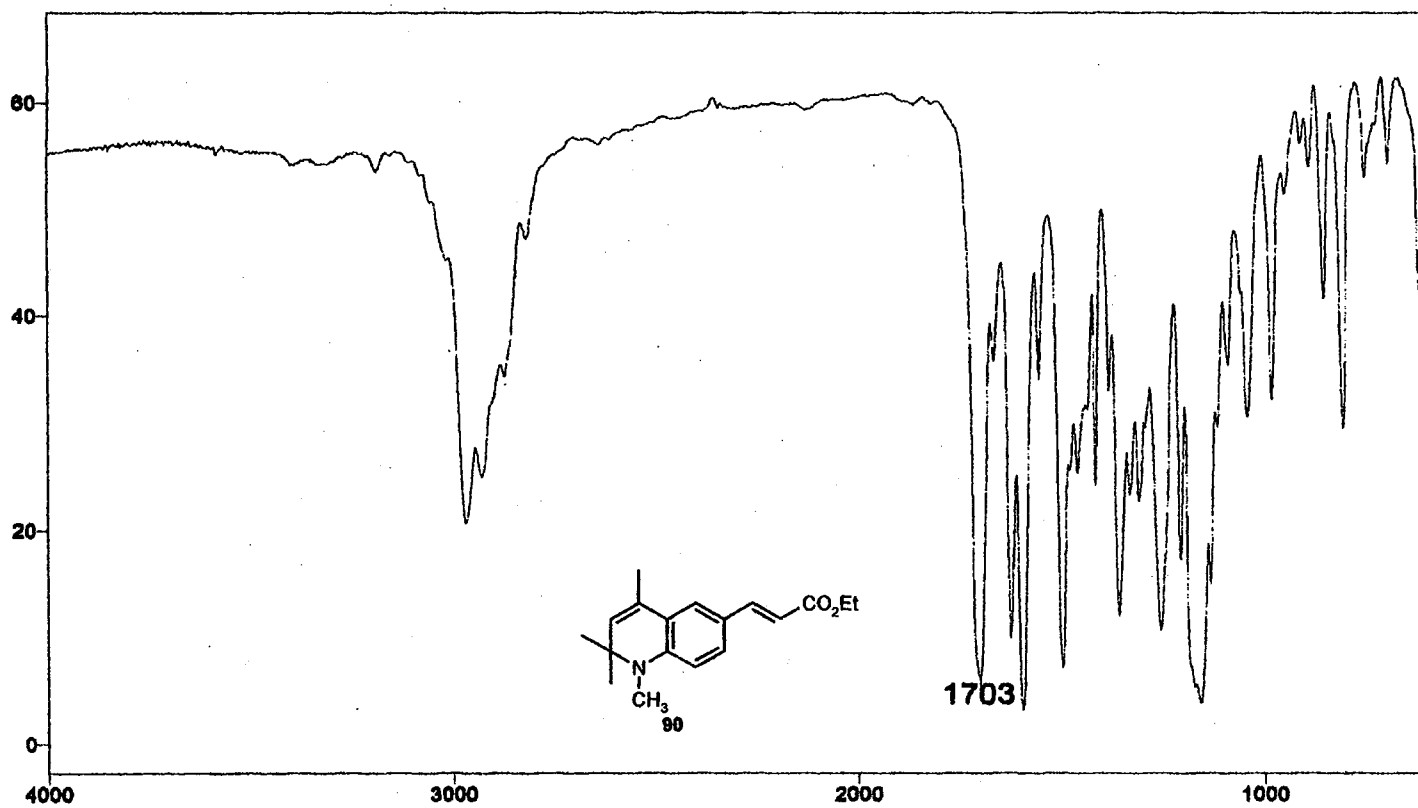
expl std13c

date	Feb 8 2000	dfrq	DEC. & VT	300.087
solvent	CDCl3	dn	H1	
file	exp	dpwr	34	
ACQUISITION				
sfrq	282.333	ds	nnn	
tn	F18	dsm	w	
at	0.800	dwt	11764	
np	30018	PROCESSING		
sw	18761.7	lb	1.00	
fb	10400	wtfile		
be	16	proc	ft	
tpwr	52	fn	not used	
pw	3.8			
dl	1.000	warr		
tof	0	wexp	wft	
nt	1024	wbs	wft	
ct	48	wnt		
alock	n			
gain	not used			
FLADS				
fl	n			
fn	y			
dp	y			
DISPLAY				
sp	-38157.3			
wp	9688.3			
vs	103			
sc	0			
wc	250			
hnm	38.75			
is	580.00			
rfl	38748.2			
rtp	0			
th	20			
ins	100.000			
nm	no ph			



¹⁹F NMR Spectrum of 89

Plate CXXVI



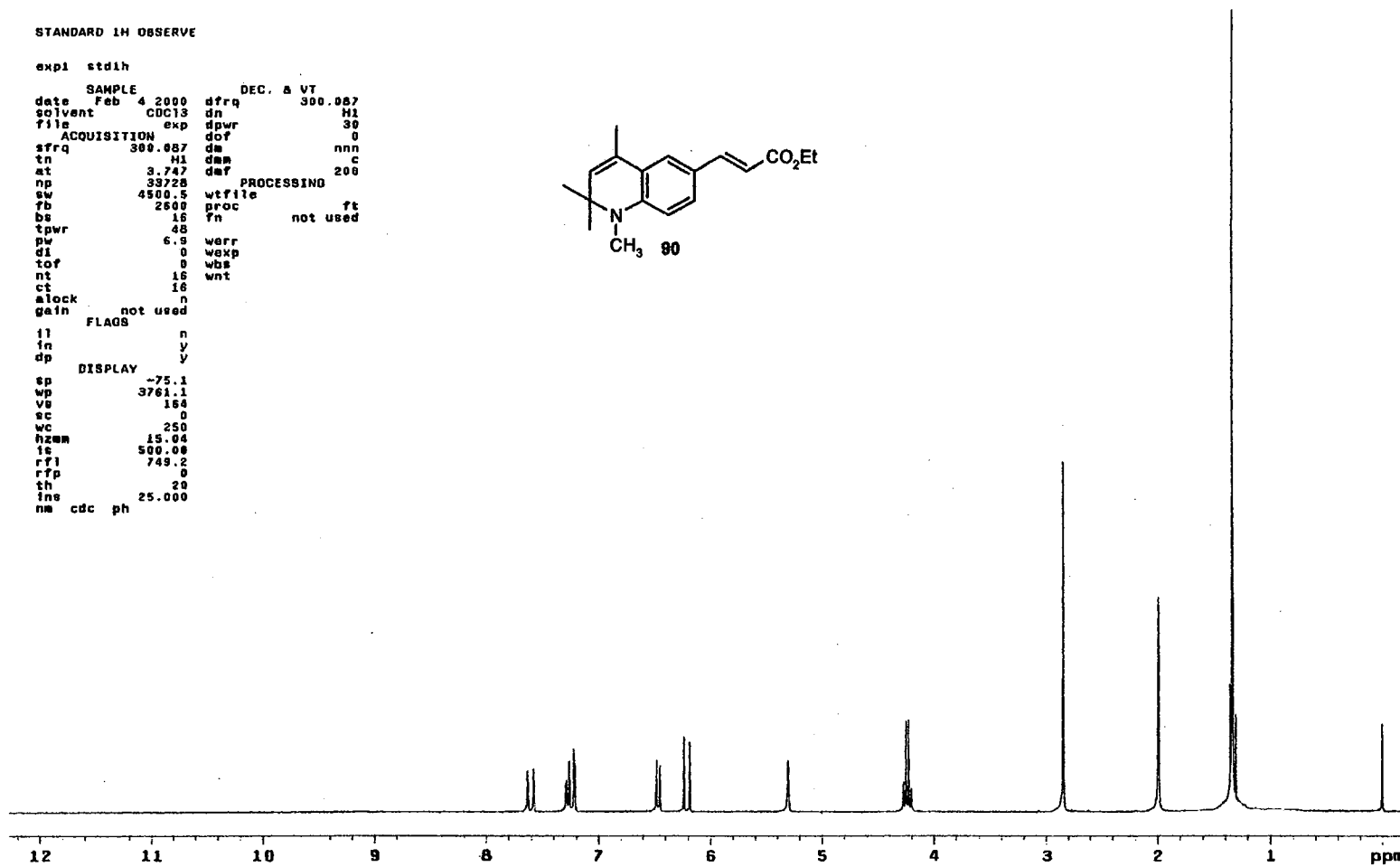
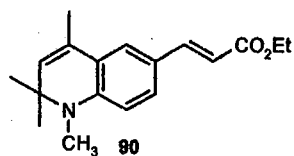
IR Spectrum of 90

Plate CXXVII

STANDARD 1H OBSERVE

```

exp1 stdih
SAMPLE
date Feb 4 2000 dfrq DEC. 8 VT 300.067
solvent CDCl3 dn H1
file exp dpwr 30
ACQUISITION dof 0
sfrq 300.067 da nnn
tn H1 dm C
at 3.747 dmf 200
np 33728 PROCESSING
sw 4500.5 wtfile
fb 2500 proc ft
bs 16 fn not used
tpwr 48
pw 6.9 werr
di 0 wexp
tof 0 wbs
nt 16 wnt
ct 16
alock n
gain not used
FLAGS
il n
in y
dp y
DISPLAY
sp -75.1
wp 3761.1
vs 164
sc 0
wc 250
hzw 15.04
ls 500.08
rfj 749.2
rfp 0
th 20
ins 25.000
nm cdc ph
    
```



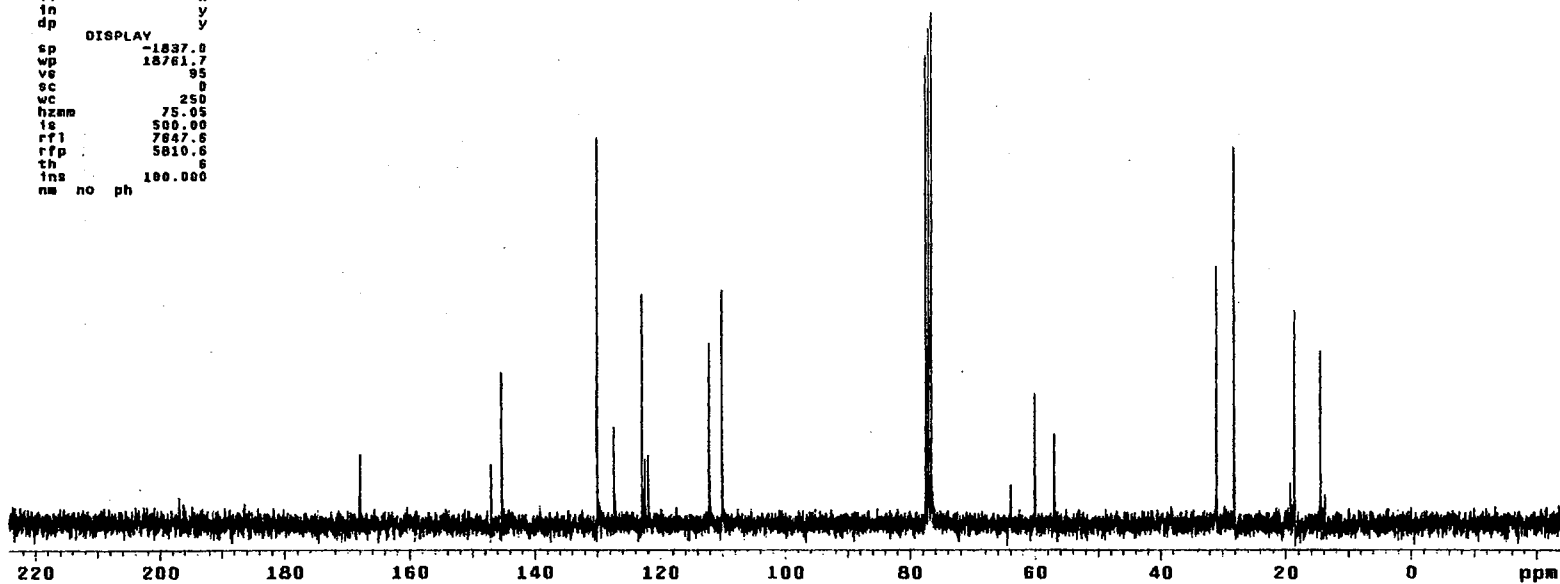
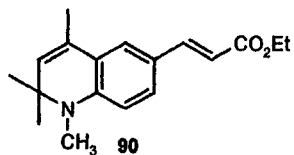
¹H NMR Spectrum of 90

Plate CXXVIII

13C OBSERVE

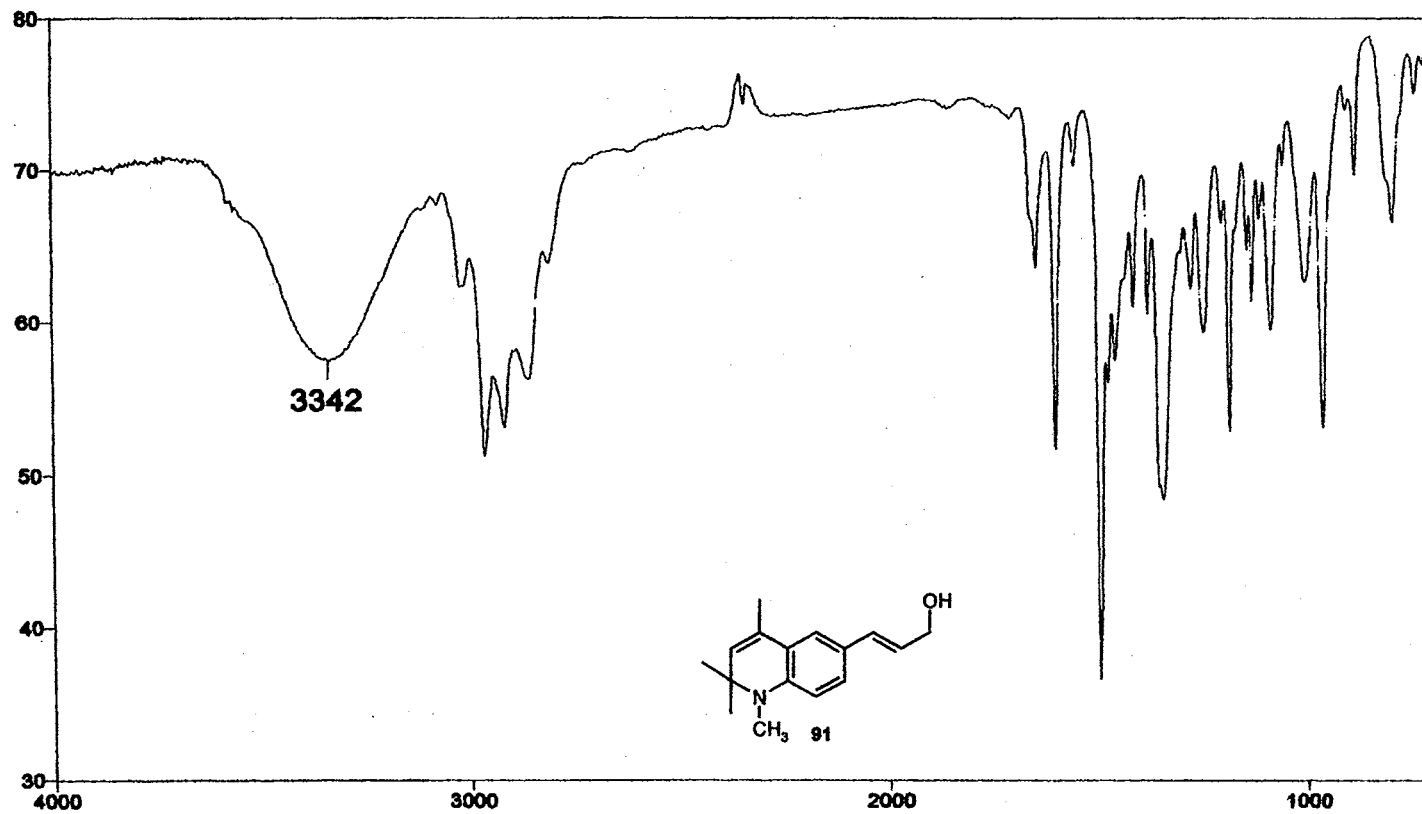
expl std13c

SAMPLE		DEC. & VT	
date	Feb 4 2000	dfrq	300.007
solvent	CDCl3	dn	41
file	exp	dpwr	34
ACQUISITION		dot	0
sfrq	75.464	dm	yyv
tn	G13	dmg	w
at	0.800	daf	11764
np	30016	PROCESSING	
sw	18761.7	lb	1.00
fb	10400	wtfile	
bs	10	proc	ft
tpwr	52	fn	not used
pw	3.2		
dl	1.000	werr	
tof	0	wexp	wft
nt	1024	wbs	wft
ct	752	wnt	
atock	s		
gain	not used		
FLAGS			
fl	n		
fn	y		
dp	y		
DISPLAY			
sp	-1837.0		
wp	18761.7		
ve	95		
sc	0		
wc	250		
hzam	75.05		
fs	500.00		
rf1	7847.6		
rfp	5810.6		
th	6		
ins	100.000		
nm	no	ph	



¹³C NMR Spectrum of 90

Plate CXXIX



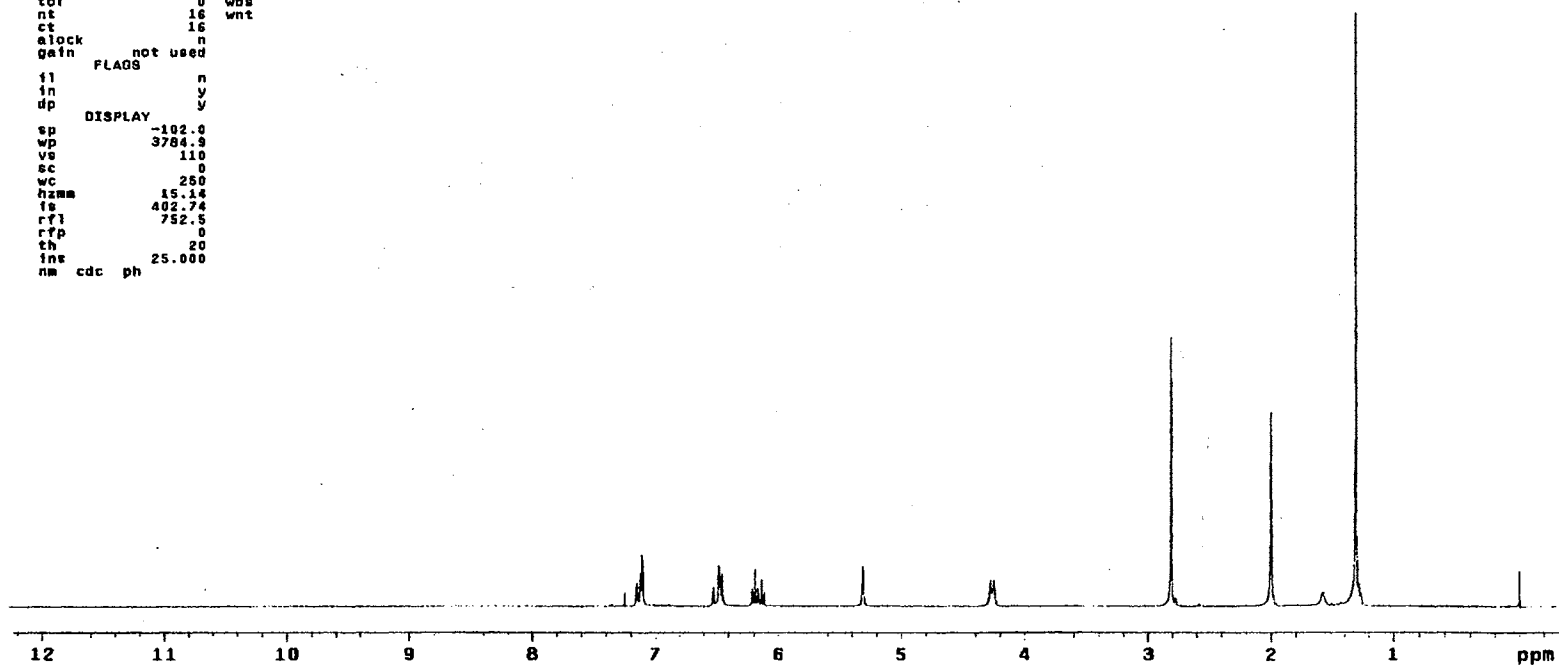
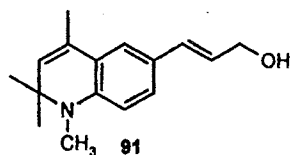
IR Spectrum of 91

Plate CXXX

STANDARD 1H OBSERVE

```

expl stdih
SAMPLE
date Feb 5 2000 dfrq DEC. & VT 300.087
solvent CDCl3 dn H1
file exp dpwr 30
ACQUISITION dof 0
sfrq 300.087 dn nnn
tn H1 dm c
at 3.747 dmf 200
np 33728 PROCESSING
sw 4500.5 wflia
fb 2880 proc ft
bs 16 tn not used
tpwr 48
pw 6.9 werr
d1 0 wekp
tof 0 wbs
nt 16 wnt
ct 16
alock n
gain not used
FLAGS
fl n
in y
dp y
DISPLAY
sp -102.0
wp 3784.9
vs 110
sc 0
wc 250
hnm 15.14
fs 402.74
rfl 752.5
rtp 0
th 20
int 25.000
nm cdc ph
    
```



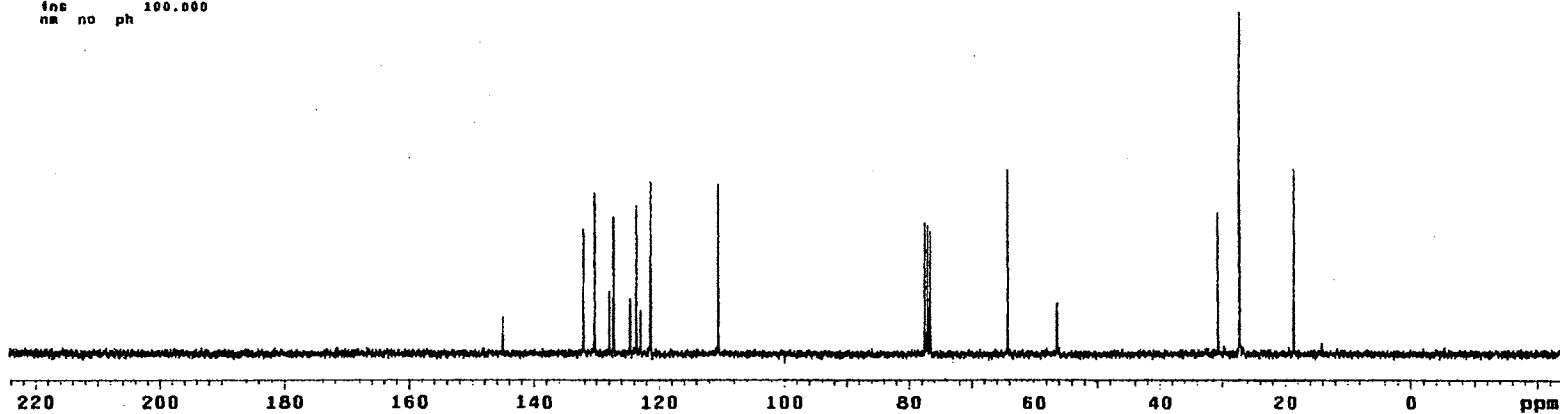
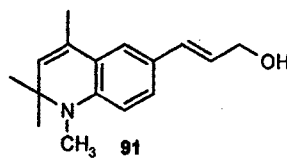
¹H NMR Spectrum of 91

Plate CXXXI

13C OBSERVE

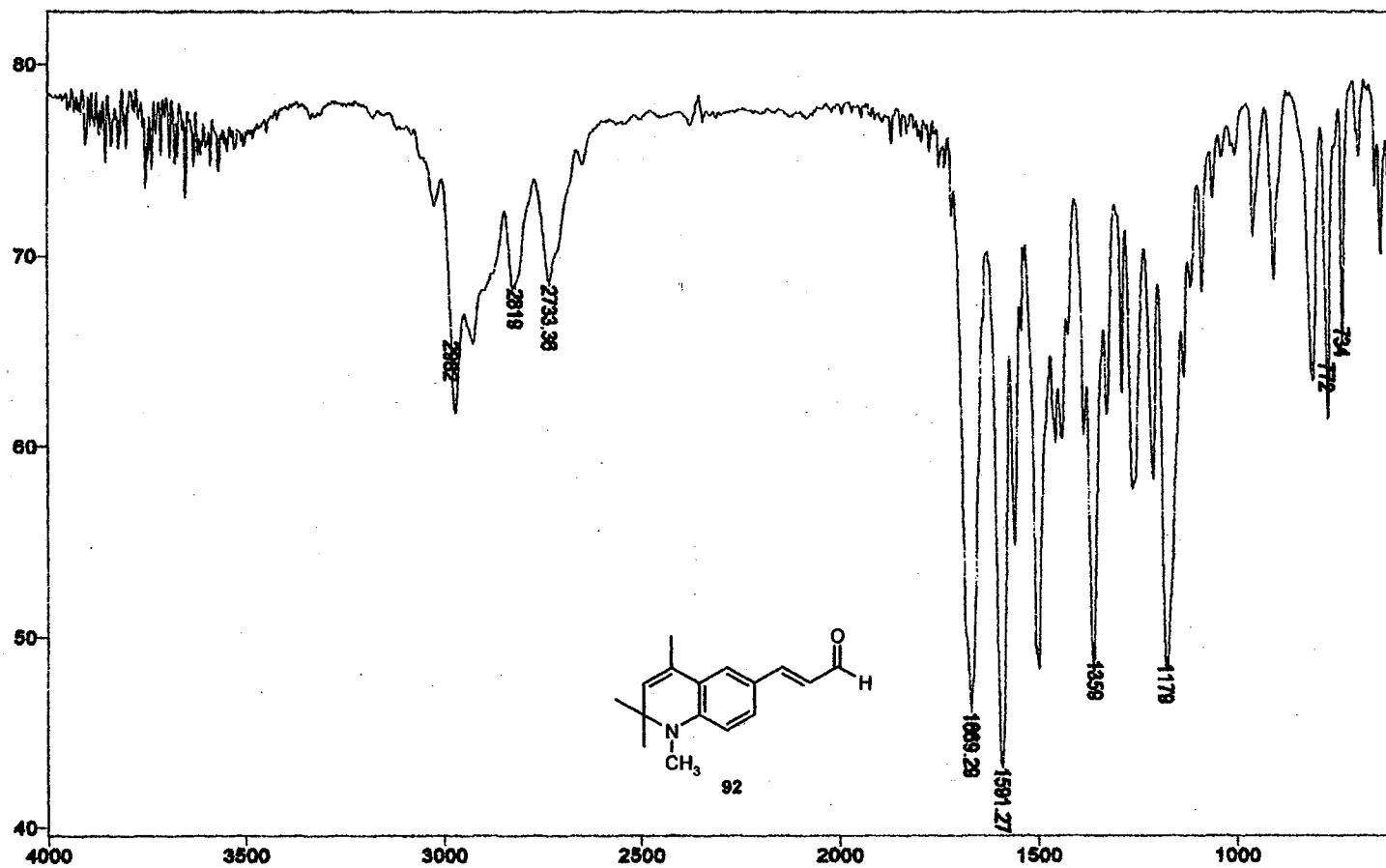
exp1 std13c

SAMPLE		DEC. & VT	
date	Feb 5 2000	dfrq	300.087
solvent	CDC13	dn	H1
files	exp	dpr	34
ACQUISITION		dot	0
sfrq	75.484	dm	vvv
tn	C13	dmm	w
at	8.800	dnt	11764
np	30018	PROCESSING	
sw	18761.7	lb	1.00
fb	10400	wffile	
bs	18	proc	ft
ipwr	52	fn	not used
pw	3.8		
d1	1.000	werr	
tof	0	wexp	wft
nt	1024	wbp	wft
ct	512	wnt	
alock	s		
gain	not used		
FLAGS			
fl	n		
in	y		
dp	y		
DISPLAY			
sp	-1839.3		
wp	18761.7		
vs	63		
sc	0		
wc	250		
hzam	75.05		
is	502.00		
rfl	7649.8		
rfp	5810.8		
th	.5		
ins	100.000		
nm	no	ph	



¹³C NMR Spectrum of 91

Plate CXXXII



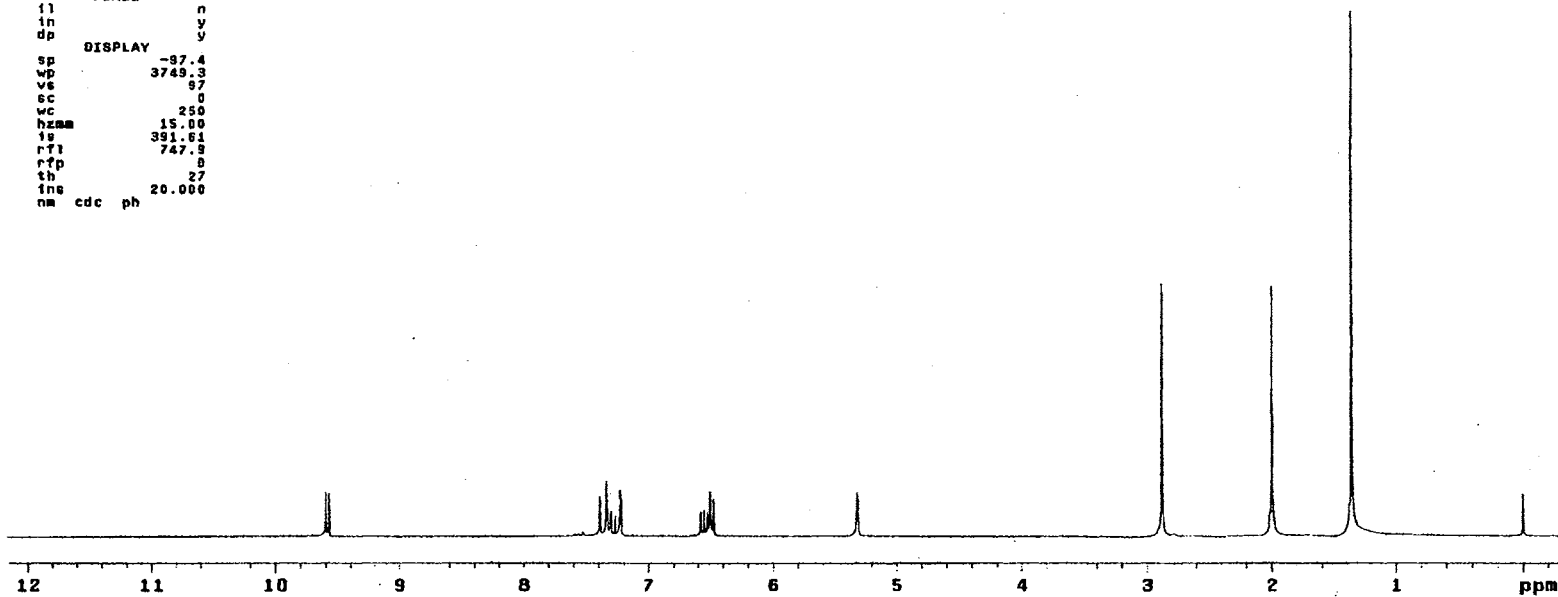
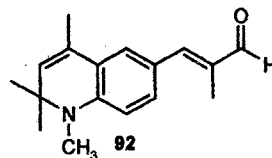
IR Spectrum of 92

Plate CXXXIII

STANDARD 1H OBSERVE

```

expl stdih
SAMPLE
date Feb 6 2000 dfrq DEC. & VT 300.087
solvent CDC13 dn H1
file exp dpwr 30
ACQUISITION dof 0
sfrq 300.087 ds nnn
tn H1 dsd c
at 3.747 dsf 200
np 39728 PROCESSING
sw 4500.5 wtfile
fb 2600 proc ft
bs 16 fn not used
tpwr 48
pw 6.9 werr
di 0 wexp
tof 0 wbs
nt 16 wnt
ct 16
alock n
gain not used
FLAGS
il n
in y
dp y
DISPLAY
sp -87.4
wp 3749.3
vs 97
sc 0
wc 250
hzmm 15.00
fs 391.61
rfl 747.9
rfp 0
th 27
ine 20.000
nm cdc ph
  
```



¹H NMR Spectrum of 92

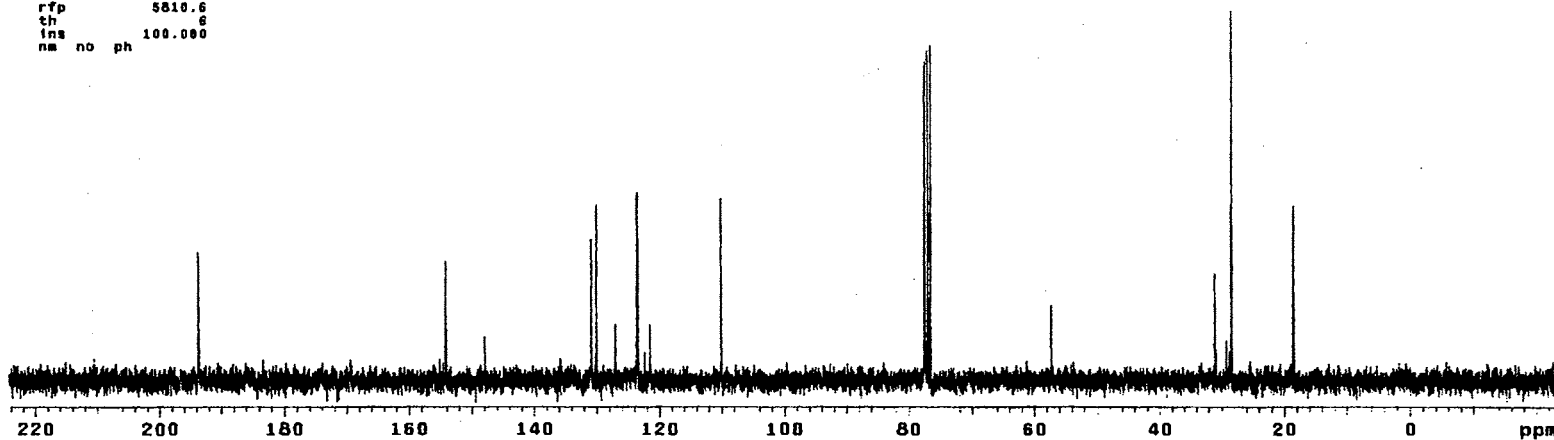
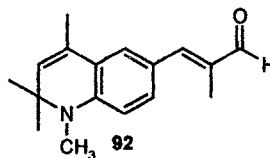
Plate CXXXIV

13C OBSERVE

expl std13c

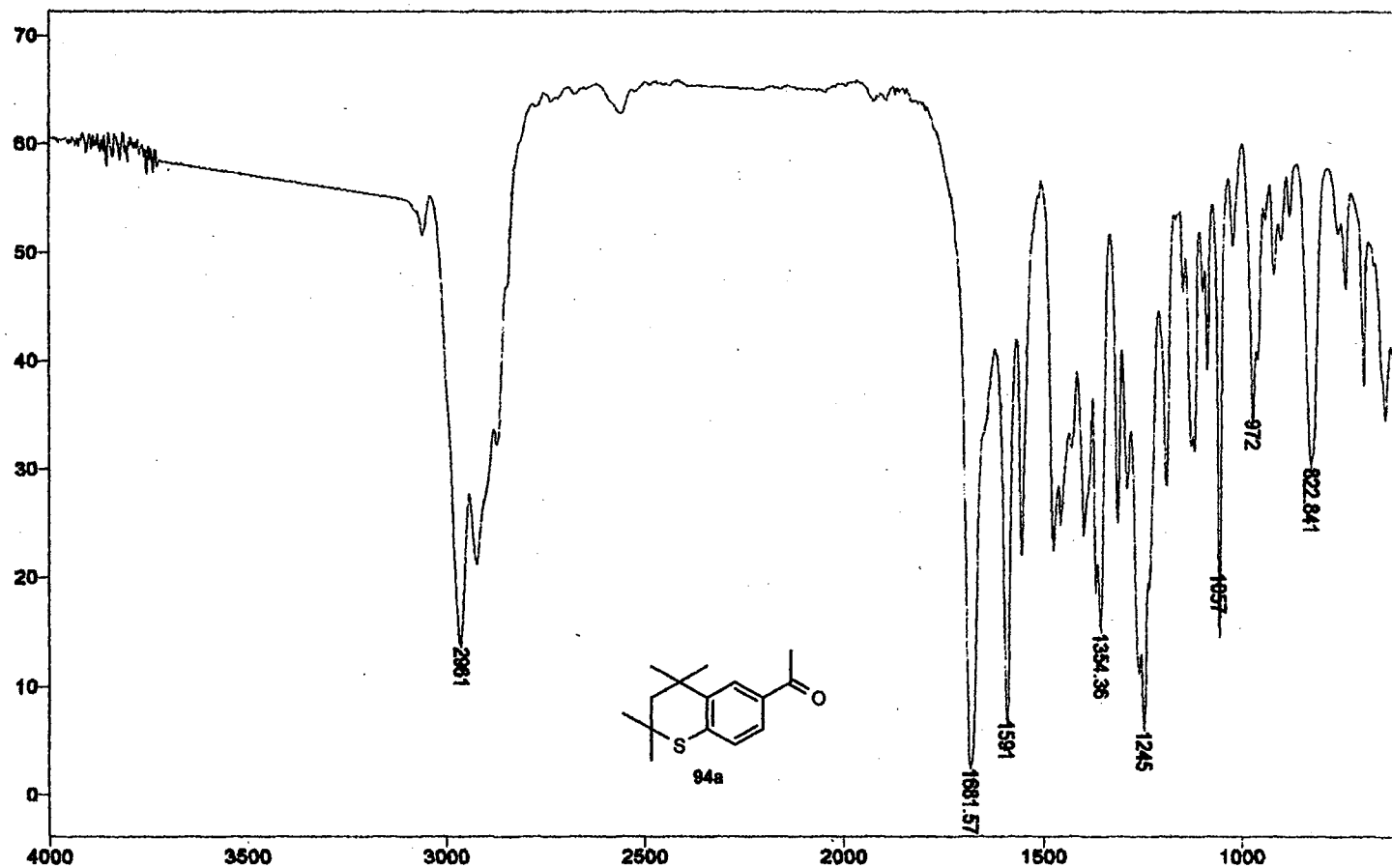
```

SAMPLE          DEC. & VT
date Feb 6 2000 dfrq          300.087
solvent CDC13      dn          M1
file          exp      dpwr         34
ACQUISITION    dof          0
sfrq          75.464  dm          yyv
tn            C13      dam          w
at            0.800   dnf         11764
np            30016   PROCESSING
sw            18761.7 lb          1.00
fb            10400  wtfile
bs            16     proc          ft
tpwr          52     fn          not used
pw            3.8
d1            1.000  werr
tof           0     wexp          wft
nt            1024  wds          wft
ct            256   wnt
alock         6
gain          not used
FLAOS
tl            n
in            y
dp            y
DISPLAY
sp            -1838.2
wp            18761.7
vs            68
ec            0
wc            250
hzmm         75.65
ls            500.00
rfl          7648.8
rtp          5810.6
th            6
ins          100.000
nm no ph
    
```



¹³C NMR Spectrum of 92

Plate CXXXV



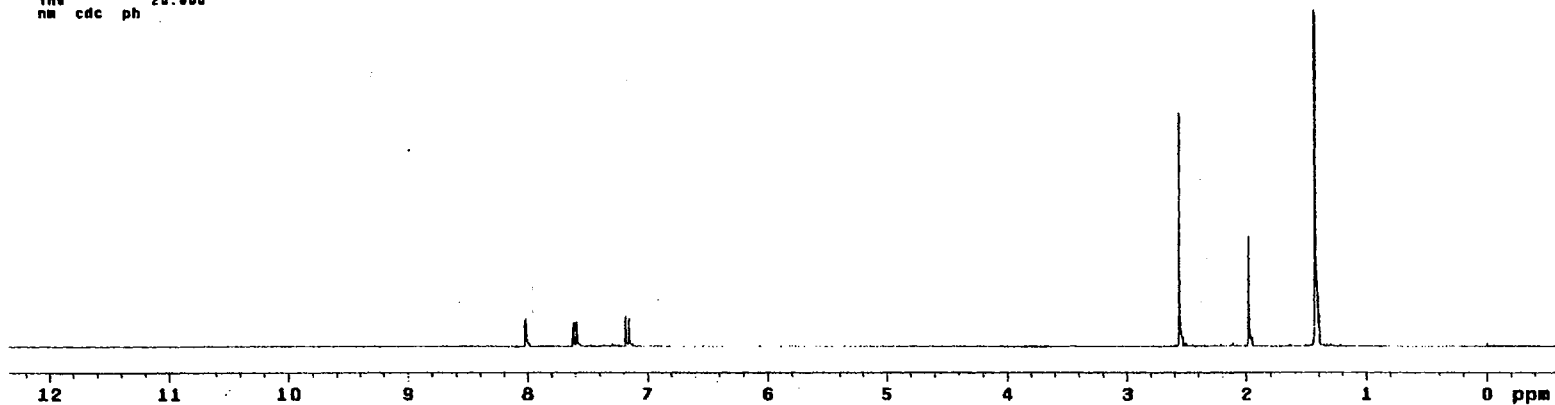
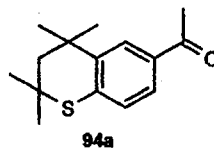
IR Spectrum of 94a

Plate CXXXVI

STANDARD 1H OBSERVE

```

expt stdih
SAMPLE
date Jul 13 1999 dfrq DEC. A VT 300.087
solvent CDCl3 dn H1
file exp dpwr 30
ACQUISITION exp dot 0
sfrq 300.087 da nnn
tn H1 dam c
at 3.747 dar 200
np 33728 PROCESSING
sw 4800.5 wtflls
fb 2600 proc ft
bs 16 fn not used
tpwr 48
pw 3.0 werr
di 0 wshp
tof 0 wbs
nt 16 wnt
ct 16
alock n
gain not used
FLAGS
fl n
in y
dp y
DISPLAY
sp -173.9
wp 3879.4
vs 62
sc 0
wc 250
hznm 15.52
fs 370.48
rf1 741.5
rfp 8
sh 24
ins 28.000
nm cdc ph
    
```



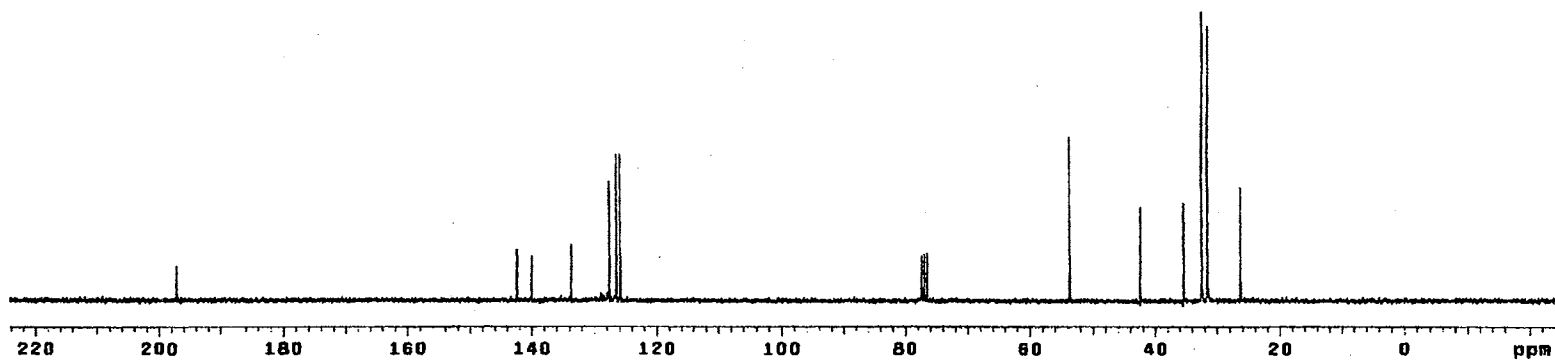
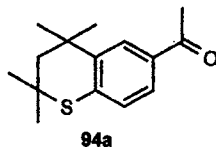
¹H NMR Spectrum of 94a

Plate CXXXVII

13C OBSERVE

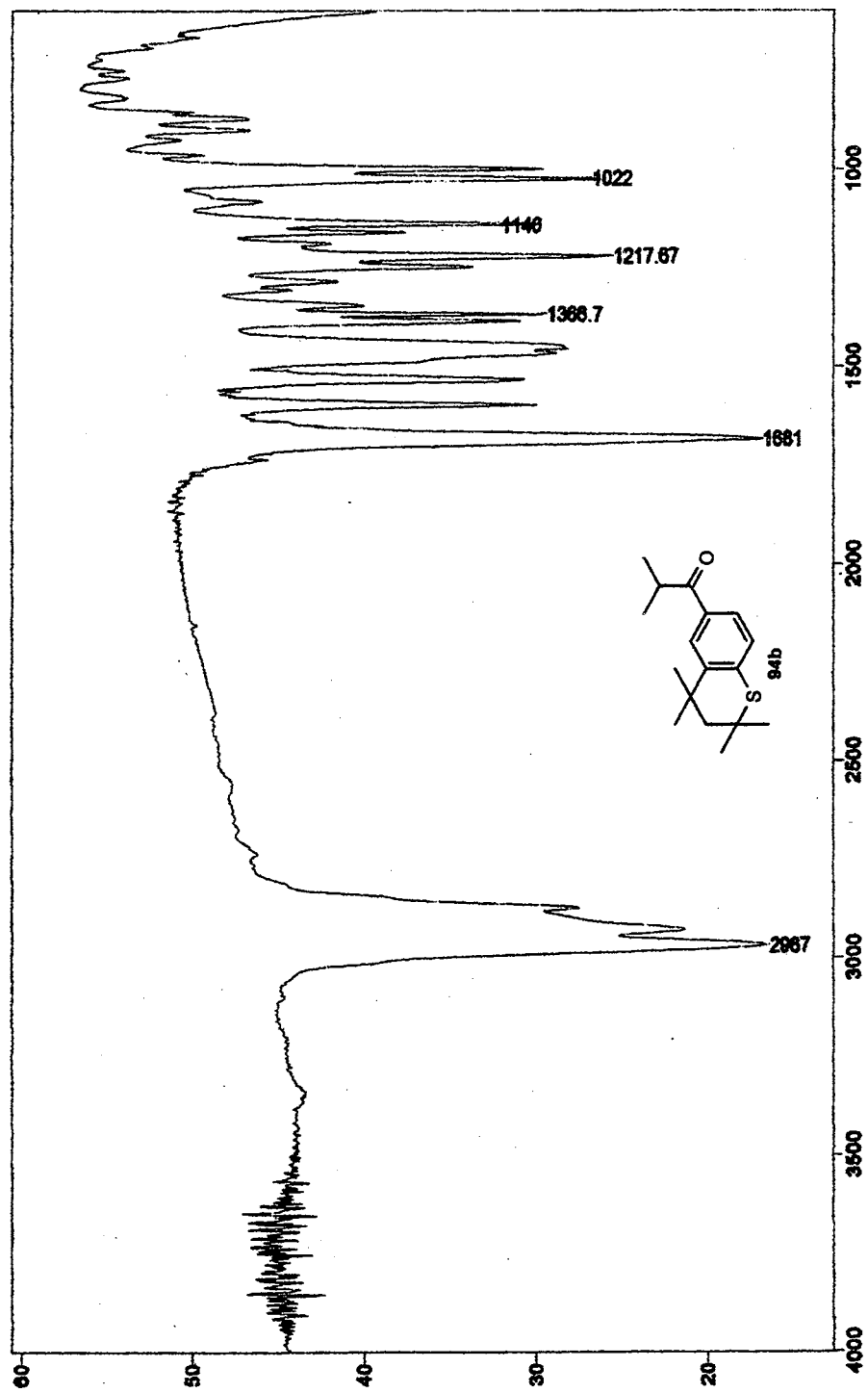
exp1 etd13c

date	Jul 13 1998	dfrq	DEC. & VT	300.087
solvent	CDCl3	dn		M1
file	exp	dgwr		34
ACQUISITION		dot		0
afrq	75.484	dm		vvv
tn	C13	dsm		w
at	0.800	dat		11754
np	30016	PROCESSING		
sw	18781.7	lb		1.00
fb	10400	wtfile		
bs	16	proc		ft
tpwr	52	fn		not used
pw	8.3			
dl	1.000	werr		
tof	0	wexp		wft
nt	1024	wbs		wft
ct	112	wnt		
alock	g			
gain	not used			
FLAGS				
ll	n			
ln	y			
dp	y			
DISPLAY				
ep	-1845.0			
wp	18781.7			
vs	53			
sc	g			
wc	250			
hzmm	75.05			
is	500.00			
rfl	7855.8			
rfp	5810.8			
th	3			
ins	100.000			
nm	no ph			



¹³C NMR Spectrum of 94a

Plate CXXXVIII



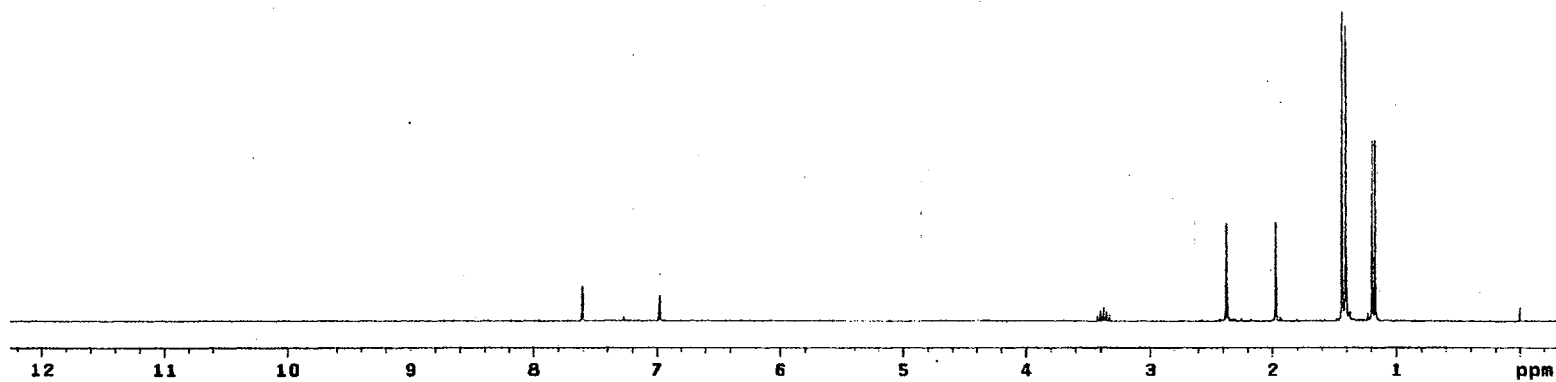
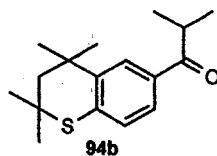
IR Spectrum of 94b

Plate CXXXIX

STANDARD 1H OBSERVE

```

expi std1h
SAMPLE
date Jul 9 1999 dfrq DEC. & VT 300.087
solvent CDC13 dn H1
file exp dpwr 30
ACQUISITION
sfrq 300.087 dm nnn
tn H1 dm c
st 3.747 day 280
np 33728 PROCESSING
sw 4500.5 wf11e
fb 2600 proc ft
bs 16 fn not used
tpwr 48
pw 6.8 werr
d1 0 wexp
tof 0 wbs
nt 16 wnt
ct 16
alock n
gain not used
FLAGS
fl n
in y
dp y
DISPLAY
sp -97.5
wp 3778.6
vs 57
sc 0
wc 250
hzam 15.12
is 282.93
rf1 746.6
rfp 0
th 20
ins cdc ph 31.250
nm
  
```



¹H NMR Spectrum of 94b

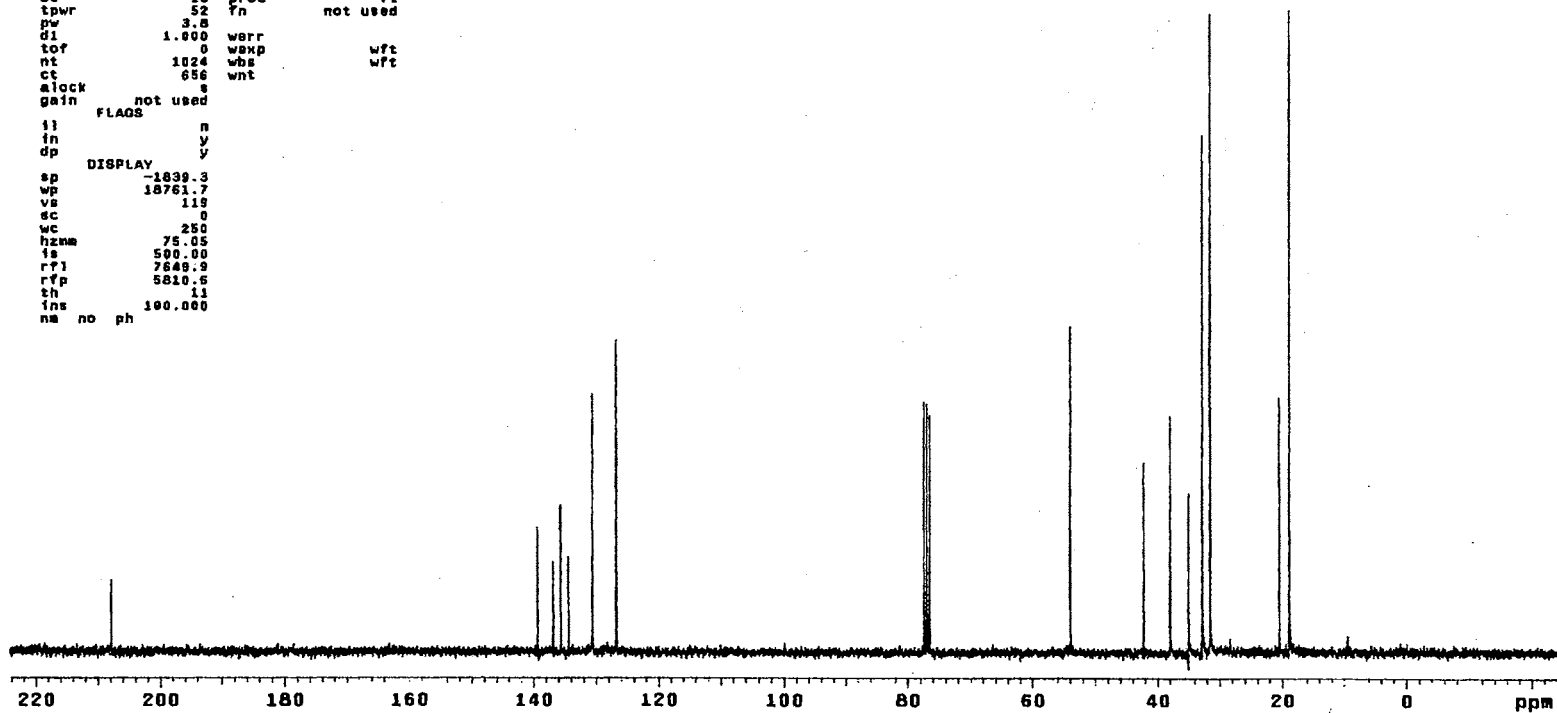
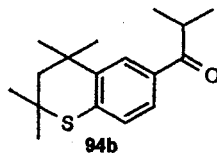
Plate CXL

13C OBSERVE

expl std13c

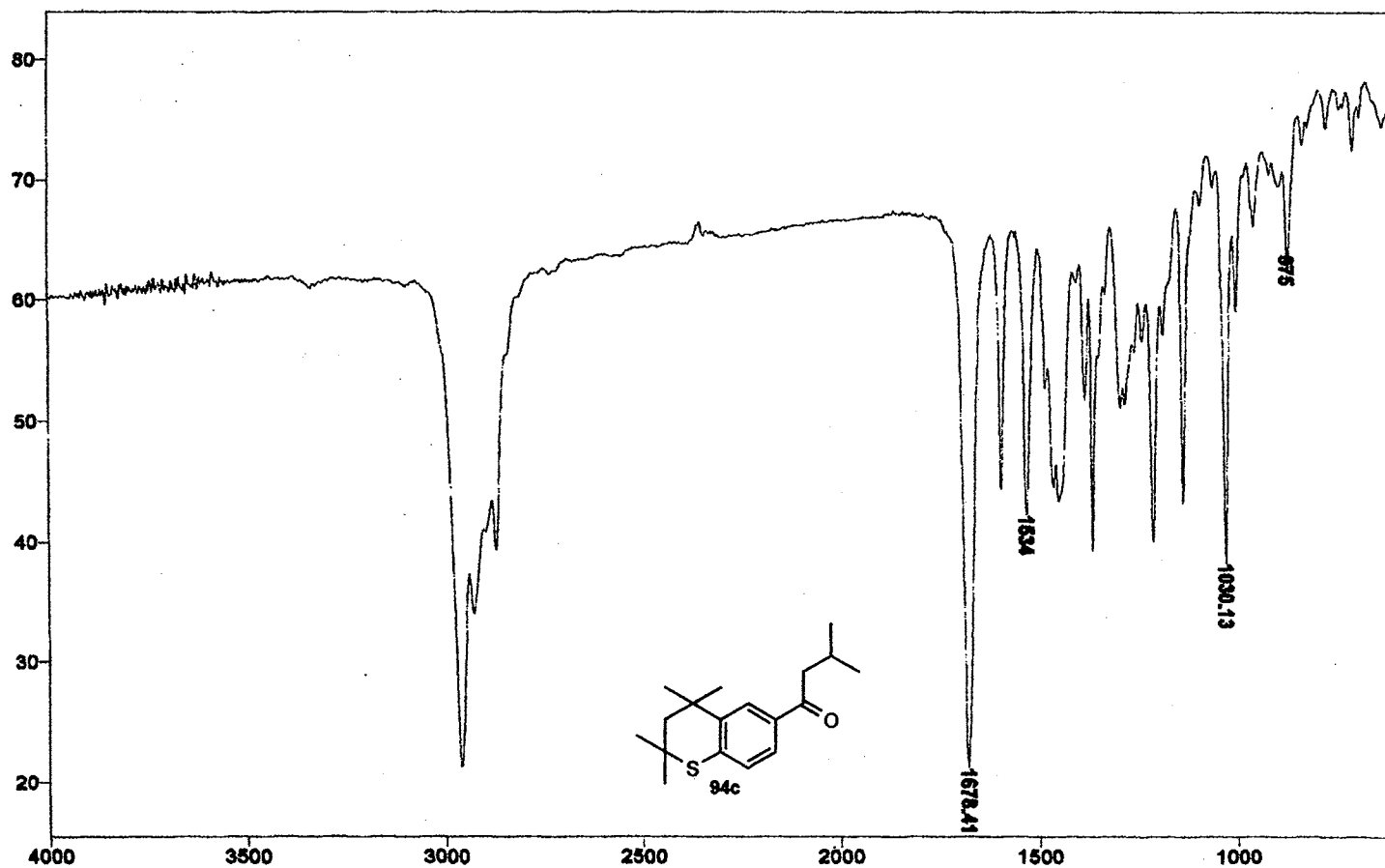
```

SAMPLE          DEC. & VT
date Jul 9 1999 dfrq 300.087
solvent CDCl3   dn      H1
f1ls exp      dpr     S4
ACQUISITION    dot     0
sfrq 75.464    dm      yyy
tn 019         dmm     w
st 0.800      dmf     11764
np 30015      PROCESSING
sw 18761.7    lb      1.00
fb 10400      wtfile
bs 18         proc    ft
tpwr 52       fn      not used
pw 3.8
d1 1.000     werr
tof 0        wexp    wft
nt 1024     wbs     wft
ct 656      wnt
elock s
gain not used
FLAQs
ii n
in y
dp y
DISPLAY
sp -1839.3
wp 18761.7
vs 119
sc 0
wc 250
hzma 75.05
fs 500.00
rfl 7648.9
rfp 5810.5
sh 11
fns 100.000
na no ph
    
```



¹³C NMR Spectrum of 94b

Plate CXLI



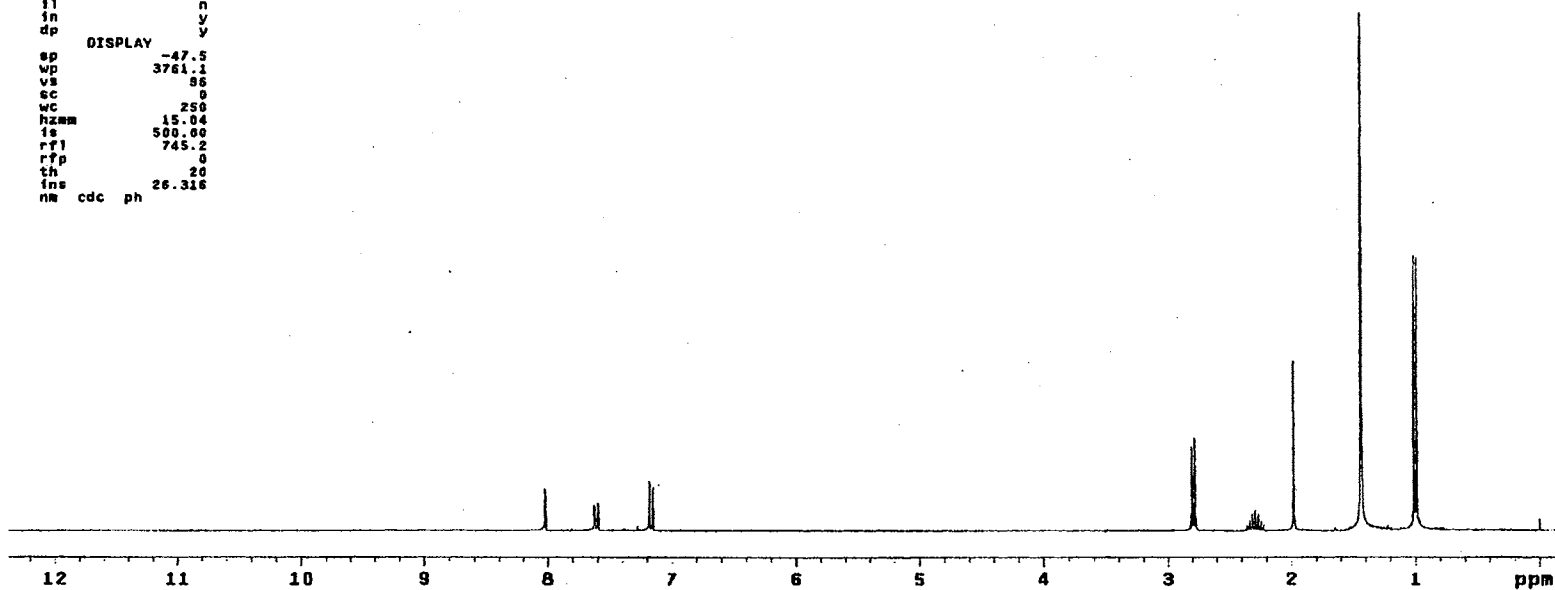
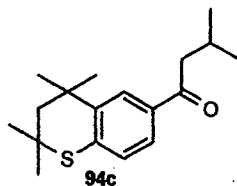
IR Spectrum of 94c

Plate CXLII

STANDARD 1H OBSERVE

```

exp1 std1h
SAMPLE
date Nov 8 1995 dfrq DEC. & VT 300.087
solvent CDC13 dn H1
file exp dpwr 30
ACQUISITION dof 0
frrq 300.087 dm nnn
tn H1 dnm c
at 3.747 dm7 200
np 33728 PROCESSING
sw 4500.5 wtfile
fb 2600 proc ft
bs 18 fn not used
tpwr 48
pw 2.0 werr
dl 0 wexp
tof 0 wbe
nt 18 wnt
ct 16
slack n
gain not used
FLAGS
il n
in y
dp y
DISPLAY
sp -47.5
wp 3761.1
vs 85
sc 0
wc 250
hzmm 15.04
is 500.00
rfj 745.2
rfp 0
th 20
ins 26.316
nm cdc ph
    
```



¹H NMR Spectrum of 94c

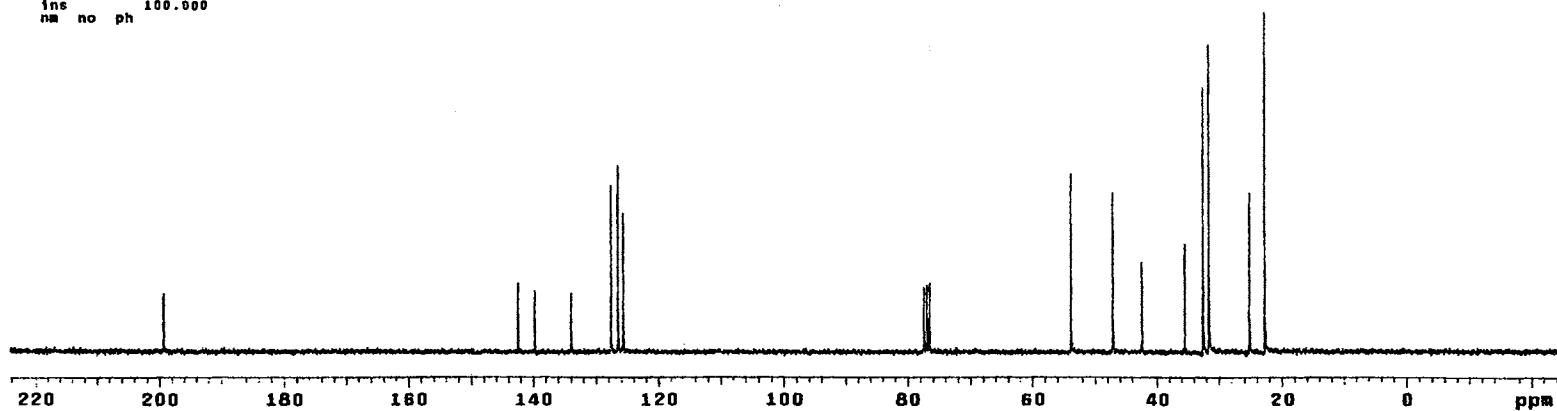
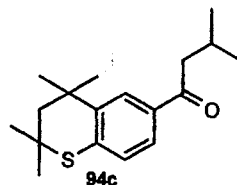
Plate CXLIII

13C OBSERVE

expl std13c

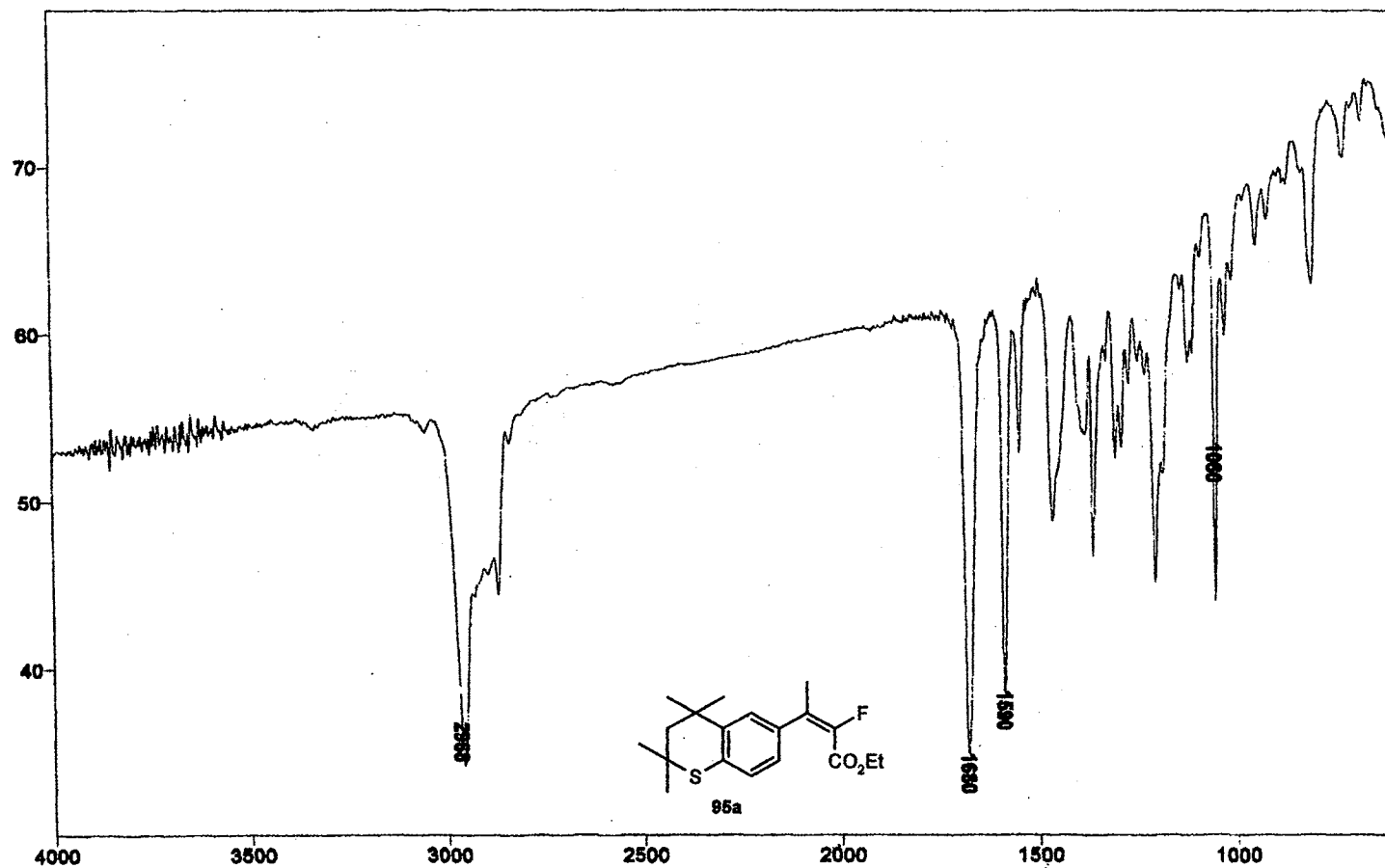
```

SAMPLE          DEC. & VT
date Nov 5 1998 dfrq 300.087
solvent CDC13   dn      H1
file          exp  dpwr   34
              dof    0
ACQUISITION    dm     vvy
sfrq 75.464    da     w
tn    C13      dam    11764
at    0.800    daF
np    30016    PROCESSING
sw    18781.7  lb     1.00
fb    10400    wtfile
bs    18      proc   ft
tpwr  52      fn     not used
pw    3.8
d1    1.000   werr
tot   0       wexp   wft
nt    1024    wbs    wft
ct    256     wnt
aLock  e
gain   not used
      FLAGS
il     n
in     y
dp     y
      DISPLAY
sp    -1840.4
wp    18781.7
vs    63
sc    0
wc    250
hzmm  75.05
ic    508.00
rf1   7851.0
rfp   5810.6
ch    11
ins   100.000
nm    no ph
    
```



¹³C NMR Spectrum of 94c

Plate CXLIV



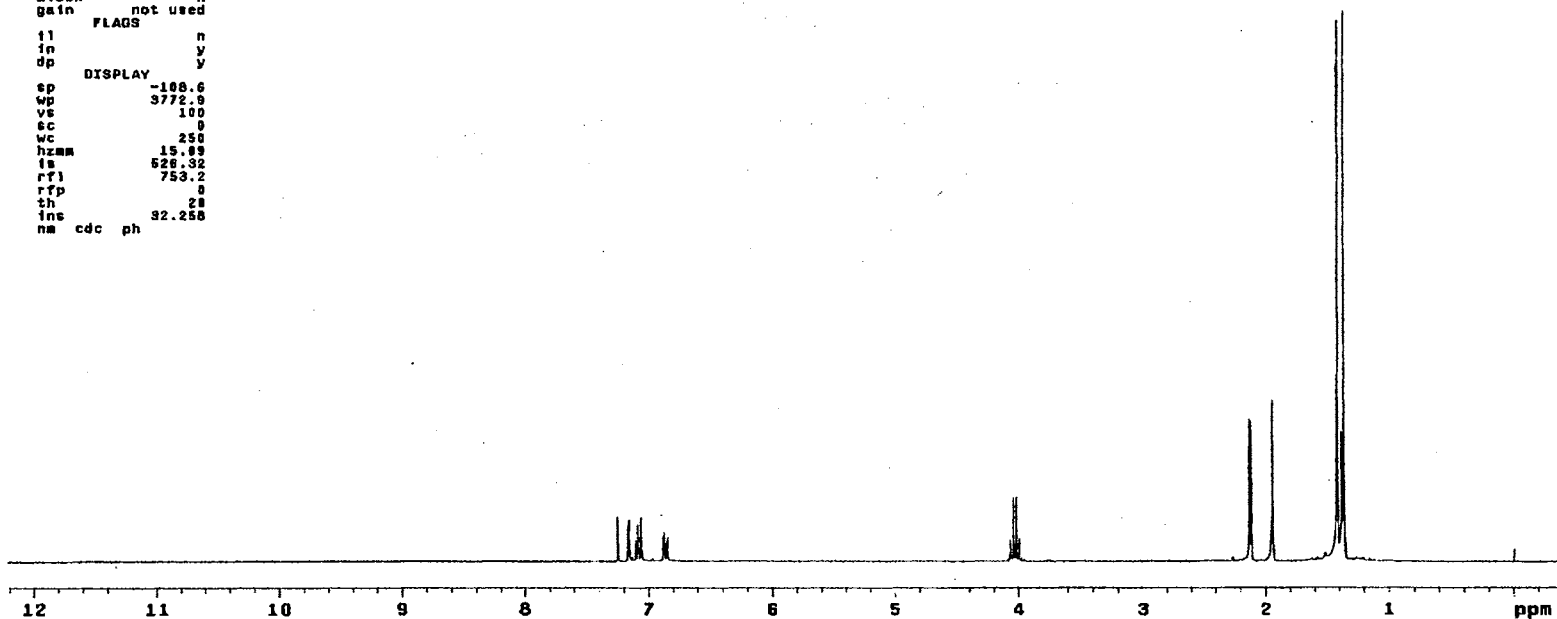
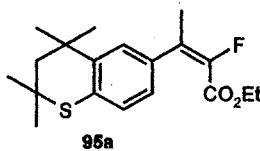
IR Spectrum of 95a

Plate CXLV

STANDARD 1H OBSERVE

```

expl stdlh
SAMPLE DEC. & VT
date Sep 28 1999 dfrq 300.087
solvent CDCl3 dn H1
f11a exp dpwr 30
ACQUISITION exp dof 0
sfrq 300.087 de nnn
tn H1 dmw c
at 3.747 dmf 200
np 33728 PROCESSING
sw 4500.5 wtf11a
fb 2600 proc .ft
bs 16 fn not used
tpwr 40
pw 6.9 werr
d1 0 wexp
tof 0 wbr
nt 32 wnt
ct 32
alock n
gain not used
FLAGS
f1 n
in y
dp y
DISPLAY
sp -108.6
wp 3772.9
vs 100
sc 0
wc 250
hzam 15.89
fs 526.32
rf1 753.2
rfp 0
sh 28
ins 32.258
nm cdc ph
    
```



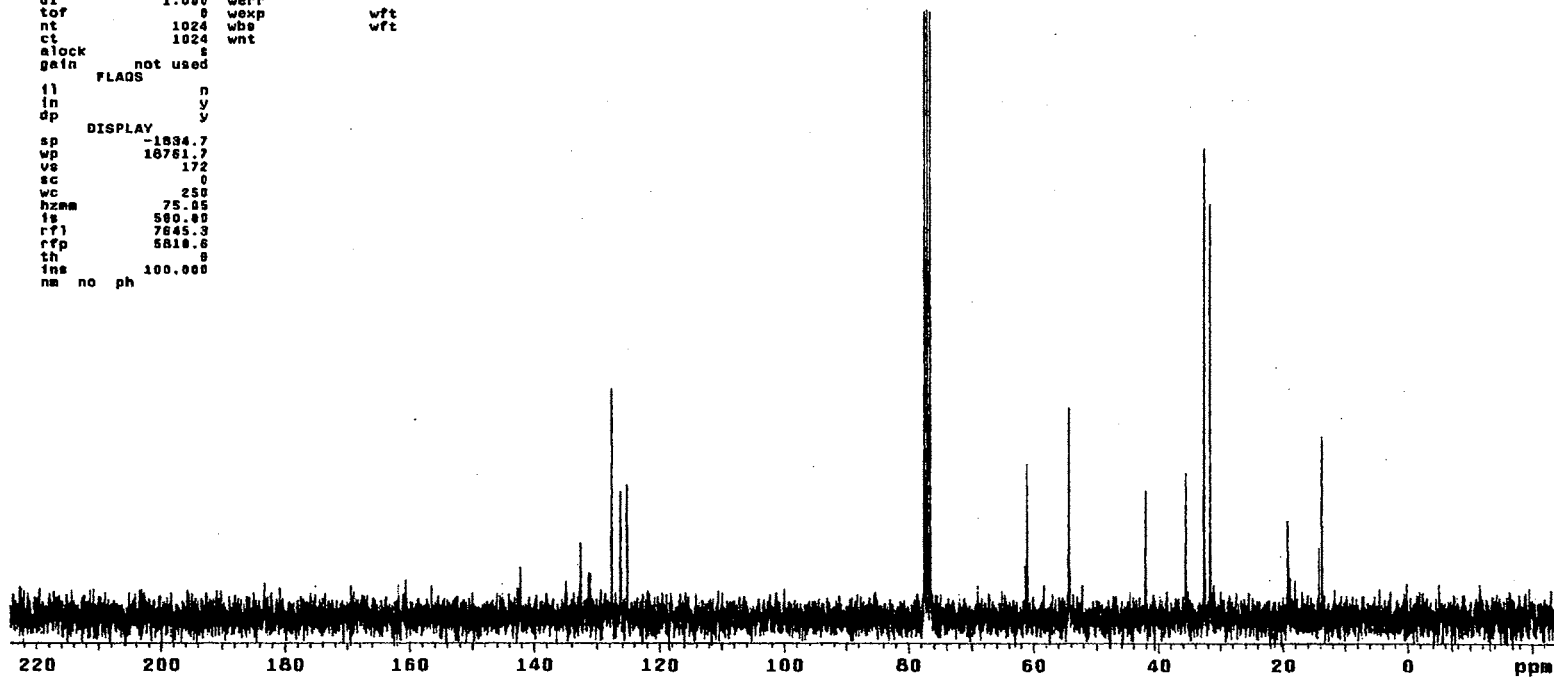
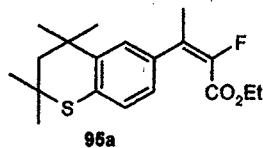
¹H NMR Spectrum of 95a

Plate CXLVI

13C OBSERVE

expl std13c

SAMPLE		DEC. & VT	
date	Sep 29 1998	dfrq	300.067
solvent	CDC13	dn	H1
file	exp	dpwr	94
ACQUISITION		dof	0
sfrq	75.464	dm	yyy
tn	C13	dsm	w
at	0.800	dwt	11764
np	30016	PROCESSING	
sw	18761.7	lb	1.00
fb	10400	wfite	
bs	16	proc	ft
tpwr	52	fn	not used
pw	3.8		
d1	1.000	werr	
tor	8	wexp	wft
nt	1024	wbs	wft
ct	1024	wnt	
alock			
gain	not used		
FLAGS			
fl	n		
in	y		
dp	y		
DISPLAY			
sp	-1834.7		
wp	18761.7		
vs	172		
sc	0		
wc	250		
hzmm	75.05		
fs	580.00		
rfl	7845.3		
rfp	5810.6		
th	8		
ins	100.000		
nm	no ph		



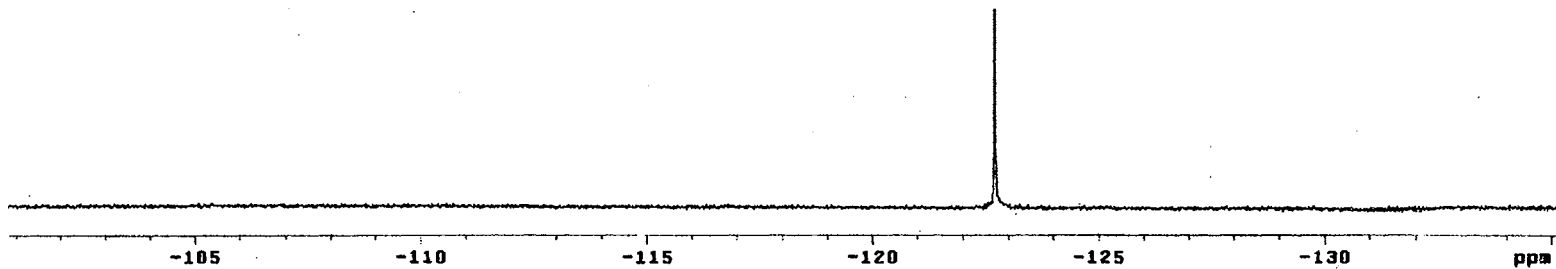
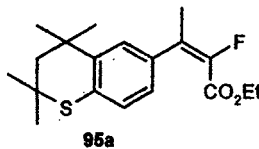
¹³C NMR Spectrum of 95a

Plate CXLVII

13C OBSERVE

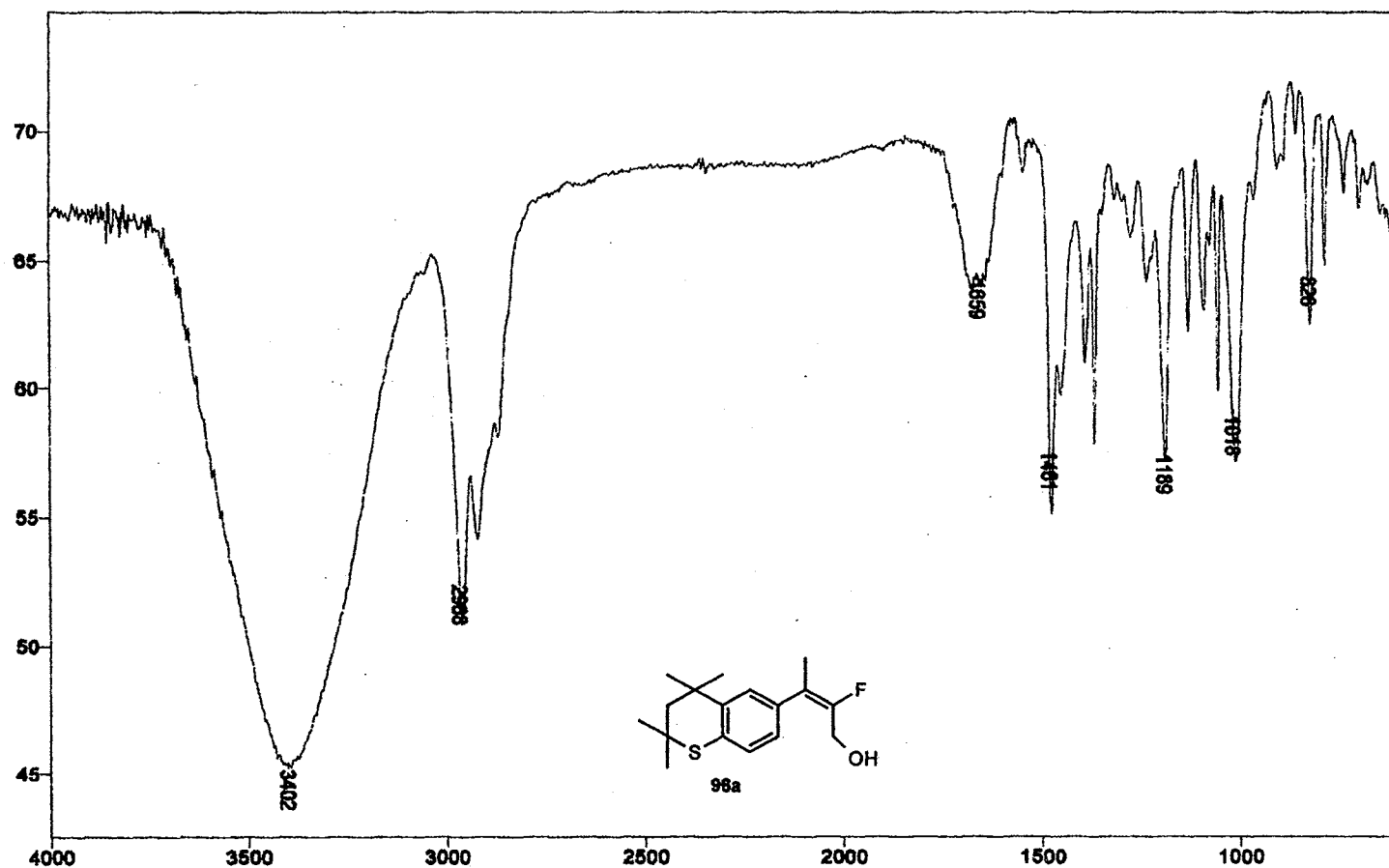
```

expt std13c
SAMPLE
date Feb 8 2000 dfrq DEC. & VT 300.067
solvent CDC13 dn H1
file exp dpwr 34
ACQUISITION dof 0
sfrq 282.333 da nnn
tn F19 dma w
at 0.800 dmf 11764
np 30018 PROCESSING
sw 18761.7 lb 1.00
fb 10400 wffile
bs 18 proc ft
tpwr 52 Tn not used
pw 3.8
dl 1.000 werr
tof 0 wskp wft
nt 1024 wss wft
ct 48 wnt
a1ock n
gain not used
FLAGS
t1 n
in y
dp y
DISPLAY
ap -38157.3
wp 5686.3
vs 103
sc 0
wc 250
hzmm 38.75
ts 500.00
rf1 38746.2
rfp 0
th 20
ins 100.000
nm no ph
  
```



¹⁹F NMR Spectrum of 95a

Plate CXLVIII



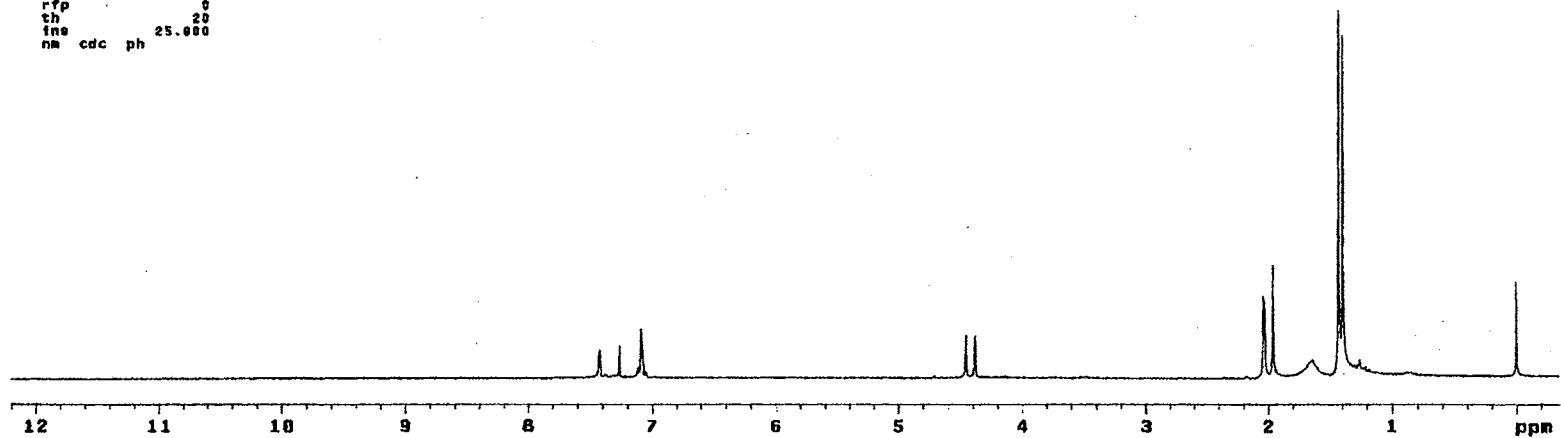
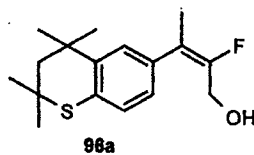
IR Spectrum of 96a

Plate CXLIX

STANDARD 1H OBSERVE

```

expt stdih
SAMPLE
date Oct 8 1999 dfrq DEC. A VT 300.087
solvent CDCl3 dn H1
file exp dpwr 30
ACQUISITION dof 0
sfrq 300.087 da nnn
tn H1 dm 200
at 3.747 daf 200
np 33728 PROCESSING
sw 4500.5 wtfile
fb 2600 proc ft
bs 16 fn not used
tpwr 48
pw 6.8 warr
dl 0 wexp
tof 0 wbs
nt 16 wnt
ct 16
slock n
gain not used
FLAGS
il n
in y
dp V
DISPLAY
sp -104.2
wp 3747.0
vs 48
sc 0
wc 250
hzmm 15.07
fs 500.00
rf1 748.8
rfp 0
th 20
fns 25.000
nm cdc ph
    
```



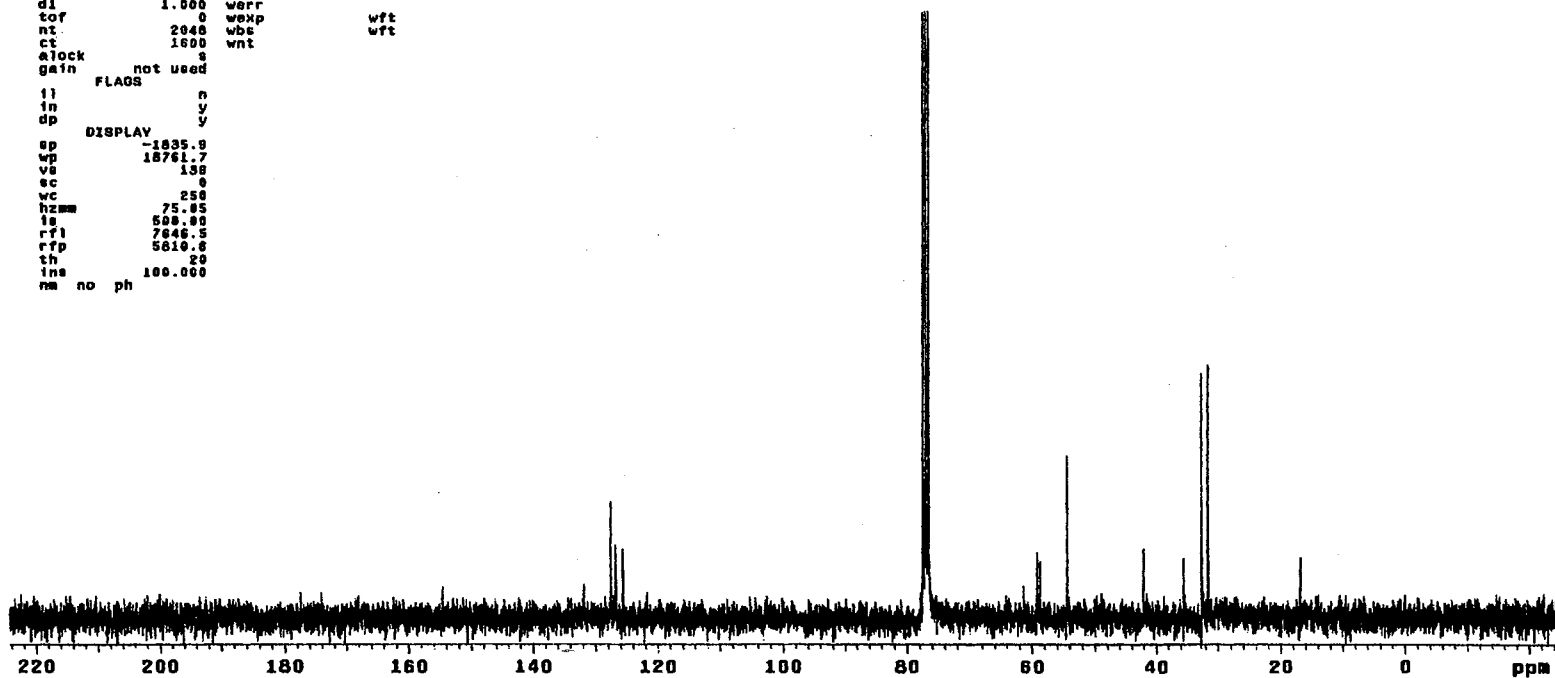
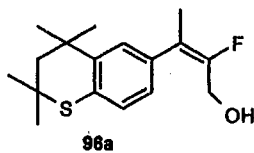
¹H NMR Spectrum of 96a

Plate CL

¹³C OBSERVE

expl std13c

SAMPLE		DEC. & VT	
date	Oct 8 1993	dfrq	300.087
solvent	CDCl3	dn	H1
file	exp	dpr	34
ACQUISITION		exp	0
efrq	75.464	de	VVY
tn	C13	dsm	W
at	0.800	dmt	11764
np	38018	PROCESSING	
sw	18761.7	lb	1.00
fb	10400	wtfile	
bs	16	proc	Yt
tpwr	52	fn	not used
pw	3.8		
d1	1.000	werr	
tof	0	wexp	wft
nt	2048	wbs	wft
ct	1600	wnt	
clock	3		
gain	not used		
FLAGS			
fl	n		
in	y		
dp	y		
DISPLAY			
ap	-1835.9		
wp	18761.7		
vs	138		
sc	0		
wc	258		
hzmm	75.05		
lg	500.00		
rfl	7646.5		
rfd	5810.6		
th	20		
ins	100.000		
nm	no	ph	



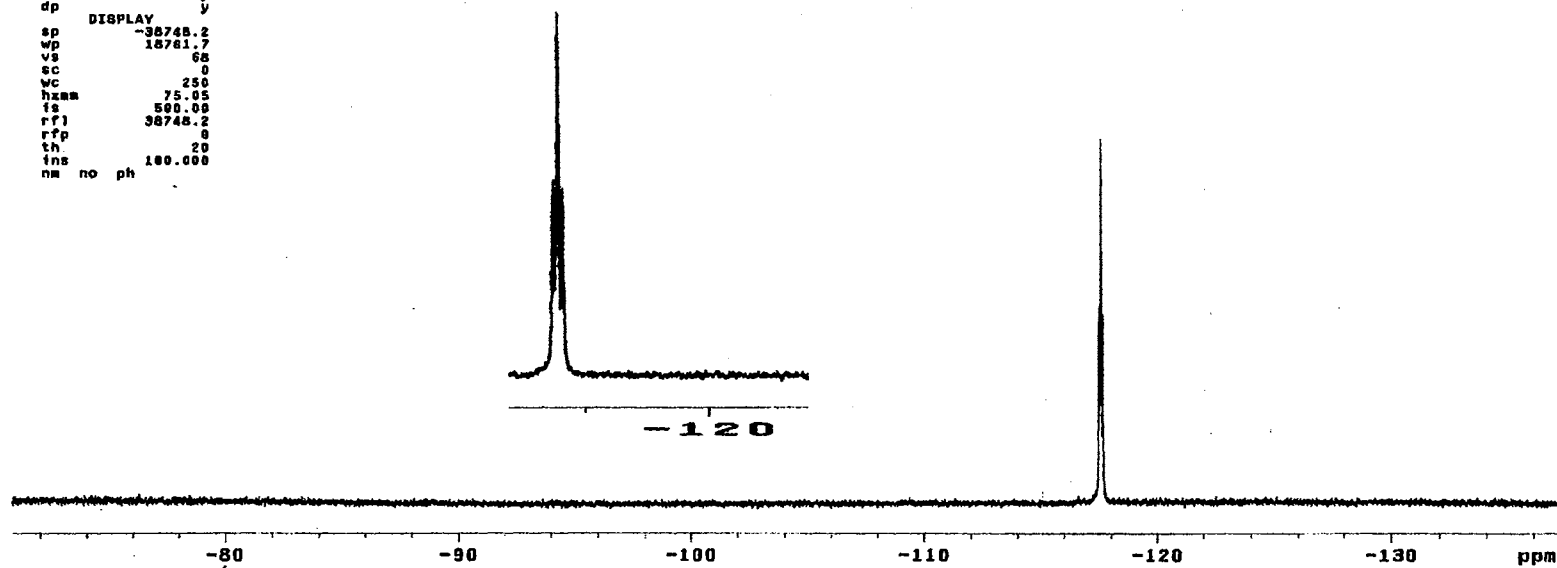
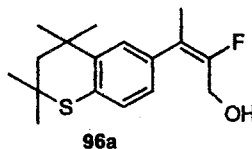
¹³C NMR Spectrum of 96a

Plate CLI

13C OBSERVE

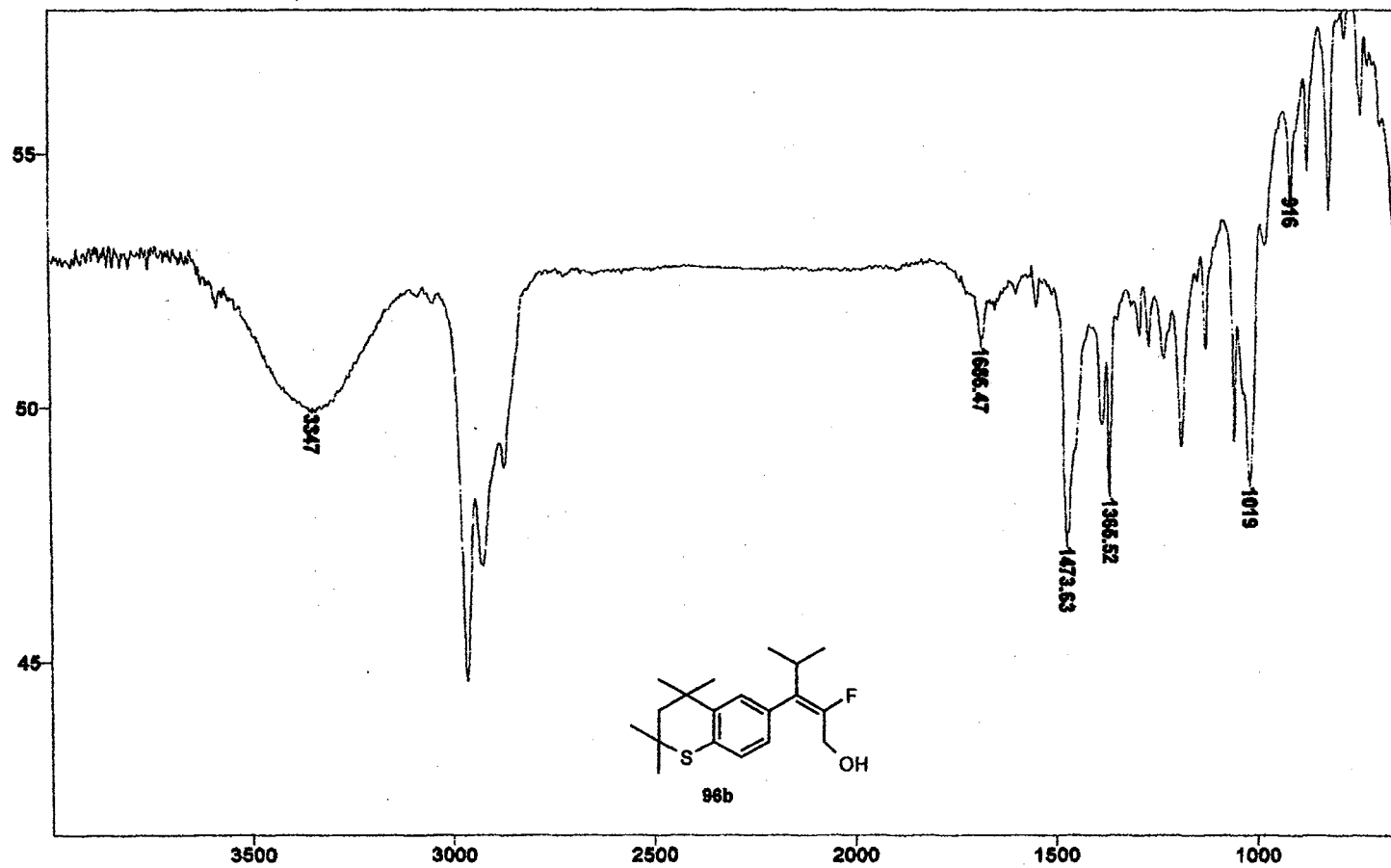
exp1 std13c

date	Oct 8 1999	dfrq	300.087	DEC. & VT
solvent	CDC13	dn	H1	
file		dpwr	36	
	ACQUISITION	exp	dof	0
sfrq	282.333	dm	nnn	
tn	F19	dsm	w	
at	8.800	dsw	11764	
np	30016	PROCESSING		
sw	18781.7	lb	1.00	
fb	10408	wtfile		
bs	16	proc	ft	
tpwr	52	fn	not used	
pw	3.8			
d1	1.008	werr		
tof	0	wexp	wft	
nt	1024	wbe	wft	
ct	396	wnt		
alock	n			
gain	not used			
	FLAGS			
fl	n			
in	y			
dp	y			
	DISPLAY			
sp	-38748.2			
wp	18781.7			
vs	0			
sc	0			
wc	250			
hzam	75.05			
is	500.00			
rfl	38748.2			
rff	0			
th	20			
ins	100.000			
nm	no ph			



¹⁹F NMR Spectrum of 96a

Plate CLII



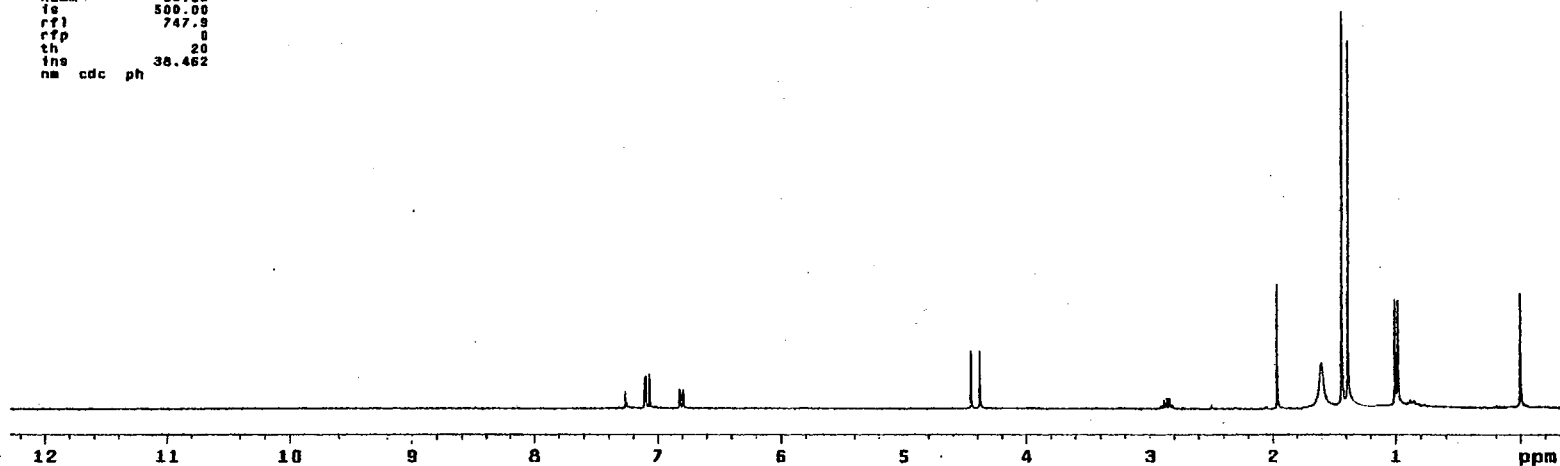
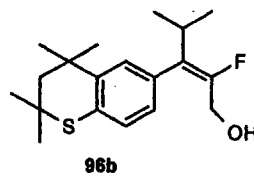
IR Spectrum of 96b

Plate CLIII

STANDARD 1H OBSERVE

```

exp1 stdih
SAMPLE
date Nov 3 1999 dfrq DEC. & VT 300.067
solvent CDC13 dn H1
file exp dpwr 30
ACQUISITION dof 0
sfrq 300.067 da nnn
tn H1 dam c
at 3.747 dmf 200
np 33728 PROCESSING
sw 4500.5 wtfile ft
fb 2600 proc not used
be 16 fn
tpwr 48
pw 6.8 warr
di 0 wexp
tof 0 wbs
nt 32 wnt
ct 32
aLock n
gain not used
FLAGS
il n
in y
dp y
DISPLAY
sp -103.3
wp 3780.6
vs 73
sc 0
wc 250
hzam 15.16
is 500.00
rf) 747.3
rfp 0
th 20
ins 38.462
na cdc ph
    
```



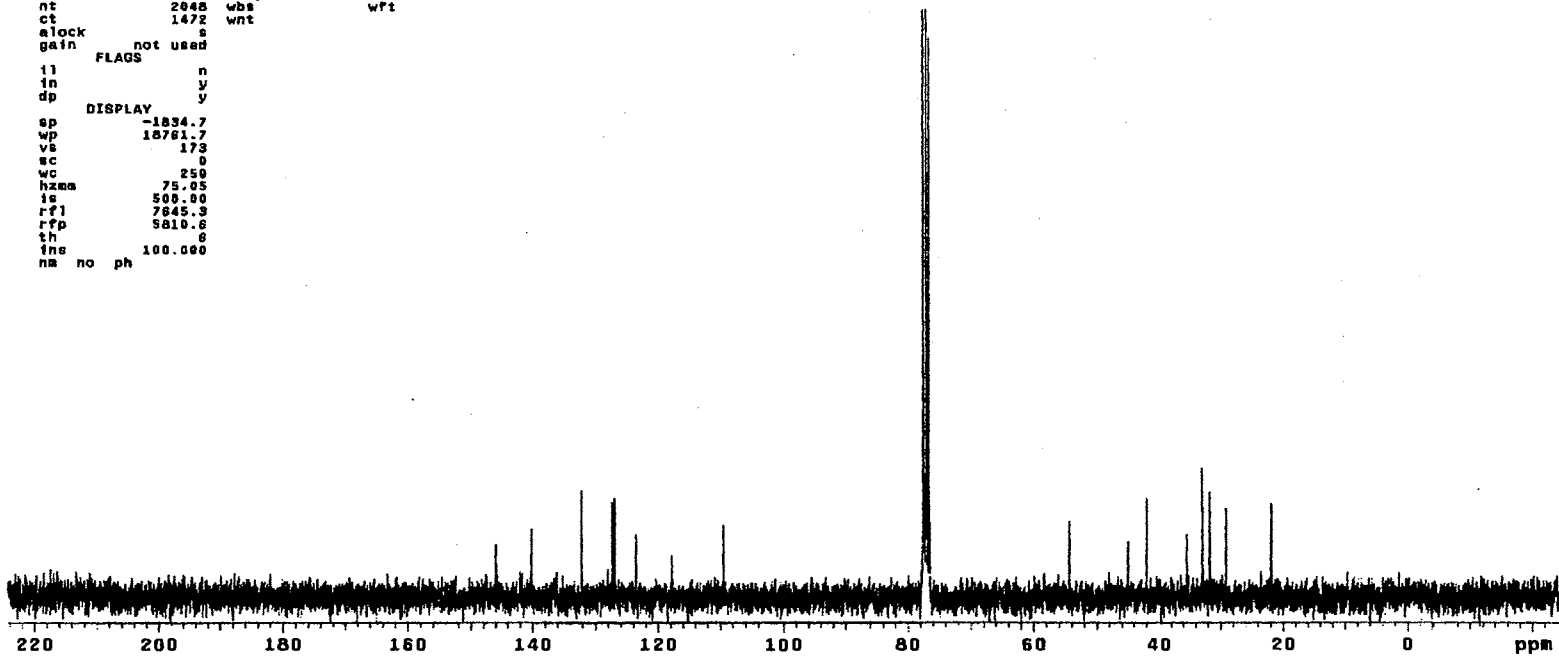
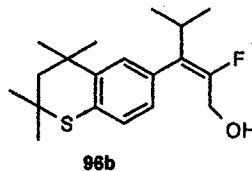
¹H NMR Spectrum of 96b

Plate CLIV

13C OBSERVE

exptl std13c

SAMPLE		DEC. & VT	
date	Nov 3 1999	dfrq	300.087
solvent	CDCl3	dn	H1
file	exp	dpr	34
ACQUISITION		dgf	0
strq	75.484	da	yyy
tn	C13	dmm	w
at	0.800	dnt	11764
np	30016	PROCESSING	
sw	18761.7	lb	1.00
fb	18408	wtfile	
bs	16	proc	ft
tpwr	52	fn	not used
pw	3.8		
dl	1.000	warr	
tof	0	wexp	wft
nt	2048	wbs	wft
ct	1472	wnt	
clock	s		
gain	not used		
FLAGS			
ll	n		
in	y		
dp	y		
DISPLAY			
sp	-1834.7		
wp	18761.7		
vs	173		
sc	9		
wc	250		
hzna	75.05		
is	500.00		
rfl	7845.3		
rfp	5810.8		
th	8		
ins	100.000		
na	no	ph	



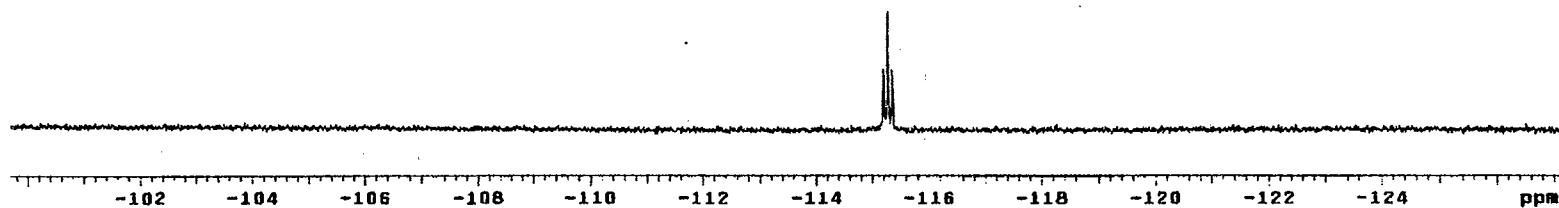
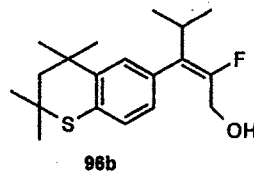
¹³C NMR Spectrum of 96b

Plate CLV

13C OBSERVE

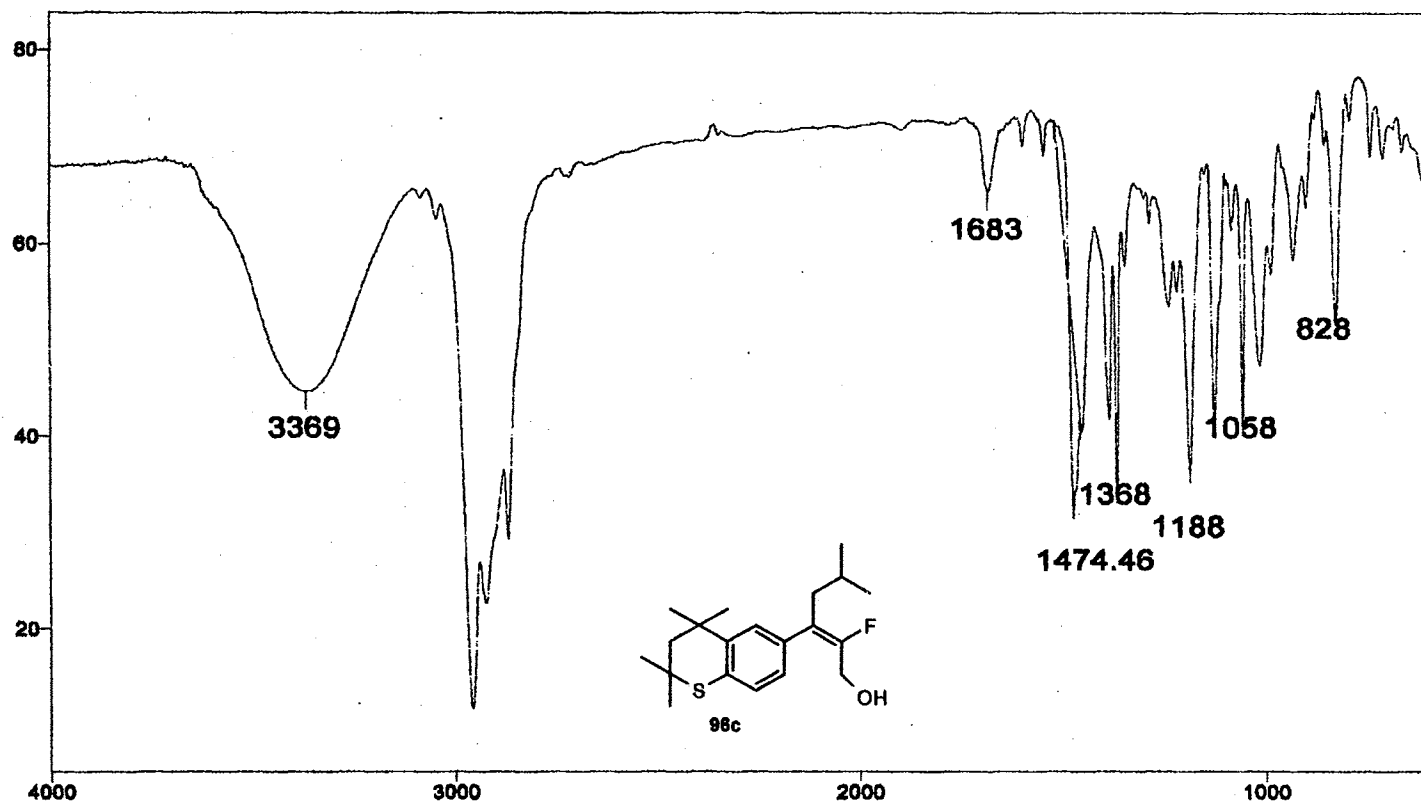
expl std13c

data	Nov 3 1999	dfrq	300.087
solvent	CDC13	dn	H1
file	exp	dpwr	34
ACQUISITION			
sfrq	282.333	da	nnn
tn	F19	dm	w
et	0.800	dmf	11764
np	30016	PROCESSING	1.00
qw	18761.7	lb	
fb	10400	wtfile	
bs	16	proc	ft
tpwr	32	fn	not used
pw	3.8		
d1	1.000	werr	
tdf	0	wexp	wft
nt	1024	wbs	wft
ct	144	wnt	
alock	n		
gain	not used		
FLAOS			
fl	n		
fn	y		
dp	y		
DISPLAY			
sp	-35913.9		
wp	7765.6		
vs	25		
sc	0		
wc	250		
hznm	31.06		
fs	500.80		
rft	38748.2		
rfp	0		
th	20		
ins	100.000		
nm	no	ph	



¹⁹F NMR Spectrum of 96b

Plate CLVI



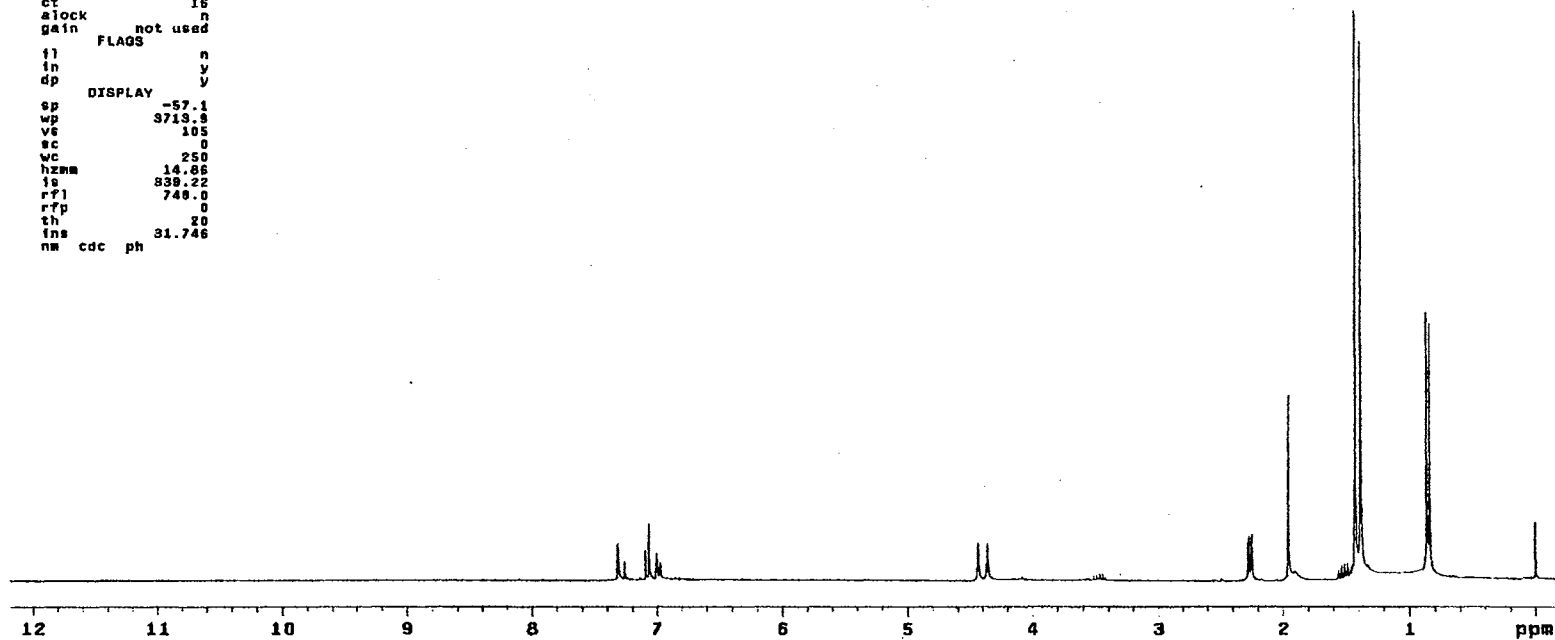
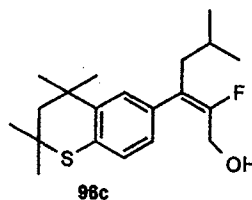
IR Spectrum of 96c

Plate CLVII

STANDARD 1H DBSERVE

```

expl stdih
SAMPLE
data Nov 23 1989 dfrq DEC. & VT 300.087
solvent CDC13 dn H1
file exp dpwr 30
ACQUISITION dot 0
sfrq 300.087 da nnn
tn H1 dm c
at 3.747 daF 200
np 33726 PROCESSING
sw 4500.5 wtfile
fb 2600 proc ft
bs 16 fn not used
tpwr 48
pw 6.8 werr
dl 0 wexp
tof 0 wba
nt 16 wnt
ot 16
alock n
gain not used
FLAGS
fl n
in y
dp y
DISPLAY
sp -57.1
wp 3719.8
vs 105
sc 0
wc 250
hzmm 14.86
ls 839.22
rf1 748.0
rfp 0
th 20
fns 31.746
nm cdc ph
    
```



¹H NMR Spectrum of 96c

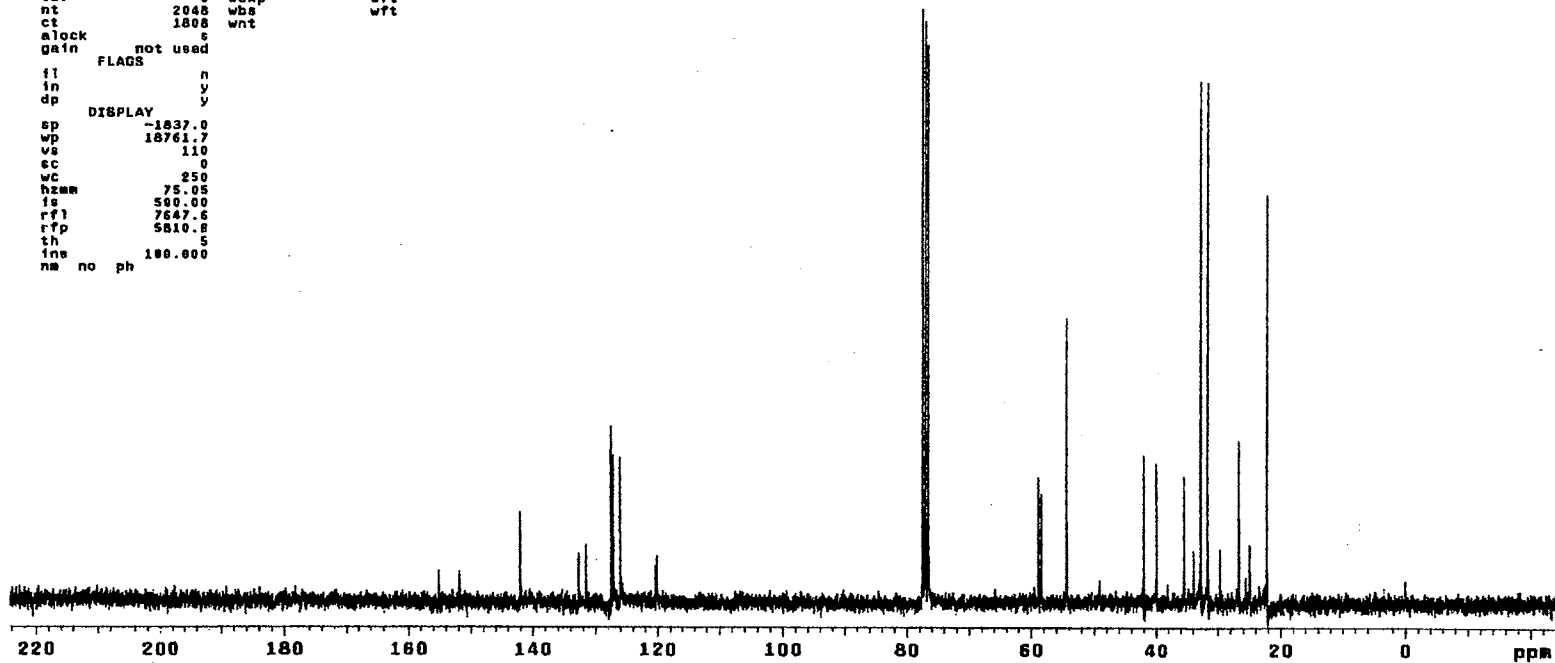
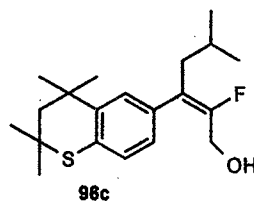
Plate CLVIII

13C OBSERVE

exp1 std13c

```

SAMPLE
data Nov 23 1998 dfrq DEC. & VT 300.087
solvent CDCl3 dn H1
file exp dpwr 34
ACQUISITION dof 0
sfrq 75.464 da vvy
tn C13 dms w
at 0.800 dm? 11764
np 30016 PROCESSING
sw 18761.7 lb 1.00
fb 10400 wfile
bs 16 proc ft
tpwr 52 fn not used
pw 3.8
di 1.000 warr
tof 0 wexp wft
nt 2048 wds wft
ct 1808 wnt
alock s
gain not used
FLAGS
fl n
in y
dp y
DISPLAY
sp -1837.0
wp 18761.7
vs 110
sc 0
wc 250
hzam 75.05
fs 500.00
rfl 7647.6
rfp 5810.8
th 5
ine 100.000
na no ph
    
```



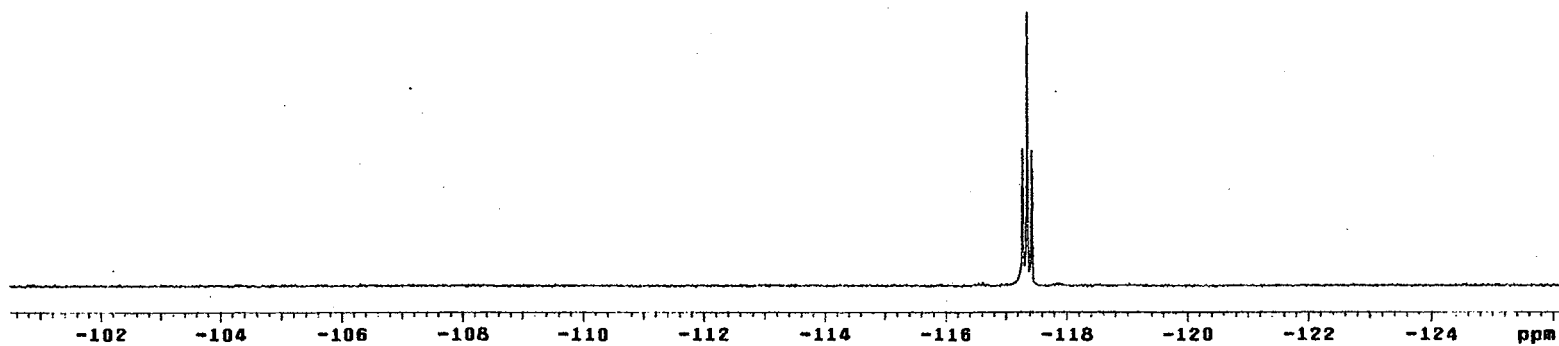
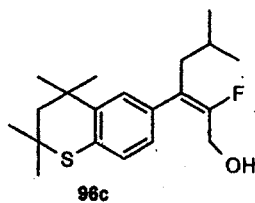
¹³C NMR Spectrum of 96c

Plate CLIX

13C OBSERVE

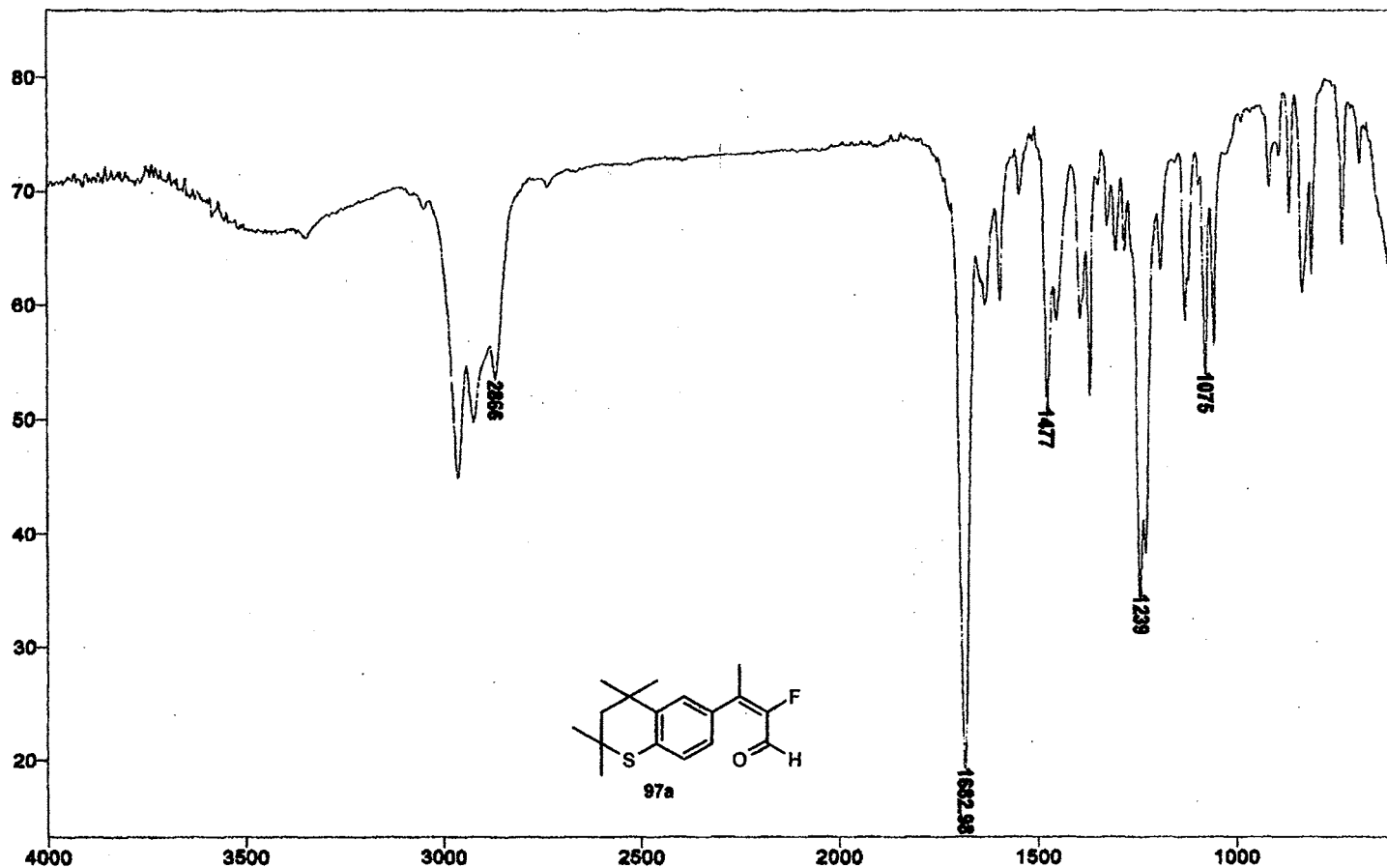
exptl std13c

date	Nov 23 1999	dfrq	DEC. & VT	300.087
solvent	CDC13	dn		H1
file		dpwr		36
ACQUISITION				
exp		dof		0
sfreq	282.333	dm		nnn
tn	F19	dnn		w
at	0.600	dnt		11764
np	30016	PROCESSING		
sw	18781.7	lb		1.00
fb	10400	wtfile		ft
bs	16	proc		ft
tpwr	52	fn		not used
pw	3.8			
d1	1.900	werr		
sof	0	wexp		wft
nt	1024	wbs		wft
ct	48	wnt		
alock	n			
gain	not used			
FLAGS				
fl		n		
in		y		
dp		y		
DISPLAY				
sp	-35617.3			
wp	7247.9			
vs	50			
sc	0			
wc	250			
hzam	28.38			
is	500.00			
rfl	38748.2			
rfp	0			
th	20			
ins	100.000			
nm	no	ph		



¹⁹F NMR Spectrum of 96cs

Plate CLX



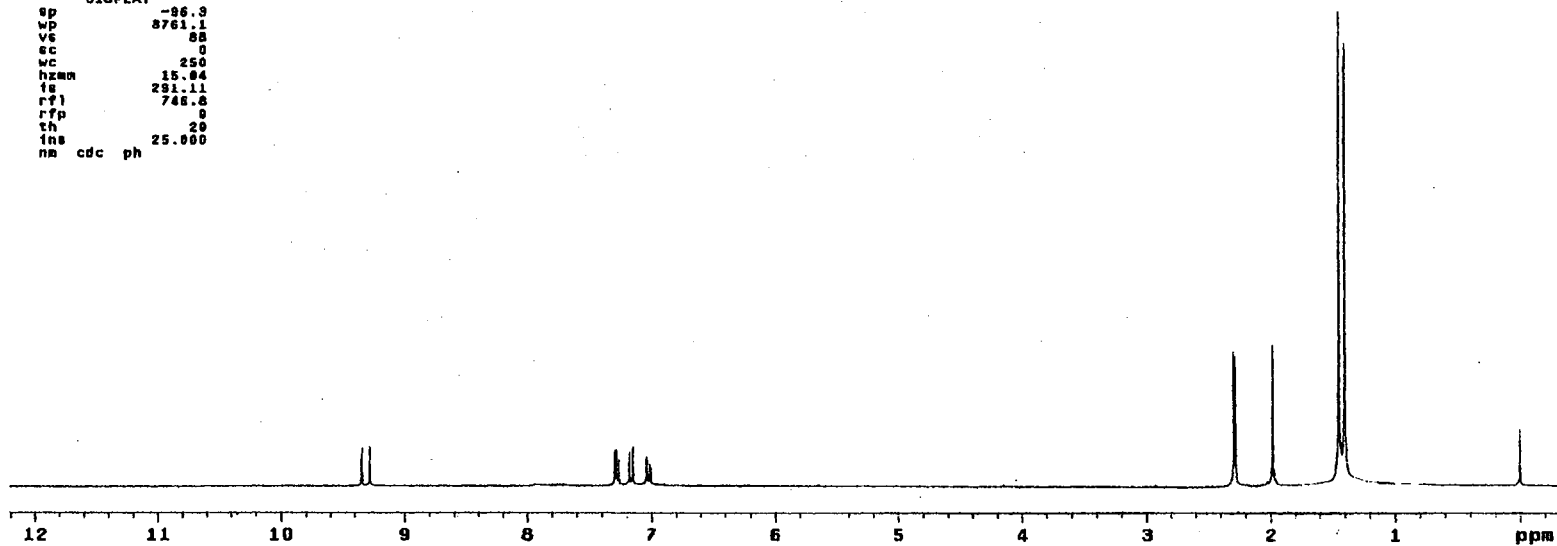
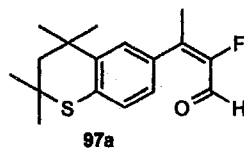
IR Spectrum of 97a

Plate CLXI

STANDARD 1H OBSERVE

```

expl stdih
SAMPLE DEC. & VT
date Oct 28 1998 dfrq 300.087
solvent CDC13 dn H1
file exp dpr 30
ACQUISITION exp dof 0
sfrq 300.087 da nnn
tn H1 dam c
at 3.747 dat 200
np 33728 PROCESSING
sw 4500.5 wtfile
fb 2500 proc ft
bs 16 fn not used
tpwr 48
pw 6.0 werr
d1 0 wexp wft
tof 0 wbs wft
nt 16 wnt
ct 16
alock n
gain not used
FLAGS
ii n
in y
dp y
DISPLAY
sp -86.3
wp 8761.1
ve 88
sc 0
wc 250
hzmm 15.04
fs 231.11
rf1 746.8
rfp 0
th 20
ins 25.000
na cdc ph
    
```



¹H NMR Spectrum of 97a

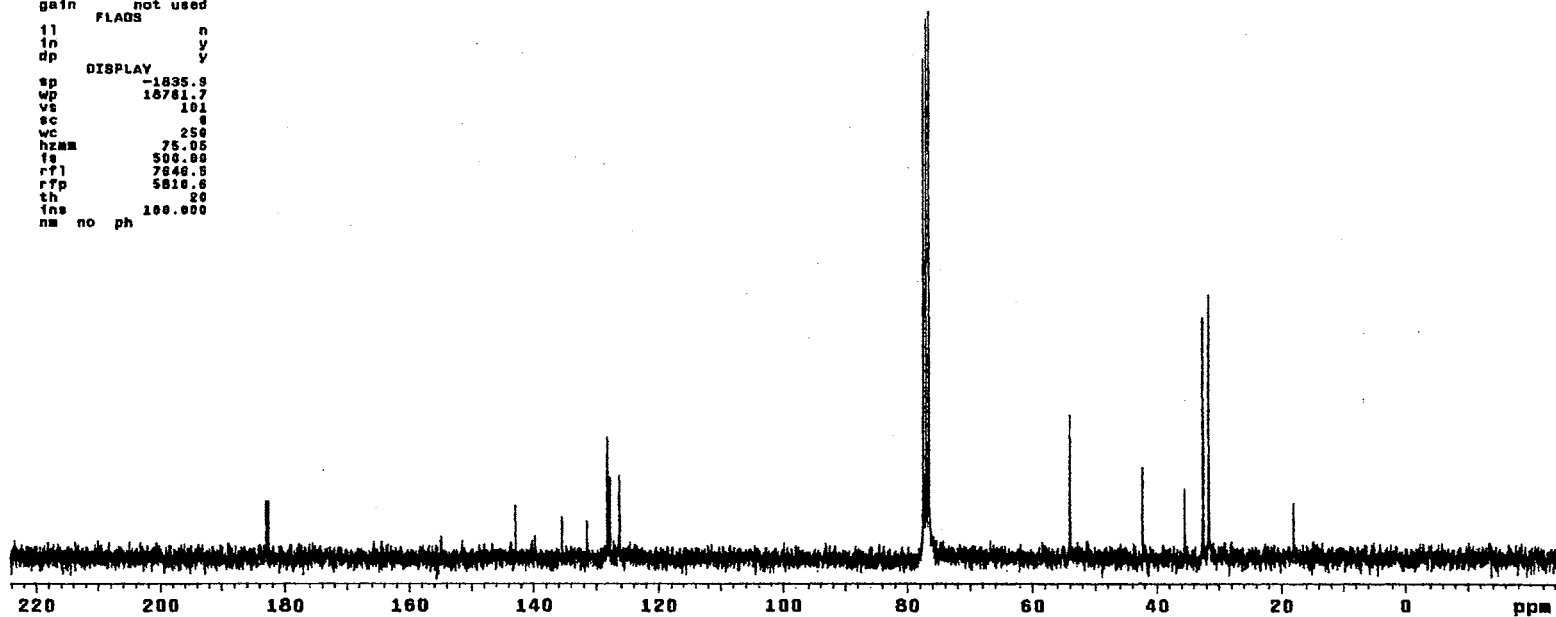
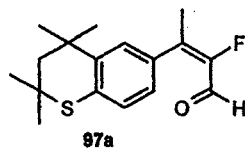
Plate CLXII

13C OBSERVE

expl std13c

```

SAMPLE
date Oct 28 1999 dfrq DEC. & VT 300.087
solvent CDCl3 dn H1
file exp dpwr 34
ACQUISITION dof 0
sfreq 75.484 dm yvy
tn 013 dnm w
at 0.000 dat 11764
np 30016 PROCESSING
sw 18781.7 lb 1.00
fb 10400 wtfile
bs 16 proc ft
tpwr 52 yn not used
pw 3.5
d1 1.000 werr
tof 8 wexp wft
nt 2048 wds wft
ct 2048 wnt
alock s
gain not used
FLAGS
il n
in y
dp y
DISPLAY
sp -1835.9
wp 18781.7
vs 101
sc 0
wc 250
hzmm 75.05
fs 500.00
rf1 7846.5
rfp 5818.6
th 20
ins no ph 100.000
    
```



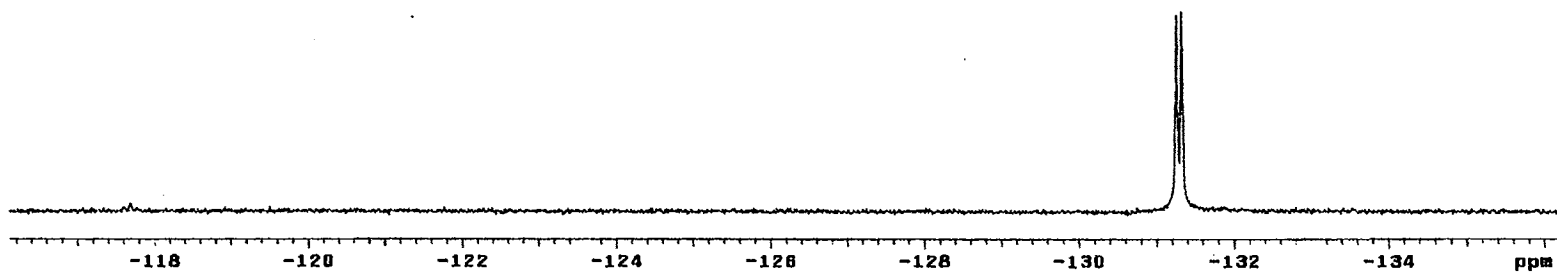
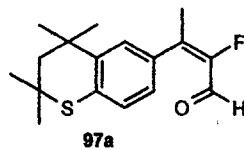
¹³C NMR Spectrum of 97a

Plate CLXIII

13C OBSERVE

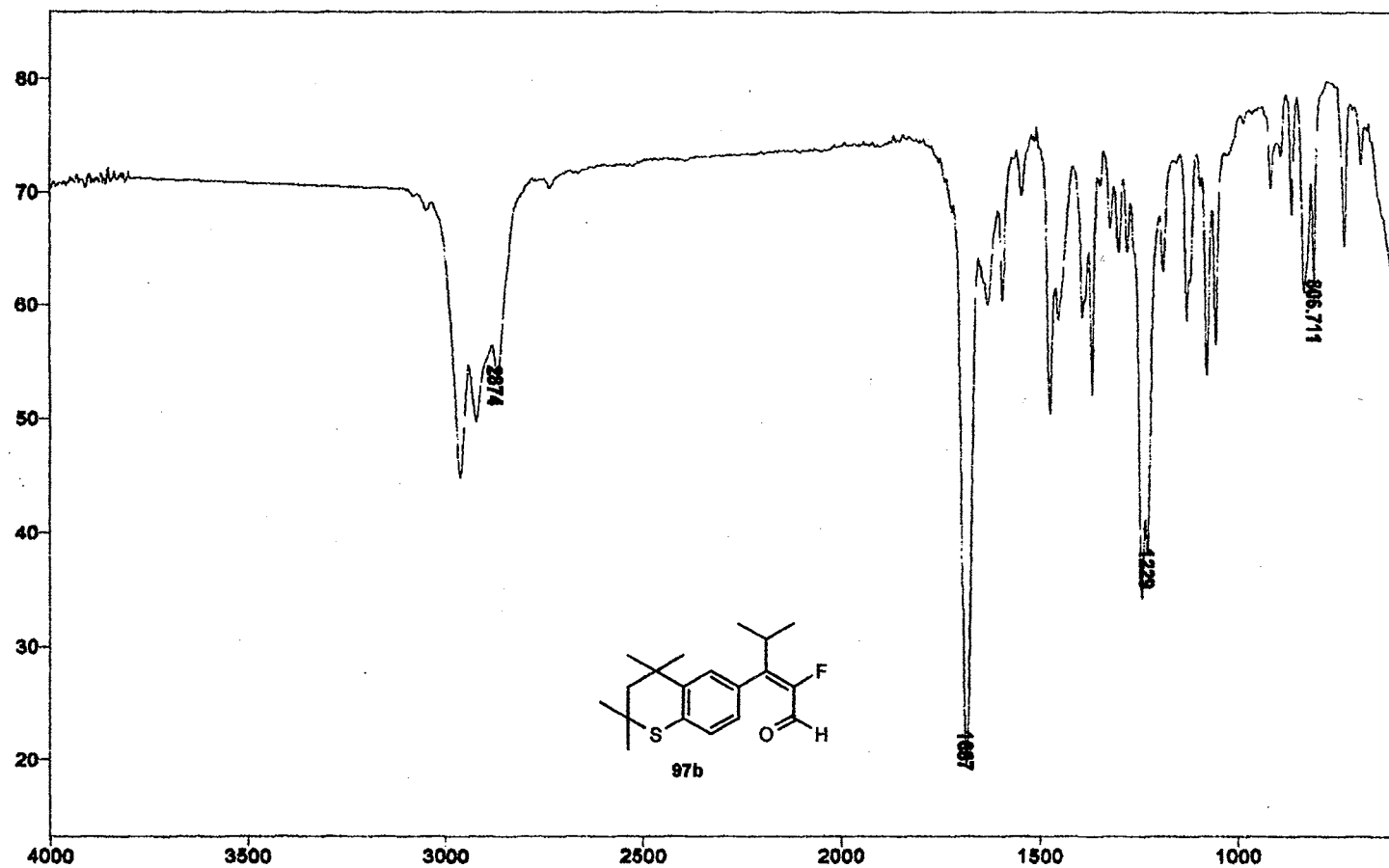
```

expt  std13c
SAMPLE
date  Oct 28 1988  dfrq  DEC. & VT  300.087
solvent  CDCl3  dn  M1
file  exp  dpwr  34
ACQUISITION  exp  dof  9
sfrq  282.333  dm  nnn
tn  F19  dm  w
at  0.800  dmf  11784
np  30016  PROCESSING
sw  18751.7  lb  wtfile  1.00
fb  10400  wtfile
bs  16  proc  ft
tpwr  52  fn  not used
pw  3.5
d1  1.000  werr
tof  0  wexp  wft
nt  1024  wbs  wft
ct  64  wnt
alock  n
gain  not used
FLAGS
il  n
in  y
dp  y
DISPLAY
sp  -38452.0
wp  5889.9
vs  37
sc  0
wc  250
hsum  22.68
fs  500.00
rfl  38746.2
rfp  0
sh  28
ins  100.000
nm  no  ph
    
```



¹⁹F NMR Spectrum of 97a

Plate CLXIV



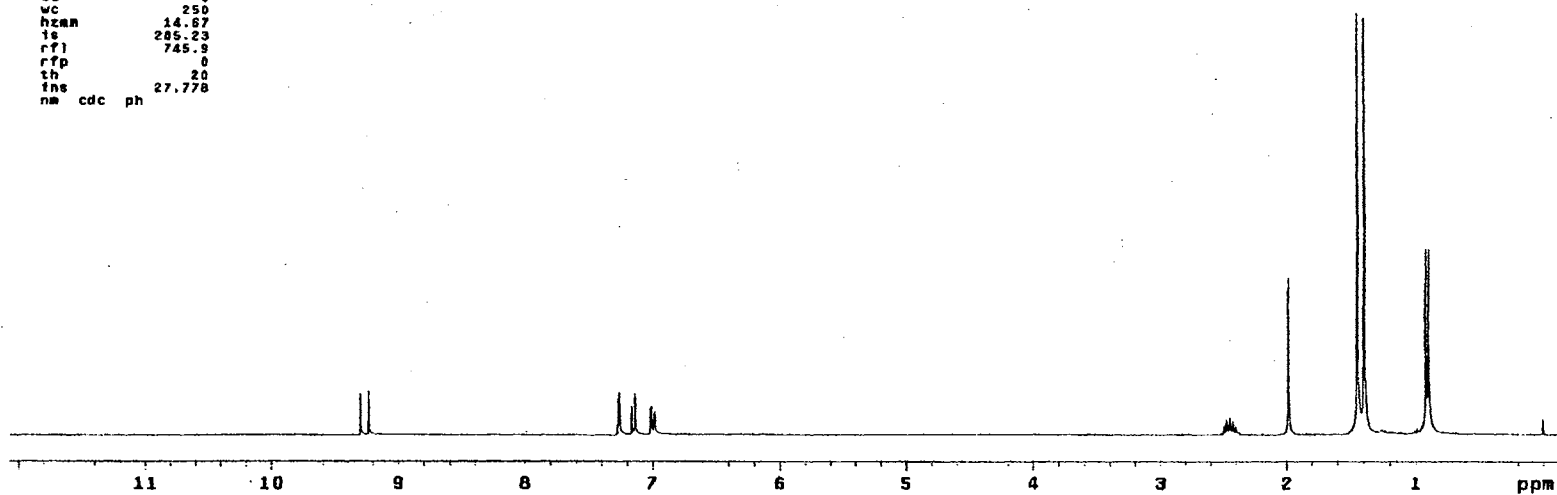
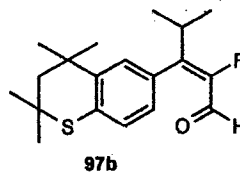
IR Spectrum of 97b

Plate CLXV

STANDARD 1H OBSERVE

```

expt  stdih
SAMPLE
date  Jan 24 2000  dfrq  300.087
solvent  CDCl3  dn  h1
file  exp  dpwr  30
ACQUISITION  dot  0
sfrq  300.087  da  nnn
tn  H1  dm  c
at  3.747  dar  200
np  33728
sw  4500.5  wifile
fb  2600  proc  ft
bs  16  fn  not used
tpwr  68
pw  6.8  warr
d1  0  wexp
tof  0  wbs
nt  16  wnt
cs  16
clock  n
gain  not used
FLAGS
ll  n
ln  y
dp  y
DISPLAY
sp  -42.3
wp  3866.5
vs  87
sc  0
wc  250
hzan  14.87
ls  285.23
rfl  745.3
rff  0
th  20
fns  27.778
nm  cdc  ph
  
```



¹H NMR Spectrum of 97b

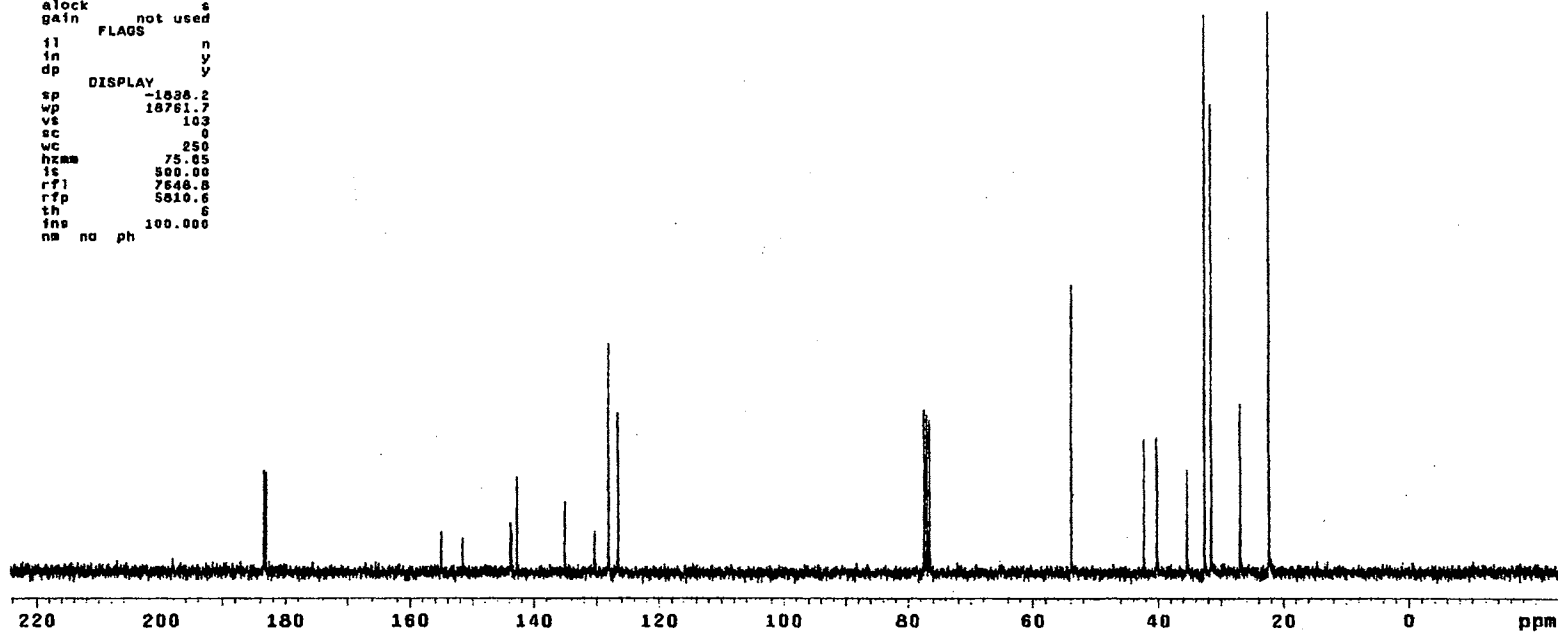
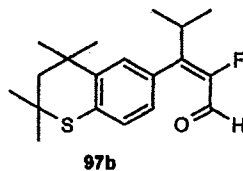
Plate CLXVI

13C OBSERVE

expl std13c

```

SAMPLE          DEC. & VT
date  Jan 24 2000  dfrq  300.007
solvent  CDC13    dn.    HI
file     exp      dpwr   34
          ACQUISITION  dof   0
sfrq    75.464   dm     vvy
tn       C13     dma     w
at       0.800   dat    11764
np       90018   PROCESSING
sw       18761.7 lb     1.00
fb       10400  wtfile
bs        15    proc
spwr     52     7n     not used
pw        3.8
dl        1.000  werr
tof        0    wexp
nt        1024  wbs
ct         203  wnt
alock     s
gain      not used
          FLAGS
fl         n
in         y
dp         y
          DISPLAY
sp       -1838.2
wp       18761.7
vs        103
sc         0
wc        250
hzam     75.05
ls        500.00
rfl       7648.8
rfp       5810.6
th         6
fns      100.000
na no ph
    
```



¹³C NMR Spectrum of 97b

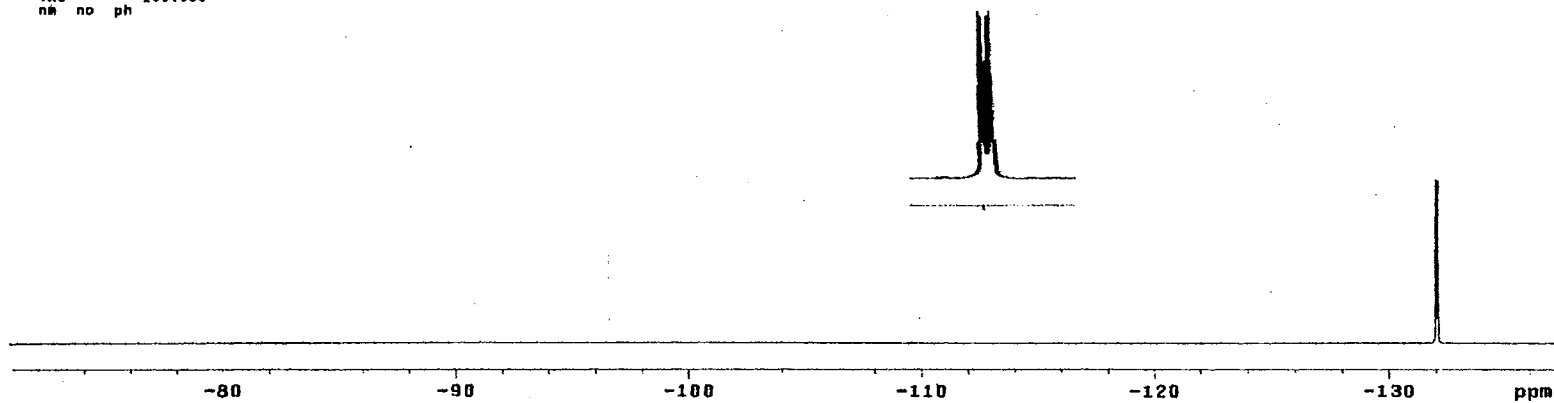
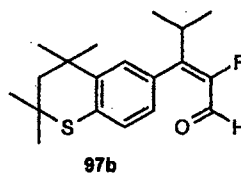
Plate CLXVII

13C OBSERVE

expl std13c

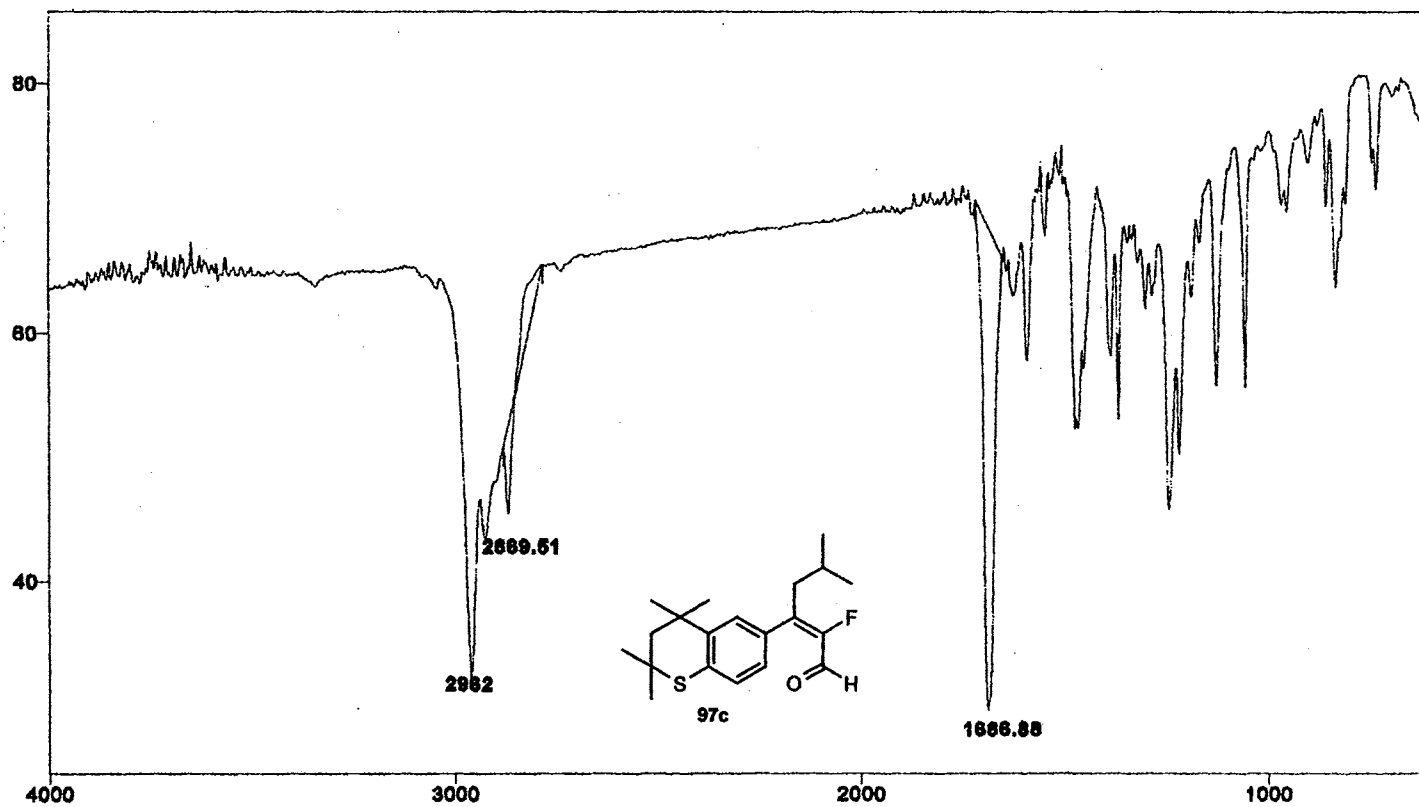
```

SAMPLE
date Jan 24 2000 dfrq DEC. & VT 300.067
solvent CDC13 dn HI
file EXP dpwr 34
ACQUISITION dof 0
sfrq 282.333 da nnn
tn F19 dma w
at 0.800 dmf 11764
np 30018 PROCESSING
sw 18761.7 lb 1.00
fb 10400 wfile
bs 16 proc ft
tpwr 52 fn not used
pw 3.8
d1 1.000 werr
tof 0 wexp wft
nt 1024 wbs wft
ct 32 wnt
alock n
gain not used
FLAGS
il n
in y
dp y
DISPLAY
sp -38748.2
wp 18761.7
vs 30
sc 0
wc 250
hznm 75.05
is 500.00
rf1 38748.2
rfp 0
th 20
ins 100.000
nm no ph
    
```



¹⁹F NMR Spectrum of 97b

Plate CLXVIII



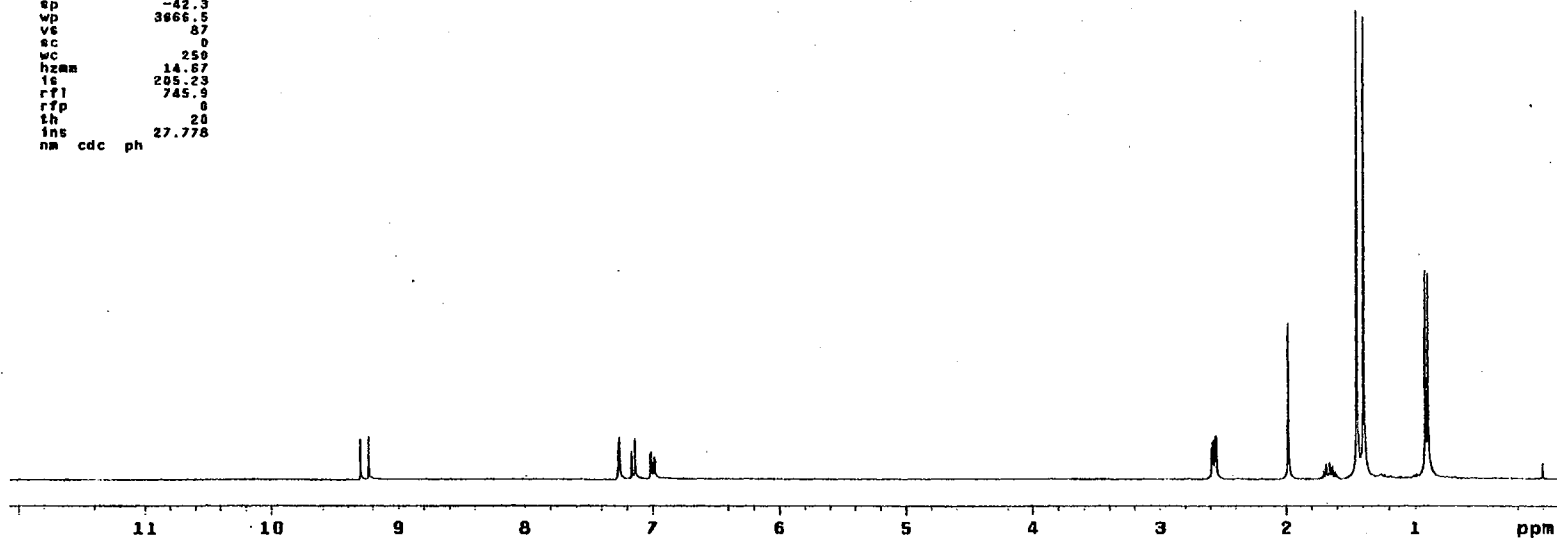
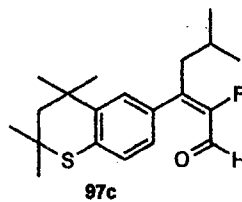
IR Spectrum of 97c

Plate CLXIX

STANDARD IN OBSERVE

```

expl stdih
SAMPLE
date Jan 24 2000 dfrq DEC. & VT 300.087
solvent CDC13 dn HI
file exp dpwr 30
ACQUISITION exp dof 0
sfrq 300.087 dm nnn
tn M1 dm c
at 3.747 dmf 200
np 33728 PROCESSING
sw 4580.5 wtf11e
fb 2800 proc ft
bs 16 fn not used
tpwr 48
pw 6.9 werr
d1 0 wexp
tof 0 wbs
nt 16 wnt
ct 16
alock n
gain not used
FLAGS
ll n
in y
dp y
DISPLAY
sp -42.3
wp 3666.5
vt 87
sc 0
wc 250
hzmm 14.57
ls 205.23
rf1 745.9
rfp 0
th 20
ins 27.778
nm cdc ph
  
```



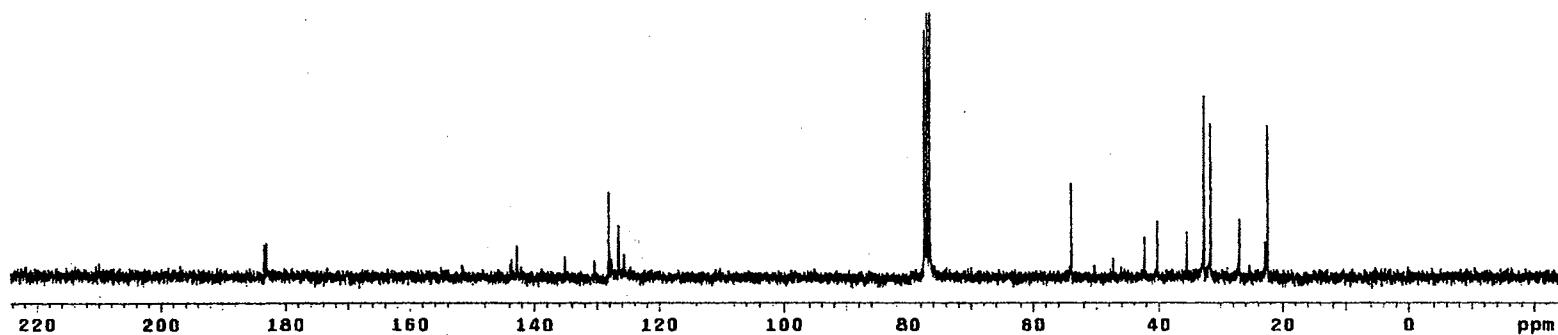
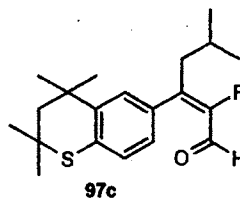
¹H NMR Spectrum of 97c

Plate CLXX

13C OBSERVE

exptl std13c

SAMPLE		DEC. & VT	
date	Dec 20 1999	dfrq	300.087
solvent	CDCl3	dn	H1
file		dpr	34
ACQUISITION		dot	0
sfrq	75.464	dm	yyy
tn	013	dms	w
at	0.000	daf	11764
np	30018	PROCESSING	
sw	18761.7	lb	1.00
fb	10400	wtfile	
bs	18	proc	ft
tpwr	52	fn	not used
pw	3.8		
d1	1.000	werr	
tof	0	wexp	wft
nt	2048	wbs	wft
ct	1744	wnt	
alock	6		
gain	not used		
FLAGS			
il		n	
in		y	
dp		y	
DISPLAY			
sp	-1835.8		
wp	18761.7		
vs	48		
sc	0		
wc	280		
hzam	75.05		
ta	500.00		
rfl	7846.5		
rfd	5810.6		
th	4		
ins	100.000		
nm	no	ph	



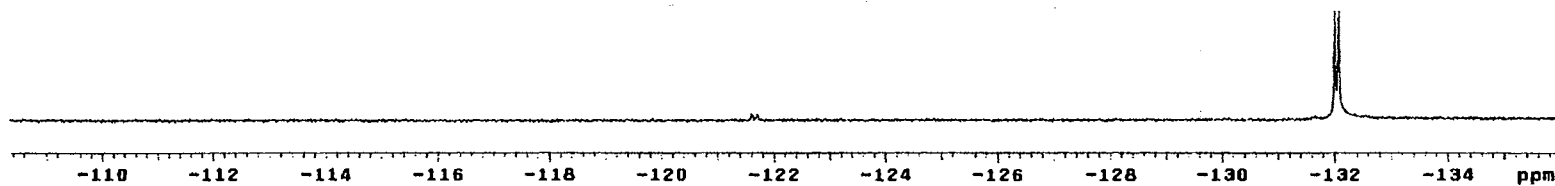
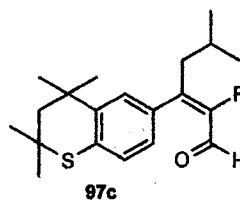
¹³C NMR Spectrum of 97c

Plate CLXXI

13C OBSERVE

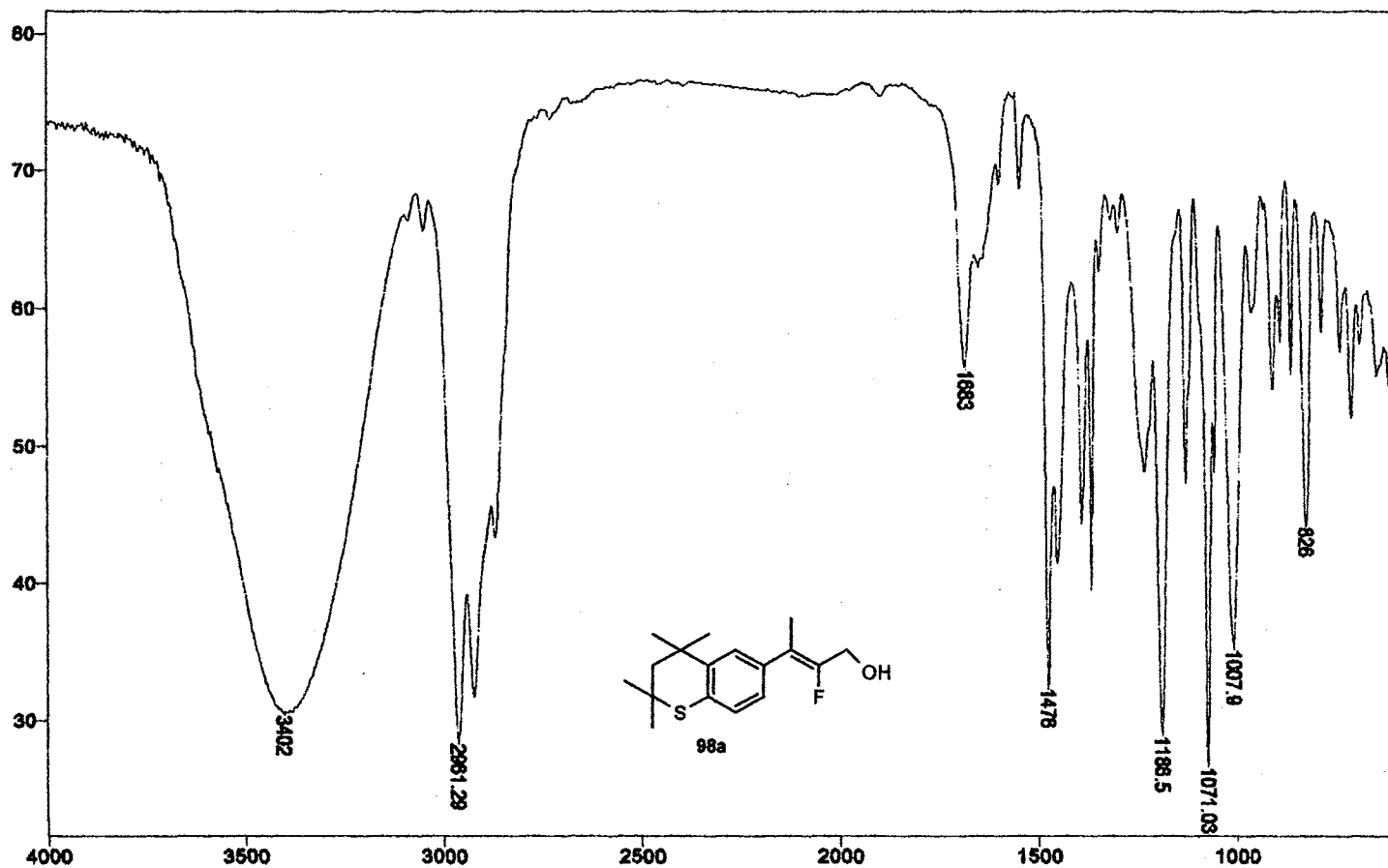
expl std13c

	SAMPLE	DEC. & VT	
date	Dec 20 1999	dfrq	300.087
solvent	CDC13	dn	H1
file	exp	dpwr	38
	ACQUISITION	dof	8
sfrq	282.333	dm	nnn
tn	F19	dsm	w
at	0.800	daf	11784
np	30018	PROCESSING	
sw	18781.7	lb	1.00
rb	19400	wffile	
bs	16	proc	ft
tpwr	52	fn	not used
pw	3.8		
d1	1.000	warr	wft
tof	8	wexp	wft
nt	1024	wbs	wft
ct	48	wnt	
clock	n		
gain	not used		
	FLAOS		
it	n		
in	y		
dp	y		
	DISPLAY		
sp	-38483.5		
wp	7814.8		
vs	20		
sc	0		
wc	250		
hzam	31.26		
is	500.00		
rfl	38748.2		
rfd	0		
th	8		
ins	100.000		
nn	no ph		



¹⁹F NMR Spectrum of 97c

Plate CLXXII



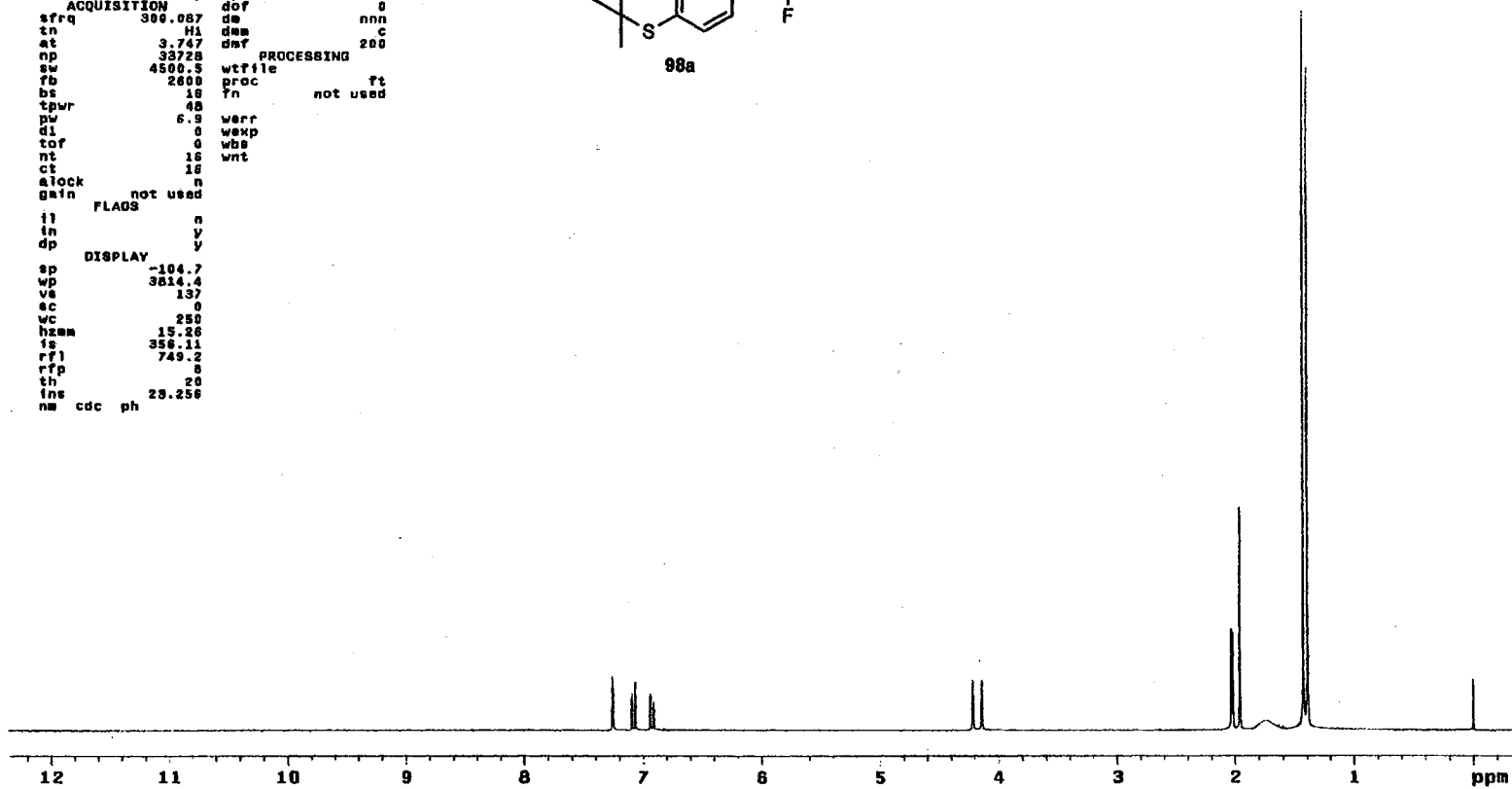
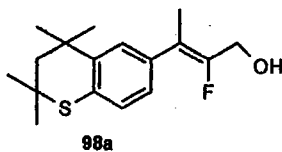
IR Spectrum of 98a

Plate CLXXIII

STANDARD 1H OBSERVE

```

exp1 std1h
SAMPLE
date Oct 8 1988 dfrq DEC. A VT 300.087
solvent CDC13 dn H1
file exp dpwr 30
ACQUISITION dof 0
sfrq 300.087 da nnn
tn H1 da c
at 3.747 dnt 200
np 33728 PROCESSING
sw 4500.5 wtfile
fb 2600 proc ft
bs 18 tn not used
tpwr 48
pw 6.9 warr
dl 0 wexp
tof 0 wba
nt 18 wnt
ct 18
slock n
gain not used
FLAGS
il n
in y
dp y
DISPLAY
sp -104.7
wp 3814.4
vs 137
sc 0
wc 250
hzmm 15.26
is 358.11
rf1 749.2
rfp 5
th 20
ins 28.256
nm cdc ph
    
```



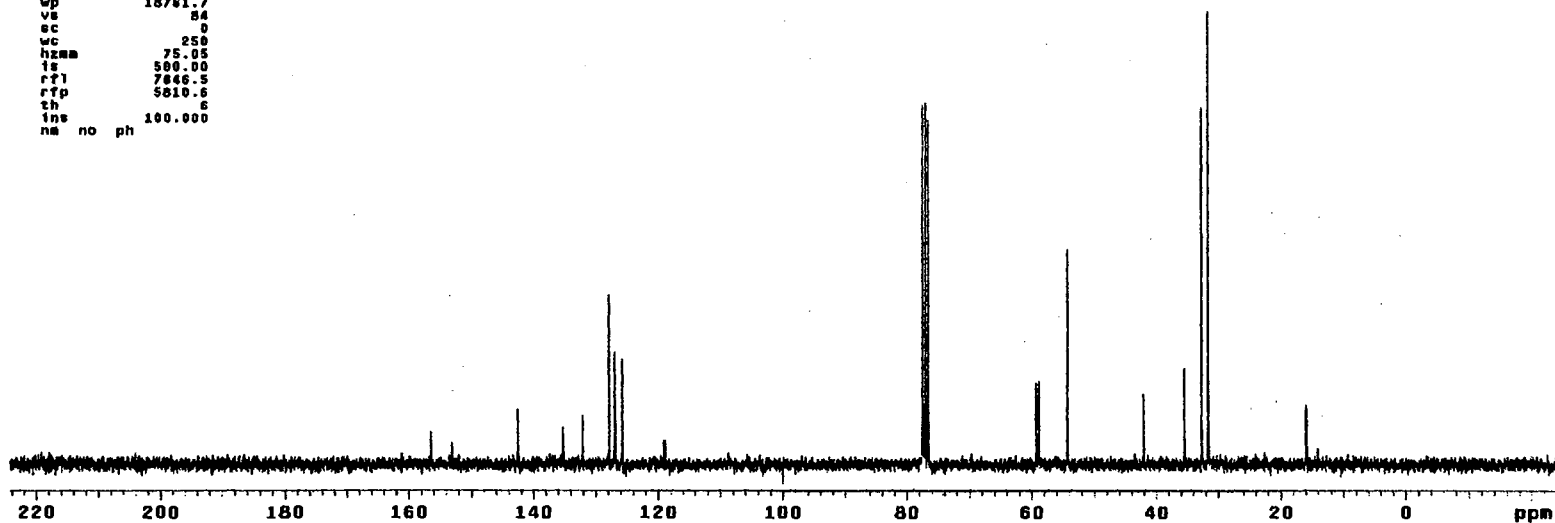
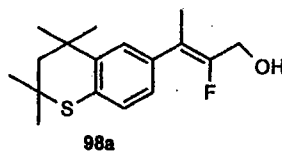
¹H NMR Spectrum of 98a

Plate CLXXIV

13C OBSERVE

expl std13c

	SAMPLE	DEC. & VT	
date	Oct 8 1999	dfrq	300.087
solvent	CDCl3	dn	H1
file	exp	dpwr	34
ACQUISITION			
	exp	dot	0
sfrq	75.464	dm	VVY
tn	C13	dms	w
at	0.800	dmt	11764
np	30016	PROCESSING	
sw	18781.7	lb	1.00
fb	10400	wtfile	
bs	16	proc	ft
tpwr	52	fn	not used
pw	3.8		
d1	1.000	warr	
tof	0	wexp	wft
nt	2048	wbs	wft
ct	1248	wnt	
alock	s		
gain	not used		
	FLABS		
ll	n		
in	y		
dp	y		
DISPLAY			
sp	-1835.9		
wp	18781.7		
vs	84		
sc	0		
wc	258		
hzmm	75.05		
is	590.00		
rfl	7846.5		
rtp	5810.6		
th	6		
ins	100.000		
nm	no	ph	



¹³C NMR Spectrum of 98a

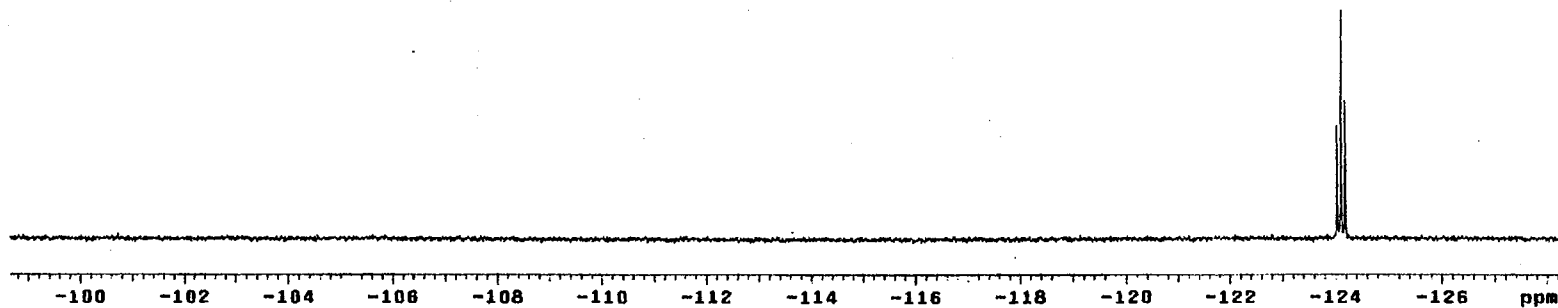
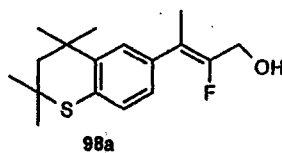
Plate CLXXV

13C OBSERVE

exptl std13c

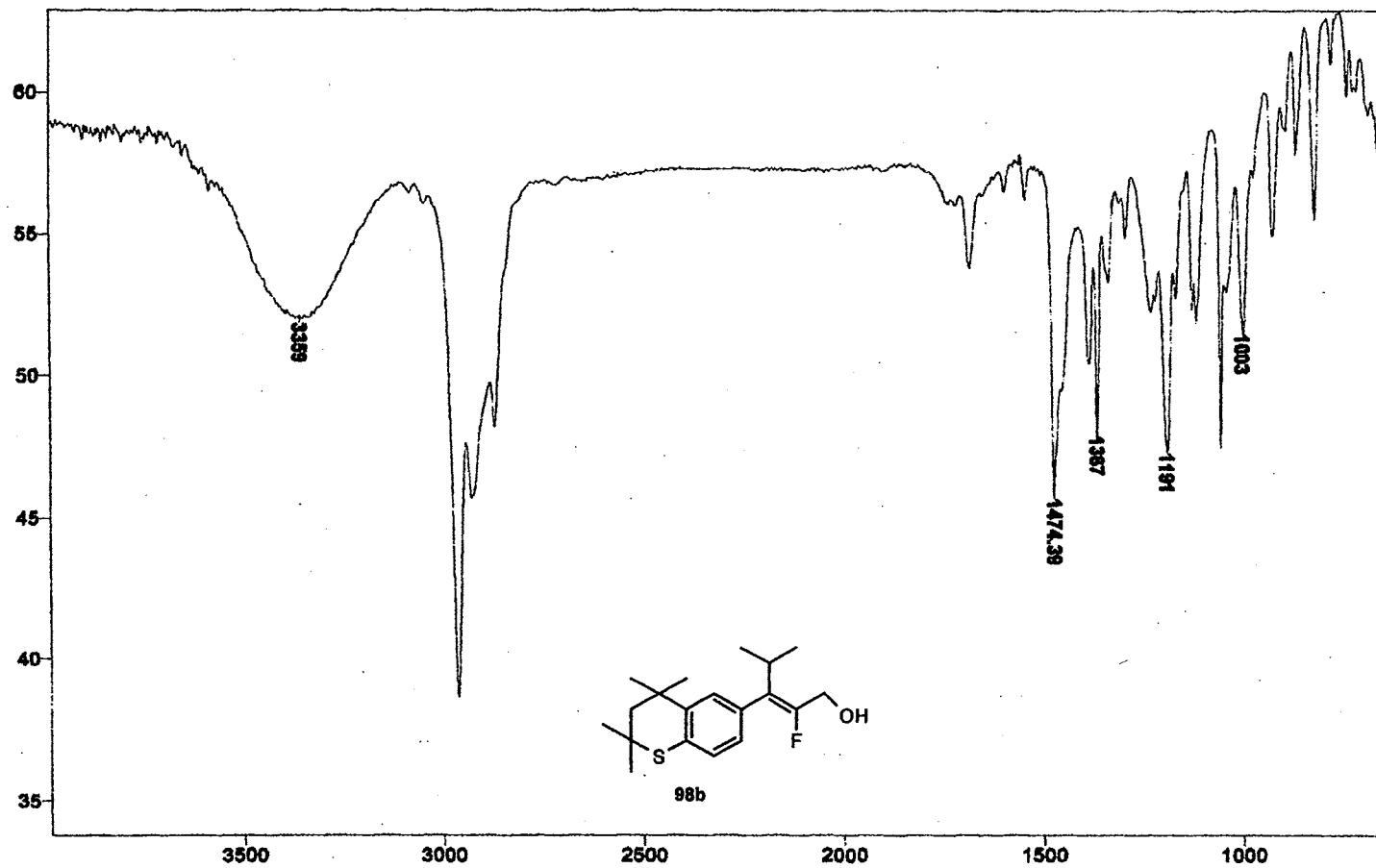
```

SAMPLE          DEC. & VT
date Nov 3 1998 dfrq 300.087
solvent CDC13   dn      HI
file          exp dpwr      34
              dof      0
ACQUISITION
sfrq 282.333 dm      nnn
tn    F19 dms      w
at    0.800 dwt 11764
np    30016 PROCESSING
sw    18761.7 lb      1.00
fb    10400 wtfile
bs    16 proc      ft
spwr  52 ?n      not used
pw    3.8
d1    1.000 werr
tof   0 wexp      wft
nt    1028 wbs
ct    48 wnt
alock n
gain  not used
      FLAGS
ii    n
in    y
dp    y
DISPLAY
sp    -38234.5
wp    6381.7
vs    32
sc    0
wc    250
hzam  33.53
is    500.00
rf1   30748.2
rfp   0
th    20
lno   100.000
nm    no ph
    
```



¹⁹F NMR Spectrum of 98a

Plate CLXXVI



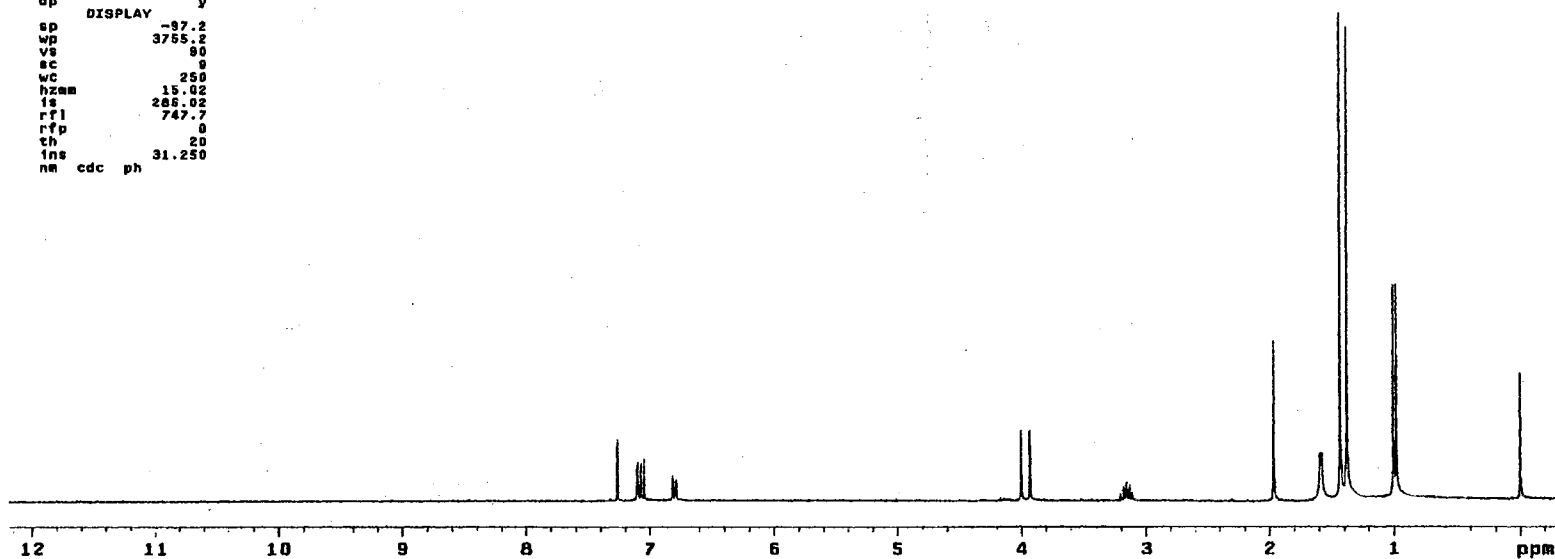
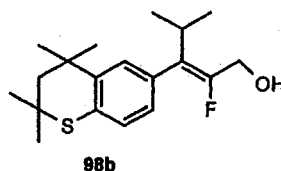
IR Spectrum of 98b

Plate CLXXVII

STANDARD IN OBSERVE

```

exp1 std1h
SAMPLE
date Nov 3 1988 dfrq DEC. & VT 300.087
solvent CDC13 dn H1
file exp dpwr 30
ACQUISITION dof 0
sfrq 300.087 dm nnn
tn H1 dm c
at 3.747 day 200
np 33720
aw 4500.8 wtfile
fb 2600 proc ft
bs 16 fn not used
tpwr 48
pw 6.9 warr
d1 0 wexp
tof 0 wgs
nt 16 wnt
ct 16
alock n
gain not used
FLAGS
tl n
in y
dp y
DISPLAY
sp -97.2
wp 3755.2
vs 90
sc 9
wc 250
hzam 15.02
fs 285.02
rf1 747.7
rfp 0
th 20
ins 31.250
nm cdc ph
    
```



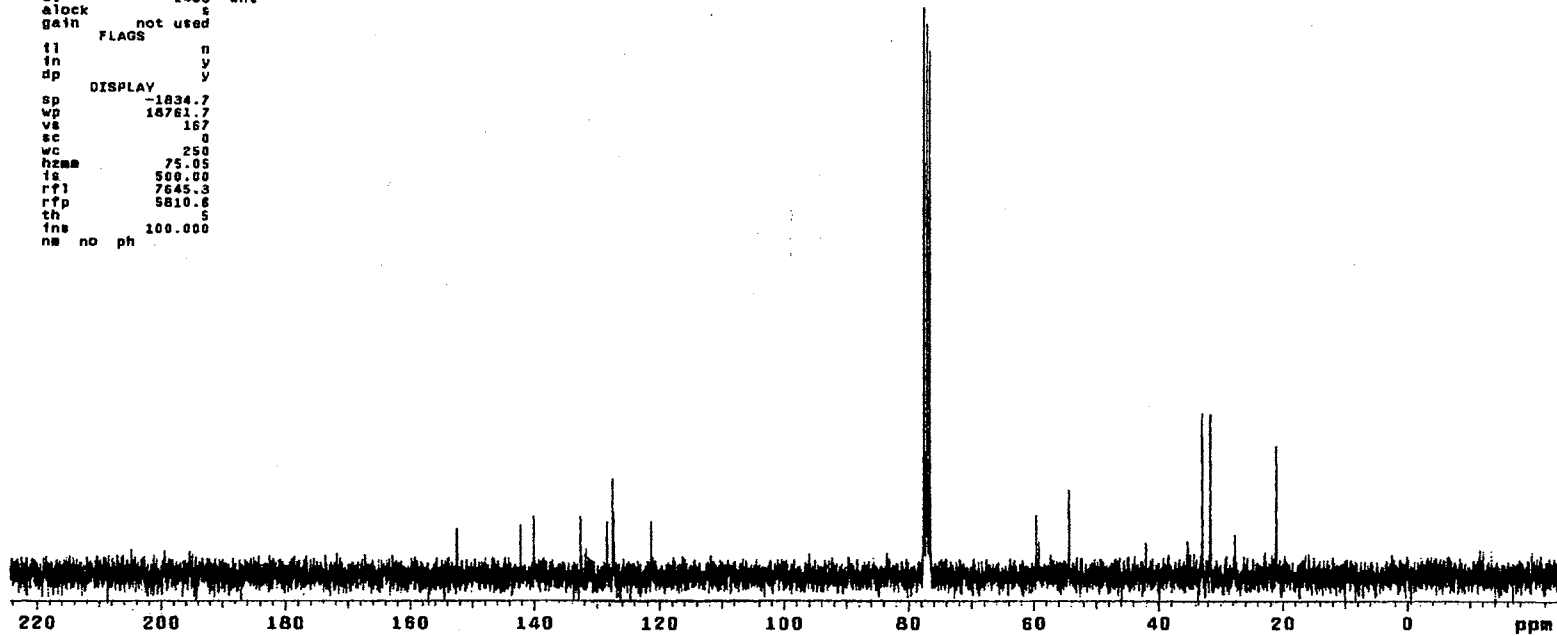
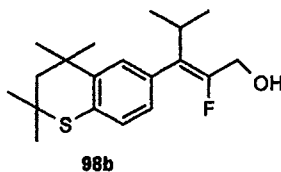
¹H NMR Spectrum of 98b

Plate CLXXVIII

13C OBSERVE

exptl std13c

date	Nov 3 1998	dfrq	300.067
solvent	CDC13	dn	H1
files		dpr	30
ACQUISITION		dof	0
sfrq	75.464	dm	yyy
tn	013	dmm	w
at	0.800	daf	11764
np	30018	PROCESSING	
ew	18761.7	lb	1.00
fb	10400	wtfile	
bs	16	proc	ft
tpwr	52	fn	not used
pw	3.8		
d1	1.000	werr	
tof	0	wexp	wft
nt	2048	wbs	wft
ct	1488	wnt	
clock	s		
gain	not used		
FLAGS			
fl		n	
fn		y	
dp		y	
DISPLAY			
sp	-1834.7		
wp	18761.7		
vs	167		
sc	0		
wc	250		
hzmm	75.05		
is	500.00		
rfl	7845.3		
rff	5810.8		
th	5		
ins	100.000		
nm	no	ph	



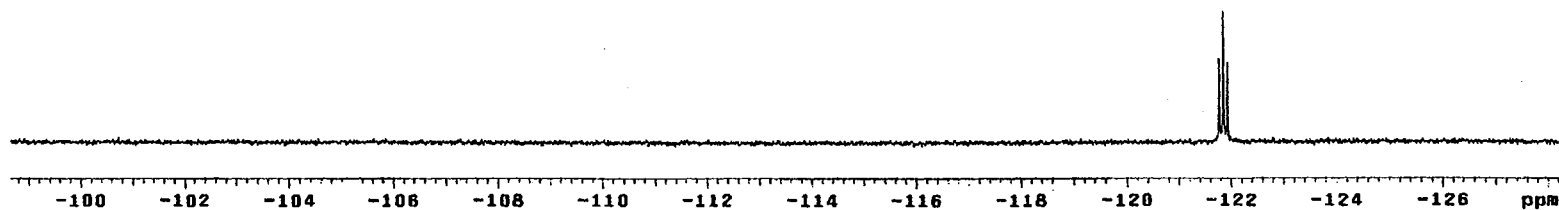
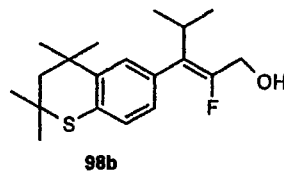
¹³C NMR Spectrum of 98b

Plate CLXXIX

13C OBSERVE

expl std13c

SAMPLE		DEC. & VT	
date	Nov 3 1999	dfrq	300.067
solvent	CDCl3	dn	H1
file	exp	dpwr	34
ACQUISITION			
sfrq	282.333	dot	0
tn	F19	dmm	nm
et	0.600	dm7	11764
np	30016	PROCESSING	
sw	18761.7	lb	1.00
fb	10400	wtfile	
be	16	proc	ft
tpwr	52	fn	not used
pw	3.8		
sl	1.000	werr	
tof	9	wexp	wft
nt	1024	wbe	wft
ct	48	wnt	
alock	n		
gain	not used		
FLAGS			
ll	n		
in	y		
dp	y		
DISPLAY			
sp	-38234.5		
wp	8381.7		
ve	32		
sc	0		
wc	250		
hzmm	33.53		
ls	500.00		
rfl	38748.2		
rff	0		
th	20		
ins	100.000		
na	no	ph	



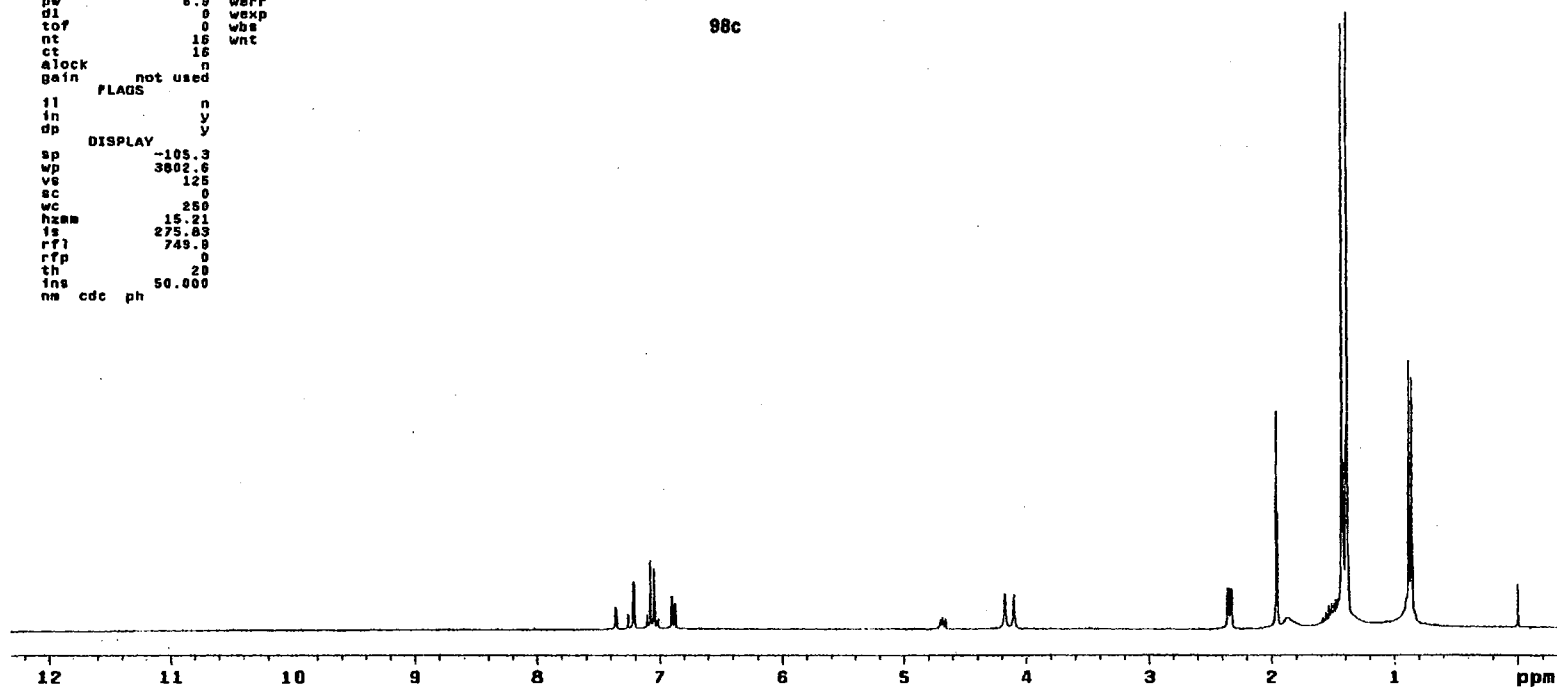
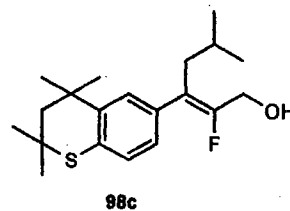
¹⁹F NMR Spectrum of 98b

Plate CLXXX

STANDARD 1H OBSERVE

```

expl stdlh
SAMPLE
date Nov 17 1988 dfrq 300.087
solvent CDC13 dn H1
f1a exp dpr 30
ACQUISITION exp dof 8
sfrq 300.087 dw nnn
tn H1 dnm c
at 3.747 dmf 200
np 33728 PROCESSING
sw 4500.5 wtfile ft
fb 2800 proc
bs 18 fn not used
tpwr 48
pw 6.3 werr
d1 0 wexp
tof 0 wbs
nt 16 wnt
ct 16
clock n
gain not used
FLAGS
fl n
in y
dp y
DISPLAY
sp -105.3
wp 3802.6
vs 125
sc 0
wc 250
hzaw 15.21
is 275.83
rfl 749.8
rtp 0
th 20
ins 50.000
nm cdc ph
    
```



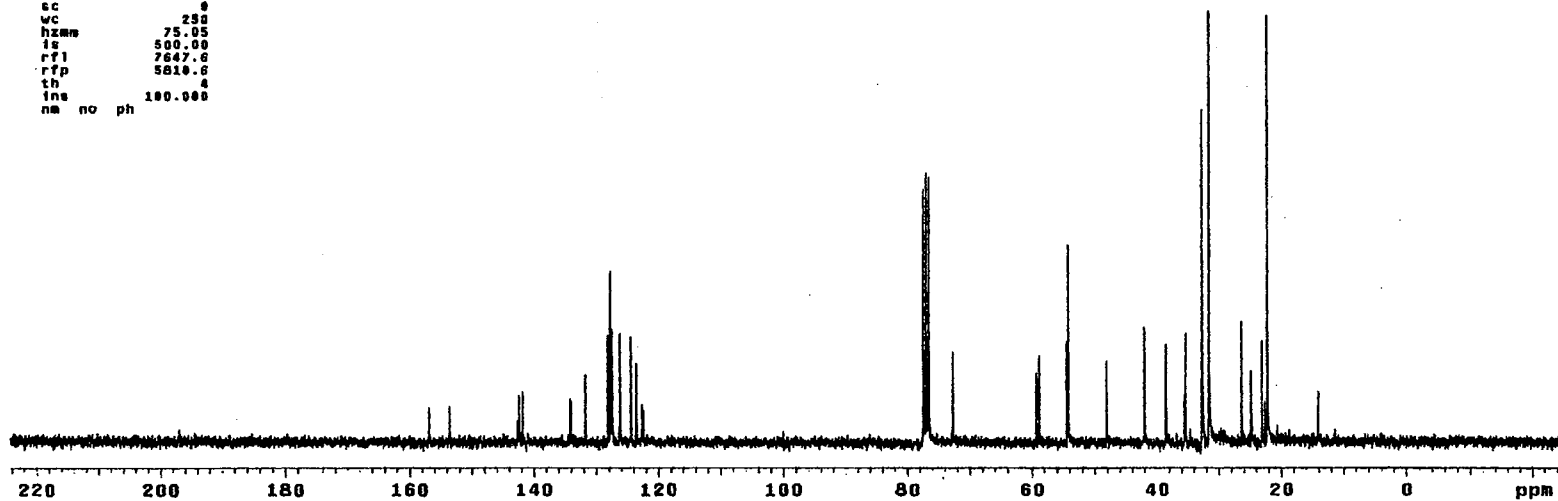
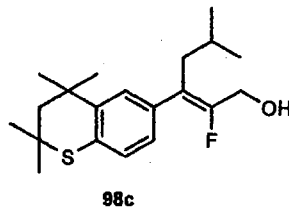
¹H NMR Spectrum of 98c

Plate CLXXXI

13C OBSERVE

expl std13c

date	Nov 17 1999	dfrq	300.007
solvent	CDCl3	dn	H1
file	ACQUISITION	exp	34
		dot	0
efrq	75.464	dm	VVY
tn	C13	dms	w
at	0.800	dnt	11764
np	30012	PROCESSING	
sw	18701.7	lb	1.00
fb	10400	wtfile	
bs	18	proc	ft
tpwr	52	fn	not used
pw	3.8		
di	1.000	werr	
tof	0	wexp	wft
nt	2006	wba	wft
ct	1120	wnt	
elock	0		
gain	not used		
flags			
ll	n		
ln	y		
dp	y		
DISPLAY			
sp	-1837.0		
wp	18701.7		
vs	0		
sc	0		
wc	232		
hzmw	75.05		
is	500.00		
rfl	7647.6		
rfp	5810.6		
th	0		
ins	100.000		
nm	no	ph	



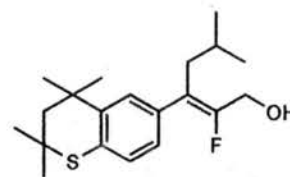
¹³C NMR Spectrum of 98c

Plate CLXXXII

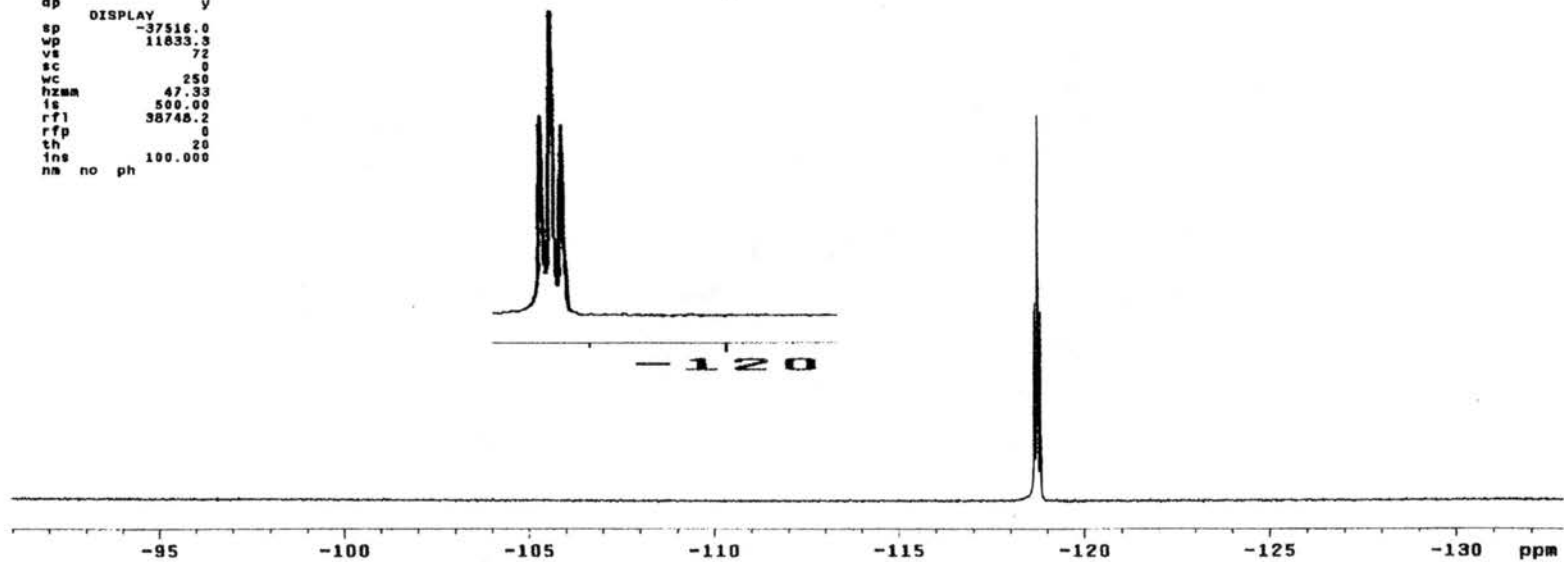
13C OBSERVE

expl std13c

date	Nov 17 1999	dfrq	DEC. & VT	300.087
solvent	CDC13	dn		H1
file	exp	dpwr		34
ACQUISITION				
sfrq	282.333	ds		0
tn	F19	dms		wnn
at	0.800	dwt		11764
np	30016	PROCESSING		
sw	18761.7	lb		1.00
fb	10400	wffile		ft
bs	16	proc		not used
tpwr	52	7n		
pw	3.0			
d1	1.000	werr		
tof	0	wexp		wft
nt	1024	wbs		wft
ct	64	wnt		
alock	n			
gain	not used			
FLAGS				
il	n			
in	y			
dp	y			
DISPLAY				
sp	-37516.0			
wp	11833.3			
vs	72			
sc	0			
wc	250			
hzam	47.33			
is	500.00			
rfl	30748.2			
rfp	0			
th	20			
ins	100.000			
na	no	ph		



98c



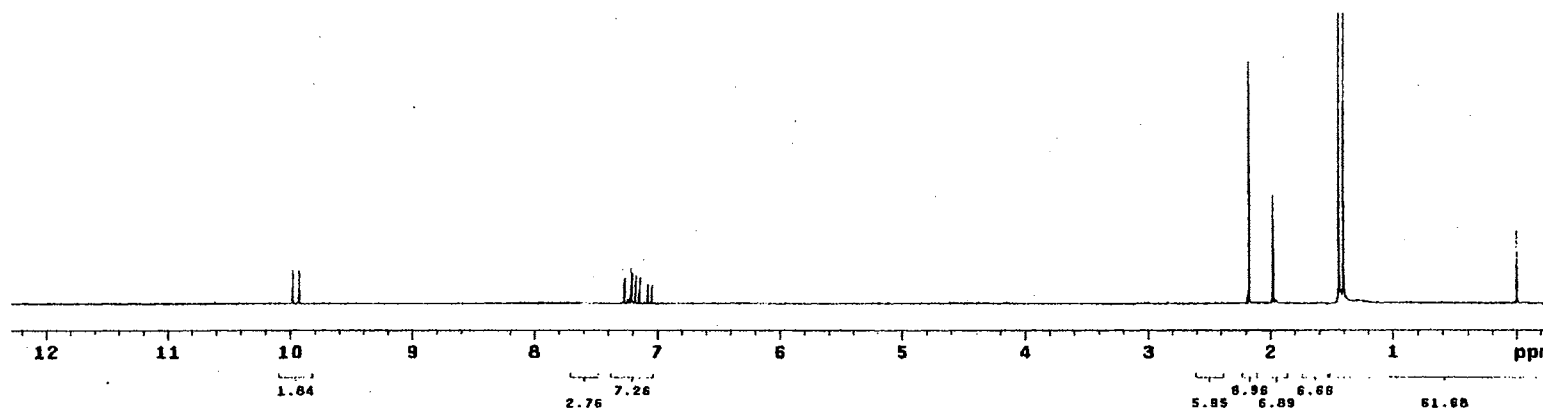
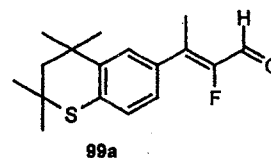
¹⁹F NMR Spectrum of 98c

Plate CLXXXIII

STANDARD 1H OBSERVE

```

expl stdih
SAMPLE DEC. & VT
date Oct 28 1999 dfrq 300.087
solvent CDCl3 dn H1
file exp dpr 30
ACQUISITION exp dof 0
sfrq 300.087 dm nnn
tn H1 dam c
at 3.747 daf 200
np 33728 PROCESSIND
sw 4580.5 wf file
fb 2600 proc ft
bs 16 fn not used
ipwr 48
pw 6.9 werr
SI 8 wexp
tof 0 wbs
nt 16 wnt
ct 16
slock n
gain not used
FLAGS
ii n
in y
dp y
DISPLAY
sp -103.1
wp 3730.6
vs 38
sc 0
wc 250
hzmm 15.18
fs 475.82
rf1 747.7
rfd 0
th 20
ins 100.000
nm cdc ph
    
```



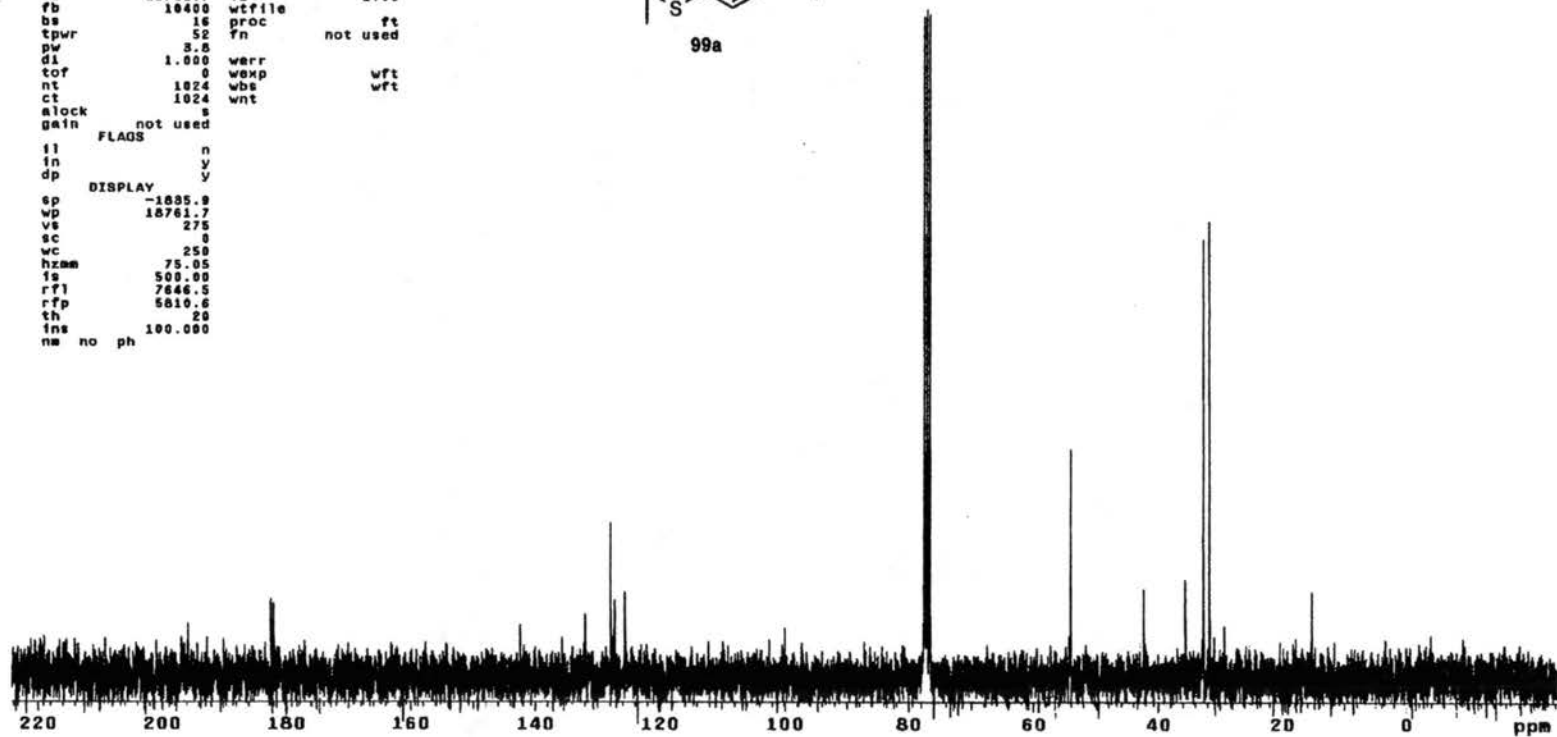
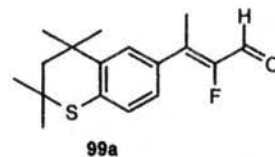
¹H NMR Spectrum of 99a

Plate CLXXXIV

13C OBSERVE

expi std13c

SAMPLE		DEC. & VT	
date	Oct 28 1999	dfrq	300.887
solvent	CDCl3	dn	H1
flfa	exp	dpr	34
ACQUISITION		doF	0
sfrq	75.464	dm	yyy
tn	C13	dmm	w
at	0.800	dM7	11764
np	39016	PROCESSING	
sw	18761.7	lb	1.00
fb	10400	wtfile	
bs	16	proc	ft
tpwr	52	fn	not used
pw	3.5		
di	1.000	werr	
tof	0	wexp	wft
nt	1024	wbe	wft
ct	1024	wnt	
alock	s		
gain	not used		
FLAGS			
il	n		
in	y		
dp	y		
DISPLAY			
sp	-1895.9		
wp	18761.7		
vs	275		
sc	0		
wc	250		
hzam	75.05		
is	500.00		
rfl	7846.5		
rff	5810.5		
th	20		
ins	100.000		
nm	no	ph	



¹³C NMR Spectrum of 99a

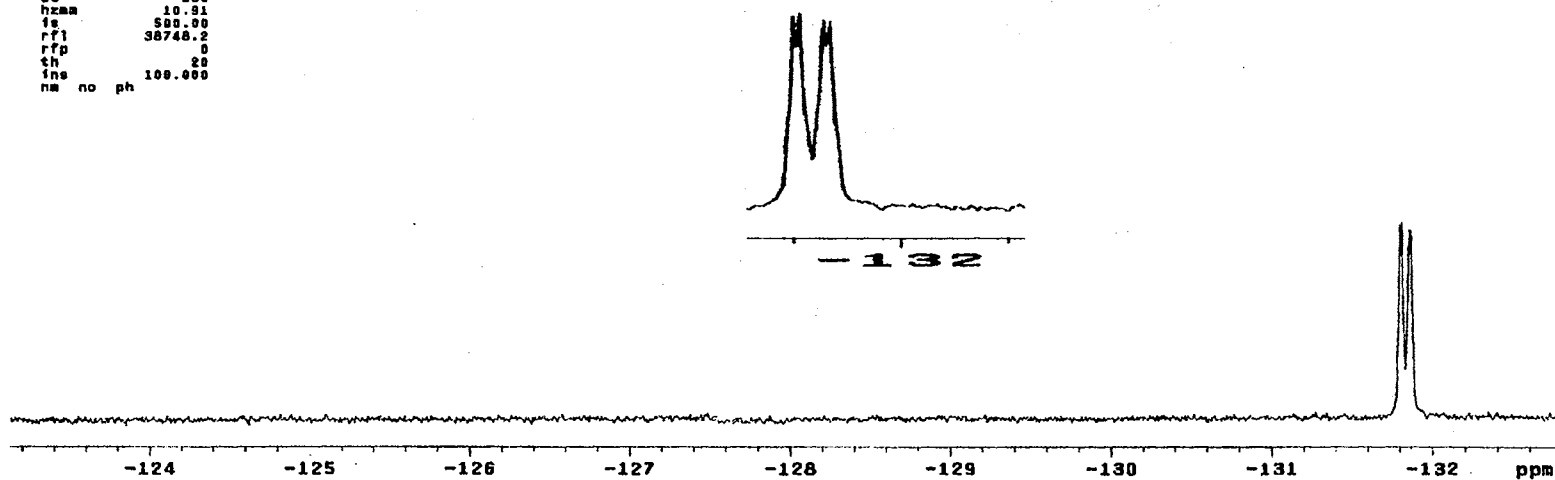
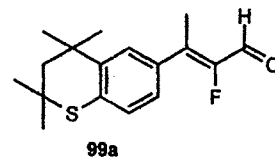
Plate CLXXXV

13C OBSERVE

exp1 std13c

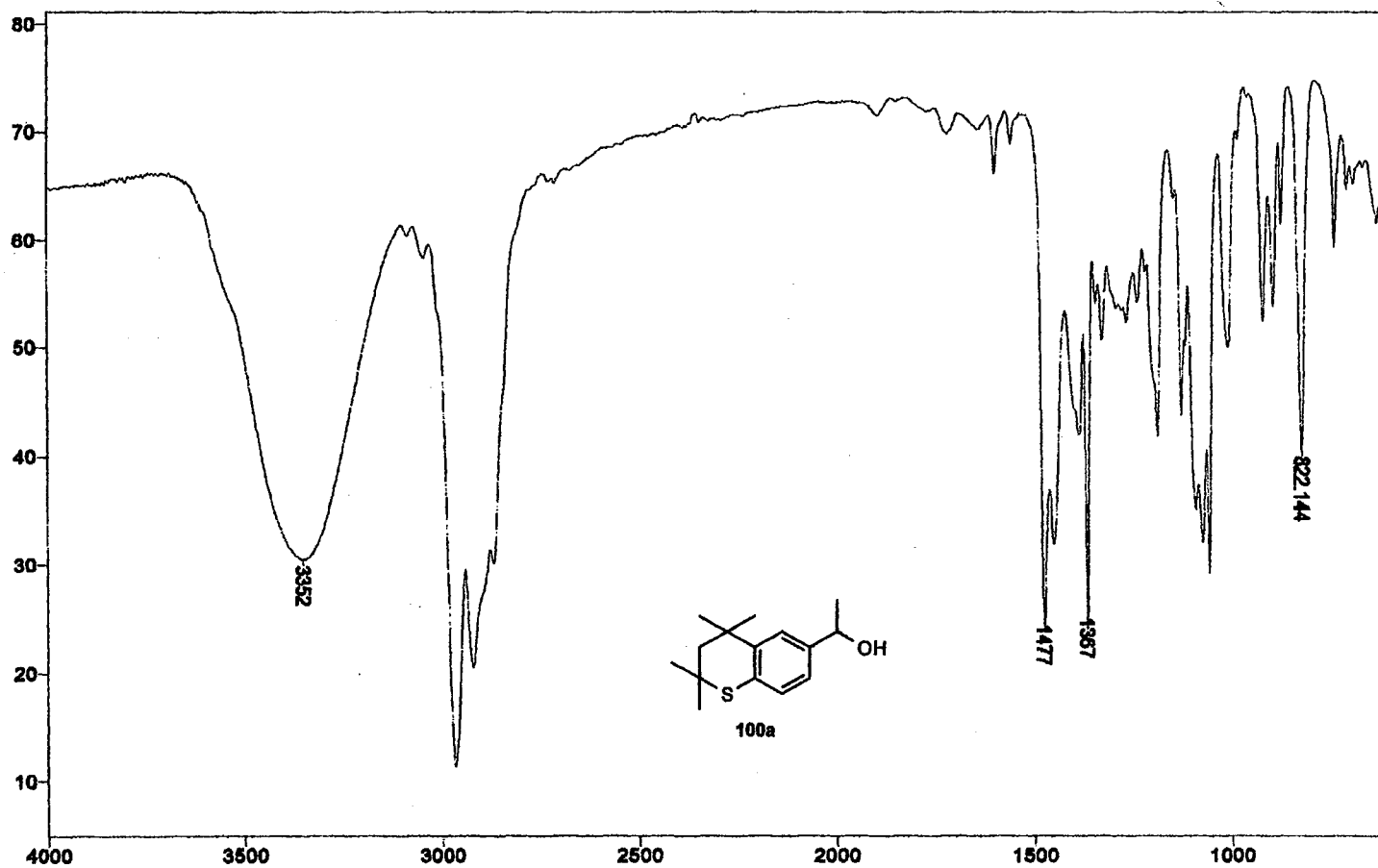
```

SAMPLE          DEC. & VT
date   Oct 28 1999   dfrq   300.087
solvent CDC13      dn      HI
file   exp         dpwr    34
          ACQUISITION dot      0
efrq   282.393    dm      nnn
tn     F13       dam      w
at     0.500     dat      11764
np     38016     PROCESSING
sw     18781.7   lb      1.00
fb     10400    wtfile
bs     15       proc      ft
tpwr   52       7n      not used
pw     3.8
di     1.000    warr
tof     0       wexp      wft
nt     1824    wbs      wft
ct     80       wnt
alock  n
gain   not used
          FLAGS
il     n
in     y
dp     y
          DISPLAY
sp     -37494.2
wp     2727.0
vs     38
sc     0
wc     250
hzma   10.81
fs     500.00
rf1    38748.2
rfp     0
th     20
ins    100.000
nm     no ph
    
```



¹⁹F NMR Spectrum of 99a

Plate CLXXXVI



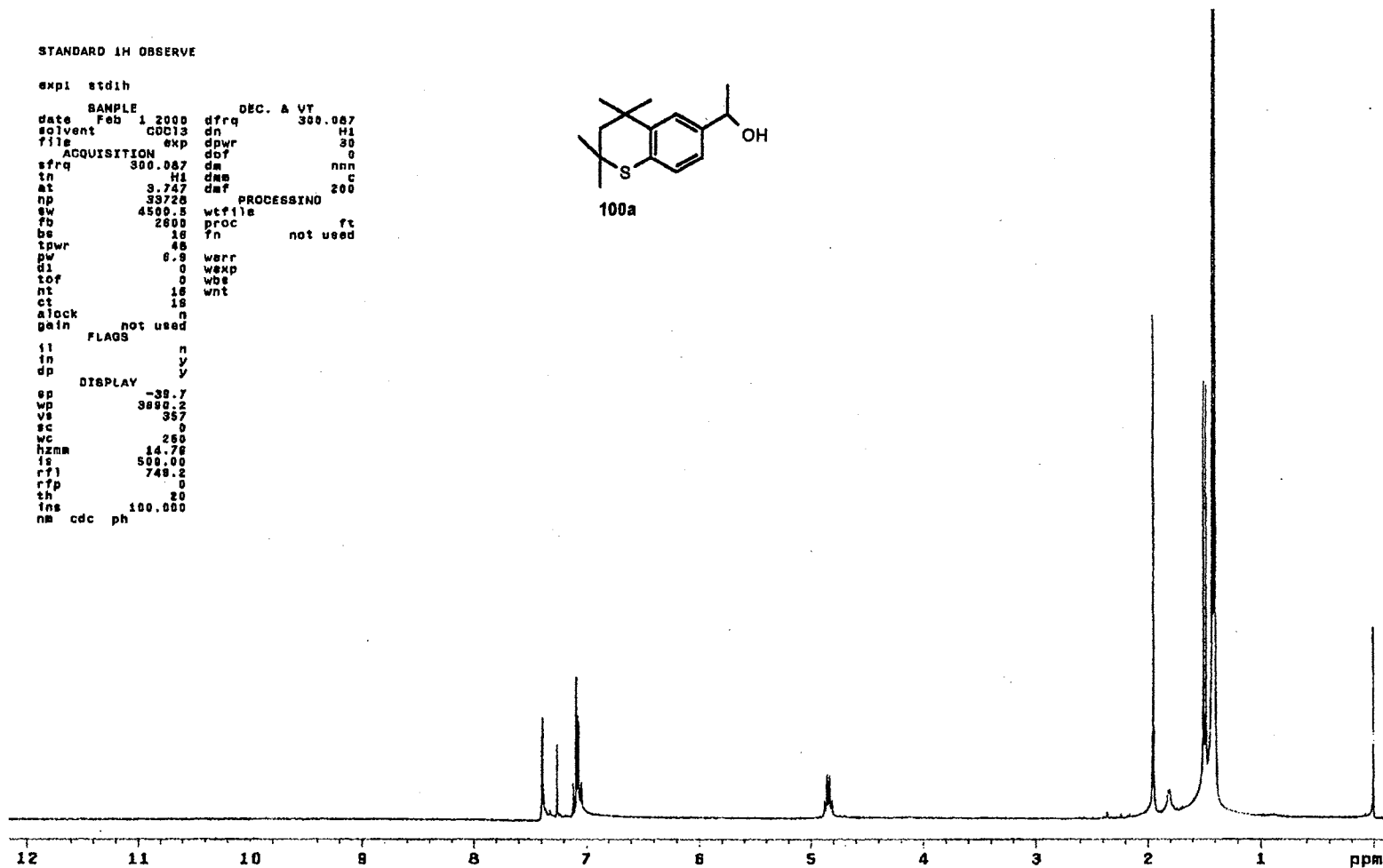
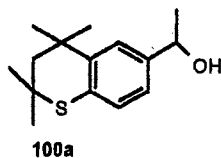
IR Spectrum of 100a

Plate CLXXXVII

STANDARD 1H OBSERVE

```

expi stdih
SAMPLE
date Feb 1 2000 dfrq DEC. A VT 300.067
solvent CDCl3 dn H1
file exp dpwr 30
ACQUISITION dof 0
sfrq 300.067 dm nnn
in H1 dm c
ax 3.747 daf 200
np 33728 PROCESSING
sw 4500.8 wfile
fb 2000 proc ft
bs 18 fn not used
tpwr 48
pw 0.9 werr
d1 0 wexp
tof 0 wbs
nt 18 wnt
ct 18
alock n
gain not used
FLAGS
i1 n
in y
dp DISPLAY y
sp -38.7
wp 3880.2
vs 357
sc 0
wc 250
hzmm 14.78
is 500.00
rf1 749.2
rfp 0
th 20
ins 100.000
nm cdc ph
    
```



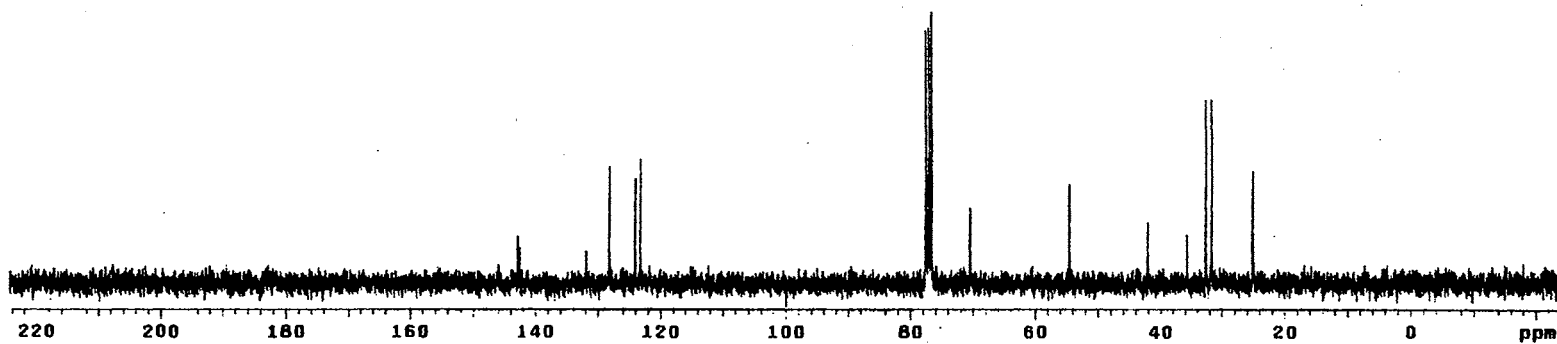
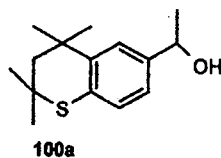
¹H NMR Spectrum of 100a

Plate CLXXXVIII

13C OBSERVE

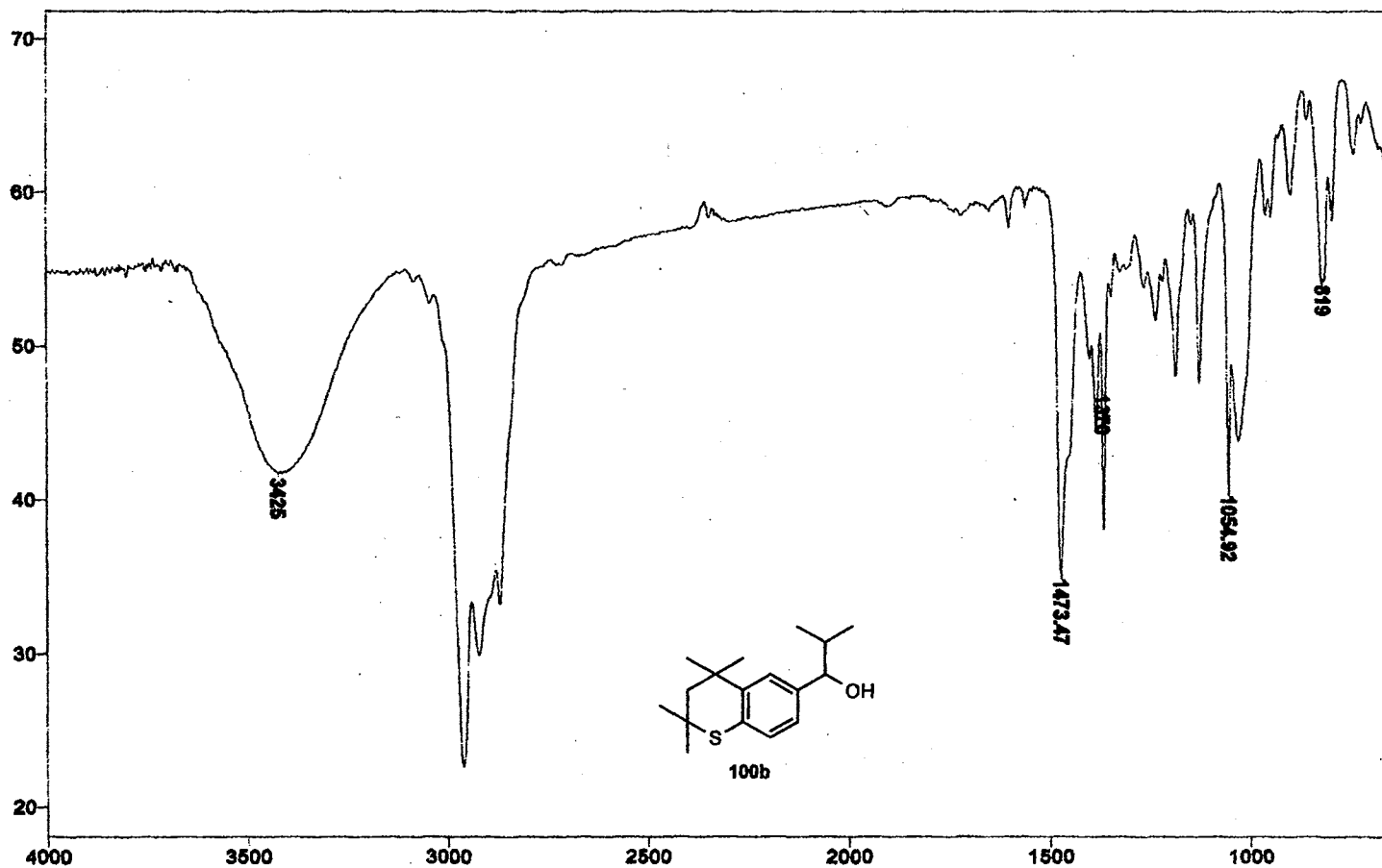
```

expt  std13c
SAMPLE
date  Feb 1 2000   dfrq  DEC. A VT 300.087
solvent CDC13      dn      H1
file    exp      dpwr     34
ACQUISITION      dof      0
efrq    75.464   dm       yy
tn      C13      dnm      w
at      0.800    dmf      11764
np      30016    PROCESSING
qs      10761.7  lb       1.00
fb      10400   wtfile
bs      16      proc      ft
tpwr    52      fn       not used
pw      3.0
d1      1.000   werr
tof     0       wexp
nt      1024   wbs
ct      256   wnt
alock   not used
gain    not used
FLAOS
f1      n
in      y
dp      y
DISPLAY
sp      -1837.0
wp      10761.7
vs      50
sc      0
wc      250
hzma    75.05
is      500.00
rf1     7647.6
rfp     5010.6
th      5
fns     100.000
nm      no ph
    
```



¹³C NMR Spectrum of 100a

Plate CLXXXIX



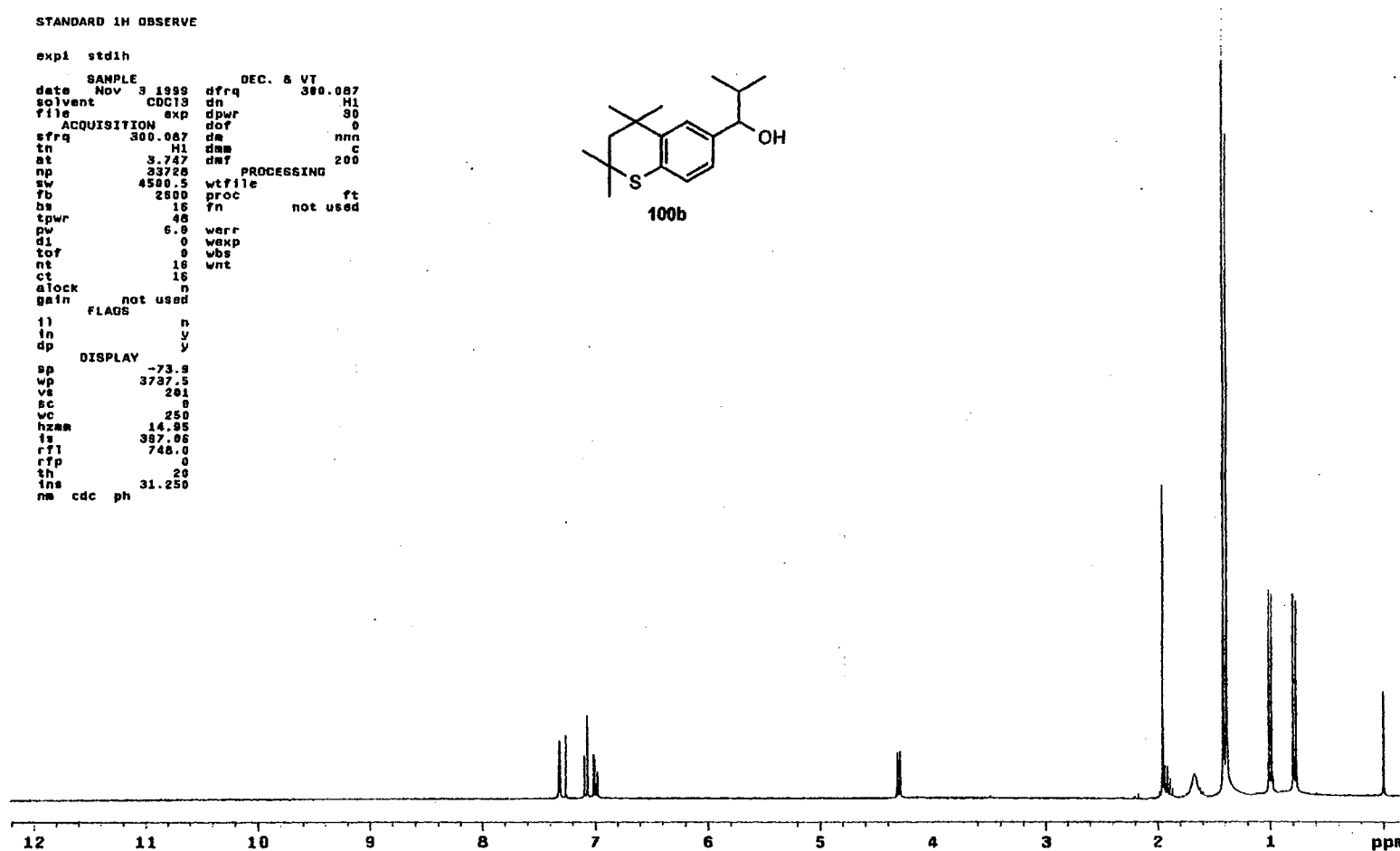
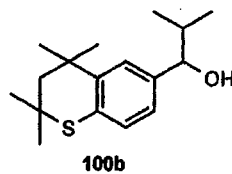
IR Spectrum of 100b

Plate CXC

STANDARD 1H OBSERVE

```

expl std1h
SAMPLE          DEC. & VT
date Nov 3 1999 dfrq 300.087
solvent CDCl3   dn      H1
file          exp dpwr    30
ACQUISITION    dof      0
sfrq 300.087  da        nnn
tn          H1  dam      c
at          3.747 dmf     200
np          33720 PROCESSING
sw          4500.5 wtfile
fb          2800 proc    ft
bs          16  fn      not used
tpwr       48
pv          6.0 werr
d1          0  wskp
tof         0  wbs
nt          16  wnt
ct          16
alock      not used
gain      not used
FLAGS
ll         n
in         y
dp         y
DISPLAY
sp         -73.8
wp         3737.5
vs         201
sc         0
wc         250
hzwr       14.95
fs         387.06
rf1        748.0
rfp         0
sh         20
ins        31.250
nm cdc ph
    
```



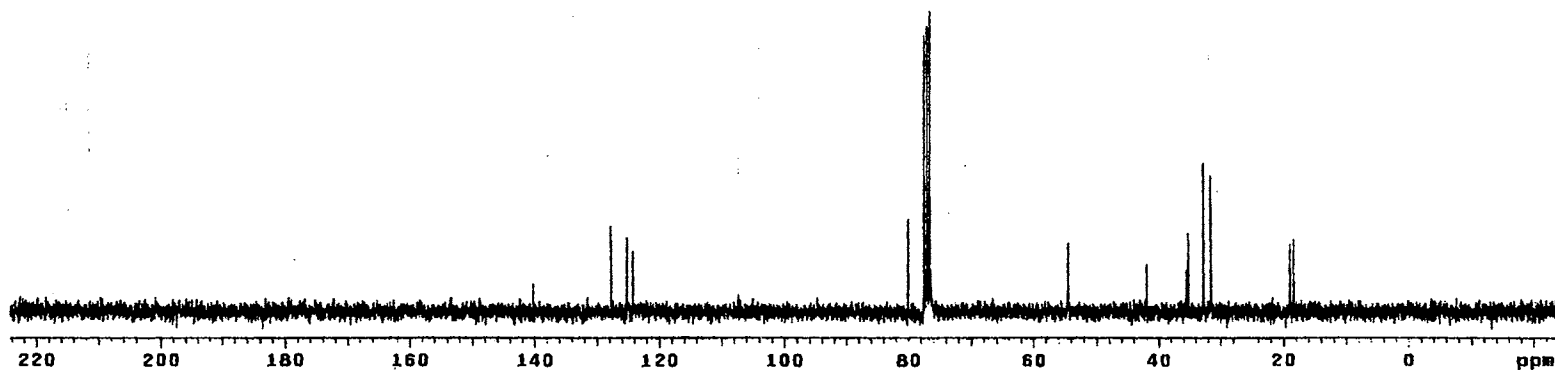
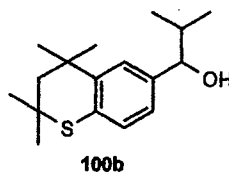
¹H NMR Spectrum of 100b

Plate CXCI

¹³C OBSERVE

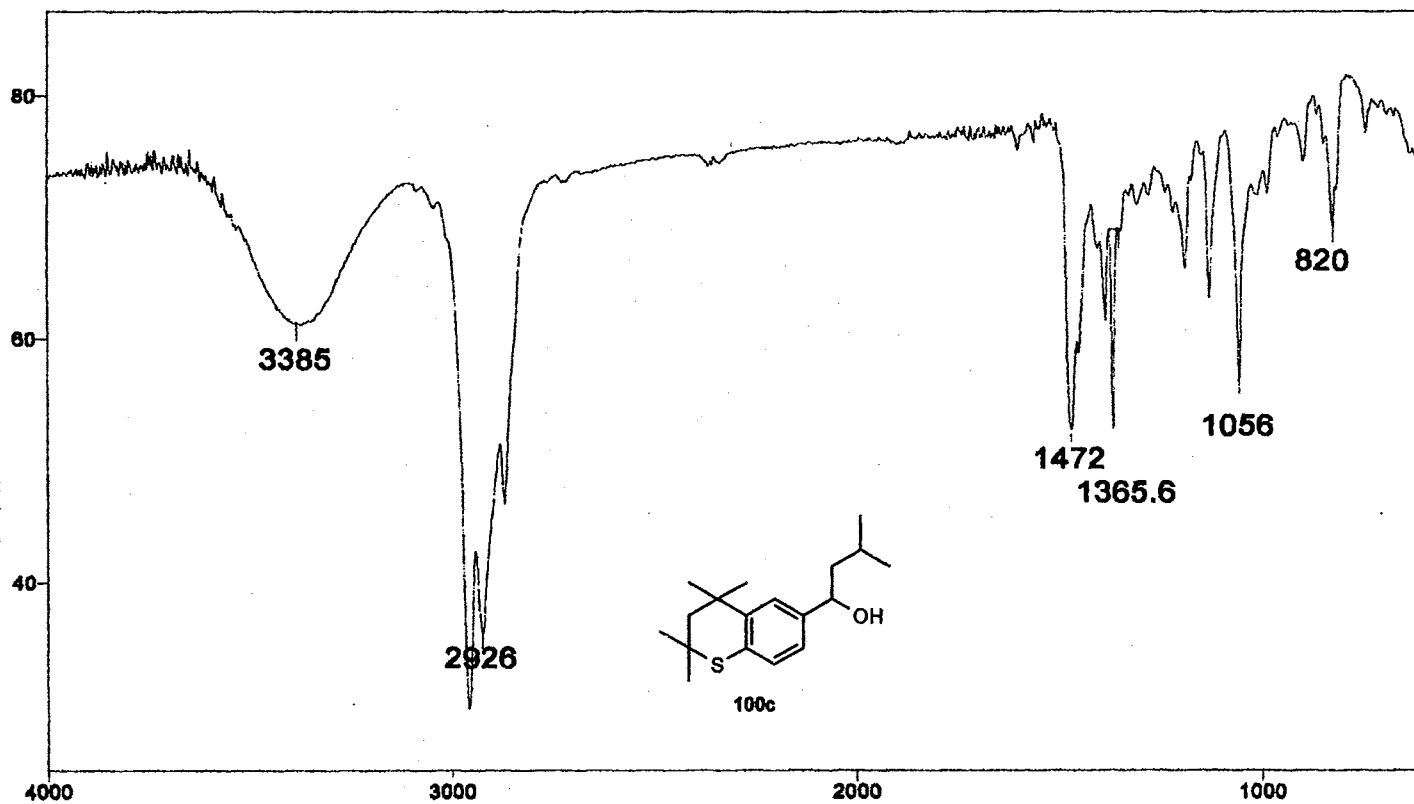
```

expl std13c
SAMPLE
date Nov 3 1999 dfrq DEC. & VT 300.087
solvent CDCl3 dn H1
file ACQUISITION exp dpwr 34
sfrq 75.484 dm dof 0
tn C13 dms vvy w
at 0.800 dmf 11764
np 38016 PROCESSING
pw 18761.7 lb wtfile 1.00
fb 10400 wtfile
bs 16 proc ft
tpwr 52 fn not used
pw 3.8
di 1.000 verr
sof 0 wexp wft
nt 2048 wbs wft
ct 512 wnt
alock not used s
gain FLADS not used
il n
in y
dp DISPLAY y
sp -1835.9
wp 18761.7
vs 56
sc 0
wc 250
hznm 75.85
ls 500.00
rfl 7848.5
rff 5810.8
th 8
ins 100.000
na no ph
    
```



¹³C NMR Spectrum of 100b

Plate CXCII



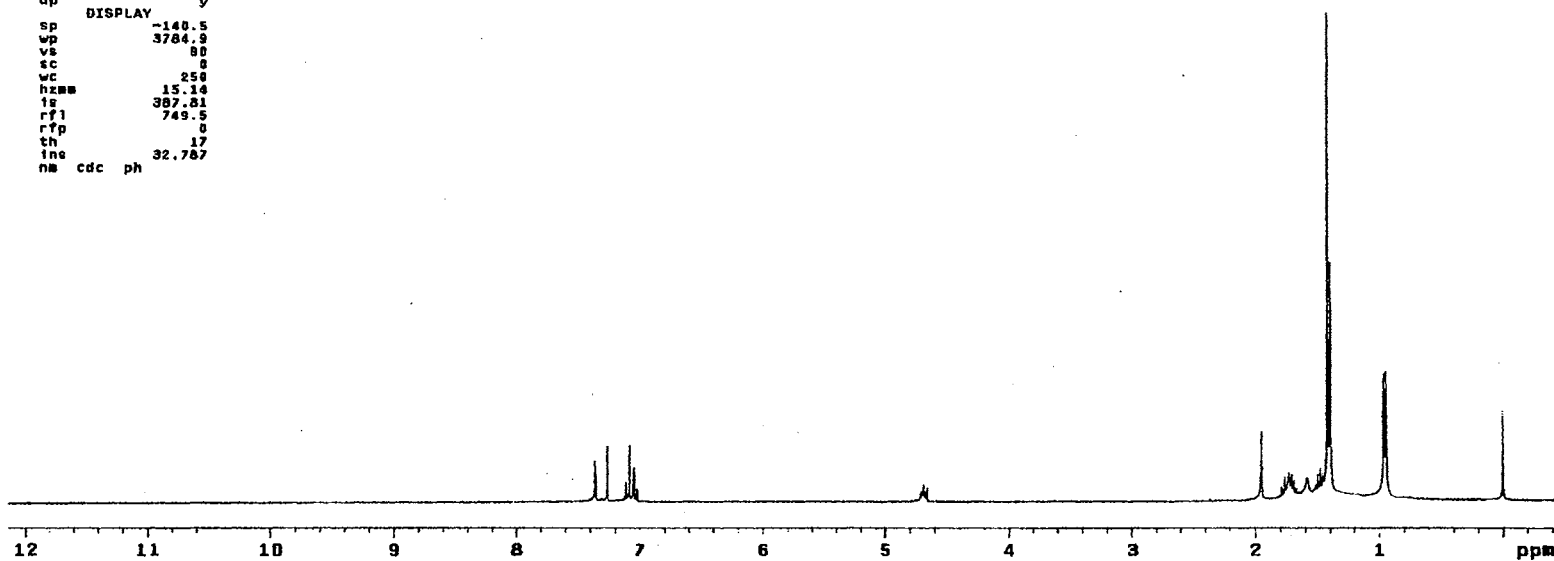
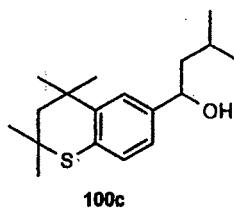
IR Spectrum of 100c

Plate CXCIII

STANDARD 1H OBSERVE

```

expl stdih
SAMPLE
date Nov 16 1999 dfrq DEC. & VT 300.087
solvent CDC13 dn H1
file exp dpwr 30
ACQUISITION dof 0
sfrq 300.087 dm nnn
dn H1 dms c
at 3.747 dmf 200
np 33726 PROCESSING
sw 4500.5 wtfile
fb 2800 proc ft
bs 16 fn not used
tpwr 48
pw 6.9 werr
d1 0 wexp
tof 0 wbs
nt 16 wnt
ct 16
alock n
gain not used
FLAGS
fl n
in y
dp y
DISPLAY
sp -140.5
wp 3784.9
vs 80
sc 0
wc 250
hzmm 15.14
lg 387.81
rf1 745.5
rfp 0
th 17
ine 32.787
nm cdc ph
    
```



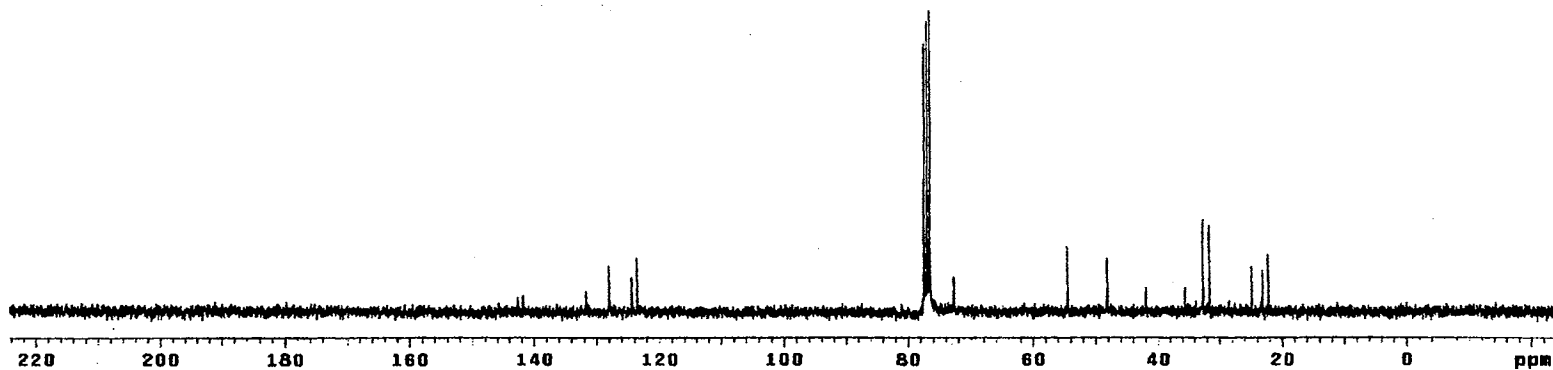
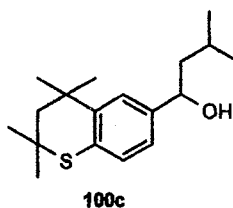
¹H NMR Spectrum of 100c

Plate CXCIV

13C OBSERVE

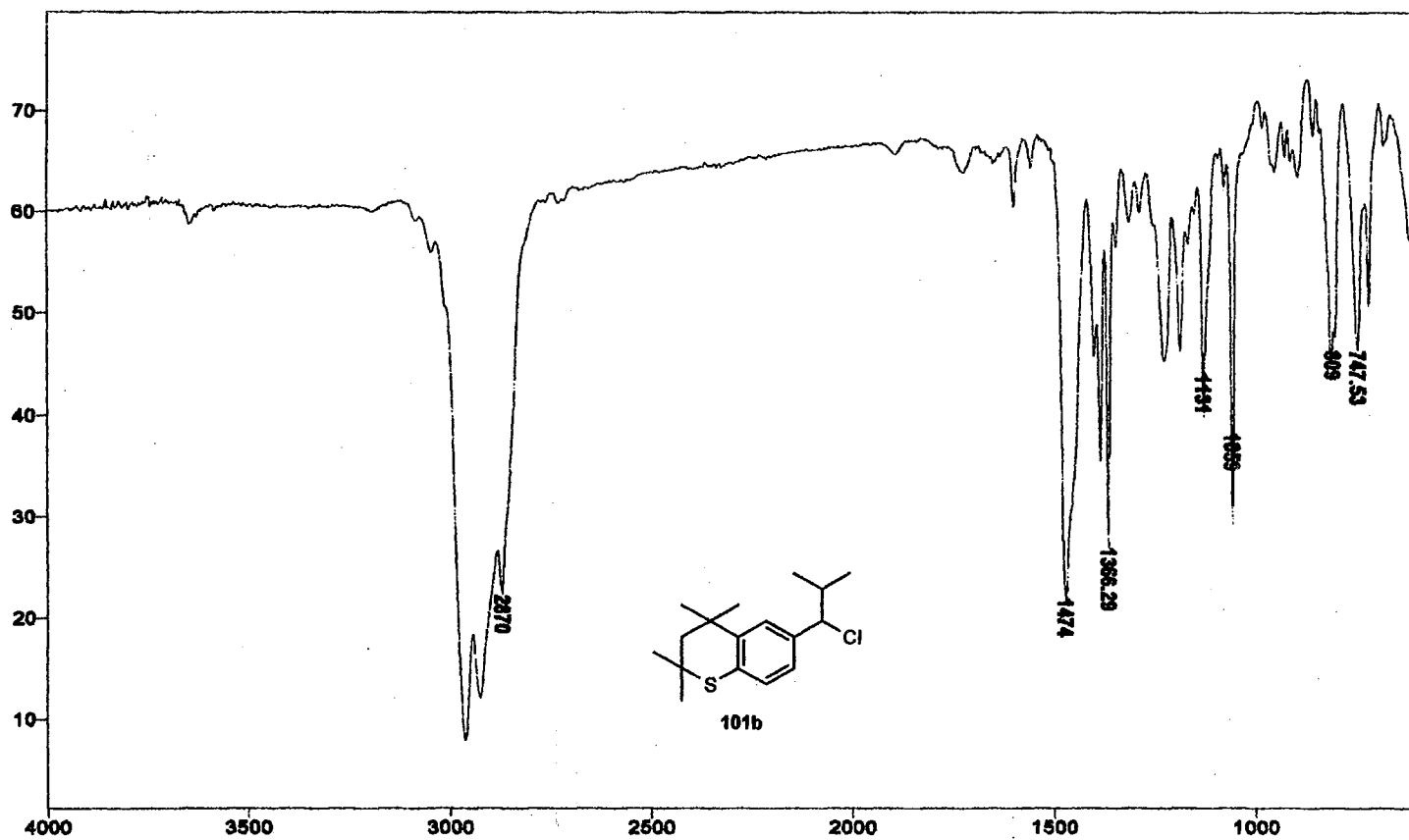
```

expl std13c
SAMPLE
date Nov 16 1999 dfrq DEC. & VT 300.087
solvent CDCl3 dn H1
file exp dpwr 34
ACQUISITION dof 0
sfrq 75.464 dm yyy
tn C13 dm w
at 0.800 daf 11764
np 30018 PROCESSING
sw 18761.7 lb 1.00
fb 10400 wtfile
bs 16 proc ft
tpwr S2 fn not used
pv 3.8
d1 1.000 warr
tof 0 wexp wft
nt 2048 wbs wft
ct 2048 wnt
alock
gain not used
FLAOS
ii n
in y
dp y
DISPLAY
sp -1835.9
wp 18761.7
vs 50
sc 0
wc 250
hzmm 75.05
is 500.08
rf1 7846.5
rfp 5819.8
th 20
fns 100.000
nm no ph
    
```



¹³C NMR Spectrum of 100c

Plate CXCIV



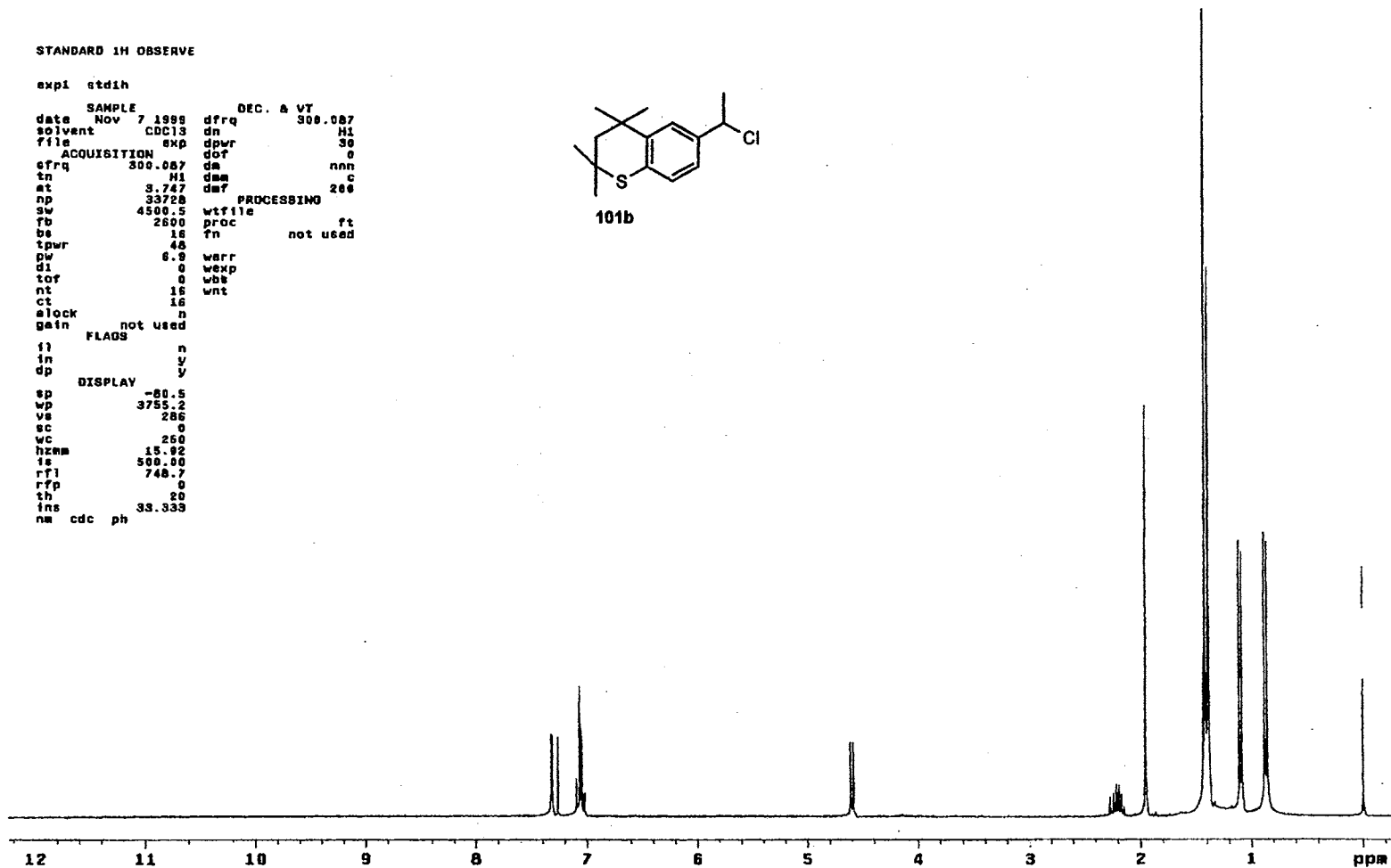
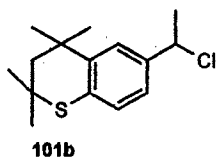
IR Spectrum of 101b

Plate CXCVI

STANDARD 1H OBSERVE

```

expi stdih
date Nov 7 1999      SAMPLE      DEC. & VT
solvent CDCl3        dn          308.087
file     EXP         dpwr         30
ACQUISITION          dof          0
cfreq    300.087    dm          nnn
tn       H1         dsm          c
at       3.747      dmf         200
np       33728      PROCESSING
sw       4500.5     wtf file
rs       2500      proc          ft
bs       16        fn          not used
tpwr     48
pw       6.9      warr
di       0        wexp
tof      0        wbb
nt       16      wnt
ct       16
elock   n
gain    not used
FLAGS
f1      n
in      y
dp      y
DISPLAY
sp      -80.5
wp      3755.2
vs      286
sc      0
wc      250
hscm    15.92
fs      500.00
rf1     748.7
rfp     0
th      20
ins     33.333
nm cdc ph
    
```



¹H NMR Spectrum of 101b

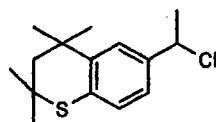
Plate CXC VII

13C OBSERVE

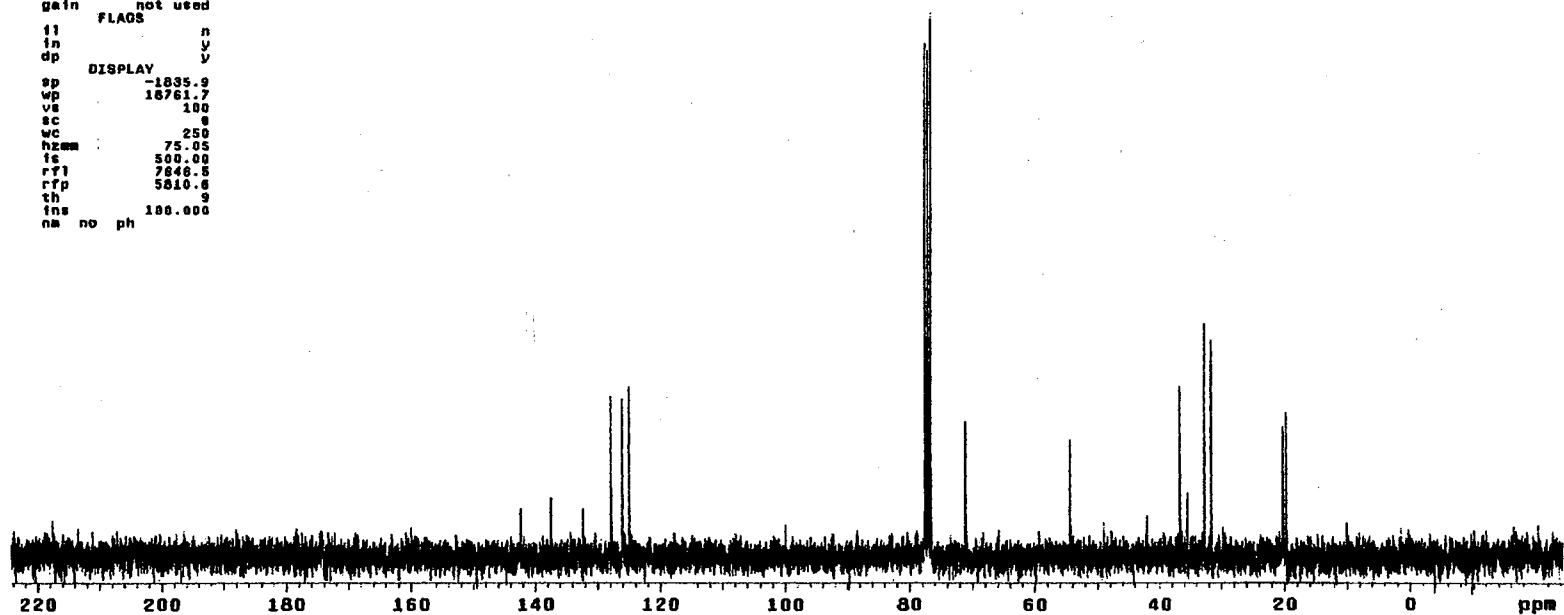
expl std13c

```

SAMPLE          DEC. & VT
date Nov 7 1998 dfrq 300.007
solvent CDCl3   dn      H1
file exp       dpwr    34
ACQUISITION    dof     0
sfrq 75.464   dm      yyy
tn    C13     dnm     w
at    0.800   dmf     11764
np    30016   PROCESSING
sw    18761.7 lb      1.00
fb    10400   wtf file
ba    16     proc    ft
tpwr  52     fn      not used
pv    3.6
d1    1.000   werr
tof   0       wexp    wft
nt    1024   wbs
ct    360    wnt
alock  s
gain  not used
FLAGS
fl    n
in    y
dp    y
DISPLAY
sp    -1895.9
wp    18761.7
vs    100
sc    0
wc    250
hzmm  75.05
fe    500.00
rfl   7848.8
rfp   5810.6
th    9
ins   100.000
na    no ph
    
```

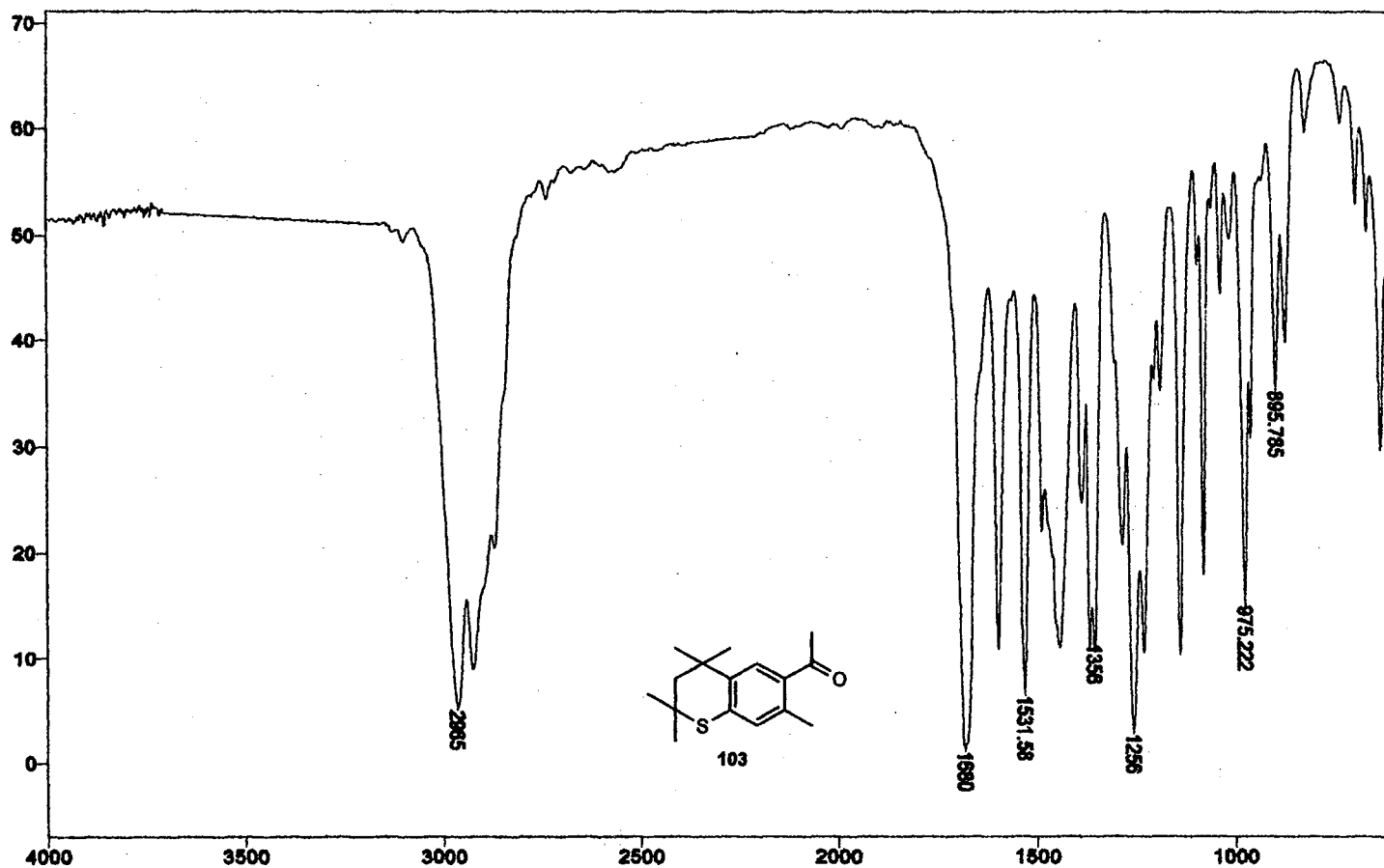


101b



¹³C NMR Spectrum of 101b

Plate CXCVIII



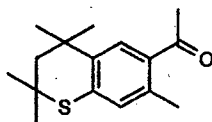
IR Spectrum of 103

Plate CXCIX

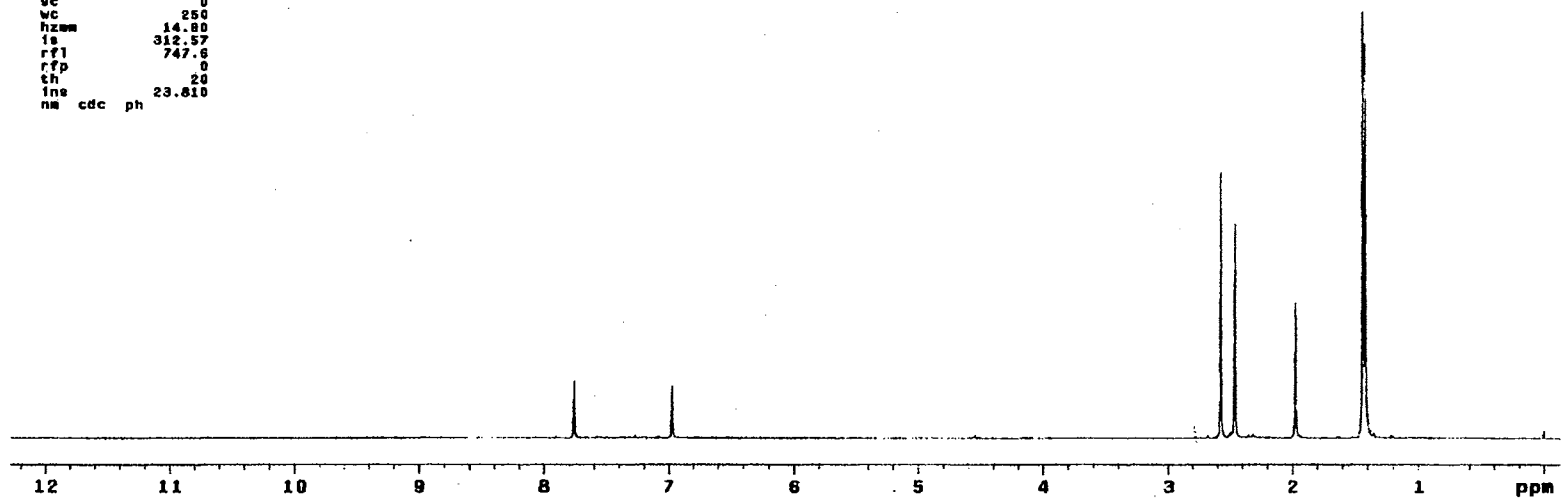
STANDARD 1H OBSERVE

```

expl stdh
date Jul 9 1998 dfrq DEC. & VT 300.087
solvent CDC13 dn H1
file ACQUISITION exp dpwr H1
sfrq 300.087 dm dof 0
tn H1 dam nnn c
at 9.747 dmf 200
rp 33728 PROCESSING
sw 4500.5 wtf1e ft
fb 2680 proc
bs 16 Th not used
tpwr 40
pw 3.0 werr
d1 0 wexp
tof 0 wbs
nt 16 wnt
ct 16
alock not used
gain FLAOS n
ii n
in y
dp DISPLAY y
sp -30.0
wp 3725.7
ve 79
ec 0
wc 250
hzmm 14.80
ia 312.57
rf1 747.6
rfp 0
ch 20
lne 23.010
na cdc ph
    
```



103



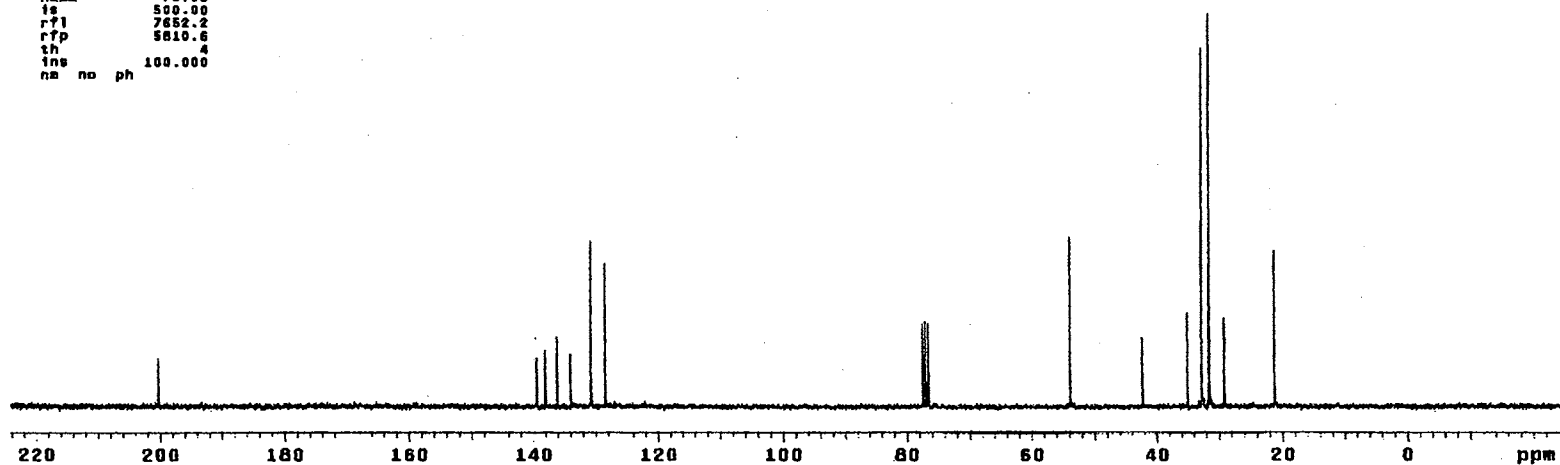
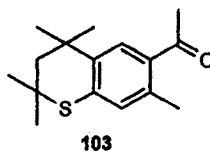
¹H NMR Spectrum of 103

Plate CC

13C OBSERVE

```

expl  std13c
date  SAMPLE      DEC. & VT
      Jul  8 1988  dfrq  300.067
solvent  CDCl3    dn      H1
file     exp     dpwr   34
ACQUISITION  dof    0
sfrq    75.464  dm     vvy
tn      C13     dm     w
at      0.800   dmf    11764
np      38015   PROCESSING
sw      16761.7  lb     1.00
fb      18400   wtf1le
bs      16     proc   ft
tpwr    52     fn     not used
pw      3.8
d1      1.000  warr
tof     0     wskp   wft
nt      1024  wbs    wft
ct      256   wnt
elock   0
gain    not used
      FLAGS
      n
      y
      y
      DISPLAY
      -1841.6
      18761.7
      73
      0
      250
      hzmm  75.05
      is   500.00
      r71  7662.2
      r7p  5610.6
      th   4
      ins  100.000
na no ph
  
```



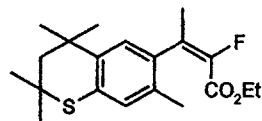
¹³C NMR Spectrum of 103

Plate CCI

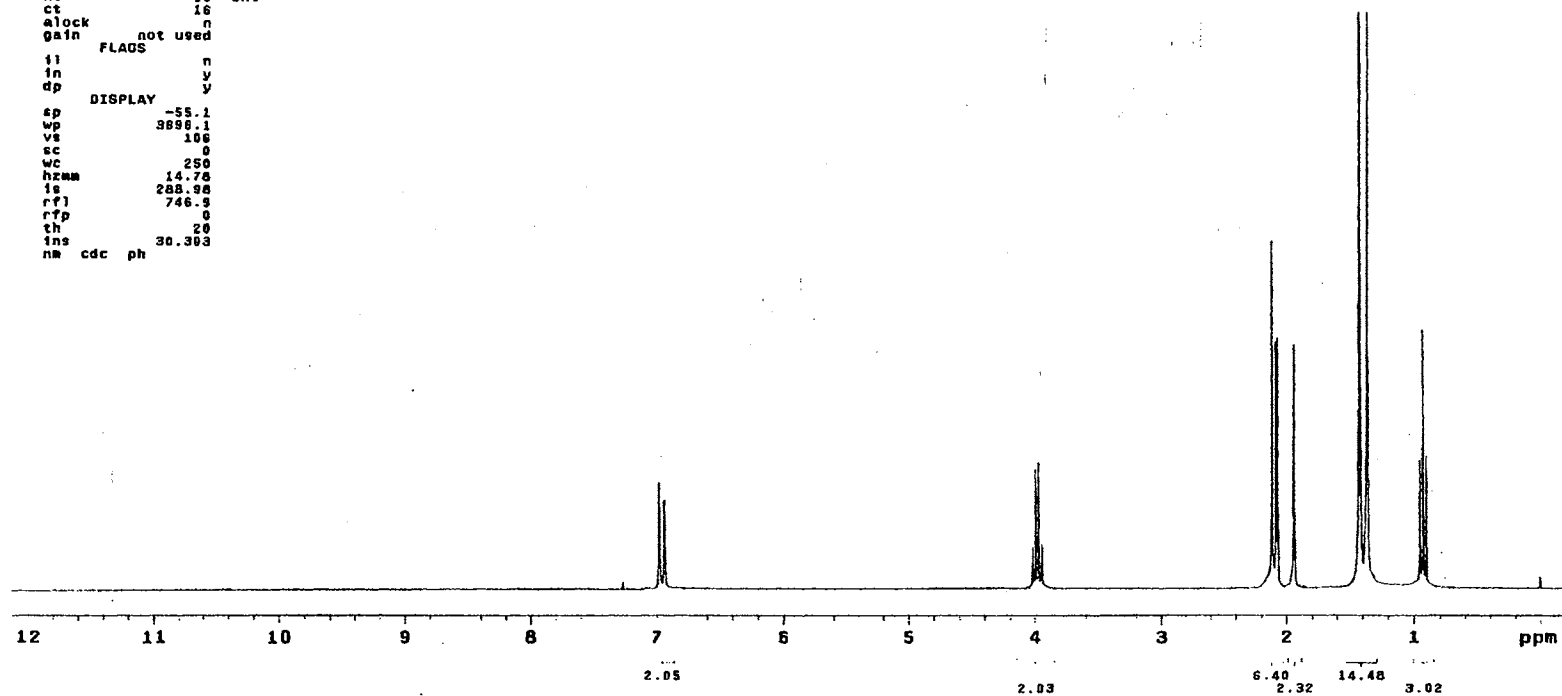
STANDARD 1H OBSERVE

```

expi stdih
SAMPLE
date Jan 24 2000 dfrq DEC. & VT 300.087
solvent CDCl3 dn H1
file exp dpwr 30
ACQUISITION exp dof 0
sfrq 300.087 da nnc
tn H1 dm c
at 3.747 dmf 200
np 33728 PROCESSING
sw 4500.5 wtf file ft
fb 2800 proc fn not used
bs 16
tpwr 48
pv 2.0 werr
dl 0 wexp
tof 9 wbs
nt 16 wnt
ct 16
alock n
gain not used
FLAOS
ii n
in y
dp y
DISPLAY
sp -55.1
wp 3888.1
vs 106
sc 0
wc 250
hcam 14.78
is 288.98
rf1 746.9
rtf 0
th 20
ins 30.363
na cdc ph
    
```



104



¹H NMR Spectrum of 104

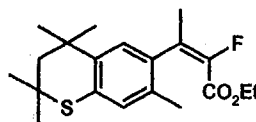
Plate CCII

13C OBSERVE

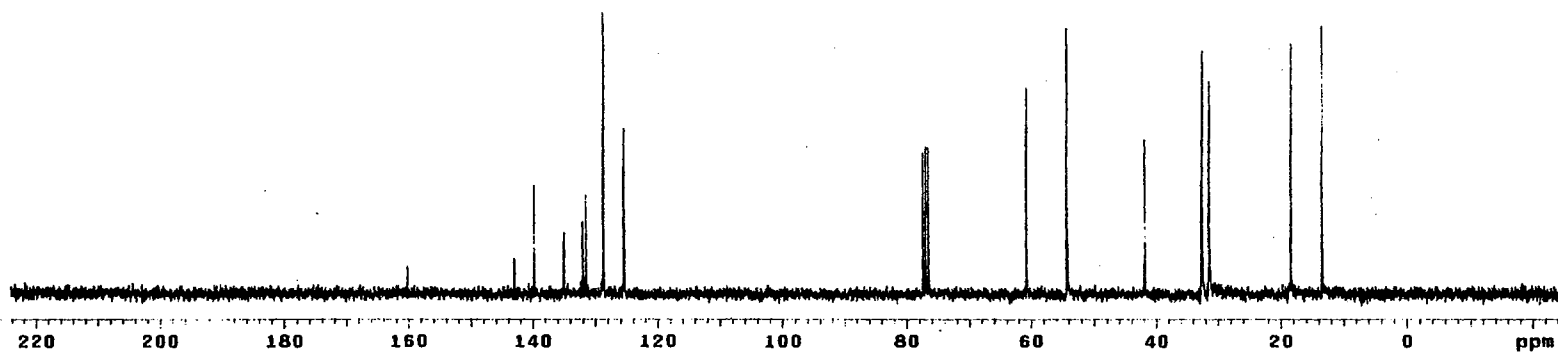
expl std13c

```

SAMPLE
date Jan 24 2000 dfrq 300.087
solvent CDCl3 dn H1
file exp dpwr 34
ACQUISITION dof 0
sfrq 75.464 dm yyy
tn C13 dsm w
at 0.800 dmf 11764
np 30016 PROCESSING
sw 18761.7 lb 1.00
fb 10400 wtf1le
bs 16 proc ft
tpwr 52 fn not used
pw 3.8
di 1.000 werr
tof 8 wexp wft
nt 1024 wbs wft
ct 112 wnt
alock s
gain not used
FLAOS
il n
in y
dp y
DISPLAY
sp -1842.7
wp 18761.7
vs 52
sc 0
wc 250
hzmm 75.05
is 500.00
rf1 7553.3
rfp 5810.6
th 7
ins 100.000
na no ph
    
```



104



¹³C NMR Spectrum of 104

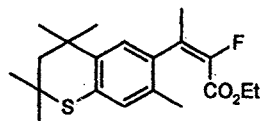
Plate CCIII

13C OBSERVE

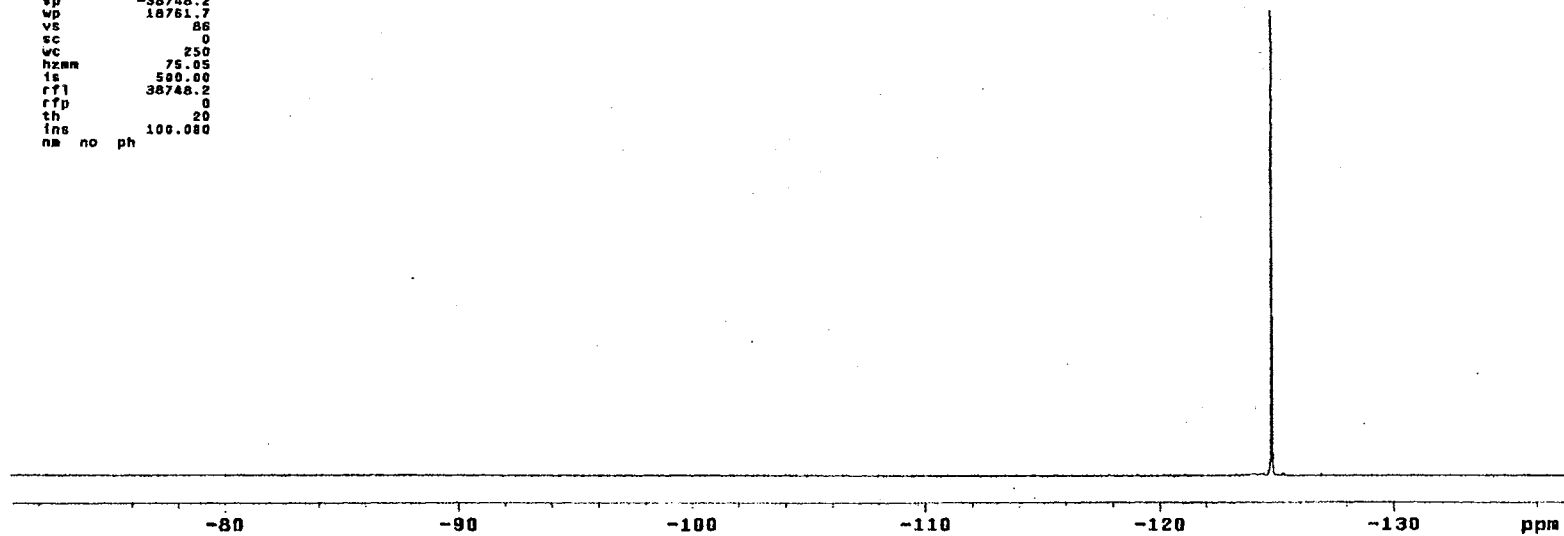
expl std13c

```

SAMPLE
date Jan 24 2008 dfrq DEC. & VT 380.067
solvent COC13 dn H1
file exp dpwr 34
ACQUISITION dof 0
sfrq 282.333 dm nnn
tn F18 dms w
at -0.500 dmf 11764
np 30016 PROCESSING
aw 18761.7 lb 1.00
fb 10400 wtfile
bs 16 proc ft
tpwr 52 fn not used
pw 3.8
dl 1.000 werr
tof 0 wexp wft
nt 1024 wss wft
ct 16 wnt
alock n
gain not used
FLAGS
il n
in y
dp y
DISPLAY
ep -38748.2
sp 18761.7
vs 86
sc 0
wc 250
hzmm 75.05
ts 500.00
rf1 38748.2
rfp 0
th 20
ins 100.080
na no ph
    
```

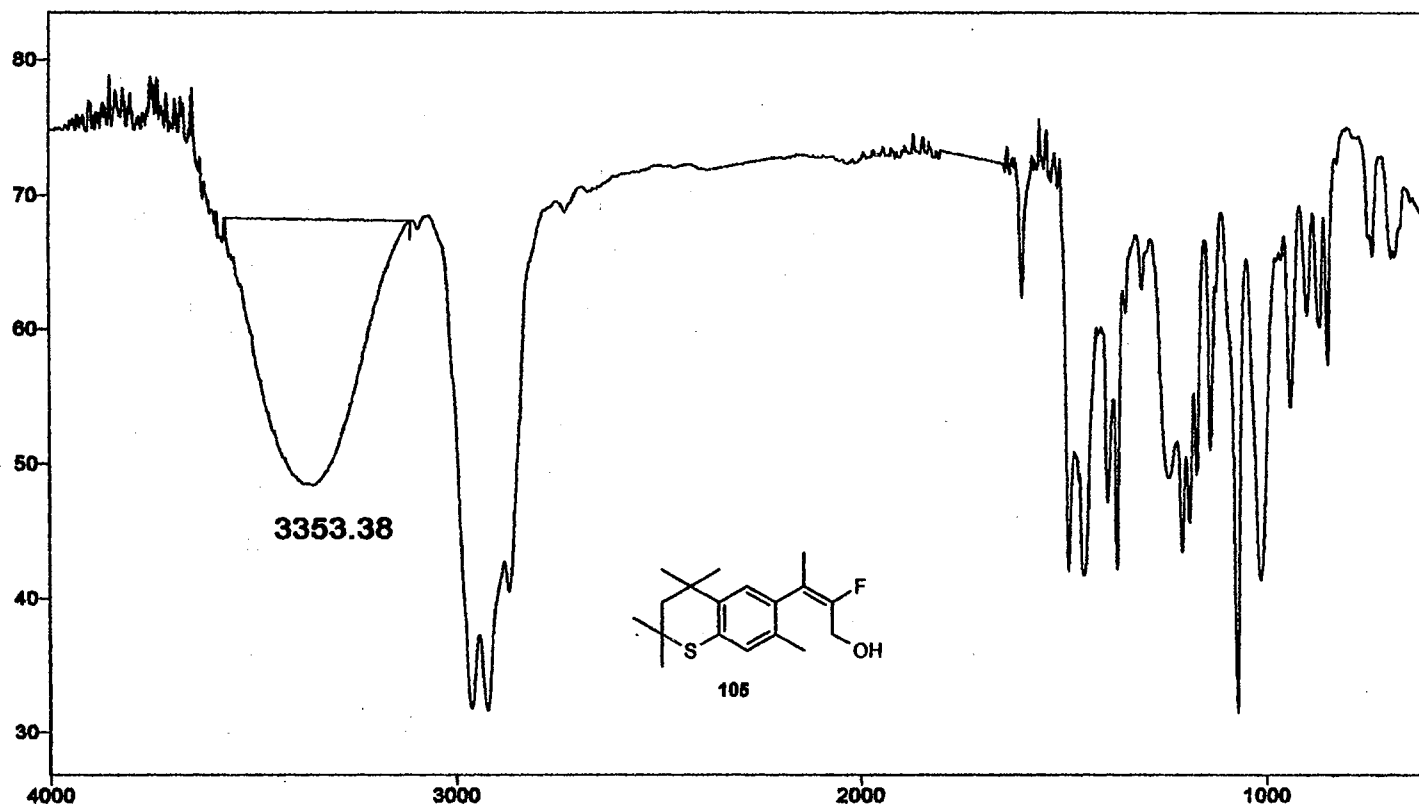


104



¹⁹F NMR Spectrum of 104

Plate CCIV



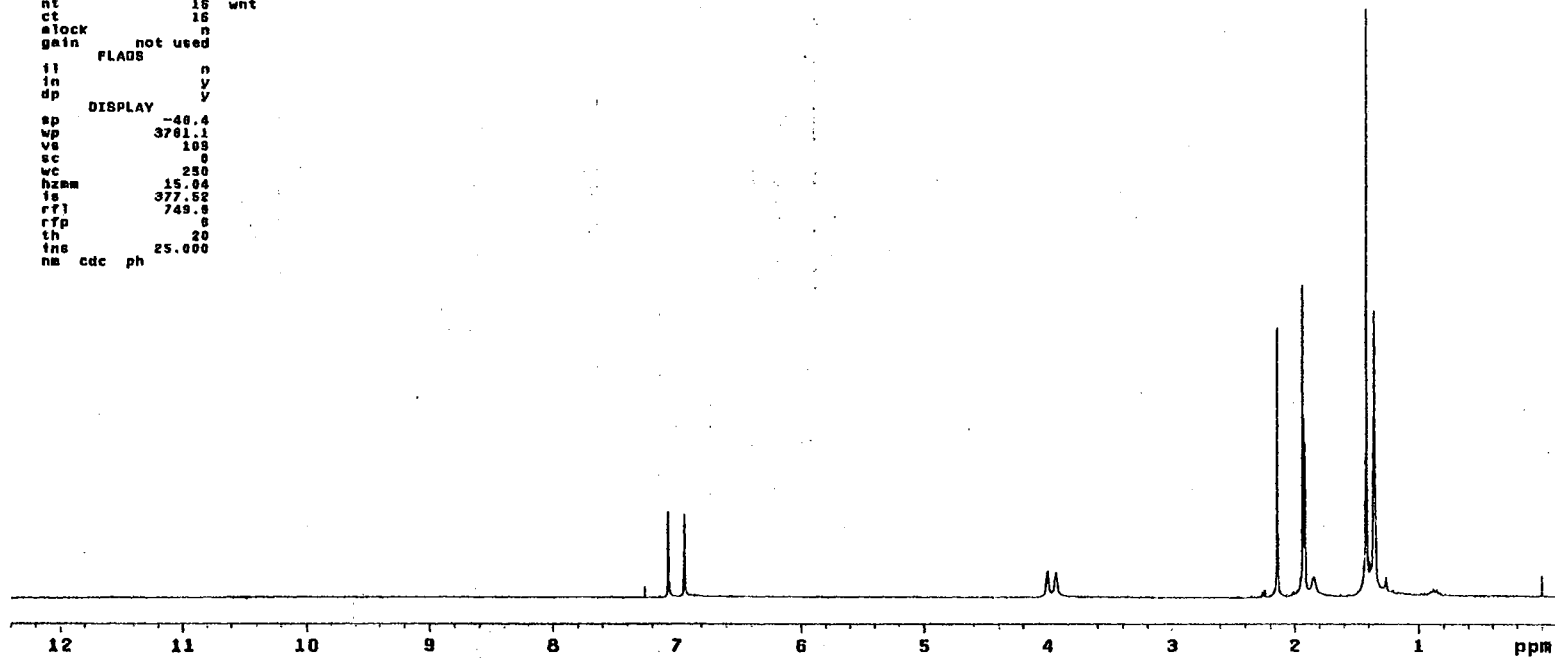
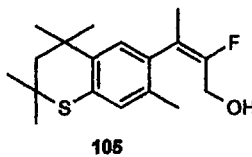
IR Spectrum of 105

Plate CCV

STANDARD 1H OBSERVE

```

expl stdih
SAMPLE
date Feb 7 2000 dfrq DEC. & VT 300.067
solvent CDC13 dn HI
fils exp dpwr 30
ACQUISITION dof 0
sfrq 300.067 dm nnn
tn HI dm c
st 3.747 dat 200
np 33726 PROCESSING
sw 4500.5 wtfile ft
fb 2600 proc not used
bs 18 fn
tpwr 48
pw 3.0 werr
qi 0 wexp
tof 0 wba
nt 18 wnt
ct 18
slock n
gain not used
FLAGS
il n
in y
dp y
DISPLAY
sp -40.4
wp 3701.1
vs 103
sc 0
wc 250
hzam 15.04
ls 377.52
rf1 745.8
rfp 8
th 20
fns 25.000
nm cdc ph
    
```



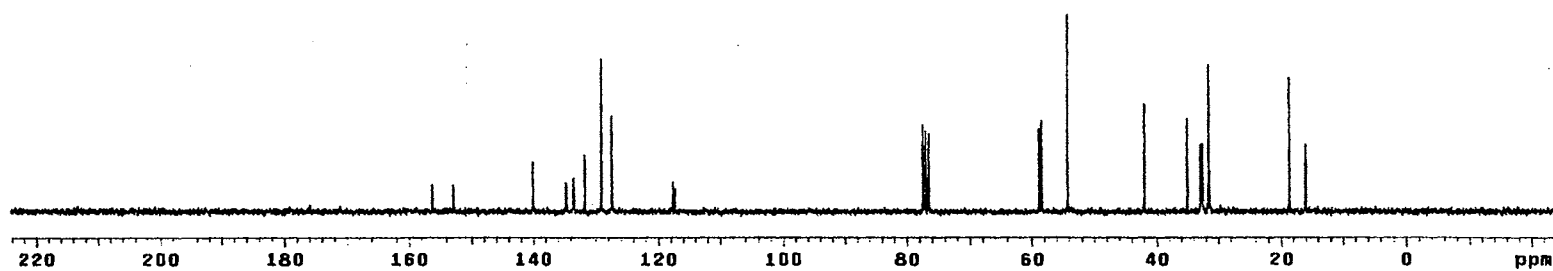
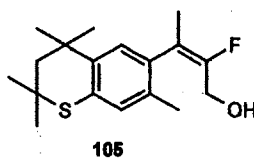
¹H NMR Spectrum of 105

Plate CCVI

13C OBSERVE

expl std13c

date	Feb 7 2000	dfrq	DEC. & VT	300.087
solvent	CDCl3	dn		H1
file	exp	dpwr		34
	ACQUISITION	dot		0
cfrq	75.464	dm		yyy
fn	C13	dsm		w
at	0.800	dmt		11764
np	30018	PROCESsing		
sw	18761.7	lb		1.00
fb	10400	wtfile		
bs	16	proc		Tt
fpwr	52	fn		not used
pw	3.8			
d1	1.000	werr		wft
tor	0	wexp		wft
nt	1024	wbs		wft
ct	272	wnt		
alock		s		
gain	not used			
	FLAGS			
il		n		
in		y		
dp		y		
	DISPLAY			
sp	-1839.9			
wp	18761.7			
vs	38			
sc	0			
wc	250			
hzm	75.05			
is	500.80			
rfl	7649.9			
rff	5810.8			
th	4			
ins	no			
na	ph			



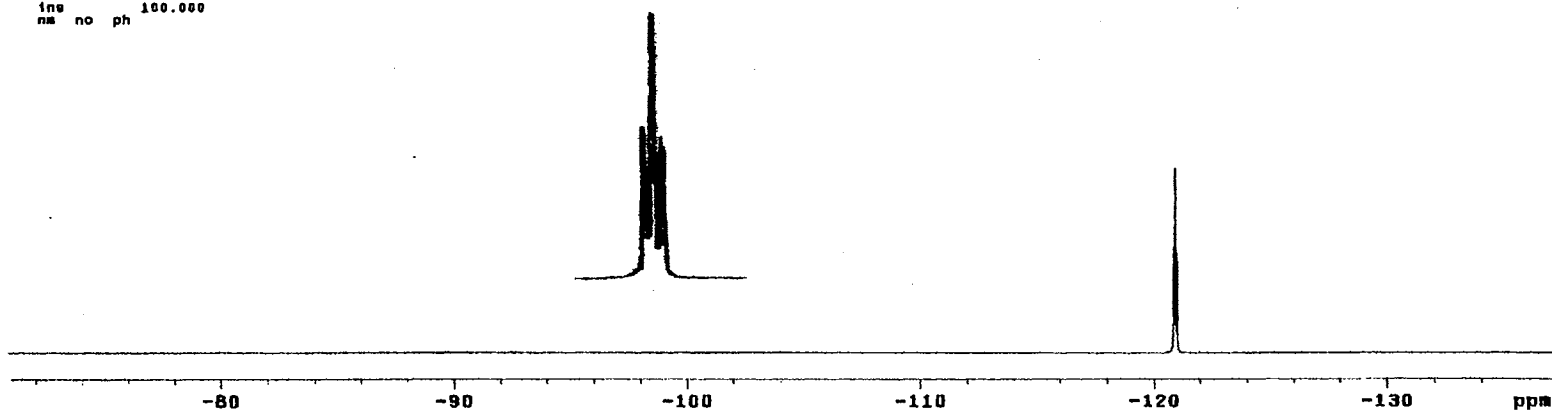
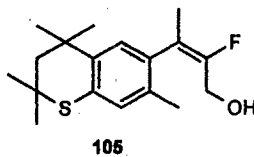
¹³C NMR Spectrum of 105

Plate CCVII

13C OBSERVE

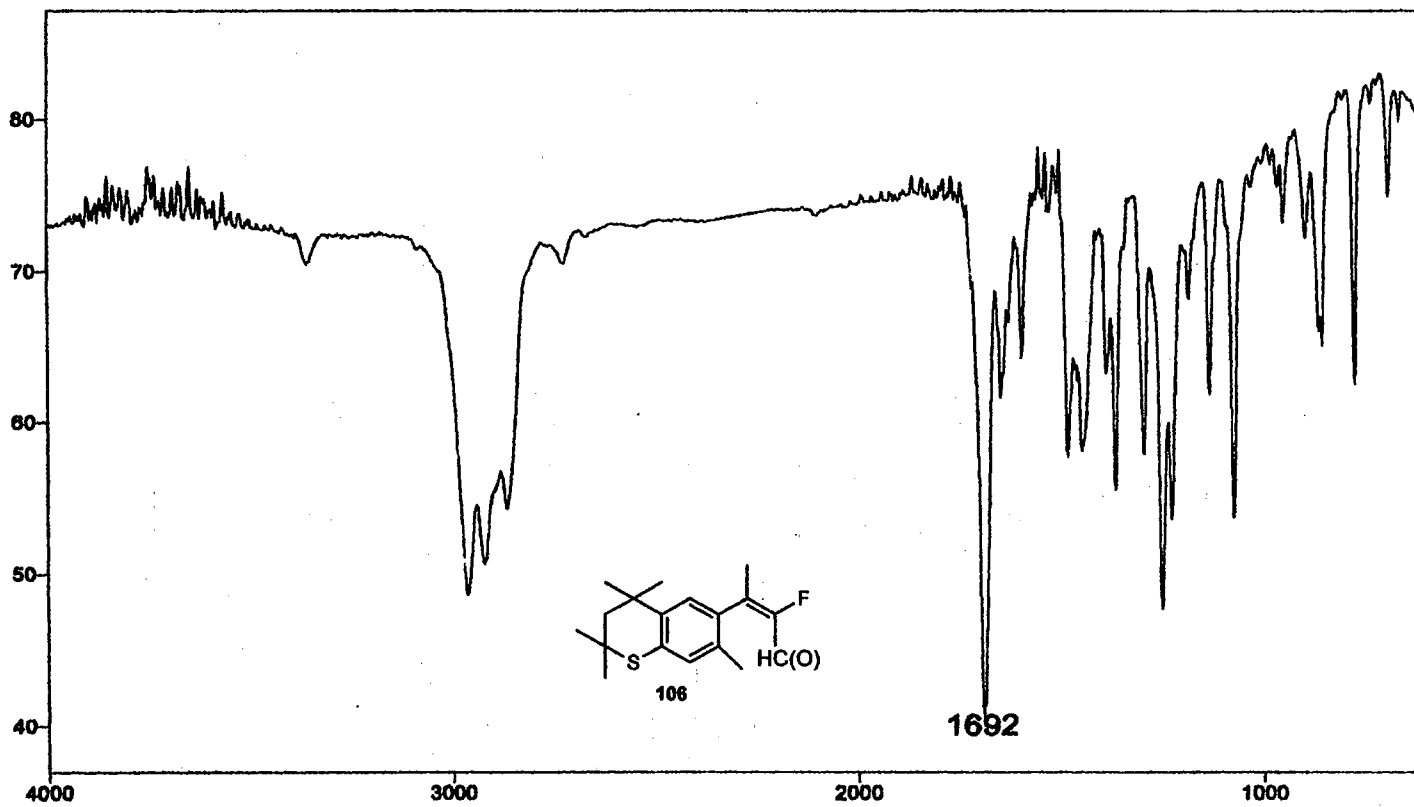
```

exp1 std13c
SAMPLE
date Feb 7 2000 dfrq DEC. & VT 300.087
solvent CDC13 dn H1
file ACQUISITION exp dpwr 34
sfrq 282.333 dm dot 0
tn F19 dma nnn w
at 0.800 dat 11784
np 30016 PROCESSING
sw 18781.7 lb 1.00
fb 10400 wtfile
bs 16 proc Ft
tpwr 52 fn not used
pw 3.8
di 1.000 werr
tof 0 wexp wft
nt 1024 wbs wft
ct 32 wnt
alock not used n
gain FLAGS n
it n
in y
dp y
DISPLAY
sp -38748.2
wp 18781.7
ve 34
sc 0
wc 259
hzms 75.05
is 500.00
rf1 38748.2
rfp a
th 28
ins 100.000
na no ph
    
```



¹⁹F NMR Spectrum of 105

Plate CCVIII



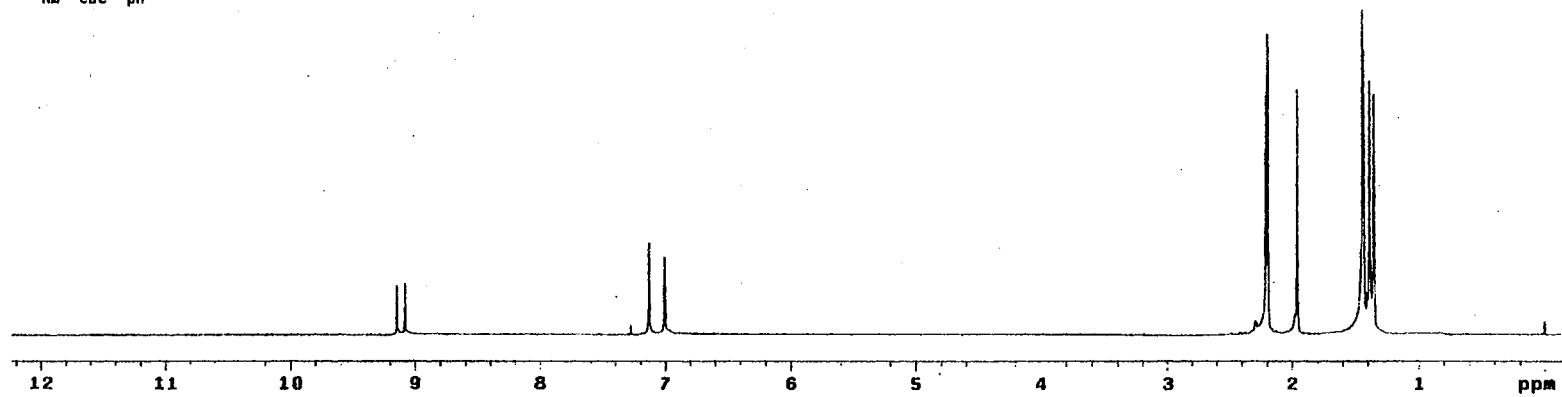
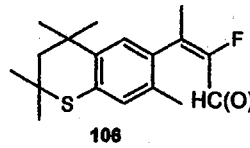
IR Spectrum of 106

Plate CCIX

STANDARD 1H OBSERVE

```

expl std1h
SAMPLE      DEC. & VT
data Feb 8 2000 dfrq 300.087
solvent CDC13 dn H1
file exp dpwr 30
ACQUISITION dof 0
sfrq 300.087 dm nnn
tn H1 dam c
at 3.747 dmf PROCESSING 200
np 33728
sw 4500.5 wtfila
fb 2800 proc ft
bs 16 Tn not used
tpwr 48
pw 3.0 wbrf
d1 0 wexp
tof 0 vbs
nt 16 wnt
ct 16
alock n
gain not used
FLAGB
fl n
in y
dp y
DISPLAY
sp -40.9
wp 3718.9
vt 60
sc 0
vc 250
hzmm 14.86
fs 318.25
rf1 744.6
rfp 0
th 20
ins
nm cdc ph
    
```



¹H NMR Spectrum of 106

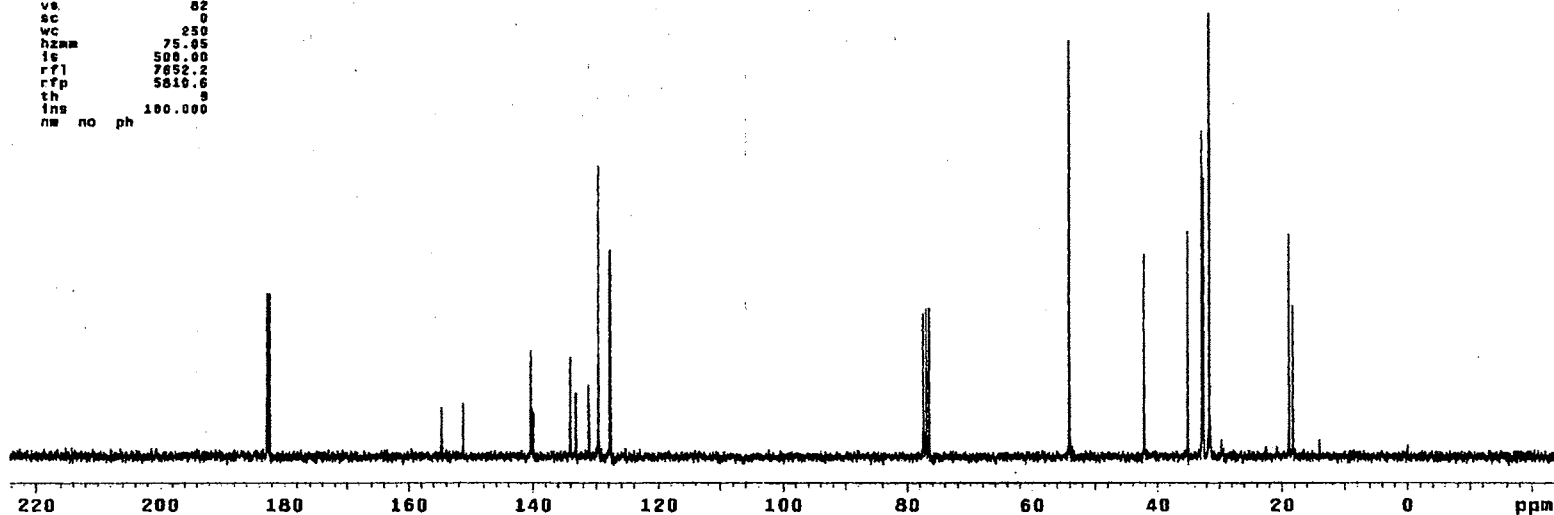
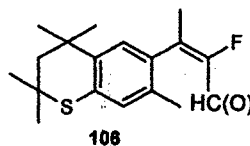
Plate CCX

13C OBSERVE

expl std13c

```

SAMPLE          DEC. & VT
date Feb 8 2000 dfrq      300.087
solvent GDC13   dn        H1
file      exp   dpr      34
ACQUISITION    dot      0
sfrq      75.464 dm      yvy
tn        C13  dms      w
at        0.888 dmf     11784
np        39916  PROCESSING
sv        18781.7 lb      1.00
fb        10400  wtfile
ba        16    proc      ft
tpwr      52    fn      not used
pw        3.8
dl        1.000 werr
tof        0    wexp      wft
nt        1024 wba      wft
ct        480  wnt
elock      s
gain      not used
FLAGS
it        n
in        y
dp        y
DISPLAY
sp      -1841.6
wp      18781.7
vs      82
sc      0
wc      250
hzmm    75.05
ic      500.00
rfl     7852.2
rff     5810.6
th      s
ins     100.000
nm no ph
    
```



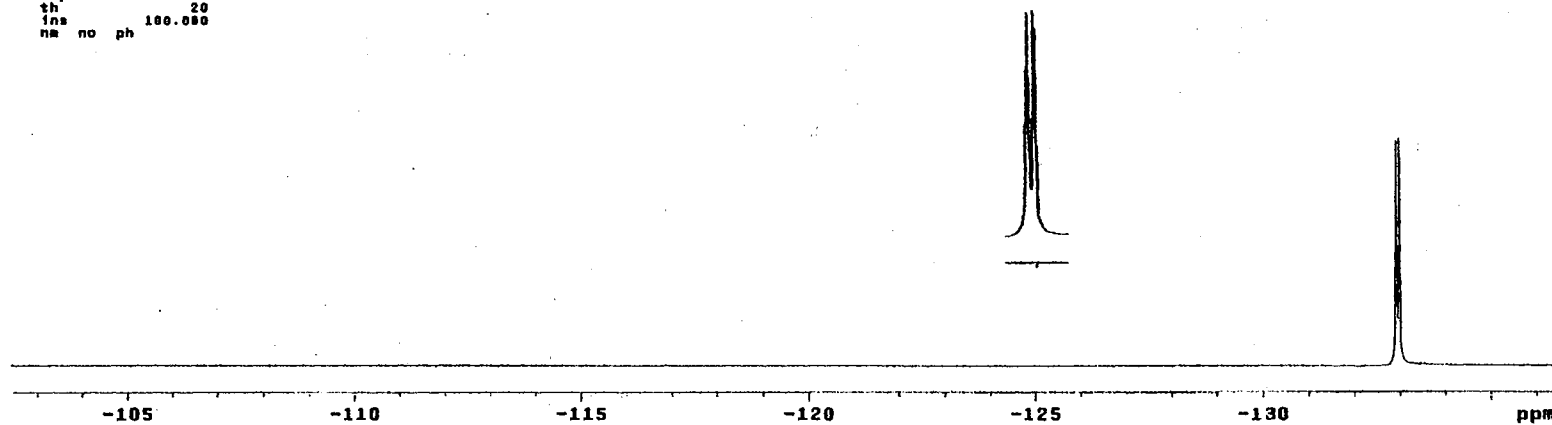
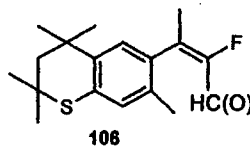
¹³C NMR Spectrum of 106

Plate CCXI

13C OBSERVE

expl std13c

SAMPLE		DEC. & VT	
date	Feb 8 2000	dfrq	300.087
solvent	CDCl3	dn	H1
file	exp	dpwr	34
ACQUISITION		dof	0
afrq	282.333	dm	nnn
tn	719	dsm	w
at	0.800	daf	11764
np	30018	PROCESSING	
sw	10761.7	lb	1.00
fb	10400	wf11e	
be	16	proc	ft
tpwr	52	fn	not used
pw	3.8		
dl	1.000	werr	
tof	0	wexp	wft
nt	1024	wbs	wft
ct	32	wnt	
atock	n		
gain	not used		
FLAGS			
fl	n		
in	y		
dp	y		
DISPLAY			
sp	-30551.2		
wp	0639.1		
vs	42		
sc	0		
wc	250		
hzmm	30.56		
ls	300.00		
rfl	30740.2		
rff	0		
th	20		
ins	100.000		
na	no	ph	



¹⁹F Spectrum of 106

BIBLIOGRAPHY

1. Araki, H.; Shidoji, Y.; Yamada, Y.; Moriwaki, H.; Muto, Y. Retinoid Agonist Activities of Synthetic Geranyl Geranoic Acid Derivatives. *Biochem. Biophys. Res. Comm.* **1995**, *209*, 66-72.
2. Bavic, C. O.; Erricksson, U.; Allen, R. A.; Peterson, P. A. Identification and Partial Characterization of Retinal Pigment Epithelial Membrane Receptors for Plasma Retinol Binding Protein. *J. Biol. Chem.* **1991**, *266*, 14978-14985.
3. Becker, A. M.; DeLamarter, J. F.; Staple, J. K.; Hooft, H.; Carlberg, C. RZR, a New Family of Retinoid-Related Orphan Receptor that Function as Both Monomers and Homodimers. *Mol. Endocrin.* **1994**, *8*, 757-770.
4. Becker-Andre, M.; Wienenberg, I.; Schaeren-Wiemers, N.; Andre, E.; Missbach, M.; Saurat, J. H.; Carlberg, C. Nuclear Receptors Activity in the Brain Tissue. *J. Biol. Chem.* **1994**, *269*, 28531-28534.
5. Benbrook, D.; Lernhardt, E.; Pfahl, M. A New Retinoic Acid Receptor Identified from a Hepatocellular Carcinoma. *Nature* **1988**, *333*, 669-672.
6. Benbrook, D. M.; Madler, M. M.; Spruce, L. W.; Birckbichler, P. J.; Nelson, E. C.; Subramanian, S.; Weerasekare, G. M.; Gale, J. B.; Patterson, M. K.; Wang, W.; Lu, S.; Rowland, T. C.; DiSivestro, P.; Lindamood, C.; Berlin, K. D. Biologically Active Heteroarotinoids Exhibit Anticancer Activity and Decreased Toxicity. *J. Med. Chem.* **1997**, *40*, 3567-3583.
7. Bennani, Y. L. Synthesis of 1-[¹³CD₃]-9-*cis*-Retinoic Acid. *Journal of Labelled Compounds and Radiopharmaceuticals*, **1995**, *8*, 755-763.
8. Berlin, K. D.; Benbrook, D. M.; Nelson, E. C.; Birckbichler, P. J.; Madler, M. M.; Liu, S.; Arindam, D.; Zacheis, D.; Ivey, R. T.; Lu, S.; Brown, C. W.; Klucik, J. Synthesis, Structure-Activity Relationship, and RAR γ -Ligand Interactions of Nitrogen Heteroarotinoids. *J. Med. Chem.* **1999**, *42*, 3602-3614.
9. Berlin, K. D.; Benbrook, D. M.; Clement, F.; Madler, M. M.; Liu, S.; Arindam, D.; Zacheis, D.; Gold, M. A.; Lu, S.; Brown, C. W.; Klucik, J.; Subramanian, S.; Weerasekare, M. G.; Fountain, K. R.; Houck, J. R. Jr. Heteroarotinoids Inhibit Head and Neck Cancer Lines In Vitro and In Vivo Through Both RAR and RXR Retinoic Acid Receptors. *J. Med. Chem.* **1999**, *42*, 4434-4445.
10. Bernard, B.; Bernardon, J. M.; Delescluse, C.; Martin, B.; Maignan, J.; Charpentier,

- B.; Pilgrim, U.; Shroot, B. Identification of Synthetic Retinoids with Selectivity for RAR. *Biochem. Biophys. Res. Comm.* **1992**, *186*, 977-983.
11. Blomhoff, R.; Green, M. H.; Green, J. B.; Berg, T.; Norum, K. R. Vitamin A Metabolism: New Perspective on Absorption, Transport, and Storage. *Physiol. Rev.* **1991**, *71*, 951-990.
 12. Boehm, M. F.; Zhang, L.; Badea, B. A.; Berger, E.; Suto, C. M.; Heyman, R. A. Synthesis and Structure-Activity Relationship of Novel Retinoid X Receptors. *J. Med. Chem.* **1994**, *37*, 2930-2941.
 13. Boerman, M. H. E.; Napoli, J. L. Cholate-Independent Retinyl Ester Hydrolysis: Stimulation by Apo-Retinol Binding Protein. *J. Biol. Chem.* **1991**, *266*, 22273-22278.
 14. Bourget, J. P.; Ruff, M.; Rochel, N.; Chambon, P.; Gronemeyer, H.; Moras, D. Crystal Structure of RAR- γ Ligand Binding Domain Bound to All-*Trans*-Retinoic Acid. *Nature* **1995**, *378*, 681-689.
 15. Bourguet, W.; Ruff, M.; Chambon, P.; Gronemeyer, H.; Moras, D. Crystal Structure of the Human Nuclear Receptor RXR- α . *Nature* **1995**, *375*, 377-385.
 16. Boylan, J. F.; Gudas, L. J. The Level of CRABP-I Expression Influences the Amounts and Types of All-*Trans*-Retinoic Acid in F9 Teratocarcinoma Stem Cells. *J. Biol. Chem.* **1992**, *267*, 21486-21491.
 17. Budowski, P.; Gross, J. Conversion of Carotenoids to 3-Dihydroretinol (Vitamin A₂) in the Mouse. *Nature* **1965**, *206*, 1254-1255.
 18. Buck, J.; Myc, A.; Garbe, A.; Cathomas, G. Differences in the Action and Metabolism Between Retinol and Retinoic Acid in B-Lymphocytes. *J. Biol. Chem.* **1991**, *115*, 851-859.
 19. Campaigne, E.; Archer, R. W. *p*-Dimethylaminobenzaldehyde. In *Organic Syntheses Coll. Vol. 3* **1961**, pp. 331-333.
 20. Chambon, P. The Retinoid Signaling Pathway: Molecular and Genetic Analysis *Semin. Cell. Biol.* **1994**, *5*, 115-125.
 21. Chambon, P.; Krust, A.; Petkovich, M.; Kastner, P.; Zelent, A. Cloning of Murine α and β Retinoic Acid Receptors and a Novel Receptor γ Predominantly Expressed in Skin. *Nature* **1989**, *339*, 714-717.
 22. Chandraratna, R. A. S. Rational Design of Receptor-Selective Retinoids. *J. Am.*

- Acad. Dermatol.* **1998**, *39*, 124-128.
23. Chandraratna, R. A. S. Tazarotene: First of a New Generation of Receptor-Selective Retinoids. *Br. J. Dermatol.* **1996**, *135*, 18-25.
 24. Chen, J. D.; Evans, R. M. A Transcriptional Co-Repressor that Interacts with Nuclear Hormone Receptors. *Nature* **1995**, *377*, 454-457.
 25. Cheng, X.; Reginato, M. J.; Andrews, N. C.; Lazar, M. A. The Transcriptional Integrator CREB-Binding Protein Mediates Positive Cross Talk Between Nuclear Hormone Receptors and the Hematopoietic bZip Protein p45/NF-E2. *Mol. Cell. Biol.* **1997**, *17*, 1407-1416.
 26. Cooper, R. J.; von Baur, E.; Zachel, C.; Heery, D.; Heine, M. J.; Garnier, J. M.; Vivat, V.; Le Douarin, B.; Gronemeyer, H.; Chambon, P.; Losson, R. Differential Ligand-Dependent Interaction Between the AF-2 Activating Domain of Nuclear Receptor and the Putative Transcriptional Intermediary Factors mSUG 1 and TIF 1. *EMBO J.* **1996**, *16*, 3241-3247.
 27. Cuvailles, V.; Dauvois, S.; L'Horset, F.; Lopez, G.; Hoare, S.; Kusner, P. J.; Parker, M. G. Nuclear Factor RIP 140 Modulates Transcription Activation. *EMBO J.* **1995**, *14*, 3741-3751.
 28. Dawson, M. I.; Okamura, W. H. In *Chemistry and Biology of Synthetic Retinoids* CRC Press: Boca Raton, FL, 1990, pp. 579-586
 29. DeKoning, A. J.; van der Merve, G. The Synthesis of a Number of Analogues of Ethoxyquinone and Their Evolution as Antioxidants in Fish Oil. *Fett. Lipid* **1996**, *98*, 14-17.
 30. Discover 97 is copyright of Molecular Simulations Inc. (MSI), 9685 Scranton Road, San Diego, Ca, 92121-2777.
 31. Eppinger, T. M.; Buck, J.; Hammerling, U. Growth Control or Terminal Differentiation: Endogenous Production and Differential Activities of Vitamin A Metabolites. *J. Exp. Med.* **1993**, *178*, 1995-2005.
 32. Evans, R. M.; Hollenberg, S. M. Zinc Fingers: Guilt by Association. *Cell* **1988**, *52*, 1-3.
 33. Evans, R. M. The Steroid and Thyroid Hormone Receptor Superfamily. *Science* **1988**, *240*, 889-895.

34. Fanjul, A. N.; Delia, D.; Pierott, M. A.; Rideout, D.; Qui, D.; Pfall, M. 4-Hydroxyphenyl Retinamide is a Highly Selective Activator of Retinoic Receptors. *J. Biol. Chem.* **1996**, *271*, 22441-22446.
35. Fawell, S. E.; Lees, J. A.; White, R.; Parker, M. G. Characterization and Co-localization of Steroid Binding and Dimerization Activities. *Cell* **1990**, *60*, 953-962.
36. Fiorella, P. D.; Napoli, J. L. Microsomal Retinoic acid Metabolism: Effects of Cellular Retinoic Acid Binding Protein (Type I) and C18-Hydroxylation as an Initial Step. *J. Biol. Chem.* **1994**, *269*, 10538-10544.
37. Fisher, G. J.; Voorhees, J. J. Molecular Mechanism of Retinoid in Skin. *FASEB J.* **1996**, *10*, 1002-1013.
38. Flannery, B. P.; Teukolsky, W. T.; Vetterling, W. T. In: *Numerical Recipes in C: The Art of Computing*. Cambridge University Press: Boston, MA, 1988, pp.301-312.
39. (a) Foglio, M. H.; Duester, G. Molecular Docking Studies on Interaction of Diverse Retinol Structures with Human Alcohol Dehydrogenase Predict a Broad Role in Retinoid Ligand System. *Biochem. Biophys. Acta* **1999**, *13*, 239-250. (b) van Aalten, D. M.; de Groot, B. L.; Berendsen, H. J.; Findlay, J. B. Conformational Analysis of Retinoids and Restriction of Their Dynamics by Retinoid Binding Protein. *Biochem. J.* **1996**, *15*, 543-550.
40. Forman, B. M.; Umesono, K.; Chen, J.; Evans, R. M. Unique Response Pathway Established by Allosteric Interaction Among Nuclear Hormone Receptors. *Cell* **1995**, *81*, 541-550.
41. Forman, B.M.; Yange, C. R.; Casanova, J.; Ghysdael, J.; Samuels, H. H. A Domain Containing Leucine-Zipper Like Motifs Mediate Novel *in vivo* Interactions Between Thyroid Hormone and Retinoic Acid Receptors. *Mol. Endocrinol.* **1989**, *3*, 1610-1626.
42. Fraydon, R.; Perlman, T.; Evans, R. M. Structural Determination of Nuclear Receptor Assembly on DNA Direct Repeats. *Nature* **1995**, *374*, 203-211.
43. Freedman, L. P.; Luisi, B. F.; Korzsun, R.; Basavappa, R.; Sigler, P. B.; Yamamoto, K. R. The Function and Structure of Metal Coordination Sites Within The Glucocorticoid Receptor DNA Binding Domain. *Nature* **1988**, *334*, 543-546.
44. French, F. A.; Blanz, J. E. The Carcinostatic Activity of α -(N)-Heterocyclic Carboxyaldehyde Thiosemicarbazones. *Cancer Res.* **1965**, *25*, 1454-1459.

45. Fujimaki, Y. Formation of Carcinoma in Albino Rats Fed on Deficient Diets. *J. Cancer* **1926**, *10*, 469-477.
46. Gaub, M. P.; Lutz, Y.; Ruberte, E.; Petkovich, M.; Brand, M.; Chambon, P. Antibodies Specific to The Retinoic Acid Human Nuclear Receptors α and β . *Proc. Natl. Acad. Sci. U.S.A.* **1989**, *86*, 3089-3093.
47. Gehin, M.; Vivat, V.; Wurtz, J. M.; Losson, R.; Chambon, P.; Moras, D.; Gronemeyer, H. Structural Basis for Engineering of Retinoic Acid Receptor Isotype-Selective Agonist and Antagonist. *Chem. Biol.* **1999**, *6*, 519-529.
48. Giguere, V.; Ong, S.; Segui, P.; Evans, R. Identification of a Receptor for Morphogen Retinoic Acid. *Nature*, **1987**, *330*, 624-629.
49. Glass, C. K. Differential Recognition of Target Genes by Nuclear Receptors Monomers, Dimers, and Heterodimers. *Endocrinal Rev.* **1994**, *15*, 391-407.
50. Green, S.; Kumar, V.; Theulas, I.; Wahli, W.; Chambon, P. The N-Terminal DNA-Binding 'Zinc Finger' of the Estrogen and Glucocorticoid Receptors Determines Target Gene Specificity. *EMBO J.* **1988**, *7*, 3037-3044.
51. Greiner, E. F.; Kirfel, J.; Greschik, H.; Dorflinger, U.; Becker, P.; Mercep, A.; Schule, R. Functional Analysis of Retinoid Z Receptor, a Brain-Specific Nuclear Orphan Receptor. *Proc. Natl. Acad. Sci. U. S. A.* **1996**, *93*, 10105-10110.
52. Halachmi, S.; Merden, E.; Martin, G.; MacKay, H.; Abbondanza, C.; Brown, M. Oestrogen Receptor-Associated Proteins: Possible Mediation of Hormone-Induced Transcription. *Science* **1994**, *264*, 1455-1458.
53. Hamamda, K.; Gleason, S. L.; Levi, B. Z.; Hirschfeld, S.; Appella, E.; Ozato, K. H- 2RIIBP a Member of the Nuclear Hormone Receptor Superfamily that Binds to Both Regulatory Elements of Major Histocompatibility Class I Genes and the Estrogen Response Element. *Proc. Natl. Acad. Sci. U.S.A.* **1989**, *86*, 8289-8293.
54. Hard, T.; Kellembach, E.; Boelens, R.; Maler, B. A.; Dahlman, K.; Freedman, L. P.; Carlstedt-Duke, J.; Yamamoto, K. R.; Gustafonn, J. A.; Kaptein, R. Solution Structure of the Glucocorticoid Receptor DNA-Binding Domain. *Science* **1990**, *249*, 157-160.
55. Hashimoto, Y.; Kegachika, H.; Shudo, K. Expression of Retinoic Acid Receptor Genes and the Ligand-Binding Selectivity of Retinoic Acid Receptors (RAR's). *Biochem. Biophys. Res. Comm.* **1990**, *166*, 1300-1307.
56. Herr, F. M.; Ong, D. E. Differential Interaction of Lecithin-Retinol Acyltransferase

- with Cellular Retinol Binding Protein. *Biochemistry* **1992**, *31*, 6748-6755.
57. Heyman, R. A.; Mangelsdorf, D. J.; Dyck, J. A.; Stein, R. B.; Eichele, G.; Evans, R. M.; Thaller, C. 9-*cis*-Retinoic Acid is a High Affinity Ligand for The Retinoid X Receptor. *Cell* **1992**, *68*, 397-406.
 58. Hibi, S.; Kikuchi, K.; Yoshimura, H.; Nagai, M.; Tai, K.; Hilda, T. Synthesis and Structure Relationship of Novel Retinoid X Receptor Agonist. *J. Med. Chem.* **1998**, *39*, 3245-3252.
 59. Horlein, A. J.; Naar, A. M.; Heinzl, T.; Gloss, B.; Kurokawa, R.; Ryan, A.; Glass, C. K. Ligand-Independent Repression by the Thyroid Hormone Receptor Mediated by Nuclear Receptor Co-repressor. *Nature* **1995**, *377*, 397-403.
 60. Itri, L. M.; Moon, R. C. Retinoids and Cancer. *The Retinoids: Biology, Chemistry and Medicine*, 2nd Edition, Raven Press Ltd.: New York, 1984, pp. 357-386.
 61. Janssen, J. J.; Kuhlmann, E. D.; van Vugt, A. H.; Winkens, H. J.; Janssen, B. P.; Deutman, A. F.; Driessen, C. A. Retinoic Acid Receptors and Retinoid X Receptors in the Mature Retina: Subtype Determination and Cellular Distribution. *Curr. Eye Res.* **1999**, *19*, 338-347.
 62. Jones, P.; Vileneuve, G. B.; Fei, C.; DeMarte, J.; Haggerty, A.; Nwe, K. T.; Martin, D. A.; Lebuis, A. M.; Finkelstein, J. M.; Gour-Salin, B.; Chan, T. H.; Leyland-Jones, B. R. Synthesis and Structure-Activity Relationship of 2-Pyrazinylcarboxamido-Benzoates and Ionylideneacetamidobenzoates with Retinoidal Activity. *J. Med. Chem.* **1998**, *41*, 3062-3077.
 63. Joore, J.; Gerard, B. L. J.; Lans, P.; Lanser, J.; Vervaart, J. M. A.; Zitkovic, D.; Kruijer, W. Effect of Retinoic Acid on the Expression of Retinoic Acid Receptors During Zebrafish Embryogenesis. *Mechanism of Development* **1994**, *46*, 137-150.
 64. Judson, R. Genetic Algorithms and Their Use in Chemistry. *Reviews in Computational Chemistry*, Vol.10, Libkowitz, K. B.; Boyd, D. B. eds., VCH Publishers: New York, 1997, pp. 67-99.
 65. Kakkad, B.; Ong, D. E. Reduction of Retinaldehyde Bound to Cellular Retinol-Binding Protein (type II) by Microsomes from Rat Small Intestine. *J. Biol. Chem.* **1988**, *263*, 12916-12919.
 66. Kato, S.; Mano, H.; Kumazawa, T.; Yoshizawa, Y.; Kojima, R.; Masushige, S. Effect of Retinoid Status on Alpha, Beta and Gamma Retinoic Acid Receptors mRNA in Various Rat Tissues. *Biochem. J.* **1992**, *286*, 755-760.

- 67 Kersten, S.; Pan, L.; Noy, N. The Role of Ligand in Retinoid Signaling: Positive Cooperativity in the Interaction of 9-*cis* Retinoic Acid with Tetramers of the Retinoid X Receptor. *Biochemistry* **1995**, *34*, 14263-14269.
68. Klaholtz, B. P.; Renaud, J. P.; Mitschler, A.; Zusi, C.; Grenemeyer, H.; Chambon, P.; Moras, D. Conformational Adaptations of Agonists in the Nuclear Receptor RAR Gamma. *Nat. Struct. Biol.* **1998**, *5*, 199-202.
69. Klein, E. S.; Pino, M. E.; Johnson, A. T.; Davies, J. A.; Nagpal, S.; Thacher, S. M.; Krasinsky, G.; Chandraratna, A. S. Identification and Functional Separation of Retinoic Acid Receptor Neutral Antagonist and Inverse Agonist. *J. Biol. Chem.* **1996**, *271*, 22692-22696.
70. Koch, S. S.C.; Dardashti, L. J.; Cesario, R. M.; Croston, G. E.; Boehm, M. F.; Heyman, R. A. Nadzan, A. M. Synthesis of Retinoid X Receptor Specific Ligands That are Potent Inducers of Adipogenesis in 3T3-L1 Cells. *J. Med. Chem.* **1999**, *42*, 742-750.
71. Kollman, P. A.; Weiner, S. J.; Case, D. A.; Singh, U. C.; Ghio, C.; Alagona, G.; Profeta, S.; Weiner, P. Force Field for Molecular Mechanical Simulations of Nucleic Acids and Proteins. *J. Am. Chem. Soc.* **1984**, *106*, 765-784.
72. Krust, A.; Kastner, P.; Petkovich, M.; Zelent, A.; Chambon, P.; Leroy, P.; Garnier, J. Murine Isoforms of Retinoic Acid Receptor γ with Specific Pattern of Expression. *Proc. Natl. Acad. Sci. U. S. A.* **1990**, *87*, 2700-2704.
73. Kurokawa, R.; Soderstrom, M.; Horlein, A.; Halachni, S.; Brown, M.; Rosenfeld, M. G.; Glass, C. K. Polarity-Specific Activities of Retinoic Acid Receptors Determined by a Co-repressor. *Nature* **1995**, *377*, 397-403.
74. Lamour, F. P.; Apfel, C. M.; Lardelli, P. Analysis of the Ligand-Binding Domain of Human Retinoic Acid Receptor Alpha by Site-Directed Mutagenesis. *Mol. Cell. Biol.* **1996**, *16*, 5386-5392.
75. Le Douarin, B.; Zechel, C.; Garnier, J. M.; Lutz, Y.; Tora, L.; Pierrat, P.; Heery, D.; Gronemeyer, H.; Chambon, P.; Losson, R. The N-Terminal Part of TIF1, a Putative Mediator of the Ligand-Dependent Activation Function (AF-2) of Nuclear Receptor is Fused to B-raf in the Oncogenic Protein T18. *EMBO J.* **1995**, *14*, 2020-2033.
76. (a) Leblanc, Y.; Zamboni, R.; Bernstein, M. A. Amination of Olefinic Compounds with Bis(2,2,2-trichloroethyl)azodicarboxylate. *J. Org. Chem.* **1991**, *56*, 1971-1972.
77. Leblanc, Y.; Zaltsgendler, I.; Bernstein, M. A. Synthesis of Aromatic Amines From

- Electron-Rich Arenes and Bis(2,2,2-trichloroethyl)azodicarboxylates. *Tetrahedron Lett.* **1993**, *34*, 2441-2444.
78. Lee, J. W.; Ryan, F.; Swafield, J. C.; Johnston, S. A.; Moore, D. A. Interaction of Thyroid Hormone Receptor with a Conserved Transcriptional Mediator. *Nature* **1995**, *374*, 91-94.
79. Leid, M.; Kastner, P.; Chambon, P. Multiplicity Generates Diversity in The Retinoic Acid Pathways. *Trends Biochem. Sci.* **1992**, *17*, 427-433.
80. Lemotte, P. K.; Keidel, S.; Apfel, C. M. Phytanic Acid is Retinoid X Receptor Ligand. *Eur. J. Biochem.* **1996**, *236*, 328-333.
81. Leroy, P.; Krust, A.; Zelent, A.; Mendelsohn, C.; Garnier, J. M.; Kastner, P.; Dierich, A.; Chambon, P. Multiple Isoforms of Mouse Retinoic Acid Receptor α Are Generated by Alternative Splicing and Differential Induction by Retinoic Acid. *EMBO J.* **1991**, *10*, 59-69.
82. Levin, M. S. Cellular Retinol-Binding Proteins are Determinants of Retinol Uptake and Metabolism in Stably Transfected Caco-2 Cells. *J. Biol. Chem.* **1993**, *268*, 8267-8276.
83. Levin, A. A.; Sturzenbecker, L. J.; Kazmer, S.; Bosakowski, T.; Huselton, C.; Allenby, G.; Speck, J.; Kratzeisen, C.; Rosenberger, M.; Lovey, A.; Grippo, J. F. 9-*cis*-Retinoic Acid Stereoisomers Bind and Activate the Nuclear Receptor RXR. *Nature* **1992**, *355*, 359-361.
84. Li, Y.; Hashimoto, Y.; Agadir, A.; Kagechika, H.; Zhang, X. Identification of Novel Class of Retinoic Acid Receptor β -Selective Retinoid Antagonist and Their Inhibitory Effects on AP-1 Activity and Retinoic Acid-Induced Apoptosis in Human Breast Cancer Cells. *J. Biol. Chem.* **1999**, *274*, 15360-15366.
85. Lotan, R.; Ong, D. E.; Chytil, F. Cellular Retinoid Binding Proteins. *Arch. Dermatol.* **1987**, *123*, 1693-1695.
86. MacDonald, P. N.; Ong D. E. Evidence for the Lecithin:Retinol Acyltransferase Activity in the Rat small Intestine. *J. Biol. Chem.* **1988**, *263*, 12478-12482.
87. Madler, M. M. In *Flexible Heteroarotinoids As Potential Anticancer Agents*. 1997, Ph D. Thesis, Oklahoma State University, pp.98-99.
88. Mangelsdorf, D. J.; Ong, E. S.; Dyck, J. A.; Evans, R. M. Nuclear Receptor that Identifies a Novel Retinoic Acid Response Pathway. *Nature* **1990**, *345*, 224-229.

89. Mangelsdorf, D. J.; Umesono, K.; Kliever, S. A.; Borgmeyer, U.; Ong, E. S.; Evans, R. M. A Direct Repeat in the Cellular Retinol Binding Protein Type II Gene Confers Differential Regulation by RXR and RAR. *Cell* **1991**, *66*, 555-561.
90. Mangelsdorf, D. J.; Borgmeyer, U.; Heyman, R. A.; Zhou, J. Y.; Ong, E. S.; Oro, A. E.; Kikazuka, A.; Evans, R. M. Characterization of Three RXR Genes that Mediate the Action of 9-*cis*-Retinoic Acid. *Genes Dev.* **1992**, *6*, 329-344.
91. Mangelsdorf, D. D.; Evans R. M. The RXR Heterodimers and Orphan Receptors. *Cell* **1995**, *83*, 841-850.
92. Marchio, A.; Tiollais, P.; Dejean, A.; de The, H. A Novel Steroid Thyroid Hormone Receptor-Related Gene Inappropriately Expressed in Human Hepatocellular Carcinoma. *Nature* **1987**, *330*, 667-670.
93. Marchio, A.; deThe, H.; Thiollais, P.; Dejean, P. Differential Expression and Ligand Regulation of Retinoic Acid Receptors α and β Genes. *EMBO J.* **1989**, *8*, 429-433.
94. Meyer, M. E.; Gronemeyer, H.; Turcotte, B.; Bocquel, M. T.; Tasset, D.; Chambon, P. Steroid Hormone Receptors Compete for Factors that Mediate Their Enhancer Function. *Cell* **1989**, *57*, 433-442.
95. Minucci, S.; Ozato, K. Retinoid Receptors in Transcriptional Regulation. *Curr. Opinions Genet. Dev.* **1996**, *6*, 567-574.
96. Missbach, M.; Jagher, B.; Sigg, I.; Nayeri, S.; Carlgerg, C.; Wiesenbergl, I. Thiazolidine Diones, Specific Ligand of the Nuclear Z Receptor/Retinoic Acid Related Orphan Receptor α with Potent Antiarthritic Activity. *J. Biol. Chem.* **1996**, *271*, 13515-13522.
97. Mitchell, P. J.; Tijian, R. Transcriptional Regulation in Mammalian Cells by Sequence- Specific DNA Binding Protein. *Science* **1989**, *245*, 371-378.
98. Morriss-Kay, G. M.; Sokolova, N. Embryonic Development and Pattern Formation. *FASEB J.* **1996**, *10*, 961-968.
99. Muccio, D. D.; Broullete, W. J.; Alam, M.; Vaezi, M. F.; Sani, B. P.; Venepally, P.; Reddy, L.; Norris, A.; Hill, D. L. Conformationally Defined 6-*s-trans*-Retinoic Acid Analogs. Structure-Activity Relationship for Nuclear Receptor Binding, Transcriptional Activity, and Cancer Chemopreventive Activity. *J. Med. Chem.* **1996**, *39*, 3625-3635.
100. (a) Murko, M. A.; Murko, A. Computational Methods to Predict Binding Free

- Energy in Ligand-Receptor Complex. *J. Med. Chem.* **1995**, *38*, 4953-4966. (b) Patterson, D. E.; Cramer, R. D.; Ferguson, A. M.; Clark, R.; Weinberger, L. E. Neighborhood Behavior: A Useful Concept for Validation of "Molecular Diversity" Description. *J. Med. Chem.* **1996**, *39*, 3049-3059. (c) Cramer, R. D.; Clark, R. D.; Patterson, D. E.; Ferguson, A. M. Bioisosterism as a Molecular Diversity Descriptor: Steric Fields of Single "Topomeric" Conformers. *J. Med. Chem.* **1996**, *39*, 3060-3069. (d) Totrow, M.; Abagyan, R. Flexible Protein-Ligand Docking by Global Energy Optimization in Internal Coordinates. *Proteins* **1997**, *1*, 215-220.
101. Napoli, J. L. Biochemical Pathways of Retinoid Transport, Metabolism, and Signal Transduction. *Clinical Immunology and Immunopathology* **1996**, *80*, S52-S62.
 102. Nesher, G.; Zucker, J. Rheumatologic Complications of Vitamin A and Retinoids. *Semin. Arthritis Rheu.* **1995**, *24*, 291-296.
 103. Norris, A. W.; Cheng, L.; Giguere, V.; Rosenberg, M.; Li, E. Measurements of Subnanomolar Retinoic Acid Binding Affinities for Cellular Retinoic Acid Binding Proteins by Fluorometric Titration. *Biochem. Biophys. Acta* **1994**, *29*, 10-18.
 104. Ostrovsky, J.; Hammer, L.; Pokornowski, K.; Roalsvig, T.; Reczek, P. R. The Terminal Portion of Domain E of Retinoic Acid Receptors Alpha and Beta is Essential for the Recognition of Retinoic Acid and Various Analogs. *Proc. Natl. Acad. Sci. U. S. A.* **1995**, *92*, 1812-1816.
 105. Pawson, B. A.; Chan, K. K.; DeNoble, J.; Piermatte, V.; Specian, A. C.; Bohoslavac, O.; Machlin, L. J.; Gabriel, E. Fluorinated Retinoic Acids and Their Analogues. *J. Med. Chem.* **1979**, *22*, 1059-1067.
 106. Petkovich, M.; Brand, N. J.; Krust, A.; Chambon, P. A Human Retinoic Acid Receptor which Belongs to the Family of Nuclear Receptors. *Nature*, **1987**, *330*, 444-450.
 107. Pignatello, M. A.; Kauffman, F. C.; Levin, A. A. Multiple Factors Contributing to the Toxicity of the Aromatic Retinoid TTNPB: Interaction with Retinoic Acid Receptors. *Toxicol. Appl. Pharmacol.* **1999**, *159*, 109-116.
 108. Posch, K. C.; Boerman, M. H. E.; Burn, R. D.; Napoli, J. L. Holo-Cellular Retinol Binding Protein as a Substrate for Microsomal Retinal Synthesis. *Biochemistry* **1991**, *30*, 6224-6230.
 109. Posch, K. C.; Burns, R. D.; Napoli, J. L. Biosynthesis of All-*Trans*-Retinoic Acid from Retinal: Recognition of Retinal Bound to the Cellular Retinol Binding Protein (Type I) as a Substrate by Purified Cytosolic Dehydrogenase. *J. Biol. Chem.* **1992**,

- Protein (Type I) as a Substrate by Purified Cytosolic Dehydrogenase. *J. Biol. Chem.* **1992**, *267*, 19676-19682.
110. Powell, M. D. J. Restart Procedures for the Conjugate Gradient Method. *Mathematical Programming*, **1977**, *12*, 241-254.
 111. Ramachandran, G. N.; Sasisekharan, V. Prediction of Protein Structure and the Principles of Protein Conformations. *Adv. Protein Chem.* **1968**, *23*, 332-345.
 112. Rastenejad, F.; Perlmann, T.; Evans, R. M.; Sigler, P. B. Structural Determination of Nuclear Receptor Assembly on DNA Direct Repeats. *Nature* **1995**, *358*, 203-211.
 113. Ren, P. D.; Dong, S. F.; Wu, S. W. The Novel Reduction Systems: NaBH₄-LiCl or NaBH₄-BiCl₃ for Conversion of Nitroarenes to Primary Amines. *Synth. Commun.* **1995**, *25*, 3799-3803.
 114. Rizvi, N.A.; Marshall, J. L.; Dahut, W.; Ness, E.; Truglia, J. A.; Loewen, G.; Gill, G. M.; Ulm, E. M.; Geiser, R.; Jaunakais, D.; Hawkins, M. J. A Phase I Study of LGD1069 in an Adult with Advanced Cancer. *Clin. Cancer Res.* **1999**, *5*, 1658-1664.
 115. Rottman, J. N.; Widom, R. L.; Nadal-Ginarg, B.; Mahdavi, V. A Retinoic Acid Responsive Element in the Apolipoprotein AI Gene Distinguishes Between Two Pathways. *Mol. Cell. Biol.* **1991**, *11*, 3814-3820.
 116. Rowe, A.; Eager, N. S. C.; Brickell, P. M. Members of the RXR Nuclear Family Receptors are Expressed in Neural-Crest-Derived Cells of the Developing Chick Peripheral Nervous System. *Development* **1991**, *111*, 771-778.
 117. Schulman, I. G.; Chakravarti, D.; Juguilon, H.; Romo, A.; Evans, R. M. Interaction Between the Retinoid X Receptor and a Conserved Region of the TATA-Binding Protein Mediates Hormone Dependent Transactivation. *Proc. Natl. Acad. Sci. U.S.A.* **1995**, *92*, 8288-8292.
 118. Schweigert, F. J.; Bonitz, K.; Siegling, C.; Buchholz, I. Distribution of Vitamin A, Retinoid-Binding Protein, Cellular Retinoic Acid Binding Protein I, and Retinoic X Receptor Beta in the Porcine Uterus During Gestation. *Biol. Reprod.* **1999**, *61*, 906-911.
 119. Shalita, A. R.; Fritsch, P. O. Review: Retinoids The Present and Future. Proceedings of a Symposium Held at the 18th World Congress of Dermatology. *J. Am. Acad. Dermatol.* **1992**, *27*, Part 2, pp. S24-S37.

- D'Alessandro, N.; Tolomeo, M. Structure-Activity Relationship of Novel Heteroarotinoids: Induction of Apoptosis in the HL-60 Cell Lines by Novel Isoxazole-Containing Heteroarotinoids. *J. Med. Chem.* **1999**, *42*, 4961-4969.
121. Starr, J. T.; Rai, G. S.; Dang, H.; McNelis, B. J. An Improved Oxidation Method for the Synthesis of Azodicarbonyl Compounds. *Synth. Comm.* **1997**, *27*, 3197-3200.
122. (a) Sporn, M. B.; Roberts, A. B. in *The Retinoids: Biology, Chemistry and Medicine*, 2nd. Edition, Raven Press Ltd.: New York, 1994, pp. 1-3. (b) *Ibid*, pp.17-20.
123. (a) Stahl, W.; Sundquist, A. R.; Hanusch, M.; Schwarz, W.; Sies, H. Separation of β -Carotene and Lycopene Geometrical Isomers in Biological Samples. *Clin. Chem.* **1993**, *39*, 810-814. (b) Canada, F. J.; Law, W. C.; Rando, R. R.; Yamamoto, T.; Derguini, F.; Nakanishi, K. Substrate Specificities and Mechanism in the Enzymatic Processing of Vitamin A into 11-*cis*-Retinol. *Biochemistry* **1990**, *29*, 9690-9697. (c) Horst, R. L.; Reinhardt, T. A.; Goff, J. P.; Nonnecke, B. J.; Gambhir, V. K.; Fiorella, P. D.; Napoli, J. L. Identification of 9,13-di-*cis*-Retinoic Acid As a Major Circulating Retinoid in Plasma. *Biochemistry* **1995**, *34*, 1203-1209.
124. Standeven, A. M.; Johnson, A. T.; Escobar, M.; Chandraratna, R. A. Specific Antagonist of Retinoid Toxicity in Mice. *Toxicol. Appl. Pharmacol.* **1996**, *138*, 169-175.
125. Subramanian, S. In *Modified Heteroarotinoids: Potential Anti-Cancer Agents*. 1993, Ph D. Thesis, Oklahoma State University, pp.70-117.
126. Sybyl 6.5 is a copyright of Tripos Inc. 1699 South Henly Road, St. Louis, Missouri, 63144, U.S.A.
127. Teng, M.; Duong, T. T.; Johnson, A. T.; Klein, E.; Wang, L.; Khalifa, B.; Chandraratna, A. S. Identification of a Potent Retinoic Acid Receptor α -Selective Antagonist. *J. Med. Chem.* **1997**, *42*, 2445-2451.
128. Tsai, S. Y.; Tsai, M. J.; O'Malley, B. W. Cooperative Binding of Steroid Hormone Receptors Contributes to Transcriptional Synergism at Target Enhancer Element. *Cell* **1989**, *57*, 1139-1146.
129. Umemiya, H.; Fukasawa, H.; Ebisawa, M.; Eyrolles, L.; Kawachi, E.; Eisenman, G.; Gronemeyer, H.; Hashimoto, Y.; Shudo, K. Regulation of Retinoidal Action by Diazepinylbenzoic Acids. Retinoid Synergists which Activate the RAR-RXR Heterodimers. *J. Med. Chem.* **1997**, *40*, 4222-4234.

Heterodimers. *J. Med. Chem.* **1997**, *40*, 4222-4234.

130. Umesono, K.; Evans, R. M. Determination of Target Gene Specificity for Steroid/Thyroid Hormone Receptor. *Cell* **1988**, *57*, 1139-1146.
131. Valee, B. L.; Coleman, J. E.; Ault, D. S. Zinc Fingers, Zinc, Clusters and Zinc Twists in DNA-Binding Protein Domains. *Proc. Natl. Acad. Sci. U. S. A.* **1991**, *88*, 999-1003.
132. Vinienti, M. P.; Clark, I. M.; Brinkerhoff, C. E. Using Inhibitors of Metalloproteinases to Treat Arthritis. *Arthritis Rheumatoidism* **1994**, *37*, 1115-1126.
133. Voet, D.; Voet, J. G. In *Biochemistry*, 2nd Edition, John Wiley & Sons: New York, NY, 1995, pp. 412-422.
134. (a) Wagner, M. In *Retinoid Protocols: Methods in Molecular Biology*, Vol. 89, Redfern, C. P. F. Editor, Humana Press: N. J., 1998, pp. 41- 52. (b) Hashimoto, Y.; Sasaki, T. In *Retinoid Protocols: Methods in Molecular Biology*, Vol 89, Redfern, C. P. F. Editor, Humana Press: N. J., 1998, pp.293-305.
135. Wolbach, S. D.; Howe, P. R. Tissue Changes Following Deprivation of Fat Soluble Vitamin A. *J. Exp. Med.* **1925**, *42*, 753-761.
136. Wu, Q.; Dawson, M. I.; Zheng, Y.; Hobbs, P. D.; Agadir, A.; Jong, L.; Li, Y.; Liu, R.; Lin, X.; Zhang, X. K. Inhibition of *trans*-Retinoic Acid-Resistant Human Breast Cancer Cell Growth by Retinoic X Receptor-Selective Retinoids. *Mol. Cell. Biol.* **1997**, *17*, 6598-6608.
137. Wurtz, J. M.; Bourget, W.; Renaud, J. P.; Vivat, V.; Chambon, P.; Moras, D.; Gronemeyer, H. A Conical Structure for the Ligand-Binding Domain of Nuclear Receptors. *Nat. Struct. Biol.* **1996**, *3*, 87-94.
138. Yang, Y.; Vacchio M. S; Ashwell, J. D. 9-*cis*-Retinoic Acid Inhibits Activation-Driven T-Cell Apoptosis: Implication of Retinoid X Receptor Involvement in Thymocyte Development. *Proc. Natl. Acad. Sci. U.S.A.* **1993**, *90*, 6170-6174.
139. Yasuyuki, E.; Takehana, S.; Ohno, M.; Driedger, P. E.; Stabel, S.; Mizutani, M. Y.; Tomioka, N.; Itai, A.; Shudo, K. Clarification of the Binding Mode of Teleocidin and Benzolactams to the Cys2 Domain of Protein Kinase C δ by Synthesis of Hydrophobically Modified, Teleocidin-Mimicking Benzolactams and Computational Docking Simulations. *J. Med. Chem.* **1998**, *41*, 1476-1496.
140. Yu, K. L.; Spinnazze, P.; Ostrowsky, J.; Currier, S. J.; Pack, E. J.; Hammer, L.;

- Retinoids. *J. Med. Chem.* **1996**, *39*, 2411-2421.
141. Zakharin, L. I.; Khorlina, I. M. Reduction of Esters of Carboxylic Acids Into Aldehydes. *Tetrahedron Lett.* **1962**, *14*, 619-620.
142. Zelent, A.; Leroy, P.; Krust, A.; Mendelsohn, C.; Garnier, J. M.; Kastner, P.; Chambon, P. Differentially Expressed Isoform of the Mouse Retinoic Acid Receptor β Are Generated by Usage of Two Promoters and Alternative Splicing. *EMBO J.* **1991**, *10*, 71- 81.
143. Zhang, J.; Zamir, I.; Lazar, M. A. Differential Recognition of Liganded and Unliganded Thyroid Hormone Receptor and Retinoic X Receptor Regulates Transcriptional Repression. *Mol. Cell. Biol.* **1997**, *17*, 6887-6897.

VITA 2

Jozef Klucik

Candidate for the Degree of

Doctor of Philosophy

**Thesis: MODIFICATION OF HETEROAROTINOIDS TO ENHANCE THEIR
RETINOIC ACID RECEPTOR-BINDING SPECIFICITY AND ANTI-CANCER
ACTIVITY**

Major Field: Chemistry

Biographical:

Personal Data: Born in Bodina, Czechoslovakia, On March 30, 1962, the son of Emil and Stefania Klucik.

Education: Received primary education in Czechoslovakia; received Bachelor of Science Degree in Chemistry from Cameron University, Lawton, Oklahoma, in May of 1996. Completed the requirements for the Doctor of Philosophy degree with a major in chemistry at Oklahoma State University in July of 2000.

Experience: Employed by Oklahoma State University, Department of Chemistry, as a graduate teaching assistant and as a research assistant from June, 1996, to present.

Professional Memberships: American Chemical Society, Phi Lambda Upsilon.